Topics in the Superconformal and Defect Conformal Bootstrap

Dissertation
zur Erlangung des Doktorgrades
an der Fakultät für Mathematik, Informatik und Naturwissenschaften
Fachbereich Physik
der Universität Hamburg

vorgelegt von

Aleix Gimenez Grau

Hamburg

2022

Eidesstattliche Versicherung / Declaration on oath

Hiermit versichere ich an Eides statt, die vorliegende Dissertationsschrift selbst verfasst und keine anderen als die angegebenen Hilfsmittel und Quellen benutzt zu haben.

Hamburg, 21.02.2022

Abstract

Conformal field theory has varied applications, ranging from critical phenomena in statistical and condensed matter physics, to formal aspects of quantum gravity. In recent years, the conformal bootstrap has become one of the most promising frameworks to study conformal field theory, both at the perturbative and non-perturbative level. In this thesis, we consider two extensions of the conformal bootstrap: the addition of supersymmetry, and the addition of conformal defects. Both of these extensions have rich physical applications, that we discuss in the two main parts of the thesis. In the first part, we present a pedagogical introduction to conformal field theory, the bootstrap program, supersymmetry and conformal defects. In the second part, we discuss several applications of these general methods.

Zusammenfassung

Die konforme Feldtheorie hat vielfältige Anwendungen, die von kritischen Phänomenen in der Statistik und der Physik der kondensierten Materie bis hin zu formalen Aspekten der Quantengravitation reichen. In den letzten Jahren hat sich der konforme Bootstrap zu einem der vielversprechendsten Frameworks zum Studium der konformen Feldtheorie entwickelt, sowohl auf störungsbezogener als auch auf nicht störungsbezogener Ebene. In dieser Arbeit betrachten wir zwei Erweiterungen des konformen Bootstrap: das Hinzufügen von Supersymmetrie und das Hinzufügen von konformen Defekten. Beide dieser Modifikationen haben reiche physikalische Anwendungen, die wir in den beiden Hauptteilen der Dissertation diskutieren. Im ersten Teil präsentieren wir eine pädagogische Einführung in die konforme Feldtheorie, das Bootstrap-Programm, Supersymmetrie und konforme Defekte. Im zweiten Teil diskutieren wir mehrere Anwendungen dieser allgemeinen Methoden.

Statement of Originality

Parts I and III review known results in the literature, although the presentation is original.

Part II is based on the following publications:

[1]   A. Gimenez-Grau and P. Liendo, *Bootstrapping Coulomb and Higgs branch operators*, *JHEP* **01** (2021) 175 [2006.01847].

[2]   A. Gimenez-Grau and P. Liendo, *Bootstrapping line defects in $\mathcal{N} = 2$ theories*, *JHEP* **03** (2020) 121 [1907.04345].

[3]   A. Gimenez-Grau, P. Liendo and P. van Vliet, *Superconformal boundaries in $4 - \epsilon$ dimensions*, *JHEP* **04** (2021) 167 [2012.00018].

[4]   A. Gimenez-Grau and P. Liendo, *Bootstrapping Monodromy Defects in the Wess-Zumino Model*, 2108.05107, (waiting review in JHEP).

[5]   J. Barrat, A. Gimenez-Grau and P. Liendo, *Bootstrapping holographic defect correlators in $\mathcal{N} = 4$ super Yang-Mills*, 2108.13432, (waiting review in JHEP).

All authors contributed equally to the above publications.

Finally, other papers by the author not included in this thesis are:

[6]   A. Gimenez Grau, C. Kristjansen, M. Volk and M. Wilhelm, *A Quantum Check of Non-Supersymmetric AdS/dCFT*, *JHEP* **01** (2019) 007 [1810.11463].

[7]   A. Gimenez-Grau, C. Kristjansen, M. Volk and M. Wilhelm, *A quantum framework for AdS/dCFT through fuzzy spherical harmonics on S^4*, *JHEP* **04** (2020) 132 [1912.02468].

x

Acknowledgments

Contents

Part I

Generalities

Chapter 1

Introduction

> *The measure of greatness in a scientific idea*
> *is the extent to which it stimulates thought*
> *and opens up new lines of research.*
>
> Paul Dirac [8]

In theoretical physics, to bootstrap means to answer physics problems using only basic consistency conditions. And according to Dirac's definition, bootstrapping is a great idea. Many exciting research directions are "bootstrappy": from high-loop scattering amplitude calculations, to constraining the space of UV-complete effective field theories. Because the bootstrap is such a varied subject, in this work we focus on one of its flavors: the conformal bootstrap.

The conformal bootstrap is a framework to study Conformal Field Theory (CFT) using general principles such as symmetry and unitarity. Because CFT describes interesting phenomena in many different branches of physics, the conformal bootstrap has found numerous applications, some of which we discuss in section 1.1. In section 1.2, we give a brief overview of the conformal bootstrap program, while in section 1.3 we discuss the advantages of applying this program to supersymmetric theories and conformal defects. We conclude in section 1.4 with a brief overview of the rest of this thesis.

1.1 Applications of conformal field theories

Conformal field theory is important due to its varied applications, which range from critical phenomena in statistical and condensed matter physics, to formal aspects such as string theory and the AdS/CFT correspondence. Below we given a list of applications of CFT.

Critical phenomena in statistical physics is one of the main applications of conformal field theory. The history of how physicists understood the connection between critical phenomena and CFT is a fascinating subject. Initially, physicists realized that second-order phase transitions can be understood from the existence of fluctuations at all length scales, or more precisely, from the existence of scale invariance. Because of long-distance correlations, it is natural to study second-order phase transitions in the continuum limit, which is described by Euclidean quantum field theory. In most situations, a scale-invariant quantum field theory is also invariant under a larger symmetry group: the conformal group. In conclusion, the modern perspective is that conformal field theories describe second-order phase transitions.

A remarkable property of critical phenomena is universality, namely that one CFT describes critical properties of several seemingly different systems. In other words, at the critical point the microscopic details of a model are not important; instead, only robust properties such as global symmetries determine which CFT describes the model. The $3d$ Ising CFT provides perhaps the simplest example. The universality class of this CFT describes the $3d$ Ising model at its critical temperature, as well as the liquid–vapor transition of water, or the phase transition of uniaxial magnets. Another example with experimental applications is the $O(2)$ CFT, which describes the critical point of the XY model, as well as the superfluid transition in ^{4}He. Finally, the $O(3)$ CFT appears at the critical temperature of the Heisenberg model, and describes ferromagnetic phase transitions in isotropic magnets. A comprehensive review of applications of CFT to critical phenomena can be found in [9].

Although the previous examples are three dimensional, critical phenomena in two dimensions is also described by conformal field theory. However, two-dimensional CFT is significantly different compared to CFT in higher dimensions, because the two-dimensional conformal algebra is infinite dimensional. The infinite-dimensional conformal symmetry was used in [10] to solve a family of two-dimensional CFTs called minimal models. Many minimal models corresponds to well-known statistical systems. For instance, one of them describes the critical $2d$ Ising model, while another describes the critical 3-state Potts

model. Although two-dimensional CFT is a fascinating subject, it will not be discussed in this thesis. The interested reader can find good introductions in [11–13].

Quantum phase transitions are another relevant application of CFT. In a quantum phase transition, one considers a many-body system that lives on a lattice, and the critical point is reached by tunning parameters in its quantum Hamiltonian. Because temperature is not involved in the process, criticality is reached due to large quantum fluctuations rather than large thermal fluctuations. As an example, consider a thin-film superconductor, which is described by a two-dimensional lattice that evolves in time by means of a Hamiltonian. The CFT that describes the quantum critical point naturally lives in $2+1$ dimensions, and it is none other than the Wick rotation of the $O(2)$ CFT. More generally, the quantum phase transition of a p-dimension lattice is described by a Lorentzian CFT in $p+1$ dimensions.

In the context of particle physics, CFT is valuable in connection to Renormalization Group (RG) flows. A QFT can be thought of as a microscopic model in the UV, that evolves under RG flow towards long distances, namely the IR. The physics in the deep IR is described either by a gapped phase, a phase with massless particles, or a scale invariant phase described by CFT. A simple example of a CFT phase is the conformal window of QCD with N_c colors and N_f flavors. By choosing $N_f \lesssim \frac{11}{2} N_c$, the beta function shows that there is an IR fixed point of the RG flow: by scale invariance, the fixed point admits a CFT description. More generally, if the space of QFTs is viewed as the as the space of RG flows, then CFTs are points where the flows can end. In this vision, QFTs can be organized in equivalence classes depending on their IR phases; this is the concept of universality previously discussed, where several microscopic models can lead to the same physics at long distances.

Finally, conformal field theory has many applications to formal aspects of theoretical physics. As a first example, the worldsheet formulation of string theory is consistent as long as the worldsheet is conformally invariant, connecting the fields of $2d$ CFT and string theory. Secondly, in the AdS/CFT correspondence CFT provides a non-perturbative definition of the meaning of quantum gravity in AdS background. Although being more than twenty years old, AdS/CFT is still a very fruitful area of research. Finally, the study of dualities is a major subject where many of the known examples are given by CFTs. This list is by no means complete; nowadays CFT is connected to so many topics, ranging from scattering amplitudes to quantum information, that giving a comprehensive review would be a formidable task.

1.2 The conformal bootstrap

The previous list of applications demonstrates that CFT explains interesting physical phenomena. It is therefore necessary to understand and solve CFT, which is unfortunately a complicated task. One challenge is that due to scale invariance, it is hard to find effective descriptions that neglect unimportant effects from higher scales. A manifestation of this is the lack of small parameters to expand on.

Several methods circumvent the lack of small parameters, and allow to study CFTs perturbatively. One such method is the high temperature expansion, that consists on expanding the partition function of a lattice model to high order in $1/T$, and then extrapolating to the critical temperature T_c. An alternative consists on formulating a continuum model in $4 - \varepsilon$ dimensions, use perturbation theory around $\varepsilon = 0$, and then extrapolate to $\varepsilon = 1$ to study three-dimensional CFT. Finally, there is the large-N expansion, where one expands observables in the $O(N)$ CFT in powers of $1/N$, and extrapolates to low values of N at the end. These three methods can be problematic because of the need of uncontrolled extrapolations to reach the physically relevant regime. That is, to reach the critical temperature T_c, the physical dimension $d = 3$, or the symmetry group $O(N)$ for $N = 1, 2, 3$, one incurs in errors that cannot be bounded accurately. Although the perturbative methods often give results consistent with each other and with experiment, one might hope to find a more rigorous approach.

Monte-Carlo simulations are a powerful alternative to perturbative methods. In Monte-Carlo simulations, observables are calculated from a lattice model by averaging over random samples. A downside of Monte-Carlo methods is the need to extrapolate to the infinite volume limit, but all in all, Monte-Carlo methods are the most reliable of the ones presented so far. However, there are two somewhat philosophical problems that apply both to the perturbative and numerical methods. First, these methods need a microscopic model from which to extract properties of the CFT, which is universal. Second, these methods do not exploit the conformal symmetry enjoyed by the critical point. Instead, it would be desirable to have a method where universality and conformal symmetry are built in from the beginning, or in other words, a method that studies CFT directly without resorting to particular microscopic models.

The conformal bootstrap is such a framework. In the conformal bootstrap approach, one uses conformal invariance to derive properties that any CFT should obey. Actually, these properties can be promoted to a set of axioms that define conformal field theory, and which

are consistent with the Wightman and Osterwalder-Schrader axioms [14, 15]. However, unlike other axiomatic approaches, the conformal bootstrap is a powerful calculational framework. Indeed, the CFT axioms imply an infinite set of equations called crossing or bootstrap equations. Pictorially, the crossing equations read

$$
\sum_{\Delta,\ell} \quad \raisebox{-1em}{$\mathcal{O}_i \; \mathcal{O}_{\Delta,\ell} \; \mathcal{O}_l$} \qquad = \qquad \sum_{\Delta,\ell} \quad \raisebox{-1em}{$\mathcal{O}_i \; \mathcal{O}_l \; \mathcal{O}_{\Delta,\ell} \; \mathcal{O}_j \; \mathcal{O}_k$} \quad . \tag{1.1}
$$

These equations are very constraining, allowing the conformal bootstrap to make quantitative predictions about CFT. For many years, however, it was not understood how to extract information from crossing equations in $d \geq 3$. In 2000 this started to change, because Dolan and Osborn [16] obtained closed-form expressions for conformal blocks, the building blocks of the crossing equation. Thanks to that, in 2008 the work of Rattazzi, Rychkov, Tonni and Vichi [17] proposed a numerical algorithm that constrains the space of solutions to crossing. Since then, the conformal bootstrap has become an extremely active research topic, which has reshaped our understanding of conformal field theory. Many of these exciting developments will be discussed in later chapters. In the rest of the introduction, we direct our attention to supersymmetry and defects, two topics that will be of central importance in this thesis.

1.3   Supersymmetry and Defects

Because the conformal bootstrap program is such a wide subject, this thesis focuses on two of its applications: superconformal field theories and conformal defects. Below we show applications of these subjects, and argue why the conformal bootstrap is a good framework to approach them.

Superconformal field theory (SCFT) is a rich subject that has attracted interest for several reasons.[1] The first reason is that the large symmetry algebra of SCFT gives analytical control on part of their dynamics. The extra control manifests itself in the existence of protected quantities: scaling dimensions and low-point functions of protected operators; the expectation value of non-local operators such as supersymmetric Wilson loops;

---

[1]Although supersymmetry has been intensively studied in connection to possible phenomenological applications, these play no role in our discussion.

the superconformal index; etc. Often, protected quantities can be computed using non-renormalization theorems, supersymmetric localization, or appealing to protected sectors such as the chiral algebra in $4d$ $\mathcal{N} \geq 2$ theories. Another reason for the interest in SCFT is that some highly-supersymmetric models have holographic duals that give a handle on their strong coupling behavior. Additionally, since SCFTs are under better analytical control, there is hope that a classification program can be accomplished. For example, some believe that $6d$ $(2,0)$ theory and $4d$ $\mathcal{N} = 4$ SYM are the unique maximally-supersymmetric models in their respective dimensions, up to a choice of Lie algebra. It would be exciting if the uniqueness is rigorously proven, or if a similar classification is found for the non-maximally supersymmetric case, where many SCFTs are known to exist. Finally, coming back to experimental applications, $3d$ SCFTs with low amount of supersymmetry might exist at the boundary of topological phases and could potentially be observed in the lab [18, 19].

There are several reasons why the conformal bootstrap works well in combination with supersymmetry. First, because many newly discovered SCFTs do not have Lagrangian descriptions, a non-perturbative method like the superconformal bootstrap is perhaps the only way to study them. Second, protected quantities can be used as input in the crossing equations, making them more constraining, and then use these crossing equations to obtain information of unprotected observables. The advantage is that the predictions for unprotected observables often could not have been obtained by any other methods. Finally, because the conformal bootstrap is a general and agnostic method, it might be the perfect tool to address the classification program for SCFTs.

Defects are the second topic that we discuss in detail throughout the thesis. In QFT defects are non-local operators, that is, operators that extend on a submanifold of space-time. In the study of CFT it is natural to focus on conformal defects, which preserve part of the conformal symmetry of the ambient CFT. However, for the purpose of illustration, we show applications of general defects, that range from gauge theory to condensed matter physics. As a first example, in gauge theories Wilson and 't Hooft operators are line defects which behave as non-local order parameters, because they allow to distinguish the confining phase. In statistical and condensed matter physics, defects describe phenomena with an interplay between micro and macroscopic properties of the critical phase. Indeed, the prime example of defect is a boundary, which captures the finite size of physical systems. A perhaps less familiar example is a point-like impurity in a quantum critical point. Because it extends through the time direction, such an impurity can be described as a line defect. Finally, open string theory provides a more formal example, where the boundary of the

string can be understood as a defect from the worldsheet perspective, while D-branes are defects from the target-space perspective.

Because of their many applications, understanding defects is a necessary endeavor. However, as is the case of regular CFT, the study of defects can be quite challenging. One one hand, perturbative methods such as ε–expansion or large-N expansion lead to uncontrolled errors. On the other hand, defects with different microscopic origin can be described by the same universal defect CFT. This calls for an extension of the conformal bootstrap program to include defects. Such a program, which extends the CFT axioms and crossing equations to incorporate defects, will be one of the recurring topics of this thesis.

1.4 Structure of the thesis

The goal of the thesis is to advance our understanding of superconformal field theories, conformal defects, and often a combination of both. Because many similar ideas are used in these studies, the purpose of part I is to give a comprehensive introduction to the needed background. Each chapter covers a topic that will be of importance later in the thesis: basics of conformal bootstrap, numerical methods, analytical methods, superconformal theories, and defects. Although some of these topics have been reviewed extensively in the literature, superconformal theories and conformal defects lack beginner-friendly reviews. Therefore, one of our goals is to introduce the subjects in a clear and simple way. Unfortunately, some of the topics are somewhat technical, and in these situations, we often sacrifice rigor to achieve greater clarity. At the end of every chapter, we list topics that we have not covered. The goal of the literature review is to guide the interested reader, as well as to give credit to the many authors that contributed to our current understanding. We apologize in advance for important omissions, which are due to the breadth of the literature on certain subjects.

In part II of the thesis, we move on to advanced applications of these methods. Each chapter in based on a publication to which the author has contributed substantially. These chapters are self-contained, with their own motivation and conclusions. In some cases, the notation might differ slightly from that in part I, but we hope it will not cause too much confusion. Finally, part III contains a brief summary of the work, and a survey of exciting directions that might become important in conformal bootstrap research in the coming years.

Chapter 2

Conformal bootstrap

The main subject of this thesis are Conformal Field Theories (CFTs). These are quantum field theories that, besides Poincare invariance, enjoy a larger symmetry group, namely the group of conformal transformations. In this chapter, we lay the foundations of conformal field theory, including conformal transformations and their algebra, their representation theory, correlation functions, the operator product expansion and the crossing equation. We conclude listing other reviews in the literature, and giving references to subjects we have not covered.

2.1 Conformal group

2.1.1 Conformal transformations

A conformal transformation is a change of coordinates $x \to x'(x)$ under which the metric is mapped to itself, up to a space dependent scale factor:

$$ds'^2 = \Omega(x)^2 ds^2 \,. \tag{2.1}$$

In other words, conformal transformations preserve angles but not distances. In order to classify conformal transformations, it is convenient to consider infinitesimal transformations around flat space. In particular, we start with a flat metric $ds^2 = \delta_{\mu\nu} dx^\mu dx^\nu$ and perform an infinitesimal change of variables $x'_\mu = x_\mu + \epsilon_\mu(x)$, with scale factor $\Omega(x) = 1 + \sigma(x)$. A simple calculation shows that conformality requires

$$\partial_\mu \epsilon_\nu + \partial_\nu \epsilon_\mu = 2\sigma \delta_{\mu\nu} \,. \tag{2.2}$$

A solution ϵ_μ of this equation is called a conformal Killing vector. It is possible to classify all conformal Killing vector, see for example [20]. Besides the obvious translations, rotations and dilatations, there is a less familiar solution called special conformal transformation. As a result, the most general conformal Killing vector reads

$$\epsilon_\mu(x) = \underbrace{a_\mu}_{\text{translation}} + \underbrace{\omega_{\mu\nu}x^\nu}_{\text{rotation}} + \underbrace{\lambda x_\mu}_{\text{dilatation}} + \underbrace{b_\mu x^2 - 2x_\mu b_\nu x^\nu}_{\text{special conformal}}, \tag{2.3}$$

where $\omega_{\mu\nu} = -\omega_{\nu\mu}$. Together, these form a $\frac{(d+2)(d+1)}{2}$–dimensional group of transformations, the conformal group.

2.1.2 Conformal algebra

In quantum field theory, symmetries act on the Hilbert space by means of operators. In particular, given a conformal Killing vector $\epsilon = \epsilon^\mu \partial_\mu$, we can define a generator Q_ϵ associated to it. The commutation relations of the conformal generators can then be obtained from those of the Killing vectors

$$[Q_{\epsilon_1}, Q_{\epsilon_2}] = Q_{-[\epsilon_1, \epsilon_2]}. \tag{2.4}$$

If we associate a transformation with parameters $\{a_\mu, \omega_{\mu\nu}, \lambda, b_\mu\}$ to the symmetry generators $\{P_\mu, M_{\mu\nu}, D, K_\mu\}$, then the resulting commutation relations read [21]

$$[M_{\mu\nu}, P_\rho] = \delta_{\nu\rho}P_\mu - \delta_{\mu\rho}P_\nu, \tag{2.5}$$

$$[M_{\mu\nu}, K_\rho] = \delta_{\nu\rho}K_\mu - \delta_{\mu\rho}K_\nu, \tag{2.6}$$

$$[M_{\mu\nu}, M_{\rho\sigma}] = \delta_{\nu\rho}M_{\mu\sigma} - \delta_{\mu\rho}M_{\nu\sigma} + \delta_{\nu\sigma}M_{\mu\rho} - \delta_{\mu\sigma}M_{\nu\rho}, \tag{2.7}$$

$$[D, P_\mu] = P_\mu, \tag{2.8}$$

$$[D, K_\mu] = -K_\mu, \tag{2.9}$$

$$[K_\mu, P_\nu] = 2\delta_{\mu\nu}D - 2M_{\mu\nu}. \tag{2.10}$$

The first three lines specify how P_μ, K_μ and $M_{\mu\nu}$ transform under rotations, while the fourth and fifth line implies that P_μ/K_μ raise/lower the eigenvalue of D by one unit. These commutation relations can be brought to a more elegant form with the following redefinition:

$$L_{d+1,\mu} = \frac{P_\mu - K_\mu}{2}, \quad L_{d+2,\mu} = \frac{P_\mu + K_\mu}{2}, \quad L_{\mu\nu} = M_{\mu\nu}, \quad L_{d+1,d+2} = D. \tag{2.11}$$

If we also introduce the metric $\eta_{AB} = \mathrm{diag}(1, \ldots, 1, -1)$ in $\mathbb{R}^{d+1,1}$, then the new generators obey the commutation relations

$$[L_{AB}, L_{CD}] = \eta_{BC} L_{AD} - \eta_{AC} L_{BD} + \eta_{BD} L_{CA} - \eta_{AD} L_{CB} \,. \tag{2.12}$$

This shows that the conformal algebra is isomorphic to the algebra of $SO(d+1, 1)$. This observation is the basis of the embedding space formalism, which exploits that the conformal group acts linearly on $\mathbb{R}^{d+1,1}$ to study conformal correlators [22–26]. We do not discuss the embedding space formalism further, since it will not play a role in this thesis.

2.1.3   Reality condition

Because symmetry generators act on the Hilbert space, it is necessary to know how they transform under Hermitian conjugation. In this work, we are mostly interested in Euclidean CFT in radial quantization, for which the natural action under Hermitian conjugation is given by

$$M_{\mu\nu}^{\dagger} = -M_{\mu\nu} \,, \quad D^{\dagger} = D \,, \quad P_{\mu}^{\dagger} = K_{\mu} \,. \tag{2.13}$$

There is a heuristic justification of the above reality condition. In radial quantization, an in-state is prepared by a local operator at the origin $|\mathcal{O}\rangle = \mathcal{O}(0)|0\rangle$, while an out-state is prepared by an operator at infinity $\langle\mathcal{O}| = \langle 0|\mathcal{O}(\infty)$. As a result, Hermitian conjugation must reverse the role of the origin and infinity, and therefore it exchanges $P_{\mu} \leftrightarrow K_{\mu}$. We say that a representation of the conformal algebra is reflection positive if it respects the Hermitian conjugation (2.13).

Let us mention that if we had chosen to work in Lorentzian signature, then the conformal group would be $SO(d, 2)$, and in this case we would be interested in self-adjoint generators

$$\text{Unitarity for } SO(d, 2): \qquad P_{\mu}^{\dagger} = P_{\mu} \,, \quad K_{\mu}^{\dagger} = K_{\mu} \,. \tag{2.14}$$

Unitary representations of $SO(d, 2)$, i.e. satisfying (2.14), are in one-to-one correspondence with reflection-positive representations of $SO(d+1, 1)$, i.e. satisfying (2.13), see for example [27].

2.1.4   Representation theory

In conformal field theories, physical operators transform in representations of the conformal group. The representation theory of the conformal group can be studied with the little

group technique, which is familiar in the case of Poincare representations, see [28] for a pedagogical discussion. For conformal field theory, the main idea is to focus on operators inserted at the origin, and then translate with the P_μ generator:

$$\mathcal{O}(x) = e^{x^\mu P_\mu}\mathcal{O}(0)e^{-x^\mu P_\mu}\,. \tag{2.15}$$

The stabilizer of the origin $x = 0$ is formed by $M_{\mu\nu}$, D and K_μ, and operators inserted at the origin must transform as an irreducible representation of the stabilizer group. We assume this operator transforms as

$$[D, \mathcal{O}(0)] = \Delta\mathcal{O}(0)\,, \qquad [M_{\mu\nu}, \mathcal{O}(0)] = \mathcal{S}_{\mu\nu}\mathcal{O}(0)\,, \tag{2.16}$$

The eigenvalue Δ of the dilatation operator is called the scaling dimension of $\mathcal{O}$. Regarding rotations, the operator transforms in a representation of $SO(d)$, so a more precise version of the second equation is $[M_{\mu\nu}, \mathcal{O}^a(0)] = (\mathcal{S}_{\mu\nu})_b{}^a\mathcal{O}^b(0)$, but in the rest of the discussion we continue to suppress indices a to simplify notation. Given an operator $\mathcal{O}(0)$, acting with P_μ/K_μ produces operators with higher/lower scaling dimension, which form a so-called conformal multiplet. In physically sensible theories, the scaling dimension is bounded below, so without loss of generality we can take $O(0)$ to be the lowest dimension operator in its conformal multiplet, which we call a conformal primary operator. As a result

$$[K_\mu, \mathcal{O}(0)] = 0 \qquad \text{(conformal primary operator)}\,. \tag{2.17}$$

Summarizing, conformal primary operators are characterized by dimension Δ, a representation under $SO(d)$ and (2.17). Starting from the primary, one obtains the full conformal multiplet acting with P_μ. This conformal multiplet forms an irreducible representation of the conformal group.

Besides the generic case just presented, there exist exceptional representations called short representations. The most important examples of short representations are the free scalar, conserved current and stress-tensor multiplets. Short representation are characterized by a combination of P's that kills the conformal primary, for example

$$[P^2, \mathcal{O}(0)] = 0 \qquad \text{(free scalar multiplet)}\,, \tag{2.18}$$

$$[P_\mu, J^\mu(0)] = 0 \qquad \text{(conserved current multiplet)}\,, \tag{2.19}$$

$$[P_\mu, T^{\mu\nu}(0)] = 0 \qquad \text{(stress-tensor multiplet)}\,. \tag{2.20}$$

Consistency with the conformal algebra fixes the dimension of these operators in terms of their spin. We defer a more detailed discussion of short representations to chapter 5, which is devoted to superconformal field theories.

As anticipated, by using (2.15) it can determined how the conformal generators act on operators at an arbitrary location:

$$[P_\mu, \mathcal{O}(x)] = \partial_\mu \mathcal{O}(x)\,, \tag{2.21}$$

$$[D, \mathcal{O}(x)] = (x^\mu \partial_\mu + \Delta)\mathcal{O}(x)\,, \tag{2.22}$$

$$[M_{\mu\nu}, \mathcal{O}(x)] = (x_\nu \partial_\mu - x_\mu \partial_\nu + \mathcal{S}_{\mu\nu})\mathcal{O}(x)\,, \tag{2.23}$$

$$[K_\mu, \mathcal{O}(x)] = (2x_\mu(x\cdot\partial) - x^2\partial_\mu + 2\Delta x_\mu - 2x^\nu \mathcal{S}_{\mu\nu})\mathcal{O}(x)\,. \tag{2.24}$$

The first equation can be obtained by taking a derivative of (2.15). The second equation can be obtained using the Baker–Campbell–Hausdorff formula as follows

$$\begin{aligned}
[D, \mathcal{O}(x)] &= e^{x^\mu P_\mu}\big[e^{-x^\mu P_\mu}De^{x^\mu P_\mu}, O(0)\big]e^{-x^\mu P_\mu} \\
&= e^{x^\mu P_\mu}\big[D + x^\mu P_\mu, O(0)\big]e^{-x^\mu P_\mu} \\
&= (x^\mu \partial_\mu + \Delta)\mathcal{O}(x)\,.
\end{aligned} \tag{2.25}$$

Similar calculations give the action of $M_{\mu\nu}$ and K_μ given in (2.23) and (2.24) respectively.

2.2 Correlation functions and the OPE

In the previous subsection we studied the conformal group and determined that physical operators transform in representations described by scaling dimensions Δ and representations under the rotation group $SO(d)$. We are now ready to look at the main observable in conformal field theories, namely correlation functions of local operators. A key role is played by the operator product expansion, which relates n- and $n-1$–point functions.

2.2.1 Index free notation

For simplicity, in this work we focus on operators in rank–ℓ symmetric-traceless representations of the rotation group $SO(d)$, which we call spin–ℓ representations. In particular, scalar operators are the zero-rank case, or equivalently $\ell = 0$. More general representations, such as mixed-symmetry or spinor operators have been studied in the literature, see e.g. [24, 25]. For our purposes, it is convenient to employ index-free notation, which we now introduce.

The goal of index-free notation is to trade objects with symmetric-traceless indices by a polynomials in an auxiliary polarization vector η_μ. This is achieved by contracting indices with the polarization vector as follows

$$\mathcal{O}(x,\eta) = \mathcal{O}(x)^{\mu_1\cdots\mu_\ell}\eta_{\mu_1}\ldots\eta_{\mu_\ell}\,. \qquad (2.26)$$

Since the ℓ indices are symmetric, we do not lose information contracting with a unique polarization vector. Furthermore, since the indices are traceless, one should consider a null polarization vector $\eta_\mu\eta_\mu = 0$. Notice that given $\mathcal{O}(x,\eta)$, the original symmetric-traceless tensor can be uniquely reconstructed as follows

$$\mathcal{O}(x)^{\mu_1\cdots\mu_\ell} = \frac{1}{\ell!(d/2-1)_\ell}D_{\mu_1}\ldots D_{\mu_\ell}\mathcal{O}(x,\eta)\,, \qquad (2.27)$$

where we introduced the so-called Todorov operator

$$D_\mu = \left(\frac{d}{2} - 1 + \eta\cdot\frac{\partial}{\partial\eta}\right)\frac{\partial}{\partial\eta^\mu} - \frac{1}{2}\eta_\mu\frac{\partial^2}{\partial\eta\cdot\partial\eta}\,. \qquad (2.28)$$

The use of index-free notation is particularly useful for correlation functions, which take a simpler form in this formalism.

2.2.2   Correlation functions

Correlation functions in CFT are highly constrained by conformal symmetry, as we now show. In order to derive these constraints, it is convenient to work in a Hilbert-space formalism, where correlation functions are vaccuum expectation values of operators. The vaccuum $|0\rangle$ is a conformal invariant state, meaning that $L|0\rangle = 0$ for any conformal generator $L \in \{D, P_\mu, K_\mu, M_{\mu\nu}\}$. Furthermore, when acting on primary operators we have $[L, \mathcal{O}(x_i)] = \mathcal{L}^{(i)}\mathcal{O}(x_i)$, where $\mathcal{L}^{(i)}$ are the differential operators in (2.21)-(2.24). As a result, conformal invariance leads to a system of partial differential equations satisfied by correlation functions:

$$0 = \langle 0|[L, \mathcal{O}_1(x_1)\ldots\mathcal{O}_n(x_n)]|0\rangle = \sum_{i=1}^{n}\mathcal{L}^{(i)}\langle\mathcal{O}_1(x_1)\ldots\mathcal{O}_n(x_n)\rangle\,. \qquad (2.29)$$

We are going to call these the conformal Ward identities. In the rest of this section, we present simple solutions of the conformal Ward identities for $n = 1, 2, 3$. However, we stress that the most efficient means to obtain correlation functions is the embedding space formalism.

The simplest correlators are one-point functions. By translation invariance, these have to be constant $\langle \mathcal{O}(x, \eta) \rangle = k$. However, requiring scale invariance $x \to \lambda x$ implies that $k \neq 0$ only if $\Delta = 0$. In other words, the identity operator $\mathbb{1}$ is the only operator in CFT with non-vanishing one-point function, which we normalize to unity $\langle \mathbb{1} \rangle = 1$.

The first non-trivial correlator is a two-point function. In this case, a two-point function can only be non-vanishing provided the dimensions of the two operators are equal $\Delta_1 = \Delta_2$. Furthermore, we are allowed to take linear combinations of degenerate operators, in order to diagonalize the matrix of two-point functions. After such a procedure is implemented, the two-point function of symmetric-traceless tensors read

$$\langle \mathcal{O}_1(x_1, \eta_1) \mathcal{O}_2(x_2, \eta_2) \rangle = \frac{\delta_{\mathcal{O}_1, \mathcal{O}_2}}{x_{12}^{2\Delta_i}} \left(\eta_1^\mu \eta_2^\mu - \frac{2\eta_1^\mu x_{12}^\mu \eta_2^\nu x_{12}^\nu}{x_{12}^2} \right)^\ell . \tag{2.30}$$

As we have shown, two-point functions are completely determined by conformal symmetry and our choice of normalization conventions.

In order to obtain dynamical information of a theory, it is necessary to look at higher-point functions. The simplest one is the three-point function of two scalars and a spin–ℓ operator:

$$\langle \mathcal{O}_1(x_1) \mathcal{O}_2(x_2) \mathcal{O}_3(x_3, \eta) \rangle = \frac{\lambda_{123}}{x_{12}^{\Delta_{123}+\ell} x_{13}^{\Delta_{132}-\ell} x_{23}^{\Delta_{231}-\ell}} \left(\frac{\eta^\mu x_{13}^\mu}{x_{13}^2} - \frac{\eta^\mu x_{23}^\mu}{x_{23}^2} \right)^\ell . \tag{2.31}$$

Here we have defined $\Delta_{ijk} = \Delta_i + \Delta_j - \Delta_k$. Unless there is there is a global symmetry preventing it, it is generically expected that all such three-point functions are non-vanishing. Since we defined the two-point functions to be unit normalized, the normalization of the three-point function λ_{123} is uniquely defined, and therefore it captures dynamical information about a CFT. Often λ_{123} is called three-point coupling, three-point OPE coefficient, or simply OPE coefficient.

One could go on and consider correlation functions with more operators, but perhaps surprisingly, they can all be reconstructed with the information of three-point functions. This is achieved by the operator product expansion, which we now introduce.

2.2.3   Operator product expansion

The Operator Product Expansion (OPE) is a general property of quantum field theory, by which the product of two operators can be approximated as an infinite sum of single local

operators:

$$\mathcal{O}_1(x_1)\mathcal{O}_2(x_2) = \sum_k \lambda_{12k} f_{12k}(x_{12}, \partial_{x_2})\mathcal{O}_k(x_2) \quad \text{as} \quad x_1 \to x_2. \tag{2.32}$$

In CFT, it is conventional to sum only over conformal primary operators, and capture the contribution of conformal descendants by taking space derivatives, which explains why f_{12k} depends on ∂_{x_2}. The fact that the contribution of $\mathcal{O}_k$ to the OPE is proportional to λ_{12k} can be seen inserting (2.32) in the three-point function (2.31). Note that in (2.32) the spin indices have been left implicit to improve readability.

There are two reasons why the OPE is more powerful in CFT than in regular QFT. The first reason is that instead of an asymptotic expansion, the OPE in CFT is a convergent expansion, see [29, 30]. The actual radius of convergence depends on the correlator under cosideration. For example, the OPE of $\mathcal{O}_1\mathcal{O}_2$ inside the n-point function $\langle \mathcal{O}_1 \ldots \mathcal{O}_n \rangle$ is convergent provided one can surround x_1 and x_2 with a sphere such that all other points $x_3, \ldots, x_n$ are outside this sphere. The second reason is that in CFT, since three-point functions are kinematically fixed up to a normalization, the functions $f_{12k}(x_{12}, \partial_{x_2})$ are also kinematically fixed. In order to see that, one inserts the OPE (2.32) in the three-point function (2.31). The result has to be equal to a two-point function of the form (2.30), which allows one to uniquely determine f_{12k}. For example, at leading order in the limit $x_1 \to x_2$ one finds

$$\mathcal{O}_1(x_1)\mathcal{O}_2(x_2) = \sum_k \frac{\lambda_{12k}}{x_{12}^{\Delta_1+\Delta_2-\Delta_k+\ell}} \left[x_{12}^{\mu_1} \ldots x_{12}^{\mu_\ell} \mathcal{O}_k^{\mu_1 \ldots \mu_\ell}(x_2) + \ldots \right]. \tag{2.33}$$

The take-home message is that two- and three-point functions fix the form of the operator product expansion. If one is interested in higher-point functions, they can be expressed as infinite sums of products of lower-point functions by repeatedly using the OPE. Since the spectrum of operators and the set of OPE coefficients fixes any higher-point function, one can say that a CFT is completely determined by $\{\Delta_i, \lambda_{ijk}\}$, which is often called CFT data. The simplest example of the power of the OPE is provided by four-point functions, which are the subject of the next section.

2.3 The Conformal Bootstrap Program

In the previous section, we argued that given a set of CFT data $\{\Delta_i, \lambda_{ijk}\}$, one can in principle construct any correlation function of local operators. However, it is natural to

ask the question whether any CFT data is valid, or instead there are some consistency conditions the CFT data should satisfy. In this section we study four-point functions, and show that associativity of the OPE puts strong constraints on the CFT data. This is demonstrated by the crossing equation, which will be the most important equation of this thesis.

2.3.1   Four-point functions

A new feature of four-point functions is the existence of conformally-invariant cross ratios:

$$u = z\bar{z} = \frac{x_{12}^2 x_{34}^2}{x_{13}^2 x_{24}^2}\,, \qquad v = (1-z)(1-\bar{z}) = \frac{x_{14}^2 x_{23}^2}{x_{13}^2 x_{24}^2}\,. \tag{2.34}$$

These two cross-ratios satisfy the conformal Ward identities (2.29) by themselves, so a four-point functions depends on a function $\mathcal{G}(u,v)$. The kinematics of four-point spinning correlators is complicated, so here and in the rest of the thesis we focus on four-point functions of scalar ($\ell = 0$) operators. There is some freedom on the overall normalization of the four-point function, but the choice which is most common in the modern CFT literature is

$$\langle \mathcal{O}_i(x_1)\mathcal{O}_j(x_2)\mathcal{O}_k(x_3)\mathcal{O}_l(x_4)\rangle = \frac{\mathcal{G}_{ijkl}(u,v)}{x_{12}^{\Delta_i+\Delta_j} x_{34}^{\Delta_k+\Delta_l}} \left(\frac{x_{24}}{x_{14}}\right)^{\Delta_{ij}} \left(\frac{x_{14}}{x_{13}}\right)^{\Delta_{kl}}\,, \tag{2.35}$$

where the notation $\Delta_{ij} = \Delta_i - \Delta_j$ is used.

As anticipated in section 2.2.3, the operator product expansion is fundamental in the study of four and higher-point functions. Indeed, by using the OPE for $\mathcal{O}_i\mathcal{O}_j$ we reduce a four-point function to an infinite sum of the form $\sum_{\mathcal{O}} \lambda_{ij\mathcal{O}} f_{ij\mathcal{O}}\langle \mathcal{O}\mathcal{O}_k\mathcal{O}_l\rangle$. Remember that both $f_{ij\mathcal{O}}$ and $\langle\mathcal{O}\mathcal{O}_k\mathcal{O}_l\rangle$ are kinematically fixed, so each term in this infinite sum can be computed, and the resulting object is called conformal block. In particular, after stripping off the prefactors in (2.35), we see that the function of the cross-ratios $\mathcal{G}_{ijkl}(u,v)$ admits the expansion

$$\mathcal{G}_{ijkl}(u,v) = \sum_{\mathcal{O}} \lambda_{ij\mathcal{O}}\lambda_{kl\mathcal{O}} \, g_{\Delta,\ell}^{\Delta_{ij},\Delta_{kl}}(u,v)\,. \tag{2.36}$$

In subsection 2.3.3, we discuss in great detail the importance of (2.36), but before we take a small detour to review basic properties of conformal blocks $g_{\Delta,\ell}^{\Delta_{ij},\Delta_{kl}}(u,v)$.

19

2.3.2 Conformal blocks

Our current understanding of conformal blocks has been shaped by the highly influential works by Dolan and Osborn [16, 31, 32]. A crucial observation by these authors is that acting with the Casimir operator on a four-point function, one selects the contribution of a single conformal family to the OPE. This implies that conformal blocks are solutions to a differential equation of the form

$$\left(\mathcal{C}_2^{(1+2)} - c_2 \right) \langle \mathcal{O}_1 \mathcal{O}_2 \mathcal{O}_3 \mathcal{O}_4 \rangle = 0 \,, \tag{2.37}$$

where $\mathcal{C}_2^{(1+2)}$ is the quadratic Casimir acting on points x_1 and x_2 defined by

$$\mathcal{C}_2^{(1+2)} = -\frac{1}{2} \sum_{A,B} (\mathcal{L}_{AB}^{(1+2)})^2 \,, \qquad \mathcal{L}_{AB}^{(1+2)} = \mathcal{L}_{AB}^{(1)} + \mathcal{L}_{AB}^{(2)} \,. \tag{2.38}$$

The differential operators $\mathcal{L}_{AB}^{(i)}$ can be read off from (2.11) and (2.21)–(2.24). Finally, the constant c_2 is the eigenvalue of the Casimir operator when acting on an operator of dimension Δ and spin ℓ, namely $c_2 = \Delta(\Delta - d) + \ell(\ell + d - 2)$.

By using the form of four-point functions (2.35), one arrives at the following differential equation for the conformal blocks

$$\left(D_z + D_{\bar{z}} + (d-2) \frac{z\bar{z}}{z - \bar{z}} ((1-z)\partial_z - (1-\bar{z})\partial_{\bar{z}}) - \frac{c_2}{2} \right) g_{\Delta,\ell}^{\Delta_{12},\Delta_{34}}(z,\bar{z}) = 0, \tag{2.39}$$

$$D_z = z^2(1-z)\partial_z^2 + \frac{\Delta_{12} - \Delta_{34} - 2}{2} z^2 \partial_z + \frac{\Delta_{12}\Delta_{34}}{4} z \,. \tag{2.40}$$

This differential equation has to be complemented with a boundary condition in order to get the unique physical solution. By using the leading-order term in the OPE (2.33), it is possible to derive the following behavior for the blocks

$$g_{\Delta,\ell}^{\Delta_{ij},\Delta_{kl}}(z,\bar{z}) \sim \frac{1}{(-2)^\ell} z^{(\Delta-\ell)/2} \bar{z}^{(\Delta+\ell)/2} \qquad \text{as} \quad 0 < z \ll \bar{z} \ll 1 \,. \tag{2.41}$$

There exist explicit solutions of (2.39)-(2.41) for any even d. For the purposes of this thesis, we only need

$$d = 2 : \quad g_{\Delta,\ell}^{\Delta_{12},\Delta_{34}}(z,\bar{z}) = \frac{1}{(-2)^\ell} \frac{1}{(1+\delta_{\ell,0})} \left(k_{\Delta+\ell}^{\Delta_{12},\Delta_{34}}(z) k_{\Delta-\ell}^{\Delta_{12},\Delta_{34}}(\bar{z}) + z \leftrightarrow \bar{z} \right) \,,$$

$$d = 4 : \quad g_{\Delta,\ell}^{\Delta_{12},\Delta_{34}}(z,\bar{z}) = \frac{1}{(-2)^\ell} \frac{z\bar{z}}{(z-\bar{z})} \left(k_{\Delta+\ell}^{\Delta_{12},\Delta_{34}}(z) k_{\Delta-\ell-2}^{\Delta_{12},\Delta_{34}}(\bar{z}) - z \leftrightarrow \bar{z} \right) \,, \tag{2.42}$$

which is written in terms of the $SL(2, \mathbb{R})$ block

$$k_\beta^{\Delta_{12}, \Delta_{34}}(x) = x^{\beta/2} {}_2F_1 \left(\frac{\beta - \Delta_{12}}{2}, \frac{\beta + \Delta_{34}}{2}, \beta; x \right) . \tag{2.43}$$

The $SL(2, \mathbb{R})$ block is an eigenfunction of the differential operator D_x with eigenvalue $\beta(\beta - 2)/2$. Alternatively, it is a one-dimensional conformal block with a normalization different from (2.41).

For odd (and non-integer) dimension d, there exist no simple closed-form expressions. This is not a problem in applications, because the differential equation (2.39)-(2.41) allows the generation of power series representations for the conformal blocks, as will be explained in detail later.

2.3.3 Crossing equation

In equation (2.36) we showed that a four-point function can be expanded in conformal blocks

$$\mathcal{G}_{ijkl}(u, v) = \sum_{\mathcal{O}} \lambda_{ij\mathcal{O}} \lambda_{kl\mathcal{O}}\, g_{\Delta, \ell}^{\Delta_{ij}, \Delta_{kl}}(u, v) . \tag{2.44}$$

The power of equation (2.44) can be seen in two complementary ways:

1. If one knows a four-point $\mathcal{G}_{ijkl}(u, v)$, then (2.44) provides a method to extract infinitely many OPE coefficients $\lambda_{ij\mathcal{O}}$.

2. Conversely, if one knows the OPE coefficients, then (2.44) provides a method to reconstruct a four-point function.

However, the logic of the conformal bootstrap program goes in a somewhat reverse way. Even when the four-point function $\mathcal{G}_{ijkl}(u, v)$ and the CFT data are *not known*, equation (2.44) leads to strong constraints on the CFT data, and in favorable situations, it allows to reconstruct the four-point function.

Let us discuss how this procedure works. Crossing symmetry is the simple observation that it is possible to reorder the position of the operators in a four-point function. For example, if we flip operators $\mathcal{O}_i \leftrightarrow \mathcal{O}_k$, then using (2.35) we see that the correlation function must satisfy

$$v^{\frac{\Delta_j + \Delta_k}{2}} \mathcal{G}_{ijkl}(u, v) = u^{\frac{\Delta_i + \Delta_j}{2}} \mathcal{G}_{kjil}(v, u) . \tag{2.45}$$

21

In the above equation the powers of u, v appear due to the prefactors in (2.35). The combination of crossing symmetry with the OPE expansion leads to the crossing equations

$$\sum_{\mathcal{O}} \left(\lambda_{ij\mathcal{O}}\lambda_{kl\mathcal{O}}\, v^{\frac{\Delta_k+\Delta_j}{2}} g_{\Delta,\ell}^{\Delta_{ij},\Delta_{kl}}(u,v) - \lambda_{kj\mathcal{O}}\lambda_{il\mathcal{O}}\, u^{\frac{\Delta_i+\Delta_j}{2}} g_{\Delta,\ell}^{\Delta_{kj},\Delta_{il}}(v,u) \right) = 0\,. \qquad (2.46)$$

The crossing equations are an infinite-dimensional system of highly non-linear equations for the CFT data $\{\Delta_i, \lambda_{ijk}\}$. The goal of the conformal bootstrap program is to solve the crossing equation, at least in selected examples or simplifying regimes.

There are mainly two approaches to extract information from the crossing equation: the numerical bootstrap, which is discussed in chapter 3, and the analytic bootstrap, which is discussed in chapter 4. For supersymmetric CFT, the extra constraints that can be imposed are discussed in chapter 5. Finally, in chapter 6 we describe how to adapt the conformal bootstrap program to the study of conformal defects.

2.4   Review of the literature

There exists a long list of excellent lecture notes [20, 21, 33, 34] and review articles [35, 36] that cover the basics of the conformal bootstrap. An important issue we have not discussed is when scale invariance and unitarity imply conformal symmetry. This has been discussed extensively in the literature, for example [37–41] but specially the review [42]. Furthermore, in this thesis we shall not discuss Gliozzi's method to solve a truncated version of crossing, instead we direct the interested reader to the literature [43–46]. Finally, it was discovered that the Casimir equation can be rephrased as a Schrodinger equation with an integrable potential, which allows the relation of conformal blocks to special functions studied in the mathematical literature [47–51].

Chapter 3

Numerical bootstrap

In this chapter, we discuss a numerical method for the crossing equation (2.46). After reviewing the importance of reflection positivity, we present the main numerical algorithms, followed by a summary on how to implement them in practice. We conclude explaining how these methods can be applied to the study of the $3d$ Ising model, and overview outstanding results in the literature.

3.1 Implications of reflection positivity

As discussed in section 2.1.3, a CFT is reflection positive when conformal generators preserve the Hermitian conjugation (2.13). Reflection positivity leads to unitarity bounds, which are constraints on the allowed values of scaling dimensions of physical operators.

General unitarity bounds are easier to understand by deriving the simplest one of them. Consider the state $|\mathcal{O}\rangle = \mathcal{O}(0)|0\rangle$, where $\mathcal{O}(0)$ is a conformal primary operator. The action of P_μ generates new states corresponding to conformal descendants, for example $|\Psi_\mu\rangle = P_\mu|\mathcal{O}\rangle$. These states should have positive norm, which implies

$$0 \leq \langle\Psi_\mu|\Psi_\mu\rangle = \langle\mathcal{O}|K_\mu P_\mu|\mathcal{O}\rangle = \langle\mathcal{O}|[K_\mu, P_\mu]|\mathcal{O}\rangle = 2\Delta\langle\mathcal{O}|\mathcal{O}\rangle \quad (\text{no } \mu \text{ sum}). \tag{3.1}$$

Because $\langle\mathcal{O}|\mathcal{O}\rangle \geq 0$, we conclude that $\Delta \geq 0$ for any operator in a reflection positive CFT. It is possible to obtain stronger bounds by considering more general states

$$|\Psi\rangle = (a_\mu P_\mu + b_{\mu\nu} P_\mu P_\nu + \ldots)|\mathcal{O}\rangle. \tag{3.2}$$

23

Positivity of the norm $\langle\Psi|\Psi\rangle \geq 0$ gives bounds that depend on the $SO(d)$ representation of the field [52–54]

$$\Delta_{\text{scalar}} \geq \frac{d-2}{2}\,, \qquad \Delta_{\text{spin-}\ell} \geq \ell + d - 2\,. \tag{3.3}$$

There are similar bounds for spinors, mixed-symmetry tensors, etc. but they play no role in the discussion that follows.

Reflection positivity also has important consequences for OPE coefficients. Key for our purposes is that whenever $\mathcal{O}_i$, $\mathcal{O}_j$ are scalars and $\mathcal{O}$ is a spin-ℓ tensor, then the OPE coefficient is real

$$\lambda_{ij\mathcal{O}} \in \mathbb{R}\,. \tag{3.4}$$

Let us give the gist of the argument, more details can be found in [35]. Take the state $|\Psi\rangle = \mathcal{O}_i(x_1)\mathcal{O}_j(x_2)\mathcal{O}(x_3)|0\rangle$, which must have positive norm in a reflection-positive CFT $\langle\Psi|\Psi\rangle \geq 0$. Roughly speaking, the adjoint state $\langle\Psi|$ is obtained by inserting the same operators at points reflected respect the unit sphere. Take $x_1, x_2, x_3 \to 0$, so the reflected points go to infinity. By the cluster decomposition principle, the norm factorizes into a product of two three-point functions, and in particular $\langle\Psi|\Psi\rangle \propto \lambda_{ij\mathcal{O}}^2 \times$ (positive), which implies (3.4).

3.2 Bounding CFT data

After the short detour to explore reflection positivity, it is time to introduce the main algorithm of this chapter. However, it is good to first rearrange the crossing equation to makes the notation consistent with the literature. Replacing $u \leftrightarrow v$ in the crossing equation (2.46), and adding and subtracting to the original equation, gives

$$\sum_{\mathcal{O}} \left(\lambda_{ij\mathcal{O}}\lambda_{kl\mathcal{O}}\, F_{\mp,\Delta,\ell}^{ij,kl}(u,v) \pm \lambda_{kj\mathcal{O}}\lambda_{il\mathcal{O}}\, F_{\mp,\Delta,\ell}^{kj,il}(u,v) \right) = 0\,, \tag{3.5}$$

where we have introduced the crossing-symmetric/antisymmetric objects

$$F_{\pm,\Delta,\ell}^{ij,kl}(u,v) \equiv v^{\frac{\Delta_k+\Delta_j}{2}} g_{\Delta,\ell}^{\Delta_{ij},\Delta_{kl}}(u,v) \pm u^{\frac{\Delta_k+\Delta_j}{2}} g_{\Delta,\ell}^{\Delta_{ij},\Delta_{kl}}(v,u)\,. \tag{3.6}$$

Instead of presenting algorithms to bound general systems of correlators, we focus on a four-point function of identical real scalars $\langle\phi\phi\phi\phi\rangle$. The crossing equation reads

$$F_{0,0}(u,v) + \sum_{\mathcal{O}} \lambda_{\phi\phi\mathcal{O}}^2\, F_{\Delta,\ell}(u,v) = 0\,, \tag{3.7}$$

24

where we abbreviate $F_{\Delta,\ell}(u,v) = F^{\phi\phi\phi\phi}_{-,\Delta,\ell}(u,v)$ to unclutter notation, and use that $\lambda_{\phi\phi\mathbb{1}} = 1$ in our conventions.

From the numerical perspective, it is convenient to think of the crossing equation as a sum rule satisfied by the *positive* coefficients $\lambda^2_{\phi\phi\mathcal{O}}$. As will become clear momentarily, it is convenient to act with a linear functional α on the crossing equation

$$\alpha[F_{0,0}] + \sum_{\mathcal{O}} \lambda^2_{\phi\phi\mathcal{O}}\, \alpha[F_{\Delta,\ell}] = 0\,. \tag{3.8}$$

The central observation of the numerical bootstrap goes as follows. If there exists a functional α such that $\alpha[F_{\Delta,\ell}] \geq 0$ for all operators in the spectrum, then (3.8) cannot be satisfied, because the left-hand side is a sum of positive terms, and the right-hand side is zero. This simple observation turns into two numerical algorithms that bound the space of allowed CFTs:

Scaling dimension bound [17]: Choose a putative spectrum of a CFT, namely specify the set $S = \{\Delta, \ell\}$ of scaling dimensions and spins of operators allowed in the $\phi \times \phi$ OPE. If there exists α such that

$$\alpha[F_{0,0}] = 1\,, \qquad \alpha[F_{\Delta,\ell}] \geq 0 \text{ for all } \Delta, \ell \in S\,, \tag{3.9}$$

the putative spectrum is ruled out. By making different assumptions about the spectrum and running this test, it is possible to carve out regions in "theory space" that admit no consistent reflection-positive CFT.

OPE bound [55]: As before, choose a putative spectrum S, but now find α that maximizes $\alpha[F_{0,0}]$ such that

$$\alpha[F_{\Delta_{\mathcal{O}},\ell_{\mathcal{O}}}] = 1\,, \qquad \alpha[F_{\Delta,\ell}] \geq 0 \text{ for all } \Delta, \ell \in S\,. \tag{3.10}$$

Then the OPE coefficient of $\mathcal{O}$ is bounded above by $\lambda^2_{\phi\phi\mathcal{O}} \leq -\alpha[F_{0,0}]$. If there exists α with $\alpha[F_{0,0}] > 0$, the bound $\lambda^2_{\phi\phi\mathcal{O}} < 0$ violates reflection positivity and the spectrum is ruled out. As small modification of the algorithm consists on maximizing $\alpha[F_{0,0}]$ with the normalization $\alpha[F_{\Delta_{\mathcal{O}},\ell_{\mathcal{O}}}] = -1$, which gives the lower bound $\lambda^2_{\phi\phi\mathcal{O}} \geq \alpha[F_{0,0}]$.

To implement these algorithms with a computer, it is necessary to make a large ansatz for the functional α, and search if $\alpha[F_{\Delta,\ell}] \geq 0$ can be satisfied in the parameter space

of α. The ansatz most used in the literature consists on taking derivatives around the crossing-symmetric point $z = \bar{z} = 1/2$:

$$\alpha[F] = \sum_{m,n=0}^{\Lambda} a_{m,n} \partial_z^m \partial_{\bar{z}}^n F(z,\bar{z})\big|_{z=\bar{z}=1/2}. \tag{3.11}$$

This is by no means the unique choice for α, but it is one that worked well so far. Notice that by increasing Λ the size of the ansatz grows, leading to stronger numerical bounds. The subject of the next subsection is how to search the parameter space $a_{m,n}$ to satisfy the positivity conditions (3.9)-(3.10).

3.3   Semidefinite programming

A recurrent question in the numerical bootstrap is whether for a given spectrum, namely a set $S = \{\Delta, \ell\}$, we can find coefficients $a_{m,n}$ such that

$$\sum_{m,n=0}^{\Lambda} a_{m,n} \partial_z^m \partial_{\bar{z}}^n F_{\Delta,\ell}(z,\bar{z})\big|_{z=\bar{z}=1/2} \geq 0 \;\; \text{for all} \;\; \Delta, \ell \in S. \tag{3.12}$$

Here $F_{\Delta,\ell}(z,\bar{z})$ is a highly non-linear function of Δ, ℓ. However, by factoring out a positive term $\chi_\ell(\Delta)$, it is possible to approximate it as [56–58]

$$\partial_z^m \partial_{\bar{z}}^n F_{\Delta,\ell}(z,\bar{z})\big|_{z=\bar{z}=1/2} \approx \chi_\ell(\Delta) P_\ell^{mn}(\Delta), \tag{3.13}$$

where $P_\ell^{mn}(\Delta)$ is a polynomial in Δ. Increasing the degree of the polynomial the approximation becomes better, keeping numerical error under control. Since $\chi_\ell(\Delta)$ is positive, our problem is rephrased as finding $a_{m,n}$ such that

$$\sum_{m,n=0}^{\Lambda} a_{m,n} P_\ell^{mn}(\Delta) \geq 0, \tag{3.14}$$

where we reiterate that $P_\ell^{mn}(\Delta)$ is a polynomial in Δ. Equation (3.14) is the simplest instance of a polynomial matrix program. This optimization problem is so indispensable for the numerical bootstrap that a specialized software `SDPB` was developed to solve it [59,60]. The most general problem that can be solved with `SDPB` is:

26

Polynomial matrix program: Consider a set of square matrices

$$
M_j^n(x) = \begin{pmatrix} P_{j,11}^n(x) & \cdots & P_{j,1m_j}^n(x) \\ \vdots & \ddots & \vdots \\ P_{j,m_j1}^n(x) & \cdots & P_{j,m_jm_j}^n(x) \end{pmatrix}, \quad 0 \le n \le N, \quad 1 \le j \le J, \tag{3.15}
$$

and a given vector $b \in \mathbb{R}^N$. Then a polynomial matrix program maximizes $b_0 + b \cdot y$ over $y \in \mathbb{R}^N$, such that

$$
M_j^0(x) + \sum_{n=1}^N y_n M_j^n(x) \succeq 0 \qquad \text{(positive semidefinite)}, \tag{3.16}
$$

for all $x \ge 0$ and $1 \le j \le J$. The simple example (3.14) corresponds to $J = 1$, $m_1 = 1$ and N is the number of coefficients a_{mn} in the ansatz.

To solve a polynomial matrix program, `SDPB` maps it to a standard semidefinite program, which is solved via an interior-point method. `SDPB` provides many features tailored to bootstrap calculations, such as arbitrary-precision arithmetic, high parallelization, or a `mathematica` interface. `SDPB` is by far the most used solver for numerical bootstrap, and it has contributed enormously to the development of this field.

The only loose end in the above discussion is how to obtain the polynomial approximations for the conformal blocks (3.13). For the applications discussed in this thesis, which take place in $d = 1, 2, 4$, there exist closed-form expressions for the conformal blocks in terms of hypergeometric functions, see (2.43) and (2.42). Taylor expanding these functions around $z, \bar{z} = 0$, evaluating the series at $z = \bar{z} = 1/2$, and factoring out a common positive prefactor, one obtains expressions of the form (3.13). A simple code that implements this in $d = 2$ is attached to `SDPB`. For the case of $d = 4$, a refinement of this idea can be found in appendix 7.B.1. For arbitrary spacetime dimension d, there exist efficient recursion relations to generate similar polynomial approximations, which have been implemented in `scalar-blocks` [61]. We do not give further details on this fascinating subject, which plays no role in the thesis.

3.4 A success story: the 3d Ising model

We conclude this chapter discussing the biggest achievement of the numerical conformal bootstrap: the determination of critical exponents of the $3d$ Ising model to the highest-to-date precision.

The $3d$ Ising model is one of the simplest non-trivial CFTs in $d > 2$. An essential feature of this model is that it preserves $\mathbb{Z}_2$ global symmetry. We call σ and ε the lowest-dimensional operators which are $\mathbb{Z}_2$ odd and even respectively. The importance of these operators is that they are the only relevant scalar operators, namely $\Delta_{\sigma,\varepsilon} < 3$ but $\Delta_{\mathcal{O}} > 3$ for any other scalar. It is clear that the $\mathbb{Z}_2$ symmetry constrains the OPEs of σ, ε to take the form

$$\sigma \times \sigma \sim \mathbb{1} + \varepsilon + \sum_{\Delta,\ell} \mathcal{O}_+ \,, \tag{3.17}$$

$$\varepsilon \times \varepsilon \sim \mathbb{1} + \varepsilon + \sum_{\Delta,\ell} \mathcal{O}_+ \,, \tag{3.18}$$

$$\sigma \times \varepsilon \sim \sigma + \sum_{\Delta,\ell} \mathcal{O}_- \,, \tag{3.19}$$

where $\mathcal{O}_\pm$ stand for operators which are $\mathbb{Z}_2$ even/odd respectively. These assumptions will be sufficient to constrain the $3d$ Ising model to high accuracy.

The simplest bootstrap bound is obtained from the four-point function of σ, with crossing equation

$$F_{0,0}(u,v) + \sum_{\mathcal{O}} \lambda_{\sigma\sigma\mathcal{O}}^2 \, F_{\Delta,\ell}(u,v) = 0 \,. \tag{3.20}$$

Since the value of Δ_σ is a priori unknown, one scans the range $\Delta_\sigma \in [0.5, 0.6]$. For each value of Δ_σ, we define ε as the lowest-dimension scalar operator in the $\sigma \times \sigma$ OPE. There are other scalar operators in the OPE, but they have $\Delta_{\mathcal{O}_+} \geq \Delta_\varepsilon$. The OPE also contains higher-spin operators, which have dimension above the unitarity bound $\Delta \geq \ell + 1$. With these assumptions, we scan different values of Δ_ε, and for each of them, we ask whether the spectrum is allowed (see *Scaling dimension bound*). The result is that Δ_ε cannot be arbitrarily large, and the shape of the allowed region in the $(\Delta_\sigma, \Delta_\varepsilon)$ plane can be seen in figure 3.1a). The most noticeable feature is that the allowed region has a kink around the values $(\Delta_\sigma, \Delta_\varepsilon) \approx (0.52, 1.4)$, which are very close to the values for the $3d$ Ising model!

After the exciting discovery that the $3d$ Ising model sits at a special point in theory space, there are many ways to proceed. Arguably the most powerful direction is to consider
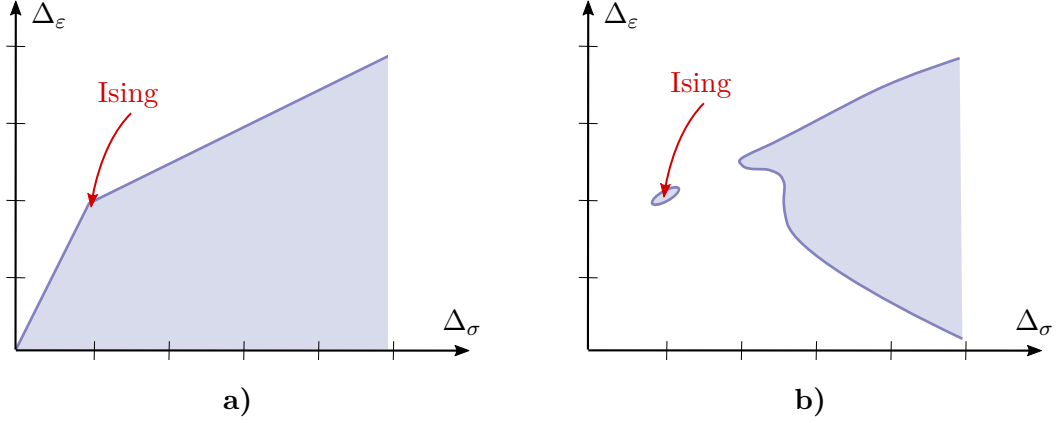
Figure 3.1: The a) kink and b) island in the bootstrap bounds for the $3d$ Ising model. The solid blue region is allowed by the bootstrap bounds. These plots are schematic, for the actual results see [59, 62–64]. With state-of-the-art results [64], the island would be too small to be visible in the plot.

crossing equations involving both σ and ε. Using (3.5) we find five crossing equations:

$$\langle\sigma\sigma\sigma\sigma\rangle: \quad 0 = \sum_{\mathcal{O}_+} \lambda^2_{\sigma\sigma\mathcal{O}} F^{\sigma\sigma,\sigma\sigma}_{-,\Delta,\ell}\,, \tag{3.21}$$

$$\langle\varepsilon\varepsilon\varepsilon\varepsilon\rangle: \quad 0 = \sum_{\mathcal{O}_+} \lambda^2_{\varepsilon\varepsilon\mathcal{O}} F^{\varepsilon\varepsilon,\varepsilon\varepsilon}_{-,\Delta,\ell}\,, \tag{3.22}$$

$$\langle\sigma\sigma\varepsilon\varepsilon\rangle: \quad 0 = \sum_{\mathcal{O}_+} \lambda_{\sigma\sigma\mathcal{O}}\lambda_{\varepsilon\varepsilon\mathcal{O}} F^{\sigma\sigma,\varepsilon\varepsilon}_{\mp,\Delta,\ell} \pm \sum_{\mathcal{O}_-} \lambda^2_{\sigma\varepsilon\mathcal{O}}(-1)^\ell F^{\varepsilon\sigma,\sigma\varepsilon}_{\mp,\Delta,\ell}\,, \tag{3.23}$$

$$\langle\sigma\varepsilon\sigma\varepsilon\rangle: \quad 0 = \sum_{\mathcal{O}_-} \lambda^2_{\sigma\varepsilon\mathcal{O}} F^{\sigma\varepsilon,\sigma\varepsilon}_{-,\Delta,\ell}\,. \tag{3.24}$$

These crossing equations can be organized in a way that can be fed into `SDPB`. We assume that Δ_σ, Δ_ε are the only relevant scalar operators, so $\Delta_{\mathcal{O}_\pm,\ell=0} \geq 3$, and spinning operators must obey unitarity bounds. As before, we scan the $(\Delta_\sigma, \Delta_\varepsilon)$ plane, and for each point `SDPB` determines if the spectrum is allowed. The resulting allowed region has the shape in figure 3.1b). In this case, even more impressively, the $3d$ Ising model lies inside a small island of allowed points! There exists an improvement of the above basic algorithm called OPE scan, which we do not discuss here. Using this and taking Λ in (3.11) as large as computationally possible, the size of the allowed island becomes extremely small. The island is so small that the allowed values of Δ_σ, Δ_ε are more accurate than any Monte-Carlo simulation to

date:

$$\Delta_\sigma = 0.5181489(10)\,, \qquad \Delta_\varepsilon = 1.412625(10)\,. \tag{3.25}$$

As a matter of fact, if we plotted the island, it would not be visible in figure 3.1b). Before we conclude, note that when a theory of interest sits close to the boundary of the allowed region, it is possible to use a technique called extremal functional method [65, 66]. This method allows to extract the approximate spectrum of the theory that saturates the bounds. For the Ising model, the extremal functional method produces results in excellent agreement with theoretical expectations.

3.5 Review of the literature

A comprehensive review of modern numerical bootstrap is [34]. Many authors have shared implementations of algorithms useful for numerical bootstrap studies, for example `autoboot` [67], `blocks_3d` [68], `CFTs4d` [26], `JuliBootS` [69], `PyCFTboot` [70], `sailboot` [71], SDPB [59, 60], `simpleboot` [72] and `spectrum-extraction` [73].[1]

Most central ideas in numerical bootstrap appeared in the early days: the dimension bound algorithm [17, 74], OPE bounds [55], central charge bounds [75], the inclusion of global symmetry [76], supersymmetry [65] and semidefinite programming [56]. After this period, the major breakthrough was the study of the $3d$ Ising using single [62, 63] and mixed correlators [58], leading to the high-precision results [64]. More recent methods include the OPE scan [64, 77], the use of Delaunay triangulation [77] and the navigator function [78], which enabled the high-precision determination of critical exponents in the $O(2)$ and $O(3)$ model [77, 79].

The numerical bootstrap has been applied to countless setups. More examples for scalar correlators include the $3d$ $O(N)$ models [57, 80–84], CFT in fractional dimension [85–87], models with cubic and hypercubic symmetry [88–90], MN symmetry [91–93], $O(M) \times O(N)$ symmetry [94], gauge theories [95–98], and many others [99–105]. The numerical bootstrap has also found applications to mathematics, such as the sphere packing problem [106], or bounding eigenvalues of the Laplacian [107–110].

Finally, all examples mentioned above considered scalar correlators. The bootstrap of spinning operators has been also performed in [25, 111–115]. These bootstrap studies were

---

[1]We want to take this occasion to thank the Bootstrap community for being so generous when it comes to sharing codes publicly.

enabled by the large number of works that studied kinematics of conformal correlators and conformal blocks [16, 22–25, 31, 32, 47–51, 68, 116–121].

Chapter 4

Analytic bootstrap

In this chapter, we change gears and extract information from the crossing equation with analytic methods. A fruitful approach is to analytically continue the CFT to Lorentzian signature, and consider kinematics with nearly lightlike-separated operators. This leads to the lightcone bootstrap, which we later formalize in terms of the Lorentzian inversion formula. These techniques have applications to perturbative CFTs, e.g. in the ε–expansion or in the large–N limit, which we also discuss.

4.1 Lightcone bootstrap

This sections starts considering the lightcone bootstrap, which gives physical intuition on why it is possible to extract analytical information from the crossing equation. The presentation is similar in spirit to the original works [122, 123]. For simplicity, throughout this chapter we consider four-point functions of identical scalars ϕ.

4.1.1 Euclidean vs Lorentzian kinematics

Before the actual bootstrap analysis, let us discuss a difference between Euclidean and Lorentzian kinematics which we glossed over in the introductory chapter. Given four points, it is possible to use conformal transformations to map three of them at zero, one and infinity, while the fourth is restricted to a two-dimensional plane:

$$x_1 = 0\,, \quad x_2 = (\tau, x)\,, \quad x_3 = (0, 1)\,, \quad x_4 = \infty\,. \tag{4.1}$$

Without loss of generality, four-point functions can always be studied in such a frame. Then the cross ratios $z, \bar{z}$ defined in (2.34) are interpreted as the complex coordinates of the two-dimensional plane, since

$$
\begin{cases} z\bar{z} = \tau^2 + x^2 \\ (1-z)(1-\bar{z}) = \tau^2 + (1-x)^2 \end{cases} \quad \Rightarrow \quad \begin{cases} z = x + i\tau \\ \bar{z} = x - i\tau \end{cases} . \tag{4.2}
$$

From this purely Euclidean discussion, we learn that the cross ratios are complex conjugate of each other $z^* = \bar{z}$. However, upon Wick rotation to Lorentzian signature $\tau = it$, the cross ratios become real and independent $z, \bar{z} = x \mp t$.

Since $z, \bar{z}$ are independent, Lorentzian signature allows for interesting kinematical regimes unavailable in Euclidean. For instance, if x_2, x_3 are almost light-like separated, then $x_{23}^2 \to 0$ and $(1-z)(1-\bar{z}) \to 0$. It is then still possible to take x_2 to be light-like from x_1 so that $z\bar{z} \propto x_{12}^2 \to 0$. This is the *lightcone limit*, described mathematically by $0 < 1 - \bar{z} \ll z \ll 1$, and graphically by
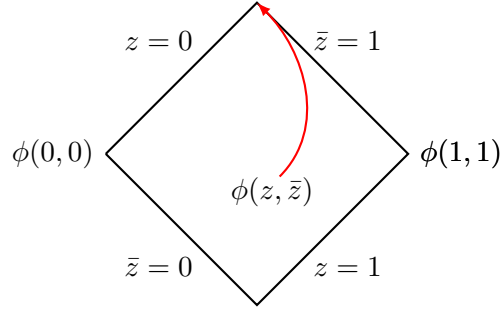
The rest of this chapter discusses how the existence of the lightcone limit constrains the spectrum of CFT.

4.1.2   Conformal blocks

Before analyzing the crossing equation in the lightcone limit, it is convenient to obtain representations for conformal blocks in this regime. Throughout this chapter, we normalize conformal blocks according to

$$
g_{\Delta,\ell}(z,\bar{z}) \sim z^{(\Delta-\ell)/2} \bar{z}^{(\Delta+\ell)/2} \qquad \text{as} \quad 0 < z \ll \bar{z} \ll 1 . \tag{4.3}
$$

The reason we deviate from (2.41) is that the results below will look simpler, and because (4.3) is becoming standard in the analytic bootstrap literature. The only downside is that

we need to modify the conformal block expansion to be

$$\mathcal{G}(z,\bar{z}) = \sum_{\mathcal{O}} \frac{1}{(-2)^\ell} \lambda^2_{\phi\phi\mathcal{O}} g_{\Delta,\ell}(z,\bar{z}), \tag{4.4}$$

but we simply use $P_{\phi\phi\mathcal{O}} = \frac{1}{(-2)^\ell} \lambda^2_{\phi\phi\mathcal{O}}$ to unclutter notation.

Coming back to conformal blocks, they admit a useful decomposition in $SL(2,\mathbb{R})$ blocks (2.43) [124]:

$$g_{\Delta,\ell}(z,\bar{z}) = \sum_{n=0}^{\infty} \sum_{q=-n}^{n} A_{n,q}(\Delta,\ell) z^{\frac{\Delta-\ell}{2}+n} k_{\Delta+\ell+2q}(\bar{z}). \tag{4.5}$$

The coefficients $A_{n,q}(\Delta,\ell)$ are unknowns that can be fixed recursively using the Casimir equation. For example, for $n \leq 1$ they read

$$A_{0,0}(\Delta,\ell) = 1, \tag{4.6}$$

$$A_{1,-1}(\Delta,\ell) = \frac{(d-2)\ell}{2\ell+d-4}, \tag{4.7}$$

$$A_{1,0}(\Delta,\ell) = \frac{\Delta-\ell}{4}, \tag{4.8}$$

$$A_{1,1}(\Delta,\ell) = \frac{(d-2)(\Delta-1)(\Delta+\ell)^2}{16(2\Delta-d+2)(\Delta+\ell-1)(\Delta+\ell+1)}. \tag{4.9}$$

It is relatively straightforward to obtain the coefficients for high values of n using a computer algebra software.

The expansion (4.5) is particularly convenient for small z, because only the first few terms are relevant. Since the formula is valid for arbitrary $\bar{z}$, it also works in the lightcone limit $0 < 1 - \bar{z} \ll z \ll 1$ that we consider below.

4.1.3 Crossing equation

After this small detour, we finally study the crossing equation for identical scalars ϕ:

$$\left(\frac{z\bar{z}}{(1-z)(1-\bar{z})}\right)^{\Delta_\phi} \sum_{\mathcal{O}} P_{\phi\phi\mathcal{O}} \, g_{\Delta,\ell}(1-z,1-\bar{z}) = \sum_{\mathcal{O}} P_{\phi\phi\mathcal{O}} \, g_{\Delta,\ell}(z,\bar{z}). \tag{4.10}$$

Remember that $P_{\phi\phi\mathcal{O}} = \frac{1}{(-2)^\ell} \lambda^2_{\phi\phi\mathcal{O}}$ is a shorthand for the OPE coefficient. The behavior of the blocks in the lightcone limit $0 < 1 - \bar{z} \ll z \ll 1$ is given by (4.5):

- On the LHS, the blocks go like $g_{\Delta,\ell}(1-z,1-\bar{z}) = (1-\bar{z})^{\frac{\Delta-\ell}{2}} k_{\frac{\Delta+\ell}{2}}(1-z)$. Thus, only the operators with lowest twist $\tau = \Delta - \ell$ contribute. For now we keep only the lowest-twist operator, which is the identity $g_{0,0} = 1$.

- On the RHS, the blocks go like $g_{\Delta,\ell}(z,\bar{z}) = z^{\frac{\Delta-\ell}{2}} k_{\Delta+\ell}(\bar{z})$. As we argue below, it is not possible to discard operators on the RHS.

As a result, the crossing equation in the lightcone limit simplifies to

$$\left(\frac{z}{(1-\bar{z})}\right)^{\Delta_\phi} \approx \sum_{\mathcal{O}} P_{\phi\phi\mathcal{O}} \, z^{\frac{\Delta-\ell}{2}} k_{\Delta+\ell}(\bar{z}), \qquad 0 < 1 - \bar{z} \ll z \ll 1. \tag{4.11}$$

Although not apparent at first, there is some tension in the above equation. The reason is that the LHS has a power law singularity $(1-\bar{z})^{-\Delta_\phi}$ as $\bar{z} \to 1$. However, each individual term on the RHS diverges only logarithmically:

$$k_\beta(\bar{z}) = -\frac{\Gamma(\beta)}{\Gamma(\beta/2)^2} \left(\log(1-\bar{z}) + 2H_{\frac{\beta-2}{2}}\right) + O(1-\bar{z}). \tag{4.12}$$

As a result, it is not possible to reproduce the singularity on the LHS with finitely many terms on the RHS. Instead, infinitely many contributions from the RHS have to resum to give the LHS. As we will show, these contributions have to take a very precise form.

Let us focus first on the z dependence of (4.11). Clearly, in order to reproduce the power z^{Δ_ϕ} on the LHS, the operators on the RHS must have scaling dimensions asymptotically close to

$$\Delta_\ell = 2\Delta_\phi + \ell. \tag{4.13}$$

Similarly, if we expand the LHS of (4.11) to higher orders in z, each power $z^{\Delta_\phi+n}$ has to be matched with an infinite family of operators with dimension

$$\Delta_{\ell,n} = 2\Delta_\phi + \ell + 2n. \tag{4.14}$$

These are called multi-twist operators, or double-twist operators only if $n = 0$. One can think of them as having the schematic form

$$[\phi\phi]_{\ell,n} \sim \phi \partial_{\mu_1} \ldots \partial_{\mu_\ell} \Box^n \phi. \tag{4.15}$$

Basic power counting shows that the bare dimension of these operators indeed agrees with (4.14). Physically, the lightcone bootstrap shows that these infinite families of multi-twist operators are present in all CFTs. Multi-twist operators are weakly coupled at large spin, in the sense that anomalous dimensions in (4.14) must be suppressed when $\ell \gg 1$.

Now, we can also consider the $\bar{z}$ dependence of (4.11). In order for the two sides of (4.11) to match, the OPE coefficients $P_{\phi\phi[\phi\phi]_{\ell,0}}$ must have a certain asymptotic behavior at large ℓ, which can be obtained as follows. Consider this identity of $SL(2,\mathbb{R})$ blocks:

$$\left(\frac{\bar{z}}{1-\bar{z}}\right)^{\Delta_\phi} = \sum_{\ell=0}^{\infty} \frac{(\Delta_\phi)_\ell^2}{\ell!(2\Delta_\phi + \ell - 1)_\ell} k_{2\Delta_\phi+2\ell}(\bar{z})\,. \tag{4.16}$$

Since the $\bar{z} \to 1$ of limit of (4.16) reduces to (4.11), the OPE coefficients $P_{\phi\phi[\phi\phi]_{\ell,0}}$ must approach (4.16) at large spin:

$$P_{\phi\phi[\phi\phi]_{\ell,0}} \approx \frac{2^{3-2\Delta_\phi-2\ell}\sqrt{\pi}}{\Gamma(\Delta_\phi)^2}\ell^{2\Delta_\phi-\frac{3}{2}} \ \text{ at large } \ell\,. \tag{4.17}$$

There is an extra factor of 2 in (4.17) which compensates the fact that (4.16) sums over all spins, while (4.11) sums over even spins. A similar discussions applies to the expansion of (4.11) to higher orders in z, which allows to reconstruct the large-spin behavior of $P_{\phi\phi[\phi\phi]_{\ell,n}}$

As a brief recap, we considered the implications of the identity operator in the lightcone limit. Matching the z dependence on the two sides of (4.11), we discovered the existence of multi-twist operators with $\Delta_{\ell,n} \approx 2\Delta_\phi + \ell + 2n$, while matching the $\bar{z}$ dependence gives their asymptotic OPE density. Going to subleading order in $1-\bar{z}$, a low-twist operator on the LHS would correct the CFT data of multi-twist operators on the RHS. The corrections $\delta\Delta_{\ell,n}$ and $\delta P_{\phi\phi[\phi\phi]_{\ell,n}}$ can be derived with methods similar to the ones above. However, it is more efficient to obtain these corrections using the Lorentzian inversion formula which we now discuss.

4.2   Lorentzian inversion formula

In this section we introduce Caron-Huot's Lorentzian Inversion Formula (LIF). The LIF captures in an elegant and compact way the main ideas of the lightcone bootstrap. However, instead of producing results that are only valid at large spin, the LIF is valid for spins $\ell \geq 2$. Furthermore, the LIF systematizes and simplifies calculations, helping the huge progress in recent years on solving CFT in perturbative regimes. In this section we discuss the formula and sketch the main steps in the original derivation, while we examine applications in the next section.

4.2.1 Euclidean inversion formula

The derivation of the Lorentzian inversion formula starts from the Euclidean inversion formula, which we now discuss. Consider a correlation function, which in Euclidean signature $z^* = \bar{z}$ must be single valued. $\mathcal{G}(z, \bar{z})$ must admit an expansion in terms of $F_{\Delta,\ell}(z, \bar{z})$, a single-valued generalization of conformal blocks

$$\mathcal{G}(z, \bar{z}) = \sum_{\ell=0}^{\infty} \int_{d/2-i\infty}^{d/2+i\infty} \frac{d\Delta}{2\pi i} c(\Delta, \ell) F_{\Delta,\ell}(z, \bar{z}) \,. \tag{4.18}$$

Since we are only sketching the derivation, it suffices to mention that $F_{\Delta,\ell}$ is a sum of a conformal block and its shadow $F_{\Delta,\ell} \sim g_{\Delta,\ell} + k g_{d-\Delta,\ell}$. The function $c(\Delta, \ell)$ is meromorphic in Δ, such that each pole sits at a physical dimension, with the residue given by the OPE coefficient of the corresponding operator

$$c(\Delta, \ell) = -\sum_{\mathcal{O}} \frac{P_{\phi\phi\mathcal{O}}}{\Delta - \Delta_{\mathcal{O}}} \,. \tag{4.19}$$

Clearly $c(\Delta, \ell)$ contains the same information as $\mathcal{G}(z, \bar{z})$, just encapsulated in a different way. By closing the contour to the right in (4.18), one recovers the usual OPE expansion. As opposed to (4.18), the purpose of an inversion formula is to determine $c(\Delta, \ell)$ as an integral over the correlator $\mathcal{G}(z, \bar{z})$.

The simplest inversion formula is the Euclidean inversion formula. The derivation of the Euclidean inversion formula uses that the Casimir operator is self adjoint with respect to the weight $(z\bar{z})^{-d}|z - \bar{z}|^{d-2}$. Since $F_{\Delta,\ell}$ are single-valued eigenfunctions of the Casimir operator, they must satisfy an orthogonality relation. By using orthogonality in (4.18), one obtains the Euclidean inversion formula

$$c(\Delta, \ell) = N(\Delta, \ell) \int_{\mathbb{C}} \frac{dz d\bar{z}}{(z\bar{z})^d} |z - \bar{z}|^{d-2} F_{\Delta,\ell}(z, \bar{z}) \mathcal{G}(z, \bar{z}) \,. \tag{4.20}$$

The precise normalization $N(\Delta, \ell)$ is unimportant for our purposes, and the integration is over complex z subject to $z^* = \bar{z}$.

4.2.2 Lorentzian inversion formula

Finally, we turn to the Lorentzian counterpart of (4.20). In the original derivation by Caron-Huot [125], he performed a contour deformation of the Euclidean inversion formula. By picking the contributions around the branch cuts of $\mathcal{G}(z, \bar{z})$, he obtained

$$c(\Delta, \ell) = \kappa_{\Delta+\ell} \frac{1 + (-1)^\ell}{4} \int_0^1 \int_0^1 \frac{dz d\bar{z}}{(z\bar{z})^d} |z - \bar{z}|^{d-2} g_{\ell+d-1,\Delta-d+1}(z, \bar{z}) \, \mathrm{dDisc}\, \mathcal{G}(z, \bar{z}) \,. \tag{4.21}$$

Alternatively, it is possible to derive the LIF by Wick rotating spacetime instead of the cross-ratios [126], see also [127] for the generalization to external spinning operators. The double discontinuity dDisc is defined as the correlator minus its analytic continuations around the branch point $\bar{z} = 1$ in the directions specified by the arrow

$$\text{dDisc}\,\mathcal{G}(z,\bar{z}) = \mathcal{G}(z,\bar{z}) - \frac{1}{2}\mathcal{G}^{\circlearrowright}(z,\bar{z}) - \frac{1}{2}\mathcal{G}^{\circlearrowleft}(z,\bar{z})\,. \tag{4.22}$$

For future reference, we also give the overall constant

$$\kappa_{\Delta+\ell} = \frac{\Gamma\left(\frac{\Delta+\ell}{2}\right)^4}{2\pi^2\Gamma(\Delta+\ell-1)\Gamma(\Delta+\ell)}\,. \tag{4.23}$$

It is good to take a pause to highlight important properties of the LIF:

1. The LIF reconstructs the CFT data $c(\Delta,\ell)$ using only the double discontinuity dDisc $\mathcal{G}$. This observation is crucial in perturbative settings, where the double discontinuity is much simpler than the correlator.

2. The LIF makes it manifest that the CFT in $c(\Delta,\ell)$ is analytic spin. There are Regge trajectories for $\ell \in \mathbb{R}$, and the physical operators are obtained setting $\ell \in \mathbb{N}$.

3. The main downside of the LIF is that, in general, it cannot be trusted for small ℓ. The reason is that the contour deformation used in its derivation is only justified for $\ell > \ell_*$. The parameter ℓ_* is theory dependent, but fortunately it is bounded in non-perturbative CFTs: It is guaranteed that the LIF is reliable at least for $\ell > 1$. However, convergence can be better for instance in supersymmetric CFT.

At first glance, it might be hard to fully appreciate the power of the Lorentzian inversion formula. We hope the applications of the next section will make this clear.

4.3 Applications

4.3.1 Double discontinuity

In order to use the Lorentzian inversion formula, it is necessary to compute the double discontinuity of the correlator $\mathcal{G}(z,\bar{z})$. Recall dDisc $\mathcal{G}$ is computed analytically continuing around the branch point $\bar{z} = 1$. It is then natural to use crossing symmetry to map

$z \to 1 - z$ and expand in conformal blocks. The double discontinuity can be applied term by term, giving:

$$\mathrm{dDisc}\,\mathcal{G}(z, \bar{z}) = \mathrm{dDisc}\left(\frac{z\bar{z}}{(1-z)(1-\bar{z})}\right)^{\Delta_\phi}\mathcal{G}(1-z, 1-\bar{z})$$

$$= \sum_{\mathcal{O}} P_{\phi\phi\mathcal{O}}\,\mathrm{dDisc}\left(\frac{z\bar{z}}{(1-z)(1-\bar{z})}\right)^{\Delta_\phi} g_{\Delta,\ell}(1-z, 1-\bar{z})$$

$$= \left(\frac{z\bar{z}}{(1-z)(1-\bar{z})}\right)^{\Delta_\phi} \sum_{\mathcal{O}} 2\sin^2\left(\frac{\Delta-2\Delta_\phi-\ell}{2}\pi\right) P_{\phi\phi\mathcal{O}}\,g_{\Delta,\ell}(1-z, 1-\bar{z})\,. \quad (4.24)$$

In order to obtain the last line, strip off the following prefactor from the conformal block

$$g_{\Delta,\ell}(1-z, 1-\bar{z}) = \left[(1-z)(1-\bar{z})\right]^{\frac{\Delta-\ell}{2}}\tilde{g}_{\Delta,\ell}(1-z, 1-\bar{z})\,. \quad (4.25)$$

Since $\tilde{g}_{\Delta,\ell}(1-z, 1-\bar{z})$ is analytic at $\bar{z} = 1$, it cannot contribute to $\mathrm{dDisc}\,\mathcal{G}$, and only powers $(1-\bar{z})^\alpha$ must be considered:

$$\mathrm{dDisc}(1-\bar{z})^\alpha = 2\sin^2(\pi\alpha)(1-\bar{z})^\alpha\,. \quad (4.26)$$

Equation (4.24) explains our claim that $\mathrm{dDisc}\,\mathcal{G}$ is simpler than the correlation function $\mathcal{G}$. Indeed, for an operator close to the multi-twist dimension $\Delta_{\ell,n} = 2\Delta_\phi + \ell + 2n + \gamma_{\ell,n}$, the contribution to the double discontinuity goes like the anomalous dimension squared:

$$\sin^2\left(\frac{\Delta_{\ell,n}-2\Delta_\phi-\ell}{2}\pi\right) \approx \frac{\pi^2\gamma_{\ell,n}^2}{4}\,. \quad (4.27)$$

In perturbative settings, anomalous dimensions are proportional to small couplings, so most contributions to $\mathrm{dDisc}\,\mathcal{G}$ are suppressed by these couplings. We present examples of this below.

4.3.2 Inversion of the identity

The simplest application of the the Lorentzian inversion formula is to reproduce and improve the results we obtained in section 4.1.3 using lightcone bootstrap. This is achieved approximating the double discontinuity by the identity operator contribution. Thus, keeping only the $\Delta = \ell = 0$ term in (4.24) gives

$$\mathrm{dDisc}\,\mathcal{G}(z, \bar{z}) \approx \mathrm{dDisc}\left(\frac{z\bar{z}}{(1-z)(1-\bar{z})}\right)^{\Delta_\phi}$$

$$= 2\sin^2(\pi\Delta_\phi)\left(\frac{z\bar{z}}{(1-z)(1-\bar{z})}\right)^{\Delta_\phi}\,. \quad (4.28)$$

It is challenging to compute the inversion integrals (4.21) in closed form, even for the simplest case (4.28). A useful strategy is to expand the integrand in the limit $z \to 0$ and integrate term by term. We focus on the leading term for clarity, although higher terms can be obtained using (4.5). The integration kernel dramatically simplifies as $z \to 0$

$$\frac{1}{z}\left(\frac{\bar{z}-z}{z\bar{z}}\right)^{d-2} g_{\ell+d-1,\Delta+1-d}(z,\bar{z}) = z^{-\frac{\Delta-\ell}{2}} k_{\Delta+\ell}(\bar{z}) + O(z), \tag{4.29}$$

where we remind the reader that $k_{\Delta+\ell}(\bar{z})$ is a Gauss hypergeometric function (2.43). As a result of the expansion, the $z, \bar{z}$ integrals factorize and can be computed in closed form. On the one hand, the $\bar{z}$ integral gives

$$\int_0^1 \frac{d\bar{z}}{\bar{z}^2} k_\beta(\bar{z}) \, \mathrm{dDisc}\left(\frac{\bar{z}}{1-\bar{z}}\right)^{\Delta_\phi} = 2\pi^2 \frac{\Gamma(\beta)}{\Gamma(\beta/2)^2} \frac{\Gamma(\beta/2+\Delta_\phi-1)}{\Gamma(\Delta_\phi)^2 \Gamma(\beta/2-\Delta_\phi+1)}, \tag{4.30}$$

which is obtained from an Euler-type representation for the hypergeometric function by swapping the order of integration. On the other hand, the simple power dependence z^a makes the remaining z integral trivial. All in all, we obtain

$$c(\Delta,\ell) = -\frac{1}{(\Delta-(2\Delta_\phi+\ell))} \frac{\left(1+(-1)^\ell\right)\Gamma\left(\frac{\Delta+\ell}{2}\right)^2 \Gamma\left(\frac{\Delta+\ell}{2}+\Delta_\phi-1\right)}{\Gamma(\Delta_\phi)^2 \Gamma(\Delta+\ell-1)\Gamma\left(\frac{\Delta+\ell}{2}-\Delta_\phi+1\right)} + \ldots \tag{4.31}$$

From here, we read off that there is a family of double-twist operators with the following dimensions and OPE coefficients:

$$\Delta_{\ell,0} = 2\Delta_\phi + \ell, \qquad P_{\phi\phi[\phi\phi]_{\ell,0}} = \frac{2(\Delta_\phi)_\ell^2}{\ell!(2\Delta_\phi+\ell-1)_\ell}. \tag{4.32}$$

In the limit $\ell \gg 1$, these reduce to the lightcone bootstrap prediction (4.17), but (4.32) is significantly more powerful, because it gives the correct answer at least for $\ell \geq 2$. Furthermore, the expansion of the LIF integrand to higher order in z gives the OPE coefficients of multi-twist operators $\Delta_{\ell,n} = 2\Delta_\phi + \ell + 2n$.

Finally, keep in mind that (4.28) approximates dDisc $\mathcal{G}$ using only the identity operator. Subleading operators in the OPE (4.28) would correct these dimensions $\delta\Delta_{\ell,n}$ and OPE coefficients $\delta P_{\phi\phi[\phi\phi]_{\ell,n}}$. For example, in the $3d$ Ising model the double discontinuity can be approximated with $\mathbb{1}, \varepsilon, T_{\mu\nu}$, giving results in excellent agreement with the numerical bootstrap.

4.3.3 Wilson-Fisher fixed point

The Wilson-Fisher fixed point is perhaps the next simplest application of the LIF. We start reviewing the main structural properties of the CFT data of the theory. At the end, we see how these properties make the Wilson-Fisher fixed point perfectly suited for a bootstrap analysis. The ε–expansion has been studied extensively in the bootstrap literature, see for example [128–133], and specially the nice review [134]. This section is a summary of [135], which illustrates the main idea behind many modern bootstrap calculations.

The Wilson-Fisher fixed point is obtained from ϕ^4 theory

$$\mathcal{L} = \frac{1}{2}(\partial\phi)^2 + \frac{\lambda}{4!}\phi^4 \,, \tag{4.33}$$

where the mass is tuned to zero $m_* = 0$ because we are interested in its IR fixed point. In $d = 4$ the coupling λ is marginally irrelevant, and as a result the only fixed point is Gaussian. On the other hand, the coupling λ is relevant for $d \leq 4$, so it triggers an RG flow that finishes at a non-trivial fixed point with critical coupling λ_*. When this model is considered in $d = 4 - \varepsilon$ dimensions, the coupling is only weakly relevant if one is sufficiently close to four dimensions. More precisely, the critical coupling is $\lambda_* \propto \varepsilon + O(\varepsilon^2)$, so perturbation theory is reliable near $d = 4$.

The two lowest-lying operators are ϕ and ϕ^2, with dimensions

$$\Delta_\phi = \frac{d-2}{2} + \gamma_\phi^{(2)}\varepsilon^2 + \dots \,, \tag{4.34}$$

$$\Delta_{\phi^2} = 2\Delta_\phi + \gamma_{\phi^2}^{(1)}\varepsilon + \gamma_{\phi^2}^{(2)}\varepsilon^2 + \dots \,. \tag{4.35}$$

By standard Feynman diagram techniques, it is not hard to obtain the precise anomalous dimensions, e.g. $\gamma_\phi^{(2)} = \frac{1}{108}$ or $\gamma_{\phi^2}^{(1)} = \frac{1}{3}$. However, the logic of the conformal bootstrap is that these constants can be fixed from consistency conditions of the four-point function $\langle\phi\phi\phi\phi\rangle$.

The main tools at our disposal are the operator product expansion and the Lorentzian inversion formula. As we have reviewed previously, the operators in a CFT are organized in twist families. The leading-twist family contains operators of the form $[\phi\phi]_{\ell,0} \sim \phi\partial_{\mu_1}\dots\partial_{\mu_\ell}\phi$. Although not obvious, the scaling dimension of these operators gets corrected at order ε^2, namely:

$$\Delta_{\ell,0} = 2\Delta_\phi + \ell + \gamma_\ell^{(2)}\varepsilon^2 + \dots \,. \tag{4.36}$$

Note that the case $\ell = 0$ is special, since there are $O(\varepsilon)$ corrections, see (4.35). There exist also multi-twist operators $[\phi\phi]_{\ell,n\geq 1} \sim \phi\partial_{\mu_1}\dots\partial_{\mu_\ell}\Box^n\phi$. However, due to the equations of motion $\Box\phi \sim \lambda_*\phi^3 \propto \varepsilon\phi^3$, these operators are subleading. This is captured in their OPE coefficients, which are order

$$\langle\!\langle P_{\phi\phi[\phi\phi]_{\ell,1}}\rangle\!\rangle = P_{\ell,1}^{(2)}\varepsilon^2 + \dots, \qquad \langle\!\langle P_{\phi\phi[\phi\phi]_{\ell,n\geq 2}}\rangle\!\rangle = P_{\ell,1}^{(3)}\varepsilon^3 + \dots. \tag{4.37}$$

Although it might seem surprising, knowing the above information allows one to bootstrap the CFT data to order $O(\varepsilon^3)$ with minimal effort.

The key idea is that an operator $\mathcal{O}$ contributes to the double discontinuity as dDisc $\mathcal{G} \propto P_{\phi\phi\mathcal{O}}\gamma_{\mathcal{O}}^2$, see section 4.3.1. For the sake of clarity, we consider each operator in the OPE separately:

1. The identity 1 has been discussed in section 4.3.2.

2. The operator ϕ^2 has anomalous dimension $\gamma_{\phi^2} \propto \varepsilon$, so it contributes to dDisc $\mathcal{G}$ at orders $O(\varepsilon^2)$ and higher.

3. The leading trajectory $[\phi\phi]_{\ell,0}$ has anomalous dimension $\gamma_{\ell,0} \propto \varepsilon^2$, which contributes at order $O(\varepsilon^4)$ and higher.

4. The subleading trajectories $[\phi\phi]_{\ell,n}$ have anomalous dimension $\gamma_{\ell,n} \propto \varepsilon$, but since their OPEs are order $O(\varepsilon^2)$, these families contribute at order $O(\varepsilon^4)$ and higher.

The conclusion is that the discontinuity of the correlator at $O(\varepsilon^3)$ is fully fixed in terms of a single conformal block:

$$\text{dDisc}\,\mathcal{G}(z,\bar{z})\big|_{O(\varepsilon^3)} = \text{Disc}\left(\frac{z\bar{z}}{(1-z)(1-\bar{z})}\right)^{\Delta_\phi}\left[1 + P_{\phi\phi\phi^2}g_{\Delta_{\phi^2},0}(z,\bar{z})\right]. \tag{4.38}$$

Here there are three unknowns, Δ_ϕ, Δ_{ϕ^2} and $P_{\phi\phi\phi^2}$, but there are several consistency conditions

1. The theory becomes free at $d = 4$.

2. The theory is local, so there exists a stress tensor. This means $\Delta_{2,0} = \Delta_{T_{\mu\nu}} = 4 - \varepsilon$ at all orders in ε.

3. The operator ϕ^2 belongs to the $[\phi\phi]_{\ell,0}$ family after a suitable analytic continuation past a pole.

While conditions 1 and 2 are self-evident, condition 3 is subtle and we have nothing else to say here. The main message, however, is that using physical assumptions one can fully fix the free coefficients. The structure of the CFT data (4.35)-(4.37) was of fundamental importance in order to derive (4.38). Although here we presented the structure of the CFT data as external input, it is possible to bootstrap it order by order in ε; the CFT obtained at a certain order serves as input to bootstrap the next order. The first challenge appears at order $O(\varepsilon^4)$, where it is necessary to solve a mixing problem to compute the discontinuity. The authors of [135,136] bypassed this by making an ansatz for the discontinuity and fixing the free coefficients from consistency conditions.

4.4 Review of the literature

There exist nice pedagogical reviews of the analytical bootstrap [137–141]. After the discovery of the lightcone bootstrap, large-spin perturbation theory was developed [142–145], which was later systematized by the Lorentzian inversion formula [125]. Besides these, there exist many analytic bootstrap methods, such as the crossing-symmetric Mellin space bootstrap [146–149], Mellin space sum rules [150, 151], superconvergence sum rules [152], the conformal dispersion relation [153, 154], or analytic functionals [155–160]. All these methods are believed to lead to equivalent dispersive sum rules [161], see also [162, 163].

The analytic bootstrap has many applications we could not cover in detail. An interesting idea is to use results from the numerical bootstrap as input for the inversion formula. This leads to very accurate predictions for the spectrum of the $3d$ Ising model [124,164,165], the $O(2)$ model [166] and the $\mathcal{N} = 1$ superIsing model [167]. The Lorentzian inversion formula and large-spin perturbation theory have been applied to weak coupling gauge theories [168], the Wilson-Fisher fixed point in the ε–expansion [135, 136] or large N [169], as well as models with more exotic symmetry groups [92, 94]. One of the main applications of the analytic bootstrap is to holographic CFTs, which has become a field of its own. A list of references to somewhat recent work is [170–178], while older work can be found in references therein.

Chapter 5

Superconformal field theories

Because the conformal bootstrap relies on symmetry and unitarity, a natural expectation is that theories preserving larger spacetime symmetry will be more amenable to conformal bootstrap. Due to the Coleman-Mandula theorem [179], supersymmetry appears to be the only possibility. The subject of this chapter is SuperConformal Field Theory (SCFT), namely the study of conformal theories that preserve supersymmetry. Our focus is on two aspects of SCFTs with a direct connection to bootstrap: representation theory of superconformal algebras, and superconformal blocks. Unfortunately, we cannot cover other interesting topics in the SCFT literature, such as localization, protected sectors, geometric engineering, etc. which are also potentially useful in bootstrap studies. Many properties of SCFTs depend on the spacetime dimension and the number of supercharges. Whenever possible, we describe general properties that apply all SCFTs; however, when it is easier to concentrate on a particular model we use $4d$ $\mathcal{N} = 1$ SCFTs as a prototypical example.

5.1 Superconformal algebra

The algebra of conformal symmetry generators was the central ingredient to develop the bootstrap equations in chapter 2. In the context of SCFT, an equally important role is played by the superconformal algebra, which is the extension of the conformal algebra by the supersymmetry generators. This section starts with an overview of the superconformal algebra, and we then give the classification of superconformal algebras in $d \geq 3$.

5.1.1   Commutation relations

Even though the (anti)commutation relations of the superconformal algebra depend on the spacetime dimension and number of supercharges, its structure remains the same. Here we discuss the universal structure of the superconformal algebra, while in appendix 5.A we present the complete set of commutation relations for the $4d$ $\mathcal{N} = 1, \ldots, 4$ case.

Our goal is to combine the $\mathcal{N}$–extended supersymmetry algebra with the conformal algebra $SO(d+1, 1)$. The supersymmetry algebra is generated by the Poincare supercharges $Q, \bar{Q}$.[1] These are fermionic generators that transform as spacetime spinors and may carry an extra index called R-symmetry index. However, here we suppress all indices to keep the results schematic but generic. The number $\mathcal{N}$ is related to the R-symmetry group, or equivalently the number of Poincare supercharges, although its precise meaning depends on the algebra under consideration. With these caveats in mind, the supersymmetry algebra reads

$$\{Q, \bar{Q}\} \sim P \,, \qquad \{Q, Q\} = \{\bar{Q}, \bar{Q}\} = [P, Q] = [P, \bar{Q}] = 0 \,. \tag{5.1}$$

We insist that there are extra indices that we suppress for clarity. Remember that Hermitian conjugation in radial quantization maps $P^\dagger = K$, so the Hermitian conjugate of (5.1) must contain new types of supercharge $S = Q^\dagger$, $\bar{S} = \bar{Q}^\dagger$. The $S, \bar{S}$ supercharges generate special superconformal transformations, and anticommute to give a special conformal transformation:

$$\{S, \bar{S}\} \sim K \,. \tag{5.2}$$

Since P and K have dimensions $\Delta_{P,K} = \pm 1$, and $Q, \bar{Q}$ and $S, \bar{S}$ are roughly their square roots, they must have scaling dimension $\Delta_{Q,S} = \pm\frac{1}{2}$:

$$[D, Q] = \frac{1}{2}Q \,, \quad [D, \bar{Q}] = \frac{1}{2}\bar{Q} \,, \quad [D, S] = -\frac{1}{2}S \,, \quad [D, \bar{S}] = -\frac{1}{2}\bar{S} \,. \tag{5.3}$$

Conservation of scaling dimension and R-symmetry can be used to fix most of the commutation relations. For example, we have $[K, Q] \sim \bar{S}$ which follows from R-symmetry and because the right-hand side must have dimension $-1/2$. In a similar way, one can proceed to obtain most of the commutation relations. A useful anticommutator that we

---

[1]In some cases there are only Q-type supercharges, in which case our formulas are valid upon setting $Q = \bar{Q}$.

mention explicitly is the one involving one Poincare and one superconformal supercharge. The right-hand side contains all possible operators of zero dimension, namely

$$\{Q, S\} \sim D + M + R, \qquad \{\bar{Q}, \bar{S}\} \sim D + M + R. \tag{5.4}$$

Note that besides the generators of dilatations D and $SO(d)$ rotations M, there are generators R called R-symmetry generators. In supersymmetric theories, the R-symmetry is an outer automorphism of the supersymmetry algebra, but in superconformal theories R-symmetry belongs to the superconformal algebra. Once more, appendix 5.A contains the commutation relations of the $4d$ superconformal algebra.

5.1.2 Classification

Given an $\mathcal{N}$-extended supersymmetry algebra and a d-dimensional conformal algebra, we just explained how to obtain its superconformal algebra. In fact, the structure is so rigid that, given d and $\mathcal{N}$, the resulting superconformal algebra is unique. This leads to the the classification of superconformal algebras for $d \geq 3$ [180]:

$$
\begin{aligned}
d = 3 \quad & OSp(\mathcal{N}|4) \supset SO(3,2) \times SO(\mathcal{N})_R\,, \\
d = 4 \quad & SU(2,2|\mathcal{N}) \supset SO(4,2) \times SU(\mathcal{N})_R \times U(1)_R\,, \\
d = 5 \quad & F_4 \supset SO(5,2) \times SU(2)_R\,, \\
d = 6 \quad & OSp(8^*|2\mathcal{N}) \supset SO(6,2) \times USp(2\mathcal{N})_R\,.
\end{aligned} \tag{5.5}
$$

Three comments are in order. First, to help the reader we also wrote in (5.5) the maximal bosonic subalgebras, which consists of the conformal and R-symmetry groups. Second, the superconformal algebras have been written in Lorentzian signature, but since in this thesis we mostly consider Euclidean CFT, we should Wick rotate them. Third, the algebra for $4d$ $\mathcal{N} = 4$ is $PSU(2,2|\mathcal{N})$, since the $U(1)_R$ commutes with the rest of generators and can be quotiented out.

Superconformal algebras in $d = 1, 2$ are infinite dimensional, a topic is outside the scope of this work. However, finite-dimensional superconformal algebras in $d = 1, 2$ have applications to superconformal defects. In this case, a full classification can be found in [181].

5.2   Representation theory

Physical operators in SCFT transform in reflection-positive irreducible representations of the superconformal algebra. The representations of the superconformal algebra can be worked out in the same way as in the non-supersymmetric case, with the only difference that here we find a richer spectrum of short representations.

5.2.1   Long representations

To construct a long representation, one starts with a superprimary operator $\mathcal{O}(0)$. Besides being a conformal primary (2.16)-(2.17), a superprimary operator is anhilated by S, $\bar{S}$

$$\text{Superprimary operator:} \qquad [S, \mathcal{O}(0)] = [\bar{S}, \mathcal{O}(0)] = 0 \,, \tag{5.6}$$

and forms a representation of the R-symmetry group. As before, spacetime or R-symmetry indices are kept implicit in $\mathcal{O}(0)$. Then, the repeated action of $P, Q, \bar{Q}$ on the superprimary forms a superconformal representation, also called superconformal multiplet or supermultiplet:

$$\text{Supermultiplet:} \quad \mathcal{O}(0), \quad [Q, \mathcal{O}(0)], \quad [Q, [Q, \mathcal{O}(0)]], \quad [Q, [\bar{Q}, \mathcal{O}(0)]], \quad [P, \mathcal{O}(0)], \quad \ldots \tag{5.7}$$

Because the Poincare supercharges are anticommuting spinors, a superconformal multiplet contains bosons and fermions related to each other by supersymmetry. Furthermore, Q, $\bar{Q}$ act at most $2^{N_Q + N_{\bar{Q}}}$ times, where $N_Q + N_{\bar{Q}}$ is the total number of supercharges. The $2^{N_Q + N_{\bar{Q}}}$ operators obtained from the superprimary are called superconformal descendants, or superdescendants for short. As discussed in more detail below, we choose a basis where superdescendants are conformal primaries on their own, namely they form an irreducible representation of the conformal group.

Let us also consider the constraints of reflection positivity. By imposing that the matrix of norms $\langle \mathcal{O}_i | \mathcal{O}_j \rangle$ is positive semidefinite, where $\mathcal{O}_i$ are the superdescendants in a multiplet, one obtains lower bounds on Δ. These lower bounds are generally stronger than the unitarity bounds obtained for non-supersymmetric theories in section 3.1.

To clarify, we treat $\mathcal{N} = 1$ theories in $d = 4$ in some detail. As mentioned above, operators are labeled by the maximal bosonic subalgebra of the superconformal algebra, which in this case is

$$SU(2, 2|1) \supset SO(4, 2) \times U(1)_R \,. \tag{5.8}$$

The operators in a multiplet are labeled by the scaling dimension Δ, Lorentz spin $[j, \bar{j}]$ and $U(1)_R$ charge r. Notice that, in these conventions, spin-ℓ symmetric-traceless tensors correspond to $[\ell, \ell]$. The $4d$ $\mathcal{N} = 1$ superconformal algebra contains four Poincare supercharges Q_α, $\bar{Q}_{\dot\alpha}$ with $\alpha, \dot\alpha = 1, 2$, so a long multiplet consists of $2^4 = 16$ superdescendants. The multiplet can be organized in a table [27, 182]

$$
\begin{array}{c}
[j; \bar{j}]^{(r)}_{\Delta} \\
\text{(diagram)}
\end{array}
\tag{5.9}
$$

$$
[j; \bar{j}]^{(r)}_{\Delta} \xrightarrow{Q} [j \pm 1; \bar{j}]^{(r-1)}_{\Delta+1/2} \quad [j; \bar{j} \pm 1]^{(r+1)}_{\Delta+1/2}
$$

$$
[j; \bar{j}]^{(r-2)}_{\Delta+1} \quad [j \pm 1; \bar{j} \pm 1]^{(r)}_{\Delta+1} \quad [j; \bar{j}]^{(r+2)}_{\Delta+1}
$$

$$
[j; \bar{j} \pm 1]^{(r-1)}_{\Delta+3/2} \quad [j \pm 1; \bar{j}]^{(r+1)}_{\Delta+3/2}
$$

$$
[j; \bar{j}]^{(r)}_{\Delta+2}
$$
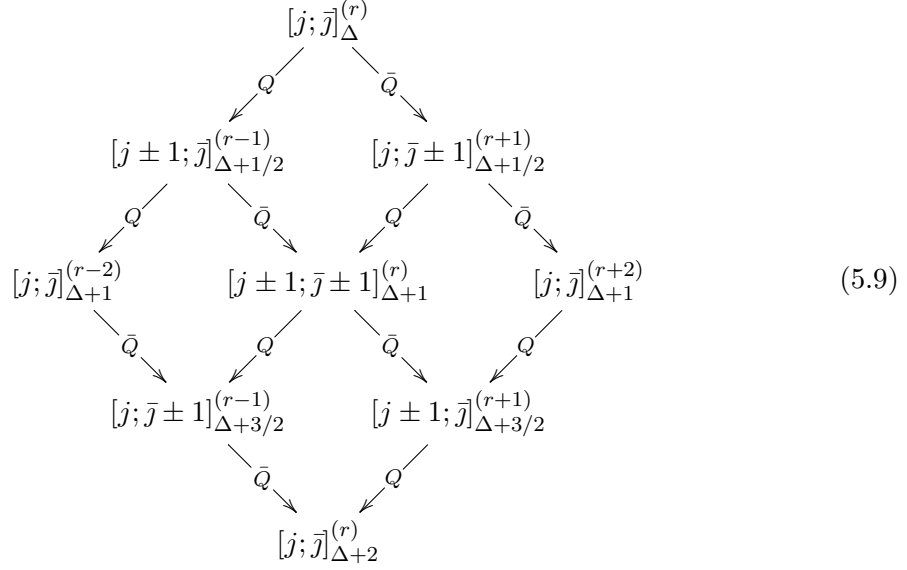
As mentioned previously, each entry corresponds to a conformal primary that, by reflection positivity, should have positive norm. A calculation similar to (3.1) leads to the unitarity bound [54, 183, 184]

$$
\Delta \geq 2 + \max\left\{ j - \tfrac{3}{2}r, \bar{j} + \tfrac{3}{2}r \right\} . \tag{5.10}
$$

For spin-ℓ representations this gives $\Delta \geq \ell + 2 + \tfrac{3}{2}|r|$, which is stronger than the non-supersymmetric unitarity bound $\Delta \geq \ell + 2$, see (3.3).

5.2.2   Short representations

Besides the long representations presented above, the superconformal algebra admits other reflection-positive representations called short representations. Short representations are characterized by the superconformal primary (5.6) being annihilated by a combination of Poincare supercharges. Consistency with the commutation relations then relates the dimension of the superprimary to its spin and R-symmetry representation. Since short representations play an important role in this thesis, we discuss them in more detail here.

Instead of trying to be general, we first discuss $4d\,\mathcal{N}=1$ and only at the end we explain general properties of short representations. For their importance in this thesis, we focus on chiral primary operators, or chirals for short. A chiral primary operator $\phi(0)$ is a scalar operator that, besides being a superprimary, is killed by the $\bar{Q}$ supercharges:

$$[\bar{Q}_{\dot{\alpha}}, \phi(0)] = 0\,. \tag{5.11}$$

This is called a shortening condition, that is, an equation stating that certain Poincare supercharges kill a superprimary operator. Similarly, there exist antichiral operators $\bar{\phi}$ which are killed by the supercharges Q_α. Because the $\bar{Q}_{\dot{\alpha}}$ supercharge annihilates the superprimary, the multiplet is obtained acting with Q_α:

$$[0;0]^{(r)}_{\Delta=\frac{3}{2}r} \;\; \xrightarrow{\;\; Q \;\;} \;\; [1;0]^{(r-1)}_{\Delta=\frac{3}{2}r+\frac{1}{2}} \;\; \xrightarrow{\;\; Q \;\;} \;\; [0;0]^{(r-2)}_{\Delta=\frac{3}{2}r+1}\,. \tag{5.12}$$

This is much smaller than the long multiplet (5.9), which explains the terminology "short multiplet".

The scaling dimension of a short multiplet is related to its Lorentz and R-symmetry representation. To derive this relation, note that the shortening condition (5.11) is equivalent to $|\Psi_{\dot{\alpha}}\rangle = \bar{Q}_{\dot{\alpha}}|\phi\rangle$ having zero norm. Using the commutation relations in 5.A, the zero-norm condition gives

$$0 = \langle\Psi_{\dot{\alpha}}|\Psi_{\dot{\alpha}}\rangle = \langle\phi|\{\bar{S}^{\dot{\alpha}},\bar{Q}_{\dot{\alpha}}\}|\phi\rangle = \frac{1}{2}\left(\Delta - \frac{3}{2}r\right)\langle\phi|\phi\rangle \quad (\text{no } \dot{\alpha} \text{ sum})\,. \tag{5.13}$$

Since the norm of the superprimary must be positive $\langle\phi|\phi\rangle > 0$, the only possibility is that

$$\Delta = \frac{3}{2}r\,. \tag{5.14}$$

An unfamiliar feature of short representations is that their scaling dimensions can be below the unitarity bound. In this example, the unitarity bound (5.10) applied to a scalar with charge r gives $\Delta = 2 + \frac{3}{2}|r|$, so the chiral operator is below it.

After this $4d\,\mathcal{N}=1$ example, it is time to discuss more general superconformal algebras, following the terminology of [182]. In SCFT, long multiplets are generated from superprimaries with generic scaling dimension above the unitarity bound. Short multiplets, on the other hand, are generated from superprimaries that satisfy a shortening condition, that is, superprimaries killed by combinations of Poincare supercharges. The scaling dimension of short multiplets is fixed in terms of the Lorentz and R-symmetry representation. If the scaling dimension of a short multiplet saturates the unitarity bound, one calls them

A-type multiplets. Instead, a short multiplet is of *B*-type when its dimension is below the unitarity bound. If more than one family of multiplets are below the unitarity bound, these are called *B*-type, *C*-type, *D*-type and so on.

5.3   Superspace

In this section we introduce superspace, a fundamental technique in the study of supersymmetric theories. For us, the main application of superspace is to study correlation functions, that can involve either long or short multiplets. In this section we consider only the $4d$ $\mathcal{N} = 1$ superspace as in [185, 186], although similar methods apply for other dimensions or number of supercharges, see e.g. [187–189].

5.3.1   Superspace and superfields

Superspace is an extension of ordinary space in which, besides the spatial directions $x^{\dot{\alpha}\alpha}$,[2] one introduces fermionic directions θ^{α}, $\bar{\theta}^{\dot{\alpha}}$. The supercharges Q_{α}, $\bar{Q}_{\dot{\alpha}}$ translate in the fermionic directions θ^{α}, $\bar{\theta}^{\dot{\alpha}}$, similarly to how $P_{\alpha\dot{\alpha}}$ translates the spatial directions $x^{\dot{\alpha}\alpha}$. Given a superconformal primary operator at the origin $O(0)$, it can be promoted to a superfield $\mathcal{O}$ by a supertranslation in space and fermionic directions:

$$\mathcal{O}(x,\theta,\bar{\theta}) \equiv e^{x^{\dot{\alpha}\alpha}P_{\alpha\dot{\alpha}}+\theta^{\alpha}Q_{\alpha}+\bar{Q}_{\dot{\alpha}}\bar{\theta}^{\dot{\alpha}}}O(0)e^{-x^{\dot{\alpha}\alpha}P_{\alpha\dot{\alpha}}-\theta^{\alpha}Q_{\alpha}-\bar{Q}_{\dot{\alpha}}\bar{\theta}^{\dot{\alpha}}} . \qquad (5.15)$$

Although superspace and superfields appear strange at first, the physical intuition behind them is simple: the role of $\theta,\bar{\theta}$ is to keep track of superconformal descendants. Because the supercharges Q_{α} and $\bar{Q}_{\dot{\alpha}}$ are anticommuting, a multiplet contains $2^4 = 16$ superdescendants, which is exactly the number of terms that appear in a Taylor expansion of θ^{α}, $\bar{\theta}^{\dot{\alpha}}$. For example, lets look at the lowest lying term in the Taylor expansion of the superfield (5.15):

$$\mathcal{O}(x,\theta,\bar{\theta}) = O(x) + \theta^{\alpha}[Q_{\alpha},O(x)] + \dots \qquad (5.16)$$

Thus, given a formula involving the superfield $\mathcal{O}$, we can recover information about the superprimary component O by setting the fermionic coordinates to zero $\theta = \bar{\theta} = 0$. Similarly, we can recover information of the superdescendant $[Q_{\alpha},O]$ by extracting the power

---

[2]Spacetime and bispinor indices are mapped to each other by $x^{\dot{\alpha}\alpha} = x^{\mu}\bar{\sigma}_{\mu}^{\dot{\alpha}\alpha}$. Here we choose bispinor indices for consistency with the superconformal algebra in appendix 5.A.

proportional to θ^α. In a similar way, one can map the 16 superdescendants in (5.9) to the 16 terms in the Taylor expansion (5.16).

5.3.2   Differential operators and Ward identities

Besides elegantly capturing superdescendants, another virtue of superspace is that the superconformal algebra acts naturally on superfields. For non-supersymmetric CFT, we showed how the conformal algebra acts on primary fields in (2.21)-(2.24). Similar formulas are valid for the superconformal algebra acting on superfields. For example, using the definition of superfield (5.15) and the commutation relations in appendix 5.A, one finds the action of translation and supertranslations:

$$[P_{\alpha\dot\alpha}, \mathcal{O}(x,\theta,\bar\theta)] = \frac{\partial}{\partial x^{\dot\alpha\alpha}} \mathcal{O}(x,\theta,\bar\theta) \,, \tag{5.17}$$

$$[Q_\alpha, \mathcal{O}(x,\theta,\bar\theta)] = \left(\frac{\partial}{\partial\theta^\alpha} + \frac{1}{2}\bar\theta^{\dot\alpha} \frac{\partial}{\partial x^{\dot\alpha\alpha}} \right) \mathcal{O}(x,\theta,\bar\theta) \,, \tag{5.18}$$

$$[\bar Q_{\dot\alpha}, \mathcal{O}(x,\theta,\bar\theta)] = \left(-\frac{\partial}{\partial\bar\theta^{\dot\alpha}} - \frac{1}{2}\theta^\alpha \frac{\partial}{\partial x^{\dot\alpha\alpha}} \right) \mathcal{O}(x,\theta,\bar\theta) \,. \tag{5.19}$$

The action of the remaining generators is obtained with the help of the Baker–Campbell–Hausdorff formula similar to (2.25). For example, the dilatation operator acts on a superfield of dimension Δ as

$$[D, \mathcal{O}(x,\theta,\bar\theta)] = \left(x^{\dot\alpha\alpha} \frac{\partial}{\partial x^{\dot\alpha\alpha}} + \frac{1}{2}\theta^\alpha \frac{\partial}{\partial\theta^\alpha} + \frac{1}{2}\bar\theta^{\dot\alpha} \frac{\partial}{\partial\bar\theta^{\dot\alpha}} + \Delta \right) \mathcal{O}(x,\theta,\bar\theta) \,. \tag{5.20}$$

Although it is possible to obtain differential operators for the remaining generators $K^{\dot\alpha\alpha}$, S^α, etc. the expressions become lengthy and we do not show them here.

Perhaps the main application of the differential operators above is to constrain superconformal correlations functions. As in the non-supersymmetric case, define $\mathcal{L}^{(i)}$ to be the differential operator corresponding to generator L acting at point x_i. Then correlation functions must satisfy the superconformal Ward identities for every possible L in the superconformal algebra:

$$\sum_{i=1}^n \mathcal{L}^{(i)} \langle \mathcal{O}_1(x_1,\theta_1,\bar\theta_1) \dots \mathcal{O}_n(x_n,\theta_n,\bar\theta_n) \rangle = 0 \,. \tag{5.21}$$

The derivation of the Ward identity is exactly as in the non-supersymmetric case (2.29). By solving these partial differential equations in $(x_i, \theta_i, \bar\theta_i)$, one can fix the form of correlators of superfields. As explained in the previous section, these correlation functions contain information about superconformal primaries and all of their descendants.

5.3.3 Covariant derivatives and short multiplets

In the previous section, we have explained how the supercharges act on superfields. To be precise, in (5.18) one starts with a superprimary operator $O(0)$, which is then translated to a superfield $\mathcal{O}$, and finally Q_α acts on the superfield. However, sometimes it is more convenient to act with the supercharges on the superprimary at the origin, and only then supertranslate. This leads to the covariant derivatives, defined as

$$D_\alpha \mathcal{O}(x,\theta,\bar\theta) \equiv e^{x\cdot P+\theta Q+\bar Q\bar\theta}[Q_\alpha, \mathcal{O}(0)]e^{-x\cdot P-\theta Q-\bar Q\bar\theta}, \tag{5.22}$$

$$\bar D_{\dot\alpha} \mathcal{O}(x,\theta,\bar\theta) \equiv e^{x\cdot P+\theta Q+\bar Q\bar\theta}[\bar Q_{\dot\alpha}, \mathcal{O}(0)]e^{-x\cdot P-\theta Q-\bar Q\bar\theta}. \tag{5.23}$$

With the commutation relations (5.57), the covariant derivative can be expressed as a differential operator acting on superfields:

$$D_\alpha \mathcal{O}(x,\theta,\bar\theta) = \left(\frac{\partial}{\partial\theta^\alpha} - \frac{1}{2}\bar\theta^{\dot\alpha}\frac{\partial}{\partial x^{\dot\alpha\alpha}}\right)\mathcal{O}(x,\theta,\bar\theta), \tag{5.24}$$

$$\bar D_{\dot\alpha} \mathcal{O}(x,\theta,\bar\theta) = \left(-\frac{\partial}{\partial\bar\theta^{\dot\alpha}} + \frac{1}{2}\theta^\alpha\frac{\partial}{\partial x^{\dot\alpha\alpha}}\right)\mathcal{O}(x,\theta,\bar\theta). \tag{5.25}$$

The usefulness of covariant derivatives is due to shortening conditions being naturally defined for superprimary operators at the origin.

The example of a chiral superprimary operator $\phi(0)$ is again illuminating. We denote $\Phi(x,\theta,\bar\theta)$ the superfield obtained from $\phi(0)$, where the chiral superprimary is defined by the shortening condition $[\bar Q_{\dot\alpha}, \phi(0)] = 0$. Comparing to the definition of covariant derivative (5.23), it is clear that the superfield obeys the shortening condition

$$\bar D_{\dot\alpha}\Phi(x,\theta,\bar\theta) = 0. \tag{5.26}$$

It is instructive to solve this shortening condition explicitly. Introducing the distance $y^{\dot\alpha\alpha} = x^{\dot\alpha\alpha} + \frac{1}{2}\theta^\alpha\bar\theta^{\dot\alpha}$, the chiral superfield can only depend on $y^{\dot\alpha\alpha}$ and θ^α, so the Taylor expansion of Φ contains only three terms

$$\Phi(x,\theta,\bar\theta) = \Phi(y,\theta) = \phi(y) + \theta^\alpha\psi_\alpha(y) + \theta^\alpha\theta_\alpha\rho(y), \tag{5.27}$$

which correspond precisely to the three operators that form a chiral multiplet, see (5.12).

The punchline is that superconformal multiplets can be constructed in two equivalent ways. In the operator language of section 5.2, one acts on a superprimary with $Q, \bar Q$ and removes null descendants. In the superspace language, a shortening condition can be imposed using covariant derivatives. The superfield that solves the shortening condition contains a smaller number of Taylor components, each of which corresponds to a member of the supermultiplet.

5.4 Superconformal blocks

One implication of supersymmetry is that OPE coefficients of operators in the same super-multiplet are related to each other. This observation leads to the concept of superconformal block, which is central in the conformal bootstrap of SCFTs. In this section, we explain two methods to compute superconformal blocks, both of which rely on superspace. These two methods are applied to the by now familiar example of $4d$ $\mathcal{N} = 1$.

5.4.1 Setup

The goal of this section is to study superconformal blocks for the four-point function of chiral and antichiral operators $\langle \phi \bar{\phi} \phi \bar{\phi} \rangle$ in $4d$ $\mathcal{N} = 1$ SCFTs. It is clear that this four-point function has two different conformal block expansions: one uses the $\phi \times \phi$ OPE, while the other uses the $\phi \times \bar{\phi}$ OPE. Although both of them are interesting, we focus on the $\phi \times \bar{\phi}$ OPE:

$$(x_{12}^2 x_{34}^2)^{\Delta_\phi} \langle \phi(x_1) \bar{\phi}(x_2) \phi(x_3) \bar{\phi}(x_4) \rangle = \mathcal{G}(z, \bar{z}) = \sum_{\mathcal{O} \in \phi \times \bar{\phi}} \lambda_{\phi\bar{\phi}\mathcal{O}}^2 g_{\Delta, \ell} \,. \tag{5.28}$$

Many terms in the infinite sum are related by superconformal symmetry, so our goal is to rearrange the sum taking these relations into account. In the next paragraphs, we explore this idea in more detail.

Any operator in the $\phi \times \bar{\phi}$ OPE satisfies two properties: it transforms in integer spin representation, because this is the only representation allowed in the OPE of two scalars; and it is uncharged $r = 0$, as follows from R-symmetry conservation. Now we take a superprimary operator A in the $\phi \times \bar{\phi}$ OPE, with scaling dimension Δ and spin ℓ. Of all the descendants of A, only three have integer spin and zero charge, as can be seen from the long multiplet (5.9):

$$A : [\ell, \ell]_\Delta^{(0)} \,, \quad J : [\ell+1, \ell+1]_{\Delta+1}^{(0)} \,, \quad N : [\ell-1, \ell-1]_{\Delta+1}^{(0)} \,, \quad D : [\ell, \ell]_{\Delta+2}^{(0)} \,. \tag{5.29}$$

For future convenience we have named these four operators, which are the only ones in the multiplet that appear in the $\phi \times \bar{\phi}$ OPE. In other words, the contribution of these operators to the conformal block expansion takes the form

$$\mathcal{G}(z, \bar{z}) \supset \lambda_{\phi\bar{\phi}A}^2 \, g_{\Delta,\ell} + \lambda_{\phi\bar{\phi}J}^2 \, g_{\Delta+1,\ell+1} + \lambda_{\phi\bar{\phi}N}^2 \, g_{\Delta+1,\ell-1} + \lambda_{\phi\bar{\phi}D}^2 \, g_{\Delta+2,\ell} \,. \tag{5.30}$$

Here supersymmetry has fixed the spin and dimension of the descendants in terms of the superprimary. Not only that, but supersymmetry also relates their OPE coefficients, so the expansion can be rewritten as

$$\mathcal{G}(z,\bar{z}) \supset \lambda_{\phi\bar{\phi}A}^2 \underbrace{\left(g_{\Delta,\ell} + k_1\, g_{\Delta+1,\ell+1} + k_2\, g_{\Delta+1,\ell-1} + k_3\, g_{\Delta+2,\ell}\right)}_{G_{\Delta,\ell}}. \tag{5.31}$$

The superconformal block $G_{\Delta,\ell}$ fixes completely contributions of descendants in terms of the superprimary A. The challenge, though, is to determine the constants $k_{1,2,3}$. Importantly, the constants $k_{1,2,3}$ depend on the superconformal algebra and multiplets under consideration, but not on dynamical information about the theory.

The rest of this section discusses two methods to compute the superblocks, or equivalently to compute $k_{1,2,3}$. For the first method, compare equations (5.30) and (5.31) to obtain the definition of $G_{\Delta,\ell}$:

$$G_{\Delta,\ell}(z,\bar{z}) = g_{\Delta,\ell} + \sum_{\mathcal{O}' \in \{J,N,D\}} \frac{1}{n_{\mathcal{O}'}} \frac{\lambda_{\phi\bar{\phi}\mathcal{O}'}^2}{\lambda_{\phi\bar{\phi}A}^2} g_{\Delta_{\mathcal{O}'},\ell_{\mathcal{O}'}}. \tag{5.32}$$

Here we allow for the descendants $\mathcal{O}'$ not to be unit-normalized: instead, their two-point functions are $\langle \mathcal{O}'\mathcal{O}' \rangle \propto n_{\mathcal{O}'}$. The calculation of equation (5.32) proceeds in three steps: first we define J, N and D in terms of supercharges in section 5.4.2; then we compute two-point norms $n_{\mathcal{O}'}$ in section 5.4.3; finally, we compute the three-point OPE coefficients $\lambda_{\phi\bar{\phi}\mathcal{O}'}$ in section 5.4.4. Our discussion follows closely the original work [65]. A second method to compute the superconformal blocks consists on solving a superconformal Casimir equation. By using an ansatz of the form (5.31), the supercasimir equation fixes $k_{1,2,3}$, as explained in section 5.4.5.

Before proceeding to the calculation, a word of caution to the reader: the derivation of superconformal blocks is a very technical subject. Here, in the same spirit as the rest of the text, we aim for clarity more than rigor, so we omit unimportant factors in many equations. These details can be reconstructed from the original literature.

5.4.2 Superconformal descendants

The first step to calculate superconformal blocks is to define precisely the superdescendants (5.29). In index free notation, the spin-ℓ superprimary is $A(x,\eta)$, while the descendants with spins $\ell\pm 1$ and ℓ, are Poincare supercharges acting on $A(x,\eta)$. More precisely, defining

$\Theta^\mu = (\bar{\sigma}^\mu)^{\dot{\alpha}\alpha}[Q_\alpha, \bar{Q}_{\dot{\alpha}}]$, the descendants are

$$J(x,\eta) \sim (\Theta^\mu \eta_\mu)A(x,\eta)\,, \tag{5.33}$$

$$N(x,\eta) \sim (\Theta^\mu \partial_{\eta^\mu})A(x,\eta)\,, \tag{5.34}$$

$$D(x,\eta) \sim (\Theta^\mu \Theta_\mu)A(x,\eta) + c_1 P^2 A(x,\eta) + c_2 (P^\mu \eta_\mu)(P^\nu \partial_{\eta^\nu})A(x,\eta)\,. \tag{5.35}$$

This definition implies that J, N and D have spin $\ell + 1$, $\ell - 1$ and ℓ respectively. Furthermore, the commutation relations in appendix 5.A imply that J and N are conformal primaries, namely special conformal transformations kill them $K_\mu J = K_\mu N = 0$. The situation for D is more complicated, because $\Theta^2 A$ is not a conformal primary. Instead, one adds the two extra terms in (5.35), and fixes the unknown coefficients requiring $K_\mu D = 0$.

Having defined the conformal primaries J, N and D, the next step is to understand them in the language of superfields. Denoting the superfield by $\mathcal{O}(x, \theta, \bar{\theta})$, then the Taylor expansion of (5.15) reads

$$\mathcal{O}(x, \theta, \bar{\theta}, \eta) \sim A(x,\eta) + \zeta^\mu \partial_{\eta^\mu} J(x,\eta) + \zeta^\mu \eta_\mu N(x,\eta) + \zeta^2 D(x,\eta) + \dots \tag{5.36}$$

where $\zeta^\mu = \theta^\alpha \sigma^\mu_{\alpha\dot{\alpha}} \bar{\theta}^{\dot{\alpha}}$. Therefore, for a given expression involving $\mathcal{O}$, the information of the descendants is recovered by Taylor expanding and keeping appropriate powers of ζ and η.[3]

5.4.3 Two-point norms

The second step in the calculation of superconformal blocks is to obtain the two-point function norms of J, N, D. In order to obtain these norms, we work in the Hilbert space formalism. For example, the operator $A(\eta)$ generates the state $|A(\eta)\rangle = A(0,\eta)|0\rangle$, which we take to be unit normalized

$$\langle A(\eta_1)|A(\eta_2)\rangle = (\eta_1 \cdot \eta_2)^\ell\,. \tag{5.37}$$

Similarly, the states corresponding to superconformal descendants can be obtained from their definition (5.33)-(5.35). Using the Hermitian conjugation in radial quantization (5.58), and the commutation relations in appendix 5.A, it is possible to obtain the two-point

---

[3] A more sophisticated method associates a differential operator to each superdescendant. Acting on the superfield with the differential operator and setting fermions to zero gives the contribution of that descendant [190, 191].

norms:

$$\langle J(\eta_1)|J(\eta_2)\rangle = 2(\Delta + \ell)(\Delta + \ell + 1)(\eta_1 \cdot \eta_2)^{\ell+1}\,, \tag{5.38}$$

$$\langle N(\eta_1)|N(\eta_2)\rangle = \frac{2(\ell+1)^2}{\ell^2}(\Delta - \ell - 2)(\Delta - \ell - 1)(\eta_1 \cdot \eta_2)^{\ell-1}\,, \tag{5.39}$$

$$\langle D(\eta_1)|D(\eta_2)\rangle = \frac{\Delta^2(\Delta - \ell - 2)(\Delta - \ell - 1)(\Delta + \ell)(\Delta + \ell + 1)}{4(\Delta - 1)^2}(\eta_1 \cdot \eta_2)^{\ell}\,. \tag{5.40}$$

These norms are calculated in a similarly way to unitarity bounds, see (3.1) and (5.13). We note in passing that positivity of these norms implies the bound $\Delta > \ell + 2$, consistent with (5.10). When the unitarity bound is saturated, the multiplet shortens and the descendants N and D drop out.

An alternative method to obtain the two-point norms is based on superspace. As described in [192], by Taylor expanding the superspace two-point function one can recovers the norms of all the superconformal descendants in a long multiplet (5.9).

5.4.4   Three-point functions

The final step in the calculation of superconformal blocks is to relate the OPE coefficients of A, J, N and D. Here we use superspace techniques, although a calculation based on the Hilbert space formalism is also possible [193]. In superspace, the chiral and antichiral multiplets are represented by superfields Φ, $\bar{\Phi}$ that satisfy a shortening condition, see (5.26). Similarly, the multiplet with superprimary A is represented by a superfield $\mathcal{O}$. In superspace, their three-point function is uniquely fixed [65, 185]

$$\langle \Phi(y_1, \theta_1)\bar{\Phi}(\bar{y}_2, \bar{\theta}_2)\mathcal{O}(x_3, \theta_3, \bar{\theta}_3, \eta_3)\rangle = F^{(3)}(x_i, \theta_i, \bar{\theta}_i, \eta_3)\,. \tag{5.41}$$

Although not extremely complicated, we refrain from showing the explicit formula for $F^{(3)}$, because for our purposes the only necessary property is that $F^{(3)}$ is unambiguously determined up to an overall normalization. Because we are interested only on the OPE coefficient of the chiral superprimaries $\phi, \bar{\phi}$, we set $\theta_1 = \bar{\theta}_2 = 0$. Furthermore, the left-hand side of equation (5.41) can be expanded using the form of the multiplets (5.36), giving

$$\langle \phi\bar{\phi}\mathcal{O}\rangle \sim \langle \phi\bar{\phi}A\rangle + \zeta^\mu \partial_{\eta^\mu}\langle \phi\bar{\phi}J\rangle + \zeta^\mu \eta_\mu\langle \phi\bar{\phi}N\rangle + \zeta^2\langle \phi\bar{\phi}D\rangle\,. \tag{5.42}$$

57

Since the right-hand side of (5.41) is fully fixed, it has a similar Taylor expansion. Matching equal powers of ζ and η in the left- and right-hand side gives

$$\langle \phi\bar{\phi}A \rangle = T^{\Delta_\phi}_{\Delta,\ell} \,, \tag{5.43}$$

$$\langle \phi\bar{\phi}J \rangle = i(\Delta + \ell)\, T^{\Delta_\phi}_{\Delta+1,\ell+1} \,, \tag{5.44}$$

$$\langle \phi\bar{\phi}N \rangle = i\frac{(\Delta - \ell - 2)(\ell + 1)}{2\ell}\, T^{\Delta_\phi}_{\Delta+1,\ell-1} \,, \tag{5.45}$$

$$\langle \phi\bar{\phi}D \rangle = -\frac{\Delta(\Delta + \ell)(\Delta - \ell - 2)}{8(\Delta - 1)}\, T^{\Delta_\phi}_{\Delta+2,\ell} \,. \tag{5.46}$$

To unclutter the notation, we introduced the three-point tensor structure $T^{\Delta_\phi}_{\Delta,\ell}$, which follows from (2.31):

$$T^{\Delta_\phi}_{\Delta,\ell} \equiv \frac{\lambda_{\phi\bar{\phi}A}}{x_{12}^{2\Delta_\phi-\Delta+\ell}x_{13}^{\Delta-\ell}x_{23}^{\Delta-\ell}} \left(\frac{\eta^\mu x_{13}^\mu}{x_{13}^2} - \frac{\eta^\mu x_{23}^\mu}{x_{23}^2} \right)^\ell \,. \tag{5.47}$$

We are finally in a position to compute the superblock of interest. The normalization of the superdescentants is found in (5.38)-(5.40), while the relation between OPE coefficients follows from (5.43)-(5.46). Inserting these results in the definition (5.32), gives:

$$
\begin{aligned}
G_{\Delta,\ell} = g_{\Delta,\ell} &- \frac{(\Delta + \ell)}{2(\Delta + \ell + 1)}g_{\Delta+1,\ell+1} - \frac{(\Delta - \ell - 2)}{8(\Delta - \ell - 1)}g_{\Delta+1,\ell-1} \\
&+ \frac{(\Delta + \ell)(\Delta - \ell - 2)}{16(\Delta + \ell + 1)(\Delta - \ell - 1)}g_{\Delta+2,\ell}
\end{aligned}
\tag{5.48}
$$

This superconformal block, which was originally obtained in [65], is the main result of this section. By now this superblock has been rederived with a variety of alternative methods [193–196], one of which we review now.

5.4.5   Four-point functions and the superconformal Casimir equation

Before concluding the chapter, we provide an alternative method to compute the superblock (5.48). For this method, the starting point is the four-point function of chiral and antichiral superfields:

$$\langle \Phi(y_1, \theta_1)\bar{\Phi}(\bar{y}_2, \bar{\theta}_2)\Phi(y_3, \theta_3)\bar{\Phi}(\bar{y}_4, \bar{\theta}_4) \rangle = \frac{1}{(\mathbf{x}_{12}^2\mathbf{x}_{34}^2)^{\Delta_\phi}}\mathcal{G}(\mathbf{u}, \mathbf{v}) \,. \tag{5.49}$$

This correlation function depends on the supersymmetric distances $\mathbf{x}_{ij}^2$ and two superconformal invariants $\mathbf{u}$ and $\mathbf{v}$, whose precise forms can be found in the literature [185, 196].

58

These objects are supersymmetrizations of the standard distances and cross-ratios, meaning that setting the Grassmann variables to zero we recover

$$\lim_{\theta,\bar\theta\to 0} \mathbf{x}_{12}^2 = x_{12}^2\,, \qquad \lim_{\theta,\bar\theta\to 0} \mathbf{u} = \frac{x_{12}^2 x_{34}^2}{x_{13}^2 x_{24}^2}\,, \qquad \text{etc.} \tag{5.50}$$

The superconformal blocks are eigenfunctions of the superconformal Casimir, analogously to conformal blocks, which are eigenfunctions of the conformal Casimir, see section 2.3.2. The superconformal Casimir operator is obtained from the conformal Casimir, by adding terms that account for the R-symmetry group and the supercharges. In the $4d$ $\mathcal{N}=1$ example the Casimir is:

$$C_{\mathcal{N}=1} = C_{SO(d+1,1)} - \frac{3}{4}R^2 + [S^\alpha, Q_\alpha] + [\bar{S}^{\dot\alpha}, \bar{Q}_{\dot\alpha}]\,. \tag{5.51}$$

From the superconformal Casimir, we can form the differential operator $\mathcal{C}_{\mathcal{N}=1}^{(1+2)}$ which acts on superspace. This notation means that one should take the Casimir (5.51) and replace each generator by the corresponding differential operator acting at the first two points. The eigenvalue problem for $\mathcal{C}_{\mathcal{N}=1}^{(1+2)}$ translates into a differential equation satisfied by the superconformal block [196, 197]:

$$\left[z^2(1-z)\partial_z^2 + \bar{z}^2(1-\bar{z})\partial_{\bar{z}}^2 + z(1-2z)\partial_z + \bar{z}(1-2\bar{z})\partial_{\bar{z}}\right.$$
$$\left. + \frac{2z\bar{z}}{z-\bar{z}}\big((1-z)\partial_z - (1-\bar{z})\partial_{\bar{z}}\big) - \frac{1}{2}\big(\Delta(\Delta-2) + \ell(\ell+2)\big)\right]G_{\Delta,\ell}(z,\bar{z}) = 0\,. \tag{5.52}$$

Notice that the eigenvalue of the superconformal Casimir is different than the one for the purely conformal case. In order to find the solution to this equation, one can simply make an ansatz of the form (5.31) to fix the coefficients $k_{1,2,3}$. As a curiosity, however, observe that the superconformal Casimir equation also admits a solution in terms of a single conformal block:

$$G_{\Delta,\ell}(z,\bar{z}) = (z\bar{z})^{-\frac{1}{2}}g_{\Delta+1,\ell}^{1,1}(z,\bar{z})\,. \tag{5.53}$$

The relation (5.53) = (5.48) is not obvious, although it is also not hard to show using hypergeometric identities. In different spacetime dimensions or number of supercharges, there exist similar expressions, where a superconformal block is equivalent to a single non-supersymmetric block with shifted arguments [1, 193, 194, 198].

5.5 Review of the literature

The numerical bootstrap for SCFT is a very rich subject, which is naturally classified by spacetime dimension and number of supersymmetries. In three dimensions, there has been work on the $\mathcal{N} = 1$ superIsing model [167, 199–201], on $\mathcal{N} = 2$ theories [193, 202–205], on $\mathcal{N} = 4$ theories and their connection to mirror symmetry [206], and on $\mathcal{N} = 6, 8$ models with holographic duals [207–211]. In four dimensions, there is work on $\mathcal{N} = 1$ [56, 65, 212–215], $\mathcal{N} = 2$ [1, 198, 216–218], $\mathcal{N} = 3$ [219], and $\mathcal{N} = 4$ [206, 220–225] models. Finally, there has also been work on $2d$ SCFT [226–228], $5d$ SCFT [229], $6d$ SCFT [230–232], and supersymmetric defects [2, 233].

Superconformal algebras and their representation theory is well understood, see [234] for a review. The early work [184] studied the representation theory of the $4d$ $\mathcal{N}$-extended superconformal algebra, which was later generalized [54] to other dimensions $d \geq 3$. The construction of long and short multiplets was initiated in [27] for $4d$ $\mathcal{N} = 2, 4$ theories, and later generalized in the very complete work [182].

The calculation of superconformal blocks has also been pursued in a large number of works, see [65, 190, 191, 193–195, 197, 235–242] for a list that gives an idea of various methods. A major omission of this chapter was the study of superconformal Ward identities for theories with eight or more supercharges [243–245]. In $4d$ $\mathcal{N} \geq 2$, these superconformal Ward identities can be understood from a protected subsector described by a chiral algebra [246], which allowed to find universal OPE bounds saturated by known theories [247, 248], see [249] for a nice review. Similar protected subsectors also exists in $3d$ $\mathcal{N} \geq 4$ [208] and $6d$ $(2, 0)$ [250].

Finally, let us mention that a more mathematical way to think of superspace is as a coset of the superconformal group by one of its subgroups. In our case, we have chosen a particular subgroup that leads to the so-called real superspace. Quotienting by different subgroups gives other types of superspace, such as chiral superspace, harmonic superspace, etc. some of which only make sense for $\mathcal{N} \geq 2$. For a complete treatment of these subjects, we refer to the pedagogical introduction [251].

5.A Four-dimensional superconformal algebra

In this appendix we show the four-dimensional superconformal algebra $SU(2, 2|\mathcal{N})$, where for physical theories $\mathcal{N} = 1, \ldots, 4$. Instead of vector indices, it is natural to use spinor

indices for P, K and M, such that the conformal algebra reads

$$[D, P_{\alpha\dot\alpha}] = P_{\alpha\dot\alpha},$$
$$[D, K^{\dot\alpha\alpha}] = -K^{\dot\alpha\alpha},$$
$$[K^{\dot\alpha\alpha}, P_{\beta\dot\beta}] = \delta^{\dot\alpha}{}_{\dot\beta} M_\beta{}^\alpha + \delta_\beta{}^\alpha \bar{M}^{\dot\alpha}{}_{\dot\beta} + \delta_\beta{}^\alpha \delta^{\dot\alpha}{}_{\dot\beta} D,$$
$$[M_\alpha{}^\beta, M_\gamma{}^\delta] = \delta_\gamma{}^\beta M_\alpha{}^\delta - \delta_\alpha{}^\delta M_\gamma{}^\beta,$$
$$[\bar{M}^{\dot\alpha}{}_{\dot\beta}, \bar{M}^{\dot\gamma}{}_{\dot\delta}] = -\delta^{\dot\gamma}{}_{\dot\beta} \bar{M}^{\dot\alpha}{}_{\dot\delta} + \delta^{\dot\alpha}{}_{\dot\delta} \bar{M}^{\dot\gamma}{}_{\dot\beta}, \tag{5.54}$$
$$[M_\alpha{}^\beta, P_{\gamma\dot\gamma}] = \delta_\gamma{}^\beta P_{\alpha\dot\gamma} - \tfrac{1}{2}\delta_\alpha{}^\beta P_{\gamma\dot\gamma},$$
$$[\bar{M}^{\dot\alpha}{}_{\dot\beta}, P_{\gamma\dot\gamma}] = \delta^{\dot\alpha}{}_{\dot\gamma} P_{\gamma\dot\beta} - \tfrac{1}{2}\delta^{\dot\alpha}{}_{\dot\beta} P_{\gamma\dot\gamma},$$
$$[M_\alpha{}^\beta, K^{\dot\gamma\gamma}] = -\delta_\alpha{}^\gamma K^{\dot\gamma\beta} + \tfrac{1}{2}\delta_\alpha{}^\beta K^{\dot\gamma\gamma},$$
$$[\bar{M}^{\dot\alpha}{}_{\dot\beta}, K^{\dot\gamma\gamma}] = -\delta^{\dot\gamma}{}_{\dot\beta} K^{\dot\alpha\gamma} + \tfrac{1}{2}\delta^{\dot\alpha}{}_{\dot\beta} K^{\dot\gamma\gamma}.$$

Besides the conformal algebra, the bosonic subgroup also includes an $SU(\mathcal{N})$ R-symmetry

$$[R^i{}_j, R^k{}_l] = \delta^k{}_j R^i{}_l - \delta^i{}_l R^k{}_j, \tag{5.55}$$

and the $U(1)_R$ charge r. There are $4\mathcal{N}$ Poincare supercharges Q^i_α and $\bar{Q}_{i\dot\alpha}$, with the indices running over $i = 1, \ldots, \mathcal{N}$ and $\alpha, \dot\alpha = 1, 2$. Under the bosonic subalgebra, these Poincare and superconformal supercharges transform as

$$[D, Q^i_\alpha] = \tfrac{1}{2}Q^i_\alpha,$$
$$[D, \bar{Q}_{i\dot\alpha}] = \tfrac{1}{2}\bar{Q}_{i\dot\alpha},$$
$$[r, Q^i_\alpha] = -Q^i_\alpha,$$
$$[r, \bar{Q}_{i\dot\alpha}] = +\bar{Q}_{i\dot\alpha},$$
$$[D, \bar{Q}_{i\dot\alpha}] = \tfrac{1}{2}\bar{Q}_{i\dot\alpha},$$
$$[K^{\dot\alpha\alpha}, Q^i_\beta] = \delta_\beta{}^\alpha \bar{S}^{i\dot\alpha},$$
$$[K^{\dot\alpha\alpha}, \bar{Q}_{i\dot\beta}] = \delta^{\dot\alpha}{}_{\dot\beta} S^\alpha_i,$$
$$[M_\alpha{}^\beta, Q^i_\gamma] = \delta_\gamma{}^\beta Q^i_\alpha - \tfrac{1}{2}\delta_\alpha{}^\beta Q^i_\gamma,$$
$$[\bar{M}^{\dot\alpha}{}_{\dot\beta}, \bar{Q}_{i\dot\gamma}] = \delta^{\dot\alpha}{}_{\dot\gamma} \bar{Q}_{i\dot\beta} - \tfrac{1}{2}\delta^{\dot\alpha}{}_{\dot\beta} \bar{Q}_{i\dot\gamma},$$
$$[R^i{}_j, Q^k_\alpha] = \delta^k{}_j Q^i_\alpha - \tfrac{1}{\mathcal{N}}\delta^i{}_j Q^k_\alpha,$$
$$[R^i{}_j, \bar{Q}_{k\dot\alpha}] = -\delta^i{}_k \bar{Q}_{j\dot\alpha} + \tfrac{1}{\mathcal{N}}\delta^i{}_j \bar{Q}_{k\dot\alpha},$$

$$[D, S^\alpha_i] = -\tfrac{1}{2}S^\alpha_i,$$
$$[D, \bar{S}^{i\dot\alpha}] = -\tfrac{1}{2}\bar{S}^{i\dot\alpha},$$
$$[r, S^\alpha_i] = +S^\alpha_i,$$
$$[r, \bar{S}^{i\dot\alpha}] = -\bar{S}^{i\dot\alpha},$$
$$[P_{\alpha\dot\alpha}, S^\beta_i] = -\delta^\beta{}_\alpha \bar{Q}_{i\dot\alpha},$$
$$[P_{\alpha\dot\alpha}, \bar{S}^{i\dot\beta}] = -\delta^{\dot\beta}{}_{\dot\alpha} Q^i_\alpha, \tag{5.56}$$
$$[M_\alpha{}^\beta, S^\gamma_i] = -\delta_\alpha{}^\gamma S^\beta_i + \tfrac{1}{2}\delta_\alpha{}^\beta S^\gamma_i,$$
$$[\bar{M}^{\dot\alpha}{}_{\dot\beta}, \bar{S}^{i\dot\gamma}] = -\delta^{\dot\gamma}{}_{\dot\beta} \bar{S}^{i\dot\alpha} + \tfrac{1}{2}\delta^{\dot\alpha}{}_{\dot\beta} \bar{S}^{i\dot\gamma},$$
$$[R^i{}_j, S^\alpha_k] = -\delta^i{}_k S^\alpha_j + \tfrac{1}{\mathcal{N}}\delta^i{}_j S^\alpha_k,$$
$$[R^i{}_j, \bar{S}^{k\dot\alpha}] = \delta^k{}_j \bar{S}^{i\dot\alpha} - \tfrac{1}{\mathcal{N}}\delta^i{}_j \bar{S}^{k\dot\alpha}.$$

Finally, the supercharges anticommute as follows:

$$
\begin{aligned}
\{Q^i_\alpha, \bar{Q}_{j\dot\alpha}\} &= \delta^i{}_j P_{\alpha\dot\alpha}, \\
\{S^\alpha_i, \bar{S}^{j\dot\alpha}\} &= \delta^j{}_i K^{\dot\alpha\alpha}, \\
\{Q^i_\alpha, S^\beta_j\} &= \delta^i{}_j \delta_\alpha{}^\beta \left(\frac{D}{2} + r\frac{4-\mathcal{N}}{4\mathcal{N}}\right) + \delta^i{}_j M_\alpha{}^\beta - \delta_\alpha{}^\beta R^i{}_j, \\
\{\bar{S}^{i\dot\alpha}, \bar{Q}_{j\dot\beta}\} &= \delta^i{}_j \delta^{\dot\alpha}{}_{\dot\beta} \left(\frac{D}{2} - r\frac{4-\mathcal{N}}{4\mathcal{N}}\right) + \delta^i{}_j \bar{M}^{\dot\alpha}{}_{\dot\beta} + \delta^{\dot\alpha}{}_{\dot\beta} R^i{}_j.
\end{aligned}
\tag{5.57}
$$

For $\mathcal{N} = 4$, the $U(1)_R$ charge can be quotiented out from the algebra, leading to the $PSU(2,2|4)$ superalgebra. Under Hermitian conjugation in radial quantization, the generators transform as

$$
\begin{aligned}
D^\dagger &= D, & P^\dagger_{\alpha\dot\alpha} &= K^{\dot\alpha\alpha}, & (R^i{}_j)^\dagger &= R^j{}_i, & r^\dagger &= r, \\
(M_\alpha{}^\beta)^\dagger &= M_\beta{}^\alpha, & (\bar{M}^{\dot\alpha}{}_{\dot\beta})^\dagger &= \bar{M}^{\dot\beta}{}_{\dot\alpha}, & (Q^i_\alpha)^\dagger &= S^\alpha_i, & (\bar{Q}_{\dot\alpha i})^\dagger &= \bar{S}^{\dot\alpha i}.
\end{aligned}
\tag{5.58}
$$

Chapter 6

Conformal defects

Conformal defects are extended operators that, when inserted in a CFT, break part of the conformal symmetry. In condensed matter theory, the most familiar examples of defects are boundaries and impurities. Here, instead of focusing on particular examples, we obtain a set of crossing equations that are satisfied by any conformal defect. This leads to the defect bootstrap program, where the goal is to constrain the space of all consistent defects, similarly to how the conformal bootstrap constrains the space of ordinary CFTs. We start this chapter with a review of the defining properties of defects, along with several physically relevant examples. In later sections, we focus on the implications of conformal symmetry, and how they can be used to constrain or even solve conformal defects.

6.1   Introduction

There exists a great variety of conformal defects: some defects admit Lagrangian description while others are intrinsically non-Lagrangian; some admit weak-coupling expansions while others are strongly coupled; some defects can break flavor symmetry; etc. To capture such diversity in a unified framework, we need to focus on the universal properties shared by all defects.

6.1.1   Geometry

The defining property of a conformal defect is the subgroup of conformal symmetry it preserves. To see how this symmetry is preserved, we start with a full fledged CFT in $\mathbb{R}^d$, which by definition preserves the full conformal group. From now on, we call this the bulk

or ambient CFT. Splitting the Cartesian coordinates as $(x^a, x^i) \in \mathbb{R}^d$, we insert an infinite flat defect that extends in the x^a directions, while it is located at $x^i = 0$. At this stage, we only need to know that the defect naturally splits space in parallel and orthogonal directions

$$\text{Parallel:} \quad a = 1, \ldots, p\,, \tag{6.1}$$

$$\text{Orthogonal:} \quad i = p+1, \ldots, d\,. \tag{6.2}$$

The dimension of the defect is denoted by p, while $q = d - p$ is its codimension. The above construction applies to any type of defect. What truly defines conformal defects is that they preserve conformal transformations along their worldvolume and rotations around them. More precisely, conformal defects preserve the following symmetry generators:

$$\text{Preserved generators:} \quad \widehat{L} \in \{D, P_a, K_a, M_{ab}, M_{ij}\}\,. \tag{6.3}$$

For an equivalent but more compact definition, one says that a conformal defect breaks conformal symmetry as

$$SO(d+1,1) \to SO(p+1,1) \oplus SO(q)\,, \qquad p+q = d\,. \tag{6.4}$$

In the previous discussion we have implicitly worked with infinite flat defects, although the symmetry-breaking pattern (6.4) is also compatible with spherical conformal defects. However, any other geometry leads to defects that are not conformal.

6.1.2 Bulk and defect operators

Another universal feature of defect CFT is the existence of two types of local operators: bulk and defect operators.

Bulk operators $\mathcal{O}$ are the local operators of the bulk CFT in the absence of conformal defects. As discussed thoroughly in section 2.1, bulk operators transform in representations of $SO(d+1,1)$ defined by the scaling dimension Δ and spin ℓ. Because of short distance singularities when bulk operators approach a defect, bulk operators must always be inserted outside the worldvolume of the defect. To obtain a well-defined operator on the defect, one needs to first renormalize these singularities. The resulting object, called a defect operator, is described below.

Defect operators $\widehat{\mathcal{O}}$ are local operators inserted in the worldvolume of the defect, which we distinguish from bulk operators with a hat. Since they are restricted to the defect, these

operators transform in representations of the broken symmetry group

$$\widehat{\mathcal{O}} : \ [\widehat{\Delta}, j, s] \ \in \ SO(p+1,1) \oplus SO(q) \,. \tag{6.5}$$

In words, the defect scaling dimension $\widehat{\Delta}$ and the parallel spin j are the quantum numbers for the p-dimensional conformal group; similarly, the transverse spin s is the quantum number for $SO(q)$ rotations. However, note that only $\widehat{\Delta}$, s are necessary for one-dimensional defects, while only $\widehat{\Delta}$, j are necessary for codimension-one defects.

6.1.3   Canonical operators

The last universal property of defects we discuss is the existence of a displacement operator. The displacement operator D^i measures the failure of the stress tensor $T_{\mu\nu}$ to be conserved in the presence of a defect. Mathematically, conservation of the stress tensor acquires a contact term supported on the defect

$$\partial_\mu T^{\mu i}(x) = D^i(x)\delta^{(q)}(x^j) \,, \qquad i,j = p+1,\ldots,d \,, \tag{6.6}$$

with the diplacement being the proportionality factor. Since the stress tensor has dimension $\Delta_{T_{\mu\nu}} = d$, equation (6.6) fixes the displacement dimension $\widehat{\Delta}_D = p+1$. Similarly, the index structure of (6.6) implies the displacement is a vector under $SO(q)$, or equivalently $s_D = 1$. The importance of the displacement operator is that it exists in any non-trivial defect in a local CFTs.

More generally, a defect operator must exist for every continuous symmetry broken by the defect. Indeed, a continuous symmetry is generated by a conserved current j^μ. The defect breaks this symmetry if the conservation equation acquires a contact term localized on the defect:

$$\partial_\mu j^\mu(x) = t(x)\delta^{(q)}(x^j) \,. \tag{6.7}$$

As before, the proportionality factor is a defect operator $t(x)$, whose existence is guaranteed in any theory with the same symmetry-breaking pattern. For example, for a defect that breaks flavor symmetry $t(x)$ is called the tilt operator [252,253], and it has scaling dimension $\widehat{\Delta}_t = p$. Another example is provided by superconformal theories, where defects break part of the R-symmetry, leading to protected defect operators.

65

6.1.4 Examples

After having reviewed the main properties of conformal defects, it is illustrative to look at examples. One can think of a defect as a non-local operator $\mathcal{D}$ that one inserts in correlation functions as $\langle \mathcal{D} \mathcal{O}_1 \ldots \widehat{\mathcal{O}}_n \rangle$. Here, we provide two different ways to construct such an operator: order and disorder defects.

Order defects

An order defect is a Lagrangian density integrated along a submanifold $\Sigma \subset \mathbb{R}^d$:

$$\mathcal{D} = \exp\left(-\int_\Sigma \mathcal{L}_{\text{defect}}(\phi)\right). \tag{6.8}$$

Above, ϕ is a collective label for the fields integrated in the path integral. For gauge theories, a familiar example of order defect is the Wilson loop, while for condensed matter systems, we provide a similar example below.

Correlation functions with an order defect insertion $\langle \mathcal{D} \mathcal{O} \ldots \rangle$ can be computed adding a term to the action localized on a submanifold:

$$S = \int_{\mathbb{R}^d} \mathcal{L}_{\text{bulk}}(\phi) + \int_\Sigma \mathcal{L}_{\text{defect}}(\phi). \tag{6.9}$$

Although the two descriptions (6.8) and (6.9) are equivalent, the second is more common in the study of RG flows. Since we want a CFT in the bulk, we look at the IR fixed point of the bulk RG flow. However, the couplings in the defect Lagrangian will typically also flow. In order to have a conformal defect in a conformal bulk, the defect RG flow must also be tuned to land on a fixed point.

This abstract discussion becomes more clear in a simple example. Consider the ϕ^4 Lagrangian (4.33) with the line defect operator

$$\mathcal{D} = \exp\left(\zeta \int d\tau \phi\right). \tag{6.10}$$

In $d = 4$ the bulk is Gaussian while the defect operator ϕ is exactly marginal, so there is a one-parameter family of conformal defects parameterized by ζ [254]. The situation is more interesting in $d = 4 - \varepsilon$. On the one hand, the bulk RG flow described below (4.33) lands on the Wilson-Fisher fixed point. On the other hand, the defect operator ϕ is weakly relevant because $\Delta_\phi = 1 - \varepsilon/2 < p = 1$, so ϕ will trigger a defect RG flow that lands on a non-trivial fixed point [253]. The result is a critical defect embedded in a critical bulk, which can be described with the framework of defect CFT.

Disorder defects

An alternative method to obtain a defect is to compute correlation functions using certain boundary conditions in the path integral:

$$\langle \mathcal{D}\mathcal{O}_1 \dots \mathcal{O}_n \rangle = \int \mathcal{O}_1 \dots \mathcal{O}_n e^{-S(\phi)} D\phi|_{\phi(\Sigma)=\phi_0} \,. \tag{6.11}$$

Defects obtained in this way are called disorder defects. Note that disorder defects are not necessarily conformal. For example, if the boundary condition has some scale associated to it, or it does not respect the isometries (6.4), the defect will typically break conformality.

In gauge theory, a well-known disorder defect is the 't Hooft line operator, while in condensed matter, monodromy defects are important examples of conformal defects. Focusing again on ϕ^4 theory (4.33), a $\mathbb{Z}_2$ monodromy defect is obtained by the boundary condition

$$\phi(r, \theta + 2\pi, \vec{y}) = -\phi(r, \theta, \vec{y}) \,. \tag{6.12}$$

The coordinate $\vec{y} \in \mathbb{R}^{d-2}$ parametrizes the $p = d-2$ dimensional worldvolume of the defect, while the polar coordinates (r, θ) parametrize the plane orthogonal to it. The boundary condition (6.12) is consistent because the $\mathbb{Z}_2$ symmetry of the bulk maps $\phi \to -\phi$. Due to the topological nature of (6.12), we expect this monodromy defect to flow to a conformal defect in the IR. The $3d$ Ising $\mathbb{Z}_2$ monodromy defect has been studied using Monte-Carlo, ε–expansion and numerical bootstrap [4, 255–258].

6.2 Kinematics

The defining property of conformal defects is the symmetry (6.4) they preserve. This symmetry constrains conformal defects in two ways, 1) fixing the form of correlation functions and 2) with operator expansions and crossing symmetry. In this section we explore the first idea, while the second is considered in section 6.3. Because our only assumption is the symmetry-breaking pattern (6.4), our discussion applies to any conformal defect, either of the order or disorder type.

6.2.1 Obtaining the Ward identities

Correlation functions in the presence of a defect satisfy a set of partial differential equations that we now derive. To account for the defect, we shall insert a non-local operator $\mathcal{D}$ in

correlation functions $\langle \mathcal{D}\mathcal{O}_1 \ldots \widehat{\mathcal{O}}_n \rangle$, and then average $\langle \cdot \rangle$ using the CFT of interest. It is natural to use the normalization

$$\langle\!\langle \mathcal{O}_1 \ldots \widehat{\mathcal{O}}_n \rangle\!\rangle \equiv \frac{\langle \mathcal{D}\mathcal{O}_1 \ldots \widehat{\mathcal{O}}_n \rangle}{\langle \mathcal{D} \rangle} \,, \tag{6.13}$$

so that the identity operator has unit one-point function $\langle\!\langle \mathbb{1} \rangle\!\rangle = 1$.

To derive the constraints of conformal symmetry, we work in the operator formalism. In this formalism, correlation functions are vacuum expectation values, the preserved generators (6.3) commute with the defect $[\widehat{L}, \mathcal{D}] = 0$, and the preserved generators kill the vacuum $\widehat{L}|0\rangle = 0$. These three properties lead to the defect Ward identities

$$0 = \frac{\langle 0|[\widehat{L}, \mathcal{D}\mathcal{O}_1(x_1) \ldots \widehat{\mathcal{O}}_n(x_n)]|0\rangle}{\langle 0|\mathcal{D}|0\rangle} = \sum_{i=1}^{n} \widehat{\mathcal{L}}^{(i)} \langle\!\langle \mathcal{O}_1(x_1) \ldots \widehat{\mathcal{O}}_n(x_n) \rangle\!\rangle \,. \tag{6.14}$$

The differential operators $\widehat{\mathcal{L}}^{(i)}$ act at point x_i and are presented in (2.21)-(2.24). There is one difference between (6.14) and the conformal Ward identities (2.29): here only the preserved generators (6.3) can be used.

6.2.2 Solving the Ward identities

The defect Ward identities (6.14) admit elegant solutions in several simple configurations. First, we consider correlation functions involving only defect operators. Remember that defect operators are labeled by a scaling dimension $\widehat{\Delta}$ and spins j, s under parallel and transverse rotations respectively. For simplicity, we use index-free notation for the defect indices:

$$\widehat{\mathcal{O}}(x,w,z) \equiv \widehat{\mathcal{O}}(x)^{i_1 \ldots i_s}_{a_1 \ldots a_j} w_{i_1} \ldots w_{i_s} z^{a_1} \ldots z^{a_j} \,, \qquad w_i w_i = z_a z_a = 0 \,. \tag{6.15}$$

Although we do not use it here, the Todorov operator (2.28) can free the indices starting from the polynomials in w, z. With these definitions, the two-point function of defect operators reads

$$\langle\!\langle \widehat{\mathcal{O}}_1(x_1, w_1, z_1) \widehat{\mathcal{O}}_2(x_2, w_2, z_2) \rangle\!\rangle = \delta_{\widehat{\mathcal{O}}_1, \widehat{\mathcal{O}}_2} \frac{(w_1^i w_2^i)^s}{|x_{12}^a|^{2\widehat{\Delta}}} \left(z_1^a z_2^a - \frac{2z_1^a x_{12}^a z_2^b x_{12}^b}{|x_{12}^a|^2} \right)^j \,. \tag{6.16}$$

As in section 2.2.2, we have redefined defect operators to make their two-point functions orthonormal. After this redefinition, the three-point functions are uniquely determined

and their normalization $\widehat{\lambda}_{ijk}$ contains dynamical information. For example, the three-point function of parallel scalars reads

$$\langle\!\langle \widehat{\mathcal{O}}_1(x_1, w_1)\widehat{\mathcal{O}}_2(x_2, w_2)\widehat{\mathcal{O}}_3(x_3, w_3)\rangle\!\rangle = \widehat{\lambda}_{123}\frac{(w_1 \cdot w_2)^{s_{123}}(w_1 \cdot w_3)^{s_{312}}(w_2 \cdot w_3)^{s_{231}}}{|x_{12}^a|^{\Delta_{123}}|x_{13}^a|^{\Delta_{312}}|x_{23}^a|^{\Delta_{231}}} \ . \quad (6.17)$$

We have introduced $\Delta_{ijk} = \Delta_i + \Delta_j - \Delta_k$ and similarly for s_{ijk}. Higher-point functions on the defect behave similarly to the bulk discussion in section 2.2.2. The only difference is that here one has to keep track of $SO(q)$ indices, which behave as flavor symmetry indices.

We can also consider correlation functions involving bulk fields. The simplest example is the one-point function of a spin-ℓ bulk operator:

$$\langle\!\langle \mathcal{O}(x, \eta)\rangle\!\rangle = \frac{a_{\mathcal{O}}}{|x^i|^{\Delta}}\left(\frac{(\eta_i x_i)^2}{|x^i|^2} - \eta_i\eta_i\right)^{\ell/2} \ . \quad (6.18)$$

Remember that bulk operators are normalized according to (2.30), so the constant $a_{\mathcal{O}}$ contains dynamical information. Another correlation function fixed by conformal symmetry is the bulk-defect two-point function. For the simpler case of a bulk scalar, conformal symmetry fixes the result

$$\langle\!\langle \mathcal{O}(x_1)\widehat{\mathcal{O}}(x_2, w)\rangle\!\rangle = b_{\mathcal{O}\widehat{\mathcal{O}}}\frac{(x_1^i w_i)^s}{(|x_1^i|^2 + |x_{12}^a|^2)^{\widehat{\Delta}}|x_1^i|^{\Delta - \widehat{\Delta} + s}} \ . \quad (6.19)$$

As before, since both $\mathcal{O}$ and $\widehat{\mathcal{O}}$ have canonical normalization, the coefficient $b_{\mathcal{O}\widehat{\mathcal{O}}}$ captures dynamical information about the theory. In fact equation (6.18) is a particular case of equation (6.19) when $\widehat{\mathcal{O}} = \widehat{\mathbb{1}}$, or equivalently $a_{\mathcal{O}} = b_{\mathcal{O}\widehat{\mathbb{1}}}$.

Although it is interesting to consider more general correlation functions, the ones above are the most relevant for practical applications. As in the case without defects, the most efficient method to obtain other correlation functions is the embedding space formalism [259]. However, for the sake of clarity, we shall not present it here.

6.3   The defect bootstrap program

In the previous section, we showed that correlation functions with low number of operators are kinematically fixed. Instead, higher-point correlation functions depend on conformal cross ratios and can be expanded using operator expansions. In this section, we show that associativity of these expansions leads to consistency conditions called crossing equations.

The defect bootstrap program is the study of solutions to the crossing equations, or equivalently, the study of consistent conformal defects. In this section we discuss the defect bootstrap program in full generality, while in section 6.4 we focus on the crossing equation for bulk two-point functions.

6.3.1 Operator expansions

Three operator expansions exist in defect CFT: the bulk-bulk, defect-defect and bulk-defect expansions. Operator expansions are useful because they allow the calculation of higher-point functions as infinite sums of lower-point functions. Furthermore, associativity of different operator expansions leads to the crossing equations.

The bulk-bulk operator product expansion has been described in detail in section 2.2.3. Because the bulk-bulk OPE is valid when two operators approach, and because in this limit the defect is negligible, the bulk-bulk OPE can be used unchanged in the presence of defects. For ease of reference, we repeat here the bulk-bulk OPE for scalar operators:

$$\mathcal{O}_1(x_1)\mathcal{O}_2(x_2) = \sum_k \lambda_{12k} f_{12k}^{\mu_1\dots\mu_\ell}(x_{12}, \partial_{x_2})\mathcal{O}_k^{\mu_1\dots\mu_\ell}(x_2) \quad \text{as} \quad x_1 \to x_2\,. \tag{6.20}$$

The differential operator f_{12k} captures the contributions of conformal descendants, such that the infinite sum runs only over conformal primaries. Figure 6.1a) shows a pictorial representation of the bulk-bulk OPE.

Similarly, the defect-defect OPE expands the product of two defect operators as an infinite sum of defect operators. The simplest example is the expansion of defect scalars, that reads

$$\widehat{\mathcal{O}}_1(x_1^a)\widehat{\mathcal{O}}_2(x_2^a) = \sum_k \widehat{\lambda}_{12k} \widehat{f}_{12k}^{a_1\dots a_j}(x_{12}^a, \partial_{x_2}^a)\widehat{\mathcal{O}}_k^{a_1\dots a_j}(x_2^a) \quad \text{as} \quad x_1^a \to x_2^a\,. \tag{6.21}$$

This OPE, shown pictorially in figure 6.1a), is analogous to the bulk-bulk OPE, with the difference that operators are restricted to live on the defect.

Finally, the bulk-defect expansion approximates a bulk operator as an infinite sum of defect operators. The physical meaning of the bulk-defect expansion is that operators sufficiently close to the defect are indistinguishable from excitations localized on the defect. For a scalar operator, the bulk-defect expansion reads

$$\mathcal{O}(x) = \sum_{\widehat{\mathcal{O}}} b_{\mathcal{O}\widehat{\mathcal{O}}} \mathcal{C}_{\widehat{\mathcal{O}}}^{i_1\dots i_s}(x^i, \partial_a)\widehat{\mathcal{O}}^{i_1\dots i_s}(x^a) \quad \text{as} \quad x^i \to 0\,. \tag{6.22}$$
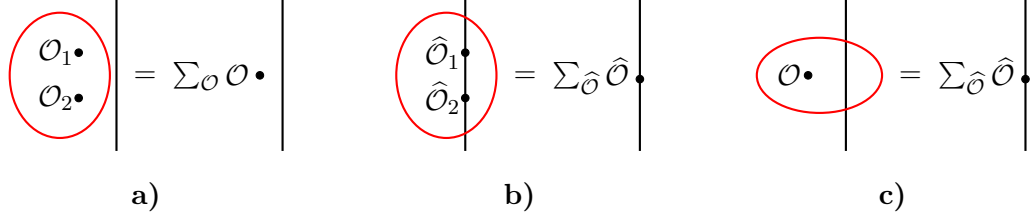
Figure 6.1: The three operator expansions in defect CFT: bulk-bulk, defect-defect and bulk-defect. The straight line represents a p-dimensional defect.

As before, the differential operator $\mathcal{C}_{\widehat{\mathcal{O}}}$ captures contributions of conformal descendants in the defect multiplet. To obtain the precise form of $\mathcal{C}_{\widehat{\mathcal{O}}}$, one inserts the bulk-defect expansion in (6.19), and compares terms order by order as $x^i \to 0$. The final result takes a simple form

$$\mathcal{C}_{\widehat{\mathcal{O}}}^{i_1 \dots i_s}(x^i, \partial_a) = \frac{x^{i_1} \dots x^{i_s}}{|x^i|^{\Delta - \widehat{\Delta} + s}} \sum_{m=0}^{\infty} \frac{(-4)^{-m}}{m!(\widehat{\Delta} + 1 - p/2)_m} \left(|x^i|^2 \partial_a^2\right)^m . \tag{6.23}$$

The bulk-defect expansion is shown in figure 6.1c).

6.3.2   Crossing equations

Repeatedly using operator expansions, one can compute any correlation function of interest. However, for the theory to be consistent, different ways to expand correlators must produce equal results, or in other words, the operator expansions must be associative.

The example of four-point functions was discussed in section 2.3.3. There, we saw that associativity of the OPE requires that four-point functions should satisfy the crossing equations (2.46). In defect CFT, four-point functions of bulk operators and four-point functions of defect operators should both be crossing symmetric:

$$\langle \mathcal{O}_i \mathcal{O}_j \mathcal{O}_k \mathcal{O}_l \rangle : \quad \sum_{\mathcal{O}} \lambda_{ij\mathcal{O}} \lambda_{kl\mathcal{O}} \, g_{\mathcal{O}}^{ijkl} = \sum_{\mathcal{O}} \lambda_{kj\mathcal{O}} \lambda_{il\mathcal{O}} \, g_{\mathcal{O}}^{kjil} , \tag{6.24}$$

$$\langle\!\langle \widehat{\mathcal{O}}_i \widehat{\mathcal{O}}_j \widehat{\mathcal{O}}_k \widehat{\mathcal{O}}_l \rangle\!\rangle : \quad \sum_{\widehat{\mathcal{O}}} \widehat{\lambda}_{ij\widehat{\mathcal{O}}} \widehat{\lambda}_{kl\widehat{\mathcal{O}}} \, \widehat{g}_{\widehat{\mathcal{O}}}^{ijkl} = \sum_{\widehat{\mathcal{O}}} \widehat{\lambda}_{kj\widehat{\mathcal{O}}} \widehat{\lambda}_{il\widehat{\mathcal{O}}} \, \widehat{g}_{\widehat{\mathcal{O}}}^{kjil} . \tag{6.25}$$

To make the notation more transparent, we have absorbed kinematical factors in the conformal blocks $g_{\mathcal{O}}^{ijkl}$ and $\widehat{g}_{\widehat{\mathcal{O}}}^{ijkl}$.

However, in defect CFT these two crossing equations are not sufficient to guarantee crossing symmetry. Indeed, the requirement that the defect couples consistently to the

bulk implies a third crossing equation. To derive this crossing equation, notice there are two ways to expand the three-point function $\langle\!\langle \mathcal{O}_i \mathcal{O}_j \widehat{\mathcal{O}}_k \rangle\!\rangle$. One option is to use a bulk-bulk OPE for $\mathcal{O}_i \mathcal{O}_j \sim \sum \mathcal{O}$ and then sum over two-point functions $\langle\!\langle \mathcal{O}\widehat{\mathcal{O}}_k \rangle\!\rangle$. Another option is to use bulk-defect expansions for $\mathcal{O}_i \sim \sum \widehat{\mathcal{O}}$ and $\mathcal{O}_j \sim \sum \widehat{\mathcal{O}}'$, and then sum over three-point functions $\langle\!\langle \widehat{\mathcal{O}}\widehat{\mathcal{O}}'\widehat{\mathcal{O}}_k \rangle\!\rangle$. The equality of the two expansions gives the crossing equation

$$\langle\!\langle \mathcal{O}_i \mathcal{O}_j \widehat{\mathcal{O}}_k \rangle\!\rangle : \quad \sum_{\mathcal{O}} \lambda_{ij\mathcal{O}} b_{\mathcal{O}k}\, h_{\mathcal{O}}^{ijk} = \sum_{\widehat{\mathcal{O}},\widehat{\mathcal{O}}'} b_{i\widehat{\mathcal{O}}} b_{j\widehat{\mathcal{O}}'} \widehat{\lambda}_{\widehat{\mathcal{O}}\widehat{\mathcal{O}}'k}\, \widehat{h}_{\widehat{\mathcal{O}},\widehat{\mathcal{O}}'}^{ijk}\,. \tag{6.26}$$

Here $h_{\mathcal{O}}^{ijk}$ and $\widehat{h}_{\widehat{\mathcal{O}},\widehat{\mathcal{O}}'}^{ijk}$ are conformal blocks, although different from the ones appearing in four-point functions. Graphically, the crossing equation is
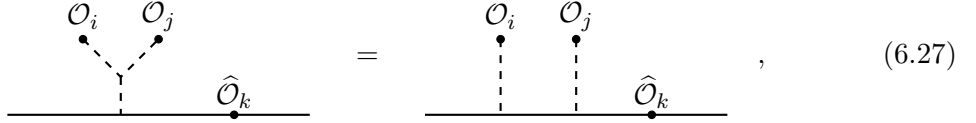
where the solid line represents the defect and the dashed lines represent operator expansions. The crossing symmetry conditions (6.24)-(6.26) are sufficient to make any higher-point correlation function crossing symmetric, as can be seen graphically using (1.1) and (6.27).

The crossing equation (6.26) can be cumbersome to work with. Therefore, most studies so far have focused on the particular case $\widehat{\mathcal{O}}_k = \widehat{\mathbb{1}}$, because then the double sum in (6.26) truncates to a single sum

$$\langle\!\langle \mathcal{O}_i \mathcal{O}_j \rangle\!\rangle : \quad \sum_{\mathcal{O}} \lambda_{ij\mathcal{O}} a_{\mathcal{O}}\, f_{\mathcal{O}}^{ij} = \sum_{\widehat{\mathcal{O}}} b_{i\widehat{\mathcal{O}}} b_{j\widehat{\mathcal{O}}}\, \widehat{f}_{\widehat{\mathcal{O}}}^{ij}\,. \tag{6.28}$$

The crossing equation (6.28) is significantly easier to use than (6.26). The goal of section 6.4 is to study this equation in detail.

6.3.3   Defect bootstrap program

After this general introduction, we are ready to state the goals of the defect bootstrap program. In its most ambitious form, the defect bootstrap program wants to answer the question: Given a bulk CFT, what is the space of consistent conformal defects?

To make the question more precise, we start with a CFT that lives in the bulk. The bulk CFT is consistent by itself, meaning that the CFT data

$$\text{Bulk:}\quad \{\Delta_i, \lambda_{ijk}\}\,, \tag{6.29}$$

satisfies the crossing symmetry equations (6.24). Then one would like to find all possible defects

$$\text{Defect:} \quad \{\widehat{\Delta}_i, \widehat{\lambda}_{ijk}, a_i, b_{ij}\}, \tag{6.30}$$

that solve the crossing equations (6.25) and (6.26).

In its most most ambitious form, the defect bootstrap program is typically too hard to address. Instead, one often focuses on a particular defect in a theory of interest, and then one studies a small number of crossing equations. For example, much work has been devoted to one-dimensional CFTs, which can be interpreted as line defects embedded in a higher-dimensional bulk, see [2, 233, 256, 260–262] for examples using bootstrap methods. In that case, one focuses on simple operators and tries to solve the four-point crossing equation (6.25). Since the techniques to do so are similar to the ones in chapters 2-5, we do not explore this direction further. Instead, we are going to focus on the crossing equation for two-point functions, which is qualitatively different from its four-point counterpart.

6.4   Bulk two-point function

In the defect bootstrap program, one studies conformal defects by solving the crossing equations (6.24)-(6.28). Because in chapters 2-5 we have presented methods to study the four-point crossing equations, here we focus instead on the two-point crossing equation (6.28). Although the lack of positivity in the bulk-channel makes numerical methods hard to use, the analytic machinery of chapter 4 can be adapted to the defect context, as we explain below.

As it stands, the crossing equation (6.28) is written schematically. Thus, we start this section reviewing the kinematics of two-point functions, and providing methods to approximate conformal blocks. After these preliminaries, we turn to the Lorentzian inversion formula, which is our main tool to solve crossing equations analytically. We conclude outlining how to apply the Lorentzian inversion formula for conformal defects in the ε–expansion and in holographic CFTs. The discussion so far applied to general defects, but from here on we restrict to codimension $q \geq 2$. The reason is that for codimension-one boundaries there are no transverse rotations and there is only one independent cross ratio, which prevents one from using the Lorentzian inversion formula. Instead, one can use the analytic methods discussed in chapter 9.

6.4.1 Kinematics

Let us start reviewing the kinematics of a two-point function of bulk operators in the presence of a defect. For simplicity we consider equal scalar operators $\phi(x)$, in which case the two-point function reads

$$\langle\!\langle \phi(x_1)\phi(x_2) \rangle\!\rangle = \frac{\mathcal{F}(z,\bar{z})}{|x_1^i|^{\Delta_\phi}|x_2^i|^{\Delta_\phi}}\,. \tag{6.31}$$

This correlator is significantly different than the standard two-point function in the absence of a defect (2.30). The reason is that with defects only the generators (6.3) are preserved, so the two-point function is no longer kinematically fixed.

The two cross ratios z, $\bar{z}$ are analogs to the four-point cross ratios (2.34), sharing with them a similar geometric interpretation. In a generic frame, the cross rations are determined from

$$\frac{1+z\bar{z}}{(z\bar{z})^{1/2}} = \frac{|x_{12}^a|^2 + |x_1^i|^2 + |x_2^i|^2}{|x_1^i||x_2^i|}\,, \qquad \frac{z+\bar{z}}{2(z\bar{z})^{1/2}} = \frac{x_1^i x_2^i}{|x_1^i||x_2^i|}\,. \tag{6.32}$$

Via conformal transformations, there exists a frame where the two operators are located on a plane orthogonal to the defect, the first sitting at $x_1 = (\tau, x)$ and the second sitting at $x_2 = (0,1)$. Then elementary algebra gives

$$z = x + i\tau\,, \qquad \bar{z} = x - i\tau\,, \tag{6.33}$$

so $z, \bar{z}$ are complex conjugate coordinates in a plane orthogonal to the defect. Alternatively, if we worked in Lorentzian signature, $z, \bar{z}$ would be real and independent. The Lorentzian regime will be useful when we consider the analytic bootstrap approach to defects.

6.4.2 Conformal blocks

The two-point function (6.31) admits expansions using the bulk-defect and the bulk-bulk OPE. Since these two expansions are completely different, the corresponding conformal blocks must be treated separately.

On the one hand, the bulk-defect expansion (6.22) leads to the defect-channel conformal block expansion:

$$\mathcal{F}(z,\bar{z}) = \sum_{\widehat{\mathcal{O}}} \frac{1}{2^s} b_{\phi\widehat{\mathcal{O}}}^2 \hat{f}_{\widehat{\Delta},s}(z,\bar{z})\,. \tag{6.34}$$

74

The bulk-defect OPE coefficient $b_{\phi\widehat{\mathcal{O}}}$ is defined in (6.19), and the factor 2^{-s} conforms with our normalization conventions. The defect-channel conformal block $\hat{f}_{\widehat{\Delta},s}$ captures contributions of defect conformal primaries and all of their descendants. To obtain the defect-channel blocks, it is possible to solve a Casimir equation in closed form [259]:

$$\hat{f}_{\widehat{\Delta},s}(z,\bar{z}) = z^{\frac{\widehat{\Delta}-s}{2}}\bar{z}^{\frac{\widehat{\Delta}+s}{2}}\, {}_2F_1\left(\widehat{\Delta},\frac{p}{2},\widehat{\Delta}+1-\frac{p}{2},z\bar{z}\right) {}_2F_1\left(-s,\frac{q}{2}-1,2-\frac{q}{2}-s,\frac{z}{\bar{z}}\right). \quad (6.35)$$

As a reminder, p is the dimension of the defect while q is its codimension.

On the other hand, the bulk-bulk OPE (6.20) leads to the bulk-channel conformal block expansion:

$$\mathcal{F}(z,\bar{z}) = \left(\frac{\sqrt{z\bar{z}}}{(1-z)(1-\bar{z})}\right)^{\Delta_\phi}\sum_{\mathcal{O}}\frac{1}{2^\ell}\lambda_{\phi\phi\mathcal{O}}a_{\mathcal{O}}f_{\Delta,\ell}(z,\bar{z}). \quad (6.36)$$

It is conventional to strip off the prefactor $\left(\frac{\sqrt{z\bar{z}}}{(1-z)(1-\bar{z})}\right)^{\Delta_\phi}$ to make the bulk-channel conformal blocks $f_{\Delta,\ell}$ independent of Δ_ϕ. Unlike the defect-channel blocks, in general no closed-form expression is known for bulk-channel blocks, but there exist instead series representations [259, 263–265]. These series representations follow from the Casimir equation that bulk-channel blocks satisfy [259]:

$$\left[(1-z)^2\left(z\partial_z^2+\partial_z\right)\right.$$
$$\left.-\frac{z(1-z)(1-\bar{z})}{z-\bar{z}}\left(p\frac{(1-z)(1+\bar{z})}{1-z\bar{z}}-(d-2)\right)\partial_z+(z\leftrightarrow\bar{z})\right]f_{\Delta,\ell} = \frac{c_2}{2}f_{\Delta,\ell}. \quad (6.37)$$

In order to solve this equation unambiguously, it must be supplemented by the boundary condition

$$f_{\Delta,\ell}(z,\bar{z}) \sim (1-z)^{(\Delta-\ell)/2}(1-\bar{z})^{(\Delta+\ell)/2} \quad \text{as} \quad 0 < 1-z \ll 1-\bar{z} \ll 1. \quad (6.38)$$

As an application of the Casimir equation, one can make the ansatz (4.5) replacing $z,\bar{z}\to 1-z,1-\bar{z}$, and solve for the coefficients recursively. This gives a convenient series representation for the bulk-channel conformal blocks around $z=1$.

Summarizing, the two-point function of scalars in the presence of a conformal defect admit bulk- and defect-channel expansions. The equality of the two expansions is called a crossing equation

$$\mathcal{F}(z,\bar{z}) = \left(\frac{\sqrt{z\bar{z}}}{(1-z)(1-\bar{z})}\right)^{\Delta_\phi}\sum_{\mathcal{O}}c_{\mathcal{O}}f_{\Delta,\ell}(z,\bar{z}) = \sum_{\widehat{\mathcal{O}}}\mu_{\widehat{\mathcal{O}}}\hat{f}_{\widehat{\Delta},s}(z,\bar{z}). \quad (6.39)$$

For convenience, here and in later chapters we use shorthand notations $c_{\mathcal{O}} \equiv 2^{-\ell}\lambda_{\phi\phi\mathcal{O}}a_{\mathcal{O}}$ and $\mu_{\widehat{\mathcal{O}}} = 2^{-s}b^2_{\phi\widehat{\mathcal{O}}}$. The two sides of the crossing equation (6.39) contain different types of CFT data, which naively suggests that the crossing equation is not very constraining. This turns out to be false in perturbative settings, where the Lorentzian inversion formula puts strong constraints on the allowed conformal defects for a given bulk. Although explicit examples are lacking, we believe crossing to be constraining also in non-perturbative theories.

6.4.3 Lorentzian inversion formula

The final topic of this chapter is the Lorentzian inversion formula. In defect CFT there are two inversion formulas, the bulk-defect formula [266] that we discuss here, and the defect-bulk formula [265] that does not play such a central role in the thesis. The bulk-defect Lorentzian inversion formula allows to efficiently solve the crossing equation (6.39) for perturbative CFTs. Here we discuss the formula, while the applications are considered in section 6.4.4.

Similarly to the four-point inversion formula (4.21), the bulk-defect inversion formula reconstructs the CFT data of defect operators using the singularities of the correlator. The derivation proceeds analogously to the four-point case in section 4.2, leading to [266]

$$\mu(\hat{\Delta}, s) = \int_0^1 \frac{dz}{2z} z^{-(\hat{\Delta}-s)/2} \int_1^{1/z} \frac{d\bar{z}}{2\pi i}(1-z\bar{z})(\bar{z}-z)\bar{z}^{-(\hat{\Delta}+s+4)/2}$$
$$\times \,_2F_1\left(s+1, 2-\frac{q}{2}, s+\frac{q}{2}; \frac{z}{\bar{z}}\right) \,_2F_1\left(1-\hat{\Delta}, 1-\frac{p}{2}, 1+\frac{p}{2}-\hat{\Delta}, z\bar{z}\right) \operatorname{Disc}\mathcal{F}(z,\bar{z}),$$
$$(6.40)$$

The first ingredient in the formula is the discontinuity of the correlator, which is computed around the branch cut $\bar{z} \in [1, \infty)$:

$$\operatorname{Disc}\mathcal{F}(z,\bar{z}) = \mathcal{F}(z, \bar{z}+i0) - \mathcal{F}(z, \bar{z}-i0), \qquad \bar{z} \geq 1\,. \qquad (6.41)$$

Differently from the four-point inversion formula, here the singularities of the correlator are captured by a single instead of a double discontinuity. The second ingredient in the inversion formula is the function $\mu(\hat{\Delta}, s)$, which contains the dimensions of defect operators as poles, and their OPE coefficients as residues:

$$\mu(\hat{\Delta}, s) = -\sum_{\widehat{\mathcal{O}}} \frac{\mu_{\mathcal{O}}}{\hat{\Delta} - \hat{\Delta}_{\widehat{\mathcal{O}}}}\,. \qquad (6.42)$$

Since (6.40) is analytic in transverse spin s, the CFT data in defect CFT is also analytic. Finally, notice that the inversion kernel in (6.40) is roughly a defect block with shifted arguments multiplied by suitable powers of $z, \bar{z}$.

6.4.4   Perturbative CFTs

This chapter concludes with two applications of the Lorentzian inversion formula to perturbative CFTs: conformal defects in the ε–expansion and holographic defects. The reason these setups can be bootstrapped is that the discontinuity of their correlators is very simple. Then, by means of the inversion formula, the full correlator can be reconstructed.

The first step is therefore to compute the discontinuity of a generic correlator. From equation (6.41), we observe that the discontinuity is computed around a cut starting $\bar{z} = 1$. Because bulk blocks have a natural expansion in powers of $(1 - \bar{z})$, it is then natural to compute the discontinuity expanding in the bulk channel. A calculations similar to (4.24) shows that the contribution of a single bulk-channel conformal block to the discontinuity reads

$$
\text{Disc} \left(\frac{\sqrt{z\bar{z}}}{(1 - z)(1 - \bar{z})} \right)^{\Delta_\phi} f_{\Delta, \ell}(z, \bar{z})
$$
$$
= -2i \sin \left(\frac{\Delta - 2\Delta_\phi - \ell}{2} \pi \right) (z\bar{z})^{\frac{\Delta_\phi}{2}} \left[(1 - z)(\bar{z} - 1) \right]^{\Delta_\phi - \frac{\Delta - \ell}{2}} \tilde{f}_{\Delta, \ell}(z, \bar{z}). \qquad (6.43)
$$

As in (4.25), we define $\tilde{f}_{\Delta, \ell}(z, \bar{z})$ to be a conformal block with a prefactor $[(1-z)(1-\bar{z})]^{\frac{\Delta - \ell}{2}}$ striped off. The sine in (6.43) suppresses operators near the multi-twist dimension $\Delta_{\mathcal{O}} = 2\Delta_\phi + \ell + 2n + \gamma$. Indeed, multi-twist operators contribute like $\text{Disc} \sim \gamma$, and in particular the discontinuity kills exact multi-twist operators. An important difference with the four-point function is that, in that case, multi-twist operators are more suppressed $\text{dDisc} \sim \gamma^2$.

It is possible to use this information to our advantage to bootstrap conformal defects. For example, the ε–expansion discussion of section 4.3.3 shows that most operators receive anomalous dimensions starting at order $O(\varepsilon^2)$. As a result, any conformal defect in the Wilson-Fisher fixed point has a discontinuity of the form

$$
\text{Disc} \, \mathcal{F} \big|_{O(\varepsilon)} \sim \text{Disc} \left(1 + c_{\phi^2} f_{\Delta_{\phi^2}, 0} \right). \qquad (6.44)
$$

Another regime where dramatic simplifications occur is planar $\mathcal{N} = 4$ SYM at strong coupling. In this case, most operators in the spectrum have exact multi-twist dimension,

so the discontinuity kills them. For example, in the two-point function of **20′** multiplets, only the **20′** itself contributes to the discontinuity:

$$\text{Disc}\,\mathcal{F}\big|_{\text{strong coupling}} \sim \text{Disc}\left(1 + c_{\mathcal{O}_{\mathbf{20'}}} F_{\mathcal{O}_{\mathbf{20'}}}\right). \tag{6.45}$$

Because of supersymmetry, $F_{\mathcal{O}_{\mathbf{20'}}}$ is a superconformal block similar to the ones presented in section 5.4.

In order to complete the bootstrap, one uses the inversion formula (6.40) to extract $\mu(\widehat{\Delta}, s)$, or equivalently, the defect CFT data. This defect CFT data can be used to resum the full correlator at the order we are interested in

$$\mathcal{F}(z, \bar{z}) \sim \sum_{\widehat{\mathcal{O}}} \left(\delta\mu_{\mathcal{O}}\hat{f}_{\widehat{\Delta},s} + \mu_{\mathcal{O}}\gamma_{\mathcal{O}}\partial_{\widehat{\Delta}}\hat{f}_{\widehat{\Delta},s}\right). \tag{6.46}$$

Finally, from the full correlator we can expand in the bulk channel, to extract information about many operators that did not originally contribute to the discontinuity. In the ε–expansion example, one finds

$$\mathcal{F}(z, \bar{z}) \propto 1 + c_{\phi^2}f_{\Delta_{\phi^2},0} + \sum_{\ell=2}^{\infty} c_{0,\ell}f_{2\Delta_\phi+\ell,\ell} + \sum_{\ell=0}^{\infty} c_{1,\ell}f_{2\Delta_\phi+\ell+2,\ell}. \tag{6.47}$$

The two families of operators take the schematic form $\phi\partial_{\mu_1}\ldots\partial_{\mu_\ell}\Box^n\phi$ for $n = 0, 1$. Note that we started only with the identity and ϕ^2, and from them we reconstructed two infinite families of operators. This example demonstrates the power of the Lorentzian inversion formula.

There are two subtleties we have not touched in the above discussion. The first subtlety is that the bootstrap cannot fix the parameters c_{ϕ^2} and $c_{\mathcal{O}_{\mathbf{20'}}}$ in (6.44) and (6.45). Thus, one should think of the above results as one-parameter families of solutions to crossing. Alternatively, one should fix the free parameters by other means, such as perturbative calculations or supersymmetric localization. The second subtlety is that the Lorentzian inversion formula can miss low-spin contributions. It is then necessary to add truncated solutions to crossing involving only low spins, which lead to further free parameters that one must fix by other means.

6.5   Review of the literature

The kinematics of conformal defects was originally studied for boundaries [267–269] and later generalized to more general defects and spinning operators [259, 263, 264, 270, 271].

Boundary CFT has been studied with analytic bootstrap [3, 269, 272–275], using Gliotzzi's method [45, 46, 252], with numerical bootstrap [252, 269], diagrammatic perturbation theory [3, 276–281], and using the large charge limit [282]. For higher codimension, many works have focused on line defects [253, 283, 284], specially in relation to Wilson lines in $\mathcal{N} = 4$ SYM [5, 233, 262, 285–289], although not exclusively [2, 4, 260, 261, 290–293]. Finally, a promising idea is the study of defects in free bulk theories [294–296]. There are geometries with similar properties as conformal defects, such two intersecting boundaries [297], CFT at finite temperature [298, 299], and CFT in projective space [300–304].

Part II

Applications

Chapter 7

Bootstrapping Coulomb and Higgs branch operators

Abstract

We apply the numerical conformal bootstrap to correlators of Coulomb and Higgs branch operators in $4d$ $\mathcal{N} = 2$ superconformal theories. We start by revisiting previous results on single correlators of Coulomb branch operators. In particular, we present improved bounds on OPE coefficients for some selected Argyres-Douglas models, and compare them to recent work where the same cofficients were obtained in the limit of large r charge. There is solid agreement between all the approaches. The improved bounds can be used to extract an approximate spectrum of the Argyres-Douglas models, which can then be used as a guide in order to corner these theories to numerical islands in the space of conformal dimensions. When there is a flavor symmetry present, we complement the analysis by including mixed correlators of Coulomb branch operators and the moment map, a Higgs branch operator which sits in the same multiplet as the flavor current. After calculating the relevant superconformal blocks we apply the numerical machinery to the mixed system. We put general constraints on CFT data appearing in the new channels, with particular emphasis on the simplest Argyres-Douglas model with non-trivial flavor symmetry.

7.1 Introduction

Four-dimensional $\mathcal{N} = 2$ superconformal theories are interesting models that despite a significant amount of symmetry, show highly non-trivial dynamics and constitute a vast landscape of theories. In this work, we use modern conformal bootstrap techniques to study a canonical set of correlators that involve *Coulomb* and *Higgs* branch operators. These are operators that sit in short multiplets of the superconformal algebra and whose vevs parameterize the moduli space vacua.

Both Coulomb and Higgs branches are a common feature of $\mathcal{N} = 2$ theories and have been used as a starting point for the ambitious program of classifying $\mathcal{N} = 2$ SCFTs. Coulomb branch geometries are characterized by their complex dimension, known as the rank, and a classification of all possible rank-one scale-invariant geometries was recently proposed in a series of papers [305–308] (for a review of later developments see [309]). The Higgs branch is also a useful organizing principle, specially when taking into account its close connection to the VOAs associated to $4d$ $\mathcal{N} = 2$ SCFTs [246]. It was conjectured in [310] that one can recover the Higgs branch by looking at the associated variety of the corresponding VOA. This observation lead to an elegant description of several VOAs in terms of free field realizations [311–313], and constitutes a first step towards a classification of VOAs associated to $4d$ $\mathcal{N} = 2$ theories.

Progress in understanding $\mathcal{N} = 2$ dynamics usually involves quantities protected by supersymmetry, and access to non-protected data is still a challenge. In this work, we will study correlators of Coulomb and Higgs branch operators using the numerical bootstrap of [17]. Even though the external operators in our analysis are protected objects, they still capture an infinite amount of non-protected data in their correlators. Our results will be naturally split into two parts: the single-correlator and the mixed-correlator bootstrap.

The single correlator bootstrap for each type of operator has already appeared in the literature [198,216,217]. Here we refine the Coulomb branch results motivated in part by the works [314, 315], where OPE coefficients of Coulomb branch operators for certain Argyres-Douglas models were calculated in the large r-charge limit. The same OPE coefficients can be estimated by obtaining upper and lower bounds using the numerical bootstrap, and our improved results show solid agreement between the two approaches.

The improved OPE-coefficient bounds also give a better idea of the non-protected spectrum of these models. This is because numerical exclusion curves correspond to solutions to crossing with a spectrum that can be extracted from the zeros of the numerical func-

tional [66]. We can then use the approximate spectrum as a guide and corner models by assuming gaps in the single correlator bootstrap, similarly to what was done in [104].

Having exhausted the single correlator analysis, we move on to the mixed-correlator bootstrap and include Higgs branch operators, which will give us access to a new region of parameter space that cannot be accessed by looking at single correlators separately. The mixed correlator setup requires the calculation of new superconformal blocks that include Coulomb and Higgs branch operators. We solve this problem by demanding that different $\mathcal{N} = 1$ decompositions of the blocks are consistent, and contribute a new entry to the superblock catalog, a result interesting on its own right. With the mixed correlator at hand we explore the landscape of theories with $SU(2)$ flavor symmetry, and also attempt to corner an individual Argyres-Douglas model, whose symmetries are consistent with our setup.

The rest of this work is organized as follows. In section 7.2 we review the properties of the Coulomb and Higgs branch operators that will be the main focus of this work. We describe to which short representations of the superconformal algebra they belong, and introduce their OPE selection rules and superconformal blocks. We also summarize the most salient features of the landscape of known $\mathcal{N} = 2$ superconformal field theories. In section 7.3 we present the crossing relations obeyed by our correlation functions. Special care is required for the four-point function of moment-map operators, where one needs to take into account the chiral algebra construction of [246]. In section 7.4 we present the results obtained from applying numerical bootstrap techniques to the single and mixed correlators. We conclude in section 7.5 with a summary of our results and an overview of possible future directions. The derivation of the new superconformal blocks and the details of our numerical bootstrap setup are relegated to appendix 7.A and 7.B.

7.2   Preliminaries

We start with a preliminary review of the two basic operators that will be the main focus of this work. We will concentrate on two types of short multiplets of the superconformal algebra, whose correlators capture "canonical data" of the theory, in the sense that it is data common to most $\mathcal{N} = 2$ superconformal theories. In particular, we will study short operators whose vevs parameterize the Coulomb and Higgs branches of the moduli space of vacua.

7.2.1 Canonical data in $\mathcal{N} = 2$ SCFTs

Coulomb branch operators

We denote Coulomb branch operators by $\varphi_r(x)$ and $\bar{\varphi}_{-r}(x)$. These are superconformal primaries killed by supercharges of the same Lorentz chirality, and their conformal dimension is fixed by supersymmetry in terms of their corresponding r charges:

$$\left[\bar{Q}_{I\dot{\alpha}}, \, \varphi_r(0)\right] = 0, \quad \left[Q_\alpha^I, \, \bar{\varphi}_{-r}(0)\right] = 0 \qquad \Rightarrow \qquad \Delta_{\varphi_r} = \Delta_{\bar{\varphi}_{-r}} = \frac{1}{2}r. \tag{7.1}$$

In the notation of [182], which we will use throughout the paper, φ is the superprimary of a $L\bar{B}[0;0]^{(0;r)}$ multiplet.[1] In the literature, they are sometimes called chiral primary operators, and we will often refer to them simply as *chiral* or *antichiral* operators. They form a ring under the OPE, called the Coulomb branch chiral ring, and the number of generators in this ring defines the rank of the theory. Canonical data associated with this ring are the $U(1)_r$ charge values of the generators. In Lagrangian theories, the chiral ring generators are given by gauge invariant combinations $\operatorname{tr}\phi^n$ of the basic vector multiplet ϕ, and their r-charges are always integer-valued. In interacting Lagrangian models, each coupling constant will have an associated chiral operator $\operatorname{tr}\phi^2$ of dimension $\Delta = 2$, which is the superconformal primary of the multiplet that contains the exactly marginal deformation responsible for the corresponding direction in the conformal manifold.

Non-lagrangian examples include Argyres-Douglas models, in which the r-charges of the Coulomb branch generators can have fractional values, and it is therefore unlikely they will have a standard Lagrangian description. One advantage of the bootstrap approach followed here is that the value of r for chiral operators is a parameter in the crossing equations, and it can take any continuous value. This makes Argyres-Douglas models prime candidates for the conformal bootstrap.

Correlators involving chiral operators have been nevertheless studied by a variety of means, and some recent results in the literature will guide our analysis. One approach is the observation that certain chiral correlators satisfy exact differential equations known as the tt^* equations [316]. This lead to a series of exciting developments [317–320], which provide an algorithmic prescription to calculate OPE coefficient among operators in the chiral ring of Lagrangian $\mathcal{N} = 2$ theories. An alternative approach is provided by the study of these correlators in the limit of large r-charge [321–324]. Of particular relevance for us will be the works [314,315], from which one can extract OPE coefficients of Coulomb

---

[1]For readers familiar with the notation of [27] this corresponds to the $\mathcal{E}_{r/2}$ multiplet.

branch operators in rank-one Argyres-Douglas models. We will be able to compare these results with our bootstrap bounds in section 7.4, showing consistent results between the two approaches.

The moment map

Complementary to the Coulomb branch there is also canonical data associated to the Higgs branch. This branch of moduli space is parameterized by another type of short multiplets killed by a different combination of supercharges, whose highest weights also form a ring under the OPE. In this work we will only consider the so-called moment map operator $M^A_{(IJ)}(x)$, which is the superconformal primary of the $B\bar{B}[0;0]^{(2;0)}$ multiplet.[2] Unlike the previous case, this multiplet satisfies a shortening condition involving supercharges of both chiralities:

$$\left[\bar{Q}_{(I}, M^A_{JK)}(0)\right] = 0, \quad \left[Q_{(I}, M^A_{JK)}(0)\right] = 0 \qquad \Rightarrow \qquad \Delta_M = 2. \tag{7.2}$$

This operator is neutral under $U(1)_r$, and transforms as a triplet under $SU(2)_R$, which we represent with two symmetric fundamental indices $I, J = 1, 2$. What makes the moment map particularly important is that it belongs to the same multiplet as the flavor current j^A_μ, this means that both transform in the adjoint of the flavor group G_F, which we indicate with an adjoint index $A = 1, \ldots, \dim G_F$. It follows from this discussion that the moment map will be present whenever there is a global (flavor) symmetry. Flavor symmetries are ubiquitous in $\mathcal{N} = 2$ superconformal theories, and correlators of flavor currents capture canonical data associated to the Higgs branch. Relevant for us is the flavor central charge k which can be considered analogous to the most common central charge c, which is associated to correlators of the stress tensor.

A fact that will play a fundamental role in our subsequent analysis is that the moment map belongs to a special class of operators whose protected data is described by a $2d$ chiral algebra [246].[3] Because the moment map sits in the adjoint of the flavor group, the corresponding operator in the $2d$ chiral algebra is an affine Kac-Moody current. The dictionary between the $4d$ and $2d$ theories is well known:

$$M^A_{(IJ)}(x) \to J^A(z), \qquad k_{4d} \to -\frac{1}{2}k_{2d}. \tag{7.3}$$

---

[2]For readers familiar with the notation of [27] this corresponds to the $\hat{\mathcal{B}}_1$ multiplet.

[3] Coulomb branch operators are not captured by the chiral algebra, and apart from protected conformal dimensions the rest of the CFT data appearing in their correlators is always dynamical.

The chiral algebra description of protected data allows to solve for an infinite number of OPE coefficients in terms of the two central charges c and k. This has two important consequences for us:

- Imposing unitarity of the parent $4d$ theory requires that the calculated OPE coefficients are positive, leading to strict analytic unitarity bounds on the central charges c and k [246–248, 325]. These unitarity bounds are a good organizing principle that we will use in the next section when we discuss the landscape of $\mathcal{N} = 2$ theories, in order to choose which theories one should focus on.

- The second consequence is that having analytic control over the protected part of the correlator gives valuable input for the numerical bootstrap, which is mostly concerned with non-protected data. In the crossing equations we present below, the infinite number of short operators appearing in the moment map four-point function can be summed and treated exactly.

Case studies

Although the bootstrap is an agnostic approach to study SCFTs, it is important to keep in mind what assumptions we are making and what theories our bounds apply to. For example, chiral operators will be present when the theory has a Coulomb branch of rank one or higher, and the moment map signals a global flavor symmetry group G_F. In this work we will consider only $G_F = SU(2)$, so our bounds will apply to any theory with a flavor symmetry that admits an $SU(2)$ subgroup. We leave the study of other flavor symmetry groups for future work.

As anticipated, a powerful organizing principle to study the space of $\mathcal{N} = 2$ SCFTs are the unitarity bounds obtained from the underlying chiral algebra. It will be important to keep in mind that the central charges of any interacting $\mathcal{N} = 2$ SCFT satisfy [246, 248]:[4]

$$k \geq \frac{24ch^\vee}{12c + \dim G_F}, \quad k(-180c^2 + 66c + 3\dim G_F) + 60c^2h^\vee - 22ch^\vee \leq 0. \qquad (7.4)$$

For theories without flavor symmetry, the first inequality does not apply and the second one reduces to $c \geq 11/30$ [247].

Perhaps the most familiar examples of $\mathcal{N} = 2$ SCFTs are Lagrangian models, the simplest one being the $SU(N)$ SYM theory coupled to an adjoint hypermultiplet. This

---

[4]The dual Coxeter number $h^\vee$ is N for $SU(N)$, $N - 2$ for $SO(N)$ and so on.

is precisely $\mathcal{N} = 4$ SYM theory, where part of the full $SU(4)_R$ symmetry is reinterpreted as an $SU(2)$ flavor symmetry. Another interesting model is $\mathcal{N} = 2$ SCQCD, namely an $SU(N)$ SYM theory coupled to $N_f = 2N$ hypermultiplets. The flavor symmetry is $SO(8)$ for $N = 2$ and $SU(2N) \times U(1)$ for $N \geq 3$. Data associated to these theories is presented in table 7.1. When restricting to rank-one or equivalently $SU(2)$ gauge group, SCQCD saturates the two bounds in (7.4), while $\mathcal{N} = 4$ SYM saturates only the first one.

	H_0	H_1	H_2	$\mathcal{N} = 4$ SYM	$\mathcal{N} = 2$ SCQCD
G_F	-	$SU(2)$	$SU(3)$	$SU(2)$	$SU(2N) \times U(1)$
Δ_φ	$\frac{6}{5}$	$\frac{4}{3}$	$\frac{3}{2}$	$2, \ldots, N$	$2, \ldots, N$
c	$\frac{11}{30}$	$\frac{1}{2}$	$\frac{2}{3}$	$\frac{N^2-1}{4}$	$\frac{2N^2-1}{6}$
k	-	$\frac{8}{3}$	3	$N^2 - 1$	$2N$

Table 7.1: $\mathcal{N} = 2$ theories that will appear in the discussion of our results.

Three non-Lagrangian models that will play an important role in our analysis are the Argyres-Douglas theories listed in the first three columns of table 7.1. These models were originally discovered as fixed points of $\mathcal{N} = 2$ $SU(2)$ supersymmetric QCD [326], and they correspond to vacua where a monopole and N_f quarks become massless.[5] These theories have a rank-one Coulomb branch, and the flavor symmetry is $SU(N_f)$ where $N_f = 1, 2, 3$ for H_0, H_1, H_2 respectively. Moreover, they saturate the bounds (7.4) and have therefore a distinguished position in the $\mathcal{N} = 2$ landscape.

These Argyres-Douglas models are isolated and strongly interacting with no standard Lagrangian description.[6] Despite this fact and thanks to superconformal symmetry, some aspects of these theories are under good analytic control. The central charges listed in the table were calculated using holography in [329], and their associated chiral algebras were conjectured in [330, 331]. They can also be obtained as low energy theories on $D3$-branes probing F-theory singularities [332], a construction that naturally generalizes our models to higher ranks. In addition to the flavor symmetry already discussed, the rank-N models will enjoy an extra $SU(2)_L$ symmetry, which will have its own flavor central charge k_L.

---

[5]The H_0 theory had been found first in [327] as a fixed point of $\mathcal{N} = 2$ $SU(3)$ super Yang-Mills.

[6]See however [328] for an interesting approach based on susy enhancement along an $\mathcal{N} = 1$ RG flow.

The central charges of the higher rank models are [329]:

$$c = \frac{1}{4}N^2\Delta_\varphi + \frac{3}{4}N(\Delta_\varphi - 1) - \frac{1}{12}, \tag{7.5}$$

$$k = 2N\Delta_\varphi, \tag{7.6}$$

$$k_L = N^2\Delta_\varphi - N(\Delta_\varphi - 1) - 1, \tag{7.7}$$

where Δ_φ is the dimension of the rank-one Coulomb branch generator in table 7.1, and the remaining generators have dimensions $2\Delta_\varphi, \ldots, N\Delta_\varphi$. This review of $\mathcal{N} = 2$ theories is by no means complete, but it will be sufficient for the discussion of our numerical results.

7.2.2 Correlators, conformal blocks and selection rules

Having reviewed the basic multiplets we are interested in, let us now have a brief review of superconformal kinematics. Conformal Ward identities imply that four-point functions depend on a function of two cross-ratios z and $\bar{z}$:

$$\langle \phi_i(x_1)\phi_j(x_2)\phi_k(x_3)\phi_l(x_4)\rangle = \frac{\mathcal{G}_{ijkl}(z,\bar{z})}{x_{12}^{\Delta_i+\Delta_j}x_{34}^{\Delta_k+\Delta_l}} \left(\frac{x_{24}}{x_{14}}\right)^{\Delta_{ij}} \left(\frac{x_{14}}{x_{13}}\right)^{\Delta_{kl}}. \tag{7.8}$$

Using the Operator Product Expansion (OPE) in the $(12) \to (34)$ channel, one obtains the conformal block decomposition:

$$\mathcal{G}_{ijkl}(z,\bar{z}) = \sum_{\mathcal{O}\in\phi_i\times\phi_j} (-1)^\ell \lambda_{ij\bar{\mathcal{O}}}\lambda_{kl\mathcal{O}}\, g_{\Delta,\ell}^{\Delta_{ij},\Delta_{kl}}(z,\bar{z}). \tag{7.9}$$

Here the sum runs only over conformal primaries that appear in the OPE $\phi_i \times \phi_j$, and the contribution of all conformal descendants is captured by the conformal blocks originally computed in [16, 31]. In our conventions, they are normalized as

$$g_{\Delta,\ell}^{\Delta_{12},\Delta_{34}}(z,\bar{z}) = \frac{z\bar{z}}{z-\bar{z}}\Big(k_{\Delta+\ell}^{\Delta_{12},\Delta_{34}}(z)k_{\Delta-\ell-2}^{\Delta_{12},\Delta_{34}}(\bar{z}) - k_{\Delta+\ell}^{\Delta_{12},\Delta_{34}}(\bar{z})k_{\Delta-\ell-2}^{\Delta_{12},\Delta_{34}}(z)\Big), \tag{7.10}$$

where the one-dimensional blocks are of the familiar form:

$$k_\beta^{\Delta_{12},\Delta_{34}}(z) = z^{\beta/2}\,_2F_1\Big(\tfrac{1}{2}(\beta - \Delta_{12}), \tfrac{1}{2}(\beta + \Delta_{34}); \beta; z\Big). \tag{7.11}$$

It will be understood from now on that $g_{\Delta,\ell} = g_{\Delta,\ell}^{0,0}$ and $k_\beta = k_\beta^{0,0}$.

When supersymmetry is present, the OPE coefficients of descendant operators can be related to the ones of the superprimary. As a result, $\mathcal{G}_{ijkl}$ can be decomposed in terms of

superconformal blocks

$$\mathcal{G}_{ijkl}(z, \bar{z}) = \sum_{\mathcal{O} \in \phi_i \times \phi_j} (-1)^\ell \lambda_{ij\bar{\mathcal{O}}} \lambda_{kl\mathcal{O}} \, G_{\Delta, \ell}^{ij,kl}(z, \bar{z}), \tag{7.12}$$

where the sum now runs only over superprimary operators in the $\phi_i \times \phi_j$ OPE, and the superconformal blocks $G_{\Delta, \ell}^{ij,kl}$ are linear combinations of non-supersymmetric blocks.

In the rest of this section we will discuss the implications of $\mathcal{N} = 2$ supersymmetry on all possible correlation functions formed with (anti)chiral operators φ, $\bar{\varphi}$ and the moment map operator M. Single correlators for chiral operators and moment maps were studied originally in [216], while mixed correlators involving both types of operators have not been studied before. In order to bootstrap this system the first necessary step is to calculate the corresponding superconformal blocks, this is done in section 7.2.2 by imposing consistency between different $\mathcal{N} = 1$ decompositions.

Chiral correlators

We focus first on the four-point function of two chirals and two antichirals:

$$\langle \varphi_r(x_1) \varphi_r(x_2) \bar{\varphi}_{-r}(x_3) \bar{\varphi}_{-r}(x_4) \rangle = \frac{1}{x_{12}^{2\Delta_\varphi} x_{34}^{2\Delta_\varphi}} \sum_{\mathcal{O} \in \varphi \times \varphi} |\lambda_{\varphi\varphi\bar{\mathcal{O}}}|^2 \, g_{\Delta,\ell}(z, \bar{z}). \tag{7.13}$$

To understand what operators appear in the sum we need to study the OPE $\varphi_r \times \varphi_r \sim \mathcal{O}$. The non-supersymmetric selection rules require that only even spin operators with $2r$-charge appear in the sum. Furthermore, the LHS is chiral and annihilated by the super-conformal charge S_α (see [65] for a proof), i.e. $\bar{Q}_{\dot{\alpha}}\mathcal{O} = S_\alpha \mathcal{O} = 0$. Tables of supermultiplets can be found in [182], where one starts with a primary operator at the top and all the Q and $\bar{Q}$-descendants are arranged in a diamond. The superselection rule implies that the only operator that contributes to the OPE is the one sitting in the right corner of this diamond. Since only one operator in each multiplet contributes to the OPE, the superconformal blocks reduce to standard bosonic blocks and we define $G_{\Delta,\ell}^{\varphi\varphi;\bar{\varphi}\bar{\varphi}} \equiv g_{\Delta,\ell}$.

Going through the tables of superconformal multiplets, we obtain all operators that can appear in the OPE. The resulting selection rule, together with the conformal blocks are summarized in table 7.2.

Similarly, we can study the same four-point function with the operators in a different order:

$$\langle \varphi_r(x_1) \bar{\varphi}_{-r}(x_2) \varphi_r(x_3) \bar{\varphi}_{-r}(x_4) \rangle = \frac{1}{x_{12}^{2\Delta_\varphi} x_{34}^{2\Delta_\varphi}} \sum_{\mathcal{O} \in \varphi \times \bar{\varphi}} |\lambda_{\varphi\bar{\varphi}\mathcal{O}}|^2 \, G_{\Delta,\ell}^{\varphi\bar{\varphi};\varphi\bar{\varphi}}(z, \bar{z}). \tag{7.14}$$

Multiplet	Block	Restrictions
$L\bar{B}[0;0]^{(0;2r)}$	$g_{2\Delta_\varphi,0}$	
$L\bar{A}[\ell;\ell\text{-}2]^{(0;2r-2)}$	$g_{2\Delta_\varphi+\ell,\ell}$	$\ell \geq 2,\ \ell$ even
$L\bar{B}[0;0]^{(2;2r-2)}$	$g_{2\Delta_\varphi+2,0}$	
$L\bar{A}[\ell;\ell\text{-}1]^{(1;2r-3)}$	$g_{2\Delta_\varphi+\ell+2,\ell}$	$\ell \geq 2,\ \ell$ even
$L\bar{L}[\ell;\ell]^{(0;2r-4)}_{\Delta-2}$	$g_{\Delta,\ell}$	$\Delta > 2\Delta_\varphi + \ell + 2,\ \ell \geq 0,\ \ell$ even

Table 7.2: List of multiplets that appear in the $\varphi_r \times \varphi_r$ OPE, where φ_r is the primary of $\mathcal{N} = 2$ chiral multiplet. For each multiplet, only one conformal descendant appears in the OPE, so we obtain non-supersymmetric bosonic blocks.

Now the sum runs over all superprimaries in the OPE $\varphi_r \times \bar{\varphi}_{-r} \sim \mathcal{O}$. Using superconformal Ward identities it is easy to prove that only multiplets with vanishing R and r charge can appear. By going through the list of $\mathcal{N} = 2$ multiplets one obtains

$$\varphi_r \times \bar{\varphi}_{-r} \sim \mathbb{1} + A\bar{A}[\ell;\ell]^{(0;0)} + L\bar{L}[\ell;\ell]^{(0;0)}_\Delta. \tag{7.15}$$

For each multiplet, all operators with $R = r = 0$ appear in $\varphi_r \times \bar{\varphi}_{-r}$, thus the superconformal blocks are linear combinations of bosonic blocks. The superconformal block for the exchange of the long multiplet was originally computed in [194], and takes a very compact form:

$$G^{\varphi\bar{\varphi};\varphi\bar{\varphi}}_{\Delta,\ell}(z,\bar{z}) = (z\bar{z})^{-1} g^{2,2}_{\Delta+2,\ell}(z,\bar{z}). \tag{7.16}$$

At the unitarity bound $\Delta = \ell + 2$, the $L\bar{L}$ multiplet shortens and we obtain the superconformal block associated to $A\bar{A}$. In particular, the stress tensor belongs to $A\bar{A}[0;0]^{(0;0)}$, and all the $A\bar{A}[\ell;\ell]^{(0;0)}$ with $\ell \geq 1$ contain higher-spin conserved currents that are absent in interacting SCFTs. Similarly, for $\ell = 0$ and $\Delta = 0$ we obtain the identity operator. Although not manifestly so, the above superconformal block can be expanded as a sum of bosonic blocks with $\Delta_{12} = 0$. We do not need the full result, but let us note for future reference the contribution of the stress-tensor multiplet:

$$G^{\varphi\bar{\varphi};\varphi\bar{\varphi}}_{2,0}(z,\bar{z}) = g_{2,0} + \frac{1}{4}g_{3,1}(z,\bar{z}) + \frac{1}{60}g_{4,2}(z,\bar{z}). \tag{7.17}$$

92

In order to study crossing symmetry, we will also need the following ordering:

$$\langle \varphi_r(x_1)\bar{\varphi}_{-r}(x_2)\bar{\varphi}_{-r}(x_3)\varphi_r(x_4)\rangle = \frac{1}{x_{12}^{2\Delta_\varphi}x_{34}^{2\Delta_\varphi}} \sum_{\mathcal{O}\in\varphi\times\bar{\varphi}} |\lambda_{\varphi\bar{\varphi}\mathcal{O}}|^2 \, \tilde{G}_{\Delta,\ell}^{\varphi\bar{\varphi};\varphi\bar{\varphi}}(z,\bar{z}). \tag{7.18}$$

The block $\tilde{G}$ is given by the same linear combination of non-supersymmetric blocks as G. However, for each term in the sum, we must include a factor $(-1)^\ell$ depending on the spin of the exchanged operator. All in all, the superconformal blocks in compact form are:

$$\tilde{G}_{\Delta,\ell}^{\varphi\bar{\varphi};\bar{\varphi}\varphi}(z,\bar{z}) = (-1)^\ell (z\bar{z})^{-1} g_{\Delta+2,\ell}^{2,-2}(z,\bar{z}). \tag{7.19}$$

The results of this section are summarized in table 7.3.

Multiplet	Block	Restrictions
$\mathbb{1}$	1	
$A\bar{A}[\ell;\ell]^{(0;0)}$	$G_{\ell+2,\ell}^{\varphi\bar{\varphi};\varphi\bar{\varphi}}$	$\ell \geq 0$
$L\bar{L}[\ell;\ell]_\Delta^{(0;0)}$	$G_{\Delta,\ell}^{\varphi\bar{\varphi};\varphi\bar{\varphi}}$	$\Delta > \ell + 2,\ \ell \geq 0$

Table 7.3: List of multiplets that appear in the $\varphi_r \times \bar{\varphi}_{-r}$ OPE, where φ_r is the primary of an $\mathcal{N} = 2$ chiral multiplet and $\bar{\varphi}_{-r}$ is its complex conjugate. The explicit form of the superconformal block is given in (7.16). The multiplets $A\bar{A}[\ell;\ell]^{(0;0)}$ for $\ell \geq 1$ contain higher-spin conserved currents and should be absent in an interacting SCFT.

Moment map correlator

Now we consider the four-point function of moment map operators. In this work, we will restrict our attention to $G_F = SU(2)$, which could represent the full flavor symmetry of the theory or an $SU(2)$ subgroup. It is convenient to contract the $SU(2)_R$ indices with auxiliary vectors t^I to unclutter the equations $M^A(x,t) = M_{IJ}^A(x)t^I t^J$. Using this notation the four-point function of moment maps can be decomposed into $SU(2)_R$ and flavor irreducible representations:

$$\langle M^A(x_1,t_1)M^B(x_2,t_2)M^C(x_3,t_3)M^D(x_4,t_4)\rangle$$
$$= \frac{(t_1\cdot t_2)^2(t_3\cdot t_4)^2}{x_{12}^4 x_{34}^4} \sum_{R=0,2,4}\sum_i P_i^{ABCD}P_R(y)\, a_{i,R}(z,\bar{z}). \tag{7.20}$$

We contract the auxiliary vectors as $t_a \cdot t_b = \varepsilon_{IJ} t_a^I t_b^J$, and the $SU(2)_R$-invariant cross ratio is

$$w = \frac{(t_1 \cdot t_2)(t_3 \cdot t_4)}{(t_1 \cdot t_3)(t_2 \cdot t_4)}, \qquad y = \frac{2}{w} - 1. \tag{7.21}$$

Since the moment map is a triplet under R-symmetry, the four-point function decomposes into $[2] \otimes [2] = [0] \oplus [2] \oplus [4]$, where $[R]$ is the $(R+1)$-dimensional representation of $SU(2)$. The projectors $P_R(y)$ are given by Legendre polynomials:

$$P_0(y) = 1, \qquad P_2(y) = y, \qquad P_4(y) = \frac{1}{2}(3y^2 - 1). \tag{7.22}$$

On the flavor symmetry side, we have an index i which runs over all irreducible representations in the product of two adjoints $i \in \operatorname{ad} G_F \times \operatorname{ad} G_F$. We use orthogonal projectors normalized as follows:

$$P_i^{ABCD} P_j^{DCEF} = \delta_{ij} P_i^{ABEF}, \qquad P_i^{ABBA} = \dim R_i. \tag{7.23}$$

For the case of interest to us $G_F = SU(2)$, the projectors are:

$$P_{\mathbf{1}}^{ABCD} = \frac{1}{3} \delta^{AB} \delta^{CD}, \tag{7.24a}$$

$$P_{\mathbf{3}}^{ABCD} = \frac{1}{2}(\delta^{AD} \delta^{BC} - \delta^{AC} \delta^{BD}), \tag{7.24b}$$

$$P_{\mathbf{5}}^{ABCD} = \frac{1}{2}(\delta^{AD} \delta^{BC} + \delta^{AC} \delta^{BD}) - P_{\mathbf{1}}^{ABCD}. \tag{7.24c}$$

A useful property of the moment map four-point function is that superconformal Ward identities relate the different R-symmetry channels. In particular, the three $a_{i,R}$ for $R = 0, 2, 4$ depend on a two-variable function $\mathcal{G}_i(z, \bar{z})$ and a meromorphic function $f_i(z)$ [243–245]:

$$a_{i,0}(z, \bar{z}) = \frac{2z\bar{z} - 3(z + \bar{z}) + 6}{6} \mathcal{G}_i(z, \bar{z}) - \frac{z\bar{z}}{2(z - \bar{z})} \left(\frac{(2 - z)f_i(z)}{z} - \frac{(2 - \bar{z})f_i(\bar{z})}{\bar{z}} \right),$$

$$a_{i,2}(z, \bar{z}) = \frac{z\bar{z}}{2(z - \bar{z})}(f_i(z) - f_i(\bar{z})) + \frac{z\bar{z} - z - \bar{z}}{2} \mathcal{G}_i(z, \bar{z}), \tag{7.25}$$

$$a_{i,4}(z, \bar{z}) = \frac{z\bar{z}}{6} \mathcal{G}_i(z, \bar{z}).$$

Since the superconformal blocks satisfy the same Ward identities as the correlator, we can also express them in terms of $\mathcal{G}(z, \bar{z})$ and $f(z)$. The selection rules for the moment map operator were first obtained in [333], and the corresponding blocks were calculated in [243]. We do not review the calculation here, but we just quote the result in table 7.4.

Multiplet	Block $\mathcal{G}(u,v)$	Block $f(z)$	Restrictions
$\mathbb{1}$	0	1	$-$
$B\bar{B}[0;0]^{(2;0)}$	0	$2k_2$	$-$
$B\bar{B}[0;0]^{(4;0)}$	$6u^{-1}g_{4,0}$	$6k_4$	$-$
$A\bar{A}[\ell;\ell]^{(0;0)}$	0	$-k_{2(\ell+2)}$	$\ell \geq 0$
$A\bar{A}[\ell;\ell]^{(2;0)}$	$-2u^{-1}g_{\ell+5,\ell+1}$	$-2k_{2(\ell+3)}$	$\ell \geq 0$
$L\bar{L}[\ell;\ell]^{(0;0)}_{\Delta}$	$u^{-1}g_{\Delta+2,\ell}$	0	$\Delta > \ell + 2$

Table 7.4: List of multiplets that appear in the $M\times M$ OPE, where M is the $\mathcal{N}=2$ moment map operator. The superconformal blocks can be expressed in terms of two functions $\mathcal{G}(z,\bar{z})$ and $f(z)$, as discussed around equation (7.25). In our conventions, the contribution from the lowest-dimension operator is always unit normalized.

Chiral and moment map

Finally, we consider the channel involving both chiral and moment map operators. In this case, the superconformal blocks are not available in the literature. Fortunately, we can leverage the knowledge of $\mathcal{N}=1$ superblocks to easily obtain the required blocks. The strategy is to build the $\mathcal{N}=2$ superblocks as a linear combination of $\mathcal{N}=1$ blocks, and by a mix of basic consistency conditions and $\mathcal{N}=2$ selection rules, it turns out all free coefficients can be fixed. We present the steps in detail in appendix 7.A.

First we consider the four-point function

$$\langle\varphi(x_1)\bar{\varphi}(x_2)M^A(x_3,t_3)M^B(x_4,t_4)\rangle = \frac{\delta^{AB}(t_3\cdot t_4)^2}{|x_{12}|^{2\Delta_\varphi}|x_{34}|^4}\sum_{\mathcal{O}}\lambda_{\varphi\bar{\varphi}\mathcal{O}}\lambda_{MM\mathcal{O}}G^{\varphi\bar{\varphi};MM}_{\Delta,\ell}(z,\bar{z}),\ (7.26)$$

where the sum runs over all even-spin superprimaries which are both in the $\varphi_r \times \bar{\varphi}_{-r}$ and $M \times M$ OPEs (see tables 7.3 and 7.4). Interestingly, the superconformal block can be written very compactly (see appendix 7.A):

$$G^{\varphi\bar{\varphi};MM}_{\Delta,\ell}(z,\bar{z}) = (z\bar{z})^{-1}g^{2,0}_{\Delta+2,\ell}(z,\bar{z}).\qquad (7.27)$$

As before, at the unitarity bound $\Delta = \ell + 2$ this block gives the contribution of the $A\bar{A}[\ell;\ell]^{(0;0)}$ multiplet. In the appendix we give an expression for $G^{\varphi\bar{\varphi};MM}_{\Delta,\ell}$ as a linear

combination of non-supersymmetric blocks (7.70). We do not need such an expression in general, only when $\Delta = 2$, $\ell = 0$ to capture the contribution of the stress tensor:

$$G_{2,0}^{\varphi\bar{\varphi};MM}(z,\bar{z}) = g_{2,0} - \frac{1}{30}g_{4,2}(z,\bar{z}). \tag{7.28}$$

These results are summarized in table 7.5.

Multiplet	Block	Restrictions
$\mathbb{1}$	1	
$A\bar{A}[\ell;\ell]^{(0;0)}$	$G_{\ell+2,\ell}^{\varphi\bar{\varphi};MM}$	$\ell \geq 0$, ℓ even
$L\bar{L}[\ell;\ell]_{\Delta}^{(0;0)}$	$G_{\Delta,\ell}^{\varphi\bar{\varphi};MM}$	$\Delta > \ell + 2$, $\ell \geq 0$, ℓ even

Table 7.5: List of multiplets that appear both in the $\varphi_r \times \bar{\varphi}_{-r}$ and $M \times M$ OPEs. For each multiplet, the superconformal block can be found in equation (7.27).

Let us now consider the four-point function in the crossed channel

$$
\begin{aligned}
&\langle \varphi(x_1) M^A(x_2, t_2) M^B(x_3, t_3) \bar{\varphi}(x_4) \rangle \\
&= \frac{\delta^{AB}(t_2 \cdot t_3)^2}{x_{12}^{\Delta_\varphi+2} x_{34}^{\Delta_\varphi+2}} \left(\frac{x_{24}}{x_{14}}\right)^{\Delta_\varphi-2} \left(\frac{x_{14}}{x_{13}}\right)^{\Delta_\varphi-2} \sum_{\mathcal{O}} |\lambda_{\varphi M\mathcal{O}}|^2 G_{\Delta,\ell}^{\varphi M;M\bar{\varphi}}(z,\bar{z}),
\end{aligned}
\tag{7.29}
$$

where the superconformal blocks derived in appendix 7.A are

$$G_{\Delta,\ell}^{\varphi M;M\bar{\varphi}}(z,\bar{z}) = (z\bar{z})^{-1/2} g_{\Delta+2,\ell}^{\Delta_\varphi-1,3-\Delta_\varphi}(z,\bar{z}). \tag{7.30}$$

The sum in (7.29) runs over the superprimaries of three different multiplets. For generic Δ it is a long multiplet $L\bar{L}$ and the block is given by (7.30). At the unitarity bound $\Delta = \Delta_\varphi + \ell + 1$ we either obtain an $L\bar{A}$ multiplet if $\ell \geq 1$, or an $L\bar{B}$ multiplet for $\ell = 0$.

When we study crossing we will also need the blocks for the $\langle \varphi M \bar{\varphi} M \rangle$ ordering. As before, we define them with a tilde:

$$\tilde{G}_{\Delta,\ell}^{\varphi M;M\bar{\varphi}}(z,\bar{z}) = (-1)^{\ell}(z\bar{z})^{-1/2} g_{\Delta+2,\ell}^{\Delta_\varphi-1,\Delta_\varphi-3}(z,\bar{z}). \tag{7.31}$$

The results in this section are summarized in table 7.6.

Multiplet	Block	Restrictions
$L\bar{B}[0;0]^{(2;r)}$	$G^{\varphi M; M\bar{\varphi}}_{\Delta_\varphi+1,0}$	
$L\bar{A}[\ell;\ell\text{-}1]^{(1;r\text{-}1)}$	$G^{\varphi M; M\bar{\varphi}}_{\Delta_\varphi+\ell+1,\ell}$	$\ell \geq 1$
$L\bar{L}[\ell;\ell]^{(0;r\text{-}2)}_\Delta$	$G^{\varphi M; M\bar{\varphi}}_{\Delta,\ell}$	$\Delta > \Delta_\varphi + \ell + 1,\ \ell \geq 0$

Table 7.6: List of multiplets that appear in the $\varphi_r \times M$ OPE. For each multiplet, the superconformal block can be found in equation (7.30).

7.3 Crossing equations

With the selection rules and superconformal blocks at hand, we are finally ready to present the crossing equations of interest. Although it is generally an easy exercise to obtain them, for the moment map four-point function one needs to take into account the contributions coming from the chiral algebra. We will review the most important results which are derived in more detail in [216].

7.3.1 Generalities

The bootstrap for four-point functions of different scalars was first studied in [58]. As usual, one demands that the OPE decomposition in the $(12) \to (34)$ channel is equivalent to the $(14) \to (23)$ channel:[7]

$$\langle \overbrace{\phi_i(x_1)\phi_j}(x_2)\overbrace{\phi_k(x_3)}\phi_l(x_4)\rangle = \langle \overbrace{\phi_i(x_1)\phi_j(x_2)\overbrace{\phi_k(x_3)}\phi_l(x_4)}\rangle\,. \tag{7.32}$$

Upon expanding in conformal blocks, this implies two independent crossing equations

$$\sum (-1)^\ell \lambda_{ij\mathcal{O}}\lambda_{kl\mathcal{O}} E^{ij,kl}_{\pm,\Delta,\ell}(z,\bar{z}) \pm \sum (-1)^\ell \lambda_{kj\mathcal{O}}\lambda_{il\mathcal{O}} E^{kj,il}_{\pm,\Delta,\ell}(z,\bar{z}) = 0\,, \tag{7.33}$$

where we have defined

$$
\begin{aligned}
E^{ij,kl}_{\pm,\Delta,\ell}(z,\bar{z}) =(z - \bar{z})\bigg[&(z\bar{z})^{-\frac{\Delta_i+\Delta_j}{2}} g^{\Delta_{ij},\Delta_{kl}}_{\Delta,\ell}(z,\bar{z}) \\
&\mp \big((1 - z)(1 - \bar{z})\big)^{-\frac{\Delta_i+\Delta_j}{2}} g^{\Delta_{ij},\Delta_{kl}}_{\Delta,\ell}(1 - z, 1 - \bar{z})\bigg]\,.
\end{aligned}
\tag{7.34}
$$

---

[7]There will also be flavor symmetry indices which for simplicity we do not consider yet.

We have multiplied by $(z - \bar{z})$ to simplify the approximation of blocks in terms of polynomials, as explained in appendix 7.B. In what follows, we will use the same notation for superblocks, for example $E^{MM;\varphi\bar{\varphi}}$ is obtained from (7.34) with $\Delta_{1,2} = 2$, $\Delta_{3,4} = \Delta_\varphi$ and $g^{\Delta_{12},\Delta_{34}}_{\Delta,\ell} \to G^{MM;\varphi\bar{\varphi}}_{\Delta,\ell}$. [8]

7.3.2 Chiral correlators

The constraints imposed by crossing symmetry on a system of $\mathcal{N} = 1$ chiral correlators in $4d$ was first studied in [65] and later improved in [56]. The analogous system with $\mathcal{N} = 2$ supersymmetry has been studied by [198,216,217]. Applying (7.33) to $\langle\varphi\bar{\varphi}\varphi\bar{\varphi}\rangle$ and $\langle\varphi\varphi\bar{\varphi}\bar{\varphi}\rangle$ one obtains three independent equations

$$\vec{I}_c + \sum_{\mathcal{O}\in A^+} |\lambda_{\varphi\bar{\varphi}\mathcal{O}}|^2\, \vec{U}_{\Delta,\ell} + \sum_{\mathcal{O}\in A^-} |\lambda_{\varphi\varphi\mathcal{O}}|^2\, \vec{V}_{\Delta,\ell} + \sum_{\mathcal{O}\in B^+} |\lambda_{\varphi\varphi\bar{\mathcal{O}}}|^2\, \vec{W}_{\Delta,\ell} = 0, \tag{7.35}$$

where

$$\vec{U}_{\Delta,\ell} = \begin{pmatrix} E^{\varphi\bar{\varphi};\varphi\bar{\varphi}}_{+,\Delta,\ell} \\ \tilde{E}^{\varphi\bar{\varphi};\varphi\bar{\varphi}}_{+,\Delta,\ell} \\ \tilde{E}^{\varphi\bar{\varphi};\varphi\bar{\varphi}}_{-,\Delta,\ell} \end{pmatrix}, \qquad \vec{V}_{\Delta,\ell} = \begin{pmatrix} E^{\varphi\bar{\varphi};\varphi\bar{\varphi}}_{+,\Delta,\ell} \\ \tilde{E}^{\varphi\bar{\varphi};\varphi\bar{\varphi}}_{+,\Delta,\ell} \\ \tilde{E}^{\varphi\bar{\varphi};\varphi\bar{\varphi}}_{-,\Delta,\ell} \end{pmatrix}, \qquad \vec{W}_{\Delta,\ell} = \begin{pmatrix} 0 \\ E^{\varphi\varphi;\bar{\varphi}\bar{\varphi}}_{+,\Delta,\ell} \\ -E^{\varphi\varphi;\bar{\varphi}\bar{\varphi}}_{-,\Delta,\ell}\, . \end{pmatrix}. \tag{7.36}$$

Furthermore, we have separated the contribution of the unit operator and the stress tensor into

$$\vec{I}_c = \vec{U}_{0,0} + \frac{\Delta_\varphi^2}{6c}\vec{U}_{2,0}\,. \tag{7.37}$$

The normalization of the stress tensor is easily obtained from (7.17) and the requirement that it is normalized as $\sim \frac{\Delta_\varphi^2}{360c}g_{4,2}$ (for details see [56,65]). The ranges of the sums in (7.35) can be read from tables 7.2 and 7.3:

$$
\begin{aligned}
A^+ &= \{\ell \geq 0,\ \ell\ \text{even},\ \Delta \geq \ell + 2\}\,, \\
A^- &= \{\ell \geq 0,\ \ell\ \text{odd},\ \Delta \geq \ell + 2\}\,, \\
B^+ &= \{\ell \geq 0,\ \ell\ \text{even},\ \Delta = 2\Delta_\varphi + \ell\} \cup \{\ell \geq 0,\ \ell\ \text{even},\ \Delta \geq 2\Delta_\varphi + \ell + 2\}\,.
\end{aligned}
\tag{7.38}
$$

The operators in the $\varphi \times \bar{\varphi}$ OPE are divided into even and odd spins $A^\pm$. Even though the distinction is not necessary at this point, we keep it in analogy to the mixed system in section 7.3.4.

---

[8]We proceed similarly for the superblocks with tilde. For example $\tilde{E}^{\varphi M;M\bar{\varphi}}$ is obtained from (7.34) with $\Delta_{2,3} = 2$, $\Delta_{1,4} = \Delta_\varphi$ and $g^{\Delta_{12},\Delta_{34}}_{\Delta,\ell} \to \tilde{G}^{\varphi M;M\bar{\varphi}}_{\Delta,\ell}$.

7.3.3 Moment map correlator

The crossing equations for the moment map are a bit more intricate than for a regular non-supersymmetric four-point function. Let us remember that this correlator is completely determined in terms of two variable functions $\mathcal{G}_i(z, \bar{z})$ and meromorphic functions $f_i(z)$. The index $i \in \operatorname{ad} G_F \times \operatorname{ad} G_F$ runs over representations that appear in the product of two flavor adjoint representations. The projectors P_i^{ABCD} transform under crossing as:

$$P_i^{ABCD} = F_i{}^j P_j^{CBAD}, \qquad F_{SU(2)} = \begin{pmatrix} \frac{1}{3} & \frac{1}{3} & \frac{1}{3} \\ 1 & \frac{1}{2} & -\frac{1}{2} \\ \frac{5}{3} & -\frac{5}{6} & \frac{1}{6} \end{pmatrix}. \tag{7.39}$$

With this definition it is a simple exercise to show that the crossing relations for $f_i(z)$ decouple from the rest, and take the simple form

$$f_i\left(\frac{z}{z-1}\right) = (-1)^{\operatorname{symm}(i)} f_i(z), \qquad F_j{}^i f_j(z) = \left(\frac{z}{z-1}\right)^2 f_i(1-z). \tag{7.40}$$

Here $\operatorname{symm}(i)$ is 0 for representations that are symmetric under the exchange of points $1 \leftrightarrow 2$, and 1 for the antisymmetric ones. For the case of $SU(2)$, $\operatorname{symm}(\mathbf{1}) = \operatorname{symm}(\mathbf{5}) = 0$ and $\operatorname{symm}(\mathbf{3}) = 1$. Interestingly, the crossing equations (7.40) determine $f_i(z)$ up to a free parameter. Alternatively, one can obtain $f^{ABCD}(z)$ as the four-point function of affine Kac-Moody currents of the chiral algebra associated to the $\mathcal{N} = 2$ theory [246]. Using either procedure, one obtains

$$f_{\mathbf{1}}(z) = \frac{3 - 6z + (5 - \frac{8}{k})z^2 - (2 - \frac{8}{k})z^3 + z^4}{(1-z)^2}, \tag{7.41a}$$

$$f_{\mathbf{3}}(z) = \frac{-\frac{8}{k}z + \frac{12}{k}z^2 + (2 - \frac{4}{k})z^3 - z^4}{(1-z)^2}, \tag{7.41b}$$

$$f_{\mathbf{5}}(z) = \frac{(2 + \frac{4}{k})(z^2 - z^3) + z^4}{(1-z)^2}. \tag{7.41c}$$

The free parameter k is the flavor central charge that appears in the four-point function of flavor currents.

Now one can expand the $f_i(z)$ in terms of one-dimensional blocks, and extract the corresponding OPE coefficients. Using table 7.4 these can be mapped to the OPE coefficients in the $\mathcal{G}(z, \bar{z})$ block expansion.[9] With this information, one can resum the contribution

---

[9] In order to do this mapping unambiguously one needs to assume the absence of higher-spin currents, or equivalently, that $A\bar{A}[\ell; \ell]^{(0;0)}$ for $\ell \geq 1$ are absent in our equations.

of the $B\bar{B}[0;0]^{(4;0)}$ and $A\bar{A}[\ell;\ell]^{(2;0)}$ multiplets to $\mathcal{G}(z,\bar{z})$, which splits into protected and unprotected pieces:

$$\mathcal{G}_i(z,\bar{z}) = \mathcal{G}_i^{\text{sh}}(z,\bar{z}) + \mathcal{G}_i^{\text{long}}(z,\bar{z}), \qquad \mathcal{G}_i^{\text{long}}(z,\bar{z}) = \sum |\lambda_{MM\mathcal{O}_i}|^2 \, u^{-1} g_{\Delta,\ell}(z,\bar{z}). \quad (7.42)$$

The conformal block decomposition of the long (unprotected) piece involves only $L\bar{L}[\ell,\ell]_{\Delta}^{(0;0)}$ multiplets, and the corresponding block appears in table 7.4. For $SU(2)$ flavor, the short (protected) pieces were computed in [216]:

$$\mathcal{G}_{\mathbf{1}}^{\text{sh}}(z,\bar{z}) = \frac{\log(1-\bar{z})}{z-\bar{z}} \left(\frac{6}{c} + \frac{8z^2}{k(1-z)} - \frac{z^2(z^2-2z+2)}{(1-z)^2} \right)$$
$$- \frac{\log(1-z)}{z-\bar{z}} \left(\frac{6}{c} + \frac{8\bar{z}^2}{k(1-\bar{z})} - \frac{\bar{z}^2(\bar{z}^2-2\bar{z}+2)}{(1-\bar{z})^2} \right)$$
$$- \frac{6\log(1-z)\log(1-\bar{z})}{cz\bar{z}}, \quad (7.43)$$

$$\mathcal{G}_{\mathbf{3}}^{\text{sh}}(z,\bar{z}) = \frac{(2-z)z\log(1-\bar{z})}{(z-\bar{z})(1-z)} \left(\frac{4}{k} - \frac{z^2}{1-z} \right) - \frac{(2-\bar{z})\bar{z}\log(1-z)}{(z-\bar{z})(1-\bar{z})} \left(\frac{4}{k} - \frac{\bar{z}^2}{1-\bar{z}} \right),$$

$$\mathcal{G}_{\mathbf{5}}^{\text{sh}}(z,\bar{z}) = -\frac{z^2\log(1-\bar{z})}{(z-\bar{z})(1-z)} \left(\frac{4}{k} + \frac{z^2-2z+2}{1-z} \right) + \frac{\bar{z}^2\log(1-z)}{(z-\bar{z})(1-\bar{z})} \left(\frac{4}{k} + \frac{\bar{z}^2-2\bar{z}+2}{1-\bar{z}} \right).$$

Keeping this information in mind, we are finally ready to write a set of crossing equations that constrain the unprotected spectrum of $\mathcal{N}=2$ theories. Besides (7.40), crossing symmetry implies

$$\left(F_j{}^i \pm \delta_j{}^i \right) \left(\mathcal{H}_j(z,\bar{z}) \pm \mathcal{H}_j(1-z,1-\bar{z}) \right) \equiv \left(F_j{}^i \pm \delta_j{}^i \right) \mathcal{H}_{\pm,j}(z,\bar{z}) = 0, \quad (7.44)$$

where

$$\mathcal{H}_i(z,\bar{z}) = (z-\bar{z})(z\bar{z})^{-2}\mathcal{G}_i(z,\bar{z}) - \frac{1}{2(z\bar{z})^2} \left(\frac{z}{z-1}f_i(\bar{z}) - \frac{\bar{z}}{\bar{z}-1}f_i(z) \right). \quad (7.45)$$

Out of the six crossing equations (7.44), only three of them are independent. When we expand them in blocks, there will be a piece which corresponds to the long operators, for which $f_i(z)$ drops out and $\mathcal{G}_i(z,\bar{z}) \to u^{-1}g_{\Delta+2,\ell}$, see table 7.4. On the other hand, for the protected part both (7.41) and (7.43) will be relevant, and we collect them in the vector $\vec{I}_{c,k}$. All in all, we get

$$\vec{I}_{c,k} + \sum_{A^+} |\lambda_{MM\mathcal{O}_{\mathbf{1}}}|^2 \, \vec{U}_{\Delta,\ell} + \sum_{C_{\mathbf{3}}^-} |\lambda_{MM\mathcal{O}_{\mathbf{3}}}|^2 \, \vec{X}_{\Delta,\ell} + \sum_{C_{\mathbf{5}}^+} |\lambda_{MM\mathcal{O}_{\mathbf{5}}}|^2 \, \vec{Y}_{\Delta,\ell} = 0. \quad (7.46)$$

with

$$\vec{U}_{\Delta,\ell} = \begin{pmatrix} 4\,E^{MM,MM}_{+,\Delta,\ell} \\ 2\,E^{MM,MM}_{+,\Delta,\ell} \\ -2\,E^{MM,MM}_{-,\Delta,\ell} \end{pmatrix}, \quad \vec{X}_{\Delta,\ell} = \begin{pmatrix} 3\,E^{MM,MM}_{+,\Delta,\ell} \\ 9\,E^{MM,MM}_{+,\Delta,\ell} \\ 3\,E^{MM,MM}_{-,\Delta,\ell} \end{pmatrix}, \quad \vec{Y}_{\Delta,\ell} = \begin{pmatrix} 5\,E^{MM,MM}_{+,\Delta,\ell} \\ -5\,E^{MM,MM}_{+,\Delta,\ell} \\ 5\,E^{MM,MM}_{-,\Delta,\ell} \end{pmatrix}. \quad (7.47)$$

For convenience we have defined

$$E^{MM,MM}_{\pm,\Delta,\ell}(z,\bar{z}) = (z-\bar{z})\Big[(z\bar{z})^{-3}g_{\Delta,\ell}(z,\bar{z}) \mp ((1-z)(1-\bar{z}))^{-3}g_{\Delta,\ell}(1-z,1-\bar{z})\Big]. \quad (7.48)$$

The contribution of all the protected operators depends only on c and k. It can be constructed by combining the definition of $\mathcal{H}$ in (7.45) with (7.41) and (7.43):

$$\vec{I}_{c,k} = \begin{pmatrix} 4\mathcal{H}^{\mathrm{sh}}_{+,\mathbf{1}} + 3\mathcal{H}^{\mathrm{sh}}_{+,\mathbf{3}} + 5\mathcal{H}^{\mathrm{sh}}_{+,\mathbf{5}} \\ 2\mathcal{H}^{\mathrm{sh}}_{+,\mathbf{1}} + 9\mathcal{H}^{\mathrm{sh}}_{+,\mathbf{3}} - 5\mathcal{H}^{\mathrm{sh}}_{+,\mathbf{5}} \\ -2\mathcal{H}^{\mathrm{sh}}_{-,\mathbf{1}} + 3\mathcal{H}^{\mathrm{sh}}_{-,\mathbf{3}} + 5\mathcal{H}^{\mathrm{sh}}_{-,\mathbf{5}} \end{pmatrix}. \quad (7.49)$$

Regarding the ranges of summation in (7.46), we have three different channels depending on the flavor symmetry representation. The singlet channel is equivalent to A^+ defined in (7.38), while the **3** and **5** channels give:

$$\begin{aligned} C^-_{\mathbf{3}} &= \{\ell \geq 0,\ \ell \text{ odd},\ \Delta > \ell + 2\}, \\ C^+_{\mathbf{5}} &= \{\ell \geq 0,\ \ell \text{ even},\ \Delta > \ell + 2\}. \end{aligned} \quad (7.50)$$

7.3.4 Full mixed system

The crossing equations for the mixed system are a simple extension of the ones presented so far. By considering $\langle \varphi M \bar{\varphi} M \rangle$ and $\langle \varphi \bar{\varphi} M M \rangle$ we obtain three extra equations and a new channel $\varphi \times M$. The full system is then

$$\vec{I}_{c,k} + \sum_{\mathcal{O}\in A^+} \left(\lambda^*_{MM\mathcal{O}}\,\lambda^*_{\varphi\bar{\varphi}\mathcal{O}}\right) \vec{U}_{\Delta,\ell} \begin{pmatrix} \lambda_{MM\mathcal{O}} \\ \lambda_{\varphi\bar{\varphi}\mathcal{O}} \end{pmatrix} + \sum_{\mathcal{O}\in A^-} |\lambda_{\varphi\bar{\varphi}\mathcal{O}}|^2 \vec{V}_{\Delta,\ell} + \sum_{\mathcal{O}\in B^+} |\lambda_{\varphi\varphi\mathcal{O}}|^2 \vec{W}_{\Delta,\ell}$$
$$+ \sum_{\mathcal{O}\in C^-_{\mathbf{3}}} |\lambda_{MM\mathcal{O}}|^2 \vec{X}_{\Delta,\ell} + \sum_{\mathcal{O}\in C^+_{\mathbf{5}}} |\lambda_{MM\mathcal{O}}|^2 \vec{Y}_{\Delta,\ell} + \sum_{\mathcal{O}\in D^\pm} |\lambda_{\varphi M\mathcal{O}}|^2 \vec{Z}_{\Delta,\ell} = 0.$$
$$(7.51)$$

101

The explicit crossing vectors are easy to obtain and are given in appendix 7.B.3. In the new channel the summation range can be obtained from table 7.6:

$$D^{\pm} = \{\ell \geq 0, \ \Delta \geq \Delta_{\varphi} + \ell + 1\}. \tag{7.52}$$

We will often refer to the different channels by the name of the crossing vector. For example, the multiplets that appear in the $\varphi \times M$ OPE will be referred to as Z-channel multiplets, and similarly for the other channels.

7.4   Numerical bounds

In this section we use the numerical bootstrap of [17] to obtain bounds on the space of $\mathcal{N} = 2$ superconformal theories. Arguably the most important numerical bootstrap result is the precise determination of the critical exponents of the three-dimensional Ising and $O(N)$ models [58, 59, 62–64, 77, 80]. In the supersymmetric literature, one can find studies of $3d$ models with minimal supersymmetry [199–201], $\mathcal{N} = 2$ supersymmetry [193, 202–205] and maximal $\mathcal{N} = 8$ supersymmetry [207–210]. Similarly, in four dimensions there have been studies of $\mathcal{N} = 1$ theories [56, 65, 212–214], $\mathcal{N} = 2$ theories [198, 216, 217], $\mathcal{N} = 3$ theories [219] and of $\mathcal{N} = 4$ SYM theory [221, 223]. Finally there have also been bootstrap studies of supersymetric theories in two [226–228], five [229] and six [230, 231] dimensions and for supersymmetric defects [2, 233]. A mixed correlator between Coulomb and moment map operators similar in spirit to our work has been studied in $3d$ $\mathcal{N} = 4$ theories in [206]. A pedagogical introduction to the modern numerical bootstrap is [34].

7.4.1   Chiral correlators

In this section we focus exclusively on chiral correlators. Some of our results are new, while others are improved versions of the ones previously obtained in [198, 216, 217]. For details of the numerical implementation for this and all subsequent sections see appendix 7.B.

OPE bounds and spectrum

As summarized in table 7.2, the OPE of two chiral fields $\varphi_r \times \varphi_r$ contains a family of protected operators captured by conformal blocks $g_{2\Delta_{\varphi}+\ell,\ell}$ for $\ell = 0, 2, 4, \ldots$. These operators should be interpreted as double traces of the chiral primary operators $\varphi \, \partial^{\mu_1} \ldots \partial^{\mu_\ell} \varphi$. For $\ell = 0$ this gives another Coulomb branch operator that we denote φ^2, while for $\ell = 2$

the exchanged operator is a level-two descendant in its multiplet which we denote $\bar{Q}^2\mathcal{O}$. In figure 7.1 we plot upper and lower bounds on the OPE coefficients λ_{φ^2} and $\lambda^2_{\bar{Q}^2\mathcal{O}}$ as a function of the dimension of the external field $\Delta_\varphi = r/2$, without making any assumptions about the spectrum. Notice that upper and lower bounds are close to each other for low values of the external dimension Δ_φ. Luckily, the Argyres-Douglas models listed in table 7.1 are characterized by a low value of Δ_φ, which means the bounds are particularly useful to constrain these theories. The equivalent bounds for $\ell \geq 4$ are qualitatively equal to the $\ell = 2$ case, in the sense that for low values of Δ_φ the OPE coefficient must be approximately given by their MFT values.
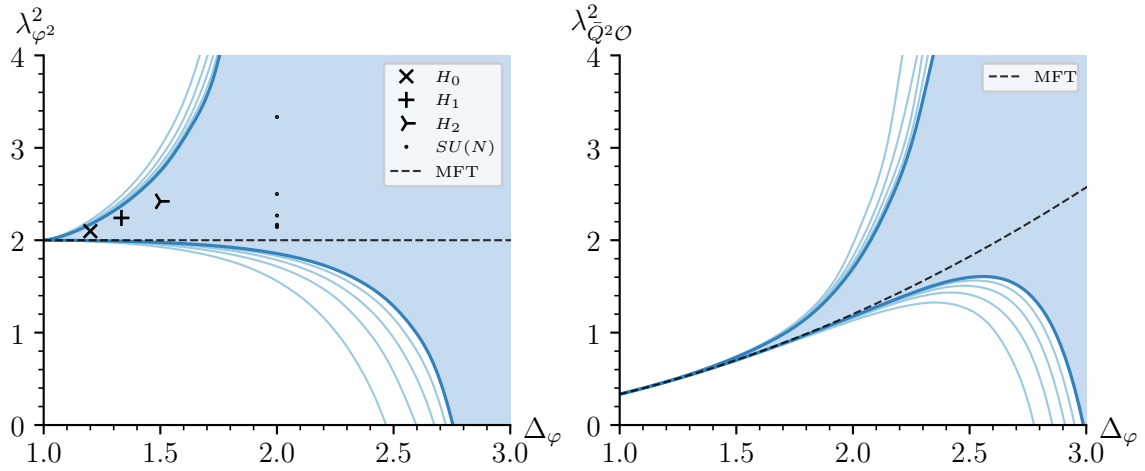
Figure 7.1: Upper and lower bounds on the OPE coefficients of operators φ^2 and $\bar{Q}^2\mathcal{O}$ in $\varphi \times \varphi$, where φ is the highest weight of a chiral multiplet. Curves are shown for $\Lambda = 16, 20, 24, 28, 32$, and the allowed region is filled. In the left figure, the values for the rank one H_0, H_1 and H_2 theories were computed in the large r-charge limit in [314, 315]. We also present free $SU(N)$ gauge theory values for $N = 2, \ldots, 6$, which as $N \to \infty$ approach the mean-field theory solution (MFT).

It is interesting now to compare our results with the works [314, 315], where analytic expressions were obtained for $\lambda^2_{\varphi^2}$ for the Argyres-Douglas theories of table 7.1. In [314] the authors obtained an expression valid to all orders in $1/r$, without taking into account exponentially-suppressed non-perturbative contributions, which could be relevant for the case of interest to us where $r = \Delta_\varphi$ is of order one.[10] The approach of [315] also relies on

---

[10]We thank D. Orlando for an interesting discussion on this point.

taking a large r-charge limit, that can be analyzed using Random Matrix Theory (RMT) techniques. The two methods give very similar results, which we have added to figure 7.1, and observe that they sit in the allowed region. Figure 7.1 is agnostic regarding the value of the central charge c, so we can refine these bounds by fixing c to the Argyres-Douglas values of table 7.1, and also by increasing the number of derivatives Λ. This allows for a better comparison between the bootstrap and large r-charge results which we present in table 7.7. There is surprising agreement between the two approaches, especially considering the analytic results were calculated using a large-r expansion, and the values of r for these operators are quite low. The values for the $\bar{Q}^2\mathcal{O}$ OPE coefficients are exclusive to the bootstrap and have not been estimated by other techniques.

	Lower bound	Upper bound	Resummed [314]	RMT [315]
$\lambda^2_{\varphi^2}$ for H_0	2.142596	2.16509	2.1181	2.0982
$\lambda^2_{\varphi^2}$ for H_1	2.216735	2.35462	2.2129	2.2412
$\lambda^2_{\varphi^2}$ for H_2	2.299679	2.69898	2.3457	2.4206
$\lambda^2_{\bar{Q}^2\mathcal{O}}$ for H_0	0.468394	0.46893	–	–
$\lambda^2_{\bar{Q}^2\mathcal{O}}$ for H_1	0.571321	0.57544	–	–
$\lambda^2_{\bar{Q}^2\mathcal{O}}$ for H_2	0.714878	0.73218	–	–

Table 7.7: Upper and lower bounds on the OPE coefficients of operators φ^2 and $\bar{Q}^2\mathcal{O}$ in $\varphi \times \varphi$, where φ is the highest weight of a chiral multiplet. The parameters Δ_φ and c are fixed to the known values of the rank-one Argyres-Douglas theories in table 7.1. All bounds have been obtained at $\Lambda = 50$. In the rightmost columns we compare with the values computed by resuming an expansion in $1/r$ to all orders [314], and using Random Matrix Theory in [315].

There is a second, less obvious motivation for looking at these bounds. Using the extremal functional method it is possible to extract the spectrum of the theory which lives at the boundary of the exclusion region [66]. This idea has been used successfully in many applications, most importantly the $3d$ Ising model [63,124]. In our case we have two numerical bounds that are quite close to each other, and the hope is that the extracted

spectrum is a good approximation of the actual spectrum of the Argyres-Douglas models. The results of the analysis are collected in table 7.8 in the appendix. We are focusing on the $\ell = 0$ operators in the U and W channels. In particular, Δ_U is the dimension of the first superprimary in the $\varphi \times \bar{\varphi}$ OPE, Δ'_U of the second superprimary, and so on. For the $\varphi \times \varphi$ OPE, Δ_W and Δ'_W denote the dimension of the exchanged operators rather than the superprimaries. For the rank-one H_0 and H_1 theories a summary of results is

$$
\begin{aligned}
H_0 &: \quad \Delta_U \sim 2.7, \quad \Delta'_U \sim 5.9, \quad \Delta''_U \sim 9.2, \qquad \Delta_W \sim 4.8, \quad \Delta'_W \sim 7, \\
H_1 &: \quad \Delta_U \sim 3.0, \quad \Delta'_U \sim 5.9, \quad \Delta''_U \sim 9 - 13, \quad \Delta_W \sim 5.3, \quad \Delta'_W \sim 6 - 8.
\end{aligned}
\tag{7.53}
$$

These are rough averages of the results in table 7.8, for which there is no rigorous way to estimate the errors. In the next section we are going to use these numbers as a guide and attempt to isolate these models using bounds on scaling dimensions, and as we will see, a consistent picture emerges.

Dimension bounds

Having obtained a rough estimate of the spectrum of operators for the H_0 and H_1 rank-one Argyres-Douglas theories, let us now try to isolate them using the numerical bootstrap for conformal dimensions. More precisely, we will fix the dimensions of the external chiral operator φ and the central charge to c to the values listed in table 7.1. We then plot the allowed region for Δ_U and Δ_W, assuming they are the dimensions of the lowest-lying operators in their respective channels. We also assume gaps for the next operator in the spectrum consistent with (7.53):

$$
\begin{aligned}
H_0 &: \quad \Delta'_U \geq \{3.0, 4.0\}, \quad \Delta'_W \geq \{5.0, 5.5\}, \\
H_1 &: \quad \Delta'_U \geq \{3.5, 4.5\}, \quad \Delta'_W \geq \{5.5, 6.0\}.
\end{aligned}
\tag{7.54}
$$

The results of this analysis can be found in figure 7.2. We observe that even for the most conservative choices of gaps, the allowed region is a fairly small island in the (Δ_U, Δ_W) plane. The effect of reducing the gaps in either channel is to allow for solutions to crossing with smaller dimensions.

An alternative but similar strategy is to focus on a particular channel, like the U-channel that contains operators neutral under all symmetries. We plot the allowed values of Δ_U and Δ'_U, assuming they are the lowest dimension operators, and assume different gaps for the next operator Δ''_U consistent with the approximate spectrum in (7.53):

$$
H_0, \, H_1 : \quad \Delta''_U \geq \{6.0, \, 7.0, \, 8.0, \, 9.0\}.
\tag{7.55}
$$
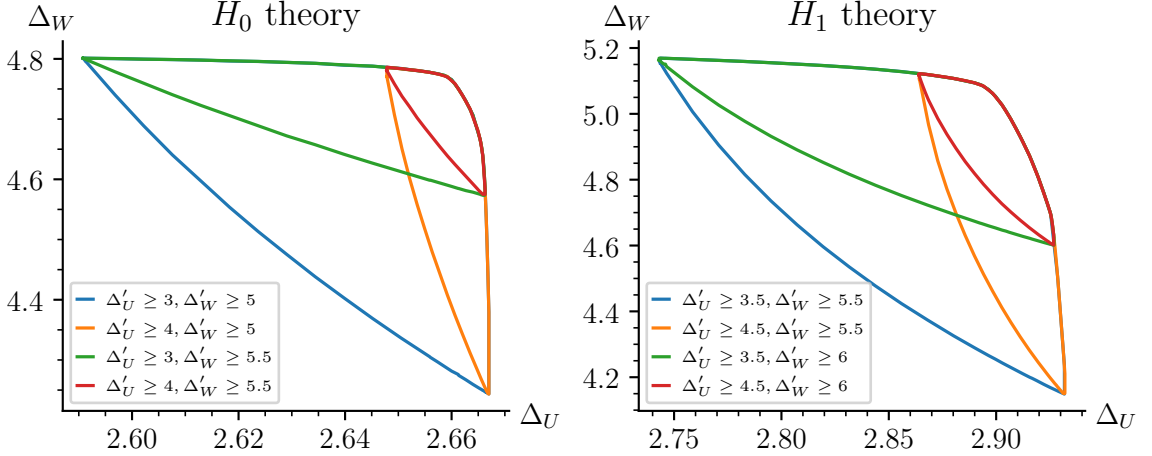
Figure 7.2: Dimension Δ_U of the lowest dimension unprotected operator in the $\varphi \times \bar{\varphi}$ channel, versus dimension Δ_W of the lowest dimension unprotected operator in the $\varphi \times \varphi$ channel. We fix the dimension of the external operator φ and the central charge c, and impose gaps with the next operators in the spectrum Δ'_U and Δ'_W. All bounds have been obtained with cutoff $\Lambda = 32$.

The results of this analysis can be found in figure 7.3. In this case we observe two qualitatively distinct behaviors. For $\Delta''_U \geq 7, 8, 9$ once again we obtain a small allowed region in the the (Δ_U, Δ'_U) plane. The estimate for Δ_U from this analysis is compatible with the one from figure 7.2. On the other hand, when the gap is lowered further to $\Delta''_U \geq 6$, the allowed region is no longer a small disconnected island. Let us focus on the H_0 plot, although the conclusion is identical for H_1. There are clearly two different regimes when $\Delta''_U \geq 6$. In the first, Δ_U can take any value between the unitarity bound 2 and ~ 2.6, provided that $\Delta'_U \sim 2.66$. In the second, Δ'_U can take any value between ~ 2.7 and ~ 6 provided that $\Delta_U \sim 2.66$. Summarizing, we are assuming there are only two operators with $\Delta_U, \Delta'_U < \Delta''_U$. If the gap Δ''_U is small enough, crossing allows one operator to have arbitrary conformal dimension as long as the other is at $\Delta_U \sim 2.66$. Thus, the bootstrap insists on having a long operator with dimension $\Delta_U \sim 2.66$, even when the gaps are lowered, but it cannot resolve the position of the next operator Δ'_U.

We should point out that these results are not on the same footing as the Ising model island [58], where the gaps were physically justified by assuming only two relevant operators in the spectrum, and moreover the island was obtained by studying mixed correlators. Our
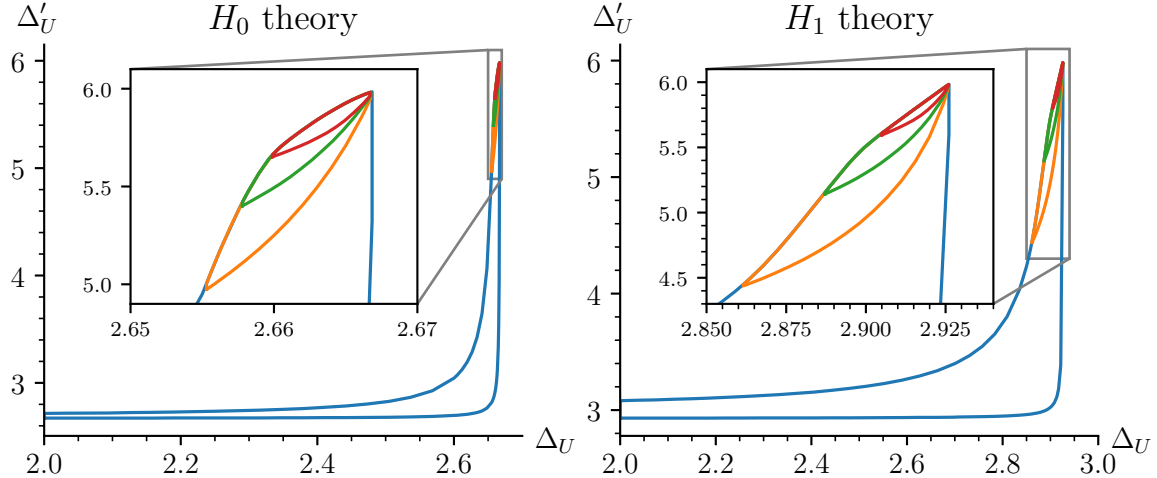
Figure 7.3: Dimensions Δ_U versus Δ'_U of the two lowest dimension unprotected operators in the $\varphi \times \bar{\varphi}$ channel. We fix the dimension of the external operator φ and the central charge c, and impose a gap with the next operator in the spectrum $\Delta''_U \geq 6, 7, 8, 9$. For Δ''_U greater than 7 we provide a zoom to the allowed region, which form small islands isolated from the continuum. All bounds have been obtained with cutoff $\Lambda = 32$.

analysis was inspired by the one in [104], where numerical islands were obtained using a single-correlator bootstrap, by assuming mild gaps around conserved currents, similar to what we did here.

We expect this single-correlator approach to give at least qualitative results for the H_0 theory, which we are assuming is in a sense "simple" and perhaps one of the models that has the best chance to be solved by bootstrap methods. Circumstantial evidence in favor of its simplicity include the fact that the theory is rank one, it has no Higgs branch, it has the minimum allowed value of c among interacting theories, and the associated chiral algebra is the Yang-Lee edge singularity, arguably the simplest non-trivial $2d$ model with Virasoro symmetry.

For H_1 on the other hand we expect more structure. This model does have some simplifying features similar to those of H_0, however there is an $SU(2)$ flavor symmetry and therefore Higgs branch operators. We will therefore consider the full mixed system of correlators in our attempts to corner this theory.

7.4.2 Moment map correlators

Before we jump to the full mixed system, let us also look at the single correlator of moment map operators, see (7.46). For later purposes, we will be mostly be interested on bounding the dimension of operators which are neutral under all symmetries, i.e. multiplets appearing in the U channel. These bounds depend heavily on the values of the central charge c and the flavor central charge k. In figure 7.4 we present upper bounds on Δ_U, the dimension of the first unprotected operator in the singlet channel of the $M \times M$ OPE. We have chosen the values of k to match some of the theories in table 7.1, for example H_1, H_2 and $SU(N)$ SCQCD, and the rest provide a convenient interpolation between them.
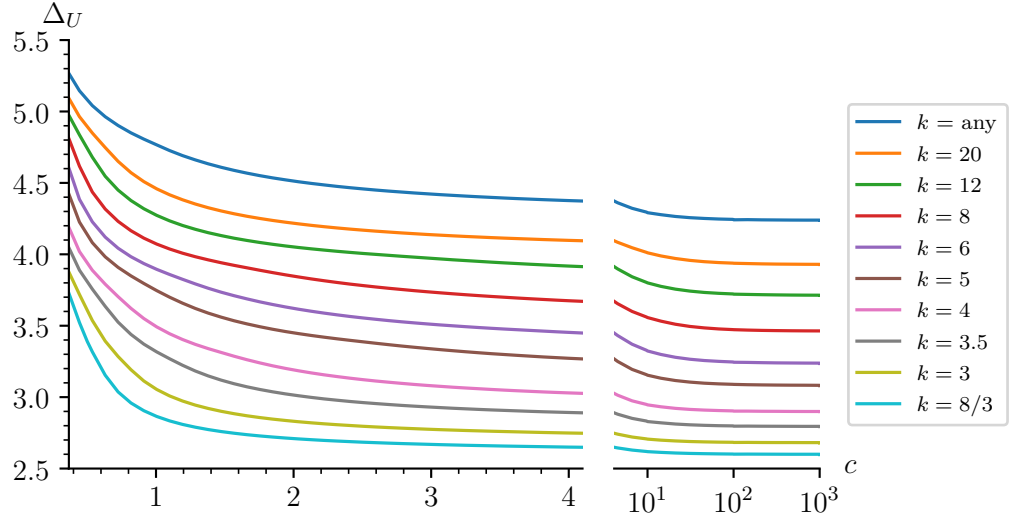
Figure 7.4: Upper bound on the dimension Δ_U of the first singlet operator in the OPE $M \times M$ of two moment map operators. The values of the flavor central charge from bottom to top are $k = 8/3, 3, 7/2, 4, 5, 6, 8, 12, 20,$ any. The bounds for $c = 10^3$ and $c = \infty$ are identical with the resolution of the plot. All results are obtained at $\Lambda = 32$.

We see that the upper bound on Δ_U decreases as we increase the central charge c, while it increases as we increase k. If we do not make assumptions about c, the upper bound is dominated by the small c values. If we do not make assumptions about k, the bound is dominated by the large k region. These considerations will be important when we look at the mixed correlator results. A more comprehensive survey of bounds from the moment

map four-point function is available in [216], including dimension bounds on the X and Y channel, as well as bounds on c and k.

7.4.3   Mixed correlators

We are finally ready to consider the full mixed system of crossing equations (7.51). The bounds we derive no longer apply to the rank-one H_0 theory, because there is no flavor symmetry and therefore no moment map operator. However, they apply to the higher rank version of H_0 with the flavor given by the $SU(2)_L$ symmetry, as well as all other theories discussed in section 7.2.1.

In general one expects the mixed correlator bootstrap to be most efficient when there is an overlap between the two types of operators. For this reason we focus in the U channel, which appears both in the $\varphi \times \bar\varphi$ and $M \times M$ OPEs, and also in the Z channel, which contains operators in the $\varphi \times M$ OPE. This last channel is of particular interest because it captures a new family of operators inaccessible from the single correlators studied so far. Numerical bounds on the central charges c and k can also be obtained, however the analytic bounds obtained from the associated chiral algebra [246,248] are quite strong, and the numerical methods used here will not improve on them.

U-channel dimension bounds

We start bounding the dimension Δ_U of the first unprotected multiplet in the $\varphi \times \bar\varphi$ and $M \times M$ OPEs. The crossing equations (7.51) contain three canonical parameters: the central charge c, the flavor central charge k and the dimension Δ_φ of the Coulomb branch operator. Ideally we would like to obtain Δ_U for all possible values of (c, k, Δ_φ), but exploring a three-dimensional parameter space is computationally intensive. Instead, in figure 7.5 we plot Δ_U for different values of (c, Δ_φ) without restrictions on k, and in figure 7.6 we plot Δ_U for different values of (k, Δ_φ) without restrictions on c.

Before we discuss the results in detail, let us summarize some of our expectations. The single correlator bound of Δ_U as a function of Δ_φ using the chiral correlators was studied in detail in [198, 216, 217]. The upper bound on Δ_U grows with Δ_φ with approximately the same slope as the mean field theory solution $\Delta_U \sim 2\Delta_\varphi$. On the other hand, from the moment map correlator the bound is $2.5 \leq \Delta_U \leq 5.5$, which is independent of Δ_φ and changes with c and k as shown in figure 7.4. It is natural to expect that for small Δ_φ the upper bound is dominated by the chiral bound, while for large Δ_φ it is dominated by the

moment map bound. This is indeed the behavior we observe in figures 7.5 and 7.6. We also know that for $c, k \to \infty$ the numerical bounds cannot rule out the intersection of the mean field theory (MFT) solutions:

$$\Delta_U = 2\Delta_\varphi \quad \text{for} \quad \Delta_\varphi \le 2, \qquad \Delta_U = 2\Delta_M = 4 \quad \text{for} \quad \Delta_\varphi \ge 2. \tag{7.56}$$

These are plotted with a black dashed line in the figures.
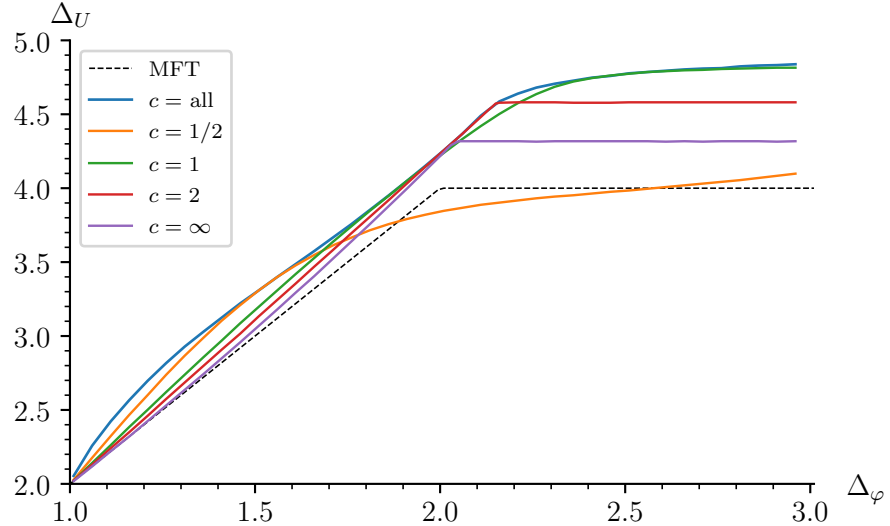
Figure 7.5: Upper bound on the dimension Δ_U of the first unprotected operator in the $\varphi \times \bar{\varphi}$ and $M \times M$ OPEs as a function of the dimension of the chiral operator Δ_φ. The flavor central charge k is not fixed to a particular value. In the top blue curve, the central charge c is also free, while it takes values $c = 1/2, 1, 2, \infty$ in the curves below it. The black dashed curve is the mean field theory value (7.56). All results are computed with $\Lambda = 24$.

In figure 7.5 the flavor central charge k is arbitrary, and as discussed in section 7.4.2, the upper bound will be dominated by the $k \to \infty$ region of parameter space. Let us first look at the $\Delta_\varphi \le 2$ regime. For low values of the central charge, the upper bound insists on staying above the mean-field theory (MFT) solution even when Λ is increased. For large values of the central charge the upper bound gets closer to the MFT value. As expected, when we approach $\Delta_\varphi = 1$ the upper bound approaches the free-theory value $\Delta_U = 2$ regardless of the central charge. The behavior is significantly different for $\Delta_\varphi \ge 2$, where the curves start flattening as dictated by the moment map crossing symmetry. For small

values of the central charge $1/2 \leq c \leq 1$ this transition is smooth. However, as we increase the central charge $c \geq 2$ the transition becomes sharp resulting in a kink around $\Delta_\varphi \sim 2$.

By extrapolating the numerics to $\Lambda \to \infty$ it seems that the kink of the $c = \infty$ curve will eventually land on $(\Delta_\varphi, \Delta_U) = (2, 4)$ which corresponds to mean field theory (MFT). The conclusion is then that for large central charge the numerical bootstrap rules out any theory with a leading gap larger than the MFT value. This is precisely what was observed in $\mathcal{N} = 4$ SYM in [221, 223]. In this case, the mean field theory solution is interpreted as the large N and large $\lambda = g_{YM}^2 N$ limit of $\mathcal{N} = 4$ SYM, whose correlators are captured by tree-level supergravity. We now have a similar phenomenon but for $\mathcal{N} = 2$ SCFTs with $SU(2)$ flavor symmetry, which incidentally also includes $\mathcal{N} = 4$ SYM. If we consider the $\mathcal{N} = 2$ decomposition of $\mathcal{N} = 4$ theories, part of the $SU(4)$ R-symmetry gets re-interpreted as a global $SU(2)$ flavor symmetry. Furthermore, the decomposition of the $\mathbf{20'}$ multiplet (the one studied in [221, 223]) into $\mathcal{N} = 2$ contains a chiral and antichiral operator of dimension $\Delta_\varphi = 2$, and a moment map multiplet [27]:

$$\mathcal{O}_{\mathbf{20'}} \sim M + \varphi + \bar{\varphi} + \dots, \tag{7.57}$$

the same multiplets that we are studying in this work. Figure 7.5 presents a bound on the lowest-dimension multiplet which has a scalar superprimary that is neutral under R-symmetry, so it should include $\mathcal{N} = 4$ SYM. The plot is however more general and valid for any $\mathcal{N} = 2$ theory with $SU(2)$ flavor. For $2 \leq c < \infty$ it is unclear to us whether the kinks corresponds to physical $\mathcal{N} = 2$ theories.

In figure 7.6 we consider the reversed situation, the central charge c is not fixed, but we allow k to take different values. In this case, we observe a behavior qualitatively similar as before. For $\Delta_\varphi \leq 1.5$, the upper bound stays above MFT and grows almost parallel to it. For $1.5 \leq \Delta_\varphi \leq 2.2$, depending on the value of k, the curves start to be dominated by the moment map part of crossing and they flatten. This flattening is smooth and we do not observe any kinks like the ones found before. The lowest upper bound in figure 7.6 is obtained by fixing both central charges c and k to the values of the H_1 theory. For H_1 we know $\Delta_\varphi = \frac{4}{3}$, which corresponds to an upper bound $\Delta_U = 2.94$. For larger Δ_φ the upper bound becomes flat at the value $\Delta_U = 3.4$ for $\Lambda = 24$. As one increases the number of derivatives Λ, the upper bound $\Delta_U = 2.94$ is very robust and does not decrease, while the asymptotic value $\Delta_U = 3.4$ has not converged and is still decreasing. Ideally, for $\Lambda \to \infty$ the two upper bounds would coincide, in which case the point $(\Delta_\varphi, \Delta_U) = (1.33, 2.94)$ would become a kink, and one could claim that the H_1 theory saturates the numerical
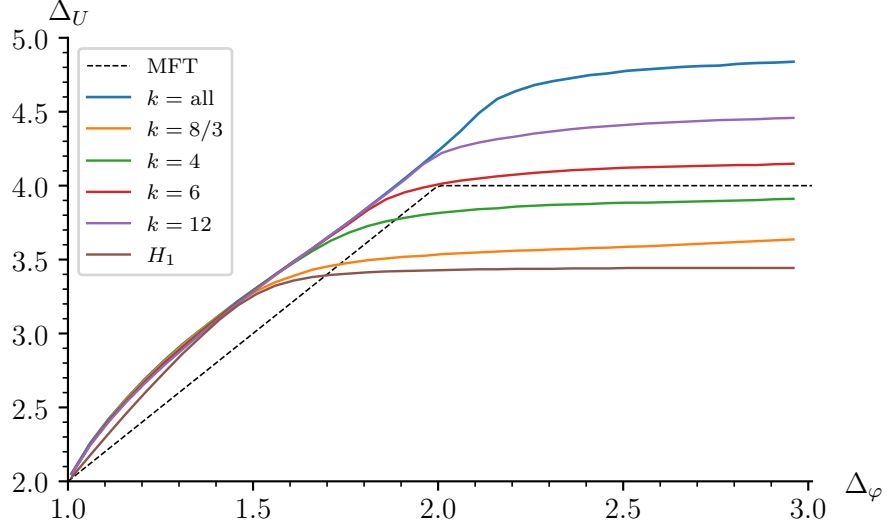
Figure 7.6: Upper bound on the dimension Δ_U of the first unprotected operator in the $\varphi \times \bar{\varphi}$ and $M \times M$ OPEs as a function of the dimension of the chiral operator Δ_φ. The central charge c is not fixed to a particular value. In the top blue curve, the flavor central charge k is also unfixed, while it takes values $k = 8/3, 4, 6, 12$ in the curves below it. For the brown curve, both central charges are fixed to the values of the H_1 theory $c = \frac{1}{2}$, $k = \frac{8}{3}$. The black dashed curve is the mean field theory value (7.56). All results are computed with $\Lambda = 24$.

bounds. Looking at the asymptotics of our numerics however it seems unlikely $\Delta_U = 3.4$ will go down below $\Delta_U \sim 3$.

Focusing on H_1

Let us now change gears for a moment. Instead of presenting bounds applicable to general $\mathcal{N} = 2$ SCFTs, we will try to use crossing symmetry to focus on the rank-one H_1 Argyres-Douglas theory. Besides the central charges c, k and the dimension of the Coulomb branch generator Δ_φ, using the superconformal index [330, 334] one can show that the short multiplet $L\bar{B}[0;0]^{(2;r)}$ that could appear in the $\varphi \times M$ OPE is missing[11] (see table 7.6). One

---

[11]We thank L. Rastelli for suggesting that this OPE coefficient might vanish in the H_1 theory, and J. Song for confirming that this is indeed the case.

should be aware that this is not a definitive proof that the multiplet is absent, and it could be a consequence of cancelations between different contributions to the index[12]. We will nevertheless assume the multiplet is absent, and try to leverage this information to learn about the spectrum of the H_1 theory.
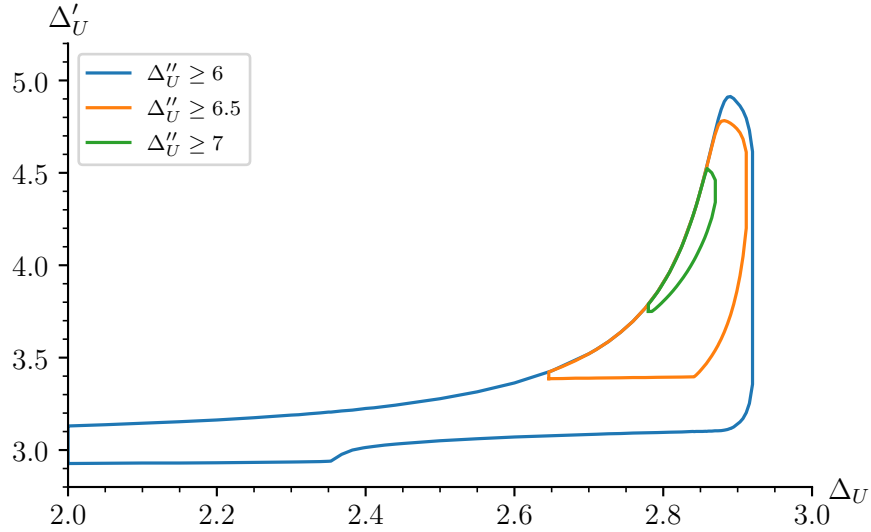
Figure 7.7: Allowed values of Δ_U versus Δ'_U, the dimensions of the first two multiplets in the $\varphi \times \bar{\varphi}$ and $M \times M$ OPEs. We assume that these are the only two operators below $\Delta''_U \geq \{6, 6.5, 7\}$ and the parameters Δ_φ, c, k are fixed to the values of the rank-one H_1 theory. The allowed region is enclosed between the upper and lower curves. The numerical optimization is using $\Lambda = 24$.

Following the approach of figure 7.3, we assume that there are only two operators in the U channel with $\Delta_U, \Delta'_U \leq \Delta''_U$, and find the allowed region in the plane (Δ_U, Δ'_U). Using only the single correlator and assuming a sparse spectrum we managed to obtain a small island. Now we will complement that result by adding constraints coming from Higgs branch operators which we know are present in the H_1 theory. Using the full mixed correlator system we observe in figure 7.7 that the gaps $\Delta''_U \geq \{6, 6.5, 7\}$ are allowed, but larger gaps are ruled out. For the smallest gap we find a change of behavior in the lower bound around $\Delta_U = 2.35$, for which we do not currently have an interpretation. To be on the safe side, in the next figure we will assume the most conservative gap $\Delta''_U \geq 6$.

---

[12]We thank Madalena Lemos for comments regarding this issue.
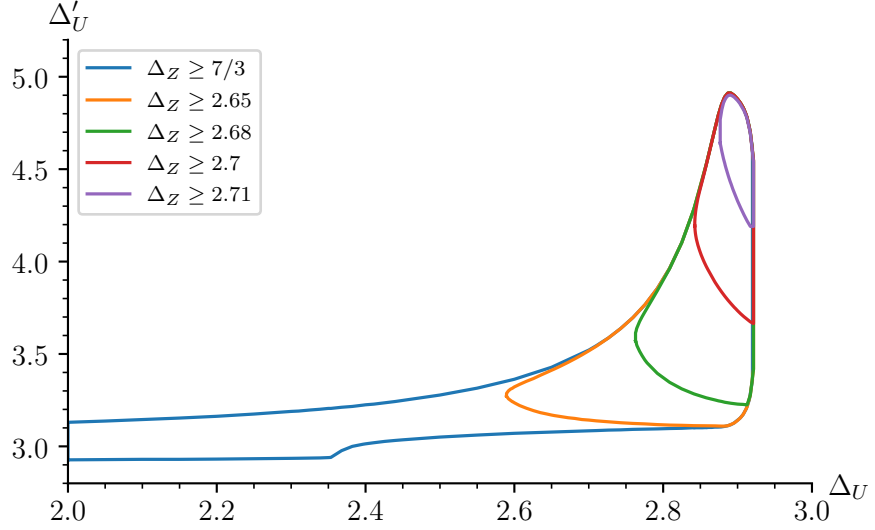
Figure 7.8: Allowed values of Δ_U versus Δ'_U, the dimensions of the first two multiplets in the $\varphi \times \bar{\varphi}$ and $M \times M$ OPEs, as a function of the gap Δ_Z in the channel $\varphi \times M$. We assume that these are the only two operators below $\Delta''_U \geq 6$, that the short multiplet φM is missing, and the parameters Δ_φ, c and k are fixed to the values of the rank-one H_1 theory. The allowed region is enclosed between the upper and lower curves. The numerical optimization is using $\Lambda = 24$.

The advantage of having the mixed correlator system is that we have a host of gap combinations we can assume. In particular, since we know that the short operator $\varphi M \in \varphi \times M$ is missing in the H_1 theory, it is natural to impose a gap in this channel until the first long operator Δ_Z. The results, shown in figure 7.8, indicate that as we increase the gap in the Z channel, the allowed region shrinks to a small island around $(\Delta_U, \Delta'_U) \sim (2.9, 5)$. In this case the value of Δ_U is saturating the upper bound in figure 7.6. We are tempted to conjecture that H_1 is characterized by a solution of crossing without the short multiplet φM and maximal gap Δ_Z, and we will see in later discussions that this seems to be indeed a distinguished point in our numerical plots. However, more work will be needed to see whether this is indeed the case.

Z-channel dimension bounds

Let us conclude the study of conformal dimensions by putting an upper bound on the dimension Δ_Z of the first unprotected operator in the $\varphi \times M$ OPE with $\ell = 0$. As discussed in the previous section, the most general situation is to have a protected operator φM at the unitarity bound $\Delta = \Delta_\varphi + 1$, after which there is a gap until the first unprotected operator at Δ_Z. In some cases however, like the H_1 theory, the short operator might be missing. One can also put gaps on the U channel on top of the Z-channel gaps, starting with the agnostic case $\Delta_U \geq 2$. In the numerical bounds of figure 7.9 we consider several possibilities. We have also explored different central charges (c, k), but the results were not significantly different and therefore we assume general values for them.
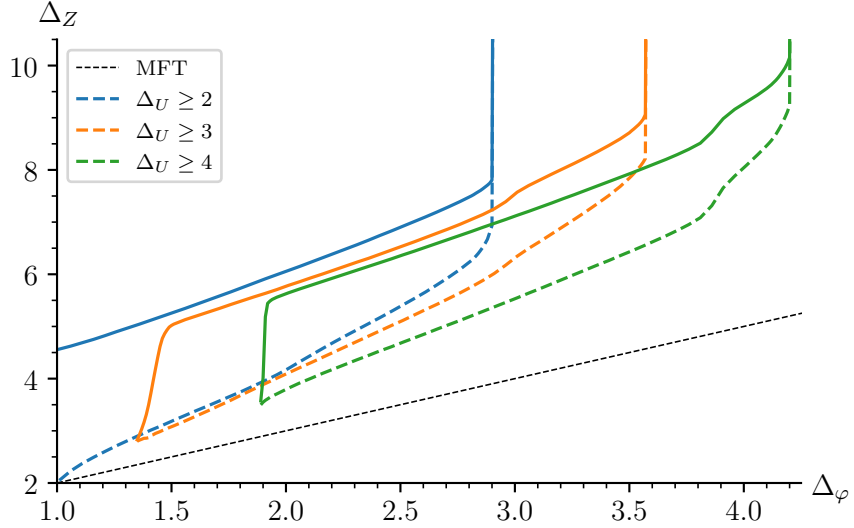
Figure 7.9: Upper bounds on the dimension of the first unprotected multiplet in the $\varphi \times M$ OPE, as a function of the dimension of the Coulomb branch operator φ and the gaps in the U channel $\Delta_U \geq \{2, 3, 4\}$. The solid line corresponds to the most general case, when the short operator φM sits at the unitarity bound $\Delta = \Delta_\varphi + 1$ and Δ_Z is the position of the first long operator. The dashed line is obtained by the further assumption that the short operator is not present. All results are obtained with $\Lambda = 24$.

The first thing that one observes in figure 7.9 is that discarding the short operator φM leads to much stronger bounds than in the general case. For theories like H_1, where the

short is indeed missing, we have

$$H_1 \quad : \quad \frac{7}{3} \approx 2.33 \leq \Delta_Z \leq 2.90 \,. \tag{7.58}$$

Note that in figure 7.8 we obtained the stronger bound $2.33 \leq \Delta_Z \leq 2.73$, but we assumed there are only two operators in the U channel with $\Delta_U, \Delta'_U \leq 6$.

It is also interesting to add a gap in the U channel. From figures 7.5 and 7.6, this restricts the dimension of the Coulomb branch operator, namely $\Delta_U \geq 3$ requires that $\Delta_\varphi \geq 1.34$ and $\Delta_U \geq 4$ requires that $\Delta_\varphi \geq 1.86$. Indeed, when in figure 7.8 we assume gaps in Δ_U the curves start at the values of Δ_φ just discussed. More importantly, at these values the upper bounds with and without short operator φM coincide. Since there is a unique solution to crossing at the boundary of the allowed region, the solutions that saturate the bound for arbitrary c and k of figure 7.5 do not have the short operator φM in the spectrum. This suggests that the H_1 theory saturates the bounds in figure 7.5.

Finally, the reader can see from figure 7.8 that for large values of Δ_φ, the upper bound of Δ_Z diverges, i.e. for Δ_φ high enough any value of Δ_Z is allowed. Increasing the gap in Δ_U moves the position of this divergence to the right, but does not remove it. We have tried different parameters of the numerical solver, either increasing the number of spins kept $\ell_{\max}$, increasing the precision used by `sdpb`, or adding more poles to improve the polynomial approximation, but none of these measures has changed the results. We currently do not know the reason of this divergence. It has been observed previously that mixed correlator bootstrap problems involving large external dimensions can be numerically unstable,[13] and perhaps we found another instance of these instabilities.

OPE bounds

Let us conclude our numerical exploration of the crossing equations (7.51) by obtaining upper and lower bounds on OPE coefficients. As mentioned previously, we will not attempt to bound the central charges c and k, because the analytic bounds obtained in [247, 248] are quite strong. We will focus our efforts on studying the operators that appear in the new channel $\varphi \times M$.

As already discussed, restricting to scalars in the $\varphi \times M$ OPE means we have two types of operators, a short protected one at the unitarity bound that we call φM, followed by

---

[13]A possibly related issue appeared in figure 6 of [214]. Instabilities in the context of mixed correlator bootstrap were discussed in [335].
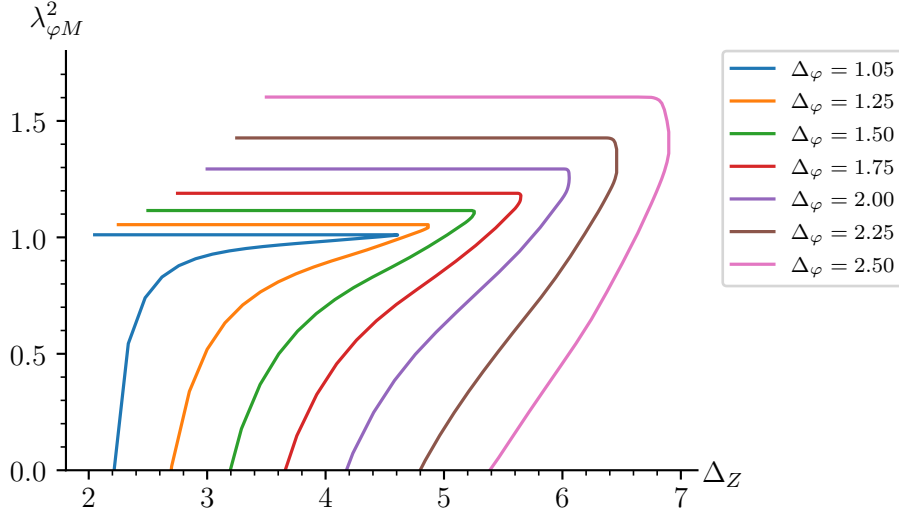
Figure 7.10: Upper and lower bounds of the protected operator φM that appears in the $\varphi \times M$ OPE, as a function of the dimension Δ_Z of the first long in the same channel. We compare the results for different dimensions of the Coulomb branch operator Δ_φ. All numerical optimizations are performed at $\Lambda = 24$.

an unprotected multiplet whose primary has dimension $\Delta_Z > \Delta_\varphi + 1$. In figure 7.10, we put upper and lower bounds on the OPE coefficient $\lambda^2_{\varphi,M,\varphi M} \equiv \lambda^2_{\varphi M}$ as a function of the dimension of the long Δ_Z. These bounds depend strongly on the dimension of the Coulomb branch generator Δ_φ; we have also experimented changing the central charges c and k but they had little influence on the final result. When the dimension of the long is close to the unitarity bound, only upper bounds are obtained, but as we increase Δ_Z we can eventually also obtain lower bounds on the OPE coefficients. The value of Δ_Z where the lower bound appears corresponds precisely to the maximum gap for a theory without the φM multiplet, namely the blue dashed line in figure 7.9. As we increase Δ_Z even more, the upper and lower bounds eventually meet, and after that point there are no solutions of crossing; this corresponds to the blue solid line in figure 7.9.

One might also be interested in the OPE coefficients of the scalar long operators in the $\varphi \times M$ OPE, which are presented in figure 7.11. In this case we are only able to obtain upper bounds because the operators belong to a continuum. We see that the value of these OPE coefficients decreases monotonically with the dimension Δ_Z of the operator. At a

117
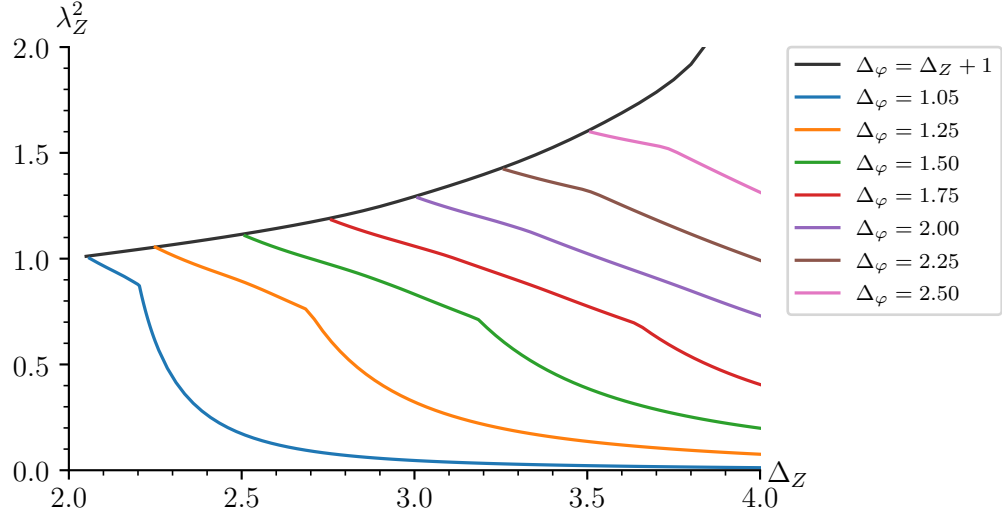
Figure 7.11: Upper bounds on the OPE coefficient of a long scalar multiplet of dimension Δ_Z in the $\varphi \times M$ OPE, for different dimensions of the Coulomb branch operator φ. Notice we do not assume that Δ_Z is the lowest dimension of an operator in the Z channel. The black line corresponds to the upper bound for the operator φM at the unitarity bound $\Delta_Z = \Delta_\varphi + 1$. All results are obtained with $\Lambda = 24$.

certain value of Δ_Z, which corresponds precisely to the point where $\lambda^2_{\varphi M}$ acquires a lower bound in figure 7.10, one can observe a kink. From the discussion around figure 7.9 this also seems to be the point that saturates the upper bounds of figures 7.5 and 7.6. Once again, it is very tempting to conjecture that the rank-one H_1 Argyres-Douglas theory lives at this kink.

7.5 Conclusions

In this work we appplied the numerical bootstrap to mixed correlators in $\mathcal{N} = 2$ superconformal theories. We refined single-correlator bounds for OPE coefficients and compared them successfully to recent results obtained in the limit of large r charge [314, 315]. The improved bounds allowed us to extract an approximate spectrum for selected Argyres-Douglas models, information that we then used to obtain numerical islands in the space of conformal dimensions.

We then proceeded to study a mixed system between Coulomb branch operators and the moment map. Even though these type of correlators had been analyzed before [198,216, 217], this is the first time mixed correlators for different types of multiplets are considered in the $4d$ $\mathcal{N} = 2$ bootstrap.

As a necessary step towards the mixed system we calculated new superconformal blocks, a result interesting on its own. Recent progress that attempts to systematize the study of superblocks include the connection to Calogero-Sutherland models [240, 241], and the analytic superspace approach of [336]. Here we have contributed a new entry to the list of known superblocks, and the simplicity of our expressions hints at a simple description within the framework of [240, 241, 336].

With the mixed system at hand we applied the numerical bootstrap machinery. Figures 7.5 and 7.6 are good examples that capture how the full system behaves. As explained in the main text, there are two regimes dominated by the individual single-correlator bounds, and the mixed system smoothly interpolates the two. The fact the interpolation is smooth is slightly disappointing, because this happens in a region where we know Argyres-Douglas models live, and there is no sharp feature signalizing their presence. The bounds are nevertheless valid and give rigorous constraints on the spectrum of these theories. The mixed system also allowed us put constraints on a region of the landscape that was unexplored until now.

One possible future direction is to continue adding information in the form of extra operators. For the H_0 theory, any additional new type of multiplet will not be of the half-BPS type considered in this work, instead it will have to be semi-short or long multiplets of the superconformal algebra, which means the four-point kinematics will be challenging. However, such studies can shed light on the validity of the numerical islands found in section 7.4. Within the realm of Coulomb and Higgs branch operators, the next natural system to consider is φ_{r_1}, φ_{r_2} and M. The rank-two (A_1, A_5) theory[14] contains precisely these type of multiplets with a $U(1)$ flavor symmetry, and although computationally this system will be more intensive than the one considered here, it is still within reach.

A long-term direction is the inclusion of the stress-tensor multiplet. The blocks for its superconformal primary operator were obtained in [337], however the numerical bootstrap has not been implemented yet. Perhaps one of the reasons this has not been done is that these this correlator is known to have nilpotent invariants [247], which means that to impose the full $\mathcal{N} = 2$ constraints one needs to include correlators of superconformal

---

[14]In this notation, the rank-one H_0, H_1 and H_2 models are (A_1, A_2), (A_1, A_3) and (A_2, A_2) respectively.

descendants. Adding the stress tensor multiplet to the correlators studied here will allow us to bootstrap all three canonical multiplets in one mixed system, and impose a huge amount of input coming from supersymmetry. Five years ago such a problem would have been clearly unfeasible, but thanks to the impressive progress on the numerical front [77], the bootstrap for correlators with several external operators is now a reality.

7.A Blocks in the mixed channel

In this appendix we compute the superconformal blocks involving mixed chiral and moment map operators. The arguments rely mostly on representation theory, and no calculations of three-point functions or Casimir equations are required.

7.A.1 Decomposition of $\mathcal{N} = 2$ into $\mathcal{N} = 1$

The $\mathcal{N} = 1$ and $\mathcal{N} = 2$ superconformal algebras share the same conformal algebra, but differ in the fermionic generators. The $\mathcal{N} = 2$ Poincare supercharges are Q_α^I, $\bar{Q}_{I\dot\alpha}$ for $I = 1, 2$ and $\alpha, \dot\alpha = 1, 2$. We can embed the $\mathcal{N} = 1$ subalgebra by keeping only the $I = 1$ component

$$(Q_\alpha)_{\mathcal{N}=1} = (Q_\alpha^1)_{\mathcal{N}=2}, \qquad (\bar{Q}_{\dot\alpha})_{\mathcal{N}=1} = (\bar{Q}_{1\dot\alpha})_{\mathcal{N}=2}, \tag{7.59}$$

and similarly for the conformal supercharges S_α and $\bar{S}_{\dot\alpha}$. The R-symmetry is reduced from $SU(2)_R \times U(1)_r$ to $U(1)_r$ as follows

$$r_{\mathcal{N}=1} = \frac{1}{3} (r - 2R_3)_{\mathcal{N}=2}, \tag{7.60}$$

and each $SU(2)_R$ representation $[R]$ decomposes into the eigenvalues $R_3 = -R, -R + 2, \ldots, R - 2, R$. Now we study the implications of this decomposition for the chiral and moment map multiplets.

Remember that a chiral operator is a scalar killed by all $\bar{Q}_{I\dot\alpha}$ supercharges, so it can also be understood as an $\mathcal{N} = 1$ chiral $\varphi_r \to \phi_{\frac{r}{3}}$, where the r charge assignment follows from (7.60). Here and in what follows, we denote the superprimary operator of an $\mathcal{N} = 1$ chiral multiplet by ϕ_r, satisfying the shortening $[\bar{Q}_{\dot\alpha}, \phi_r(0)] = 0$. The r denotes its $U(1)_r$ charge, which is related to the conformal dimension by $\Delta_\phi = \frac{3}{2}r$.

On the other hand, the moment map operator is a scalar satisfying the shortening conditions (7.2). We can reduce them to $\mathcal{N} = 1$ shortening conditions, noting $Q_{2\alpha} \to -Q_\alpha$

and $\bar{Q}_{1\dot{\alpha}} \to \bar{Q}_{\dot{\alpha}}$:

$$[\bar{Q}_{\dot{\alpha}}, M_{11}(0)] = 0, \qquad [Q^2, M_{12}(0)] = [\bar{Q}^2, M_{12}(0)] = 0, \qquad [Q_\alpha, M_{22}(0)] = 0. \qquad (7.61)$$

Thus the components M_{11}, M_{12} and M_{22} are $\mathcal{N} = 1$ chiral, $\mathcal{N} = 1$ current and $\mathcal{N} = 1$ antichiral operators:

$$M_{11} \to \phi_{\frac{4}{3}}, \qquad M_{12} \to J, \qquad M_{22} \to \bar{\phi}_{-\frac{4}{3}}. \qquad (7.62)$$

Finally, we will use repeatedly the decomposition of $\mathcal{N} = 2$ long multiplets without $SU(2)_R$ charge into $\mathcal{N} = 1$ multiplets:

$$
\begin{aligned}
L\bar{L}[j,\bar{\jmath}]_\Delta^{(0;r)} \to & L\bar{L}[j,\bar{\jmath}]_\Delta^{(\frac{1}{3}r)} \\
& + \sum_{s=\pm 1} L\bar{L}[j+s,\bar{\jmath}]_{\Delta+\frac{1}{2}}^{(\frac{1}{3}(r+1))} + \sum_{\bar{s}=\pm 1} L\bar{L}[j,\bar{\jmath}+\bar{s}]_{\Delta+\frac{1}{2}}^{(\frac{1}{3}(r-1))} \\
& + \sum_{s,\bar{s}=\pm 1} L\bar{L}[j+s,\bar{\jmath}+\bar{s}]_{\Delta+1}^{(\frac{1}{3}r)} + \sum_{s=\pm 1} L\bar{L}[j,\bar{\jmath}]_{\Delta+1}^{(\frac{1}{3}(r+2s))} \\
& + \sum_{s=\pm 1} L\bar{L}[j+s,\bar{\jmath}]_{\Delta+\frac{3}{2}}^{(\frac{1}{3}(r-1))} + \sum_{\bar{s}=\pm 1} L\bar{L}[j,\bar{\jmath}+\bar{s}]_{\Delta+\frac{3}{2}}^{(\frac{1}{3}(r+1))} \\
& + L\bar{L}[j,\bar{\jmath}]_{\Delta+2}^{(\frac{1}{3}r)}.
\end{aligned}
\qquad (7.63)
$$

This decomposition can be obtained combining the tables in [182] with the rule (7.60).

7.A.2 $\langle \varphi\bar{\varphi}MM \rangle$ correlator

In order to compute the blocks it is convenient to switch back to component notation for the moment map. In this section we suppress the adjoint flavor indices to simplify the notation. We start with the four point function (7.26):

$$\langle \varphi(x_1)\bar{\varphi}(x_2)M_{IJ}(x_3)M_{KL}(x_4) \rangle = \frac{\epsilon_{I(K}\epsilon_{J|L)}}{|x_{12}|^{2\Delta_\varphi}|x_{34}|^4} \sum_{\mathcal{O}\in A^+} \lambda_{\varphi\bar{\varphi}\mathcal{O}}\lambda_{MM\mathcal{O}} G_{\Delta,\ell}^{\varphi\bar{\varphi};MM}(z,\bar{z}). \quad (7.64)$$

The sum runs over all even spin supermultiplets that appear in the chiral-antichiral and moment map OPEs:

$$\varphi \times \bar{\varphi}, \ M \times M \ \sim \ \mathbb{1} + A\bar{A}[\ell;\ell]^{(0;0)} + L\bar{L}[\ell;\ell]_\Delta^{(0;0)}, \qquad \ell \text{ even}. \qquad (7.65)$$

By looking at the $(I,J) = (1,1)$ and $(K,L) = (2,2)$ components, we can think of (7.64) as a correlator of different $\mathcal{N} = 1$ chiral and antichiral operators $\langle \phi_1\bar{\phi}_1\phi_2\bar{\phi}_2 \rangle$. The selection

rules and superconformal blocks for this correlator are well understood [65, 194, 195]. The $\mathcal{N} = 1$ OPE is

$$\phi_{r_i} \times \bar{\phi}_{-r_i} \sim \mathbb{1} + A\bar{A}[\ell; \ell]^{(0)} + L\bar{L}[\ell; \ell]^{(0)}_\Delta, \tag{7.66}$$

and the contribution of the long multiplet is captured by the following superconformal block:

$$
\begin{aligned}
G^{\phi_1 \bar{\phi}_1, \phi_2 \bar{\phi}_2}_{\Delta, \ell} &= g_{\Delta, \ell} + \frac{(\Delta + \ell)}{4(\Delta + \ell + 1)} g_{\Delta+1, \ell+1} + \frac{(\Delta - \ell - 2)}{4(\Delta - \ell - 1)} g_{\Delta+1, \ell-1} \\
&\quad + \frac{(\Delta + \ell)(\Delta - \ell - 2)}{16(\Delta + \ell + 1)(\Delta - \ell - 1)} g_{\Delta+2, \ell}.
\end{aligned}
\tag{7.67}
$$

The contribution for the exchanged $A\bar{A}[\ell; \ell]^{(0)}$ short multiplet is obtained setting this block at the unitarity bound $\Delta = \ell + 2$. Notice that the $\mathcal{N} = 2$ long exchanged in (7.65) decomposes in $\mathcal{N} = 1$ language as

$$L\bar{L}[\ell; \ell]^{(0;0)}_\Delta \to L\bar{L}[\ell; \ell]^{(0)}_\Delta + L\bar{L}[\ell+1; \ell+1]^{(0)}_{\Delta+1} + L\bar{L}[\ell-1; \ell-1]^{(0)}_{\Delta+1} + L\bar{L}[\ell; \ell]^{(0)}_{\Delta+2}, \tag{7.68}$$

where we have omitted all $\mathcal{N} = 1$ multiplets that are not allowed by the selection rule (7.66). Thus, we must have the following decomposition:

$$G^{\varphi\bar{\varphi};MM}_{\Delta, \ell} = a_0 G^{\phi_1 \bar{\phi}_1; \phi_2 \bar{\phi}_2}_{\Delta, \ell} + a_1 G^{\phi_1 \bar{\phi}_1; \phi_2 \bar{\phi}_2}_{\Delta+1, \ell+1} + a_2 G^{\phi_1 \bar{\phi}_1; \phi_2 \bar{\phi}_2}_{\Delta+1, \ell-1} + a_3 G^{\phi_1 \bar{\phi}_1; \phi_2 \bar{\phi}_2}_{\Delta+2, \ell}. \tag{7.69}$$

We are going to fix the coefficients a_i in two different ways leading to the same result. First, in the OPE of two moment maps only operators with even spin can appear. Inserting (7.67) in (7.69) and demanding that only even spin descendants contribute fixes the block completely:

$$
\begin{aligned}
G^{\varphi\bar{\varphi};MM}_{\Delta, \ell} &= g_{\Delta, \ell} - \frac{(\Delta - \ell)(\Delta - \ell - 2)}{16(\Delta - \ell + 1)(\Delta - \ell - 1)} g_{\Delta+2, \ell-2} - \frac{(\Delta + \ell)(\Delta + \ell + 2)}{16(\Delta + \ell + 1)(\Delta + \ell + 3)} g_{\Delta+2, \ell+2} \\
&\quad + \frac{(\Delta - \ell)(\Delta - \ell - 2)(\Delta + \ell)(\Delta + \ell + 2)}{256(\Delta - \ell + 1)(\Delta - \ell - 1)(\Delta + \ell + 1)(\Delta + \ell + 3)} g_{\Delta+4, \ell}.
\end{aligned}
\tag{7.70}
$$

As discussed, this block corresponds to the exchange of a generic long multiplet. The contribution of $A\bar{A}[\ell; \ell]^{(0;0)}$ is obtained by evaluating the block at the unitarity bound $\Delta = \ell + 2$. By using hypergeometric identities one can check that (7.70) is identical to the compact expression provided in the main text (7.27).

Let us derive the same result in an alternative way. Looking at the $(I, J) = (K, L) = (1, 2)$ component of (7.64) we get a correlation function of $\mathcal{N} = 1$ chirals and currents $\langle \phi\bar{\phi}JJ \rangle$. As before, the selection rules and superconformal blocks are well understood [195, 212, 239]. In particular, the only multiplet relevant in the OPE is $J \times J \sim L\bar{L}[\ell; \ell]_{\Delta}^{(0)}$, for which the conformal block is

$$G_{\Delta,\ell \text{ even}}^{\phi\bar{\phi},JJ} = g_{\Delta,\ell} - \frac{(\Delta - 2)(\Delta - \ell - 2)(\Delta + \ell)}{16\Delta(\Delta - \ell - 1)(\Delta + \ell + 1)} g_{\Delta+2,\ell}, \tag{7.71}$$

$$G_{\Delta,\ell \text{ odd}}^{\phi\bar{\phi},JJ} = g_{\Delta+1,\ell+1} - \frac{(\ell + 2)(\Delta - \ell - 2)(\Delta + \ell + 1)}{\ell(\Delta - \ell - 1)(\Delta + \ell)} g_{\Delta+1,\ell-1}. \tag{7.72}$$

Following the same reasoning as before, the $\mathcal{N} = 2$ block should decompose as

$$G_{\Delta,\ell}^{\varphi\bar{\varphi};MM} = b_0 G_{\Delta,\ell,\text{even}}^{\phi\bar{\phi};JJ} + b_1 G_{\Delta+1,\ell+1,\text{odd}}^{\phi\bar{\phi};JJ} + b_2 G_{\Delta+1,\ell-1,\text{odd}}^{\phi\bar{\phi};JJ} + b_3 G_{\Delta+2,\ell,\text{even}}^{\phi\bar{\phi};JJ}. \tag{7.73}$$

Demanding that the two decompositions (7.69) and (7.73) are equal uniquely determines the superconformal block (7.70).

7.A.3 $\langle \varphi MM\bar{\varphi} \rangle$ correlator

Now we move on to the calculation of the blocks in the crossed channel:

$$\langle \varphi(x_1) M_{IJ}(x_2) M_{KL}(x_3) \bar{\varphi}(x_4) \rangle$$
$$= \frac{\epsilon_{I(K}\epsilon_{J|L)}}{x_{12}^{\Delta_\varphi+2} x_{34}^{\Delta_\varphi+2}} \left(\frac{x_{24}}{x_{14}}\right)^{\Delta_\varphi-2} \left(\frac{x_{14}}{x_{13}}\right)^{\Delta_\varphi-2} \sum_{\mathcal{O}} |\lambda_{\varphi M\mathcal{O}}|^2 \, G_{\Delta,\ell}^{\varphi M;M\bar{\varphi}}(z, \bar{z}). \tag{7.74}$$

The first important question is what multiplets appear in the sum over superdescendants. Using the superspace calculation of [338], we obtain the following selection rule:

$$\varphi_r \times M \sim L\bar{B}[0; 0]^{(2;r)} + L\bar{A}[\ell; \ell - 1]^{(1;r-1)} + L\bar{L}[\ell; \ell]_{\Delta}^{(0;r-2)}. \tag{7.75}$$

The strategy to compute the conformal blocks is the same as before. Consider the component $(I, J) = (2, 2)$ and $(K, L) = (1, 1)$ of the four-point function and interpret it as a correlator of $\mathcal{N} = 1$ chirals and antichirals $\langle \phi_1\bar{\phi}_2\phi_2\bar{\phi}_1 \rangle$. The selection rules and blocks are once again in the literature [198]. Restricting to the case of interest to us, we have

$$\phi_{\frac{r}{3}} \times \bar{\phi}_{-\frac{4}{3}} \sim L\bar{B}[0; 0]^{(\frac{r-4}{3})} + L\bar{A}[\ell; \ell]^{(\frac{r-4}{3})} + L\bar{L}[\ell; \ell]_{\Delta}^{(\frac{r-4}{3})}, \tag{7.76}$$

and the contribution of the long is given by the superconformal block:

$$G_{\Delta,\ell}^{\phi_1\bar{\phi}_2;\phi_2\bar{\phi}_1}(z, \bar{z}) = (z\bar{z})^{-1/2} g_{\Delta+1,\ell}^{1+\Delta_{12},1-\Delta_{12}}(z, \bar{z}). \tag{7.77}$$

As before, we want to write our $\mathcal{N} = 2$ block as a linear combination of $\mathcal{N} = 1$ ones. For concreteness, let us focus on the exchange of the long in (7.75), which has the following decomposition:

$$L\bar{L}[\ell;\ell]_{\Delta}^{(0;r-2)} \;\rightarrow\; L\bar{L}[\ell;\ell]_{\Delta+1}^{(\frac{r-4}{3})} . \tag{7.78}$$

We have dropped all terms that are not compatible with the $\mathcal{N} = 1$ selection rule (7.76). Since there is only one $\mathcal{N} = 1$ multiplet in the decomposition, the block must be equal to its $\mathcal{N} = 1$ counterpart:

$$G_{\Delta,\ell}^{\varphi M;M\bar{\varphi}}(z,\bar{z}) = G_{\Delta+1,\ell}^{\phi_1\bar{\phi}_2;\phi_2\bar{\phi}_1}(z,\bar{z}) = (z\bar{z})^{-1/2}g_{\Delta+2,\ell}^{\Delta_\varphi-1,3-\Delta_\varphi}(z,\bar{z}) . \tag{7.79}$$

Naturally, this can be expanded into non-supersymmetric blocks

$$G_{\Delta,\ell}^{\varphi M;M\bar{\varphi}} = g_{\Delta+1,\ell}^{\Delta_\varphi-2,2-\Delta_\varphi} + c_1 g_{\Delta+2,\ell+1}^{\Delta_\varphi-2,2-\Delta_\varphi} + c_2 g_{\Delta+2,\ell-1}^{\Delta_\varphi-2,2-\Delta_\varphi} + c_1 c_2 g_{\Delta+3,\ell}^{\Delta_\varphi-2,2-\Delta_\varphi}, \tag{7.80}$$

with

$$\begin{aligned}
c_1 &= \frac{(\Delta - \Delta_\varphi + \ell + 3)(\Delta + \Delta_\varphi + \ell - 1)}{4(\Delta + \ell + 1)(\Delta + \ell + 2)}, \\
c_2 &= \frac{(\Delta - \Delta_\varphi - \ell + 1)(\Delta + \Delta_\varphi - \ell - 3)}{4(\Delta - \ell - 1)(\Delta - \ell)}.
\end{aligned} \tag{7.81}$$

As a non-trivial sanity check, we can instead look at the $(I,J) = (K,L) = (1,2)$ component of the four-point function, and interpret it as a $\mathcal{N} = 1$ correlator $\langle\phi JJ\phi\rangle$. The selection rule in this case is [214]

$$\phi_r \times J \sim L\bar{L}[\ell;\ell+1]_{\Delta}^{(r-1)} + L\bar{L}[\ell;\ell-1]_{\Delta}^{(r-1)} + L\bar{L}[\ell;\ell]_{\Delta}^{(r-2)} + \text{shorts.} \tag{7.82}$$

Only the first two will play a role, and the associated blocks are

$$\begin{aligned}
L\bar{L}[\ell;\ell+1]_{\Delta}^{(r-1)} : \quad &\hat{G}_{\Delta,\ell} = \hat{c}_1\, g_{\Delta+1/2,\ell}^{\Delta_\phi-2,2-\Delta_\phi} + \hat{c}_2\, g_{\Delta+3/2,\ell+1}^{\Delta_\phi-2,2-\Delta_\phi}, \\
L\bar{L}[\ell;\ell-1]_{\Delta}^{(r-1)} : \quad &\check{G}_{\Delta,\ell} = \check{c}_1\, g_{\Delta+1/2,\ell}^{\Delta_\phi-2,2-\Delta_\phi} + \check{c}_2\, g_{\Delta+3/2,\ell-1}^{\Delta_\phi-2,2-\Delta_\phi},
\end{aligned} \tag{7.83}$$

124

with coefficients [214]:

$$\hat{c}_1 = \frac{(\ell + 2)}{(\ell + 1)(2\Delta - 2\Delta_\phi - 2\ell - 3)},$$

$$\hat{c}_2 = \frac{(2\Delta - 3)(2\Delta - 2\Delta_\phi + 2\ell + 5)(2\Delta + 2\Delta_\phi + 2\ell - 3)}{4(2\Delta - 1)(2\Delta + 2\ell + 1)(2\Delta + 2\ell + 3)(2\Delta - 2\Delta_\phi - 2\ell - 3)},$$

$$\check{c}_1 = \frac{1}{(2\Delta - 2\Delta_\phi + 2\ell + 1)},$$

$$\check{c}_2 = \frac{(2\Delta - 3)(\ell + 1)(2\Delta - 2\Delta_\phi - 2\ell + 1)(2\Delta + 2\Delta_\phi - 2\ell - 7)}{4(2\Delta - 1)\ell(2\Delta - 2\ell - 1)(2\Delta - 2\ell - 3)(2\Delta - 2\Delta_\phi + 2\ell + 1)}. \tag{7.84}$$

Decomposing the $\mathcal{N} = 2$ long multiplet and keeping only terms compatible with the OPE (7.82) we get

$$L\bar{L}[\ell; \ell]_\Delta^{(0;r\text{-}2)} \to L\bar{L}[\ell; \ell + 1]_{\Delta + \frac{1}{2}}^{(\frac{r\text{-}3}{3})} + L\bar{L}[\ell; \ell - 1]_{\Delta + \frac{1}{2}}^{(\frac{r\text{-}3}{3})}$$
$$+ L\bar{L}[\ell + 1; \ell]_{\Delta + \frac{3}{2}}^{(\frac{r\text{-}3}{3})} + L\bar{L}[\ell - 1; \ell]_{\Delta + \frac{3}{2}}^{(\frac{r\text{-}3}{3})}, \tag{7.85}$$

so we find the following decomposition:

$$G_{\Delta,\ell}^{\varphi M; M\bar{\varphi}} = d_0\, \hat{G}_{\Delta+1/2,\ell}^{\phi J; J\bar{\phi}} + d_1\, \check{G}_{\Delta+1/2,\ell}^{\phi J; J\bar{\phi}} + d_2\, \check{G}_{\Delta+3/2,\ell+1}^{\phi J; J\bar{\phi}} + d_3\, \hat{G}_{\Delta+3/2,\ell-1}^{\phi J; J\bar{\phi}}. \tag{7.86}$$

There is a linear relation between the four $\mathcal{N} = 1$ blocks above, and we fix it by setting $d_0 = 0$. It is an easy exercise to check that using the remaining coefficients we can indeed obtain the decomposition (7.86):

$$d_1 = 2(\Delta - \Delta_\varphi + \ell + 1),$$

$$d_2 = \frac{(\Delta + \Delta_\varphi + \ell - 1)(\Delta - \Delta_\varphi + \ell + 3)^2}{2(\Delta + \ell + 1)(\Delta + \ell + 2)},$$

$$d_3 = -\frac{(\Delta + \Delta_\varphi - \ell - 3)(\Delta - \Delta_\varphi - \ell + 1)^2}{2\Delta(\ell + 1)(\Delta - \ell)}. \tag{7.87}$$

The reader can check that any minor change to the $\mathcal{N} = 2$ or $\mathcal{N} = 1$ superblocks prevents this decomposition from being possible. This provides a very non-trivial check for our superblock (7.80), as well as for the results in [214].

7.B   Numerical implementation

7.B.1   Approximating blocks by polynomials

In order to build polynomial approximations of the four-dimensional conformal blocks we use the recursion relations originally obtained in [56, 65], and later generalized in [214].

The quantities we need to approximate are derivatives of one-dimensional conformal blocks, evaluated at the crossing-symmetric point:

$$C^n_{\alpha,\beta,\gamma,\delta} = \frac{\partial^n}{\partial z^n} \left(z^{1-\delta} k^{\beta,\gamma}_\alpha(z) \right)_{z=1/2}. \tag{7.88}$$

We take β, γ, δ and n to have fixed numerical values, and we wish to approximate $C_{\alpha,\beta,\gamma,\delta}$ as a polynomial in α times a positive function of α. Using the differential equation satisfied by $k^{\beta,\gamma}_\alpha(z)$, one obtains the following recursion relation [214]:

$$
\begin{aligned}
C^n_{\alpha,\beta,\gamma,\delta} = & -(2n + \beta - \gamma + 4\delta - 10)C^{n-1}_{\alpha,\beta,\gamma,\delta} \\
& + \big(4n(n - \beta + \gamma - 3) \\
& \qquad + 2\alpha(\alpha - 2) - \beta(\gamma + 2\delta - 10) + \gamma(2\delta - 10) - 4\delta(\delta - 4) - 4 \big)C^{n-2}_{\alpha,\beta,\gamma,\delta} \\
& + 2(n - 2)(2n - \beta + 2\delta - 8)(2n + \gamma + 2\delta - 8)C^{n-3}_{\alpha,\beta,\gamma,\delta}.
\end{aligned}
\tag{7.89}
$$

Applying the recursion repeatedly, we can write

$$C^n_{\alpha,\beta,\gamma,\delta} = P_n(\alpha,\beta,\gamma,\delta)\, k^{\beta,\gamma}_\alpha(1/2) + Q_n(\alpha,\beta,\gamma,\delta)\frac{\partial k^{\beta,\gamma}_\alpha}{\partial z}(1/2) , \tag{7.90}$$

where P_n and Q_n are polynomials in α. Next, we should approximate $k^{\beta,\gamma}_\alpha(1/2)$ and its first derivative as polynomials in α times a positive prefactor. We introduce the radial coordinate ρ [117]

$$z = \frac{4\rho}{(1+\rho)^2}, \tag{7.91}$$

and expand the one-dimensional blocks in a power series in ρ up to order w. Finally, we evaluate the expansion at the crossing symmetric point $\rho_* = 3 - 2\sqrt{2} \approx 0.17$. Remember that the one-dimensional blocks are schematically $z^{\alpha/2}$ times a $_2F_1$ hypergeometric, so the

expansion will have the form

$$k_\alpha^{\beta,\gamma}(1/2) \approx (4\rho_*)^{\alpha/2} \sum_{j=0}^{w} R_j(\alpha)\rho_*^j = \frac{(4\rho_*)^{\alpha/2}}{D_{\beta,\gamma,w}(\alpha)} N_{\beta,\gamma,w}(\alpha), \tag{7.92}$$

$$\frac{\partial k_\alpha^{\beta,\gamma}}{\partial z}(1/2) \approx (4\rho_*)^{\alpha/2} \sum_{j=0}^{w-1} S_j(\alpha)\rho_*^j = \frac{(4\rho_*)^{\alpha/2}}{D_{\beta,\gamma,w}(\alpha)} L_{\beta,\gamma,w}(\alpha), \tag{7.93}$$

where the terms $R_j(\alpha), S_j(\alpha)$ are rational functions of α, and so we can factor a common term $(4\rho_*)^{\alpha/2}/D(\alpha)$. The zeros of $D(\alpha)$ are at $\alpha = 0, -1, -2, \ldots$, and one can see that the prefactor is always positive provided the unitary bounds are satisfied. Combining these ingredients it is a simple exercise to construct the polynomial approximation of the conformal blocks.

There are other possible approaches to compute the polynomial approximations. One idea would be to use the Zamolodchikov-like recursion relations for $k_\alpha^{\beta,\gamma}(z)$ derived in [112]. Another option would be to use the recursion relations directly in $4d$ [339], which are already implemented in `scalar_blocks`. It would be interesting to compare the different approaches in terms of performance, accuracy of the blocks and size of the polynomial approximation.

7.B.2   SDPB parameters

In this work, we have computed mixed correlator bounds at $\Lambda = 24$ and single correlator bounds at $\Lambda = 32, 50$ using `sdpb` [59, 60]. As we increase the number of derivatives it is necessary to increase the spins included to ensure numerical stability:

$$
\begin{aligned}
S_{\Lambda=24} &= \{0, \ldots, 26\} \cup \{29, 30, 33, 34, 37, 38, 41, 42, 45, 46\}, \\
S_{\Lambda=32} &= \{0, \ldots, 44\} \cup \{47, 48, 51, 52, 55, 56, 59, 60, 63, 64, 67, 68\}, \\
S_{\Lambda=50} &= \{0, \ldots, 64\} \cup \{67, 68, 71, 72, 75, 76, 79, 80, 83, 84, 87, 88\}.
\end{aligned}
\tag{7.94}
$$

Furthermore, it is also important to increase the accuracy of the polynomial approximation w and the precision used by `sdpb`:

	$\Lambda = 24$	$\Lambda = 32$	$\Lambda = 50$
w	18	18	26
`prec`	768	768	1024.

(7.95)

We have observed that the polynomial approximation of section 7.B.1 works better for single correlators. This is the reason why for the single correlator bootstrap at $\Lambda = 32$

we can keep the same number of poles as for the mixed bootstrap at $\Lambda = 24$. For the dimension bounds, we rely heavily on the hot-starting procedure introduced in [67], which speeds up the computations significantly. We instruct `sdpb` to stop as soon as a primal or dual feasible solutions is found:

$$\begin{aligned}
&\texttt{findPrimalFeasible} = \texttt{findDualFeasible} = \text{true}, \\
&\texttt{detectPrimalFeasibleJump} = \texttt{detectDualFeasibleJump} = \text{true}.
\end{aligned} \tag{7.96}$$

In practice, we observed that the algorithm always stopped after a primal or dual jump. For the OPE optimizations, in order to speed them up, we have lowered the default `dualityGapThreshold` to

$$\texttt{dualityGapThreshold} = 10^{-10}. \tag{7.97}$$

For the remaining parameters, we have found that the defaults of `sdpb` lead to stable results.

7.B.3 Crossing vectors

In this appendix we write the explicit crossing vectors that appear in equation (7.51). The $\vec{I}_{c,k}$ term captures all the known contributions, either from the identity, stress-tensor or flavor current exchanges. The normalization of the stress-tensor contribution for the mixed blocks can be obtained from (7.28). The rest has already been discussed in the main text:

$$\vec{I}_{c,k} = \begin{pmatrix}
4\mathcal{H}^{\text{short}}_{+,\mathbf{1}} + 3\mathcal{H}^{\text{short}}_{+,\mathbf{3}} + 5\mathcal{H}^{\text{short}}_{+,\mathbf{5}} \\[6pt]
2\mathcal{H}^{\text{short}}_{+,\mathbf{1}} + 9\mathcal{H}^{\text{short}}_{+,\mathbf{3}} - 5\mathcal{H}^{\text{short}}_{+,\mathbf{5}} \\[6pt]
-2\mathcal{H}^{\text{short}}_{-,\mathbf{1}} + 3\mathcal{H}^{\text{short}}_{-,\mathbf{3}} + 5\mathcal{H}^{\text{short}}_{-,\mathbf{5}} \\[6pt]
E^{\varphi\bar\varphi;\varphi\bar\varphi}_{+,0,0} + \frac{\Delta_\varphi^2}{6c} E^{\varphi\bar\varphi;\varphi\bar\varphi}_{+,2,0} \\[6pt]
E^{\varphi\bar\varphi;\varphi\bar\varphi}_{+,0,0} + \frac{\Delta_\varphi^2}{6c} \tilde{E}^{\varphi\bar\varphi;\varphi\bar\varphi}_{+,2,0} \\[6pt]
E^{\varphi\bar\varphi;\varphi\bar\varphi}_{-,0,0} + \frac{\Delta_\varphi^2}{6c} \tilde{E}^{\varphi\bar\varphi;\varphi\bar\varphi}_{-,2,0} \\[6pt]
0 \\[6pt]
E^{MM;\varphi\bar\varphi}_{+,0,0} - \frac{\Delta_\varphi}{6c} E^{MM;\varphi\bar\varphi}_{+,2,0} \\[6pt]
E^{MM;\varphi\bar\varphi}_{-,0,0} - \frac{\Delta_\varphi}{6c} E^{MM;\varphi\bar\varphi}_{-,2,0}
\end{pmatrix} \tag{7.98}$$

The remaining crossing vectors can be easily obtained as discussed in the main text:

$$
U_{\Delta,\ell} = \begin{pmatrix} \begin{pmatrix} 4E^{MM,MM}_{+,\Delta,\ell} & 0 \\ 0 & 0 \end{pmatrix} \\ \begin{pmatrix} 2E^{MM,MM}_{+,\Delta,\ell} & 0 \\ 0 & 0 \end{pmatrix} \\ \begin{pmatrix} -2E^{MM,MM}_{-,\Delta,\ell} & 0 \\ 0 & 0 \end{pmatrix} \\ \begin{pmatrix} 0 & 0 \\ 0 & E^{\varphi\bar\varphi;\varphi\bar\varphi}_{+,\Delta,\ell} \end{pmatrix} \\ \begin{pmatrix} 0 & 0 \\ 0 & \tilde E^{\varphi\bar\varphi;\varphi\bar\varphi}_{+,\Delta,\ell} \end{pmatrix} \\ \begin{pmatrix} 0 & 0 \\ 0 & \tilde E^{\varphi\bar\varphi;\varphi\bar\varphi}_{-,\Delta,\ell} \end{pmatrix} \\ 0 \\ \begin{pmatrix} 0 & \frac12 E^{MM,\varphi\bar\varphi}_{+,\Delta,\ell} \\ \frac12 E^{MM,\varphi\bar\varphi}_{+,\Delta,\ell} & 0 \end{pmatrix} \\ \begin{pmatrix} 0 & \frac12 E^{MM,\varphi\bar\varphi}_{-,\Delta,\ell} \\ \frac12 E^{MM,\varphi\bar\varphi}_{-,\Delta,\ell} & 0 \end{pmatrix} \end{pmatrix} , \quad
V_{\Delta,\ell} = \begin{pmatrix} 0 \\ 0 \\ 0 \\ E^{\varphi\bar\varphi;\varphi\bar\varphi}_{+,\Delta,\ell} \\ \tilde E^{\varphi\bar\varphi;\varphi\bar\varphi}_{+,\Delta,\ell} \\ \tilde E^{\varphi\bar\varphi;\varphi\bar\varphi}_{-,\Delta,\ell} \\ 0 \\ 0 \\ 0 \end{pmatrix} , \quad
W_{\Delta,\ell} = \begin{pmatrix} 0 \\ 0 \\ 0 \\ 0 \\ E^{\varphi\varphi;\bar\varphi\bar\varphi}_{+,\Delta,\ell} \\ -E^{\varphi\varphi;\bar\varphi\bar\varphi}_{-,\Delta,\ell} \\ 0 \\ 0 \\ 0 \end{pmatrix} ,
\tag{7.99}
$$

$$
X_{\Delta,\ell} = \begin{pmatrix} 3\,E^{MM,MM}_{+,\Delta,\ell} \\ 9\,E^{MM,MM}_{+,\Delta,\ell} \\ 3\,E^{MM,MM}_{-,\Delta,\ell} \\ 0 \\ 0 \\ 0 \\ 0 \\ 0 \\ 0 \end{pmatrix} , \quad
Y_{\Delta,\ell} = \begin{pmatrix} 5\,E^{MM,MM}_{+,\Delta,\ell} \\ -5\,E^{MM,MM}_{+,\Delta,\ell} \\ 5\,E^{MM,MM}_{-,\Delta,\ell} \\ 0 \\ 0 \\ 0 \\ 0 \\ 0 \\ 0 \end{pmatrix} , \quad
Z_{\Delta,\ell} = \begin{pmatrix} 0 \\ 0 \\ 0 \\ 0 \\ 0 \\ 0 \\ \tilde E^{\varphi M;M\bar\varphi}_{+,\Delta,\ell} \\ E^{\varphi M;M\bar\varphi}_{+,\Delta,\ell} \\ -E^{\varphi M;M\bar\varphi}_{-,\Delta,\ell} \end{pmatrix} .
\tag{7.100}
$$

7.B.4 Spectrum extraction

In table 7.8 we present the results from extracting the spectrum that saturates the OPE bounds in table 7.7. We use the package `spectrum-extraction` developed for [73], which is available online in the Bootstrap Collaboration website. Although we have not collected the spectrum for $\ell > 0$ operators, we are happy to provide the data upon request. For a detailed analysis of the spectrum in the large-ℓ limit for the H_0 theory we refer to [217].

Theory	Bound	Type	Δ_U	Δ'_U	Δ''_U	Δ_W	Δ'_W
H_0	φ^2	upper	2.70	5.94	9.28	4.82	7.82
H_0	φ^2	lower	2.66	5.82	9.14	4.95	7.57
H_0	$\bar{Q}^2\mathcal{O}$	upper	2.69	5.88	9.16	4.81	7.79
H_0	$\bar{Q}^2\mathcal{O}$	lower	2.66	5.79	9.07	4.69	6.49
H_1	φ^2	upper	3.05	6.12	13.11	5.28	8.27
H_1	φ^2	lower	2.92	5.79	12.79	5.79	7.74
H_1	$\bar{Q}^2\mathcal{O}$	upper	3.03	5.98	9.12	5.27	8.28
H_1	$\bar{Q}^2\mathcal{O}$	lower	2.92	5.76	12.65	4.78	6.35
H_2	φ^2	upper	3.45	6.41	9.66	5.88	8.96
H_2	φ^2	lower	3.23	5.91	8.98	6.88	9.89
H_2	$\bar{Q}^2\mathcal{O}$	upper	3.42	6.29	9.49	5.85	8.95
H_2	$\bar{Q}^2\mathcal{O}$	lower	3.21	3.75	5.97	6.86	9.38

Table 7.8: Approximate spectrum from OPE bounds at $\Lambda = 50$.

Chapter 8

Bootstrapping line defects in $\mathcal{N} = 2$ theories

Abstract

We study half-BPS line defects in $\mathcal{N} = 2$ superconformal theories using the bootstrap approach. We concentrate on local excitations constrained to the defect, which means the system is a $1d$ defect CFT with $\mathfrak{osp}(4^*|2)$ symmetry. In order to study correlation functions we construct a suitable superspace, and then use the Casimir approach to calculate a collection of new superconformal blocks. Special emphasis is given to the displacement operator, which controls deformations orthogonal to the defect and is always present in a defect CFT. After setting up the crossing equations we proceed with a numerical and analytical bootstrap analysis. We obtain numerical bounds on the CFT data and compare them to known solutions. We also present an analytic perturbative solution to the crossing equations, and argue that this solution captures line defects in $\mathcal{N} = 2$ gauge theories at strong coupling.

8.1 Introduction

Defects are important observables in quantum field theory: they serve as probes that allow to extract physics otherwise inaccessible from the study of local operators. In four-dimensional gauge theories, it is well understood by now that models with the same local correlators might have different line operators, and therefore correspond to distinct physical

131

theories [340]. In this work, we concentrate on line defects in $4d$ superconformal theories with $\mathcal{N} = 2$ supersymmetry. In particular, we consider half-BPS defects that preserve an $\mathfrak{osp}(4^*|2)$ subalgebra of the full $\mathfrak{su}(2,2|2)$ superconformal algebra.

An important example of such a defect is a Wilson line operator, which describes a charged heavy particle moving in the vacuum of a gauge theory. Due to the high amount of supersymmetry preserved by the configuration, it is possible to obtain exact formulas using localization and related matrix model techniques [341]. For example, the Bremsstrahlung function, which captures the energy radiated by the particle, can be calculated exactly [342–345]. A way to understand this is that the Bremsstrahlung is proportional to the one-point function of the stress tensor in the presence of the line, and the latter can be obtained from localization. This relation between Bremsstrahlung and the stress tensor was conjectured in [345] for $\mathcal{N} = 2$ theories, and later proven in [290] using only superconformal symmetry.

The literature on Wilson operators in $\mathcal{N} = 2$ theories is vast, however work on configurations with insertions along the contour has been scarce. Here we study this system from the $1d$ CFT perspective by analyzing correlators of operators inserted on the line. Although $1d$ theories are non-local due to the absence of a stress tensor, they are consistent when interpreted as defect theories. Correlators on a defect can be thought of as describing a lower dimensional CFT embedded in a higher dimensional bulk. In particular, four-point functions exhibit crossing symmetry and have a conformal block expansion with positive coefficients. Thanks to this positivity property, one can use the numerical bootstrap of [17] to constrain the CFT data. We should mention that if one considers operators outside the defect the positivity property is lost, and the numerical bootstrap does not apply. One can nevertheless use analytical bootstrap techniques, see [265, 266] for recent progress.

The canonical operator that is always present on a defect CFT is the displacement operator. This operator measures deformations orthogonal to the defect, and is the closest one can have to a conserved stress tensor. Indeed, the stress tensor and the displacement are related by a Ward identity [259]. Due to its universal character, in this work we concentrate on the four-point function of the displacement operator. Because the system we are considering is supersymmetric, in order to study the displacement operator, it will be necessary to study the corresponding superconformal multiplet. Our bootstrap analysis is based on symmetry and we will not commit to any particular theory. This work is complementary to the bulk $\mathcal{N} = 2$ superconformal bootstrap program [198, 216, 217],

where the main focus is the study of correlators of local operators.[1]

In $\mathcal{N} = 4$ SYM, the corresponding line defect with insertions has been studied recently using a variety of techniques. These include explicit holographic calculations [346], the conformal bootstrap [233, 285], truncations to the topological sector [288, 289], and perturbative calculations at weak coupling [347, 348]. Another related system is the monodromy line of the $3d$ Ising model [255], which was studied using bootstrap techniques in [256]. Apart from their intrinsic interest, $1d$ CFTs are also a useful laboratory in which bootstrap ideas can be explored. Recent work includes exact functionals that allow to extract the spectrum analytically [155–157], inversion formulas [126, 349] (see also [272, 274] for the closely related case of BCFT), and intriguing positivity properties [350].

The structure of the paper is as follows. In section 8.2 we review the geometry of our setup and present the preserved $\mathfrak{osp}(4^*|2)$ superconformal algebra. We find all its unitary representations and explicitly construct the multiplets of long and short operators that will play a role in later discussions. In section 8.3 we construct correlation functions using superspace, concentrating on those containing the multiplet of the displacement operator. With the superspace at hand, in section 8.4 we use the Casimir approach to calculate the superconformal blocks involving four displacement multiplets. We write the associated crossing equations, and find a solution that interpolates between bosonic and fermionic free-field theory. We apply standard numerical bootstrap techniques to our crossing equations in section 8.5, and we find that the free-field solutions sit in interesting points of the allowed regions of the plots, where they saturate the numerical bounds. In section 8.6 we employ analytic techniques to find a solution to crossing which we interpret as a perturbative first-order correction to the strong-coupling limit of our line defect. Finally, we conclude in section 8.7 by giving an outlook on possible future directions of research. We complement the text with our conventions (appendix 8.A), and a compendium of superconformal blocks of unprotected long operators (appendix 8.B), which can be useful in future studies of this setup. We also attach a `Mathematica` file with a number of technical results.

8.2 Preliminaries

There are several configurations one can consider when studying defect CFTs: correlation functions of local operators in the presence of the defect, correlators of defect operators, i.e.

---

[1]We should also mention that $\mathcal{N} = 2$ theories admit a wide variety of codimension-2 surface operators, but here we only concentrate on codimension-3 defects.

local excitations that are constrained to live on the defect, and also mixed configurations with both local and defect operators (see figure 8.1). Because defects break some of the conformal symmetry, even low-point correlators tend to have non-trivial structure. One-point functions of local operators are generically non-zero, and two-point functions have a non-trivial dependence on two conformal invariants [259], which makes them analogous to four-point functions in bulk CFTs with no defects.
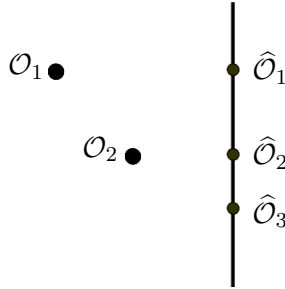
Figure 8.1: In the presence of a defect, one can consider correlators of local and defect operators. Because the defect breaks the conformal algebra down to a subalgebra, even low-point functions can acquire non-trivial coordinate dependence. In this work we will concentrate exclusively on defect excitations (hatted operators in the figure) which define a lower dimensional CFT.

In this work we will study line defects in four dimensions, and we concentrate exclusively on defect excitations. We will consider correlators of the canonical operator that is always present on a defect CFT: the *displacement operator*. This universal operator measures deformations orthogonal to the defect. Intuitively, it can be thought of as the orthogonal components of the stress tensor, which is the generator of translations. Since we are resticting ourselves to the line, our system is described by a $1d$ CFT and all the usual bootstrap techniques apply[2]. In particular, four-point functions have a conformal block expansion with positive coefficients and they satisfy a crossing symmetry equation.

The symmetry algebra preserved by our defect is $\mathfrak{osp}(4^*|2)$[3], which is a subalgebra of the full $\mathcal{N} = 2$ superconformal algebra. This is the maximal possible superalgebra consistent with the geometry of the configuration. In Lagrangian theories, special boundary conditions can be chosen in order to preserve $\mathfrak{osp}(4^*|2)$, but here we will not consider any particular model and we rely only on algebraic and symmetry constraints: the $\mathfrak{osp}(4^*|2)$ symmetry

---

[2]See appendix A of [351] for a general introduction to $1d$ CFTs.

[3]A very complete presentation of superalgebras and their real forms can be found in [352].

algebra will be our starting point.

In four dimensions a line defect has three orthogonal directions, and therefore the displacement is a vector. In the supersymmetric setup we are considering, the displacement sits in a supermultiplet whose highest weight is a scalar. This means that after taking into account all the constraints coming from supersymmetry, our analysis will be similar to the $1d$ bosonic bootstrap. In the next subsection we review the $\mathfrak{osp}(4^*|2)$ superalgebra together with its representation theory, with special emphasis on the multiplets which will be relevant when studying crossing symmetry in section 8.4.

8.2.1   The superalgebra

We are interested in line defects that preserve the maximum amount of supersymmetry $\mathfrak{osp}(4^*|2)$, with bosonic subalgebra $\mathfrak{sl}(2;\mathbb{R}) \oplus \mathfrak{su}(2)_j \oplus \mathfrak{su}(2)_R$. In addition to the $\mathfrak{sl}(2;\mathbb{R})$ factor which captures the $1d$ conformal symmetry, there is an extra $\mathfrak{so}(3) \cong \mathfrak{su}(2)_j$ which can be interpreted as rotations around the defect. The quantum number associated to it, which we label by j, is called transverse spin. The last $\mathfrak{usp}(2) \cong \mathfrak{su}(2)_R$ is the leftover R-symmetry preserved by the configuration. For transverse-spin indices we will use $a = 1, 2$, and for R-symmetry indices $\mathbf{A} = 1, 2$. The fermionic generators are given by supercharges $\mathcal{Q}$ and $\mathcal{S}$, and carry both types of indices. The bosonic part of the superalgebra is given by

$$
\begin{aligned}
[\mathcal{D}, \mathcal{P}] &= \mathcal{P}, \\
[\mathcal{D}, \mathcal{K}] &= -\mathcal{K}, \\
[\mathcal{K}, \mathcal{P}] &= 2\mathcal{D}, \\
[\mathcal{M}_a{}^b, \mathcal{M}_c{}^d] &= -\delta_a{}^d \mathcal{M}_c{}^b + \delta_c{}^b \mathcal{M}_a{}^d, \\
[\mathcal{R}^{\mathbf{A}}{}_{\mathbf{B}}, \mathcal{R}^{\mathbf{C}}{}_{\mathbf{D}}] &= -\delta^{\mathbf{A}}{}_{\mathbf{D}} \mathcal{R}^{\mathbf{C}}{}_{\mathbf{B}} + \delta^{\mathbf{C}}{}_{\mathbf{B}} \mathcal{R}^{\mathbf{A}}{}_{\mathbf{D}}.
\end{aligned}
\tag{8.1}
$$

The fermionic generators anticommute as follows

$$
\begin{aligned}
\{\mathcal{Q}_a^{\mathbf{A}}, \mathcal{Q}_b^{\mathbf{B}}\} &= \varepsilon^{\mathbf{AB}} \varepsilon_{ab} \mathcal{P}, \\
\{\mathcal{S}_{\mathbf{A}}^a, \mathcal{S}_{\mathbf{B}}^b\} &= \varepsilon_{\mathbf{AB}} \varepsilon^{ab} \mathcal{K}, \\
\{\mathcal{Q}_a^{\mathbf{A}}, \mathcal{S}_{\mathbf{B}}^b\} &= -2\delta_a{}^b \mathcal{R}^{\mathbf{A}}{}_{\mathbf{B}} + \delta^{\mathbf{A}}{}_{\mathbf{B}} (\mathcal{M}_a{}^b + \delta_a{}^b \mathcal{D}).
\end{aligned}
\tag{8.2}
$$

Finally, the fermionic generators have the following commutation relations with the bosonic subalgebra

$$
\begin{aligned}
[\mathcal{D}, \mathcal{Q}_a^{\mathbf{A}}] &= \tfrac{1}{2}\mathcal{Q}_a^{\mathbf{A}}, & [\mathcal{D}, \mathcal{S}_{\mathbf{A}}^a] &= -\tfrac{1}{2}\mathcal{S}_{\mathbf{A}}^a, \\
[\mathcal{P}, \mathcal{Q}_a^{\mathbf{A}}] &= 0, & [\mathcal{P}, \mathcal{S}_{\mathbf{A}}^a] &= -\varepsilon_{\mathbf{A}\mathbf{B}}\varepsilon^{ab}\mathcal{Q}_b^{\mathbf{B}}, \\
[\mathcal{K}, \mathcal{Q}_a^{\mathbf{A}}] &= \varepsilon^{\mathbf{A}\mathbf{B}}\varepsilon_{ab}\mathcal{S}_{\mathbf{B}}^b, & [\mathcal{K}, \mathcal{S}_{\mathbf{A}}^a] &= 0, \\
[\mathcal{M}_a{}^b, \mathcal{Q}_c^{\mathbf{C}}] &= \delta_c{}^b\mathcal{Q}_a^{\mathbf{C}} - \tfrac{1}{2}\delta_a{}^b\mathcal{Q}_c^{\mathbf{C}}, & [\mathcal{M}_a{}^b, \mathcal{S}_{\mathbf{C}}^c] &= -\delta_a{}^c\mathcal{S}_{\mathbf{C}}^b + \tfrac{1}{2}\delta_a{}^b\mathcal{S}_{\mathbf{C}}^c, \\
[\mathcal{R}^{\mathbf{A}}{}_{\mathbf{B}}, \mathcal{Q}_c^{\mathbf{C}}] &= \delta^{\mathbf{C}}{}_{\mathbf{B}}\mathcal{Q}_c^{\mathbf{A}} - \tfrac{1}{2}\delta^{\mathbf{A}}{}_{\mathbf{B}}\mathcal{Q}_c^{\mathbf{C}}, & [\mathcal{R}^{\mathbf{A}}{}_{\mathbf{B}}, \mathcal{S}_{\mathbf{C}}^c] &= -\delta^{\mathbf{A}}{}_{\mathbf{C}}\mathcal{S}_{\mathbf{B}}^c + \tfrac{1}{2}\delta^{\mathbf{A}}{}_{\mathbf{B}}\mathcal{S}_{\mathbf{C}}^c.
\end{aligned}
\tag{8.3}
$$

The above superalgebra is compatible with the natural hermitian conjugation in radial quantization

$$
\mathcal{D}^{\dagger} = \mathcal{D}, \quad \mathcal{P}^{\dagger} = \mathcal{K}, \quad \left(\mathcal{M}_a{}^b\right)^{\dagger} = \mathcal{M}_b{}^a, \quad \left(\mathcal{R}^{\mathbf{A}}{}_{\mathbf{B}}\right)^{\dagger} = \mathcal{R}^{\mathbf{B}}{}_{\mathbf{A}}, \quad \left(\mathcal{Q}_a^{\mathbf{A}}\right)^{\dagger} = \mathcal{S}_{\mathbf{A}}^a.
\tag{8.4}
$$

8.2.2   Unitary multiplets

Let us now turn to the study of unitary representations of $\mathfrak{osp}(4^*|2)$. The multiplet that contains the displacement operator has been constructed in [290], and a similar analysis for the case of Wilson loops in ABJM can be found in [353,354]. Unitary representations of $\mathfrak{osp}(4^*|2)$ have been previously discussed in [355], although here we give a more complete treatment following the work of [182].

Highest-weight representations of superconformal algebras are constructed starting from a superconformal primary field $\mathcal{V}$, which is anhilated by the $\mathcal{K}$ and $\mathcal{S}$ generators, and transforms in some representation of the bosonic subalgebra. For the case of interest to us, we label the primary by $[\Delta, j, R]$, where Δ is the conformal dimension, and j, R are positive half-integers that label the transverse spin and R-symmetry respectively. Acting with $\mathcal{Q}$ supercharges on $\mathcal{V}$, one obtains the conformal descendants, which are conformal primary fields, i.e. fields anhilated by the $\mathcal{K}$ generator. It is then clear that the conformal descendants form representations of the conformal algebra (but not of the superconformal algebra) on their own. Requiring positivity of the the norm of these descendants at levels 1 and 2, imposes the unitarity bounds and shortening conditions summarized in table 8.1. To our knowledge, these results have not been presented systematically elsewhere, but we do not derive them here. Instead, we refer the reader to the works [54, 182], which give a detailed treatment on how to obtain unitarity bounds for all superconformal theories in $d \geq 3$.

Name	**P**rimary	**U**nitarity Bound	**N**ull State
L	$[\Delta, j, R]$	$\Delta > 2R + j + 1$	$-$
A_1	$[\Delta, j, R], j > 0$	$\Delta = 2R + j + 1$	$[\Delta + \frac{1}{2}, j - \frac{1}{2}, R + \frac{1}{2}]$
A_2	$[\Delta, 0, R]$	$\Delta = 2R + 1$	$[\Delta + 1, 0, R + 1]$
B_1	$[\Delta, 0, R]$	$\Delta = 2R$	$[\Delta + \frac{1}{2}, \frac{1}{2}, R + \frac{1}{2}]$

Table 8.1: Shortening conditions in one-dimensional $\mathcal{N} = 2$ SCFTs.

Given a superconformal primary field transforming in one of the representations of table 8.1, it will be important for our analysis to know the explicit quantum numbers of all the conformal descendants. This can be achieved efficiently by means of the Racah-Speiser algorithm [27], which has been described in great detail in [182]. Note that the weights of the supercharges in our conventions are

$$
\begin{aligned}
\mathcal{Q}_1^{\mathbf{1}} &\sim \left[+\tfrac{1}{2}, +\tfrac{1}{2}, +\tfrac{1}{2} \right], \quad \mathcal{Q}_2^{\mathbf{1}} \sim \left[+\tfrac{1}{2}, -\tfrac{1}{2}, +\tfrac{1}{2} \right], \\
\mathcal{Q}_1^{\mathbf{2}} &\sim \left[+\tfrac{1}{2}, +\tfrac{1}{2}, -\tfrac{1}{2} \right], \quad \mathcal{Q}_2^{\mathbf{2}} \sim \left[+\tfrac{1}{2}, -\tfrac{1}{2}, -\tfrac{1}{2} \right].
\end{aligned}
\tag{8.5}
$$

For a long multiplet, we act on the highest weight in all possible ways with the four $\mathcal{Q}$'s, so we obtain a representation of dimension

$$
\dim L = 16(2j + 1)(2R + 1).
\tag{8.6}
$$

In order to construct the A_1 supermultiplet, we need to set $\mathcal{Q}_2^{\mathbf{1}} = 0$, since this supercharge has the weights that correspond to the null state in table 8.1. The corresponding representation has dimension

$$
\dim A_1 = 8(1 + j + 3R + 4jR).
\tag{8.7}
$$

In a similar way, the A_2 multiplet is obtained by setting $\mathcal{Q}_1^{\mathbf{1}} \mathcal{Q}_2^{\mathbf{1}} = 0$, and the B_1 multiplet by setting $\mathcal{Q}_1^{\mathbf{1}} = 0$. The corresponding dimensions are

$$
\dim A_2 = 8(3R + 1), \qquad \dim B_1 = 8R.
\tag{8.8}
$$

In this work, we will be mostly concerned with the displacement operator which has protected conformal dimension $\Delta = 2$, and transforms as a vector under rotations orthogonal

to the defect. Therefore, it must have quantum numbers $[2, 1, 0]$, and it has to sit at the bottom component of the short multiplet that contains it. A careful analysis of the representation theory shows that it can only be contained in the $[A_2]_{R=0}$ multiplet [290]

$$[A_2]_{R=0} \; : \; [1, 0, 0] \to [\tfrac{3}{2}, \tfrac{1}{2}, \tfrac{1}{2}] \to [2, 1, 0]. \tag{8.9}$$

Of special relevance will be the following multiplets, some of which will appear in the OPE of two displacement multiplets

$$
\begin{aligned}
[B_1]_{R=1} \quad &: \; [2, 0, 1] \to [\tfrac{5}{2}, \tfrac{1}{2}, \tfrac{1}{2}] \to [3, 0, 0], \\
[A_1]_{R=0}^{j=1} \quad &: \; [2, 1, 0] \to [\tfrac{5}{2}, \tfrac{3}{2}, \tfrac{1}{2}] \to [3, 2, 0], \\
[A_1]_{R=1/2}^{j=1/2} &: \; [\tfrac{5}{2}, \tfrac{1}{2}, \tfrac{1}{2}] \to [3, 0, 0] \oplus [3, 1, 0] \oplus [3, 1, 1] \to [\tfrac{7}{2}, \tfrac{1}{2}, \tfrac{1}{2}] \oplus [\tfrac{7}{2}, \tfrac{3}{2}, \tfrac{1}{2}] \to [4, 1, 0], \\
[L]_{R=0}^{j=0} \quad &: \; [\Delta, 0, 0] \to [\Delta + \tfrac{1}{2}, \tfrac{1}{2}, \tfrac{1}{2}] \to [\Delta + 1, 1, 0] \oplus [\Delta + 1, 0, 1] \to \\
&\qquad \to [\Delta + \tfrac{3}{2}, \tfrac{1}{2}, \tfrac{1}{2}] \to [\Delta + 2, 0, 0], \\
[L]_{R=0}^{j=1} \quad &: \; [\Delta, 1, 0] \to \left[\Delta + \tfrac{1}{2}, \tfrac{1}{2}, \tfrac{1}{2}\right] \oplus \left[\Delta + \tfrac{1}{2}, \tfrac{3}{2}, \tfrac{1}{2}\right] \to \\
&\qquad \to [\Delta + 1, 0, 0] \oplus [\Delta + 1, 1, 0] \oplus [\Delta + 1, 1, 1] \oplus [\Delta + 1, 2, 0] \to \\
&\qquad \to \left[\Delta + \tfrac{3}{2}, \tfrac{1}{2}, \tfrac{1}{2}\right] \oplus \left[\Delta + \tfrac{3}{2}, \tfrac{3}{2}, \tfrac{1}{2}\right] \to [\Delta + 2, 1, 0].
\end{aligned}
\tag{8.10}
$$

When the above long operators approach the unitarity bound, we get the following recombinations rules:

$$
\begin{aligned}
\lim_{\Delta \to 1} [L]_{R=0}^{j=0} &= [A_2]_{R=0} \oplus [B_1]_{R=1}, \\
\lim_{\Delta \to 2} [L]_{R=0}^{j=1} &= [A_1]_{R=0}^{j=1} \oplus [A_1]_{R=1/2}^{j=1/2}.
\end{aligned}
\tag{8.11}
$$

Therefore, we can think of the $[A_2]_{R=0}$ and $[A_1]_{R=0}^{j=1}$ multiplets as the longs $[L]_{R=0}^{j=0}$ and $[L]_{R=0}^{j=1}$ at their respective unitarity bounds, and $[A_1]_{R=1/2}^{j=1/2}$ as the leftover part after the recombination of $[L]_{R=0}^{j=1}$.

As we pointed out in the introduction, our setup is closely related to the work [233], which considered line defects in four-dimensional $\mathcal{N} = 4$ theories preserving $\mathfrak{osp}(4^*|4)$ symmetry. By carefully studying how our $\mathfrak{osp}(4^*|2)$ algebra is embedded in $\mathfrak{osp}(4^*|4)$, we can decompose the multiplets of $\mathcal{N} = 4$ into their $\mathcal{N} = 2$ counterparts. The most important multiplets in the $\mathcal{N} = 4$ case are $\mathcal{B}_1$, which contains the diplacement operator, and $\mathcal{B}_2$, which is the lowest dimension multiplet in the OPE of two diplacements. They decompose

in the following way

$$
\begin{aligned}
\mathcal{B}_1 &\to [A_2]_{R=0} + 2[B_1]_{R=1/2}, \\
\mathcal{B}_2 &\to [L]_{j=R=0}^{\Delta=2} + 2[A_2]_{R=1/2} + 3[B_1]_{R=1}.
\end{aligned}
\tag{8.12}
$$

Therefore, the analogous of the $\mathcal{B}_1$ multiplet in our setup is $[A_2]_{R=0}$, since they both contain the displacement operator. Moreover, the role that was played by the $\mathcal{B}_2$ multiplet will be played now by $[L]_{j=R=0}^{\Delta=2}$. With the numerical results, it will become clear that this intuition is correct.

8.3 Superspace

Having reviewed the symmetry algebra and its representation theory, we now proceed to construct a superspace suitable for the type of correlators we want to study. There are several kinds of superspaces in the literature, and which one to use usually depends on the type of multiplet being studied. Harmonic superspace is quite useful to study half-BPS multiplets, while chiral superspace is more efficient for chiral multiplets. In this work we are interested in the displacement operator, which sits in a multiplet which is neither half-BPS nor chiral, however it has the simplifying feature that its highest weight is neutral under $\mathfrak{su}(2)_j \oplus \mathfrak{su}(2)_R$. We therefore use the most standard superspace in which we add one fermionic coordinate for each conserved $\mathcal{Q}$ supercharge. In this section we will follow closely [185, 186].

8.3.1 Basic definitions

Since we study a $1d$ CFT which preserves the supersymmetry algebra $\mathfrak{osp}(4^*|2)$, the superspace must have one generator $\mathcal{P}$ for translations, and four generators $\mathcal{Q}_a^{\mathbf{A}}$ for supertranslations. These supercharges have to satisfy the algebra

$$
\{\mathcal{Q}_a^{\mathbf{A}}, \mathcal{Q}_b^{\mathbf{B}}\} = \varepsilon_{ab}\varepsilon^{\mathbf{AB}}\mathcal{P}, \qquad [\mathcal{P}, \mathcal{Q}_a^{\mathbf{A}}] = 0,
\tag{8.13}
$$

where $\mathbf{A} = 1, 2$ and $a = 1, 2$. In this section we will show how to build a superspace consistent with these commutation relations, and how to obtain the natural differential and covariant derivative. We take the coordinates of superspace to be $z^M = (x, \theta_{\mathbf{A}}^a)$, and a finite supertranslation to be implemented by the operator

$$
g(z) = g(x, \theta) = \exp\left(x\mathcal{P} + \theta_{\mathbf{A}}^a \mathcal{Q}_a^{\mathbf{A}}\right).
\tag{8.14}
$$

139

The composition of two supertranslations $g(\varepsilon, \xi)g(z) = g(z')$ can be evaluated using the Baker-Campbell-Hausdorff formula $e^X e^Y \approx e^{X+Y+\frac{1}{2}[X,Y]}$, giving

$$
\begin{aligned}
x' &= x + \varepsilon - \tfrac{1}{2}\xi\theta, \\
\theta' &= \theta + \xi\,.
\end{aligned}
\tag{8.15}
$$

Here and in what follows, we use the index-free notation introduced in appendix 8.A, where for example $\xi\theta \equiv \varepsilon_{ab}\varepsilon^{\mathbf{AB}}\xi^a_{\mathbf{A}}\theta^b_{\mathbf{B}} = \xi^a_{\mathbf{A}}\theta^{\mathbf{A}}_a$. The differential of a function in superspace is defined as

$$
\dot{\delta} \equiv \dot{\delta}z^M \frac{\partial}{\partial z^M} \quad \Rightarrow \quad \dot{\delta}f = \dot{\delta}x\frac{\partial f}{\partial x} + \dot{\delta}\theta^a_{\mathbf{A}}\frac{\partial f}{\partial \theta^a_{\mathbf{A}}}\,.
\tag{8.16}
$$

It will prove convenient to rewrite it in terms of the covariant derivative $D^{\mathbf{A}}_a$ and the "covariant one-form" $e(z)$. Looking at the differential of a supertranslation (8.15)

$$
\begin{aligned}
\dot{\delta}x' &= \dot{\delta}x - \tfrac{1}{2}\xi\dot{\delta}\theta, \\
\dot{\delta}\theta' &= \dot{\delta}\theta,
\end{aligned}
\tag{8.17}
$$

we see that it is natural to define the one-form $e(z) \equiv \dot{\delta}x + \frac{1}{2}\theta\dot{\delta}\theta$, which has the property $e(z') = e(z)$ for any constant supertranslation. By rewriting the differential in terms of $e(z)$, we get

$$
\dot{\delta} = e(z)\frac{\partial}{\partial x} + \dot{\delta}\theta^a_{\mathbf{A}}D^{\mathbf{A}}_a,
\tag{8.18}
$$

where the covariant derivative is

$$
D^{\mathbf{A}}_a \equiv \frac{\partial}{\partial \theta^a_{\mathbf{A}}} + \frac{1}{2}\theta^{\mathbf{A}}_a\frac{\partial}{\partial x}, \qquad \{D^{\mathbf{A}}_a, D^{\mathbf{B}}_b\} = \varepsilon_{ab}\varepsilon^{\mathbf{AB}}\frac{\partial}{\partial x}.
\tag{8.19}
$$

The covariant one-form $e(z)$ will be important in the next section in order to derive the Killing equation satisfied by superconformal changes of coordinates. The covariant derivative will be important as well, when we implement shortening conditions in superspace, see section 8.3.1.

Killing equation

After having defined the one-form $e(z)$, we are now ready to derive the equation satisfied by a superconformal change of coordinates, which will be analogous to the conformal Killing equations in standard CFT.

A superconformal transformation is defined as a change of coordinates $z \to z'(z)$ such that $e(z)$ transforms as

$$e(z')^2 = \Omega^2(z)e(z)^2. \tag{8.20}$$

Under a generic change of coordinates $z \to z'(z)$, we have

$$e(z') = e(z) \left(\frac{\partial x'}{\partial x} - \frac{1}{2} \frac{\partial \theta'}{\partial x} \theta' \right) + \dot{\delta}\theta_{\mathbf{A}}^a \left(D_a^{\mathbf{A}} x' - \frac{1}{2} \left(D_a^{\mathbf{A}} \theta' \right) \theta' \right). \tag{8.21}$$

Therefore, it is clear that the superconformal Killing equations are given by

$$D_a^{\mathbf{A}} x' = \frac{1}{2} \left(D_a^{\mathbf{A}} \theta' \right) \theta', \qquad \Omega(z) = \frac{\partial x'}{\partial x} - \frac{1}{2} \frac{\partial \theta'}{\partial x} \theta'. \tag{8.22}$$

We will see that the usual superconformal transformations solve these constraints, but it is instructive to first expand the first equation for infinitesimal transformations $x' = x + \delta x$ and $\theta' = \theta + \delta\theta$:

$$D_a^{\mathbf{A}} \left(\delta x - \tfrac{1}{2} \delta\theta\, \theta \right) = \delta\theta_a^{\mathbf{A}}. \tag{8.23}$$

In this form, it is clear that there is an infinite family of superconformal transformations. In particular, given any function $h(z)$, we can construct a solution of the Killing equation (8.23) with

$$\delta x = h - \tfrac{1}{2}\theta(Dh), \qquad \delta\theta_{\mathbf{A}}^a = D_{\mathbf{A}}^a h. \tag{8.24}$$

It is not surprising that there is an infinite number of solutions, since this is analogous to the statement that in an ordinary one-dimensional space any change of coordinates $x' = f(x)$ is conformal.

There are three particularly simple solutions to the Killing equation (8.22), which can be associated with translations, supertranslations and dilatations:

$$
\begin{aligned}
\exp(a\mathcal{P}) \;&: \quad x' = x + a, \qquad \theta' = \theta, \\
\exp(\xi\mathcal{Q}) \;&: \quad x' = x - \tfrac{1}{2}\xi\theta, \quad \theta' = \theta + \xi, \\
\exp(\lambda\mathcal{D}) \;&: \quad x' = \lambda x, \qquad\quad \theta' = \tfrac{1}{2}\lambda\theta.
\end{aligned}
\tag{8.25}
$$

Here a and ξ are not necessarily infinitesimal parameters, and λ does not need to be close to one. In the following sections we will describe how to obtain the full set of $\mathfrak{osp}(4^*|2)$ transformations starting from the above three.

Inversion

Inversions are special types of superconformal transformations with the property $I^2 = 1$, but such that $\det I = -1$. Since they belong to the disconnected component of the superconformal group, they cannot be expanded infinitesimally around the identity. To find an inversion we must require that it squares to one and satisfies the finite Killing equation (8.22). In our superspace, such a transformation is

$$x \xrightarrow{\ I\ } x_I = \frac{x}{x^2 + \frac{1}{8}\theta^4}, \qquad \theta_{\mathbf{A}}^a \xrightarrow{\ I\ } (\theta_I)_{\mathbf{A}}^a = \frac{(\sigma_3)^a{}_b (x\,\theta_{\mathbf{A}}^b - \frac{1}{2}(\theta^3)_{\mathbf{A}}^b)}{x^2 + \frac{1}{8}\theta^4}, \tag{8.26}$$

where $(\sigma_3)^a{}_b$ denotes the components of the third Pauli matrix, and the fermionic contractions θ^3 and θ^4 are defined in appendix 8.A. Using equation (8.22) we can find the reescaling associated with the previous inversion

$$\Omega(z) = \frac{-1}{x^2 + \frac{1}{8}\theta^4} \,. \tag{8.27}$$

Inversions provide a simple way to generate new solutions to the Killing equation (8.22). Imagine $\mathcal{L}$ is a solution, then one can compose it with two inversions to obtain a new superconformal transformation $\mathcal{L}' = I\,\mathcal{L}\,I$. Using this procedure we obtain the special superconformal transformations

$$\mathcal{K} = I\mathcal{P}I, \quad \mathcal{S} = I\mathcal{Q}I, \quad \Rightarrow \quad e^{b\mathcal{K}} = Ie^{b\mathcal{P}}I, \quad e^{\eta\mathcal{S}} = Ie^{\eta\mathcal{Q}}I. \tag{8.28}$$

Notice that this provides a definition of the finite action of $\mathcal{K}$ and $\mathcal{S}$ which is not limited to infinitesimal transformations.

Differential operators

Given a solution of the infinitesimal Killing equation (8.23), we can use it to build a differential operator that implements the corresponding infinitesimal transformation

$$\mathcal{L} = \delta x\,\partial_x + \delta\theta_{\mathbf{A}}^a \partial_a^{\mathbf{A}}. \tag{8.29}$$

If we compose two transformations as $[\mathcal{L}_1, \mathcal{L}_2] = -\mathcal{L}_3$, one can show that δx_3 and $\delta\theta_3$ still satisfy the Killing equation. From the commutation relations of the superalgebra (8.2), we see that we can obtain $\mathcal{M}$ and $\mathcal{R}$ by looking at the anticommutator of $\mathcal{Q}$ with $\mathcal{S}$, schematically

$$\{\mathcal{Q}, \mathcal{S}\} \sim \mathcal{R} + \mathcal{M} + \mathcal{D}. \tag{8.30}$$

In this way we can construct all the differential operators $\mathcal{P}, \mathcal{K}, \ldots$ of our superconformal algebra. However, before doing so, we need to consider a slight generalization.

In general, we are interested in the action of differential operators on superfields $\mathcal{O}^{I,i}(z)$ which have a conformal dimension Δ, transverse-spin index i, and R-symmetry index I. If such a field is evaluated at $z = 0$, then the action of the generators simplifies

$$\mathcal{D}\mathcal{O}^{I,i}(0) = \Delta\mathcal{O}^{I,i}(0), \quad \mathcal{M}_a{}^b \mathcal{O}^{I,i}(0) = \left(M_a{}^b\right)^i{}_j \mathcal{O}^{I,j}(0), \quad \mathcal{R}^{\mathbf{A}}{}_{\mathbf{B}}\mathcal{O}^{I,i}(0) = \left(R^{\mathbf{A}}{}_{\mathbf{B}}\right)^I{}_J \mathcal{O}^{J,i}(0),$$

$$(8.31)$$

where $M_a{}^b$ and $R^{\mathbf{A}}{}_{\mathbf{B}}$ form representations of the transverse-spin and R-symmetry subalgebras. Demanding that the differential operators act on operators at the origin as (8.31), and that they act on the coordinates as described in this section, we obtain[4]

$$\mathcal{P} = \partial_x,$$

$$\mathcal{D} = x\partial_x + \tfrac{1}{2}\theta^a_{\mathbf{A}}\partial^{\mathbf{A}}_a + \Delta,$$

$$\mathcal{K} = \left(x^2 - \tfrac{1}{8}\theta^4\right)\partial_x + \left(x\theta^a_{\mathbf{A}} + \tfrac{1}{2}(\theta^3)^a_{\mathbf{A}}\right)\partial^{\mathbf{A}}_a + 2\Delta x + \tfrac{1}{2}\theta^a_{\mathbf{A}}\theta^{\mathbf{A}}_b M_a{}^b - \theta^a_{\mathbf{A}}\theta^{\mathbf{B}}_a R^{\mathbf{A}}{}_{\mathbf{B}},$$

$$\mathcal{M}_a{}^b = \theta^b_{\mathbf{A}}\partial^{\mathbf{A}}_a - \tfrac{1}{2}\delta_a{}^b \theta^c_{\mathbf{C}}\partial^{\mathbf{C}}_c + M_a{}^b,$$

$$\mathcal{R}^{\mathbf{A}}{}_{\mathbf{B}} = \theta^a_{\mathbf{B}}\partial^{\mathbf{A}}_a - \tfrac{1}{2}\delta^{\mathbf{A}}{}_{\mathbf{B}} \theta^c_{\mathbf{C}}\partial^{\mathbf{C}}_c + R^{\mathbf{A}}{}_{\mathbf{B}},$$

$$\mathcal{Q}^{\mathbf{A}}_a = \partial^{\mathbf{A}}_a - \tfrac{1}{2}\theta^{\mathbf{A}}_a \partial_x,$$

$$\mathcal{S}^a_{\mathbf{A}} = -\tfrac{1}{2}\left(x\theta^a_{\mathbf{A}} + \tfrac{1}{2}(\theta^3)^a_{\mathbf{A}}\right)\partial_x + x\partial^b_{\mathbf{B}} - \tfrac{1}{2}\left(\theta^a_{\mathbf{A}}\theta^b_{\mathbf{B}} + 3\theta^b_{\mathbf{A}}\theta^a_{\mathbf{B}}\right)\partial^{\mathbf{B}}_b - \Delta\theta^a_{\mathbf{A}} - \theta^b_{\mathbf{A}}M_b{}^a + 2\theta^a_{\mathbf{B}}R^{\mathbf{B}}{}_{\mathbf{A}}.$$

$$(8.32)$$

Notice also that $\{\mathcal{Q}^{\mathbf{A}}_a, D^{\mathbf{B}}_b\} = 0$. This standard property of the covariant derivative ensures that shortening conditions constructed with it are invariant under supersymmetry.

---

[4]Here we are abusing notation by using the same symbols for the differential operators and the generators of the superalgebra. Moreover, as usual in this type of superspace constructions, the differential operators (8.32) follow the commutation relations (8.1)-(8.3) with an extra minus sign, i.e. $[\mathcal{L}_1, \mathcal{L}_2] = -\mathcal{L}_3$. In principle, one would need to be careful with these extra minus signs, however for the problems we will study this will not be an issue.

Multiplets in superspace

A generic multiplet with transverse spin j and R-symmetry R can be represented in terms of a superfield

$$\mathcal{O}^{\mathbf{A}_1 \ldots \mathbf{A}_{2R}}_{a_1 \ldots a_{2j}}(z) = \mathcal{O}^{(\mathbf{A}_1 \ldots \mathbf{A}_{2R})}_{(a_1 \ldots a_{2j})}(z), \tag{8.33}$$

where we use $(a_1 \ldots a_m)$ to denote symmetrization of the indices. The superspace dependence is obtained by applying a supertranslation to the superfield at the origin

$$\mathcal{O}^{\mathbf{A}\cdots}_{a\cdots}(x, \theta) = \exp\left(x\mathcal{P} + \theta\mathcal{Q}\right)\mathcal{O}^{\mathbf{A}\cdots}_{a\cdots}(0). \tag{8.34}$$

The short multiplets from table 8.1 can be obtained by setting the conformal dimension Δ to the appropriate value, and then imposing extra shortening conditions in terms of covariant derivatives

$$A_1 \; : \; \varepsilon^{ab} D^{(\mathbf{A}}_a \mathcal{O}^{\mathbf{B}_1)\ldots\mathbf{B}_{2R}}_{bb_2\ldots b_{2j}} = 0, \tag{8.35a}$$

$$A_2 \; : \; \varepsilon^{ab} D^{(\mathbf{A}}_a D^{\mathbf{B}}_b \mathcal{O}^{\mathbf{C}_1)\ldots\mathbf{C}_{2R}} = 0, \tag{8.35b}$$

$$B_1 \; : \; D^{(\mathbf{A}}_a \mathcal{O}^{\mathbf{B}_1)\ldots\mathbf{B}_{2R}} = 0. \tag{8.35c}$$

It is not hard to check that the content of these shortened multiplets is in perfect agreement with the decompositions in terms of conformal primaries given by the Racah-Speiser algorithm of section 8.2.2. In the rest of this section we will work out explicitly the example of the displacement multiplet $[A_2]_{R=0}$.

We start with a long scalar multiplet of conformal dimension Δ, namely a superfield that carries no transverse-spin or R-symmetry indices. In equation (8.10) one can see the decomposition of this multiplet in terms of conformal primaries, which in superspace takes the form

$$\mathcal{O}(x, \theta) = A(x) + \theta^a_{\mathbf{A}} B^{\mathbf{A}}_a(x) + \theta^a_{\mathbf{A}} \theta^b_{\mathbf{B}} \left(C^{\mathbf{AB}}_{ab}(x) + E^{\mathbf{AB}}_{ab}(x) \right) + (\theta^3)^a_{\mathbf{A}} F^{\mathbf{A}}_a(x) + \theta^4 G(x), \tag{8.36}$$

where $C^{\mathbf{AB}}_{ab} = C^{[\mathbf{AB}]}_{(ab)}$ and $E^{\mathbf{AB}}_{ab} = E^{(\mathbf{AB})}_{[ab]}$. Expanding equation (8.34) and comparing terms,

one can obtain the explicit form of the components

$$
\begin{aligned}
B_a^{\mathbf{A}}(x) &= \mathcal{Q}_a^{\mathbf{A}} A(x), \\
C_{ab}^{\mathbf{AB}}(x) &= -\tfrac{1}{2} \mathcal{Q}_{(a}^{[\mathbf{A}} \mathcal{Q}_{b)}^{\mathbf{B}]} A(x), \\
E_{ab}^{\mathbf{AB}}(x) &= -\tfrac{1}{2} \mathcal{Q}_{[a}^{(\mathbf{A}} \mathcal{Q}_{b]}^{\mathbf{B})} A(x), \\
F_a^{\mathbf{A}}(x) &= -\tfrac{1}{9} \left((\mathcal{Q}^3)_a^{\mathbf{A}} + \tfrac{1}{2} \mathcal{Q}_a^{\mathbf{A}} \mathcal{P} \right) A(x), \\
G(x) &= +\tfrac{1}{144} \left(\mathcal{Q}^4 + \mathcal{P}^2 \right) A(x).
\end{aligned}
\tag{8.37}
$$

Some of these terms are not annihilated by $\mathcal{K}$ and therefore do not correspond to conformal primaries. By using the commutation relations (8.1)-(8.3), we see that A, $B_a^{\mathbf{A}}$, $C_{ab}^{\mathbf{AB}}$ and $E_{ab}^{\mathbf{AB}}$ are indeed primaries, but we need to take

$$
F^{\mathrm{p}}(x) = F(x) - \frac{1}{2(2\Delta + 1)} \mathcal{P} B(x), \qquad G^{\mathrm{p}}(x) = G(x) + \frac{1}{16(2\Delta + 1)} \mathcal{P}^2 A(x). \tag{8.38}
$$

The displacement superfield $\mathcal{D}(z)$ corresponds to the short multiplet $[A_2]_{R=0}$, so from table 8.1 and equation (8.9) it is clear that we need to send $\Delta \to 1$, and remove the conformal descendants $E = F^{\mathrm{p}} = G^{\mathrm{p}} = 0$. We are then left with the superfield

$$
\mathcal{D}(x, \theta) = A(x) + \theta_{\mathbf{A}}^a B_a^{\mathbf{A}}(x) + \theta_{\mathbf{A}}^a \theta_{\mathbf{B}}^b C_{ab}^{\mathbf{AB}}(x) + \tfrac{1}{6} (\theta^3)_{\mathbf{A}}^a \partial_x B_a^{\mathbf{A}}(x) - \tfrac{1}{48} \theta^4 \partial_x^2 A(x). \tag{8.39}
$$

One can obtain the same expression by making an ansatz for $\mathcal{D}(z)$ of the form (8.36) and imposing the shortening condition (8.35b)

$$
\varepsilon^{ab} D_a^{(\mathbf{A}} D_b^{\mathbf{B})} \mathcal{D}(z) = 0 \,. \tag{8.40}
$$

Then equation (8.39) is the most general solution to this condition, or equivalently, it implies that $E = F^{\mathrm{p}} = G^{\mathrm{p}} = 0$.

8.3.2   Correlation functions

Having introduced the basics of our superspace, we are now ready to construct correlation functions of long and short operators. In general, superconformal theories have additional kinematical structures when compared to standard CFTs. A well known example is that already at the three-point level there can be non-trivial superconformal invariants [185]. We start by constructing all such invariants up to four points in section 8.3.2, and then compute the correlation functions for scalar long operators in section 8.3.2. We finish by specifying our results to the displacement operator multiplet in section 8.3.2.

Invariants

The superconformal invariants that will form the bulding blocks of our correlators can be obtained as described in [185]. The most general case we will consider in this work is that of four points $z_1, \ldots, z_4$. Notice that these points can be fixed to standard values in the following way

1. Fix $z = 0$ by doing a translation $\mathcal{P}$ with parameter $a = -x$ followed by a supertranslation $\mathcal{Q}$ with parameter $\xi = -\theta$.

2. Fix $x = \infty$ by doing a special conformal transformation $\mathcal{K}$ with parameter $b = -x_I$, and then fix $\theta = 0$ using an $\mathcal{S}$ transformation of parameter $\eta = -\theta_I$. Here we are denoting $z_I = (x_I, \theta_I)$ the coordinates obtained from z by an inversion, see equation (8.26).

We can combine these two types of transformations to go to a frame where two of the points are fixed to $z = 0$ and $z' = (\infty, 0)$. For our purposes, it will be convenient to work in two different frames

$$
\begin{aligned}
\mathscr{F}_1 &: z_1, \, z_2 \text{ unfixed}, \, z_3 = 0, \, z_4 = (\infty, 0), \\
\mathscr{F}_2 &: z_1 = 0, \, z_2 = (\infty, 0), \, z_3, \, z_4 \text{ unfixed}.
\end{aligned}
\tag{8.41}
$$

In either frame, one can construct the invariants as the combinations of the unfixed z_i which are invariant under the leftover symmetry generators $\mathcal{D}$, $\mathcal{M}$ and $\mathcal{R}$.

Consider first the case of three points in the frame $\mathscr{F}_2$, where the only unfixed coordinates are $z_3 = (x_3, \theta_3)$. If there is a quantity built from θ_3 which is invariant under $\mathcal{M}$ and $\mathcal{R}$, then it must not have any uncontracted indices. As discussed in appendix 8.A, the only such object is $(\theta_3)^4$. On the other hand, x_3 is automatically invariant under $\mathcal{M}$ and $\mathcal{R}$, and the only independent combinations of both that is also invariant under dilatations $\mathcal{D}$ is

$$
J\big|_{\mathscr{F}_2} = \frac{\theta_3^4}{x_3^2}.
\tag{8.42}
$$

One can invert the transformations that led to the frame $\mathscr{F}_2$, to obtain the general expression of the three-point invariant

$$
J = \left(\frac{\theta_{12}^4}{y_{12}^2} + \frac{2\,\theta_{12}\theta_{12}\theta_{23}\theta_{23}}{y_{12}\,y_{23}} + \text{cycl. perms.} \right) + \frac{2(\theta_{12}\theta_{23}\theta_{31})(\theta_{12}\theta_{31}\theta_{23})}{y_{12}\,y_{23}\,y_{31}},
\tag{8.43}
$$

146

where y_{ij} and θ_{ij} are the supertranslation invariant combinations

$$y_{ij} = x_i - x_j - \tfrac{1}{2}\theta_i\theta_j, \qquad \theta_{ij} = \theta_i - \theta_j. \tag{8.44}$$

We do not provide details on how to carry out this calculation, but one can find a similar setup in Appendix A of [356]. It is worth stressing how from a very simple expression for the invariant in a certain frame (8.42), we obtain a much more complicated equation in the general case (8.43).

Let us now consider the four-point case, in which one of the invariants is the standard $1d$ cross-ratio, and the remaining ones correspond to nilpotent quantities. Unlike the three-point case, with four points there is freedom in how to choose the invariants, and we fix it by working with a basis which is simple in the frame $\mathscr{F}_1$. In our conventions, we take the bosonic invariant to be

$$z\big|_{\mathscr{F}_1} = 1 - \frac{x_2}{x_1}, \tag{8.45}$$

which corresponds to the supersymmetric generalization of the standard $1d$ cross-ratio $\chi = \frac{x_{12}x_{34}}{x_{13}x_{24}}$. From the discussion of appendix 8.A, more precisely equations (8.128) and (8.129), one can see that a complete basis for the nilpotent invariants is[5]

$$
\begin{aligned}
I_1\big|_{\mathscr{F}_1} &= \frac{\theta_1\theta_2}{x_1}, & I_2\big|_{\mathscr{F}_1} &= \frac{\theta_1\theta_1\theta_1\theta_1}{x_1^2}, & I_3\big|_{\mathscr{F}_1} &= \frac{\theta_1\theta_1\theta_1\theta_2}{x_1^2}, \\
I_4\big|_{\mathscr{F}_1} &= \frac{\theta_1\theta_1\theta_2\theta_2}{x_1^2}, & I_5\big|_{\mathscr{F}_1} &= \frac{\theta_1\theta_2\theta_1\theta_2}{x_1^2}, & I_6\big|_{\mathscr{F}_1} &= \frac{\theta_1\theta_2\theta_2\theta_2}{x_1^2}, \\
I_7\big|_{\mathscr{F}_1} &= \frac{\theta_2\theta_2\theta_2\theta_2}{x_1^2}, & I_8\big|_{\mathscr{F}_1} &= \frac{(\theta_1\theta_2)^3}{x_1^3}, & I_9\big|_{\mathscr{F}_1} &= \frac{\theta_1^4\theta_2^4}{x_1^4}.
\end{aligned}
\tag{8.46}
$$

As before, one could undo the transformation that led to the frame $\mathscr{F}_1$, and find expressions for I_i in a completely general frame. The resulting expressions are rather involved, and we do not present them here. Actually, for the discussions in this paper, we will mostly need I_i in the frame $\mathscr{F}_1$, and we will only need the expressions in the frame $\mathscr{F}_2$ to obtain the shortening conditions of equation (8.61). The readers interested in this calculation can find the $I_i|_{\mathscr{F}_2}$ in the attached `Mathematica` notebook.

In order to study crossing symmetry, we will be interested in the invariants $\tilde{I}_i$ obtained from I_i with the replacement $z_1 \leftrightarrow z_3$. They take simple forms when expressed in terms of

---

[5]We remind the reader that we are using an index-free notation for the contractions of anticommuting variables, which we describe in detail in appendix 8.A.

the original invariants, for example the bosonic cross-ratio becomes

$$\tilde{z} = 1 - z + \frac{I_1}{2}, \tag{8.47}$$

while the nilpotent invariants become

$$
\begin{aligned}
\tilde{I}_i &= I_i \quad \text{for} \quad i = 1, 2, 8, 9, \\
\tilde{I}_3 &= I_2 - I_3, \\
\tilde{I}_4 &= I_2 - 2I_3 + I_4, \\
\tilde{I}_5 &= I_2 - 2I_3 + I_5, \\
\tilde{I}_6 &= I_2 - 3I_3 + \tfrac{3}{2}I_4 + \tfrac{3}{2}I_5 - I_6, \\
\tilde{I}_7 &= I_2 - 4I_3 + 3I_4 + 3I_5 - 4I_6 + I_7.
\end{aligned}
\tag{8.48}
$$

Scalar long multiplets

We are finally ready to write our first correlators. In analogy with standard CFT, the building block of scalar correlators are combinations Z_{ij}^2 of the coordinates z_i and z_j such that

$$Z_{ij}^2 = \frac{(Z'_{ij})^2}{\Omega(z'_i)\Omega(z'_j)}. \tag{8.49}$$

Here z'_i represent the coordinates obtained from z_i by a superconformal transformation with conformal factor $\Omega(z)$, see equation (8.22). The combination Z_{ij}^2 must be built out of the supertranslation invariant intervals y_{ij} and θ_{ij}, defined in equation (8.44). At order x^2, the most general combination we can build from them which transforms correctly under $\mathcal{D}$, $\mathcal{M}$ and $\mathcal{R}$ is $y_{12}^2 + k\theta_{12}^4$. We can fix the relative coefficient by requiring that (8.49) holds also for inversions I, and we find

$$Z_{ij}^2 \equiv y_{ij}^2 + \tfrac{1}{8}\theta_{ij}^4. \tag{8.50}$$

Notice that we only defined Z_{ij}^2 because $|Z_{ij}| = (Z_{ij}^2)^{1/2}$ does not have a simple form in terms of y_{ij} and θ_{ij}. From the above discussion, it is clear that the two-point function of long scalar fields is

$$\langle \mathcal{O}_1(z_1)\mathcal{O}_2(z_2) \rangle = \frac{\delta_{\Delta_1,\Delta_2}}{\left(Z_{12}^2\right)^{\Delta_1}}, \tag{8.51}$$

148

while the three-point function is

$$\langle \mathcal{O}_1(z_1)\mathcal{O}_2(z_2)\mathcal{O}_3(z_3)\rangle = \frac{\lambda_{\mathcal{O}_1\mathcal{O}_2\mathcal{O}_3}(1 + c\,J)}{(Z_{12}^2)^{\frac{1}{2}(\Delta_1+\Delta_2-\Delta_3)}(Z_{13}^2)^{\frac{1}{2}(\Delta_1+\Delta_3-\Delta_2)}(Z_{23}^2)^{\frac{1}{2}(\Delta_2+\Delta_3-\Delta_1)}}. \tag{8.52}$$

This has the usual form of a three-point function, except for the presence of the three-point invariant J defined in (8.43), and the free parameter c that cannot be fixed by superconformal symmetry. Finally, the four-point function of long scalar fields is

$$\langle \mathcal{O}_1(z_1)\mathcal{O}_2(z_2)\mathcal{O}_3(z_3)\mathcal{O}_4(z_4)\rangle = \frac{F(I_a)}{(Z_{12}^2)^{\frac{1}{2}(\Delta_1+\Delta_2)}(Z_{34}^2)^{\frac{1}{2}(\Delta_3+\Delta_4)}} \left(\frac{Z_{24}^2}{Z_{14}^2}\right)^{\frac{1}{2}\Delta_{12}} \left(\frac{Z_{14}^2}{Z_{13}^2}\right)^{\frac{1}{2}\Delta_{34}} \tag{8.53}$$

where $\Delta_{ij} = \Delta_i - \Delta_j$ and $F(I_a)$ is an arbitrary function of the four-point superconformal invariants. We can expand $F(I_a)$ in the nilpotent basis as

$$F(I_a) = f_0(z) + \sum_{i=1}^{9} f_i(z)I_i, \tag{8.54}$$

where $f_0(z), \ldots, f_9(z)$ are arbitrary functions not fixed by superconformal symmetry.

The displacement operator

Our main objective in this work is to bootstrap the four-point function of the displacement operator. This operator can be obtained as the $\Delta \to 1$ limit of a long scalar, provided that the shortening condition (8.40) is satisfied.

For example, the two point function of the displacement multiplet is

$$\langle \mathcal{D}(z_1)\mathcal{D}(z_2)\rangle = \frac{1}{Z_{12}^2}, \tag{8.55}$$

which is compatible with the shortening condition (8.40)

$$\varepsilon^{ab} D_{1,a}^{(\mathbf{A}} D_{1,b}^{\mathbf{B})} \langle \mathcal{D}(z_1)\mathcal{D}(z_2)\rangle = \varepsilon^{ab} D_{2,a}^{(\mathbf{A}} D_{2,b}^{\mathbf{B})} \langle \mathcal{D}(z_1)\mathcal{D}(z_2)\rangle = 0. \tag{8.56}$$

Similarly, the three-point function of two displacements and one long scalar $\mathcal{O}$ of dimension Δ is

$$\langle \mathcal{D}(z_1)\mathcal{D}(z_2)\mathcal{O}(z_3)\rangle = \frac{\lambda_{\mathcal{D}\mathcal{D}\mathcal{O}}\left(1 - \frac{\Delta(\Delta-2)}{48}J\right)}{(Z_{12}^2)^{\frac{1}{2}(2-\Delta)}(Z_{13}^2)^{\frac{1}{2}\Delta}(Z_{23}^2)^{\frac{1}{2}\Delta}}, \tag{8.57}$$

where the coefficient $c = -\frac{1}{48}\Delta(\Delta - 2)$ is fixed by the the shortening conditions at points 1 and 2. We could also consider the three-point function of displacement operators, in which case we set $\Delta = 1$ in equation (8.57), and the shortening condition at z_3 is automatically satisfied. The previous study of the three-point functions implies the following OPE selection rule

$$[A_2]_{R=0} \times [A_2]_{R=0} \sim 1 + [A_2]_{R=0} + \sum_{\Delta > 1} [L]_{R=j=0}^{\Delta} + \dots, \tag{8.58}$$

where the $\dots$ represent long or short multiplets such that $R, j \neq 0$. One way to complete the right-hand side of this equation would be study more general three-point functions. In section 8.4.1 below we will follow a different route, and derive the full OPE selection rule by solving the Casimir equations.

Finally, let us consider the four-point function of displacement multiplets, which in the frame $\mathscr{F}_1$ takes the form

$$\langle \mathcal{D}(z_1)\mathcal{D}(z_2)\mathcal{D}(0)\mathcal{D}(\infty, 0)\rangle = \frac{F(I_a)}{Z_{12}^2}. \tag{8.59}$$

In this frame it is simple to impose the shortening condition (8.40) at points z_1 and z_2, leading to the constraints

$$
\begin{aligned}
f_2(z) &= \frac{(z+2)(1-z)f_0'(z)}{24z} - \frac{1}{48}(1-z)^2 f_0''(z), \\
f_3(z) &= -\frac{(1-z)f_0'(z)}{6z} + \frac{(z+2)f_1(z)}{6z} - \frac{1}{6}(1-z)f_1'(z), \\
f_4(z) &= \frac{(1-z)f_0'(z)}{8z} + \frac{f_1(z)}{4z} - \frac{1}{2}(z+1)f_6(z) + \frac{1}{4}(1-z)zf_6'(z) + zf_8(z), \\
f_5(z) &= -\frac{f_1(z)}{2z}, \\
f_6(z) &= -\frac{f_0'(z)}{6z} + \frac{f_1(z)}{3z} - \frac{1}{6}f_1'(z), \\
f_7(z) &= \frac{f_0'(z)}{12z} - \frac{1}{48}f_0''(z), \\
f_8(z) &= \frac{f_0'(z)}{24} + \frac{(5z-12)f_0''(z)}{96} - \frac{(z+4)(z-1)f_0^{(3)}(z)}{96} - \frac{z(z-1)^2 f_0^{(4)}(z)}{192} \\
&\quad - \frac{f_1'(z)}{4} + \frac{(1-z)f_1''(z)}{8} + 12zf_9(z).
\end{aligned}
\tag{8.60}
$$

One should also impose shortening at the points z_3 and z_4. The simplest way to achieve this is to consider the four-point function in the frame $\mathscr{F}_2$, but now special care is needed

since equations (8.45)-(8.46) are no longer valid in this frame. All in all, one obtains one extra constraint

$$
\begin{aligned}
f_9(z) = &-\frac{\left(z^2 + z + 2\right) f_0'(z)}{288z^3} + \frac{(z(4 - 5z) + 8)f_0''(z)}{1152z^2} + \frac{(z + 4)(z - 1)f_0{}^{(3)}(z)}{1152z} \\
&+ \frac{(z - 1)^2 f_0{}^{(4)}(z)}{2304} - \frac{(z + 2)f_1(z)}{144z^3} + \frac{(z + 2)f_1'(z)}{144z^2} + \frac{(z - 1)f_1''(z)}{144z}.
\end{aligned}
\tag{8.61}
$$

Summarizing, we have found that the four-point function of displacements depends on two unfixed functions $f_0(z)$ and $f_1(z)$. These two functions will be the subject of the bootstrap analysis of the following sections.

8.4   Superconformal blocks

Armed with the four-point functions in superspace we can now calculate the relevant superconformal blocks. There are several approaches that have been used to calculate superblocks with varying degrees of success. These include explicit calculation of three-point couplings of descendants [65, 239], the shadow formalism [194, 337], Ward identities in harmonic superspace [219, 244, 336, 357], the Casimir operator [194, 196, 228, 237], and the connection to Calogero-Sutherland models [240]. Because the multiplets we are considering are scalars with no R-symmetry or transverse-spin indices, we will use the most conventional of these methods, which is to consider superblocks as eigenfunctions of the Casimir operator.[6] In the main text we will concentrate on the blocks for the displacement multiplet, however in appendix 8.B we present more general correlators that also include non-protected long operators.

8.4.1   From the Casimir equation

Superconformal blocks are given by a finite sum of $1d$ bosonic blocks, that capture the contributions of the $\mathfrak{sl}(2; \mathbb{R})$ primaries in the conformal multiplets:

$$
g_\Delta^{\Delta_{12}, \Delta_{34}}(z) = z^\Delta {}_2F_1(\Delta - \Delta_{12}, \Delta + \Delta_{34}, 2\Delta, z). \tag{8.62}
$$

The coefficients in this sum are fixed by supersymmetry, so we can make an ansatz for the functions f_i in terms of bosonic blocks. After acting with the Casimir operator on

---

[6]In some selected cases we will also calculate three-point couplings of descendants as a non-trivial check for our computations.

the four-point function, we will obtain a coupled system of equations for the functions f_i that we will use to fix the coefficients in our ansatz. Since we will use the coupled set of differential equations only to fix these coefficients, the superblocks will automatically satisfy the correct boundary conditions.

The Casimir of the $\mathfrak{osp}(4^*|2)$ superalgebra is given by

$$\mathcal{C}^2 = +\mathcal{D}^2 - \tfrac{1}{2}(\mathcal{P}\mathcal{K} + \mathcal{K}\mathcal{P}) + \tfrac{1}{2}\mathcal{M}_a{}^b\mathcal{M}_b{}^a - \mathcal{R}^{\mathbf{A}}{}_{\mathbf{B}}\mathcal{R}^{\mathbf{B}}{}_{\mathbf{A}} - \tfrac{1}{2}[\mathcal{Q}_a^{\mathbf{A}}, \mathcal{S}_{\mathbf{A}}^a]. \tag{8.63}$$

When it acts on an operator $\mathcal{O}$ with quantum numbers $[\Delta, j, R]$ it has the following eigenvalue

$$\mathcal{C}^2\mathcal{O} = \mathfrak{c}_{\Delta,j,R}\mathcal{O}, \qquad \mathfrak{c}_{\Delta,j,R} = \Delta(\Delta+1) + j(j+1) - 2R(R+1). \tag{8.64}$$

Given a four-point function, we can evaluate it by taking OPEs in the $(12) \to (34)$ channel, leading to the usual expansion in terms of superconformal blocks

$$\langle \mathcal{D}(z_1)\mathcal{D}(z_2)\mathcal{D}(z_3)\mathcal{D}(z_4)\rangle = \frac{1}{Z_{12}^2 Z_{34}^2} \sum_{\mathcal{O} \in \mathcal{D} \times \mathcal{D}} \lambda_{\mathcal{D}\mathcal{D}\mathcal{O}}^2 \, \mathcal{G}_{\mathcal{O}}(I_a). \tag{8.65}$$

In order to obtain a superconformal block, we act with the Casimir on the four-point function and find the solution to the eigenvalue problem[7]

$$\mathcal{C}_{12}^2 \, \mathcal{G}_{\Delta,j,R}(I_a) = \mathfrak{c}_{\Delta,j,R} \, \mathcal{G}_{\Delta,j,R}(I_a). \tag{8.66}$$

The differential operator $\mathcal{C}_{12}^2$ is constructed from the Casimir (8.63) and the symmetry generators in differential form (8.32). Note that the operators need to be evaluated at points z_1 and z_2, namely $\mathcal{L}_{12} = \mathcal{L}_1 + \mathcal{L}_2$. In order to solve the above equation, we take $\mathcal{G}$ to be of the form (8.54) with the shortening conditions (8.60) and (8.61). Furthermore, we evaluate the Casimir equation in the frame $\mathscr{F}_1$ where the calculations are simpler. The resulting system of differential equations is

$$-z^2\big[(z-1)f_0''(z) + f_0'(z)\big] - 4zf_1(z) = \mathfrak{c}_{\Delta,j,R}\, f_0(z), \tag{8.67a}$$

$$-(z-1)z\big(zf_1''(z) + 4f_1'(z)\big) + (2-z)\big(\tfrac{1}{2}f_0'(z) + 2f_1(z)\big) = \mathfrak{c}_{\Delta,j,R}\, f_1(z). \tag{8.67b}$$

Notice the similarity of (8.67a) with the usual non-supersymmetric $1d$ Casimir equation. To solve these equations one should make an ansatz for the f_i in terms of $1d$ bosonic blocks. However, as discussed in [228], it is simpler to first "change basis" to a set of functions $G_i(z)$,

---

[7]Notice that the dependence on Z_{12}^2 drops from the eigenvalue problem since $\mathcal{C}_{12}^2 Z_{12}^2 = 0$.

where each of the G_i captures the contribution of the external superconformal descendants, and build an ansatz for the G_i instead. Let us review in detail how to implement this idea.

We start by expanding the displacement multiplets in terms of their conformal descendants (8.39), so that the four-point function becomes

$$
\begin{aligned}
\langle \mathcal{D}(z_1)\mathcal{D}(z_2)\mathcal{D}(0)\mathcal{D}(\infty,0) \rangle &= \langle A(x_1)A(x_2)A(0)A(\infty) \rangle \\
&\quad - \theta_{1,\mathbf{A}}^a \theta_{2,\mathbf{B}}^b \langle B_a^{\mathbf{A}}(x_1)B_b^{\mathbf{B}}(x_2)A(0)A(\infty) \rangle + \dots
\end{aligned}
\tag{8.68}
$$

Note that since we work in the frame $\mathscr{F}_1$, we have $\theta_3 = \theta_4 = 0$, so only the superconformal primary A at points 3 and 4 will appear. There are only three four-point functions of descendants that contribute to the above expansion, and for each of them we define a new function G_i as

$$
\begin{aligned}
\langle A(x_1)A(x_2)A(0)A(\infty) \rangle &\;\rightarrow\; \frac{1}{|x_{12}|^2} G_0(z), \\
\langle B_a^{\mathbf{A}}(x_1)B_b^{\mathbf{B}}(x_2)A(0)A(\infty) \rangle &\;\rightarrow\; \frac{x_{12}\,\varepsilon^{\mathbf{AB}}\varepsilon_{ab}}{|x_{12}|^4} G_1(z), \\
\langle C_{ab}^{\mathbf{AB}}(x_1)C_{cd}^{\mathbf{CD}}(x_2)A(0)A(\infty) \rangle &\;\rightarrow\; \frac{\varepsilon^{\mathbf{AB}}\varepsilon^{\mathbf{CD}}(\varepsilon_{ac}\varepsilon_{bd} + \varepsilon_{ad}\varepsilon_{bc})}{|x_{12}|^4} G_2(z),
\end{aligned}
\tag{8.69}
$$

On one hand, we can introduce (8.69) in the expansion (8.68), and on the other, we can expand the four-point function of displacements (8.59) in terms of θ_1 and θ_2. By matching the components of the two sides, we get that the change of basis is

$$
f_0(z) = G_0(z), \qquad f_1(z) = -\tfrac{1}{z}[G_0(z) + G_1(z)].
\tag{8.70}
$$

Furthermore, we see that G_2 must be related to G_0 and G_1 by

$$
G_2(z) = \tfrac{1}{8}G_0(z) + \tfrac{1}{48}z(z-4)G_0'(z) - \tfrac{1}{48}z^2(z-1)G_0''(z) + \tfrac{1}{2}G_1(z) + \tfrac{1}{12}z(z-2)G_1'(z).
\tag{8.71}
$$

It is natural that G_2 is related to G_0 and G_1, since the four-point function of displacements contains only two unfixed functions $f_0(z)$ and $f_1(z)$. However, we still had to include G_2 in (8.69), because a priori we did not know what this relation was.

The virtue of the G_i basis is that now the ansatz in terms of $1d$ bosonic blocks is very simple

$$
G_i(z) = a_i\, g_\Delta^{0,0}(z) + b_i\, g_{\Delta+\frac{1}{2}}^{0,0}(z) + c_i\, g_{\Delta+1}^{0,0}(z) + d_i\, g_{\Delta+\frac{3}{2}}^{0,0}(z) + e_i\, g_{\Delta+2}^{0,0}(z).
\tag{8.72}
$$

We finally have all the ingredients to solve the Casimir equations (8.67). If we consider the case of an exchanged multiplet $[\Delta, 0, 0]$, then the Casimir eigenvalue is $\mathfrak{c} = \Delta(\Delta + 1)$, and the equations are solved by

$$
\begin{aligned}
G_0(z) &= g_\Delta^{0,0}(z) + \frac{(\Delta - 1)\Delta(\Delta + 1)}{4(\Delta + 2)(2\Delta + 1)(2\Delta + 3)} g_{\Delta+2}^{0,0}(z), \\
G_1(z) &= \frac{1}{2}(\Delta - 2)g_\Delta^{0,0}(z) - \frac{(\Delta - 1)\Delta(\Delta + 1)(\Delta + 3)}{8(\Delta + 2)(2\Delta + 1)(2\Delta + 3)} g_{\Delta+2}^{0,0}(z).
\end{aligned}
\tag{8.73}
$$

From now on, we will sometimes use vectorial notation $G(z) = (G_0(z), G_1(z))$. Depending on the value of Δ, the solution (8.73) is interpreted as follows:

- For $\Delta = 0$ the block reduces to $G_{\mathbb{1}}(z) = (1, -1)$, and corresponds to the identity operator being exchanged.

- For $\Delta = 1$ the block reduces to $G_{A_2}(z) = (g_1^{0,0}(z), -\frac{1}{2}g_1^{0,0}(z))$, and corresponds to a displacement multiplet $[A_2]_{R=0}$ being exchanged.

- For $\Delta > 1$ the block $G_\Delta^{[0,0]}(z)$ is given by (8.73), and corresponds to a long scalar multiplet $[L]_\Delta^{j=R=0}$ being exchanged.

One can also consider an exchanged multiplet $[\Delta, 1, 0]$, in which case the Casimir eigenvalue is $\mathfrak{c} = \Delta(\Delta + 1) + 2$, and the equations are solved by

$$
G_0(z) = g_{\Delta+1}^{0,0}(z), \qquad G_1(z) = -\frac{1}{2}g_{\Delta+1}^{0,0}(z).
\tag{8.74}
$$

The solution (8.74) is interpreted as follows:

- For $\Delta = 2$ the block reduces to $G_{A_1}(z) = (g_3^{0,0}(z), -\frac{1}{2}g_3^{0,0}(z))$. Note that from the recombination rules (8.11), we could interpret the solution as either an $[A_1]_{R=0}^{j=1}$ or an $[A_1]_{R=1/2}^{j=1/2}$. The correct interpretation is that it is actually $[A_1]_{R=1/2}^{j=1/2}$ which is exchanged, in particular its descendant with quantum numbers $[3, 0, 0]$, see equation (8.10).

- For $\Delta > 2$ the block $G_\Delta^{[1,0]}(z)$ is given by (8.74), and corresponds to a long scalar multiplet $[L]_\Delta^{j=1, R=0}$ being exchanged.

We have tried solving the Casimir equation considering other possible exchanges, but in all cases there were no new solutions found, so the above are all the operators that can appear in the OPE of two displacement multiplets.

OPE selection rule.   Summarizing the above results, we obtain the following selection rule

$$[A_2]_{R=0} \times [A_2]_{R=0} \sim 1 + [A_2]_{R=0} + [A_1]^{j=1/2}_{R=1/2} + \sum_{\Delta>1} [L]^{[0,0]}_\Delta + \sum_{\Delta>2} [L]^{[1,0]}_\Delta, \qquad (8.75)$$

which completes the partial selection rule (8.58) obtained from the three-point function analysis.

8.4.2   From two- and three-point functions

In this section, we calculate the superconformal blocks in the $[\Delta, 0, 0]$ channel (8.73) following the approach of [65]. This provides a non-trivial consistency check for our results, and sheds light on the structure of such blocks. The key insight is that the coefficients appearing in the superconformal blocks are OPE coefficients and norms of conformal descendants

$$\begin{aligned}
G_0(z) &= \frac{\lambda^2_{AAA}}{\langle A|A\rangle} \, g^{0,0}_\Delta(z) + \frac{\lambda^2_{AAG}}{\langle G|G\rangle} \, g^{0,0}_{\Delta+2}(z), \\
G_1(z) &= \frac{\lambda_{AAA}\lambda_{BBA}}{\langle A|A\rangle} \, g^{0,0}_\Delta(z) + \frac{\lambda_{AAG}\lambda_{BBG}}{\langle G|G\rangle} \, g^{0,0}_{\Delta+2}(z).
\end{aligned} \qquad (8.76)$$

Here $\lambda_{O_1 O_2 O_3}$ denotes the OPE coefficient of two fields from the displacement multiplet with one operator from a long scalar multiplet, namely $O_1, O_2 \in \mathcal{D}$ and $O_3 \in \mathcal{O}$, see equations (8.36) and (8.39) for more details. On the other hand, $\langle O|O\rangle$ denotes the norm of an operator that belongs to the long multiplet $\mathcal{O}$, and can be computed from the two-point function as explained below.

The procedure to obtain the OPE coefficients resembles the way we obtained the change of basis in equation (8.70). Let us take the three-point function (8.57) of two displacement operators and a long scalar of dimension Δ. On one hand, we expand it in the fermionic variables, while on the other we expand the external superfields in terms of their conformal descendants (8.36) and (8.39)

$$\begin{aligned}
\langle \mathcal{D}(z_1)\mathcal{D}(z_2)\mathcal{O}(z_3)\rangle &= \frac{\lambda_{\mathcal{DDO}}}{|x_{12}|^{2-\Delta}|x_{13}|^\Delta|x_{23}|^\Delta} - \theta^a_{1,\mathbf{A}}\theta^b_{2,\mathbf{B}} \frac{\frac{1}{2}(\Delta-2)\lambda_{\mathcal{DDO}}\varepsilon_{ab}\varepsilon^{\mathbf{AB}}}{|x_{12}|^{3-\Delta}|x_{13}|^\Delta|x_{23}|^\Delta} + \dots \\
&= \langle A(x_1)A(x_2)A(x_3)\rangle \quad - \theta^a_{1,\mathbf{A}}\theta^b_{2,\mathbf{B}} \langle B^{\mathbf{A}}_a(x_1)B^{\mathbf{B}}_b(x_2)A(x_3)\rangle + \dots
\end{aligned}$$

$$(8.77)$$

Mapping the two sides one can obtain all the OPE coefficients of the descendant fields. The relevant ones for us will be

$$\lambda_{AAA} = \lambda_{\mathcal{DDO}}, \qquad\qquad \lambda_{AAG} = -\frac{(\Delta - 1)\Delta(\Delta + 1)\lambda_{\mathcal{DDO}}}{24(2\Delta + 1)},$$

$$\lambda_{BBA} = \frac{1}{2}(\Delta - 2)\lambda_{\mathcal{DDO}}, \qquad \lambda_{BBG} = \frac{(\Delta - 1)\Delta(\Delta + 1)(\Delta + 3)\lambda_{\mathcal{DDO}}}{48(2\Delta + 1)},$$

$$\lambda_{CCA} = -\frac{1}{16}(\Delta - 3)(\Delta - 2)\lambda_{\mathcal{DDO}}, \quad \lambda_{CCG} = \frac{(\Delta - 1)\Delta(\Delta + 1)(\Delta + 3)(\Delta + 4)\lambda_{\mathcal{DDO}}}{384(2\Delta + 1)}.$$

$$(8.78)$$

Notice how λ_{AAG}, λ_{BBG}, λ_{CCG} vanish for $\Delta = 1$, as expected from the shortening $\mathcal{O} \to \mathcal{D}$ and the fact that $G \notin \mathcal{D}$. We can do a similar analysis for the two-point function (8.51) of scalar longs of dimension Δ. In this case we obtain the norms of the descendants

$$\langle A|A \rangle = 1, \qquad\qquad \langle E|E \rangle = \frac{1}{8}(\Delta - 1)\Delta,$$

$$\langle B|B \rangle = \Delta, \qquad\qquad \langle F|F \rangle = \frac{2(\Delta - 1)\Delta(\Delta + 1)(\Delta + 2)}{9(2\Delta + 1)}, \qquad (8.79)$$

$$\langle C|C \rangle = \frac{1}{8}\Delta(\Delta + 2), \qquad \langle G|G \rangle = \frac{(\Delta - 1)\Delta(\Delta + 1)(\Delta + 2)(2\Delta + 3)}{144(2\Delta + 1)}.$$

It is a simple exercise to check that inserting (8.78) and (8.79) in (8.76) leads to the superconformal blocks (8.73). One could do a similar analysis to compute the blocks in the $[\Delta, 1, 0]$ channel, but it would be more involved, since then an expression for the three-point functions of external operators with transverse spin would be needed.

8.4.3 Crossing equations

In the previous sections we have studied the four-point function of displacement operators in the $(12) \to (34)$ channel. Demanding that it is equivalent to the four-point function in the $(14) \to (23)$ channel leads to the crossing equation

$$\frac{1}{Z_{12}^2 Z_{34}^2}\left(f_0(z) + \sum_{i=1}^{9} I_i f_i(z)\right) = \frac{1}{Z_{14}^2 Z_{23}^2}\left(f_0(\tilde{z}) + \sum_{i=1}^{9} \tilde{I}_i f_i(\tilde{z})\right), \qquad (8.80)$$

where the $\tilde{I}_i$ invariants appear in equation (8.48), and are obtained from the I_i by the replacement $z_1 \leftrightarrow z_3$. Since $\tilde{z} = 1 - z + \frac{1}{2}I_1$, we can Taylor expand the f_i's in the right-hand side around $\tilde{z} = 1 - z$, and insert the expressions for the $\tilde{I}_i$. By looking at independent

terms, one can see that the crossing equation reduces to

$$(1 - z)^2 H(z) - z^2 H(1 - z) = 0, \tag{8.81}$$

where $H(z)$ is a two-dimensional vector with components

$$
\begin{aligned}
H_0(z) &= G_0(z), \\
H_1(z) &= -2zG_0(z) + z(z - 1)G_0'(z) - 4(z - 1)G_1(z).
\end{aligned}
\tag{8.82}
$$

Notice that from the first component we obtain the usual $1d$ bosonic crossing equation, but the second mixes $G_0(z)$ and $G_1(z)$ in a non-trivial way.

8.4.4   An exact solution

In this section we present a family of exact solutions to the crossing equations in terms of free fields. We will argue in section 8.6 that one solution in this family describes the strong coupling limit of line defects that admit a holographic description. Furthermore, these solutions will play a prominent role in the next two sections, where we will apply numerical and analytical bootstrap techniques to this correlator.

The most general solution of crossing that we have found built from Wick contractions contains one free parameter ξ. Since it is a valid correlator, it can be expanded in terms of superconformal blocks as in equation (8.65)

$$
\begin{aligned}
\langle \mathcal{D}(z_1)\mathcal{D}(z_2)\mathcal{D}(z_3)\mathcal{D}(z_4) \rangle &= \frac{1}{Z_{12}^2 Z_{34}^2} \left[1 + \xi \frac{Z_{12}^2 Z_{34}^2}{Z_{13}^2 Z_{24}^2} + \frac{Z_{12}^2 Z_{34}^2}{Z_{14}^2 Z_{23}^2} \right] \\
&= \frac{1}{Z_{12}^2 Z_{34}^2} \left[1 + c\,\mathcal{G}_{A_1} + \sum_{\Delta \geq 2} a_\Delta \mathcal{G}_{L_\Delta^{[0,0]}} + \sum_{\Delta \geq 3} b_\Delta \mathcal{G}_{L_\Delta^{[1,0]}} \right].
\end{aligned}
\tag{8.83}
$$

Notice how the block $\mathcal{G}_{A_2}$, which a priori could appear in the expansion, has vanishing OPE coefficient $\lambda_{A_2}^2 = 0$ for any value of ξ. The other OPE coefficients are given by

$$
a_\Delta = \frac{\left(1 + (-1)^\Delta \xi\right) \sqrt{\pi}\,\Gamma(\Delta + 3)}{2^{2\Delta+1}\Gamma\left(\Delta + \frac{1}{2}\right)}, \qquad b_\Delta = \frac{3(\Delta - 1)}{2(\Delta + 1)} \frac{\left(1 + (-1)^{\Delta+1}\xi\right) \sqrt{\pi}\,\Gamma(\Delta + 3)}{2^{2\Delta+1}\Gamma\left(\Delta + \frac{1}{2}\right)},
\tag{8.84}
$$

and $c = b_{\Delta=2} = (1 - \xi)/2$. Positivity of the OPE coefficients requires $-1 \leq \xi \leq 1$. The theory with $\xi = 1$ corresponds to free bosons, $\xi = -1$ corresponds to free fermions, and

certain values $-1 < \xi < 1$ correspond to free gauge theories, as discussed in [233]. We will argue in section 8.6 that the bosonic theory with $\xi = 1$ corresponds to the displacement operator at leading order in the strong-coupling limit. The physical interpretation of the fermionic $\xi = -1$ theory is less clear, since we know that the displacement must be a bosonic operator. Nevertheless, it will be important as a valid solution of crossing that will sit in interesting corners of the allowed regions of the numerical results in next section.

8.5   Numerical results

In this section we use numerical boostrap techniques [17,56,58] to bound conformal dimensions and OPE coefficients of operators that appear in the four-point function of displacement operators. We start each subsection with a short review of the numerical algorithm, and then we proceed to discuss the results. We have generated tables of derivatives of superconformal blocks with `Mathematica`, which are then used by the semidefinite program solver `SDPB` [59][8]. The results are analyzed using `python`, and the plots are generated with `matplotlib` [358].

In section 8.4.3 we derived the crossing equations (8.81), which take the simple form $F(z) = 0$ in terms of the two-dimensional vector

$$F(z) \equiv (1 - z)^2 H(z) - z^2 H(1 - z) \,. \tag{8.85}$$

We can expand $F(z)$ summing the contributions of the operators that appear in the OPE of two displacements (8.75)

$$F(z) = F_{\mathbb{1}}(z) + \lambda_{A_1}^2 F_{A_1}(z) + \lambda_{A_2}^2 F_{A_2}(z) + \sum_{\Delta > 1} \lambda_{L_\Delta^{[0,0]}}^2 F_\Delta^{[0,0]}(z) + \sum_{\Delta > 2} \lambda_{L_\Delta^{[1,0]}}^2 F_\Delta^{[1,0]}(z) = 0 \,, \tag{8.86}$$

where by unitarity the OPE coefficients are real, hence $\lambda_{\mathcal{O}}^2 \geq 0$. Here and in what follows we are using a shorthand notation where it is implicitly understood that $\lambda_{\mathcal{O}}^2 = \lambda_{\mathcal{D}\mathcal{D}\mathcal{O}}^2$.

In order to explore the numerical constraints implied by crossing we will make some structural assumptions about the CFT data. In some of our plots we will assume that $\lambda_{A_2}^2 = 0$, or equivalently, that the displacement multiplet does not appear in the OPE of

---

[8]An alternative to `Mathematica` to compute the tables is `PyCFTBoot` [70], which then relies on `SDPB` to carry out the optimizations. On the other hand, one can generate the tables in `Mathematica`, but then perform the numerics in `JuliBoots` [69].

two displacements. Notice that this is the case for the mean-field solutions of the previous section, as well as for $\mathcal{N} = 4$ theories that are interpreted as $\mathcal{N} = 2$ SCFT [346]. This is also true whenever the displacement is odd under a $\mathbb{Z}_2$ symmetry. One could relax this condition, however we found that the numerical results become significantly weaker. It will be interesting to explore this further in the future. The second assumption is that the low-lying spectrum is somehow sparse, with gaps in between the local operators. More precisely, we will assume an isolated long operator with dimension $\Delta_{[0,0]}$ separated by a finite gap from the unitarity bound, and a second gap between $\Delta_{[0,0]}$ and a continuum of long operators with dimensions $\Delta \geq \Delta'_{[0,0]}$. Similar assumptions will also be made for the longs in the $[1,0]$ channel.

The most general case we will be studying is then

$$F_{\mathbb{1}}(z) + \lambda_{A_1}^2 F_{A_1}(z) + \lambda_{A_2}^2 F_{A_2}(z) + \lambda_{L_{\Delta_{[0,0]}}}^2 F_{\Delta_{[0,0]}}^{[0,0]}(z) + \lambda_{L_{\Delta_{[1,0]}}}^2 F_{\Delta_{[1,0]}}^{[1,0]}(z) +$$
$$+ \sum_{\Delta \geq \Delta'_{[0,0]}} \lambda_{L_{\Delta}^{[0,0]}}^2 F_{\Delta}^{[0,0]}(z) + \sum_{\Delta \geq \Delta'_{[1,0]}} \lambda_{L_{\Delta}^{[1,0]}}^2 F_{\Delta}^{[1,0]}(z) = 0\,.$$

(8.87)

When we discuss the results, it will be instructive to compare with the free-field solutions (8.83). In the plots we will represent these solutions with a solid bullet $\bullet$ or dashed line ......, accompanied by a letter representing the type of solution

- B : Free boson, $\xi = 1$,
- F : Free fermion, $\xi = -1$, (8.88)
- G : Free gauge theory, $-1 < \xi < 1$.

Currently, the only $\mathcal{N} = 2$ line defect with insertions that has been studied in the literature is the one in $\mathcal{N} = 4$ SYM. The leading-order correlation function of $\mathcal{D}$'s at strong coupling was computed in [346], and it is given by the free bosonic solution. In that work, the first-order correction in $\frac{1}{\sqrt{\lambda}}$ to the correlator was also obtained. It would be an interesting problem for the future to study an $\mathcal{N} = 2$ line defect with insertions either using holography or perturbation theory and compare with our numerical bounds.

8.5.1 Dimension bounds

The algorithm for bounding operator dimensions works in the following way. First, one assumes a spectrum of operator dimensions. In the case of interest to us (8.87), this boils

down to fixing the dimension of the isolated longs $\Delta_{[0,0]}$ and $\Delta_{[1,0]}$, and also the dimension of the first longs in the continuum $\Delta'_{[0,0]}$ and $\Delta'_{[1,0]}$. Then one tries to find a functional α such that

$$\alpha(F_{\mathbb{1}}) = 1 \,, \quad \alpha(F_{\mathcal{I}}) \geq 0 \,, \quad \alpha\big(F_\Delta^{[0,0]}\big) \geq 0 \ \text{ for } \ \Delta \geq \Delta'_{[0,0]} \,, \quad \alpha\big(F_\Delta^{[1,0]}\big) \geq 0 \ \text{ for } \ \Delta \geq \Delta'_{[1,0]} \,, \tag{8.89}$$

where $\mathcal{I} = A_1$, A_2, $L_{\Delta_{[0,0]}}^{[0,0]}$, $L_{\Delta_{[1,0]}}^{[1,0]}$ runs over all the operators with fixed conformal dimensions. If such functional α exists, then it is not possible to satisfy equation (8.87), and the spectrum is ruled out.

As is customary we consider functionals of the form

$$\alpha(F_\Delta) = \sum_{i=0}^{1} \sum_{m=0}^{\Lambda} a_{i,m} \left. \frac{\partial^m F_{i,\Delta}(z)}{\partial z^m} \right|_{z=1/2} \approx \chi(\Delta) P(\Delta) \,, \tag{8.90}$$

where $i = 0, 1$ runs over the two components of $F_\Delta(z)$, and the number of derivatives Λ needs to be increased in order to obtain stronger bounds. In the last step we have approximated the conformal blocks by a positive function $\chi(\Delta) \geq 0$ multiplying a linear combination of polynomials in Δ

$$P(\Delta) = \sum_{i=0}^{1} \sum_{m=0}^{\Lambda} a_{i,m} P_{i,m}(\Delta) \,. \tag{8.91}$$

This approximation can be obtained as described in [57, 58]. Thanks to (8.90) and (8.91), we can reformulate the optimization problem (8.89) as finding a set of coefficients $a_{i,m}$ such that

$$\alpha(F_{\mathbb{1}}) = 1 \,, \qquad \alpha(F_{\mathcal{I}}) \geq 0 \,, \qquad P^{[0,0]}\left(\Delta'_{[0,0]} + x\right) \geq 0 \,, \qquad P^{[1,0]}\left(\Delta'_{[1,0]} + x\right) \geq 0 \,, \tag{8.92}$$

for all $x \geq 0$. This is a semidefinite programming problem which can be solved using SDPB [59].

In figure 8.2 we present upper bounds on the dimension $\Delta'_{[0,0]}$ of the first long in the continuum, as a function of the dimension of the isolated long $\Delta_{[0,0]}$, while keeping all the operators in the $[1, 0]$ channel slightly above their unitarity bound. In an exactly analogous way, we also present the upper bound of $\Delta'_{[1,0]}$ as a function of $\Delta_{[1,0]}$ without imposing gaps in the $[0, 0]$ channel. The first interesting feature is that regardless of where the continuum
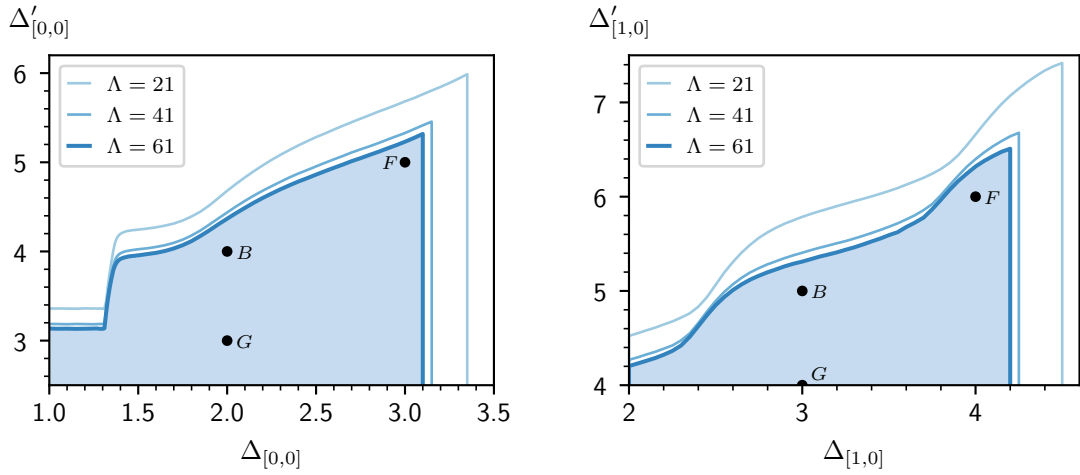
Figure 8.2: Left: Upper bounds on the dimension $\Delta'_{[0,0]}$ of the first long in the continuum as a function of the dimension $\Delta_{[0,0]}$ of the isolated long. Only the allowed region for $\Lambda = 61$ is shaded. There is a sudden jump in the upper bound for $\Delta_{[0,0]} \simeq 1.31$. We are not imposing any gaps in the channel $[1,0]$, and we keep the operators slightly above the unitarity bound, i.e. $\Delta_{[1,0]} = \Delta'_{[1,0]} \gtrsim 2$. Right: Upper bounds on $\Delta'_{[1,0]}$ as a function of the dimension $\Delta_{[1,0]}$ keeping $\Delta_{[0,0]} = \Delta'_{[0,0]} \gtrsim 1$. The free theory solutions are represented by bullets $\bullet$, as explained in (8.88).

sits, there is an upper bound on the dimension $\Delta_{[a,b]}$ of the first long. The plots suggest that in the limit $\Lambda \to \infty$ the maximum dimension is approximately[9]

$$\Delta_{[0,0]} \lesssim 3.0 \,, \qquad \Delta_{[1,0]} \lesssim 4.0 \,. \tag{8.93}$$

These bounds are almost saturated by the fermionic free theory of equation (8.83) with $\xi = -1$. Moreover, the fermionic theory sits very close to the upper bound for $\Delta'_{[0,0]}$ and $\Delta'_{[1,0]}$ when (8.93) is saturated. Similarly, we also see that when $\Delta_{[0,0]} = 2.0$ or $\Delta_{[1,0]} = 3.0$, the free bosonic theory almost saturates the upper bounds for $\Delta'_{[0,0]}$ and $\Delta'_{[1,0]}$ respectively. Finally, the free gauge theories (8.83) with $-1 < \xi < 1$ are far from the boundary of the allowed region.

Another feature is the sudden jump in the upper bound for $\Delta'_{[0,0]}$ starting at

$$\Delta_{[0,0],\mathrm{jump}} \simeq 1.31 \,. \tag{8.94}$$

As we will discuss in more detail in the following section, this seems to be related to certain OPE coefficients becoming unbounded for $\Delta_{[0,0]} < \Delta_{[0,0],\mathrm{jump}}$.

8.5.2 OPE bounds

One can find upper and lower bounds for the OPE coefficient $\lambda_{\mathcal{O}}^2$ using a very similar algorithm as the one described above. We use a functional α of the form (8.90), and maximize $\alpha(F_{\mathbb{1}})$ such that $\alpha(F_{\mathcal{O}}) = 1$ and

$$\alpha(F_{\mathcal{I}}) \geq 0, \qquad P^{[0,0]} \left(\Delta'_{[0,0]} + x \right) \geq 0 \ \text{ for } \ x \geq 0 \,, \qquad P^{[1,0]} \left(\Delta'_{[1,0]} + x \right) \geq 0 \ \text{ for } \ x \geq 0 \,. \tag{8.95}$$

Then we obtain the upper bound $\lambda_{\mathcal{O}}^2 \leq -\alpha(F_{\mathbb{1}})$. Similarly, if we find α that maximizes $\alpha(F_{\mathbb{1}})$ such that $\alpha(F_{\mathcal{O}}) = -1$ and (8.95) holds, we obtain the lower bound $\lambda_{\mathcal{O}}^2 \geq \alpha(F_{\mathbb{1}})$. As before, such optimization problems can be solved using SDPB.

First, we would like to understand the nature of the jump observed in figure 8.2 and discussed around equation (8.94). In figure 8.3 we obtain upper and lower bounds on the OPE coefficients $\lambda_{L_{\Delta_{[0,0]}}}^2$ and $\lambda_{A_1}^2$ as a function of the dimension of the first long $\Delta_{[0,0]}$. Here, we are not assuming a double gap in any of the two long channels, i.e. we take

---

[9]It would be interesting to confirm that for larger values of Λ the bounds indeed converge to $\Delta_{[0,0]} = 3$ and $\Delta_{[1,0]} = 4$, but at this stage the assumption is very plausible.
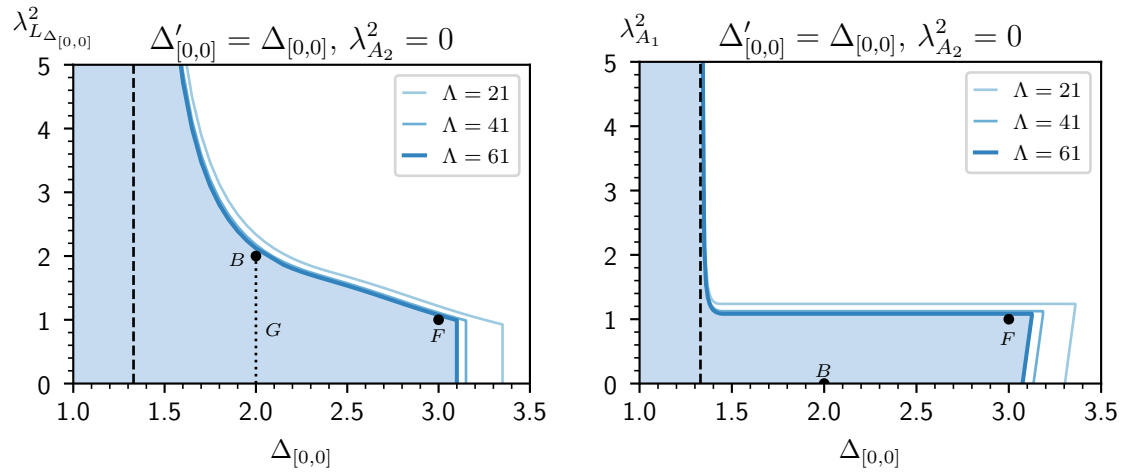
Figure 8.3: Left: Upper bound on the OPE coefficient of the isolated long as a function of its dimension $\Delta_{[0,0]}$. Right: Upper bound on the OPE coefficient of the $[A_1]_{R=1/2}^{j=1/2}$ multiplet, as a function of the dimension of the first long $\Delta_{[0,0]}$. In both plots, we keep $\Delta'_{[0,0]} \gtrsim \Delta_{[0,0]}$ and $\Delta_{[1,0]} = \Delta'_{[1,0]} \gtrsim 2$. The upper bound of both OPE coefficients diverges for $\Delta_{[0,0]} \simeq 1.33$, which is represented with a vertical dashed line.
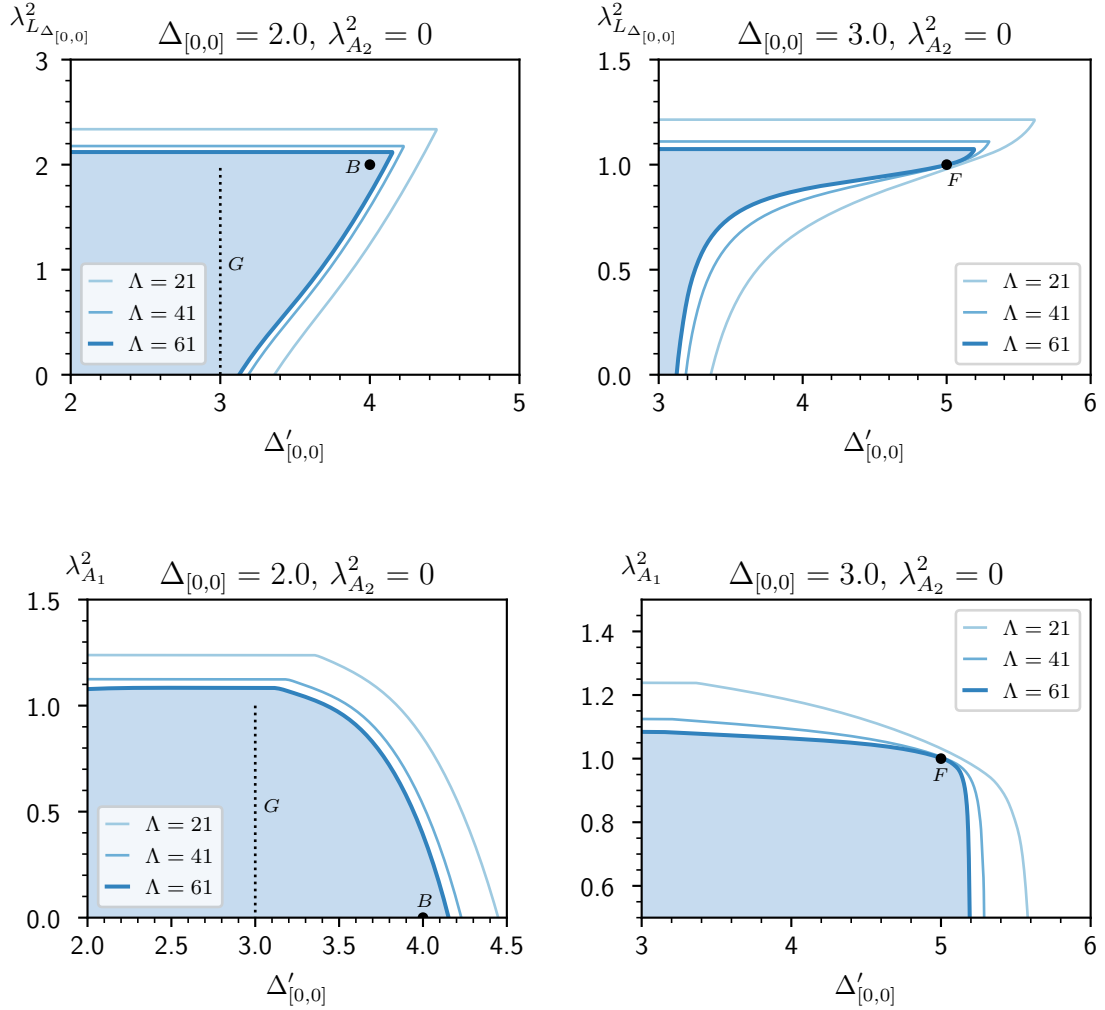
Figure 8.4: Upper and lower bounds for $\lambda^2_{L_{\Delta}^{[0,0]}}$ (first row) and $\lambda^2_{A_1}$ (second row) as a function of $\Delta'_{[0,0]}$ when $\lambda^2_{A_2} = 0$. In the first column, $\Delta_{[0,0]} = 2.0$ and by increasing $\Delta'_{[0,0]}$ the bosonic free theory sits at the boundary of the allowed region. In the second column, $\Delta_{[0,0]} = 3.0$ and by increasing $\Delta'_{[0,0]}$ the fermionic free theory sits at the boundary.
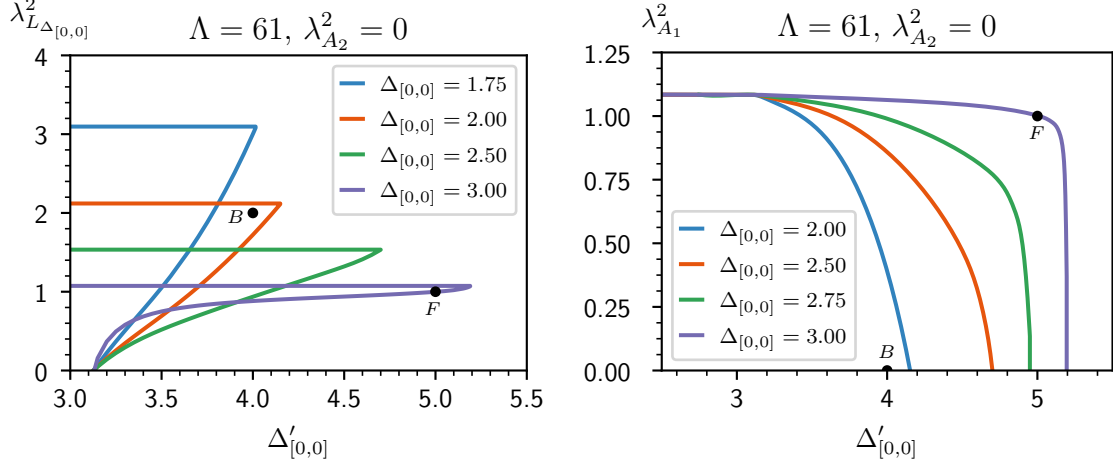
Figure 8.5: Comparison of the upper and lower bounds of λ_L^2 (left) and $\lambda_{A_1}^2$ (right) as a function of $\Delta'_{[0,0]}$ and for different values of $\Delta_{[0,0]}$. All the optimizations have been run for $\Lambda=61$ and assuming $\lambda_{A_2}^2=0$.

$\Delta_{[a,b]}=\Delta'_{[a,b]}$, but we do assume $\lambda_{A_2}^2=0$. Somehow unexpectedly, both OPE coefficients become unbounded for $\Delta_{[0,0]}$ less than

$$\Delta_{[0,0],\text{jump}} \simeq 1.33 \,. \tag{8.96}$$

Even though there is a slight mismatch between the values of $\Delta_{[0,0],\text{jump}}$ in (8.94) and (8.96), we believe it is only due to the numerical nature of the calculation, and that the two values would be the same for large enough Λ. A very similar situation was observed in [233], where a sudden drop in the upper bound of a conformal dimension was related to the appearence of an upper bound of a related OPE coefficient. For the $3d$ Ising model it is known that the dimensions and OPE coefficients of certain operators suffered a sudden jump around the Ising model point [63]. It would be interesting to see if the region $\Delta_{[0,0]}\sim\Delta_{[0,0],\text{jump}}$ corresponds to a line defect of an interesting $\mathcal{N}=2$ superconformal theory.

In order to obtain further constraints on OPE coefficients we will assume the existence of gaps, in particular, $\Delta_{[0,0]}\geq\Delta_{[0,0],\text{jump}}$, because otherwise the optimization problems are unbounded. As an important example, we study in more detail the exact bosonic and fermionic solutions of crossing. We fix the dimension of the first long to $\Delta_{[0,0]}=2.0/3.0$ for the bosonic/fermionic theories, and then bound the OPE coefficients as we increase the

second gap $\Delta'_{[0,0]}$. The results are plotted in figure 8.4. In the first row we observe that the OPE coefficient of the long at $\Delta_{[0,0]}$ has upper bounds which are essentially constant, and lower bounds appear only when the second gap is $\Delta'_{[0,0]} \gtrsim 3$. The lower bounds grow as we increase $\Delta'_{[0,0]}$, until they meet the upper bound precisely where the bosonic and fermionic theories sit. For this reason, we expect that the bosonic and fermionic theories are unique provided that the second gap is large enough. Indeed, our plots are almost identical to the ones obtained for the $\mathcal{N} = 4$ analogous case [233]. In order to map results, one simply needs to note that their $\mathcal{B}_2$ multiplet is identified with our isolated long of dimension $\Delta_{[0,0]} = 2$ (see the discussion around equation (8.12)). A mixed-correlator bootstrap study for $\mathcal{N} = 4$ revealed the appearence of an island around the bosonic free theory. We are confident that a similar analysis can be done in our setup, which would give evidence that our free-field solutions of crossing are unique if one assumes appropriate gaps.

In the second row of figure 8.4 we show bounds on the OPE coefficient of the $[A_1]^{j=1/2}_{R=1/2}$ multiplet. There is no analogous of this multiplet for line defects in $\mathcal{N} = 4$ theories, so we will not be able to borrow any intuition from the results of [233]. The primary of A_1 has dimension $\Delta = 5/2$, so it sits inside the continuum of $[1,0]$ long operators. Intuitively, in order for lower bounds to appear, there needs to be enough distance between the dimension of the operator and the dimension of the first operator in the continuum, and that explains why we do not obtain any lower bounds for $\lambda^2_{A_1}$. In any case, when $\Delta_{[0,0]} = 2$ the upper bound keeps decreasing until it crosses zero, exactly at the position where the bosonic free theory sits. When $\Delta_{[0,0]} = 3$, the bounds seems to converge to the rectangular region $\lambda^2_{A_1} \leq 1$ and $\Delta'_{[0,0]} \leq 5$, and the fermionic theory sits exactly at the upper right corner of this region.

Summarizing, figure 8.4 provides ample evidence that the numerical bootstrap is isolating the bosonic and fermionic free theories when we assume large gaps in the spectrum of long operators. Interestingly, one can allow the dimension for the first long to be in the range

$$\Delta_{\text{jump},[0,0]} \leq \Delta_{[0,0]} \leq 3, \tag{8.97}$$

and compute bounds on OPE coefficients as a function of $\Delta'_{[0,0]}$. The results are plotted in figure 8.5. There is an entire family of plots that share similar qualitative features to the ones we just discussed. This can be thought of as an one-parameter family of theories interpolating between the fermionic and bosonic free-field theories, and which would extend all the way up to the critical theory where the OPE coefficients are diverging.

166
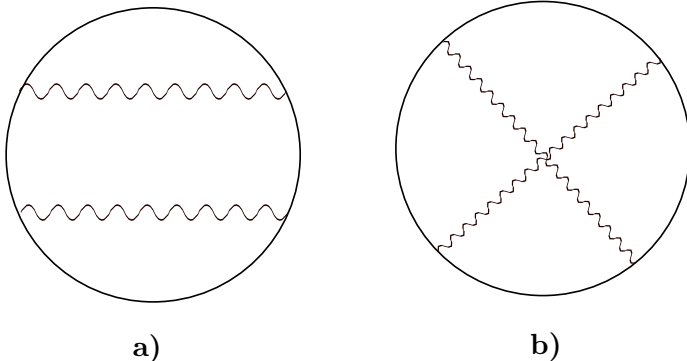
Figure 8.6: Disconnected and connected Witten diagrams in the dual AdS_2 description. The disconnected piece corresponds to a mean-field theory correlator, while the connected piece is bootstrapped in the current section.

8.6   Analytical results

8.6.1   Introduction

In this section we study perturbations around the bosonic mean-field solution (8.83), similar to the analysis of section 6 in [233]. We will interpret the bosonic solution as the strong-coupling limit of line defects in $\mathcal{N} = 2$ theories which admit a holographic description. From the holographic perspective, the leading contribution to a four-point function at strong coupling is a disconnected Witten diagram in AdS_2, while the first-order correction is given by a four-point connected Witten diagram, see figure 8.6. The disconnected piece can be obtained by Wick contractions, and leads to our solution (8.83) with $\xi = 1$. Our goal is to use superconformal blocks and crossing symmetry to bootstrap the contribution from the connected Witten diagram. We will see that under mild assumptions, the correlator is uniquely determined in terms of two normalization constants c_1, c_2, which cannot be fixed by our symmetry arguments. From the correlator it is then possible to extract the first-order corrections to the anomalous dimensions and OPE coefficients of the operators in the spectrum. In the analogous $\mathcal{N} = 4$ case, perfect agreement was found between the explicit holographic calculation [346] and the bootstrap result [233].

Let us remind the reader that in section 8.4.3 we wrote the crossing equation (8.81) in terms of the two-dimensional vector $H(z)$. This function can be expressed in a superblock-

like expansion

$$H(z) = \sum_{\Delta \in S^{[0,0]}} a_\Delta H_\Delta^{[0,0]}(z) + \sum_{\Delta \in S^{[1,0]}} b_\Delta H_\Delta^{[1,0]}(z), \tag{8.98}$$

where $H_\Delta^{[a,b]}$ are also two-dimensional vectors that can be computed from the definition of $H(z)$ in (8.82) and the superconformal blocks in the two channels (8.73) and (8.74). One can think of $H_\Delta^{[a,b]}$ as a superblock expressed in a new basis, such that the crossing equation takes a particularly simple form.

The solution to crossing we want to perturb around has OPE coefficients given in equation (8.84) with $\xi = 1$, and the spectrum of dimensions is

$$S_{[0,0]} = \{2, 4, 6, \dots\} \qquad \text{and} \qquad S_{[1,0]} = \{3, 5, 7, \dots\}. \tag{8.99}$$

The idea is to start with this free theory and consider a perturbation of the CFT data to leading order in the perturbation parameter ϵ. On the one hand, the correlator will receive a correction

$$H(z) = H^{(0)}(z) + \varepsilon H^{(1)}(z), \tag{8.100}$$

which by equation (8.98) will translate into the operators acquiring anomalous dimensions

$$S_{[0,0]}^{(1)} = \{\Delta + \varepsilon \gamma_\Delta^{[0,0]}\}_{\Delta \in S_{[0,0]}}, \qquad S_{[1,0]}^{(1)} = \{\Delta + \varepsilon \gamma_\Delta^{[1,0]}\}_{\Delta \in S_{[1,0]}}, \tag{8.101}$$

and the OPE coefficients receiving first-order corrections

$$a_\Delta = a_\Delta^{(0)} + \varepsilon a_\Delta^{(1)}, \qquad b_\Delta = b_\Delta^{(0)} + \varepsilon b_\Delta^{(1)}. \tag{8.102}$$

Schematically, we have that $H_\Delta^{[a,b]} \sim z^\Delta f(\Delta, z)$, so if we give an anomalous dimension to Δ the first-order correlator $H^{(1)}(z)$ must contain a log term. As a result, we take it to be of the form

$$H^{(1)}(z) = R(z) \log(z) + P(z), \tag{8.103}$$

where $R(z)$ and $P(z)$ are a priory completely arbitrary functions. Comparing this with the block expansion we obtain

$$R(z) = \sum_{\Delta \in S_{[0,0]}} a_\Delta^{(0)} \gamma_\Delta^{[0,0]} H_\Delta^{[0,0]}(z) + \sum_{\Delta \in S_{[1,0]}} b_\Delta^{(0)} \gamma_\Delta^{[1,0]} H_\Delta^{[1,0]}(z), \tag{8.104a}$$

$$\begin{aligned} P(z) = &\sum_{\Delta \in S_{[0,0]}} a_\Delta^{(1)} H_\Delta^{[0,0]}(z) + \sum_{\Delta \in S_{[0,0]}} a_\Delta^{(0)} \gamma_\Delta^{[0,0]} z^\Delta \partial_\Delta \left(z^{-\Delta} H^{[0,0]}(z) \right) \\ &+ \sum_{\Delta \in S_{[1,0]}} b_\Delta^{(1)} H_\Delta^{[1,0]}(z) + \sum_{\Delta \in S_{[1,0]}} b_\Delta^{(0)} \gamma_\Delta^{[1,0]} z^\Delta \partial_\Delta \left(z^{-\Delta} H^{[1,0]}(z) \right), \end{aligned} \tag{8.104b}$$

In the analysis below, the "brading" transformation

$$z \to \frac{z}{z-1} \tag{8.105}$$

will play a crucial role to provide extra constraints for the functions $R(z)$ and $P(z)$. The one-dimensional bosonic blocks $g_\Delta = g_\Delta^{0,0}$ of equation (8.62) have clean transformation properties under braiding. In our analysis, only chiral blocks with even Δ will appear, for which we have[10]

$$g_\Delta \left(\frac{z}{z-1} \right) = g_\Delta(z), \qquad g'_\Delta \left(\frac{z}{z-1} \right) = -(1-z)^2 g'_\Delta(z), \qquad \text{etc.} \tag{8.106}$$

From the form of the superconformal blocks $G_i(z)$, it is clear that they inherit these nice transformation properties under braiding. However, when we work in the H-basis, the transformations become more complicated and instead of writing them here we will only present their consequences. Using the transformation (8.106) combined with the expansions (8.104), we obtain non-trivial constraints for the two components of $R(z)$

$$R_0 \left(\frac{z}{z-1} \right) - R_0(z) = 0, \qquad R_1 \left(\frac{z}{z-1} \right) - \mathcal{B}[R](z) = 0, \tag{8.107}$$

and for the two components of $P(z)$

$$P_0 \left(\frac{z}{z-1} \right) - P_0(z) - \log(1-z) R_0(z) = 0, \tag{8.108a}$$

$$P_1 \left(\frac{z}{z-1} \right) - \mathcal{B}[P](z) - \log(1-z) \mathcal{B}[R](z) + \frac{z}{z-1} R_0(z) = 0. \tag{8.108b}$$

Here we have defined a functional $\mathcal{B}$, which takes as argument a two-component function $F(z)$ and mixes its two components as follows:

$$\mathcal{B}[F](z) = -\frac{2z(z-2)}{(z-1)^2} F_0(z) - \frac{z^2}{z-1} \partial_z F_0(z) + \frac{1}{(z-1)^2} F_1(z) \,. \tag{8.109}$$

In the next section we will study how these constraints fix the functions $R(z)$ and $P(z)$ up to overall coefficients.

---

[10]For generic values of Δ, the chiral block will have an extra branch cut due to the prefactor z^Δ, and one has to be careful on how to analytically continue the block under (8.105). See [272] for a careful analysis in the BCFT setup.

8.6.2 Corrections to the anomalous dimension

We are now ready to find solutions to crossing which are consistent with the relations just presented. In order to do so, we take the function $P(z)$ to be of the form

$$P(z) = \frac{z^2}{(1-z)^2} R(1-z) \log(1-z) + Q(z), \tag{8.110}$$

and we assume that $R(z)$ and $Q(z)$ are rational functions. This assumption is inspired by the holographic calculation of [346], and can also be justified a posteriori if a solution is actually found. The idea is that the contribution from the connected Witten diagram in figure 8.6 is given by an integral of four bulk-to-boundary propagators living in AdS_2, which is denoted by $D_{\Delta_1\Delta_2\Delta_3\Delta_4}$ in [346]. For the case of interest to us, the conformal dimensions of the external operators are all identical and take integer values, in which case the only transcendental functions appearing in D are $\log(z)$ and $\log(1-z)$. Therefore, our ansatz (8.103) and (8.110) is the most general one representing a first order correction in the holographic dual.

Due to the form of our ansatz, crossing symmetry does not impose conditions on the function $R(z)$, however the braiding property does impose non-trivial relations on both $R(z)$ and $Q(z)$. It turns out that it is sufficient to solve (8.108) and that (8.107) does not impose extra constraints. Also, recall that under the assumption of rationality the coefficients of possible log terms have to cancel separately. Now we insert our ansatz (8.110) in (8.108a), and by extracting the coefficient of the log term, we obtain the following relation for the function $R_0(z)$:

$$- z^2 R_0 \left(\frac{1}{1-z} \right) - \frac{z^2 R_0(1-z)}{(z-1)^2} - R_0(z) = 0. \tag{8.111}$$

Similarly, by looking at (8.108b) we obtain an equation that mixes the two components of $R(z)$

$$-(z-1)z^4 R_0'(1-z) + 2(z-3)z^3 R_0(1-z) + (z-1)^3 z^2 R_0'(z) + 2(z-2)(z-1)^2 z R_0(z)$$
$$-z^2(z-1)^4 R_1 \left(\frac{1}{1-z} \right) - z^2 R_1(1-z) + \left(-z^2 + 2z - 1 \right) R_1(z) = 0. \tag{8.112}$$

In addition to these relations, the function $R(z)$ is constrained by the block expansion (8.104). In particular, in the limit $z \sim 0$ it should satisfy

$$(R_0(z), R_1(z)) \sim (z^2, -2z^2), \tag{8.113}$$

where the relative factor of -2 comes from the explicit normalization of the conformal blocks in the basis we employ. As discussed in [233], these conditions are not enough to fix the function $R(z)$, and we need to look at the behavior of the function around $z \sim 1$, which is correlated with the behavior of anomalous dimensions at large Δ. Because we are looking for a solution that can be interpreted as a holographic correlator, we will borrow some intuition from [359, 360]. The idea is that the growth of anomalous dimensions is governed by how irrelevant the interaction is in the putative *AdS* dual. Because we are trying to bootstrap a *leading* correction to the holographic correlator, we should keep the solution with the *weakest* growth. Therefore, we impose that anomalous dimensions grow no faster than $\gamma_\Delta^{[a,b]} \sim \Delta^2$ for large values of Δ. This last condition fixes the function $R(z)$ up to two normalization constants. The explicit answer reads

$$R_0(z) = -\frac{z^2}{z-1}c_1 - \frac{(2z^2 - 7z + 7)\,z^4}{2(z-1)^3}c_2\,, \tag{8.114}$$

$$R_1(z) = -\frac{z^2\,(2z^2 - 3z - 6)}{3(z-1)}c_1 + \frac{z^4\,(8z^2 - 28z + 35)}{3(z-1)^3}c_2\,. \tag{8.115}$$

It is instructive to compare this result with the analysis of [233] for line defects in $\mathcal{N} = 4$ theories. In the $\mathcal{N} = 4$ case, there is only one function and the solution could be fixed up to an overall coefficient. Moreover, this coefficient is associated to a three-point function of half-BPS operators and can be fixed using localization [288]. In our case of line defects in $\mathcal{N} = 2$ theories, we have two overall constants associated to each independent channel. Unlike $\mathcal{N} = 4$ SYM, which seems to be unique, we know that there is an extensive catalog of $\mathcal{N} = 2$ theories, and it is then no surprise that our solution has more freedom.

From the explicit solution for $R(z)$, the anomalous dimensions can be read off from the block expansion in (8.104a):

$$\gamma_\Delta^{[0,0]} = \frac{\Delta(\Delta+1)}{3(\Delta-1)(\Delta+2)}c_1 + \frac{(\Delta-2)(\Delta+3)\big(3\Delta(\Delta+1) - 4\big)}{12(\Delta-1)(\Delta+2)}c_2\,, \tag{8.116}$$

$$\gamma_\Delta^{[1,0]} = -\frac{(\Delta-1)(\Delta+2)}{9\Delta(\Delta+1)}c_1 + \frac{(\Delta-1)(\Delta+2)\big(9\Delta(\Delta+1) + 4\big)}{36\Delta(\Delta+1)}c_2\,. \tag{8.117}$$

From this expression is clear that they scale as Δ^2 for large Δ.

8.6.3 Corrections to the OPE coefficients

With the explicit solution for $R(z)$ at hand, we can proceed to compute $Q(z)$, which will allow us to extract the first-order correction to the OPE coefficients. The crossing equation

gives non-trivial constraints for both components of $Q(z)$, namely

$$Q(z) - \frac{z^2}{(1-z)^2}Q(1-z) = 0. \tag{8.118}$$

The equations coming from braiding will provide extra conditions, in particular if we insert the ansatz (8.110) in (8.108b) and now extract the term with no logs, we get

$$(z-1)^4 Q_1\left(\frac{z}{z-1}\right) - 2(2-z)z(z-1)^2 Q_0(z) - (z-1)^2 Q_1(z)$$
$$+z(z-1)^3 R_0(z) + z^2\left((z-1)^3 Q_0'(z) + z^2 R_0(1-z)\right) = 0. \tag{8.119}$$

As before, the other braiding equations do not provide extra conditions. It only remains to impose the boundary conditions for $z \sim 0$ similarly to what we did for $R(z)$. Our final solution for $Q(z)$ is given by

$$Q_0(z) = \frac{\left(z^2 - z + 1\right)^2}{(z-1)^2}c_2, \tag{8.120}$$

$$Q_1(z) = \frac{2z^2}{3}c_1 - \frac{(16z^4 - 32z^3 + 97z^2 - 81z + 30)}{6(z-1)^2}c_2. \tag{8.121}$$

Having both $R(z)$ and $Q(z)$, we can now use the block expansion (8.104b) to extract corrections to the OPE coefficients, similarly to what we did for the anomalous dimension. It turns out that the corrections $a_\Delta^{(1)}$ and $b_\Delta^{(1)}$ can be elegantly written in terms of the derivatives of the anomalous dimensions times the zeroth-order values for $a_\Delta^{(0)}$ and $b_\Delta^{(0)}$:

$$a_\Delta^{(1)} = \frac{\partial}{\partial\Delta}(a_\Delta^{(0)}\gamma_\Delta^{[0,0]}), \qquad b_\Delta^{(1)} = \frac{\partial}{\partial\Delta}(b_\Delta^{(0)}\gamma_\Delta^{[1,0]}). \tag{8.122}$$

Similar relations were originally observed in [359, 361]. It is not clear to us which of our assumptions implies these relations, but in any case it is reassuring to see that they are satisfied.

Let us finish with some comments. From the start we are assuming that the spectrum of the perturbed solution is the same as the spectrum of the zeroth-order starting point. In principle, there could be degenerate families that are lifted at first order. However, because we are looking at a single correlator, possible degeneracies are invisible at this stage of the calculation. The more correct way to interpret our results is as weighted averages [362, 363]. In order to resolve possible degeneracies it is necessary to study a mixed correlator system. For example, one could use the correlators involving long multiplets that we present in appendix 8.B, although perhaps more general correlators are needed in which the external

operators carry non-zero quantum numbers under $\mathfrak{su}(2)_j \times \mathfrak{su}(2)_R$. We leave this interesting problem for future work.

Let us also point out that this solution to crossing is interesting in its own right. It would be ideal to compare our result with other approaches and explicit holographic calculations in some selected $\mathcal{N} = 2$ model, as it would allow us to understand the origin of the coefficients c_1 and c_2. Finally, a similar calculation to ours was done in [157] using the exact functional method, where possible deformations of a free theory were bootstrapped by explicitly constructing the exact functionals that give the optimal bound. It would be interesting to adapat the approach of [157] to our crossing constraints (8.81).

8.7   Conclusions

In this work we have initiated the bootstrap program for line defects in $\mathcal{N} = 2$ theories. We studied the $1d$ CFT that lives in a line defect using a collection of bootstrap techniques. Our results are for the most part very general, as they rely on basic symmetry principles and consistency requirements, and are therefore valid for standard Wilson and 't Hooft lines in gauge theories, but also for more exotic constructions like line defects in non-Lagrangian models [364–366].

We concentrated mostly on correlators of the displacemente operator, but one can also consider more general external multiplets and study a mixed correlator bootstrap. Partial progress towards this goal is already presented in appendix 8.B, where conformal blocks for correlators that include scalar long multiplets as external operators are shown. The analysis of this paper shows that not only scalar long multiplets, but also multiplets charged under transverse spin, are generated in the OPE of two displacements. Therefore, it would be interesting to consider crossing involving long operators that sit in non-trivial representations of the bosonic subalgebra.

As a longer term goal, one could include local operators outside the defect. This is particularly interesting when considering that theories with the same local spectrum can support different line defects [340]. Basic kinematics constraints on two-point functions in the presence of an $\mathcal{N} = 2$ line have not been calculated yet. A project for the not so distant future would be to consider a mixed system between the bulk stress tensor and the displacement operator, generalizing the analysis of [290] where the coupling between the displacement and the stress tensor was studied. It would also be interesting to see bootstrap constraints on possible line defects when assuming a given bulk CFT.

Another interesting follow-up would be to perform holographic calculations in some specific $\mathcal{N} = 2$ model, in order to compare with our analytic correlator from section 8.6. There seems to be no calculation of this sort in the $\mathcal{N} = 2$ literature. In $\mathcal{N} = 4$ SYM the holographic calculation of [346] and the bootstrap analysis of [233] are in perfect agreement. We are confident that there will be a similar match in the $\mathcal{N} = 2$ case.

One more possible avenue is to push the analytic analysis to higher orders in the perturbative expansion. This was done in [233] for $\mathcal{N} = 4$, but in order to resolve the important issue of degeneracies a bigger collection of correlators has to be considered. In addition, one could also try to adapt the exact functional machinery developed in [155–157]. The systems studied in this work have interesting simplifying features, i.e. $1d$ CFTs with a high amount of supersymmetry, and perhaps exact solutions to the crossing equations are within reach.

Acknowledgments

8.A   Conventions

In this appendix, we define an index-free notation to contract the fermionic coordinates $\theta_{\mathbf{A}}^a$ of our superspace. These objects have one transverse-spin and one R-symmetry index, and since both groups are $\mathfrak{su}(2)$, we will need to use the totally antisymmetric symbol

$$\varepsilon^{12} = -\varepsilon^{21} = -\varepsilon_{12} = \varepsilon_{21} = 1, \qquad \varepsilon^{\mathbf{12}} = -\varepsilon^{\mathbf{21}} = -\varepsilon_{\mathbf{12}} = \varepsilon_{\mathbf{21}} = 1. \tag{8.123}$$

As usual, the conventions to raise or lower indices are as follows

$$\theta_{\mathbf{A},a} = \varepsilon_{ab}\theta_{\mathbf{A}}^b, \qquad \theta^{\mathbf{A},a} = \varepsilon^{\mathbf{AB}}\theta_{\mathbf{B}}^a, \qquad \text{etc.} \tag{8.124}$$

There is only one meaningful way to contract two coordinates and form a scalar

$$\theta\xi \equiv \varepsilon_{ab}\varepsilon^{\mathbf{AB}}\theta_{\mathbf{A}}^a\xi_{\mathbf{B}}^b. \tag{8.125}$$

Note that $\theta\xi = -\xi\theta$ and therefore $\theta\theta = 0$. Given three coordinates θ, ξ and ζ, they can be contracted as

$$(\theta\xi\zeta)^a_{\mathbf{A}} = \varepsilon_{bc}\varepsilon^{\mathbf{BC}}\theta^b_{\mathbf{A}}\xi^a_{\mathbf{B}}\zeta^c_{\mathbf{C}}. \tag{8.126}$$

This contraction is interesting because it is inequivalent to contracting two coordinates as in (8.125) and then multiplying by the third one. As a result, it does not vanish even if two or three coordinates are the same: $(\theta\theta\theta)^a_{\mathbf{A}} \equiv (\theta^3)^a_{\mathbf{A}} \neq 0$. Finally, given four Grassmann variables there is one contraction such that it cannot be decomposed as a product of terms of the form (8.125)

$$\theta\xi\zeta\eta = \varepsilon_{ac}\varepsilon_{bd}\varepsilon^{\mathbf{AB}}\varepsilon^{\mathbf{CD}}\theta^a_{\mathbf{A}}\xi^b_{\mathbf{B}}\zeta^c_{\mathbf{C}}\eta^d_{\mathbf{D}}. \tag{8.127}$$

As before, this does not vanish even in the case of four identical coordinates $\theta\theta\theta\theta \equiv \theta^4 \neq 0$. Note also that we could have defined it as $\theta\xi\zeta\eta \equiv \theta^a_{\mathbf{A}}(\xi\zeta\eta)^{\mathbf{A}}_a$.

When we classify all possible fermionic invariants, the following relations will be useful

$$\begin{aligned}
\theta\xi\theta\xi &= \xi\theta\xi\theta, \\
\theta\theta\xi\xi &= \xi\xi\theta\theta, \\
\theta\xi\xi\theta &= \xi\theta\theta\xi = \tfrac{1}{2}(\theta\xi\theta\xi + \theta\theta\xi\xi), \\
\xi\theta\theta\theta &= \theta\xi\theta\theta = \theta\theta\xi\theta = \theta\theta\theta\xi,
\end{aligned} \tag{8.128}$$

and also

$$(\theta\xi)^2 = \tfrac{1}{2}(\theta\xi\theta\xi - \theta\theta\xi\xi), \qquad (\theta\xi)^3 = -\tfrac{2}{3}\theta^3\xi^3. \tag{8.129}$$

8.B   Long blocks

In this appendix, we compute superconformal blocks involving unprotected operators. We start by obtaining the blocks of two displacements and two longs in the $(12) \to (34)$ channel, and then proceed to compute the same blocks involving four long operators. In order to study crossing for the full mixed system, one would still need to compute the blocks $\langle \mathcal{DDOO} \rangle$ in the $(14) \to (23)$ channel, but we expect this not to be hard using the techniques presented in the paper.

8.B.1 Two displacements and two longs

We will start by computing the superconformal blocks of two displacements $\mathcal{D}(z)$ with two identical long scalar operators $\mathcal{O}(z)$ of dimension $\Delta_{\mathcal{O}}$ in the $(12) \to (34)$ channel

$$\langle \mathcal{D}(z_1)\mathcal{D}(z_2)\mathcal{O}(z_3)\mathcal{O}(z_4)\rangle = \frac{1}{Z_{12}^2 Z_{34}^{2\Delta_{\mathcal{O}}}} \sum_{\mathcal{O}'} \lambda_{\mathcal{D}\mathcal{D}\mathcal{O}'} \lambda_{\mathcal{O}\mathcal{O}\mathcal{O}'} \, \mathcal{G}_{\mathcal{O}'}(I_a). \tag{8.130}$$

The steps of the calculation are analogous to section 8.4.1, with the exception that now the shortening conditions are given by (8.60) only. Therefore, there are three free functions $f_0(z)$, $f_1(z)$ and $f_9(z)$, and there must be an extra independent Casimir equation. As before, we apply the Casimir operator $\mathcal{C}_{12}^2$ to the four-point function in the frame $\mathscr{F}_1$ to simplify the computations. We get one of the original Casimir equations (8.67a), together with two new constraints:

$$-z^2\big[(z-1)f_0''(z) + f_0'(z)\big] - 4z f_1(z) = \mathfrak{c}\, f_0(z), \tag{8.131a}$$

$$\begin{aligned}
&+ 2304z^3 f_9(z) - 16(2\mathfrak{c} + 3z - 10)f_1(z) + 48(2 - 3z)z f_1'(z) - 48(z-1)z^2 f_1''(z) \\
&\quad + 8\big[(z-1)z + 6\big]f_0'(z) + 2\big[z(5z - 4) - 8\big]z f_0''(z) \\
&\quad - 2(z-1)(z+4)z^2 f_0^{(3)}(z) - (z-1)^2 z^3 f_0^{(4)}(z) = 0,
\end{aligned} \tag{8.131b}$$

$$\begin{aligned}
&(\mathfrak{c} - 2)^2 \mathfrak{c} f_0(z) + z^2\big[3\mathfrak{c}^2 + 2\mathfrak{c}(6z - 5) + 4z(9z - 8)\big]f_0'(z) \\
&\quad + z^2\big[3\mathfrak{c}^2(z-1) + 2\mathfrak{c}(z(21z - 23) + 5) + 4z(7z - 6)(9z - 4)\big]f_0''(z) \\
&\quad + 2z^3\big[6\mathfrak{c}(z-1)(2z - 1) + z(z(165z - 284) + 138) - 16\big]f_0^{(3)}(z) \\
&\quad + (z-1)z^4\big[3\mathfrak{c}(z-1) + 2z(69z - 79) + 38\big]f_0^{(4)}(z) \\
&\quad + 3(z-1)^2(7z - 4)z^5 f_0^{(5)}(z) + (z-1)^3 z^6 f_0^{(6)}(z) = 0.
\end{aligned} \tag{8.131c}$$

As discussed in the main text, we need to first "change basis" from the functions $f_i(z)$ to the $G_i(z)$, and then make an ansatz as a sum of bosonic blocks in order to solve the Casimir equations. We start by expanding the external fields in terms of their conformal descendants, and we obtain the same expansion as in the right-hand side of (8.68). Even though the operators at points z_3 and z_4 are longs, there are no new terms is the expansion because we work in the frame $\mathscr{F}_1$, where $\theta_3 = \theta_4 = 0$, and therefore we can only get contributions from the superconformal primary field A. As a result, the mapping (8.69) is

still valid, and we find that the change of basis must be given by (8.70) together with

$$
\begin{aligned}
f_9(z) &= \frac{G_0(z)}{48z^4} - \frac{(z^2 + 6)\, G_0'(z)}{288z^3} - \frac{(5z^2 - 12)\, G_0''(z)}{1152z^2} + \frac{(z+4)(z-1)G_0^{(3)}(z)}{1152z} \\
&\quad + \frac{(z-1)^2 G_0^{(4)}(z)}{2304} - \frac{G_1(z)}{24z^4} - \frac{G_1'(z)}{144z^2} - \frac{(z-1)G_1''(z)}{144z^2} + \frac{G_2(z)}{6z^4}.
\end{aligned}
\tag{8.132}
$$

The final step is to insert the change of basis (8.70) and (8.132) in the Casimir equations (8.67) and (8.131a), and use the resulting equations to fix the coefficients that apear in the ansatz (8.72). If we consider the block for an exchanged operator with quantum numbers $[\Delta, 0, 0]$, the solution to the equations is

$$
\begin{aligned}
a_1 &= \tfrac{1}{2}a_0\,(\Delta - 2)\,, & e_1 &= -\tfrac{1}{2}e_0\,(\Delta + 3)\,, \\
a_2 &= -\tfrac{1}{16}a_0\,(\Delta - 3)\,(\Delta - 2)\,, & e_2 &= -\tfrac{1}{16}e_0\,(\Delta + 3)\,(\Delta + 4)\,,
\end{aligned}
\tag{8.133}
$$

and $b_i = c_i = d_i = 0$. Note that one of the free parameters, say a_0, can be fixed by choosing an overall normalization of the conformal block, as we did in (8.73). However, the new feature is that there is still a free parameter e_0 that cannot be fixed by superconformal symmetry.

As a consistency check, we can take the OPE coefficients and norms of section 8.4.2 to rederive this result. The superblocks are given by

$$
\begin{aligned}
G_0(z) &= \frac{\lambda_{AAA}\tilde{\lambda}_{AAA}}{\langle A|A \rangle}\, g_\Delta^{0,0}(z) + \frac{\lambda_{AAG}\tilde{\lambda}_{AAG}}{\langle G|G \rangle}\, g_{\Delta+2}^{0,0}(z), \\
G_1(z) &= \frac{\lambda_{BBA}\tilde{\lambda}_{AAA}}{\langle A|A \rangle}\, g_\Delta^{0,0}(z) + \frac{\lambda_{BBG}\tilde{\lambda}_{AAG}}{\langle G|G \rangle}\, g_{\Delta+2}^{0,0}(z), \\
G_2(z) &= \frac{\lambda_{CCA}\tilde{\lambda}_{AAA}}{\langle A|A \rangle}\, g_\Delta^{0,0}(z) + \frac{\lambda_{CCG}\tilde{\lambda}_{AAG}}{\langle G|G \rangle}\, g_{\Delta+2}^{0,0}(z),
\end{aligned}
\tag{8.134}
$$

As in section 8.4.2, $\lambda_{O_1 O_2 O_3}$ denotes the OPE coefficient of two fields from the displacement multiplet with one operator from a long scalar multiplet, namely $O_1, O_2 \in \mathcal{D}$ and $O_3 \in \mathcal{O}'$. However, now one needs to consider also $\tilde{\lambda}_{O_1 O_2 O_3}$, where O_1 and O_2 are descendents of the external long $\mathcal{O}$, but O_3 is a descendant of the exchanged long $\mathcal{O}'$. To recover equation (8.133) we fix

$$
a_0 = \frac{\lambda_{AAA}\tilde{\lambda}_{AAA}}{\langle A|A \rangle}, \qquad e_0 = \frac{\lambda_{AAG}\tilde{\lambda}_{AAG}}{\langle G|G \rangle}.
\tag{8.135}
$$

Then, for example, $a_1 = a_0 \lambda_{BBA}/\lambda_{AAA}$, and using (8.78) we recover the blocks (8.133). This works in an identical way for the other a_i and e_i.

As in the case of four displacements, we can also have an exchange $[\Delta, 1, 0]$, with solution given by

$$c_1 = -\tfrac{1}{2}c_0, \qquad c_2 = \tfrac{1}{48}c_0 \left(\Delta - 2\right)\left(\Delta + 3\right), \tag{8.136}$$

where $a_i = b_i = d_i = e_i = 0$ and we could fix the normalization of the block by $c_0 = 1$.

8.B.2   Four longs

Finally, we compute the superconformal blocks that appear in the four-point function of long scalar operators in the $(12) \to (34)$ channel

$$\langle \mathcal{O}(z_1)\mathcal{O}(z_2)\mathcal{O}'(z_3)\mathcal{O}'(z_4) \rangle = \frac{1}{Z_{12}^{2\Delta_{\mathcal{O}}} Z_{34}^{2\Delta'_{\mathcal{O}}}} \sum_{\mathcal{O}''} \lambda_{\mathcal{O}\mathcal{O}\mathcal{O}''} \lambda_{\mathcal{O}'\mathcal{O}'\mathcal{O}''} \, \mathcal{G}_{\mathcal{O}''}(I_a), \tag{8.137}$$

where for simplicity we assume that $\Delta_1 = \Delta_2 = \Delta_{\mathcal{O}}$ and $\Delta_3 = \Delta_4 = \Delta'_{\mathcal{O}}$. The steps in the calculation are very similar to the other studied cases, but the equations soon become quite long. For this reason, we will skip some intermediate results in our presentation, but the interested reader can find the details in an attached `Mathematica` notebook. The authors are also happy to provide further details on request.

First, we consider the four-point function of interest, which is given by (8.53), and act on it with the Casimir operator $\mathcal{C}_{12}^2$. Since we do not impose any shortening conditions to the four-point function, the full system of Casimir equations involves ten independent functions $f_0(z), \ldots, f_9(z)$. The explicit differential equations, which are not particularly illuminating, can be found in the attached notebook.

In order to solve these equations, we need to first "change basis" to functions G_i that capture the contribution of the conformal descendants in our multiplets. In addi-

tion to (8.69), we need to make the following identifications:

$$
\begin{aligned}
\langle E^{\mathbf{AB}}_{ab}(x_1) E^{\mathbf{CD}}_{cd}(x_2) A(0) A(\infty)\rangle &\to \frac{\varepsilon_{ab}\varepsilon_{cd}(\varepsilon^{\mathbf{AC}}\varepsilon^{\mathbf{BD}} + \varepsilon^{\mathbf{AD}}\varepsilon^{\mathbf{BC}})}{|x_{12}|^{2\Delta_{\mathcal{O}}+2}} G_3(z), \\
\langle A(x_1) G^{\mathrm{p}}(x_2) A(0) A(\infty)\rangle &\to \frac{1}{|x_{12}|^{2\Delta_{\mathcal{O}}+2}} G_4(z), \\
\langle G^{\mathrm{p}}(x_1) A(x_2) A(0) A(\infty)\rangle &\to \frac{1}{|x_{12}|^{2\Delta_{\mathcal{O}}+2}} G_5(z), \\
\langle B^{\mathbf{A}}_a(x_1) F^{\mathrm{p}\mathbf{B}}_b(x_2) A(0) A(\infty)\rangle &\to \frac{\varepsilon^{\mathbf{AB}}\varepsilon_{ab}}{|x_{12}|^{2\Delta_{\mathcal{O}}+2}} G_6(z), \\
\langle F^{\mathrm{p}\mathbf{A}}_a(x_1) B^{\mathbf{B}}_b(x_2) A(0) A(\infty)\rangle &\to \frac{\varepsilon^{\mathbf{AB}}\varepsilon_{ab}}{|x_{12}|^{2\Delta_{\mathcal{O}}+2}} G_7(z), \\
\langle F^{\mathrm{p}\mathbf{A}}_a(x_1) F^{\mathrm{p}\mathbf{B}}_b(x_2) A(0) A(\infty)\rangle &\to \frac{\varepsilon^{\mathbf{AB}}\varepsilon_{ab}}{|x_{12}|^{2\Delta_{\mathcal{O}}+3}} G_8(z), \\
\langle G^{\mathrm{p}}(x_1) G^{\mathrm{p}}(x_2) A(0) A(\infty)\rangle &\to \frac{1}{|x_{12}|^{2\Delta_{\mathcal{O}}+4}} G_9(z).
\end{aligned}
\tag{8.138}
$$

Here one needs to be careful to map the $G_i(z)$ with the true conformal descendants in the $\mathcal{O}(z)$ superfield, namely one needs to use F^{p} and G^{p} defined in (8.38). With the above identifications, and following the obvious generalization of the steps in the main text, one can find the explicit change of basis $f_i(z) \to G_i(z)$. Again, this transformation is a bit involved, and the interested reader can find it in the attached notebook.

Finally, we make an ansatz for the functions $G_i(z)$ as a finite sum of $\mathfrak{sl}(2;\mathbb{R})$ blocks, as in equation (8.72). Unlike the cases described so far, some of the G_i represent four-point functions of descendants where the operators at x_1 and x_2 have different dimensions. In these cases, the sum of bosonic blocks must be given by the blocks (8.62) with $\Delta_{12} \neq 0$. More specifically, we use the ansatz

$$
G_i(z) = a_i\, g^{\Delta_{12},0}_{\Delta}(z) + b_i\, g^{\Delta_{12},0}_{\Delta+\frac{1}{2}}(z) + c_i\, g^{\Delta_{12},0}_{\Delta+1}(z) + d_i\, g^{\Delta_{12},0}_{\Delta+\frac{3}{2}}(z) + e_i\, g^{\Delta_{12},0}_{\Delta+2}(z), \tag{8.139}
$$

where

$$
\Delta_{12} = \begin{cases} -2 & \text{for } G_4(z) \\ +2 & \text{for } G_5(z) \\ -1 & \text{for } G_6(z) \\ +1 & \text{for } G_7(z) \\ 0 & \text{otherwise} \end{cases} . \tag{8.140}
$$

With these ingredients, one can fix the coefficients $a_i, \ldots, e_i$ by solving the Casimir equations as we previously did. Before we present the solutions, let us make some comments. First, compared to the cases studied before, there is a new solution corresponding to an exchanged operator with quantum numbers $[\Delta, 0, 1]$, namely without transverse spin but with R-symmetry. Similarly to the discussion of the $\langle \mathcal{D}\mathcal{D}\mathcal{O}\mathcal{O} \rangle$ blocks, there are free parameters left in the solution. Some of them can be fixed by choosing an appropriate normalization, but superconformal symmetry is not powerful enough to fix the rest.

Scalar exchange   For an exchanged operator with quantum numbers $[\Delta, 0, 0]$, the Casimir eigenvalue is $\mathfrak{c} = \Delta(\Delta + 1)$ and the blocks are given by

$$
a_1 = \frac{1}{2}a_0 \left(\Delta - 2\Delta_{\mathcal{O}}\right),
$$

$$
a_3 = -\frac{1}{16}a_0 \left(\Delta - 2\Delta_{\mathcal{O}} - 1\right)\left(\Delta - 2\Delta_{\mathcal{O}}\right) - a_2,
$$

$$
a_4 = +a_5 = \frac{a_0 \left(\Delta_{\mathcal{O}} + 2\right)\left(2\Delta_{\mathcal{O}} - \Delta\right)\left(-\Delta + 2\Delta_{\mathcal{O}} + 1\right)}{24 \left(2\Delta_{\mathcal{O}} + 1\right)} + \frac{2a_2}{3},
$$

$$
a_6 = -a_7 = \frac{a_0 \left(\Delta_{\mathcal{O}} + 2\right)\left(2\Delta_{\mathcal{O}} - \Delta\right)\left(-\Delta + 2\Delta_{\mathcal{O}} + 1\right)}{6 \left(2\Delta_{\mathcal{O}} + 1\right)} + \frac{8a_2}{3},
$$

$$
a_8 = \frac{a_0 \left(2\Delta_{\mathcal{O}} - \Delta\right)\left(-\Delta + 2\Delta_{\mathcal{O}} + 1\right)\left(-\Delta + 2\Delta_{\mathcal{O}} + 2\right)\left(\Delta_{\mathcal{O}} + 2\right)^2}{18 \left(2\Delta_{\mathcal{O}} + 1\right)^2}
$$

$$
+ \frac{8a_2 \left(-\Delta + 2\Delta_{\mathcal{O}} + 2\right)}{3 \left(2\Delta_{\mathcal{O}} + 1\right)},
$$

$$
a_9 = \frac{a_0 \left(2\Delta_{\mathcal{O}} - \Delta\right)\left(-\Delta + 2\Delta_{\mathcal{O}} + 1\right)\left(-\Delta + 2\Delta_{\mathcal{O}} + 2\right)\left(-\Delta + 2\Delta_{\mathcal{O}} + 3\right)\left(\Delta_{\mathcal{O}} + 2\right)^2}{576 \left(2\Delta_{\mathcal{O}} + 1\right)^2}
$$

$$
+ \frac{a_2 \left(-\Delta + 2\Delta_{\mathcal{O}} + 2\right)\left(-\Delta + 2\Delta_{\mathcal{O}} + 3\right)}{12 \left(2\Delta_{\mathcal{O}} + 1\right)},
$$

$$
\tag{8.141}
$$

and

$$e_1 = \frac{1}{2} e_0 \left(-\Delta - 2\Delta_{\mathcal{O}} - 1 \right),$$

$$e_3 = -\frac{1}{16} e_0 \left(\Delta + 2\Delta_{\mathcal{O}} + 1 \right) \left(\Delta + 2\Delta_{\mathcal{O}} + 2 \right) - e_2,$$

$$e_4 = +e_5 = \frac{e_0 (\Delta + 2)(\Delta + 3) \left(\Delta_{\mathcal{O}} + 2 \right) \left(\Delta + 2\Delta_{\mathcal{O}} + 1 \right) \left(\Delta + 2\Delta_{\mathcal{O}} + 2 \right)}{24\Delta(\Delta + 1) \left(2\Delta_{\mathcal{O}} + 1 \right)}$$

$$+ \frac{2(\Delta + 2)(\Delta + 3)e_2}{3\Delta(\Delta + 1)},$$

$$e_6 = -e_7 = -\frac{e_0 (\Delta + 2) \left(\Delta_{\mathcal{O}} + 2 \right) \left(\Delta + 2\Delta_{\mathcal{O}} + 1 \right) \left(\Delta + 2\Delta_{\mathcal{O}} + 2 \right)}{6(\Delta + 1) \left(2\Delta_{\mathcal{O}} + 1 \right)} - \frac{8(\Delta + 2)e_2}{3(\Delta + 1)}, \quad (8.142)$$

$$e_8 = \frac{e_0 \left(\Delta + 2\Delta_{\mathcal{O}} + 1 \right) \left(\Delta + 2\Delta_{\mathcal{O}} + 2 \right) \left(\Delta + 2\Delta_{\mathcal{O}} + 3 \right) \left(\Delta_{\mathcal{O}} + 2 \right)^2}{18 \left(2\Delta_{\mathcal{O}} + 1 \right)^2}$$

$$+ \frac{8e_2 \left(\Delta + 2\Delta_{\mathcal{O}} + 3 \right)}{3 \left(2\Delta_{\mathcal{O}} + 1 \right)},$$

$$e_9 = \frac{e_0 \left(\Delta + 2\Delta_{\mathcal{O}} + 1 \right) \left(\Delta + 2\Delta_{\mathcal{O}} + 2 \right) \left(\Delta + 2\Delta_{\mathcal{O}} + 3 \right) \left(\Delta + 2\Delta_{\mathcal{O}} + 4 \right) \left(\Delta_{\mathcal{O}} + 2 \right)^2}{576 \left(2\Delta_{\mathcal{O}} + 1 \right)^2}$$

$$+ \frac{e_2 \left(\Delta + 2\Delta_{\mathcal{O}} + 3 \right) \left(\Delta + 2\Delta_{\mathcal{O}} + 4 \right)}{12 \left(2\Delta_{\mathcal{O}} + 1 \right)},$$

with all other coefficients vanishing: $b_i = c_i = d_i = 0$.

Transverse-spin charged exchange   For an exchanged operator with quantum numbers $[\Delta, 1, 0]$, the Casimir eigenvalue is $\mathfrak{c} = \Delta(\Delta + 1) + 2$ and the blocks are given by

$$c_1 = \frac{1}{2}c_0 \left(1 - 2\Delta_{\mathcal{O}}\right),$$

$$c_2 = \frac{1}{48}c_0\big(\Delta(\Delta + 1) - 6\Delta_{\mathcal{O}}(\Delta_{\mathcal{O}} + 1) + 6\big),$$

$$c_3 = -\frac{1}{8}c_0 \left(\Delta_{\mathcal{O}} - 1\right)^2,$$

$$c_4 = +c_5 = -\frac{c_0(\Delta + 1)(\Delta + 2)\left(\Delta_{\mathcal{O}} - 1\right)}{24\left(2\Delta_{\mathcal{O}} + 1\right)},$$

$$c_6 = -c_7 = -\frac{c_0(\Delta + 1)\left(\Delta_{\mathcal{O}} - 1\right)}{3\left(2\Delta_{\mathcal{O}} + 1\right)},$$

$$c_8 = \frac{c_0\left(\Delta_{\mathcal{O}} - 1\right)^2\left(2\Delta_{\mathcal{O}} + 3\right)\left(2\Delta_{\mathcal{O}} - \Delta + 1\right)\left(2\Delta_{\mathcal{O}} + \Delta + 2\right)}{18\left(2\Delta_{\mathcal{O}} + 1\right)^2},$$

$$c_9 = \frac{c_0\left(\Delta_{\mathcal{O}} - 1\right)^2\left(2\Delta_{\mathcal{O}} - \Delta + 1\right)\left(2\Delta_{\mathcal{O}} - \Delta + 2\right)\left(2\Delta_{\mathcal{O}} + \Delta + 2\right)\left(2\Delta_{\mathcal{O}} + \Delta + 3\right)}{576\left(2\Delta_{\mathcal{O}} + 1\right)^2},$$

$$(8.143)$$

with all other coefficients vanishing: $a_i = b_i = d_i = e_i = 0$.

R-symmetry charged exchange   Finally, when the exchanged operator has quantum numbers $[\Delta, 0, 1]$, the Casimir eigenvalue is $\mathfrak{c} = \Delta(\Delta + 1) - 4$ and the solution is

$$c_1 = -c_0 \left(\Delta_{\mathcal{O}} + 1\right),$$

$$c_2 = -\frac{1}{8}c_0 \left(\Delta_{\mathcal{O}} + 2\right)^2,$$

$$c_3 = \frac{1}{48}c_0\big(\Delta(\Delta + 1) - 6\Delta_{\mathcal{O}}(\Delta_{\mathcal{O}} + 1)\big),$$

$$c_4 = c_5 = \frac{c_0(\Delta + 1)(\Delta + 2)\left(\Delta_{\mathcal{O}} + 2\right)}{24\left(2\Delta_{\mathcal{O}} + 1\right)},$$

$$c_6 = -c_7 = -\frac{c_0(\Delta + 1)\left(\Delta_{\mathcal{O}} + 2\right)}{6\left(2\Delta_{\mathcal{O}} + 1\right)},$$

$$c_8 = \frac{c_0\Delta_{\mathcal{O}}\left(\Delta_{\mathcal{O}} + 2\right)^2\left(2\Delta_{\mathcal{O}} - \Delta + 1\right)\left(2\Delta_{\mathcal{O}} + \Delta + 2\right)}{9\left(2\Delta_{\mathcal{O}} + 1\right)^2},$$

$$c_9 = \frac{c_0\left(\Delta_{\mathcal{O}} + 2\right)^2\left(2\Delta_{\mathcal{O}} - \Delta + 1\right)\left(2\Delta_{\mathcal{O}} - \Delta + 2\right)\left(2\Delta_{\mathcal{O}} + \Delta + 2\right)\left(2\Delta_{\mathcal{O}} + \Delta + 3\right)}{576\left(2\Delta_{\mathcal{O}} + 1\right)^2},$$

$$(8.144)$$

with $a_i = b_i = d_i = e_i = 0$.

Chapter 9

Superconformal boundaries in $4 - \varepsilon$ dimensions

Abstract

Boundaries in three-dimensional $\mathcal{N} = 2$ superconformal theories may preserve one half of the original bulk supersymmetry. There are two possibilities which are characterized by the chirality of the leftover supercharges. Depending on the choice, the remaining $2d$ boundary algebra exhibits $\mathcal{N} = (0, 2)$ or $\mathcal{N} = (1, 1)$ supersymmetry. In this work we focus on correlation functions of chiral fields for both types of supersymmetric boundaries. We study a host of correlators using superspace techniques and calculate superconformal blocks for two- and three-point functions. For $\mathcal{N} = (1, 1)$ supersymmetry, some of our results can be analytically continued in the spacetime dimension while keeping the codimension fixed. This opens the door for a bootstrap analysis of the ϵ-expansion in supersymmetric BCFTs. Armed with our analytically-continued superblocks, we prove that in the free theory limit two-point functions of chiral (and antichiral) fields are unique. The first order correction, which already describes interactions, is universal up to two free parameters. As a check of our analysis, we study the Wess-Zumino model with a supersymmetric boundary using Feynman diagrams, and find perfect agreement between the perturbative and bootstrap results.

9.1   Introduction

Conformal field theories with boundaries have a wide variety of applications that range from condensed matter to string theory. In recent years the conformal bootstrap has emerged as a powerful tool to study CFTs and has also been applied to boundary conformal theories (BCFTs). The numerical bootstrap for BCFTs was originally implemented in [45, 269], while analytical approaches, which include the ϵ-expansion bootstrap [269, 272], and the construction of exact linear functionals [273, 274], have also been explored. A closely related line of research is to study the dynamics of free bulk theories with non-trival dynamics localized in the boundary [276, 278, 279, 295, 367, 368].

In this work we study supersymmetric boundaries for three-dimensional models with $\mathcal{N} = 2$ supersymmetry, a setup that has received particular attention in the context of infrared dualities [369–372], and localization [373, 374]. There are two ways in which supersymmetry can be preserved when a boundary is introduced: one choice preserves supercharges of the same chirality which define a $2d$ $\mathcal{N} = (0, 2)$ subalgebra, while the other choice is non-chiral and describes a $2d$ $\mathcal{N} = (1, 1)$ subalgebra. We will study the kinematical constraints on correlators for both choices, with a particular emphasis on two-point functions. As is well known, in the presence of a boundary two-point correlators are not fixed by symmetry, but depend on a conformal invariant. They contain non-trivial dynamics akin to four-point functions in homogeneous CFTs, which is captured by the existence of two inequivalent conformal block expansions. One possibility is to fuse the two local operators together and calculate the resulting one-point functions in the presence of the boundary. Another option is to expand a local operator as an infinite sum of boundary excitations, and calculate the resulting two-point functions on the boundary. Consistency between the two decompositions is the starting point of the bootstrap program for BCFT.

Our main focus will be chiral fields, which are short operators of the bulk superconformal algebra killed by half of the supercharges, and whose conformal dimension is fixed by the R-symmetry. As usual in the bootstrap, it is essential to calculate the relevant superconformal blocks. Bosonic blocks for BCFT two-point functions have been known for a long time [268], however less work has been done on supersymmetric models, the sole exception being boundaries in $\mathcal{N} = 4$ SYM [285]. Attempts to formalize the study of superconformal blocks include analytic superspace [336] and the connection to Calogero-Sutherland models [240, 241]. Here we start our analysis using standard superspace techniques, and calculate superblocks using the Casimir approach [31]. The superspace analysis will be uni-

form for the $\mathcal{N} = (0,2)$ and $\mathcal{N} = (1,1)$ subalgebras, but it turns out that the $\mathcal{N} = (1,1)$ blocks have the interesting property that they can be analytically continued across dimensions. In more detail, there is a unique half-BPS boundary in $4d$ $\mathcal{N} = 1$ which is non-chiral, and that can be interpolated to the $\mathcal{N} = (1,1)$ boundary in $3d$. This is the BCFT counterpart of the results obtained in [193], where the bulk superconformal blocks were continued in d. Even though conformal symmetry is subtle in non-integer dimensions,[1] conformal blocks are usually analytic in all their quantum numbers.[2]

Armed with the analytic continuation we tackle the ϵ-expansion for models that satisfy our constraints. Using minimal assumptions, we prove that two-point functions of free chiral and antichiral fields are completely fixed. At leading order in ϵ, which already corresponds to an interacting fixed point, we prove that the two-point functions are universal up to two free parameters: the anomalous dimension of the lowest-lying bulk field, and the anomalous dimension of the lowest-lying boundary field. The solution is non-trivial and contains an infinite number of conformal blocks, and therefore can be used to extract an infinite amount of CFT data.

As a check of our general order ϵ result, we concentrate on the Wess-Zumino model with cubic superpotential, which is a prime example of a critical system that preserves four supercharges. Using the results of [376], we construct an explicit Lagrangian model with boundary degrees of freedom that exhibits all the symmetries of our setup. We use this model to perform a Feynman diagram calculation at one-loop order, and confirm that the perturbative result is in perfect agreement with our bootstrap prediction.

The outline of the paper is as follows. In section 9.2 we summarize the differences between the $\mathcal{N} = (0,2)$ and $\mathcal{N} = (1,1)$ boundaries and introduce the crossing equations for BCFT. In section 9.3 we carry out a detailed study of correlation functions and superconformal blocks of these $3d$ models. In section 9.4 we rederive the superconformal blocks with a new method that is applicable to any $3 \leq d \leq 4$, and use them to bootstrap two-point functions of chiral operators in the ϵ expansion. Finally, in section 9.5 we compute the same two-point functions for the Wess-Zumino model using Feynman diagrams. We conclude with some possible future directions in section 9.6 and we relegate some technical details to the appendices.

---

[1] See [129] for discussions on non-integer d and [375] for non-integer N (in the context of $O(N)$ models).

[2] In the case of the defects both dimension and codimension appear as parameters in the blocks [259, 264].

9.2   Preliminaries

In this preliminary section we introduce the symmetry algebra in the bulk, and the two possible half-BPS subalgebras preserved by a supersymmetric boundary. We also introduce chiral fields and review the standard bootstrap equations for two-point functions in BCFT.

9.2.1   Superconformal boundaries in $3d$

There are two inequivalent half-BPS boundaries that one can consider in $3d$ $\mathcal{N} = 2$ superconformal theories, which are commonly denoted as $\mathcal{N} = (0, 2)$ and $\mathcal{N} = (1, 1)$ boundaries (see [369–374, 377] for related work). The cleanest way to understand their differences is at the level of the commutation relations of their algebras.

Let us start by reminding the reader about the main features of $3d$ $\mathcal{N} = 2$ superconformal symmetry. Besides the conformal generators $\mathcal{D}, \mathcal{P}_\mu, \mathcal{K}_\mu, \mathcal{M}_{\mu\nu}$, the superconformal algebra has four Poincaré supercharges $\mathcal{Q}_\alpha, \bar{\mathcal{Q}}_\alpha$, and four superconformal partners $\mathcal{S}_\alpha, \bar{\mathcal{S}}_\alpha$. There is an extra $U(1)$ symmetry generated by $\mathcal{R}$ under which $\mathcal{Q}_a, \mathcal{S}_a$ have charge -1, and $\bar{\mathcal{Q}}_a, \bar{\mathcal{S}}_a$ have charge $+1$. The precise commutation relations with a summary of our conventions are presented in appendix 9.A. The representation theory of $3d$ $\mathcal{N} = 2$ is well known and can be found for example in [182].

When we restrict ourselves to three dimensions, we take the superconformal boundary to be located at $x_2 \equiv x_\perp = 0$. It is clear that the bosonic subalgebra is generated by $\mathcal{P}_a$, $\mathcal{K}_a$, $\mathcal{M}_{ab}$, and $\mathcal{D}$, where $a = 0, 1$ runs over directions parallel to the boundary. We are now ready to introduce the two inequivalent boundary-preserving superalgebras, which differ only by the choice of fermionic generators.

The $\mathcal{N} = (0, 2)$ boundary: The first possibility is to choose the following fermionic generators: $\mathcal{Q}_2, \bar{\mathcal{Q}}_2, \mathcal{S}^2, \bar{\mathcal{S}}^2$. The precise commutation relations can be obtained by restricting the full superconformal algebra presented in appendix 9.A.2. The following ones are of particular importance:

$$
\begin{aligned}
\{\mathcal{Q}_2, \bar{\mathcal{Q}}_2\} &= -2(\mathcal{P}_0 + \mathcal{P}_1), \\
\{\mathcal{Q}_2, \bar{\mathcal{S}}^2\} &= -2i\mathcal{D} + 2\mathcal{R} + 2i\mathcal{M}_{01}, \\
\{\bar{\mathcal{Q}}_2, \mathcal{S}^2\} &= -2i\mathcal{D} - 2\mathcal{R} + 2i\mathcal{M}_{01}.
\end{aligned}
\tag{9.1}
$$

From the first equation, we notice that $\mathcal{P}_2$ does not appear on the right-hand side. This was to be expected, since translations in the $x_2 = x_\perp$ direction are not preserved. Regarding

the second and third equations, it is crucial to notice the appearence of $\mathcal{R}$. Physically, it means that the $\mathcal{N} = (0,2)$ boundary preserves R-symmetry, a property that strongly constrains which correlation functions are non-vanishing. For example, we will often be concerned with bulk operators $\mathcal{O}_r$ with charge r. From the above discussion, it follows that one-point functions $\langle \mathcal{O}_r \rangle = 0$ unless $r = 0$, and similarly two-point functions $\langle \mathcal{O}_{r_1} \mathcal{O}_{r_2} \rangle = 0$ unless $r_1 + r_2 = 0$.

The $\mathcal{N} = (1,1)$ boundary: The second possibility is to choose the following fermionic generators:

$$
\begin{aligned}
\tilde{\mathcal{Q}}_1 &\equiv \frac{1}{\sqrt{2}} \left(\mathcal{Q}_1 + \bar{\mathcal{Q}}_1 \right), \quad \tilde{\mathcal{Q}}_2 \equiv \frac{i}{\sqrt{2}} \left(\mathcal{Q}_2 - \bar{\mathcal{Q}}_2 \right), \\
\tilde{\mathcal{S}}^1 &\equiv \frac{1}{\sqrt{2}} \left(\mathcal{S}^1 + \bar{\mathcal{S}}^1 \right), \quad \tilde{\mathcal{S}}^2 \equiv \frac{i}{\sqrt{2}} \left(\mathcal{S}^2 - \bar{\mathcal{S}}^2 \right).
\end{aligned}
\tag{9.2}
$$

Once again, the full set of commutation relations can be obtained from the formulas in appendix 9.A.2. The non-vanishing anticommutators are

$$
\begin{aligned}
\{\tilde{\mathcal{Q}}_\alpha, \tilde{\mathcal{Q}}_\beta\} &= 2(\gamma^a)_{\alpha\beta} \mathcal{P}_a \,, \\
\{\tilde{\mathcal{Q}}_1, \tilde{\mathcal{S}}^1\} &= -2i(\mathcal{D} + \mathcal{M}_{01}) \,, \\
\{\tilde{\mathcal{Q}}_2, \tilde{\mathcal{S}}^2\} &= -2i(\mathcal{D} - \mathcal{M}_{01}) \,.
\end{aligned}
\tag{9.3}
$$

As before, $\mathcal{P}_2$ is not part of the algebra since $a = 0, 1$. Interestingly, the second anticommutator does not contain $\mathcal{R}$, since R-symmetry is broken by the $\mathcal{N} = (1,1)$ boundary. In this case, charged bulk operators can have one- and two-point functions that would be forbidden by charge conservation, namely $\langle \mathcal{O}_r \rangle \neq 0 \neq \langle \mathcal{O}_{r_1} \mathcal{O}_{r_2} \rangle$ for any values of the charges.

9.2.2 Chiral primaries in superconformal theories

As announced before, we will mostly focus on chiral primary operators ϕ and their complex conjugates. Often, we will call these operators "chirals" and "antichirals" for simplicity. These are short multiplets of the superconformal algebra killed by half of the supercharges:

$$
[\bar{\mathcal{Q}}_\alpha, \phi(0)] = 0 \,, \qquad [\mathcal{Q}_\alpha, \bar{\phi}(0)] = 0 \,,
\tag{9.4}
$$

and whose conformal dimension and R-charge are related to each other. For general spacetime dimension one obtains

$$
\Delta_\phi = \frac{d-1}{2} r_\phi \,, \qquad \Delta_{\bar{\phi}} = -\frac{d-1}{2} r_{\bar{\phi}} \,.
\tag{9.5}
$$

There is a consistent way to define chiral multiplets in any, in principle continuous, number of dimensions, a fact that will play a significant role in section 9.4.

Chiral operators are ubiquitous in the study of SCFTs and they are present in most known models. A textbook example of a $4d$ Lagrangian with $\mathcal{N} = 1$ supersymmetry is to consider chiral fields in superspace with some non-linear interaction. We will consider a simple example of this in section 9.5, where we study the Wess-Zumino model, i.e. a single chiral multiplet with a cubic superpotential. This model flows to an interacting fixed point, which can be described perturbatively in the ϵ-expansion using weakly-coupled chiral fields. It turns out that the ϵ-expansion can be generalized to include boundaries, a fact that we will explore using the bootstrap results obtained in this work.

An important property of chiral operators is that they often satisfy non-trivial chiral-ring relations. These relations are dynamic and imply that certain chiral operators might disappear from an OPE, for example $\phi_3 \notin \phi_1 \times \phi_2$, even if this is not forbidden by superconformal symmetry. The Wess-Zumino model in $3d$ is a simple SCFT with chiral-ring relations. The chiral ring of this model is generated by ϕ together with the relation $\phi^2 \notin \phi \times \phi$. In the numerical bootstrap analysis of [193, 378], the chiral-ring relation provided strong evidence that a kink in the numerical plots described the Wess-Zumino model. In section 9.5.3 we will notice that our perturbative results are also consistent with the same chiral-ring relation. More complicated examples of chiral-ring relations can be found in [205] where the authors studied numerically a $3d$ conformal manifold parametrized by the complex gauge coupling τ. Chiral-ring relations of bulk operators could also be used to extract information of a theory living on the boundary, similar in spirit to the work of [294, 295].[3]

In this work we will not explore all these questions yet, but they motivated us to study this setup. Here we will work out basic kinematical constraints and use the bootstrap to study the dynamics of a single chiral field. Possible future directions and applications of our results will be discussed in the conclusions. Before we jump to the main analysis, let us first review the bootstrap approach for BCFT, which will be one of our main tools.

9.2.3 Crossing symmetry in BCFT

In this section we will review crossing symmetry for generic, non-supersymmetric boundary CFTs. There are two relevant symmetry algebras to study BCFT. The first one contains

---

[3]We thank Edo Lauria for discussions on this idea.

the d-dimensional conformal group, and it describes physics far away from the boundary. In particular, bulk local operators $\mathcal{O}(x)$ transform in irreducible representations of this algebra, and are labeled by a conformal dimension Δ and spin ℓ. There can also be physical excitations localized on the boundary, which are represented by local operators $\hat{\mathcal{O}}(x_a, x^\perp = 0)$. These boundary operators transform as irreducible representations of the symmetry algebra that preserves the boundary, namely they have conformal dimension $\hat{\Delta}$ and $d - 1$ dimensional spin j.

Correlation functions can be constructed with arbitrary combinations of bulk and boundary operators. As usual, conformal symmetry puts strong constraints on the form of these correlation functions. For example, the one-point function and the bulk-to-boundary correlator of a bulk scalar are fixed up to a constant [268]

$$\langle \mathcal{O}(x) \rangle = \frac{a_{\mathcal{O}}}{(2x^\perp)^\Delta}, \qquad \langle \mathcal{O}(x_1)\hat{\mathcal{O}}(x_2^a) \rangle = \frac{b_{\mathcal{O}\hat{\mathcal{O}}}}{(2x_1^\perp)^{\Delta - \hat{\Delta}} \left((x_{12}^a)^2 + (x_1^\perp)^2 \right)^{\hat{\Delta}}} . \tag{9.6}$$

For more general correlation functions the situation is more involved, because they can depend on conformal invariants. For example, a two-point function of bulk scalars depends on an arbitrary function of the invariant ξ:

$$\langle \mathcal{O}_1(x_1)\mathcal{O}_2(x_2) \rangle = \frac{\mathcal{F}(\xi)}{(2x_1^\perp)^{\Delta_1}(2x_2^\perp)^{\Delta_2}}, \qquad \xi = \frac{(x_1 - x_2)^2}{4x_1^\perp x_2^\perp} . \tag{9.7}$$

Knowledge of $\mathcal{F}(\xi)$ is equivalent to knowing the full two-point correlator. The function $\mathcal{F}(\xi)$ is far from arbitrary; it is heavily constrained by crossing symmetry and it is the main subject of study in the bootstrap program for BCFT.

The main ingredient to derive the crossing equation is the operator product expansion (OPE). It is well known that one can rewrite a product of two bulk local operators as an infinite sum of individual bulk local operators using the standard OPE. In the presence of a boundary there is a second possible expansion, the boundary operator expansion (BOE), in which one bulk local operator is replaced by a sum of operators that are localized in the boundary. In terms of equations, these two OPEs are

$$\mathcal{O}_1(x)\mathcal{O}_2(0) = \frac{1}{x^{2\Delta}} + \sum_{\mathcal{O}} \lambda_{\mathcal{O}_1\mathcal{O}_2\mathcal{O}} C[x, \partial_x]\mathcal{O}(0) ,$$
$$\mathcal{O}(x) = \frac{a_{\mathcal{O}}}{(2x_\perp)^\Delta} + \sum_{\hat{\mathcal{O}}} b_{\mathcal{O}\hat{\mathcal{O}}} D[x_\perp, \partial_a]\hat{\mathcal{O}}(x^a) . \tag{9.8}$$

The sums run only over conformal primaries, and the contributions of the descendants are captured by the differential operators C and D which are completely fixed by conformal symmetry.

The power of the OPE is that it allows us to evaluate higher-point functions using lower-point correlators, provided we know the spectrum of the theory and all the OPE coefficients a, b and λ. In the example of a bulk two-point function, there are two different decompositions possible:

$$\mathcal{F}(\xi) = \sum_{\mathcal{O}} a_{\mathcal{O}} \lambda_{\mathcal{O}_1 \mathcal{O}_2 \mathcal{O}} f_\Delta(\xi) = \sum_{\hat{\mathcal{O}}} b_{\mathcal{O}_1 \hat{\mathcal{O}}} b_{\mathcal{O}_2 \hat{\mathcal{O}}} \hat{f}_{\hat{\Delta}}(\xi) \,. \tag{9.9}$$

The objects $f_\Delta(\xi)$ and $\hat{f}_{\hat{\Delta}}(\xi)$ are called conformal blocks, which we review in appendix 9.B. Equation (9.9) is called the "crossing equation", and it provides non-trivial constraints on the spectrum and CFT data of boundary conformal field theories.

The above discussion was completely general, and it applies to any conformal field theory with a conformal boundary. The main goal of the present paper is to specialize it to superconformal boundaries, in which case the crossing equation (9.9) can be constrained even further. The reason is that supersymmetry relates the OPE coefficients of different conformal primaries that belong to the same supermultiplet, which means that we can organize the expansion in terms of superconformal blocks $F_\Delta(\xi)$ and $\hat{F}_{\hat{\Delta}}(\xi)$. These new objects are linear combinations of the bosonic blocks $f_\Delta(\xi)$ and $\hat{f}_{\hat{\Delta}}(\xi)$ with coefficients fixed by supersymmetry. In sections 9.3 and 9.4 we will compute these objects in $d = 3$ and in $3 \leq d \leq 4$ respectively, which will allow us to study the bootstrap equations analytically in section 9.4.4.

9.3 Boundaries in three dimensions

9.3.1 Superspace analysis

Let us start by studying correlators for both types of boundary conditions using superspace techniques. We introduce a standard Minkowski superspace in which each supercharge $\mathcal{Q}_\alpha, \bar{\mathcal{Q}}_\alpha$, where $\alpha = (1,2) = (-,+)$, has a Grassmann variable θ^α, $\bar{\theta}^\alpha$ associated to it. This setup is enough for our purposes, because we will mostly study correlators of scalar operators in a system with minimal supersymmetry.[4] Our superspace then consists of three spacetime coordinates x^μ and four Grassmann coordinates θ^α and $\bar{\theta}^\alpha$ which we collect as follows:

$$z = (x^\mu, \theta^\alpha, \bar{\theta}^\alpha) \,, \tag{9.10}$$

---

[4]See [270, 271] for studies of non-supersymmetric two-point functions of arbitrary spin.

where $\mu = 0, 1, 2$. We can convert spinor indices α, β into vector indices μ, ν by means of the gamma matrices $(\gamma^\mu)_{\alpha\beta}$. The form of these matrices, together with further conventions regarding raising, lowering and contracting indices, can be found in appendix 9.A.1.

The differential form of the (super)translations acting on fields $\mathcal{O}(z)$ is standard

$$[\mathcal{P}_\mu, \mathcal{O}(z)] = i\partial_\mu \mathcal{O}(z), \tag{9.11}$$

$$[\mathcal{Q}_\alpha, \mathcal{O}(z)] = \left(\partial_\alpha + i(\gamma^\mu)_{\alpha\beta}\bar{\theta}^\beta \partial_\mu\right)\mathcal{O}(z), \tag{9.12}$$

$$\left[\bar{\mathcal{Q}}_\alpha, \mathcal{O}(z)\right] = -\left(\bar{\partial}_\alpha + i(\gamma^\mu)_{\alpha\beta}\theta^\beta \partial_\mu\right)\mathcal{O}(z). \tag{9.13}$$

From the bulk algebra it is easy to derive the form of all the other differential operators, which we list in appendix 9.A.3. The action of the covariant derivatives is also standard

$$D_\alpha \mathcal{O}(z) = \left(\partial_\alpha - i(\gamma^\mu)_{\alpha\beta}\bar{\theta}^\beta \partial_\mu\right)\mathcal{O}(z), \quad \bar{D}_\alpha \mathcal{O}(z) = -\left(\bar{\partial}_\alpha - i(\gamma^\mu)_{\alpha\beta}\theta^\beta \partial_\mu\right)\mathcal{O}(z), \tag{9.14}$$

and as usual, they anticommute with the action of supertranslations. The main focus of this paper is on chiral and antichiral operators (see section 9.2), which are defined in superspace as

$$\bar{D}_\alpha \Phi(z) = 0, \qquad D_\alpha \bar{\Phi}(z) = 0. \tag{9.15}$$

In order to work with chiral operators it is useful to work with chiral/antichiral coordinates defined as

$$y^\mu = x^\mu - i\gamma^\mu_{\alpha\beta}\theta^\alpha \bar{\theta}^\beta, \qquad \bar{y}^\mu = x^\mu + i\gamma^\mu_{\alpha\beta}\theta^\alpha \bar{\theta}^\beta. \tag{9.16}$$

In terms of these coordinates, a chiral field depends only on $\Phi(y, \theta)$ and similarly for the antichiral field $\bar{\Phi}(\bar{y}, \bar{\theta})$. If we consider two points, we can also define supersymmetric invariant distances with well-defined chirality:[5]

$$y^\mu_{12} = x^\mu_{12} - i(\gamma^\mu)_{\alpha\beta}\left(\theta^\alpha_1\bar{\theta}^\beta_1 + \theta^\alpha_2\bar{\theta}^\beta_2 - 2\theta^\alpha_1\bar{\theta}^\beta_2\right), \tag{9.17}$$

$$\bar{y}^\mu_{12} = x^\mu_{12} + i(\gamma^\mu)_{\alpha\beta}\left(\theta^\alpha_1\bar{\theta}^\beta_1 + \theta^\alpha_2\bar{\theta}^\beta_2 + 2\bar{\theta}^\alpha_1\theta^\beta_2\right). \tag{9.18}$$

These distances are chiral at one point and antichiral at the other, namely

$$\bar{D}^{(1)}_\alpha y^\mu_{12} = D^{(2)}_\alpha y^\mu_{12} = 0, \qquad D^{(1)}_\alpha \bar{y}^\mu_{12} = \bar{D}^{(2)}_\alpha \bar{y}^\mu_{12} = 0. \tag{9.19}$$

---

[5]Note that $y^\mu_{12} \neq y^\mu_1 - y^\mu_2$, we hope the notation will not create confusion.

Introducing a boundary will generally break supersymmetry in the bulk. In this paper we study a special class of boundaries that preserve one half of the supersymmetry. As already discussed, they are characterized by $2d$ algebras with $\mathcal{N} = (0,2)$ and $\mathcal{N} = (1,1)$ supersymmetry respectively. The two boundaries have distinct features that we discuss in detail below, the most prominent being that the $\mathcal{N} = (1,1)$ boundary breaks R-symmetry, while it is kept intact in the $\mathcal{N} = (0,2)$ case.

9.3.2   The $\mathcal{N} = (0,2)$ boundary

The $\mathcal{N} = (0,2)$ boundary preserves the supercharges $\mathcal{Q}_+, \bar{\mathcal{Q}}_+$, resulting in the algebra given in (9.1). The bulk superspace can be split into coordinates parallel and perpendicular to the boundary. The parallel coordinates are

$$\left(\theta^+, \bar{\theta}^+, x^a \right), \quad a = 0, 1, \tag{9.20}$$

while the perpendicular coordinates read

$$\left(\theta^-, \bar{\theta}^-, x^\perp \equiv x^2 \right). \tag{9.21}$$

As was the case for the bulk theory, it is convenient to define supersymmetric, chiral, and antichiral perpendicular distances. The supersymmetric distance is

$$z^\perp = x^\perp - i\theta^\alpha \bar{\theta}_\alpha \tag{9.22}$$

and the chiral $y^\perp \equiv y^2$ and antichiral $\bar{y}^\perp \equiv \bar{y}^2$ perpendicular distances can be read off from (9.16). Note that $z^\perp$ is invariant under the boundary (super)translations $\mathcal{P}_a, \mathcal{Q}_+$ and $\bar{\mathcal{Q}}_+$, while $y^\perp$ and $\bar{y}^\perp$ are not. The component expansion of a chiral field Φ takes the familiar form

$$\Phi(y, \theta) = \phi(y) + \theta^+ \psi_+(y) + \theta^- \psi_-(y) + \theta^+ \theta^- F(y), \tag{9.23}$$

where ϕ is a complex boson, ψ_α a complex fermion, and F a complex auxiliary field. It will be convenient to decompose this bulk chiral supermultiplet Φ in terms boundary supermultiplets, that transform irreducibly under the $(0,2)$ subalgebra [372,377]

$$\Phi = \hat{\Phi} + \theta^- \hat{\Psi} + \ldots, \tag{9.24}$$

where $\hat{\Phi}$ is a boundary chiral field, $\hat{\Psi}$ a boundary Fermi field, and the ... stand for derivatives of $\hat{\Phi}$ parallel to the boundary. A similar expansion can be written for the antichiral

bulk supermultiplet $\bar{\Phi}$. From now on, we will denote boundary multiplets and boundary fields with a hat. One can straightforwardly derive a similar expansion for $\hat{\Phi}$ and $\hat{\Psi}$:

$$\hat{\Phi} = \Phi\Big|_{\theta^- = \bar{\theta}^- = 0} = \phi + \theta^+ \psi_+ + \dots, \tag{9.25}$$

$$\hat{\Psi} = D_- \Phi\Big|_{\theta^- = \bar{\theta}^- = 0} = \psi_- + \theta^+ F + \dots, \tag{9.26}$$

where $F \sim \partial_\perp \phi$ on-shell and the $\dots$ stand for terms with derivatives. The usual Neumann and Dirichlet boundary conditions can be neatly represented in terms of these superfields:

$$\text{Neumann:} \quad \partial_\perp \phi\Big|_\partial = 0, \quad \psi_-\Big|_\partial = 0 \quad \rightarrow \quad \hat{\Psi}|_\partial = 0, \tag{9.27}$$

$$\text{Dirichlet:} \quad \phi\Big|_\partial = 0, \quad \psi_+\Big|_\partial = 0 \quad \rightarrow \quad \hat{\Phi}|_\partial = 0. \tag{9.28}$$

One-point functions

As reviewed in section 9.2, scalar bulk operators can acquire a one-point function in the presence of a boundary. In the superspace setup we are considering, we expect on general grounds one-point functions of the form

$$\langle \mathcal{O}(z) \rangle = \frac{a_\mathcal{O}}{(z^\perp)^\Delta}, \tag{9.29}$$

where $z^\perp$ is given in (9.22). For chiral fields, the chirality condition (9.15) and conservation of R-symmetry imply that the one-point function vanishes: $a_\Phi = 0$.

Bulk-to-boundary correlator

Similarly to the one-point function, we expect bulk-to-boundary correlators to be of the form

$$\langle \mathcal{O}(z_1) \hat{\mathcal{O}}(z_2) \rangle = \frac{1}{(z_1^\perp)^{\Delta - \hat{\Delta}} |y_{12}^2 \, \bar{y}_{12}^2|^{\hat{\Delta}/2}} \, g(\Theta_i), \tag{9.30}$$

where g is a function of possible nilpotent invariants Θ_i.

Again, the chirality condition (9.15) is extremely powerful and severely constrains the possible defect operators that can appear in the boundary OPE of a chiral field. From the expansion in (9.24) we expect two types of boundary multiplets, and indeed there are two possible correlators consistent with all the symmetry constraints. One choice involves a

scalar boundary multiplet[6]

$$\langle \Phi(y,\theta)\hat{\bar{\Phi}}_r(0) \rangle = \frac{b_{\Phi\hat{\bar{\Phi}}}}{|y^\mu|^{2\Delta}}, \tag{9.31}$$

where $|y^\mu|$ is the norm of the chiral distance (9.16), and the conformal dimensions are constrained by conservation of R-symmetry $\hat{\Delta} = \Delta_\phi = r_\phi = r_{\hat{\phi}}$.

The other bulk-to-boundary two-point function involves the Fermi multiplet $\hat{\bar{\Psi}}$ whose highest weight carries spin:

$$\langle \Phi(y,\theta)\hat{\bar{\Psi}}(0) \rangle = \frac{b_{\Phi\hat{\bar{\Psi}}}\gamma^\mu_{1\beta}y_\mu\theta^\beta}{(y^\perp)^{\Delta - \hat{\Delta} + \frac{1}{2}}|y^\mu|^{2(\hat{\Delta} + \frac{1}{2})}}. \tag{9.32}$$

Charge conservation implies $r_\psi = 1 - r_\phi$ but $\hat{\Delta}$ is not constrained to take a specific value, which means these multiplets are responsible for most of the operators that appear in the boundary block expansion of the two-point function of chiral fields. The power $\hat{\Delta} + \frac{1}{2}$ indicates that the contributing field is not the primary, but a descendant (see equation (9.45) below).

Two-point functions

As reviewed in section 9.2, bosonic two-point functions depend on a conformal invariant and therefore contain a large amount of dynamical information through their conformal block decompositions. As evident from our analysis so far, correlators of chiral fields are severely constrained by superconformal symmetry and their chirality condition. There is actually only one possible two-point invariant that satisfies all the superspace constraints:

$$\xi = \frac{y_{12}^2}{4y_1^\perp \bar{y}_2^\perp}\left(1 + 2i\frac{(y_{12}^0 + y_{12}^1)\theta_1^-\bar{\theta}_2^-}{y_1^\perp \bar{y}_2^\perp} + 2i\frac{\theta_1^+\bar{\theta}_2^-}{\bar{y}_2^\perp}\right). \tag{9.33}$$

This is the unique "supersymmetrization" of the standard bosonic invariant. The most general two-point function of a chiral and an antichiral field then reads

$$\langle \Phi(y_1,\theta_1)\bar{\Phi}(0,\bar{y}_2^\perp,\bar{\theta}_2^-) \rangle = \left(\frac{\xi}{y_{12}^2}\right)^\Delta \mathcal{F}(\xi), \tag{9.34}$$

where $\mathcal{F}$ is an abitrary function of the superconformal invariant ξ. In equations (9.33) and (9.34) we work in a frame where $\bar{y}_2^a = \bar{\theta}_2^+ = 0$, $(a = 0, 1)$, but we keep the dependence

---

[6]Whenever possible we supertranslate point 2 to the origin to simplify our formulas, but if necessary one can easily supertranslate back to a general frame.

on $\bar{y}_2^{\perp}$ and $\bar{\theta}_2^{-}$, since they are perpendicular coordinates and cannot be set to zero. Using a supertranslation one can find the two-point function in a frame with completely general z_1 and z_2, as will be needed below. Two-point functions of two chiral (or two antichiral) fields are zero due to R-symmetry. For more general external operators, for example long multiplets of the superconformal algebra, we expect a more complicated correlator involving nilpotent invariants, which then translates into superconformal blocks that have free parameters (see for example [228]). We will not consider more general correlators in this work, however our superspace setup could be used to study them in the future.

Superconformal blocks

We are now ready to obtain one of the main results of this section: the superconformal blocks associated to the two-point correlator $\mathcal{F}(\xi)$. As reviewed in section 9.2, there are two conformal block expansions associated to the bulk and defect channel respectively. Bulk conformal blocks are eigenfunctions of the two-point bulk Casimir operator, while defect blocks are eigenfunctions of the defect Casimir.

Bulk channel: Let us start with the bulk channel,

$$\mathcal{C}_{\text{susy}}^{(12)} \langle \Phi(z_1) \bar{\Phi}(z_2) \rangle = C_{\Delta, \ell, r} \langle \Phi(z_1) \bar{\Phi}(z_2) \rangle \,, \tag{9.35}$$

where the supersymmetric bulk Casimir is given by

$$\mathcal{C}_{\text{susy}}^{(12)} = -\mathcal{D}^2 - \frac{1}{2}\{\mathcal{K}^{\mu}, \mathcal{P}_{\mu}\} + \frac{1}{2}\mathcal{M}^{\mu\nu}\mathcal{M}_{\mu\nu} - \frac{1}{2}\mathcal{R}^2 + \frac{1}{4}[\mathcal{S}^{\alpha}, \bar{\mathcal{Q}}_{\alpha}] + \frac{1}{4}[\bar{\mathcal{S}}^{\alpha}, \mathcal{Q}_{\alpha}]. \tag{9.36}$$

The superscript (12) indicates that the operator acts on points z_1 and z_2. To avoid cluttering we wrote the superscript only on the Casimir, and omit it from the operators on the RHS. The eigenvalue reads

$$C_{\Delta, \ell, r} = \Delta(\Delta - 1) + \ell(\ell + 1) - \frac{r^2}{2} \,. \tag{9.37}$$

Evaluating (9.35) leads to a differential equation for the corresponding block $F_{\Delta}(\xi)$. Our analysis implies the absence of nilpotent invariants when chiral fields are involved. This means that full superspace correlators can be reconstructed from those of the superprimaries and implies that a multiplet contributes only if its superprimary contributes. Because only scalars can acquire a one-point function in BCFT, we can safely set $\ell = 0$ when looking for solutions to the Casimir equation. A standard approach to solve these

equations is to recognize that superconformal blocks can be written as linear combinations of bosonic blocks. The superdescendants of a field $\mathcal{O}(z)$ can be generated by acting on the superprimary $\mathcal{O}(z)$ with the supercharges $\mathcal{Q}, \bar{\mathcal{Q}}$. This creates superdescendants of the schematic form $\mathcal{Q}_1 \dots \bar{\mathcal{Q}}_n \mathcal{O}(z)$.[7] We therefore make the following ansatz

$$F_\Delta(\xi) = f_\Delta(\xi) + c_0 f_{\Delta + \frac{1}{2}} + c_1 f_{\Delta + 1}(\xi) + c_2 f_{\Delta + \frac{3}{2}}(\xi) + c_3 f_{\Delta + 2}(\xi) , \tag{9.38}$$

where $f_\Delta(\xi)$ are the bosonic blocks given in (9.175), and we fix the relative coefficients using (9.35). The solution is easy to find

$$F_\Delta(\xi) = f_\Delta(\xi) - \frac{(\Delta - 1)\Delta}{(2\Delta - 1)(2\Delta + 1)} f_{\Delta + 2}(\xi) , \tag{9.39}$$

which corresponds to a long operator being exchanged in the $\phi \times \bar{\phi}$ OPE. There are also contributions from short multiplets, but they can be obtained from (9.39) evaluating Δ at the unitarity bound. The selection rules of this OPE have been studied in the context of bulk four-point functions [193] and our results are in perfect agreement with the literature. The block in equation (9.39) can be written as a single hypergeometric funtion

$$F_\Delta(\xi) = \xi^{\Delta/2} \, {}_2F_1\left(1 + \frac{\Delta}{2}, \frac{\Delta}{2}; \Delta + \frac{1}{2}; -\xi\right). \tag{9.40}$$

We will see that all of the two-point blocks derived in this section have this feature.

Boundary channel: In the boundary channel the blocks are eigenfunctions of the boundary Casimir

$$\hat{\mathcal{C}}_{\text{susy}} = -\mathcal{D}^2 - \frac{1}{2}\{\mathcal{K}^a, \mathcal{P}_a\} + \frac{1}{2}\mathcal{M}^{ab}\mathcal{M}_{ab} - \frac{1}{2}\mathcal{R}^2 + \frac{1}{4}\left([\bar{\mathcal{S}}^+, \mathcal{Q}_+] + [\mathcal{S}^+, \bar{\mathcal{Q}}_+]\right) , \tag{9.41}$$

where now the operator acts at a single point:

$$\hat{\mathcal{C}}_{\text{susy}}^{(1)} \langle \Phi(z_1) \bar{\Phi}(z_2) \rangle = \hat{C}_{\hat{\Delta}, j, r} \langle \Phi(z_1) \bar{\Phi}(z_2) \rangle . \tag{9.42}$$

The eigenvalue depends on the conformal dimension $\hat{\Delta}$ of the exchanged boundary operator, as well as its parallel spin j and its R-charge:

$$\hat{C}_{\hat{\Delta}, j, r} = \hat{\Delta}(\hat{\Delta} - 1) + j(j - 1) - \frac{r^2}{2} . \tag{9.43}$$

---

[7]In order to obtain proper conformal primaries (killed by $\mathcal{K}$) the action of the $\mathcal{Q}_i$ has to be corrected by terms containing the momentum generator $\mathcal{P}$.

Proceeding as before we make an ansatz for $\hat{F}_{\hat{\Delta}}$ in terms of bosonic blocks and fix the relative coefficients using (9.42). Note that we only have to include conformal blocks up to dimension $\hat{\Delta} + 1$ in our ansatz, since the boundary only preserves half of the supercharges. From section 9.3.2 we know there are two types of boundary multiplets that can appear in the boundary expansion of a chiral field: a scalar $\hat{\Phi}$ and the Fermi multiplet $\hat{\Psi}$. We therefore expect two classes of solutions to the Casimir equation. Indeed, the solution corresponding to a chiral primary with $r = r_\phi$, $j = 0$ and $\hat{\Delta} = \Delta_\phi = r_\phi$, is given by

$$\hat{F}_{\hat{\Delta}}^{\hat{\Phi}}(\xi) = \hat{f}_{\Delta_\phi}(\xi) \,. \tag{9.44}$$

The second solution, with $r = r_\phi - 1$, $j = \frac{1}{2}$ corresponds to the Fermi field

$$\hat{F}_{\hat{\Delta}}^{\hat{\Psi}}(\xi) = \hat{f}_{\hat{\Delta}+\frac{1}{2}}(\xi) \,. \tag{9.45}$$

Notice that the $\frac{1}{2}$ in the argument indicates that the highest weight does not contribute, but a descendant (as expected).

Three-point functions

Although not our main topic, let us also analyze three-point correlators involving one bulk field and two boundary fields. An interesting application for these correlators is to impose that the bulk field is free, and to study the corresponding constraints on the boundary three-point couplings [294, 295]. For the rest of this section we will choose a frame where $x_2^a = \theta_2^+ = \bar{\theta}_2^+ = \theta_3^+ = \bar{\theta}_3^+ = 0, x_3^a \to \infty$. By imposing that the bulk field is chiral we obtain

$$\langle \Phi(y, \theta) \hat{\mathcal{O}}_{2,j}(0, \omega) \hat{\mathcal{O}}_3(\infty) \rangle = \frac{(y^a \omega_a)^j}{(y^\perp)^{\Delta + \hat{\Delta}_{23}} |y^a|^j} \mathcal{F}^{3\mathrm{pt}}(\chi) \,. \tag{9.46}$$

The second operator has arbitrary parallel spin j, and we use an index-free notation where $\hat{\mathcal{O}}_{2,j}(z, \omega) = \hat{\mathcal{O}}_{2,j}(z)^{a_1 \ldots a_j} \omega_{a_1} \ldots \omega_{a_j}$ and ω_a is a null vector in the parallel directions. For brevity we define $\hat{\Delta}_{23} \equiv \hat{\Delta}_2 - \hat{\Delta}_3$, and y^a is defined in (9.16), where one should remember that $a = 0, 1$ are the parallel coordinates. Conservation of R-symmetry implies $r_\phi + r_2 + r_3 = 0$. The function $\mathcal{F}^{3\mathrm{pt}}(\chi)$ depends on the superconformal three-point invariant χ. Like in the two-point function case, there is a unique, non-nilpotent, three-point invariant:

$$\chi = \frac{|y^a|^2}{(y^\perp)^2} \,. \tag{9.47}$$

The function $\mathcal{F}_{3\mathrm{pt}}(\chi)$ can be expanded in three-point superconformal blocks which are in turn sums of three-point bosonic blocks (reviewed in appendix 9.B.2). Notice that there is

no crossing equation for this correlator. We can act with the boundary Casimir on point z_1 and obtain the eigenvalue equation

$$\hat{\mathcal{C}}^{(1)}_{\text{susy}} \langle \Phi(y, \theta) \hat{\mathcal{O}}_{2,j}(0, \omega) \hat{\mathcal{O}}_3(\infty) \rangle = \hat{C}_{\hat{\Delta}, j, r} \langle \Phi(y, \theta) \hat{\mathcal{O}}_{2,j}(0, \omega) \hat{\mathcal{O}}_3(\infty) \rangle . \tag{9.48}$$

By now the story is familiar; we give an ansatz in terms of bosonic blocks and obtain a solution with $r = r_\phi$, $j_{\text{chiral}} = 0$, $\hat{\Delta} = \Delta_\phi = r_\phi$:

$$\hat{F}^{\text{3pt}}_{\Delta_\phi}(\chi) = \hat{f}^{\text{3pt}, \hat{\Delta}_{23}}_{\Delta_\phi, j}(\chi) , \tag{9.49}$$

which describes the exchange of a boundary chiral field. The other possible solution has $r = r_\phi - 1$, $j_{\text{fermi}} = \frac{1}{2}$ and generic $\hat{\Delta}$:

$$\hat{F}^{\text{3pt}}_{\hat{\Delta}}(\chi) = \hat{f}^{\text{3pt}, \hat{\Delta}_{23}}_{\hat{\Delta} + \frac{1}{2}, j}(\chi) , \tag{9.50}$$

and corresponds to the exchange of a Fermi multiplet. Let us also consider the case where the second operator is a Fermi field. The three-point function is given by

$$\langle \Phi(y, \theta) \hat{\bar{\Psi}}(0) \hat{\mathcal{O}}(\infty) \rangle = \frac{(\gamma_{1\beta})^\mu y_\mu \theta^\beta}{(y^\perp)^{\Delta + \hat{\Delta}_{23} + \frac{3}{2}}} \mathcal{F}_{\text{3pt}}(\chi) , \tag{9.51}$$

where χ is the same invariant as before. There are again two solutions to the eigenvalue equation, the first one corresponds to the exchange of a boundary chiral

$$\hat{F}^{\text{3pt}}_{\Delta_\phi}(\chi) = \hat{f}^{\text{3pt}, \hat{\Delta}_{23} + \frac{1}{2}}_{\Delta_\phi, 0}(\chi) , \tag{9.52}$$

while the second describes a Fermi field

$$\hat{F}^{\text{3pt}}_{\hat{\Delta}}(\chi) = f^{\text{3pt}, \hat{\Delta}_{23} + \frac{1}{2}}_{\hat{\Delta} + \frac{1}{2}, 0}(\chi) . \tag{9.53}$$

The supersymmetric block corresponds to a bosonic block with shifted external conformal dimensions $\hat{\Delta}_{23} \to \hat{\Delta}_{23} + \frac{1}{2}$ and with spin $j = 0$. Like in the two-point case, the shift can be understood as a contribution coming from a superconformal descendant of $\hat{\bar{\Psi}}$.

Free theory in the bulk

Having obtained a handful of correlators, let us investigate the possible constraints that a free theory in the bulk imposes on the boundary data. In superspace the free field equations of motion take the form

$$D^\alpha D_\alpha \Phi(y, \theta) = 0 , \tag{9.54}$$

which is the supersymmetric version of the more familiar $\partial^2 \phi(x) = 0$. As usual, a free chiral field has dimension $\Delta_\phi = r_\phi = \frac{1}{2}$. Imposing this condition on the two bulk-to-boundary correlators (9.31) and (9.32), we obtain two solutions:

$$\langle \Phi(y,\theta) \hat{\bar{\Phi}}_{\hat{\Delta}=\frac{1}{2}}(0) \rangle = \frac{b_{\Phi\hat{\bar{\Phi}}}}{|y^\mu|}, \qquad \langle \Phi(y,\theta) \hat{\bar{\Psi}}_{\hat{\Delta}=1}(0) \rangle = \frac{b_{\Phi\hat{\bar{\Psi}}} \gamma^\mu_{1\beta} y_\mu \theta^\beta}{|y^\mu|^3}. \tag{9.55}$$

This is not surprising. The first solution corresponds to a boundary chiral field of dimension $\hat{\Delta} = \frac{1}{2}$, which corresponds to the operator $\hat{\phi}$ and describes Neumann boundary conditions. The second solution is a Fermi field with $\hat{\Delta} = 1$, which has a scalar descendant with dimension $\hat{\Delta} + \frac{1}{2} = \frac{3}{2}$ (recall the discussion below (9.32)). The descendant can be identified with $\partial_\perp \hat{\phi}$ as expected for Dirichlet boundary conditions. We have therefore proven that the boundary expansion of a bulk free field has a finite number of contributions.

We now turn to the three-point function to see if there are extra constraints on the boundary operators from a free bulk chiral field. Let us expand the correlation function (9.46) in bosonic blocks, where we take Φ to be a free bulk chiral. From equation (9.55) we know that there are two independent contributions coming from a chiral and a Fermi boundary field:

$$\mathcal{F}^{\text{3pt}}(\chi) = b_{\phi\hat{\phi}} \lambda_{\hat{\phi}\hat{O}_2\hat{O}_3} \hat{f}^{\text{3pt},\hat{\Delta}_{23}}_{\hat{\Delta}=\frac{1}{2},j}(\chi) + b_{\phi\partial_\perp\hat{\phi}} \lambda_{\hat{\partial}_\perp\hat{\phi}\hat{O}_2\hat{O}_3} \hat{f}^{\text{3pt},\hat{\Delta}_{23}}_{\hat{\Delta}=\frac{3}{2},j}(\chi). \tag{9.56}$$

Note that we have written the OPE coefficients explicitly in terms of the operators that appear in the OPE and not in terms of the superprimaries. Equation (9.56) is identical to the conformal block expansion of a non-supersymmetric free scalar in the bulk, which has been studied in detail in [294, 295]. In the limit $\chi \to 0$ there are unphysical singularities, which can only be removed provided the OPE coefficients satisfy the following relation:

$$b_{\phi\partial_\perp\hat{\phi}} \lambda_{\hat{\partial}_\perp\hat{\phi}\hat{O}_2\hat{O}_3} = -\frac{2\Gamma\left(\frac{2j-2\hat{\Delta}_{23}+3}{4}\right)\Gamma\left(\frac{2j+2\hat{\Delta}_{23}+3}{4}\right)}{\Gamma\left(\frac{2j-2\hat{\Delta}_{23}+1}{4}\right)\Gamma\left(\frac{2j+2\hat{\Delta}_{23}+1}{4}\right)} b_{\phi\hat{\phi}} \lambda_{\hat{\phi}\hat{O}_2\hat{O}_3}. \tag{9.57}$$

This constraint is equivalent to the constraints on non-supersymmetric three-point functions with a free bulk. We can go one step further and look at the three-point function involving a boundary Fermi multiplet (9.51) in the hope that we will find additional constraints on the CFT data from supersymmetry. Once again, we expect the two solutions in equation (9.55) to contribute to the Fermi three-point function. If we act with the equations of motion, the resulting differential equation can only be solved if $\hat{\Delta}_{23} = 1$, excluding

the solution $\hat{\Delta} = \frac{1}{2}$. The resulting correlator corresponds to a single bosonic block

$$\mathcal{F}_{3\text{pt}}(\chi) \propto \hat{f}_{\hat{\Delta}=\frac{3}{2},0}^{3\text{pt},\frac{3}{2}}(\chi) = \frac{1}{(\chi+1)^{\frac{3}{2}}} \, . \tag{9.58}$$

In this case the correlator is manifestly non-singular as $\chi \to 0$. Having a free bulk implies that there is only one operator in the OPE $\hat{\phi} \times \hat{\psi}$, which has fixed dimension $\hat{\Delta}_3 = \hat{\Delta}_2 - 1$. This is a new, additional constraint coming from the superspace analysis that was not present in the non-supersymmetric case. It would be interesting to see if a more systematic analysis allows us to find more general constraints.

9.3.3   The $\mathcal{N} = (1,1)$ boundary

We now present the superspace analysis for the $\mathcal{N} = (1,1)$ boundary, and since it is quite similar to what we have done so far, we will mostly state the results. We again divide the superspace into parallel and perpendicular coordinates, the bosonic coordinates are split as usual, and for the fermionic variables we define

$$\text{parallel:} \quad \tilde{\theta}^1 \equiv \tilde{\theta}^- = -i(\theta^- - \bar{\theta}^-) \, , \quad \tilde{\theta}^2 \equiv \tilde{\theta}^+ = -(\theta^+ + \bar{\theta}^+) \, , \tag{9.59}$$

$$\text{perpendicular:} \quad \theta_\perp^1 \equiv \theta_\perp^- = -(\theta^- + \bar{\theta}^-) \, , \quad \theta_\perp^2 \equiv \theta_\perp^+ = -i(\theta^+ - \bar{\theta}^+) \, , \tag{9.60}$$

There are two useful ways to construct supersymmetric perpendicular distances

$$z^\perp = y^\perp + 2i\theta^- \theta^+ \, , \qquad \bar{z}^\perp = \bar{y}^\perp + 2i\bar{\theta}^- \bar{\theta}^+ \, , \tag{9.61}$$

with the property that they are chiral and antichiral respectively $\bar{D}_\alpha z^\perp = D_\alpha \bar{z}^\perp = 0$. These distances will be the natural objects to appear in correlators of (anti)chiral fields. The decomposition of a bulk (anti)chiral field for the $\mathcal{N} = (1,1)$ boundary contains only one boundary supermultiplet instead of the two possibilities present in the $(0,2)$ boundary

$$\Phi = \hat{\Phi} + \dots \, , \tag{9.62}$$

where the dots stand for derivatives of $\hat{\Phi}$. The field $\hat{\Phi}$ can be decomposed into bosonic components, schematically (see [377] for the precise coefficients)

$$\hat{\Phi} = \hat{\phi} + \tilde{\theta}^+ \hat{\psi}_+ + \tilde{\theta}^- \hat{\psi}_- + \tilde{\theta}^2 \partial_\perp \hat{\phi} + \tilde{\theta}^2 \hat{F} \, . \tag{9.63}$$

We see that $\hat{\phi}$ and $\partial_\perp \hat{\phi}$ belong to the same boundary multiplet, which implies the unexpected feature that Neumann and Dirichlet boundary conditions are related by supersymmetry.

One-point functions

Due to the absence of R-symmetry, (anti)chiral bulk fields can now acquire a one-point function. The only correlators consistent with the symmetry constraints are given by

$$\langle \Phi(y, \theta) \rangle = \frac{a_\Phi}{(2z^\perp)^\Delta} \,, \qquad \langle \bar{\Phi}(\bar{y}, \bar{\theta}) \rangle = \frac{a_{\bar{\Phi}}}{(2\bar{z}^\perp)^\Delta} \,, \tag{9.64}$$

where $z^\perp, \bar{z}^\perp$ were defined in (9.61), and a_Φ is the one-point coupling that appears as the coefficient of the "boundary identity" in the conformal block expansion.

Bulk-to-boundary correlator

Since a chiral bulk supermultiplet decomposes into one boundary supermultiplet, we expect only one correlator:

$$\langle \Phi(y, \theta) \hat{\mathcal{O}}(0) \rangle = \frac{b_{\Phi \hat{\mathcal{O}}}}{(2z^\perp)^{\Delta - \hat{\Delta}} |y^\mu|^{2\hat{\Delta}}} \,, \tag{9.65}$$

where $z^\perp$ is the same as above and $|y^\mu|$ is the norm of the chiral coordinate (9.16). Notice that $\hat{\Delta}$ is unconstrained so these are the operators captured by the boundary conformal blocks to be calculated below.

Two-point functions

Due to the broken R-symmetry there is now no selection rule implying that correlators with fields of the same chirality vanish. Thus, we should consider the two-point functions $\langle \Phi_1 \bar{\Phi}_2 \rangle$ and $\langle \Phi_1 \Phi_2 \rangle$ where the R-charges are arbitrary. The two-point functions in the presence of the $\mathcal{N} = (1, 1)$ boundary have the same structure as in the $\mathcal{N} = (0, 2)$ case. Each of them depends on a single superconformal invariant ξ which has the appropriate chirality properties:

$$\langle \Phi_1(y_1, \theta_1) \bar{\Phi}_2(\bar{y}_2, \bar{\theta}_2) \rangle = \frac{\mathcal{F}^{\phi\bar{\phi}}(\xi)}{(2z_1^\perp)^{\Delta_1}(2\bar{z}_2^\perp)^{\Delta_2}}, \qquad \xi = \frac{(y_{12})^2}{4z_1^\perp \bar{z}_2^\perp} \,, \tag{9.66}$$

$$\langle \Phi_1(y_1, \theta_1) \Phi_2(y_2, \theta_2) \rangle = \frac{\mathcal{F}^{\phi\phi}(\xi)}{(2z_1^\perp)^{\Delta_1}(2z_2^\perp)^{\Delta_2}}, \qquad \xi = \frac{(\tilde{y}_{12})^2 + 2i\theta_{12}^2(z_1^\perp + z_2^\perp)}{4z_1^\perp z_2^\perp} \,. \tag{9.67}$$

201

The perpendicular distances $z^\perp, \bar{z}^\perp$ are given in equation (9.61), the chiral-antichiral distance y_{12}^μ can be found in (9.17), and we have defined the following chiral-chiral distance:

$$
\begin{aligned}
\tilde{y}_{12}^0 &= y_1^0 - y_2^0 - 2i(\theta_1^+ \theta_2^+ - \theta_1^- \theta_2^-)\,, \\
\tilde{y}_{12}^1 &= y_1^1 - y_2^1 - 2i(\theta_1^+ \theta_2^+ + \theta_1^- \theta_2^-)\,, \\
\tilde{y}_{12}^2 &= z_1^\perp - z_2^\perp \,.
\end{aligned}
\tag{9.68}
$$

Let us now calculate the corresponding superblocks for the functions $\mathcal{F}^{\phi\bar{\phi}}(\xi)$ and $\mathcal{F}^{\phi\phi}(\xi)$.

Superconformal blocks

We now calculate the superconformal blocks using the same approach we used in the $\mathcal{N} = (0,2)$ case in section 9.3.2. We use the Casimir to obtain a differential equation that we then solve using a finite combination of bosonic blocks.

Bulk channel: We first act wit the bulk Casimir

$$
\mathcal{C}_{\text{susy}}^{(12)} \langle \Phi_1(y_1, \theta_1) \bar{\Phi}_2(\bar{y}_2, \bar{\theta}_2) \rangle = C_{\Delta,\ell,r} \langle \Phi_1(y_1, \theta_1) \bar{\Phi}_2(\bar{y}_2, \bar{\theta}_2) \rangle\,,
\tag{9.69}
$$

where $\mathcal{C}_{\text{susy}}^{(12)}$ and $C_{\Delta,\ell,r}$ were already given in (9.36) and (9.37) respectively. The solution to this equation in terms of bosonic blocks is easy to find. Only $\ell = 0$ and $r = r_1 - r_2$ contributes

$$
\begin{aligned}
F_\Delta^{\phi_1 \bar{\phi}_2}(\xi) &= f_\Delta^{\Delta_{12}}(\xi) + \frac{(\Delta - \Delta_{12})(\Delta + \Delta_{12})}{(2\Delta - 1)(2\Delta + 1)} f_{\Delta+2}^{\Delta_{12}}(\xi) \\
&= \xi^{\frac{\Delta - \Delta_1 - \Delta_2}{2}}\, {}_2F_1\Big(\frac{\Delta - \Delta_{12}}{2}, \frac{\Delta + \Delta_{12}}{2}; \Delta + \frac{1}{2}; -\xi\Big),
\end{aligned}
\tag{9.70}
$$

which in general corresponds to a long operator being exchanged in the $\phi_1 \times \bar{\phi}_2$ OPE. The contributions of short operators can be found by evaluating Δ at the unitarity bound, as discussed below equation (9.39). For the two-point function $\langle \Phi_1 \Phi_2 \rangle$, which was not present in the $\mathcal{N} = (0,2)$ case, the solution to the Casimir equation

$$
\mathcal{C}_{\text{susy}}^{(12)} \langle \Phi_1(y_1, \theta_1) \Phi_2(y_2, \theta_2) \rangle = C_{\Delta,\ell,r} \langle \Phi_1(y_1, \theta_1) \Phi_2(y_2, \theta_2) \rangle\,,
\tag{9.71}
$$

can be written in terms of single bosonic blocks with shifted arguments $F_\Delta^{\phi\phi} = f_{\Delta + \frac{n}{2}}$. This is a well-known result which has been described in detail for $d = 3$ in [193]. We will review the analysis in detail in section 9.4.1.

Boundary channel: Let us now move on to the boundary channel. The boundary Casimir is now given by

$$\hat{\mathcal{C}}_{\text{susy}} = -\mathcal{D}^2 - \frac{1}{2}\{\mathcal{K}^a, \mathcal{P}_a\} + \frac{1}{2}\mathcal{M}^{ab}\mathcal{M}_{ab} + \frac{1}{4}[\tilde{\mathcal{S}}^\alpha, \tilde{\mathcal{Q}}_\alpha] \,, \tag{9.72}$$

with eigenvalue

$$\hat{C}_{\hat{\Delta},j} = \hat{\Delta}(\hat{\Delta} - 1) + j^2 \,. \tag{9.73}$$

We can only find consistent solutions when the superprimary has no parallel spin: $j = 0$. For the chiral-antichiral correlator we find

$$\begin{aligned}
\hat{F}_{\hat{\Delta}}^{\phi_1 \bar{\phi}_2}(\xi) &= \hat{f}_{\hat{\Delta}}(\xi) + \frac{1}{4}\hat{f}_{\hat{\Delta}+1}(\xi) \\
&= \xi^{-\hat{\Delta}} \, {}_2F_1\left(\hat{\Delta} - \frac{1}{2}, \hat{\Delta}; 2\hat{\Delta}; -\frac{1}{\xi}\right).
\end{aligned} \tag{9.74}$$

while for the chiral-chiral correlator we have

$$\begin{aligned}
\hat{F}_{\hat{\Delta}}^{\phi_1 \phi_2}(\xi) &= \hat{f}_{\hat{\Delta}}(\xi) - \frac{1}{4}\hat{f}_{\hat{\Delta}+1}(\xi) \\
&= \xi^{-\hat{\Delta}} \, {}_2F_1\left(\hat{\Delta} + \frac{1}{2}, \hat{\Delta}; 2\hat{\Delta}; -\frac{1}{\xi}\right).
\end{aligned} \tag{9.75}$$

These two blocks describe the exchange of operators whose correlator (9.65) is non-vanishing. This concludes our analysis of two-point blocks in the $\mathcal{N} = (1,1)$ boundary. We will generalize these results for arbitrary $3 \leq d \leq 4$ in section 9.4. The superspace analysis of this section will give supporting evidence that the blocks of section 9.4 are a consistent continuation of the $3d$ results presented here.

Three-point functions

Let us now study the correlator of a chiral bulk field and two boundary fields. We allow the first boundary operator to have arbitrary spin j, and we will work in a frame where we set $x_2^a, \tilde{\theta}_2^a, \tilde{\theta}_3^a$ to zero, and x_3^a to infinity. Unlike the situations studied so far, there is a nilpotent invariant consistent with all the symmetries, which implies the following structure

$$\langle \Phi(y, \theta)\hat{\mathcal{O}}_{2,j}(0, \omega)\hat{\mathcal{O}}_3(\infty) \rangle = \frac{(y^a \omega_a)^j}{(y^\perp)^{\Delta_\phi + \hat{\Delta}_{23}}|y^a|^j}\left(\mathcal{F}_1^{\text{3pt}}(\chi) + \frac{\theta^+ \theta^-}{y^\perp}\mathcal{F}_2^{\text{3pt}}(\chi)\right). \tag{9.76}$$

All the dependence of the correlator is in terms of the chiral coordinates y and θ, see (9.16). The superconformal invariant χ is the same as for the $\mathcal{N} = (0, 2)$ boundary in (9.47).

The superfields $\Phi, \hat{\mathcal{O}}_i$ appearing in the three-point function can be expanded into bosonic components, whose correlators are captured by $\mathcal{F}_i^{\text{3pt}}$. Let us look at this expansion with more details. Since we chose a frame where $\theta_2 = \bar{\theta}_2 = \theta_3 = \bar{\theta}_3 = 0$, only the superprimary in the θ-expansion of $\hat{\mathcal{O}}_i$ will contribute, then

$$\Phi(y, \theta) = \phi(y) + \theta^\alpha \psi_\alpha(y) + \theta^+ \theta^- F(y), \quad \hat{\mathcal{O}}_2(0, \omega) = \hat{O}_2(0, \omega), \quad \hat{\mathcal{O}}_3(\infty) = \hat{O}_3(\infty).$$
(9.77)

Comparing the correlator (9.76) with the expansion (9.77) we read off

$$\langle \phi(x) \hat{O}_2(0, \omega) \hat{O}_3(\infty) \rangle = \frac{(x^a w_a)^j}{(x^\perp)^{\Delta_\phi + \hat{\Delta}_{23}} |x^\mu|^j} \mathcal{F}_1^{\text{3pt}}(\chi),$$
(9.78)

$$\langle \psi_\alpha(x) \hat{O}_2(0, \omega) \hat{O}_3(\infty) \rangle = 0,$$
(9.79)

$$\langle F(x) \hat{O}_2(0, \omega) \hat{O}_3(\infty) \rangle = \frac{(x^a w_a)^j}{(x^\perp)^{(\Delta_\phi + 1) + \hat{\Delta}_{23}} |x^\mu|^j} \mathcal{F}_2^{\text{3pt}}(\chi),$$
(9.80)

so indeed $\mathcal{F}_{1,2}^{\text{3pt}}$ capture the correlators of the top and bottom components of the chiral multiplet. To find the corresponding superconformal blocks we act with the boundary supersymmetric Casimir in point z_1:

$$\hat{\mathcal{C}}_{\text{susy}}^{(1)} \langle \Phi(y, \theta) \hat{\mathcal{O}}_{2,j}(0, \omega) \hat{\mathcal{O}}_3(\infty) \rangle = \hat{C}_{\hat{\Delta}, 0, r} \langle \Phi(y, \theta) \hat{\mathcal{O}}_{2,j}(0, \omega) \hat{\mathcal{O}}_3(\infty) \rangle,$$
(9.81)

where $\hat{C}_{\hat{\Delta}, 0, r}$ is given in equation (9.73). This results in two coupled differential equations, which we can solve by assuming that the superconformal blocks are given in terms of the bosonic blocks $\hat{f}_{\hat{\Delta}}^{\text{3pt}}$ given in (9.182). The final result reads

$$F_{1, \hat{\Delta}}^{\text{3pt}}(\chi) = f_{\hat{\Delta}, j}^{\text{3pt}, \hat{\Delta}_{23}}(\chi) + c_{\hat{\Delta}} f_{\hat{\Delta}+1, j}^{\text{3pt}, \hat{\Delta}_{23}}(\chi),$$

$$F_{2, \hat{\Delta}}^{\text{3pt}}(\chi) = -2i(r_\phi - \hat{\Delta}) f_{\hat{\Delta}, j}^{\text{3pt}, \hat{\Delta}_{23}}(\chi) + 2i c_{\hat{\Delta}}(r_\phi + \hat{\Delta} - 1) f_{\hat{\Delta}+1, j}^{\text{3pt}, \hat{\Delta}_{23}}(\chi),$$
(9.82)

where $c_{\hat{\Delta}}$ is a free parameter, related to the OPE coefficients of the exchanged operator, see equation (9.83) below.

Free bulk theory

We now repeat the analysis of section 9.3.2, and see how the bulk equations of motion constrain the spectrum of boundary operators. Imposing that the chiral field is free in (9.65) fixes the dimension of the boundary field to $\hat{\Delta} = \frac{1}{2}$. Unlike in the $\mathcal{N} = (0, 2)$ case

there is only solution, since both Neumann and Dirichlet boundary conditions are related by supersymmetry, and belong to the same supermultiplet.

Let us now focus on to the three-point function (9.76). It is well known that the free equations of motion for a chiral field imply $F(x) = 0$, so it is sufficient to focus on $\mathcal{F}_1^{3\text{pt}}(\chi)$. From the analysis of the free bulk-to-boundary correlator we conclude that there can only be one multiplet in the bulk-to-boundary OPE. The superprimary has dimension $\hat{\Delta} = \frac{1}{2}$, which we will call $\hat{\phi}$. The multiplet also contains a superdescendant of dimension $\hat{\Delta} + 1 = \frac{3}{2}$, which we denote by $\partial_\perp \hat{\phi}$. Both operators contribute to the superconformal block (9.82), and the resulting correlation function is

$$\mathcal{F}_1^{3\text{pt}}(\chi) = b_{\phi\hat{\phi}} \lambda_{\hat{\phi}\hat{O}_2\hat{O}_3} \hat{f}_{\hat{\Delta}=\frac{1}{2},j}^{3\text{pt},\hat{\Delta}_{23}}(\chi) + b_{\phi\partial_\perp\hat{\phi}} \lambda_{\partial_\perp\hat{\phi}\hat{O}_2\hat{O}_3} \hat{f}_{\hat{\Delta}=\frac{3}{2},j}^{3\text{pt},\hat{\Delta}_{23}}(\chi) \,, \tag{9.83}$$

where the OPE coefficients are written in terms of the superdescendants, not the superprimaries. Due to the presence of a free coefficient $c_{\hat{\Delta}}$ in the superconformal block (9.82), the relative coefficient in this expansion is not fixed by supersymmetry. Equation (9.83) is identical to the non-supersymmetric case of a free scalar in the bulk and to equation (9.56) for the $\mathcal{N} = (0, 2)$ boundary. Thus, the analysis below (9.56) applies here as well and we find the same OPE relations (9.57). There are no extra constraints coming from supersymmetry.

9.4 Boundaries across dimensions

In this section we study superconformal theories with boundaries in any, in principle continuous, number of dimensions $3 \leq d \leq 4$, keeping the codimension fixed. We obtain superconformal blocks using similar techniques as were developed originally for bulk four-point functions in [193, 236].[8] Conformal blocks in an arbitrary number of dimensions allow us to use analytical techniques like the ϵ-expansion, a subject that we explore in this section inspired by previous work [269, 272] .

9.4.1 Superconformal blocks

Superconformal algebra

In the entire section we follow the same conventions as [193], which we review briefly. The notation will differ from the one in section 9.3, but our main results, the superconformal

---

[8]Another example of blocks across dimensions was uncovered in the context of Parisi-Sourlas supersymmetry [379, 380].

blocks, will be convention-independent. We hope this does not cause too much confusion. The reader is welcome to look at the original reference for more details. The conformal part of the algebra is generated by the usual operators D, P_i, K_i and M_{ij}. We also have four Poincaré supercharges Q_α^+ and $Q_{\dot\alpha}^-$ and four conformal supercharges $S^{\dot\alpha+}$ and $S^{\alpha-}$ with anticommutation relations

$$\{Q_\alpha^+, Q_{\dot\alpha}^-\} = \Sigma_{\alpha\dot\alpha}^i P_i\,, \qquad \{S^{\dot\alpha+}, S^{\alpha-}\} = \bar\Sigma_i^{\dot\alpha\alpha} P_i\,, \qquad i = 1, \ldots, d\,. \tag{9.84}$$

Finally, there is a generator R of $U(1)_R$ symmetry, under which Q_α^+ and $Q_{\dot\alpha}^-$ have charge $+1$ and -1 respectively. Provided that $\Sigma_{\alpha\dot\alpha}^i$ satisfies certain formal identities, the superjacobi identites are satisfied for arbitrary d. The full set of commutation relations, the Casimir operator C_{bulk}, and many other important relations can be found in [193].

In what follows, we will focus our attention on chiral primary operators ϕ and their complex conjugates $\bar\phi$. These operators are killed by supercharges of the same chirality, and using the superconformal algebra their conformal dimension is related to the R-charge:

$$\left[Q_\alpha^+, \phi(0)\right] = \left[Q_{\dot\alpha}^-, \bar\phi(0)\right] = 0 \quad \Rightarrow \quad \Delta_\phi = \Delta_{\bar\phi} = \frac{d-1}{2} r_\phi = -\frac{d-1}{2} r_{\bar\phi}\,. \tag{9.85}$$

The chirality property, as well as the relation between Δ and r, will be important in the calculation of superconformal blocks in the next section.

The subalgebra of conformal transformations that preserve the boundary is generated by D, P_a, K_a and M_{ab}, where $a, b = 2, \ldots, d$. We chose P_1 not to be part of this subalgebra, which physically means that the boundary sits at $x_1 \equiv x^\perp = 0$. Only half of the original supercharges belong to the algebra, and they anticommute as:

$$\{Q_A^{\text{bdy}}, Q_B^{\text{bdy}}\} = (\Sigma_{bdy})_{AB}^a P_a\,, \qquad \{S_A^{\text{bdy}}, S_B^{\text{bdy}}\} = (\Sigma_{bdy})_{AB}^a K_a\,, \qquad A, B = 1, 2. \tag{9.86}$$

For arbitrary d we embbed the boundary subalgebra into the full superconformal algebra as

$$Q_1^{\text{bdy}} = Q_1^+ + Q_2^-\,, \quad Q_2^{\text{bdy}} = Q_2^+ + Q_1^-\,, \quad S_1^{\text{bdy}} = S_2^+ + S_1^-\,, \quad S_2^{\text{bdy}} = S_1^+ + S_2^-\,. \tag{9.87}$$

It is easy to check explicitly in $d = 3$ and $d = 4$ that (9.87) indeed generate a subalgebra and that all the superjacobi identities are satisfied, provided that we use the following Clifford algebra representation:

$$\Sigma_{\alpha\dot\alpha}^i = (\bar\Sigma_i^{\dot\alpha\alpha})^* = (\sigma_3, \sigma_1, \sigma_2, i\mathbb{1})\,. \tag{9.88}$$

Notice that the generator R is not part of the boundary superalgebra. In physical terms the R charge is not conserved near the boundary, and both $\langle \phi_1 \phi_2 \rangle$ and $\langle \phi_1 \bar{\phi}_2 \rangle$ are non-vanishing two-point functions for any $r_{1,2}$. These two-point functions have different superconformal block decompositions that we treat separately in the next section.

In order to compute superconformal blocks, we will need the explicit form of the superconformal Casimir of the boundary superalgebra:

$$C_{\text{bdy}} = -D^2 - \frac{1}{2}\{P_a, K^a\} + \frac{1}{2}M_{ab}M^{ab} + \frac{1}{4}[S_A^{\text{bdy}}, Q_A^{\text{bdy}}]. \tag{9.89}$$

If we consider a boundary operator with quantum numbers $\hat{\Delta}, j$, then it will be an eigenstate of the superconformal Casimir with eigenvalue

$$\hat{C}_{\hat{\Delta},j} = \hat{\Delta}(\hat{\Delta} - d + 2) + j(j - d + 3). \tag{9.90}$$

Boundary channel

As discussed at length in the superspace section, the boundary channel blocks for a two-point function are eigenfunctions of the boundary superconformal Casimir (9.89). We can naturally split the Casimir operator into a non-supersymmetric piece and a contribution coming from supersymmetry:

$$C_{\text{bdy}} = C_{\text{bdy,non-susy}} + C_{\text{bdy,susy}}, \qquad C_{\text{bdy,susy}} \equiv \frac{1}{4}[S_A^{\text{bdy}}, Q_A^{\text{bdy}}]. \tag{9.91}$$

We worked out the non-supersymmetric contribution in equation (9.176). Focusing only on the supersymmetric part and using the anticommutation relations we obtain:

$$
\begin{aligned}
[C_{\text{bdy,susy}}, \phi_1(x)]|0\rangle &= \left(\frac{d-1}{2}[R, \phi_1(x)] - \frac{1}{2}\left\{ Q_2^-, \left[S^{1-}, \phi_1(x) \right] \right\} \right)|0\rangle \\
&= \left(\Delta_1 \phi_1(x) + ix^\perp \{ Q_1^-, [Q_2^-, \phi_1(x)] \} \right)|0\rangle.
\end{aligned}
\tag{9.92}
$$

In appendix 9.C we use superconformal Ward identities to rewrite the piece with $Q_1^- Q_2^-$ as a term that can be included in a differential equation. Unfortunately, we have not been able to find a strategy to use these Ward identities for general d. Instead, we focus on the particular cases of $d = 3, 4$ where the explicit Clifford algebra representation (9.88) is valid. Since the final result does not depend on d, we claim it is also valid for $3 \leq d \leq 4$.[9]

---

[9] It is likely that our blocks are valid for $2 \leq d \leq 4$ but we have not checked explicitly the $d = 2$ case. Notice that below $d \leq 3$ on has to take into account the operators $M_{\hat{i},\hat{j}}$ with $\hat{i}, \hat{j} = d, \dots, 4$, and the calculation is slightly more complicated.

The fact that we can find solutions to the Casimir equations with the expected properties for any continuous d confirms that our assumption is justified. The ϵ-expansion results, to be described below and in the next section, also give supporting evidence that the whole picture is consistent.

$\langle \phi_1 \bar{\phi}_2 \rangle$ **correlator:** When we consider the two-point function of a chiral and antichiral operator, the contribution from supersymmetry is given by

$$\frac{C_{\text{bdy,susy}} \langle \phi_1(x_1) \bar{\phi}_2(x_2) \rangle}{(2x_1^\perp)^{-\Delta_1} (2x_2^\perp)^{-\Delta_2}} = -\xi \partial_\xi \hat{F}_{\hat{\Delta}}^{\phi_1 \bar{\phi}_2}(\xi) \,. \tag{9.93}$$

Combining the supersymmetric and non-supersymmetric pieces, and using the appropriate value of the Casimir, we get the following differential equation:

$$\left[\xi(\xi + 1) \partial_\xi^2 + \left(\frac{d}{2} + (d-1)\xi \right) \partial_\xi - (\hat{\Delta}(\hat{\Delta} - d + 2) + j(j - d + 3)) \right] \hat{F}_{\hat{\Delta}}^{\phi_1 \bar{\phi}_2}(\xi) = 0 \,. \tag{9.94}$$

A priori, there are two independent solutions of this equation for arbitrary values $\hat{\Delta}$ and j. However, we must also require that the solutions can be decomposed into non-supersymmetric blocks, and we find that this is only possible whenever $j = 0$ for arbitrary $\hat{\Delta}$. The solution can be expressed either as a linear combination of bosonic blocks, or as a single hypergeometric function with a prefactor:

$$\begin{aligned}
\hat{F}_{\hat{\Delta}}^{\phi_1 \bar{\phi}_2}(\xi) &= \hat{f}_{\hat{\Delta}}(\xi) + \frac{\hat{\Delta}}{2(2\hat{\Delta} - d + 3)} \hat{f}_{\hat{\Delta}+1}(\xi) \,, \\
&= \xi^{-\hat{\Delta}} \, {}_2F_1 \left(\hat{\Delta}, \hat{\Delta} + 1 - \frac{d}{2}; 2\hat{\Delta} - d + 3; -\frac{1}{\xi} \right) \,.
\end{aligned} \tag{9.95}$$

Even though we considered a general two-point function $\langle \phi_1 \bar{\phi}_2 \rangle$, the superconformal blocks are the same as for a two-point function of identical (anti)chiral operators $\langle \phi \bar{\phi} \rangle$. A nice consistency check is that the relative coefficient between the non-supersymmetric blocks is positive, as we expect in the defect channel of $\langle \phi \bar{\phi} \rangle$, because the coefficients that appear in the OPE are $|b_{\phi \hat{\mathcal{O}}}|^2$. When we restrict to $d = 3$ we find perfect agreement with the explicit superspace calculation (9.74).

$\langle \phi_1 \phi_2 \rangle$ **correlator:** In a similar way, we can work out the Ward identities for the $\langle \phi_1 \phi_2 \rangle$ two-point function. The new contribution to the Casimir equation is:

$$\frac{C_{\text{bdy,susy}} \langle \phi_1(x_1) \phi_2(x_2) \rangle}{(2x_1^\perp)^{-\Delta_1} (2x_2^\perp)^{-\Delta_2}} = -(\xi + 1) \partial_\xi \hat{F}_{\hat{\Delta}}^{\phi_1 \phi_2}(\xi) \,. \tag{9.96}$$

Combining the non-supersymmetric and supersymmetric pieces with the eigenvalue (9.90), the Casimir equation reads

$$\left[\xi(\xi+1)\partial_\xi^2 + \left(\frac{d-2}{2} + (d-1)\xi\right)\partial_\xi - (\hat{\Delta}(\hat{\Delta} - d + 2) + j(j - d + 3))\right]\hat{F}_{\hat{\Delta}}^{\phi_1\phi_2}(\xi) = 0\,.$$
(9.97)

Once again, we only find physically acceptable solutions whenever $j = 0$:

$$\hat{F}_{\hat{\Delta}}^{\phi_1\phi_2}(\xi) = \hat{f}_{\hat{\Delta}}(\xi) - \frac{\hat{\Delta}}{2(2\hat{\Delta} - d + 3)}\hat{f}_{\hat{\Delta}+1}(\xi)\,,$$
$$= \xi^{-\Delta}\,{}_2F_1\left(\hat{\Delta}, \hat{\Delta} + 2 - \frac{d}{2}; 2\hat{\Delta} - d + 3; -\frac{1}{\xi}\right)\,.$$
(9.98)

The decompositions into non-supersymmetric blocks in (9.98) and (9.95) are identical up to a relative minus sign. We know this must be the case, since the boundary OPE of $\langle\phi\phi\rangle$ contains $b_{\phi\hat{\mathcal{O}}}^2$, which is not necesarily positive definite, but instead $b_{\phi\hat{\mathcal{O}}}^2 = \pm|b_{\phi\hat{\mathcal{O}}}|^2$. When we restrict to $d = 3$ we find perfect agreement with the explicit superspace calculation (9.75).

Bulk channel

Now we proceed to calculate the blocks that appear in the bulk decomposition using the bulk Casimir.

$\langle\phi_1\bar{\phi}_2\rangle$ **correlator:** To obtain bulk channel blocks we act with the full Casimir once more focusing on the part that is new from supersymmetry:

$$C_{\text{bulk,susy}} = -\frac{d-1}{2}R^2 + \frac{1}{2}[S^{\dot{\alpha}+}, Q_{\dot{\alpha}}^-] + \frac{1}{2}[S^{\alpha-}, Q_\alpha^+]\,.$$
(9.99)

We can simplify the action of the superconformal Casimir using the commutation relations, the chirality properties of ϕ_1 and $\bar{\phi}_2$, and equation (51) from [193]:

$$\left[C_{\text{bulk,susy}}, \phi_1(x_1)\bar{\phi}_2(x_2)\right]|0\rangle = ix_{12}^\mu \bar{\Sigma}_\mu^{\dot{\alpha}\alpha}\left[Q_{\dot{\alpha}}^-, \phi_1(x_1)\right]\left[Q_\alpha^+, \bar{\phi}_2(x_2)\right]|0\rangle$$
$$+ \left(2(\Delta_1 + \Delta_2) - \frac{d-1}{4}r_{12}^2\right)\phi_1(x_1)\bar{\phi}_2(x_2)|0\rangle\,.$$
(9.100)

Here we assume ϕ_i has charge r_i, we define $r_{12} = r_1 - r_2$ and we use chirality to relate $\Delta_i = \frac{1}{2}(d-1)r_i$. We can use Ward identities to rewrite the Q-dependent part in a way

209

that can be put in a Casimir equation. After some algebra we get[10]

$$\frac{C_{\text{bulk,susy}}\langle \phi_1(x_1)\bar{\phi}_2(x_2)\rangle}{(2x_1^\perp)^{-\Delta_1}(2x_2^\perp)^{-\Delta_2}\xi^{-(\Delta_1+\Delta_2)/2}} = \left(4\xi\partial_\xi - \frac{d-1}{4}r_{12}^2\right)G_\Delta^{\phi_1\bar{\phi}_2}(\xi). \tag{9.101}$$

Now we can combine all the pieces to form the differential equation

$$\left[4\xi^2(\xi+1)\partial_\xi^2 + 2\xi(2\xi - d + 4)\partial_\xi - \Delta(\Delta - d + 2)\right.$$

$$\left. - \ell(\ell + d - 2) - \frac{d-1}{4}(r_{12}^2 - r^2) - \Delta_{12}^2\xi\right]G_\Delta^{\phi_1\bar{\phi}_2}(\xi) = 0. \tag{9.102}$$

The superselection rules in the $\phi_1 \times \bar{\phi}_2$ OPE were worked out in four dimensions [65] and in any d [193]. For our setup, they imply that only superprimaries with $r = r_{12}$ and $\ell = 0$ can appear[11]. Indeed, we can solve the Casimir equation in this case to find:

$$G_\Delta^{\phi_1\bar{\phi}_2}(\xi) = g_\Delta^{\Delta_{12}}(\xi) + \frac{(\Delta - \Delta_{12})(\Delta + \Delta_{12})}{(2\Delta - d + 2)(2\Delta - d + 4)}g_{\Delta+2}^{\Delta_{12}}(\xi)$$

$$= \xi^{\Delta/2} \, {}_2F_1\left(\frac{\Delta + \Delta_{12}}{2}, \frac{\Delta - \Delta_{12}}{2}; \Delta + 2 - \frac{d}{2}; -\xi\right). \tag{9.103}$$

For generic values of Δ these blocks capture the exchange of a long operator, while they can be interpreted as short operators when Δ saturates the unitarity bounds. The classification of possible short multiplets in $d = 3, 4$ is well known and can be found for example in [27, 182].

$\langle\phi_1\phi_2\rangle$ **correlator:** It is well know that when the two operators are chiral the bulk blocks are equal to non-supersymmetric blocks. The precise selection rules for $\phi_1 \times \phi_2$ are known [193], but we review them here for convenience:

- Consider a superprimary $\mathcal{O}$ that has R-charge $r = r_1 + r_2 - 2$ and dimension Δ. The descendant $(Q^+)^2\mathcal{O}$ has charge $r_1 + r_2$, dimension $\Delta + 1$ and is killed by Q_α^+, so it appears in the $\phi_1 \times \phi_2$ OPE.

- Alternatively, consider the chiral superprimary operator $(\phi_1\phi_2)$, with $r = r_1 + r_2$ and $\Delta = \Delta_1 + \Delta_2$. In this case the superprimary itself is exchanged in the OPE.

---

[10]We find it more convenient to work in terms of $G(\xi) = \xi^{(\Delta_1+\Delta_2)/2}F(\xi)$, but one can easily map the results between the two conventions.

[11]Superprimaries with $\ell \geq 1$ also appear in the OPE but they have zero one-point function, so they are not relevant in our analysis.

- Finally, consider an anti-chiral superprimary operator $\bar{\Psi}$ whose dimension is related to its charge and given by $\Delta = -\frac{d-1}{2}r = d - 1 - (\Delta_1 + \Delta_2)$. The descendant operator $(Q^+)^2 \bar{\Psi}$ is exchanged in the OPE.

In what follows, whenever we consider bulk channel $\phi\phi$ superconformal blocks, Δ will be the dimension of the actual exchanged operator, and not the dimension of the superprimary.

9.4.2 An aside: codimension-two defects

In the present paper we are mostly concerned with boundaries that interpolate between $3 \leq d \leq 4$ models. In the same way there exist codimension-two defects that interpolate between a line in $d = 3$ and a surface in $d = 4$. A familiar example is the $3d$ Ising twist defect, which was studied using Feynman diagrams in $4 - \epsilon$ dimensions [256] (see also [255] for a Monte-Carlo analysis in exactly $d = 3$). These results were later reproduced and generalized using analytic bootstrap technology [265]. Similar techniques should be applicable to half-BPS codimension-two defects in supersymmetric theories like the Wess-Zumino model. We plan to come back to this problem in the future, but for now we describe how the superconformal blocks can be obtained within our framework.

The notation in this subsection will be different from the rest of the section; we hope this does not cause confusion. We insert the codimension-two defect at $x_i = 0$ for $i = 1, 2$ and label the parallel directions as x_a for $a = 3, \ldots, d$. The defect will naturally preserve parallel translations and special conformal transformations P_a, K_a, dilatations D, as well as parallel and perpendicular rotations M_{ab}, M_{ij}. The two-point function of local operators depends on two cross-ratios. To study the defect channel it is convenient to use coordinates (χ, ϕ), while the bulk channel simplifies using coordinates $(x, \bar{x})$:[12]

$$
\begin{aligned}
\frac{|x_{12}^a|^2 + |x_1^i|^2 + |x_2^i|^2}{|x_1^i||x_2^i|} &= \chi = \frac{2 - x - \bar{x}}{\sqrt{(1-x)(1-\bar{x})}} \,, \\
\frac{x_1^i x_2^i}{|x_1^i||x_2^i|} &= \cos\phi = \frac{2 - x - \bar{x} + x\bar{x}}{2\sqrt{(1-x)(1-\bar{x})}} \,.
\end{aligned}
\tag{9.104}
$$

The non-supersymmetric as well as the supercoformal blocks are given below.

Besides the bosonic generators described above, a half-BPS defect preserves two Poincaré supercharges:

$$
Q_1^{\text{defect}} = Q_1^+ \,, \qquad Q_2^{\text{defect}} = Q_1^- \,, \qquad S_1^{\text{defect}} = S^{1+} \,, \qquad S_2^{\text{defect}} = S^{1-} \,.
\tag{9.105}
$$

---

[12]Our cross-ratios are related to the ones in [266] by $z = 1 - x$ and $\bar{z} = (1 - \bar{x})^{-1}$.

Our system does not preserve R-symmetry or transverse rotations independently, but only a linear combination of them that we call twisted transverse rotations:[13]

$$M^{\text{defect}} = M_{12} + \frac{d-1}{2}R \,. \tag{9.106}$$

With these conventions in mind, we proceed to obtain the superconformal blocks.

Defect channel

When supersymmetry is not present, the defect operators are labeled by the conformal dimension $\hat{\Delta}$ and the transverse spin s. One can write down a Casimir equation which is solved by the following conformal blocks [259]:

$$\hat{f}_{\hat{\Delta},s}(\chi, \phi) = e^{is\phi}\chi^{-\hat{\Delta}} \, {}_2F_1\Big(\frac{\hat{\Delta}}{2}, \frac{\hat{\Delta}+1}{2}; \hat{\Delta}+2-\frac{d}{2}; \frac{4}{\chi^2}\Big) \,. \tag{9.107}$$

In the supersymmetric case the only difference is that s denotes the twisted transverse spin (9.106). One can work out the selection rules, and find that only one operator in each multiplet contributes to the OPE, so the superconformal blocks are just (9.107) with the arguments shifted appropriately.

Bulk channel

Similarly, one can obtain a Casimir equation for the non-supersymmetric bulk channel. It was observed in [259] that for codimension-two the Casimir equation is identical to the one found by Dolan and Osborn (D&O) for bulk four-point functions [31]. Therefore, the bulk-channel blocks of a defect two-point function are equal to the familiar four-point blocks:

$$f_{\Delta,\ell}(x, \bar{x}) = G^{0,0}_{\Delta,\ell,\text{D\&O}}(x, \bar{x}) \,. \tag{9.108}$$

When supersymmetry is included, the Casimir equation has an extra term $C_{\text{bulk,susy}}$ that can be simplified using Ward identites, as described in appendix 9.C. When the dust settles, it turns out that the blocks are described by non-supersymmetric blocks with shifted arguments:

$$F_{\Delta,\ell}(x, \bar{x}) = (x\bar{x})^{-\frac{1}{2}} G^{-1,-1}_{\Delta+1,\ell,\text{D\&O}}(x, \bar{x}) \,. \tag{9.109}$$

Even more surprisingly, these blocks are exactly the same that were found in [193] for a four-point function of chiral and antichiral operators!

---

[13]For the particular case of a line defect in $d = 3$, the subalgebra has been written explicitly in [181].

9.4.3   Free theory

After the small codimension-two detour let us come back to the boundary setup. As a first consistency check of our superconformal blocks, we consider a free chiral multiplet in the bulk in the presence of a half-BPS boundary. It is well known that a free scalar has dimension $\Delta_\phi = \frac{d-2}{2}$, and the bulk equations of motion have a simple solution:

$$\partial_x^2 \langle \phi(x) \bar{\phi}(x') \rangle = 0 \quad \Rightarrow \quad \mathcal{F}^{\phi\bar{\phi}}(\xi) = \frac{c_1^{\phi\bar{\phi}}}{\xi^{(d-2)/2}} + \frac{c_2^{\phi\bar{\phi}}}{(\xi+1)^{(d-2)/2}}\,. \tag{9.110}$$

For the two-point function $\langle \phi\phi \rangle$ we find the same solution with free coefficients $c_{1,2}^{\phi\phi}$. In order to impose supersymmetry, we must require that these correlators have consistent superconformal block decompositions in the bulk and boundary channels. It is a simple exercise to show that this fixes $c_1^{\phi\phi} = c_2^{\phi\bar{\phi}} = 0$. We can also fix $c_1^{\phi\bar{\phi}} = 1$ requiring that far away from the boundary, the two-point function $\langle \phi\bar{\phi} \rangle$ is unit normalized: it is normalized such that the OPE coefficient of the bulk identity block is 1. Finally, after an appropriate redefinition $\phi \to e^{i\delta}\phi$ we can always chose the normalization $c_2^{\phi\phi} = 1$. All in all,

$$\begin{aligned}
\mathcal{F}^{\phi\bar{\phi}}(\xi) &= \frac{1}{\xi^{(d-2)/2}} = F_{\mathrm{Id}}^{\phi\bar{\phi}}(\xi) = \hat{F}_{(d-2)/2}^{\phi\bar{\phi}}(\xi)\,, \\
\mathcal{F}^{\phi\phi}(\xi) &= \frac{1}{(\xi+1)^{(d-2)/2}} = F_{d-2}^{\phi\phi}(\xi) = \hat{F}_{(d-2)/2}^{\phi\phi}(\xi)\,.
\end{aligned} \tag{9.111}$$

In the above equation we also present the expansion of the correlation functions in terms of superconformal blocks. Interestingly, only one superconformal block contributes to each channel, and with our normalization conventions all OPE coefficients are equal to one.

The above solution to crossing has a clear physical interpretation if we split the chiral primary operator in terms of its real and imaginary parts $\phi = \phi_1 + i\phi_2$. Then we see that ϕ_1 satisfies Neumann boundary conditions, whereas ϕ_2 satisfies Dirichlet boundary conditions. Indeed, from (9.111) we obtain

$$\lim_{x\to\mathrm{bdy}} \langle \partial_\perp \phi_1(x)\phi_1(x') \rangle = 0\,, \qquad \lim_{x\to\mathrm{bdy}} \langle \phi_2(x)\phi_2(x') \rangle = 0\,. \tag{9.112}$$

We can think of our free correlation functions as linear combinations of the Neumann and Dirichlet boundary CFTs studied in [269], with the precise relative coefficients fixed by supersymmetry.

9.4.4 The ϵ-expansion bootstrap

It was originally observed in [269] that the crossing equation for boundary CFTs can be used to extract information about the Wilson-Fischer fixed point in the epsilon expansion. In particular, they bootstrapped the one-loop correlators at order $\mathcal{O}(\epsilon)$, and the analysis was generalized to $\mathcal{O}(\epsilon^2)$ using different techniques in later works [272, 274, 381]. In this section we apply the same ideas to our supersymmetric two-point functions, and we obtain the full correlation functions at order $\mathcal{O}(\epsilon)$.

In the supersymmetric setup there are two relevant crossing equations, one for $\phi\bar{\phi}$ and the other for $\phi\phi$:

$$F_{\text{Id}}^{\phi\bar{\phi}}(\xi) + \sum_n c_n F_{\tilde{\Delta}_n}^{\phi\bar{\phi}}(\xi) = \sum_n \mu_n \hat{F}_{\hat{\Delta}_n}^{\phi\bar{\phi}}(\xi), \quad \sum_n d_n F_{\Delta_n}^{\phi\phi}(\xi) = \sum_n \rho_n \hat{F}_{\hat{\Delta}_n}^{\phi\phi}(\xi). \qquad (9.113)$$

Notice that the spectrum of operators in the boundary channel is the same for the two correlators. The boundary OPE coefficients are given in terms of bulk-to-boundary coefficients as $\mu_n = |b_{\phi\mathcal{O}_n}|^2$ and $\rho_n = b_{\phi\mathcal{O}_n}^2$, so they must be equal up to possible signs $\mu_n = \pm\rho_n$. The precise signs as a function of n will be an outcome of our bootstrap analysis. The bulk channel OPE coefficients are products of one- and three-point coefficients $c_n = a_{\mathcal{O}_n}\lambda_{\phi\bar{\phi}\mathcal{O}_n}$ and $d_n = a_{\mathcal{O}_n}\lambda_{\phi\phi\mathcal{O}_n}$ so we do not expect any relations between them.

Our analysis starts in $d = 4$, where the SCFT is free and the correlators are given in (9.111). We assume that the coupling of the theory is of order $g \sim \epsilon$, so as we lower the dimension to $d = 4 - \epsilon$ the CFT data acquires small corrections. In particular, we expect the external chiral operator to acquire an anomalous dimension:

$$\Delta_\phi = \frac{d-2}{2} + \Delta_\phi^{(1)}\epsilon + \Delta_\phi^{(2)}\epsilon^2 + \dots . \qquad (9.114)$$

We should think of $\Delta_\phi^{(1)}$ as being related to the strenght of the coupling $g \propto \Delta_\phi^{(1)}\epsilon$, and the precise constant depends on the model under consideration. In the bulk four-point function ϵ-expansion bootstrap, see for example [135], conservation of the stress tensor allows one to fix the precise value of $\Delta_\phi^{(1)}$. Unfortunately this will not be possible in our setup because the stress-tensor multiplet does not appear in the bulk OPE.

Another consequence of turning on the couplings is that we expect that new infinite families of operators will enter our crossing equations. In the bulk channel, from the intuition gained from the usual four-point function analytic bootstrap, we expect double-trace operators of the form $\phi\Box^n\phi$ with dimensions

$$\Delta_n = d - 2 + 2n + \Delta_n^{(1)}\epsilon + \Delta_n^{(2)}\epsilon^2 + \dots , \qquad (9.115)$$

and similarly operators $\phi \Box^n \bar\phi$ with dimensions $\tilde\Delta_n$. In the boundary channel, we expect operators of the schematic form $\Box^m \partial_\perp^{n-2m} \phi$ so they have dimension

$$\hat\Delta_n = \frac{d-2}{2} + n + \hat\Delta_n^{(1)} \epsilon + \hat\Delta_n^{(2)} \epsilon^2 + \dots . \tag{9.116}$$

Finally, the OPE coefficients will also get corrections as a power series in ϵ, namely

$$c_n = c_n^{(0)} + c_n^{(1)} \epsilon + c_n^{(2)} \epsilon^2 + \dots , \tag{9.117}$$

and similarly for d_n, μ_n and ρ_n. With the above conventions, the free theory solution when $d = 4$ is given by

$$d_0^{(0)} = \mu_0^{(0)} = \rho_0^{(0)} = 1, \qquad c_{n\geq 0}^{(0)} = d_{n\geq 1}^{(0)} = \mu_{n\geq 1}^{(0)} = \rho_{n\geq 1}^{(0)} = 0 . \tag{9.118}$$

In what follows we derive the first order correction to the CFT data.

$\langle \phi\phi \rangle$ correlator

We start by studying the two-point function $\langle \phi\phi \rangle$, because in this case we can reuse many results from [272]. We will very closely follow the notation and manipulations from this reference, and we refer the reader there for further details. The similarity is a consequence of the $\phi\phi$ bulk channel superconformal blocks being equal to non-supersymmetric ones: $F_\Delta^{\phi\phi} = f_\Delta$.

The first step in the construction of [272] is to divide the crossing equation in two terms called G and H:

$$\mathcal{F}^{\phi\phi}(\xi) = G_{\text{blk}}(\xi) + H_{\text{blk}}(\xi) = G_{\text{bdy}}(\xi) + H_{\text{bdy}}(\xi) . \tag{9.119}$$

In G we collect the contributions that appeared at order ϵ^0, but we allow them to acquire anomalous dimensions:

$$
\begin{aligned}
G_{\text{blk}}(\xi) &= F_{2-\epsilon+\Delta_0^{(1)}\epsilon}^{\phi\phi}(\xi) = \frac{1}{\xi+1} + \frac{(\Delta_0^{(1)} - 2\Delta_\phi^{(1)})\log\xi + \log(\xi+1)}{2(\xi+1)}\epsilon + \mathcal{O}(\epsilon^2) , \\
G_{\text{bdy}}(\xi) &= \hat{F}_{1-\frac{\epsilon}{2}+\epsilon\hat\Delta_0^{(1)}}^{\phi\phi}(\xi) = \frac{1}{\xi+1} + \frac{\log(\xi+1) - 2\hat\Delta_0^{(1)}\log\xi}{2(\xi+1)}\epsilon + \mathcal{O}(\epsilon^2) .
\end{aligned}
\tag{9.120}
$$

On the other hand, we collect in H all the contributions where the anomalous dimensions do not contribute, so the blocks are evaluated at integer values of the dimensions:

$$H_{\text{blk}}(\xi) = \epsilon \sum_{n=0}^\infty d_n^{(1)} F_{2n+2}^{\phi\phi}(\xi) , \qquad H_{\text{bdy}}(\xi) = \epsilon \sum_{n=0}^\infty \rho_n^{(1)} \hat{F}_{n+1}^{\phi\phi}(\xi) . \tag{9.121}$$

215

Note that an operator can contribute to both G and H, for instance the anomalous dimension $\Delta_0^{(1)}$ of the leading bulk operator $\mathcal{O}_0$ appears in G_{blk}, while the correction to its OPE coefficient $d_0^{(1)}$ appears in H_{blk}.

The key observation of [272] was that one can eliminate H_{bdy} from the crossing equation by applying the following discontinuity:

$$\text{Disc } f(z) = f(ze^{i\pi}) - f(ze^{-i\pi}), \qquad z \equiv \xi + \frac{1}{2} \in (\tfrac{1}{2}, \infty). \tag{9.122}$$

Indeed, from (9.122) one sees that $\text{Disc } \hat{f}_n(\xi) = 0$ for integer n, which implies $\text{Disc } H_{\text{bdy}}(\xi) = 0$. It is an easy exercise to take the discontinuity of (9.120), and using the crossing equation we find

$$\text{Disc } H_{\text{blk}}(\xi) = \text{Disc } G_{\text{bdy}}(\xi) - \text{Disc } G_{\text{blk}}(\xi) = \frac{i\pi\epsilon}{\xi} \left(2\hat{\Delta}_0^{(1)} - 2\Delta_\phi^{(1)} + \Delta_0^{(1)} \right). \tag{9.123}$$

The authors of [272] reconstructed the full correlator by expanding (9.123) in terms of discontinuities of bulk blocks, extracting the CFT data, and then resumming the bulk OPE expansion. Note that since our expansion in the bulk has non-supersymmetric blocks, we can reuse their results without problems. In particular, comparing their equations (4.8) and (4.14) with our expression we obtain

$$H_{\text{blk}}(\xi) = -\frac{\epsilon \log(\xi + 1)}{2(\xi + 1)} \left(2\hat{\Delta}_0^{(1)} - 2\Delta_\phi^{(1)} + \Delta_0^{(1)} \right). \tag{9.124}$$

From this calculation we can reconstruct the full correlator $\mathcal{F}^{\phi\phi}(\xi) = G_{\text{blk}}(\xi) + H_{\text{blk}}(\xi)$ and extract CFT data to $\mathcal{O}(\epsilon)$. Before we do that, however, let us also reconstruct the $\langle \phi\bar{\phi} \rangle$ correlator using the same technique.

$\langle \phi\bar{\phi} \rangle$ correlator

As before, let us divide the contributions of the crossing equations into two pieces, where

$$
\begin{aligned}
G_{\text{blk}}(\xi) &= F_{\text{Id}}^{\phi\bar{\phi}}(\xi) = \frac{1}{\xi} + \frac{(1 - 2\Delta_\phi^{(1)}) \log \xi}{2\xi} \epsilon + \mathcal{O}(\epsilon^2), \\
G_{\text{bdy}}(\xi) &= \hat{F}_{1-\frac{\epsilon}{2}+\epsilon\hat{\Delta}_0^{(1)}}^{\phi\bar{\phi}}(\xi) = \frac{1}{\xi} + \frac{\log \xi - 2\hat{\Delta}_0^{(1)} \log(\xi + 1)}{2\xi} \epsilon + \mathcal{O}(\epsilon^2),
\end{aligned}
\tag{9.125}
$$

and the functions H are the same we defined in (9.121), replacing $(d_n, \rho_n) \to (c_n, \mu_n)$ and using the appropriate superconformal blocks for $\phi\bar{\phi}$. Again, the discontinuity removes

$H_{\text{bdy}}(\xi)$ and we are left with

$$\text{Disc}\, H_{\text{blk}}(\xi) = \text{Disc}\, G_{\text{bdy}}(\xi) - \text{Disc}\, G_{\text{blk}}(\xi) = -\frac{2\pi i \epsilon}{\xi + 1} \left(\Delta_\phi^{(1)} - \hat{\Delta}_0^{(1)} \right) . \tag{9.126}$$

This can be expanded in terms of discontinuities of superconformal blocks. In principle, we should repeat the analysis of [272] using our superconformal blocks. However, the first term in the expansion captures the entire correlator:

$$\text{Disc}\, F_2^{\phi\bar\phi}(\xi) = -\frac{2\pi i}{\xi + 1} = \frac{\text{Disc}\, H_{\text{blk}}(\xi)}{\epsilon \left(\Delta_\phi^{(1)} - \hat{\Delta}_0^{(1)} \right)} . \tag{9.127}$$

We can remove the discontinuity from this equation[14] to obtain

$$H_{\text{blk}}(\xi) = \epsilon \left(\Delta_\phi^{(1)} - \hat{\Delta}_0^{(1)} \right) F_2^{\phi\bar\phi} = \epsilon \left(\Delta_\phi^{(1)} - \hat{\Delta}_0^{(1)} \right) \frac{\log(\xi + 1)}{\xi} . \tag{9.128}$$

The full correlator is $\mathcal{F}^{\phi\bar\phi}(\xi) = G_{\text{blk}}(\xi) + H_{\text{blk}}(\xi)$. Equation (9.127) implies that the bulk channel of $\phi\bar\phi$ contains only the identity and another block, unlike the $\phi\phi$ expansion which contained infinitely many blocks.

Correlation functions and CFT data

The solution of crossing we have found to $\mathcal{O}(\epsilon)$ has three free parameters. However, as discussed below equation (9.113), the boundary OPE coefficients in the two channels should be equal up to a sign $\rho_n = \pm \mu_n$. Expanding $\mathcal{F}^{\phi\phi}(\xi)$ and $\mathcal{F}^{\phi\bar\phi}(\xi)$ in boundary superblocks and comparing the expansions we find one last constraint:

$$\Delta_0^{(1)} = 2 \left((s+1)\Delta_\phi^{(1)} - \hat{\Delta}_0^{(1)} \right) , \qquad s = \pm . \tag{9.129}$$

Hence, our solution depends on the anomalous dimension $\Delta_\phi^{(1)}$ of the external chiral operator, the anomalous dimension of the leading boundary operator $\hat{\Delta}_0^{(1)}$, and a choice of signs

---

[14] The discontinuities of superblocks are schematically $\text{Disc}\, F_{2n}^{\phi\bar\phi} \sim P_n$, where P_n are certain orthogonal polynomials. Since any function has a unique expansion in terms of P_n, it is safe to remove Disc from (9.127).

$s = \pm$. Using this relation, the one-loop correlation functions take a very simple form[15]

$$
\begin{aligned}
\mathcal{F}^{\phi\bar{\phi}}(\xi) &= \frac{1}{\xi} + \frac{\left(1 - 2\Delta_\phi^{(1)}\right)\log\xi + 2\left(\Delta_\phi^{(1)} - \hat{\Delta}_0^{(1)}\right)\log(\xi + 1)}{2\xi}\epsilon + \mathcal{O}(\epsilon^2), \\
\mathcal{F}^{\phi\phi}(\xi) &= \frac{1}{\xi + 1} + \frac{\left(1 - 2s\Delta_\phi^{(1)}\right)\log(\xi + 1) + 2\left(s\Delta_\phi^{(1)} - \hat{\Delta}_0^{(1)}\right)\log\xi}{2(\xi + 1)}\epsilon + \mathcal{O}(\epsilon^2).
\end{aligned}
\tag{9.130}
$$

From the correlation functions we can extract the CFT data at one-loop:[16]

$$
\begin{aligned}
c_0^{(1)} &= \Delta_\phi^{(1)} - \hat{\Delta}_0^{(1)}, \qquad c_{n\geq1}^{(1)} = 0, \qquad d_0^{(1)} = 0, \qquad \mu_0^{(1)} = \rho_0^{(1)} = 0, \\
\mu_n^{(1)} &= s(-1)^n\rho_n^{(1)} = s(-1)^n d_n^{(1)} = \frac{(n - 1)!}{2^{n-1}(2n - 1)!!}\Delta_\phi^{(1)}, \qquad n \geq 1.
\end{aligned}
\tag{9.131}
$$

Although we lack a conclusive proof, we believe it is very likely that the unfixed sign is always $s = +1$. One argument is that the correlators (9.130) are related to each other under $\xi \leftrightarrow \xi + 1$, provided $s = +1$. Another argument is that only for $s = +1$ the signs of the coefficients in the BOE are alternating, namely $(\rho_0, \rho_1, \rho_2, \ldots) = (\mu_0, -\mu_1, \mu_2, \ldots)$, and otherwise they are alternating only for $n \geq 1$. Finally, we will do an explicit perturbative calculation for a specific model in the next section and we will find again that $s = +1$.

An interesting feature of the CFT data (9.131) is that the bulk and boundary OPE coefficients are identical for the two-point function $\langle\phi\phi\rangle$. This is a very non-trivial relation, since $\rho_n = b_{\phi\mathcal{O}_n}^2$, but $d_n = a_{\mathcal{O}_n}\lambda_{\phi\phi\mathcal{O}_n}$. It would be interesting to see if this is just a coincidence of the order $\mathcal{O}(\epsilon)$ result, or if it actually persists at higher orders in perturbation theory.

Going to order ϵ^2

From the structure of the order ϵ CFT data (9.131), there is hope that one can push the bootstrap analysis to order ϵ^2. Indeed, only two blocks contribute at order ϵ in the $\phi\bar{\phi}$ bulk channel. We expect infinitely many operators at order ϵ^2, but the majority of

---

[15]We can also write $\langle\phi(x)\bar{\phi}(y)\rangle = (x - y)^{-2\Delta_\phi}(\xi + 1)^{\epsilon(\Delta_\phi^{(1)} - \hat{\Delta}_0^{(1)})}$ and similarly for $\langle\phi\phi\rangle$. This is very similar to the non-supersymmetric case, see equation (2.32) of [276]. We thank A. Söderberg for pointing this out.

[16] Our solution of crossing splits naturally into a pice involving only boundary blocks with $n = 0$ and a piece that includes all $n \geq 1$. This resembles the four-point analytic bootstrap where our n plays the role of the bulk spin ℓ. In particular, our $n = 0$ solution corresponds to the solutions with finite support in spin found in [145]. We thank F. Alday for pointing this out.

them will contribute as conformal blocks of even dimension $F_{2n+2}(\xi)$. One can construct a discontinuity, different than (9.122), that kills bulk blocks $\widetilde{\text{Disc}}\, F_{2n+2} = 0$, see [273]. From here there are several possible directions one can pursue:

- Following the ideas of the present section and [272], one can calculate $\widetilde{\text{Disc}}\, H_{\text{bdy}} = \widetilde{\text{Disc}}\, G_{\text{blk}} - \widetilde{\text{Disc}}\, G_{\text{bdy}}$. One should now expand $\widetilde{\text{Disc}}\, H_{\text{bdy}}$ in terms of discontinuities of boundary blocks to extract the relevant CFT data. However, at this order in ϵ, the discontinuities of the blocks cannot be easily rewritten in terms orthogonal polynomials, and it is not clear how to proceed.

- The authors of [273] studied an inversion formula that would reconstruct the boundary data from the two discontinuities $\text{Disc}\,\mathcal{F}$ and $\widetilde{\text{Disc}}\,\mathcal{F}$ of a correlator. Unfortunately, they were unable to determine its precise form for the case of interest here, and even if the relevant inversion formula is found, calculating $\text{Disc}\,\mathcal{F}^{\phi\bar{\phi}}$ in our setup would be challenging.

- Finally, one can make an ansatz for the full correlator based on trascendentality and demand consistency with the above discontinuities to fix coefficients. With this approach it is possible to rederive the order ϵ^2 correlator of the Wilson-Fischer fixed point calculated in [272]. In our supersymmetric setup, we have found a consistent solution to crossing at order ϵ^2 that depends on a number of free parameters. However, it is not clear to us yet whether this correlator is physical or whether it is part of a more general solution of crossing yet to be found.

9.5 Wess-Zumino model with a boundary

In this section we study the Wess-Zumino (WZ) model with a cubic superpotential in the presence of half-BPS boundary conditions. The WZ model has a stable fixed point in $4 - \epsilon$ dimensions, which has been studied in the context of emergent supersymmetry [382, 383]. The two-loop calculation of [384] showed that supersymmetry is preserved perturbatively, provided the gamma matrix algebra is evaluated in $d = 4$, but using a $4 - \epsilon$ dimensional spacetime otherwise. Here we adopt the same regularization procedure, which is reminiscent of the way we obtained the blocks in section 9.4, using a superconformal algebra with $4d$ spinor representations, but allowing arbitrary $d \leq 4$ spacetime dimensions. Furthermore, we assume that the boundary is exactly codimension-one for any d.

9.5.1 Action and boundary conditions

Our model consists of a single chiral multiplet interacting with a cubic superpotential, so the degrees of freedom are the real and imaginary parts of $\phi = \phi_1 + i\phi_2$, a four-component Majorana fermion Ψ, and the real and imaginary parts of the auxiliary fields $F = F_1 + iF_2$. The action is obtained by integrating the Lagrangian density over a half-space, with parallel coordinates $\mathbf{x} \in \mathbb{R}^{d-1}$ and perpendicular coordinate $y \in \mathbb{R}^+$:[17]

$$
S_{blk} = \int d^{d-1}\mathbf{x} \, dy \left(\frac{1}{2}(\partial_\mu \phi_1)^2 + \frac{1}{2}(\partial_\mu \phi_2)^2 + \frac{1}{2}\bar{\Psi}\gamma^\mu \partial_\mu \Psi - \frac{1}{2}F_1^2 - \frac{1}{2}F_2^2 \right.
$$
$$
\left. - \frac{\lambda}{2\sqrt{2}}\Big(F_1(\phi_1^2 - \phi_2^2) + 2F_2\phi_1\phi_2 - \bar{\Psi}(\phi_1 + i\gamma_5\phi_2)\Psi \Big) \right). \tag{9.132}
$$

In order to compute Feynman diagrams, it will be simpler to integrate out the auxiliary fields F_i, producing the following interaction vertices:

$$
S_{int} = \int d^{d-1}\mathbf{x} \, dy \left(\frac{1}{16}\lambda^2 \left(\phi_1^2 + \phi_2^2 \right)^2 + \frac{\lambda}{2\sqrt{2}}\bar{\Psi}(\phi_1 + i\gamma_5\phi_2)\Psi \right). \tag{9.133}
$$

However, it is easier to work with the off-shell action to study how the boundary breaks supersymmetry. The supersymmetry transformations are parametrized by a Majorana spinor ϵ and they are well known:

$$
\begin{aligned}
\delta\phi_1 &= -\bar{\epsilon}\Psi, & \delta\Psi &= \left(-\slashed{\partial}\phi_1 - i\gamma_5\slashed{\partial}\phi_2 - F_1 + i\gamma_5 F_2 \right)\epsilon, & \delta F_1 &= -\bar{\epsilon}\slashed{\partial}\Psi, \\
\delta\phi_2 &= i\bar{\epsilon}\gamma_5\Psi, & \delta\bar{\Psi} &= \bar{\epsilon}\left(\slashed{\partial}\phi_1 - i\gamma_5\slashed{\partial}\phi_2 - F_1 + i\gamma_5 F_2 \right), & \delta F_2 &= i\bar{\epsilon}\gamma_5\slashed{\partial}\Psi.
\end{aligned} \tag{9.134}
$$

If we integrated the Lagrangian (9.132) over $\mathbb{R}^d$, the supersymmetry transformations (9.134) would be an exact symmetry of the action. However, the situation is more complicated in the presence of the boundary. On the one hand, we know that not all supersymmetries can be preserved, because that would imply that translations orthogonal to the boundary are also preserved. We can preserve at most half of the supersymmetry, namely the transformations generated by spinors satisfying [278]

$$
\Pi_+\epsilon = \epsilon \quad \Leftrightarrow \quad \Pi_-\epsilon = 0, \qquad \Pi_\pm \equiv \frac{1}{2}\left(1 \pm i\gamma_5\gamma^n \right). \tag{9.135}
$$

On the other hand, to check invariance under supersymmetry of (9.132), we have to integrate by parts, which generates extra boundary terms. Supersymmetry will only be

---

[17] We work in Euclidean signature with $\{\gamma^\mu, \gamma^\nu\} = 2\delta^{\mu\nu}$ and $\gamma_5 = \gamma^1\gamma^2\gamma^3\gamma^4$. The Majorana reality condition is $\Psi^T \mathcal{C} = \bar{\Psi}$, where the charge conjugation matrix satisfies $\gamma^\mu = -\mathcal{C}^{-1}(\gamma^\mu)^T\mathcal{C}$.

preserved for an action containing extra boundary degrees of freedom $S = S_{blk} + S_{bdy}$, provided we choose S_{bdy} to cancel the terms generated by the supersymmetry variation of S_{blk}. A systematic study of all possible boundary actions for a generic $4d$ $\mathcal{N} = 1$ theory appeared in [376], and we can easily translate their results to our conventions. For the purposes of this section, we will pick the minimal boundary action that preserves supersymmetry, although more general options would be possible:

$$S_{bdy} = \int d^{d-1}\mathbf{x} \left(\frac{1}{2} \Big(\phi_1 \partial_n \phi_1 + \phi_2 \partial_n \phi_2 + \phi_1 F_2 + \phi_2 F_1 \Big) - \frac{\lambda}{2\sqrt{2}} \Big(\tfrac{1}{3}\phi_2^3 - \phi_1^2 \phi_2 \Big) \right). \quad (9.136)$$

It is an easy but tedious exercise to check that the combination of bulk and boundary actions indeed preserves half of the original supersymmetries.

Next we address the problem of determining the boundary conditions of our fields. Demanding that the Euler-Lagrange variation of the total action vanishes produces a bulk term which is zero, provided that the fields satisfy the equations of motion (EOM). However, we also get terms localized in the boundary

$$\delta(S_{bulk} + S_{bdy}) = \int d^{d-1}\mathbf{x}\, dy\, (\,\mathrm{EOM}\,) + \int d^{d-1}\mathbf{x} \left(\frac{1}{2}\phi_1\, \delta(F_2 + \partial_n \phi_1) \right.$$
$$\left. + \frac{1}{2}\phi_2\, \delta(F_1 + \partial_n \phi_2) - \frac{1}{2}\delta\phi_1(F_2 + \partial_n \phi_1) - \frac{1}{2}\delta\phi_2(F_1 + \partial_n \phi_2) + \frac{1}{2}\delta\bar{\Psi}\gamma^n\Psi \right), \quad (9.137)$$

and the boundary conditions must be chosen such that they are zero. Moreover, one must check that the boundary conditions are closed under the supersymmetry transformations (9.134). In [376] it was shown that there is only one possible supersymmetric boundary condition, up to R-symmetry redefinitions $\phi \to e^{i\delta}\phi$. In conventions that match the bootstrap analysis of section 9.4 this boundary condition is

$$\partial_n \phi_1 = -F_2 = \frac{\lambda}{\sqrt{2}}\phi_1\phi_2\,, \qquad \phi_2 = 0, \qquad \Pi_- \Psi = 0\,. \quad (9.138)$$

In equations (9.137) and (9.138) we used the bulk equations of motion that relate $F \sim \lambda\phi^2$. Since we will work in perturbation theory, the free propagators are obtained for $\lambda = 0$, where ϕ_1 satisfies Neumann boundary conditions $\partial_n \phi_1 = 0$. As pointed out in [385], these boundary conditions are a good description near the free theory, but are not meant to describe the boundary condition of the fields at the interacting fixed point.

9.5.2 Using susceptibility

The calculation of correlation functions in the presence of boundaries using Feynman diagrams is typically challenging. An important observation that dates back to the work of

McAvity and Osborn [268,386] is that the calculations simplify in terms of susceptibilities, defined as

$$\chi_{\mathcal{O}_1\mathcal{O}_2}(y,y') = \int d^{d-1}\mathbf{x} \, \langle \mathcal{O}_1(\mathbf{x},y)\mathcal{O}_2(0,y') \rangle \,. \tag{9.139}$$

Crucially, this integral transform is invertible and one can recover the two-point function in terms of the susceptibility. This idea has been recently used to compute the one-loop two-point function of the order parameter in the extraordinary phase transition of the $O(N)$ model [280, 281]. One can also apply it to the $O(N)$ model in the large-N limit, see [277] for the three-dimensional case with a ϕ^6 potential.

In susceptibility space the role of the cross ratio ξ is played by a new object ζ, which is defined as follows:

$$\zeta = \frac{\min(y,y')}{\max(y,y')} \,. \tag{9.140}$$

The importance of ζ was noted in [280], where they observed that the contribution of a single conformal block in the boundary expansion is proportional to $\zeta^{\hat{\Delta} - \frac{d-1}{2}}$. This allows one to extract the boundary CFT data directly from the susceptibility without the need to reexpress everything in terms of the correlation function $F(\xi)$. To be more precise, the susceptibility can be expanded as

$$\chi_{\mathcal{O}\mathcal{O}}(y,y') = (4yy')^{\frac{d-1}{2} - \Delta_{\mathcal{O}}} \sum_{\hat{\mathcal{O}}} \mu_{\hat{\mathcal{O}}} \pi^{\frac{d-1}{2}} \frac{\Gamma\left(\hat{\Delta} - \frac{d-1}{2}\right)}{\Gamma(\hat{\Delta})} (4\zeta)^{\hat{\Delta} - \frac{d-1}{2}} \,, \tag{9.141}$$

where $\Delta_{\mathcal{O}}$ is the dimension of the external operator, $\mu_{\hat{\mathcal{O}}}$ is the boundary OPE coefficient and $\hat{\Delta}$ is the dimension of the exchanged operator.

Even though the bootstrap analysis used the chiral field and its complex conjugate, for the purposes of the current section it is more convenient to work with its real and imaginary parts $\phi = \phi_1 + i\phi_2$. The susceptibilities of the two descriptions are related by

$$
\begin{aligned}
\chi^+(y,y') &\equiv \chi_{\phi_1\phi_1}(y,y') = \frac{1 + \frac{\epsilon}{2}(\gamma + \log \pi)}{4\pi^2} \left(\chi_{\phi\bar{\phi}}(y,y') + \chi_{\phi\phi}(y,y') \right) \,, \\
\chi^-(y,y') &\equiv \chi_{\phi_2\phi_2}(y,y') = \frac{1 + \frac{\epsilon}{2}(\gamma + \log \pi)}{4\pi^2} \left(\chi_{\phi\bar{\phi}}(y,y') - \chi_{\phi\phi}(y,y') \right) \,,
\end{aligned}
\tag{9.142}
$$

where the prefactor translates from the natural normalization in the bootstrap calculation to the natural normalization using Lagrangians. It is an easy exercise to check that our

prediction for the order ϵ correlator (9.130) leads to

$$
\begin{aligned}
\chi^+(y, y') &= \frac{-1}{2\sqrt{\zeta}} (4yy')^{\frac{1}{2} - \Delta_\phi^{(1)} \epsilon} \Big[1 + 2\hat{\Delta}_0^{(1)} \epsilon + \hat{\Delta}_0^{(1)} \epsilon \log \zeta \\
&\qquad - \Delta_\phi^{(1)} \epsilon \big((1 + \zeta) \log(1 + \zeta) + (1 - \zeta) \log(1 - \zeta) \big) + \mathcal{O}(\epsilon^2) \Big], \\
\chi^-(y, y') &= \frac{\sqrt{\zeta}}{2} (4yy')^{\frac{1}{2} - \Delta_\phi^{(1)} \epsilon} \Big[1 + 2 \left(2\Delta_\phi^{(1)} - \hat{\Delta}_0^{(1)} \right) \epsilon + \hat{\Delta}_0^{(1)} \epsilon \log \zeta \\
&\qquad - \Delta_\phi^{(1)} \epsilon \left(\frac{(1 + \zeta)}{\zeta} \log(1 + \zeta) - \frac{(1 - \zeta)}{\zeta} \log(1 - \zeta) \right) + \mathcal{O}(\epsilon^2) \Big].
\end{aligned}
\tag{9.143}
$$

In the rest of this section we will check that perturbation theory gives a result consistent with this prediction, and we will find the explicit values of $\Delta_\phi^{(1)}$ and $\hat{\Delta}_0^{(1)}$ for the Wess-Zumino model.

9.5.3 Susceptibility at one-loop

Tree level

To compute the scalar propagators we have to solve the Klein-Gordon equation in position space. It is well known that in the presence of a boundary one has to add a "mirror" term to the propagator to satisfy the correct boundary conditions at $y = 0$. Since ϕ_1/ϕ_2 satisfy Neumann/Dirichlet boundary conditions we have:

$$
\begin{aligned}
\langle \phi_1(x) \phi_1(x') \rangle_0 &= \kappa_s \left(\frac{1}{|x - x'|^{d-2}} + \frac{1}{|\bar{x} - x'|^{d-2}} \right), \\
\langle \phi_2(x) \phi_2(x') \rangle_0 &= \kappa_s \left(\frac{1}{|x - x'|^{d-2}} - \frac{1}{|\bar{x} - x'|^{d-2}} \right).
\end{aligned}
\tag{9.144}
$$

Here $\langle \ldots \rangle_0$ indicates the two-point functions are evaluated in the free theory. For each $x = (\mathbf{x}, y)$ we defined the mirror point $\bar{x} = (\mathbf{x}, -y)$, and the overall normalization is $\kappa_s = \frac{\Gamma(\frac{d}{2})}{(d-2)2\pi^{d/2}}$. We will be mostly interested in the susceptibilities, which can be readily obtained from (9.139) and (9.144):

$$
\begin{aligned}
\chi_0^+(y, y') &= \chi_{\langle \phi_1 \phi_1 \rangle_0}(y, y') = -\max(y, y'), \\
\chi_0^-(y, y') &= \chi_{\langle \phi_2 \phi_2 \rangle_0}(y, y') = +\min(y, y').
\end{aligned}
\tag{9.145}
$$

Similarly, solving the Dirac equation and adding a "mirror" term dictated by the boundary conditions one gets [278]

$$
\langle \Psi(x) \bar{\Psi}(x') \rangle_0 = \kappa_f \left(\frac{\gamma \cdot (x - x')}{|x - x'|^d} + i\gamma_5 \gamma^n \frac{\gamma \cdot (\bar{x} - x')}{|\bar{x} - x'|^d} \right), \qquad \kappa_f = \frac{\Gamma(\frac{d}{2})}{2\pi^{d/2}}.
\tag{9.146}
$$

It is not hard to check that the fermion propagator satisfies the correct boundary conditions:

$$\Pi_- \langle \Psi(\mathbf{x}, 0) \bar{\Psi}(\mathbf{x}', y') \rangle_0 = \langle \Psi(\mathbf{x}, y) \bar{\Psi}(\mathbf{x}', 0) \rangle_0 \, \Pi_- = 0 \,. \tag{9.147}$$

Tadpole diagram

First we consider the quartic interaction terms in (9.133) and we use them to form loop diagrams with either ϕ_1 or ϕ_2 running in the loop. These diagrams would vanish if the boundary was not present, or equivalently if we studied physics far away from the boundary. As a result, we expect them to be finite in the limit $\epsilon \to 0$. Taking symmetry factors into account the total contribution is

$$\chi^{\pm}(y, y')|_{\text{tadpole}} = \quad \text{----} \vee \text{----} \quad = \mp 2^{-3+\epsilon} \lambda^2 \kappa_s I_b^{\pm}(y, y') \,. \tag{9.148}$$

The propagator that runs in the loop is defined as the finite part of $\langle \phi_i(\mathbf{x}, y) \phi_i(\mathbf{x}', y') \rangle_0$ when $\mathbf{x}' \to \mathbf{x}$, and can be obtained from (9.144). With this prescription, the Feynman integrals we must compute are [281]

$$
\begin{aligned}
I_b^+(y, y') &= \int_0^\infty dz \, \chi_0^+(y, z) \, z^{-2+\epsilon} \, \chi_0^+(z, y') = \frac{y^\epsilon y'}{\epsilon - 1} - \frac{y'(y^\epsilon - y'^\epsilon)}{\epsilon} - \frac{y'^{\epsilon+1}}{\epsilon + 1} \,, \\
I_b^-(y, y') &= \int_0^\infty dz \, \chi_0^-(y, z) \, z^{-2+\epsilon} \, \chi_0^-(z, y') = -\frac{yy'^\epsilon}{\epsilon - 1} - \frac{y(y^\epsilon - y'^\epsilon)}{\epsilon} + \frac{y^{\epsilon+1}}{\epsilon + 1} \,.
\end{aligned}
\tag{9.149}
$$

For simplicity we assumed here and in the rest of the section that $y < y'$, but one can obtain the integral for $y > y'$ replacing $y \leftrightarrow y'$.

Fermion bubble

Similarly, we can use the Yukawa interactions in (9.133) to form diagrams with fermions running in the loop. If the boundary was not present, these diagrams would be UV divergent and would contribute to the renormalization of ϕ. Since the boundary does not change the UV behaviour of the theory, we expect a divergence as $\epsilon \to 0$ which is canceled by the counterterm δ_ϕ:

$$\chi^{\pm}(y, y')|_{\text{bubble}} = \quad \text{----} \bigcirc \text{----} \quad + \quad \text{----} \bigstar \text{----}$$
$$= \lambda^2 \kappa_f^2 I_f^{\pm}(y, y') - \delta_\phi \chi_0^{\pm}(y, y') \,. \tag{9.150}$$

Using the identities

$$
\begin{aligned}
\operatorname{tr}\left[\langle\Psi(x)\bar{\Psi}(x')\rangle_0\langle\Psi(x')\bar{\Psi}(x)\rangle_0\right] &= -4\kappa_f^2\left(\frac{1}{|x-x'|^{2(d-1)}} + \frac{1}{|\bar{x}-x'|^{2(d-1)}}\right), \\
\operatorname{tr}\left[\langle\Psi(x)\bar{\Psi}(x')\rangle_0\gamma_5\langle\Psi(x')\bar{\Psi}(x)\rangle_0\gamma_5\right] &= 4\kappa_f^2\left(\frac{1}{|x-x'|^{2(d-1)}} - \frac{1}{|\bar{x}-x'|^{2(d-1)}}\right),
\end{aligned}
\tag{9.151}
$$

we see that the Feynman integral is

$$
I_f^{\pm}(y,y') = \int_0^\infty dz \int_0^\infty dz' \chi^{\pm}(y,z) b^{\pm}(z,z') \chi^{\pm}(z',y'),
\tag{9.152}
$$

where we have defined

$$
\begin{aligned}
b^{\pm}(z,z') &= \int d^{d-1}\mathbf{r}\left(\frac{1}{(\mathbf{r}^2+(z-z')^2)^{d-1}} \pm \frac{1}{(\mathbf{r}^2+(z+z')^2)^{d-1}}\right) \\
&= \frac{2^{2-d}\pi^{d/2}}{\Gamma\left(\frac{d}{2}\right)}\left(|z-z'|^{-3+\epsilon} \pm |z+z'|^{-3+\epsilon}\right).
\end{aligned}
\tag{9.153}
$$

We will evaluate this integral with a trick that has been used in the literature in similar situations [280, 281, 387]. The idea is to split the integration region between $z > z'$ and $z < z'$. By changing variables to $Z = \frac{z}{z'}$ and $Z = \frac{z'}{z}$, one can carry out the first integration in terms of $I_b^{\pm}$ defined in the previous section. The result is:

$$
\begin{aligned}
I_f^{\pm}(y,y') = y^{\epsilon+1}\Bigg[&\int_1^\infty dZ I_b^{\pm}(1,Z/\zeta) b^{\pm}(1,Z) Z^{-\epsilon} + \int_1^{1/\zeta} dZ I_b^{\pm}(1,(Z\zeta)^{-1}) b^{\pm}(1,Z) Z \\
&+ \zeta^{-1-\epsilon}\int_{1/\zeta}^\infty dZ I_b^{\pm}(1,\zeta Z) b^{\pm}(1,Z) Z^{-\epsilon}\Bigg].
\end{aligned}
\tag{9.154}
$$

Remember that we are assuming $y < y'$, such that $\zeta = y/y'$. Finally, all terms in (9.154) can be integrated using `Mathematica`[18]. The result for general ϵ is not particularly illuminating and will not be needed later, instead we focus on the result in the limit $\epsilon \to 0$. First, the divergent piece is canceled in $\overline{\text{MS}}$ with the following counterterm:

$$
\delta_\phi = -\frac{\lambda^2}{(4\pi)^2}\left(\frac{1}{\epsilon} + \frac{1}{2}(\gamma + \log\pi) + 1\right).
\tag{9.155}
$$

---

[18]The only exception are integrals of the form $\int_1^\infty dZ(Z-1)^a$, but they are zero in dimensional regularization.

The total diagram is now finite:

$$
\chi^{+}(y, y')|_{\text{bubble}} = \frac{\lambda^2}{64\pi^2} \frac{\sqrt{4yy'}}{\sqrt{\zeta}} \Big(\log(4yy') - \log\zeta - 2
$$
$$
+ (1 + \zeta)\log(1 + \zeta) + (1 - \zeta)\log(1 - \zeta) \Big) + \mathcal{O}(\epsilon) ,
$$
$$
\chi^{-}(y, y')|_{\text{bubble}} = \frac{-\lambda^2}{64\pi^2} \sqrt{4yy'\zeta} \Big(\log(4yy') - \log\zeta - 2
$$
$$
+ \frac{(1 + \zeta)}{\zeta}\log(1 + \zeta) - \frac{(1 - \zeta)}{\zeta}\log(1 - \zeta) \Big) + \mathcal{O}(\epsilon) .
$$

$$(9.156)$$

Final result

We can obtain the full susceptibility at order ϵ by combining the tree-level result (9.145), the tadpole diagram (9.149), and the fermion bubble (9.156). We should evaluate the sum at the fixed point coupling $\lambda_*^2 = \frac{16\pi^2}{3}\epsilon$, and keep only terms up to order ϵ. The result is perfectly consistent with the bootstrap prediction (9.143), and we identify

$$
\Delta_\phi^{(1)} = \frac{1}{6} , \qquad \hat{\Delta}_0^{(1)} = 0 , \qquad s = +1 . \tag{9.157}
$$

The anomalous dimension of ϕ in the Wess-Zumino model is well known in the literature. One can obtain it by demanding that the superpotential has R-charge $R(W) = 3r_\phi = 2$, so we find that $r_\phi = 2/3$. Using the relation between the R-charge and conformal dimension we find $\Delta_\phi = \frac{d-1}{3}$, in perfect agreement with (9.157). From this argument it is clear that Δ_ϕ is one-loop exact.

An interesting prediction of our calculation is the anomalous dimension of the leading bulk operator in the OPE $\phi \times \phi \sim \mathcal{O}_0 + \dots$. We calculated this for a general model in (9.129), and for the Wess-Zumino case we get

$$
\Delta_0^{(1)} = \frac{2}{3} \qquad \Rightarrow \qquad \Delta_0 = \frac{d+2}{3} = d - 2\Delta_\phi . \tag{9.158}
$$

Recalling the selection rules of section 9.4.1, we see that the exchanged operator is of the form $\mathcal{O}_0 \sim (Q^+)^2\bar{\Psi}$ where $\bar{\Psi}$ is an antichiral primary operator. Indeed, the numerical bootstrap applied to the Wess-Zumino model in [193, 378] also provides strong evidence that the leading operator in the $\phi \times \phi$ OPE is of this form. The agreement of our results with the predictions from [193, 378] provides a non-trivial sanity check of our perturbative calculation. It would be interesting to consider other particular models, for instance with

extra boundary interactions or a more complicated bulk, and see whether the anomalous dimension of the defect operator changes. We hope to come back to this question in the future.

9.6   Conclusions

In this work we studied supersymmetric boundaries for $3d$ $\mathcal{N} = 2$ superconformal theories. There are two possible choices characterized by $2d$ $\mathcal{N} = (0, 2)$ and $\mathcal{N} = (1, 1)$ boundary algebras respectively. After performing a careful superspace analysis of correlators involving chiral fields, we observed in section 9.4 that the $\mathcal{N} = (1, 1)$ choice can be analytically continued in the spacetime dimension. This allowed us to compute superconformal blocks across dimensions and opened the door for the ϵ-expansion bootstrap in our supersymmetric setup. We proved uniqueness of the first two orders in ϵ, and confirmed our general prediction for one specific model using perturbation theory. We used standard perturbative and bootstrap techniques in this analysis, but one could also try using alternative approaches, such as Mellin space [274] or the equations of motion method of [381].

An interesting follow up to our BCFT analysis is to consider higher codimension defects. The algebraic approach to calculate superblocks of section 9.4 is applicable to higher codimension, where the spacetime and defect dimensions are allowed to change while the codimension is kept fixed. In particular, the codimension-two blocks calculated in section 9.4.2 are applicable to known examples, such as the Wess-Zumino model in the presence of twist defects. In the same spirit of the present work, one can use the ϵ-expansion to study two-point functions of local operators. In principle one can do explicit perturbative calculations as in [256], however it is perhaps simpler to set up a bootstrap problem and attempt to solve it using the technology of inversion formulas [265, 266]. One could also concentrate exclusively on three dimensions and apply the numerical bootstrap on the line, analogous to what was done for the twist defect in the $3d$ Ising model [256] (the $1d$ bootstrap for superconformal line defects has been studied in [2, 233, 260]).

A longer term goal is to include multi-point correlators in the analysis; this is a program that has been underexplored even in the bosonic case, although significant progress can be made using Calogero-Sutherland technology [388]. Finally, the study of free theories in the presence of interacting defects has gotten some attention recently; in particular the results of [295] suggest the existence of a new conformal boundary condition for the free scalar field. It would be interesting to repeat their analysis in our supersymmetric setup, either

for boundaries or higher codimension defects.

9.A   Details on three-dimensional boundaries

9.A.1   Conventions

In section 9.3 we work in Lorentzian signature with mostly plus metric $\eta_{\mu\nu} = \text{diag}(-1, +1, +1)$. The gamma matrices are defined in terms of the identity matrix $\mathbf{1}$ and Pauli matrices σ^i as

$$(\gamma^\mu)_{\alpha\beta} \equiv \left(-\mathbf{1}_{\alpha\beta}, (\sigma^3)_{\alpha\beta}, (\sigma^1)_{\alpha\beta} \right) , \quad (\gamma^\mu)_\alpha{}^\beta = (\gamma^\mu)_{\alpha\gamma} \varepsilon^{\gamma\beta}, \quad (\gamma^\mu)^{\alpha\beta} = \varepsilon^{\alpha\gamma} (\gamma^\mu)_\gamma{}^\beta . \quad (9.159)$$

With these conventions the gamma matrices are real and symmetric. Here and in what follows we are raising and lowering spinor indices as $\theta^\alpha = \varepsilon^{\alpha\beta} \theta_\beta$ and $\theta_\alpha = \varepsilon_{\alpha\beta} \theta^\beta$, where

$$\varepsilon^{12} = 1, \quad \varepsilon_{12} = -1 . \quad (9.160)$$

The contraction of two spinors is defined as $\theta^2 = \varepsilon_{\alpha\beta} \theta^\alpha \theta^\beta$. Finally, the spacetime Levi-Civita tensor is defined by:

$$\varepsilon_{012} = -1, \quad \varepsilon^{012} = 1 . \quad (9.161)$$

9.A.2   Superconformal algebra

The three dimensional Lorentz group $SO(2,1)$ is generated by $\mathcal{M}_{\mu\nu}$. A generic element of the algebra $\mathcal{J}$ contains vector indices $\mu, \nu, \lambda, \ldots$ and spinor indices $\alpha, \beta, \ldots$, and each of them transforms under rotations as:

$$\begin{aligned}
[\mathcal{M}_{\mu\nu}, \mathcal{J}_{\lambda\ldots}] &= i \left(\eta_{\mu\lambda} \mathcal{J}_{\nu\ldots} - \eta_{\nu\lambda} \mathcal{J}_{\mu\ldots} \right) , \\
[\mathcal{M}_{\mu\nu}, \mathcal{J}_{\alpha\ldots}] &= +\frac{i}{2} \varepsilon_{\mu\nu\lambda} (\gamma^\lambda)_\alpha{}^\beta \mathcal{J}_{\beta\ldots}, \\
[\mathcal{M}_{\mu\nu}, \mathcal{J}^{\alpha\ldots}] &= -\frac{i}{2} \varepsilon_{\mu\nu\lambda} (\gamma^\lambda)_\beta{}^\alpha \mathcal{J}^{\beta\ldots} .
\end{aligned} \quad (9.162)$$

With these identities it is easy to write down any commutator involving $\mathcal{M}_{\mu\nu}$. The rest of the $3d$ conformal algebra is:

$$[\mathcal{D}, \mathcal{P}_\mu] = i\mathcal{P}_\mu, \quad [\mathcal{D}, \mathcal{K}_\mu] = -i\mathcal{K}_\mu, \quad [\mathcal{K}_\mu, \mathcal{P}_\nu] = -2i \left(\mathcal{M}_{\mu\nu} + \eta_{\mu\nu} \mathcal{D} \right) . \quad (9.163)$$

The $3d$ $\mathcal{N} = 2$ superconformal algebra is given by $OSP(2|4)$. Besides the conformal and R-symmetry generators, it contains four Poincaré supercharges and four superconformal

supercharges that anticommute as

$$\{\mathcal{Q}_\alpha, \bar{\mathcal{Q}}_\beta\} = 2(\gamma^\mu)_{\alpha\beta}\mathcal{P}_\mu, \quad \{\mathcal{S}^\alpha, \bar{\mathcal{S}}^\beta\} = 2(\gamma^\mu)^{\alpha\beta}\mathcal{K}_\mu,$$
$$\{\mathcal{Q}_\alpha, \bar{\mathcal{S}}^\beta\} = -i\left(2\delta_\alpha{}^\beta(\mathcal{D} + i\mathcal{R}) - \varepsilon^{\mu\nu\lambda}(\gamma_\lambda)_\alpha{}^\beta\mathcal{M}_{\mu\nu}\right), \tag{9.164}$$
$$\{\bar{\mathcal{Q}}_\alpha, \mathcal{S}^\beta\} = -i\left(2\delta_\alpha{}^\beta(\mathcal{D} - i\mathcal{R}) - \varepsilon^{\mu\nu\lambda}(\gamma_\lambda)_\alpha{}^\beta\mathcal{M}_{\mu\nu}\right).$$

The commutation relations between the conformal group and the supercharges are

$$[\mathcal{D}, \mathcal{Q}_\alpha] = \frac{1}{2}i\mathcal{Q}_\alpha, \quad [\mathcal{D}, \mathcal{S}^\alpha] = -\frac{1}{2}i\mathcal{S}^\alpha, \quad [\mathcal{K}_\mu, \mathcal{Q}_\alpha] = (\gamma_\mu)_{\alpha\beta}\mathcal{S}^\beta, \quad [\mathcal{P}_\mu, \mathcal{S}^\alpha] = -(\gamma_\mu)^{\alpha\beta}\mathcal{Q}_\beta,$$
$$[\mathcal{D}, \bar{\mathcal{Q}}_\alpha] = \frac{1}{2}i\bar{\mathcal{Q}}_\alpha, \quad [\mathcal{D}, \bar{\mathcal{S}}^\alpha] = -\frac{1}{2}i\bar{\mathcal{S}}^\alpha, \quad [\mathcal{K}_\mu, \bar{\mathcal{Q}}_\alpha] = (\gamma_\mu)_{\alpha\beta}\bar{\mathcal{S}}^\beta, \quad [\mathcal{P}_\mu, \bar{\mathcal{S}}^\alpha] = -(\gamma_\mu)^{\alpha\beta}\bar{\mathcal{Q}}_\beta.$$
$$\tag{9.165}$$

Lastly, all generators are neutral under R-symmetry, except the eight supercharges:

$$[\mathcal{R}, \mathcal{Q}_\alpha] = -\mathcal{Q}_\alpha, \quad [\mathcal{R}, \bar{\mathcal{Q}}_\alpha] = \bar{\mathcal{Q}}_\alpha, \quad [\mathcal{R}, \mathcal{S}^\alpha] = -\mathcal{S}^\alpha, \quad [\mathcal{R}, \bar{\mathcal{S}}^\alpha] = \bar{\mathcal{S}}^\alpha. \tag{9.166}$$

9.A.3   Differential operators

In this appendix we present the action of our generators in terms of differential operators in superspace. We consider an operator $\mathcal{O}(z)$ of dimension Δ and charge r that transforms under rotations in a representation dictated by matrices $s_{\mu\nu}$, which satisfy the same

commutation relations as $\mathcal{M}_{\mu\nu}$. Then, the generators of the algebra act as:

$$[\mathcal{D}, \mathcal{O}(z)] = i \left(\Delta + x^\mu \partial_\mu + \frac{1}{2} \theta^\alpha \partial_\alpha + \frac{1}{2} \bar{\theta}^\alpha \bar{\partial}_\alpha \right) \mathcal{O}(z) , \tag{9.167}$$

$$\begin{aligned}[\mathcal{K}_\mu, \mathcal{O}(z)] = \Big(&- 2i\Delta x_\mu - 2ix_\mu x^\nu \partial_\nu + ix^2 \partial_\mu \\
&- ix_\mu(\theta^\alpha \partial_\alpha + \bar{\theta}^\alpha \bar{\partial}_\alpha) + i\epsilon_{\mu\nu\rho}(\gamma^\nu)_\alpha{}^\beta x^\rho(\theta^\alpha \partial_\beta + \bar{\theta}^\alpha \bar{\partial}_\beta) \\
&+ (\gamma_\mu)_{\alpha\beta}\theta^\alpha \bar{\theta}^\beta(\theta^\gamma \partial_\gamma - \bar{\theta}^\gamma \bar{\partial}_\gamma) - \frac{i}{2}\theta^2 \bar{\theta}^2 \partial_\mu \\
&- 2r(\gamma_\mu)_{\alpha\beta}\theta^\alpha \bar{\theta}^\beta - 2x^\nu s_{\mu\nu} - i\eta_{\mu\nu}\varepsilon^{\nu\rho\sigma} s_{\rho\sigma}\theta^\alpha \bar{\theta}_\alpha \Big)\mathcal{O}(z) , \end{aligned} \tag{9.168}$$

$$[\mathcal{M}_{\mu\nu}, \mathcal{O}(z)] = \left(\frac{i}{2}\varepsilon_{\mu\nu\rho}(\gamma^\rho)_\alpha{}^\beta(\theta^\alpha \partial_\beta + \bar{\theta}^\alpha \bar{\partial}_\beta) + ix_\mu \partial_\nu - ix_\nu \partial_\mu + s_{\mu\nu} \right)\mathcal{O}(z) , \tag{9.169}$$

$$[\mathcal{R}, \mathcal{O}(z)] = \left(\bar{\theta}^\alpha \bar{\partial}_\alpha - \theta^\alpha \partial_\alpha + r \right)\mathcal{O}(z) , \tag{9.170}$$

$$\begin{aligned}[\mathcal{S}^\alpha, \mathcal{O}(z)] = \Big(&- i(\gamma_\mu)^{\alpha\beta} x^\mu \partial_\beta + \bar{\theta}^\alpha x^\mu \partial_\mu + \frac{1}{2}(\gamma^\mu)^{\alpha\beta}(\gamma^\nu)_{\beta\gamma}\bar{\theta}^\gamma(x_\mu \partial_\nu - x_\nu \partial_\mu) \\
&- \theta^\alpha \bar{\theta}^\beta \partial_\beta + \bar{\theta}^\alpha \theta^\beta \partial_\beta - 2\bar{\theta}^\alpha \bar{\theta}^\beta \bar{\partial}_\beta \\
&- i(\gamma^\mu)_{\beta\gamma}\theta^\beta \bar{\theta}^\gamma \bar{\theta}^\alpha \partial_\mu + 2\Delta\bar{\theta}^\alpha - 2r\bar{\theta}^\alpha + i\varepsilon^{\mu\nu\rho}(\gamma_\rho)_\beta{}^\alpha \bar{\theta}^\beta s_{\mu\nu} \Big)\mathcal{O}(z) , \end{aligned} \tag{9.171}$$

$$\begin{aligned}\left[\bar{\mathcal{S}}^\alpha, \mathcal{O}(z) \right] = \Big(&i(\gamma^\mu)^{\alpha\beta} x_\mu \bar{\partial}_\beta - \theta^\alpha x^\mu \partial_\mu - \frac{1}{2}(\gamma^\mu)^{\alpha\beta}(\gamma^\nu)_{\beta\gamma}\theta^\gamma(x_\mu \partial_\nu - x_\nu \partial_\mu) \\
&+ \bar{\theta}^\alpha \theta^\beta \bar{\partial}_\beta - \theta^\alpha \bar{\theta}^\beta \bar{\partial}_\beta + 2\theta^\alpha \theta^\beta \partial_\beta \\
&+ i(\gamma^\mu)_{\beta\gamma}\bar{\theta}^\beta \theta^\gamma \theta^\alpha \partial_\mu - 2\Delta\theta^\alpha - 2r\theta^\alpha - i\varepsilon^{\mu\nu\rho}(\gamma_\rho)_\beta{}^\alpha \theta^\beta s_{\mu\nu} \Big)\mathcal{O}(z) . \end{aligned} \tag{9.172}$$

9.B Non-supersymmetric conformal blocks

In this appendix, we will derive the non-supersymmetric bulk and boundary blocks for bulk two-point functions and bulk-boundary-boundary correlators.

9.B.1 Two-point function

The conformal blocks for a two-point function were first derived in [268] but we will follow [269] in our approach.

Bulk channel: The bulk-channel blocks can be found by acting on the two-point function (9.7) with the bulk Casimir operator:

$$\mathcal{C}^{(12)}_{\text{bulk,bos}} = -\mathcal{D}^2 - \frac{1}{2}\{\mathcal{K}^\mu, \mathcal{P}_\mu\} + \frac{1}{2}\mathcal{M}^{\mu\nu}\mathcal{M}_{\mu\nu} . \tag{9.173}$$

The differential operators are well know, but they can also be obtained from section 9.A.3 by setting all Grassmann coordinates to zero. The Casimir eigenvalues is $C_{\Delta,\ell} = \Delta(\Delta - d) + \ell(\ell + d - 2)$, but only operators with $\ell = 0$ can appear in the bulk OPE. For the bulk channel, it is convenient to define the blocks in terms of $g_\Delta^{\Delta_{12}}(\xi) = \xi^{(\Delta_1 + \Delta_2)/2} f_\Delta^{\Delta_{12}}(\xi)$. The resulting differential equation is

$$
\frac{(\mathcal{C}_{\text{bulk,bos}} - C_{\Delta,\ell}) \langle \phi_1(x_1) \phi_2(x_2) \rangle}{(2x_1^\perp)^{-\Delta_1} (2x_2^\perp)^{-\Delta_2} \xi^{-(\Delta_1 + \Delta_2)/2}} = \Big[4\xi^2(\xi + 1)\partial_\xi^2 + 2\xi(2\xi - d + 2)\partial_\xi
$$
$$
- (\Delta(\Delta - d) + \Delta_{12}^2 \xi) \Big] g_\Delta^{\Delta_{12}}(\xi) = 0 \,, \tag{9.174}
$$

which is solved by

$$
g_\Delta^{\Delta_{12}}(\xi) = \xi^{\Delta/2} \, {}_2F_1\Big(\frac{\Delta + \Delta_{12}}{2}, \frac{\Delta - \Delta_{12}}{2}; \Delta + 1 - \frac{d}{2}; -\xi \Big). \tag{9.175}
$$

Whenever the superscript Δ_{12} is omitted, it is assumed that $\Delta_{12} = 0$.

Boundary channel: In the boundary channel, the conformal blocks are eigenfunctions of the boundary Casimir that acts on a single point

$$
\hat{\mathcal{C}}_{\text{non-susy}}^{(1)} = -\mathcal{D}^2 - \frac{1}{2}\{\mathcal{K}^a, \mathcal{P}_a\} + \frac{1}{2}\mathcal{M}^{ab}\mathcal{M}_{ab} \,, \tag{9.176}
$$

where the index a, b runs only on directions parallel to the boundary. The eigenvalue of the boundary Casimir is $\hat{C}_{\Delta,j} = \Delta(\Delta - d + 1) + j(j + d - 1)$, but once more we have to take $j = 0$ because only scalar operators appear in the BOE of a bulk scalar. The resulting differential equation is

$$
\frac{\left(\hat{\mathcal{C}}_{\text{non-susy}} - \hat{C}_{\Delta,0} \right) \langle \phi_1(x_1) \phi_2(x_2) \rangle}{(2x_1^\perp)^{-\Delta_1} (2x_2^\perp)^{-\Delta_2}} = \Big[\xi(\xi + 1)\partial_\xi^2 + \frac{d}{2}(2\xi + 1)\partial_\xi
$$
$$
- \hat{\Delta}(\hat{\Delta} - d + 1) \Big] \hat{f}_{\hat{\Delta}}(\xi) = 0 \,, \tag{9.177}
$$

which is solved by

$$
\hat{f}_{\hat{\Delta}}(\xi) = \xi^{-\hat{\Delta}} \, {}_2F_1\Big(\hat{\Delta}, \hat{\Delta} - \frac{d}{2} + 1; 2\hat{\Delta} - d + 2; -\frac{1}{\xi} \Big). \tag{9.178}
$$

9.B.2 Three-point bosonic blocks

In this section we restrict to $d = 3$. We start with considering the bosonic correlator

$$
\langle \mathcal{O}_1(x) \hat{\mathcal{O}}_{2,j}(0) \hat{\mathcal{O}}_3(\infty) \rangle = \frac{(x^a \omega_a)^j}{(x^\perp)^{\Delta_1 + \hat{\Delta}_{23}} |x^a|^j} \mathcal{F}^{\text{3pt}}(\chi), \qquad \chi = \frac{|x^a|^2}{(x^\perp)^2} \,, \tag{9.179}
$$

where the second operator has parallel spin j. We used index-free notation to contract all vector indices, and ω_a is a null-vector. We need to evaluate the eigenvalue equation

$$\hat{\mathcal{C}}_{\text{bos}}^{(1)}\langle\mathcal{O}_1(x)\hat{\mathcal{O}}_{2,j}(0)\hat{\mathcal{O}}_3(\infty)\rangle = \hat{C}_{\hat{\Delta},0}\langle\mathcal{O}_1(x)\hat{\mathcal{O}}_{2,j}(0)\hat{\mathcal{O}}_3(\infty)\rangle\,, \tag{9.180}$$

where $\hat{C}_{\hat{\Delta},0}$ is the boundary Casimir eigenvalue when the parallel spin of the exchanged operator is zero. This gives us the differential equation

$$\left[4\chi(\chi+1)\partial_\chi^2 + 4\left((\hat{\Delta}_{23}+2)\chi+1\right)\partial_\chi - \hat{\Delta}(\hat{\Delta}-2) + \hat{\Delta}_{23}(\hat{\Delta}_{23}+2) - \frac{j^2}{\chi}\right]\hat{f}_{\hat{\Delta},j}^{\text{3pt},\hat{\Delta}_{23}} = 0\,. \tag{9.181}$$

The solution to equation (9.181) is once more given by a hypergeometric function

$$\hat{f}_{\hat{\Delta},j}^{\text{3pt},\hat{\Delta}_{23}}(\chi) = \chi^{-\frac{1}{2}(\hat{\Delta}+\hat{\Delta}_{23})}\,_2F_1\left(\frac{1}{2}\left(\hat{\Delta}+\hat{\Delta}_{23}-j\right),\frac{1}{2}\left(\hat{\Delta}+\hat{\Delta}_{23}+j\right);\hat{\Delta};-\frac{1}{\chi}\right)\,. \tag{9.182}$$

9.C   More on blocks across dimensions

In this appendix, we provide more details on the derivation of the superconformal blocks in any number of dimension. In section 9.4 we showed that the supersymmetric part of the Casimir acting on a two-point function can be written in terms of Q supercharges acting on the two-point function. Our current goal is to find equivalent expressions where the supercharges are replaced by a differential operator, for example

$$\langle 0|\left[Q_{\dot{\alpha}}^-,\phi_1(x_1)\right]\left[Q_\alpha^+,\bar{\phi}_2(x_2)\right]|0\rangle \sim \mathcal{D}_x\langle 0|\phi_1(x_1)\bar{\phi}_2(x_2)|0\rangle\,. \tag{9.183}$$

It was proposed in [193] that this can be achieved with supersymmetric Ward identities. Here we give a quick summary of the strategy. In our setup the supercharges $\mathcal{Q}_A$ and $\mathcal{S}_A$ are preserved by the boundary, so the following Ward identities are satisfied:

$$\langle 0|\{Q_1^{\text{bdy}},\left[Q_1^-,\phi_1(x_1)\right]\bar{\phi}_2(x_2)\}|0\rangle = 0\,, \qquad \langle 0|\{S_1^{\text{bdy}},\left[Q_1^-,\phi_1(x_1)\right]\bar{\phi}_2(x_2)\}|0\rangle = 0\,,$$

$$\langle 0|\{Q_1^{\text{bdy}},\left[Q_2^-,\phi_1(x_1)\right]\bar{\phi}_2(x_2)\}|0\rangle = 0\,, \qquad \langle 0|\{S_1^{\text{bdy}},\left[Q_2^-,\phi_1(x_1)\right]\bar{\phi}_2(x_2)\}|0\rangle = 0\,. \tag{9.184}$$

$$\langle 0|\{Q_2^{\text{bdy}},\left[Q_1^-,\phi_1(x_1)\right]\bar{\phi}_2(x_2)\}|0\rangle = 0\,,$$

There are other Ward identities that can be considered, but these five are sufficient for our purposes. At this point, it is hard to continue without an explicit matrix representation for the Clifford algebra, so we focus on $d = 3$ where $\Sigma_\mu = (\sigma_3,\sigma_1,\sigma_2)$. Let us consider explicitly the simplest Ward identity to show how to replace the supercharges with differential

operators in the general case. With elementary manipulations we find:

$$
\begin{aligned}
0 &= \langle 0|\{Q_2^{\mathrm{bdy}}, \left[Q_1^-, \phi_1(x_1)\right] \bar{\phi}_2(x_2)\}|0\rangle \\
&= \langle 0|\{Q_2^{\mathrm{bdy}}, \left[Q_1^-, \phi_1(x_1)\right] \}\bar{\phi}_2(x_2)|0\rangle - \langle 0|\left[Q_1^-, \phi_1(x_1)\right]\left[Q_2^{\mathrm{bdy}}, \bar{\phi}_2(x_2)\right]|0\rangle \\
&= \langle 0|\left[\{Q_2^+, Q_1^-\}, \phi_1(x_1)\right]\bar{\phi}_2(x_2)|0\rangle - \langle 0|\left[Q_1^-, \phi_1(x_1)\right]\left[Q_2^+, \bar{\phi}_2(x_2)\right]|0\rangle .
\end{aligned}
\tag{9.185}
$$

In our conventions $\{Q_2^+, Q_1^-\} = P_2 + iP_3$ and also $[P_\mu, \mathcal{O}(x)] = -i\partial_\mu \mathcal{O}(x)$, so we conclude

$$
\left\langle 0\left|\left[Q_1^-, \phi_1(x_1)\right]\left[Q_2^+, \bar{\phi}_2(x_2)\right]\right|0\right\rangle = (-i\partial_2 + \partial_3)\left\langle 0\left|\phi_1(x_1)\bar{\phi}_2(x_2)\right|0\right\rangle .
\tag{9.186}
$$

The other Ward identities can be manipulated identically, but unlike the example we showed they do not decouple, so one has to solve a simple linear system of equations to obtain the terms we are interested in.

These steps can be automated in `Mathematica` and applied to all cases of interest in $d = 3, 4$. The resulting differential operators $\mathcal{D}_x$ depend on x_i^μ and $\partial_{\mu,i}$ and take a complicated looking form. However, we know that the Casimir operator $C_{\mathrm{bulk/bdy,susy}}$ has to respect conformal invariance, so when we combine all the contributing terms, the result has to be a differential operator of the cross-ratio ξ. Indeed, in $d = 3, 4$ we find the following results:

$$
\begin{aligned}
ix_{12}^\mu \bar{\Sigma}_\mu^{\dot{\alpha}\alpha} \left\langle 0\left|\left[Q_{\dot{\alpha}}^-, \phi_1(x_1)\right]\left[Q_\alpha^+, \bar{\phi}_2(x_2)\right]\right|0\right\rangle &\to (4\xi\partial_\xi - 2(\Delta_1 + \Delta_2))\mathcal{G}(\xi), \\
ix_1^\perp \left\langle 0\left|\left\{Q_1^-, \left[Q_2^-, \phi_1(x_1)\right]\right\} \bar{\phi}_2(x_2)\right|0\right\rangle &\to (-\xi\partial_\xi - \Delta_1)\mathcal{F}(\xi), \\
ix_1^\perp \left\langle 0\left|\left\{Q_1^-, \left[Q_2^-, \phi_1(x_1)\right]\right\} \phi_2(x_2)\right|0\right\rangle &\to (-(\xi+1)\partial_\xi - \Delta_1)\mathcal{F}(\xi) .
\end{aligned}
\tag{9.187}
$$

From these results we can obtain (9.93), (9.96) and (9.101). Although the intermediate differential operators were complicated, the final result takes a remarkably simple form. Perhaps one could find a more direct method of obtaining these results, and at the same time make it more manifest that the result is indeed independent of d.

Chapter 10

Bootstrapping Monodromy Defects

Abstract

We use analytical bootstrap techniques to study supersymmetric monodromy defects in the critical Wess-Zumino model. In preparation for this result we first study two related systems which are interesting on their own: general monodromy defects (no susy), and the ε–expansion bootstrap for the Wess-Zumino model (no defects). For general monodromy defects, we extend previous work on codimension-two conformal blocks and the Lorentzian inversion formula in order to accommodate parity-odd structures. In the Wess-Zumino model, we bootstrap four-point functions of chiral operators in the ε–expansion, with the goal of obtaining spectral information about the bulk theory. We then proceed to bootstrap two-point functions of chiral operators in the presence of a monodromy defect, and obtain explicit expressions in terms of novel special functions which we analyze in detail. Several of the results presented in this paper are quite general and should be applicable to other setups.

10.1 Introduction and summary

Conformal defects are extended objects in conformal field theories that preserve a fraction of the full conformal symmetry. They are important physical observables and their properties should be studied with the same emphasis as the spectrum of local operators. In three

dimensions, the critical Ising model has been the subject of intensive research during the past years, and part of this work has focused on its spectrum of defects: conformal boundary conditions were studied using bootstrap techniques in [45, 269], while the existence of a monodromy defect was proposed in [255], and further studied in [256].

The motivation behind this work is the study of monodromy defects in the $\mathcal{N} = 2$ Wess-Zumino model, which can be considered a supersymmetric counterpart to the standard $3d$ Ising model which preserves four supercharges.[1] In order to achieve our goal, several intermediate results are necessary, and some of them are interesting on their own right. In particular, our analysis contains applications valid for non-supersymmetric monodromy defects, for general codimension-two defects and for the Wess-Zumino model without defects. The purpose of this detailed introduction is to summarize the paper and provide an outlook of the most relevant results.

Consider a d-dimensional Euclidean conformal field theory. Whenever there is a complex scalar $\phi(x)$ invariant under $U(1)$ transformations $\phi(x) \to e^{i\alpha}\phi(x)$, a monodromy defect is introduced demanding that the scalar picks a phase when it goes around the origin as follows

$$\phi(r, \theta + 2\pi, \vec{y}) = e^{2\pi i v}\phi(r, \theta, \vec{y}) \, . \tag{10.1}$$

Here $0 \leq v < 1$ is a real parameter that characterizes the monodromy, and we are using polar coordinates (r, θ) in the plane orthogonal to the defect. The critical Ising model provides the simplest example: since the global symmetry is $\mathbb{Z}_2$, there exists a monodromy defect with $v = 1/2$. This defect was studied in [255, 256] using Monte-Carlo simulations, ε–expansion calculations and numerical bootstrap (see also [389]). For the case of the $O(N)$ models, there exist monodromy defects with general v, which were studied in the ε–expansion in [257], and recently the very systematic study of [258] has extended these results and obtained new ones in the large-N limit.[2]

In the present work, an important observable we consider are two-point correlation functions of scalar fields in the presence of a monodromy defect. Since the monodromy partly breaks conformal symmetry, the correlator depends on two conformal cross ratios

$$\langle \phi(x_1)\bar{\phi}(x_2)\rangle = \frac{\mathcal{G}(x, \bar{x})}{(r_1 r_2)^{\Delta_\phi}} \, . \tag{10.2}$$

---

[1]The $\mathcal{N} = 1$ super Ising model can also be formulated as a Wess-Zumino model [383], and has been studied successfully using the numerical bootstrap [199, 200].

[2] The monodromy defect geometry is reminiscent of two interesecting boundaries at an angle $\theta = 2\pi v$, although the later setup breaks more symmetry [297].

Analogously to four-point functions in homogeneous CFT, the correlator $\mathcal{G}(x, \bar{x})$ captures an infinite amount of CFT data thanks to the Operator Product Expansion (OPE). In the presence of a defect, two different OPEs are possible, one as a sum of bulk operators, the other in terms of operators localized on the defect [259]. For two-point functions, these OPEs give two conformal block decompositions which must be equal:[3]

$$\mathcal{G}(x, \bar{x}) = \sum_{\widehat{\Delta}, s} \mu_{\widehat{\Delta}, s} \hat{f}_{\widehat{\Delta}, s}(x, \bar{x}) = \left(\frac{\sqrt{x\bar{x}}}{(1-x)(1-\bar{x})} \right)^{\Delta_\phi} \sum_{\Delta, \ell} c_{\Delta, \ell} f_{\Delta, \ell}(x, \bar{x}) \,. \tag{10.3}$$

In this paper, we follow the bootstrap philosophy which uses the crossing equation (10.3) as the starting point. Indeed, we will see that in favorable situations, (10.3) together with basic structural properties of the bulk theory and mild physical assumptions, can be used to fully determine the correlator $\mathcal{G}(x, \bar{x})$. In the case of conformal boundaries, this approach has been successfully carried out in a number of interesting examples [3, 269, 272–275].

The main technical tool we will use to solve crossing analytically is the so-called Lorentzian inversion formula (LIF). Because defect correlators have two different operator product expansions, there exist two inversion formulas, one for each channel. These formulas were obtained in [265, 266] and were already used to study the $\mathbb{Z}_2$ Ising monodromy defect. In this work, we continue with this program and use the LIF to solve more general monodromy defects in the ε–expansion.

We start in section 10.2 with the Wilson-Fisher (WF) fixed point with global $O(2N)$ symmetry. This model is described in $d = 4 - \varepsilon$ dimensions by the following Lagrangian

$$L_{\text{WF}} = \frac{1}{2} (\partial_\mu \phi_i)^2 + \frac{\lambda}{4!} (\phi_i \phi_i)^2 \,, \qquad i = 1, \ldots, 2N \,. \tag{10.4}$$

We define the complex scalar $\phi = \phi_1 + i\phi_2$ and impose a monodromy v under rotations (10.1). Since this model is weakly coupled for $0 < \varepsilon \ll 1$, one can use the Lagrangian description to compute CFT data using Feynman diagrams [256–258]. However, this is not the approach we follow on this work. Although still perturbative in nature, our analysis relies solely on modern analytical bootstrap techniques. The bootstrap has several advantages which allow us to present improvements on previous results. On the one hand, we obtain closed-form expressions for the correlation function $\mathcal{G}(x, \bar{x})$ to order $O(\varepsilon)$, which allows us to extract previously unknown bulk CFT data in an efficient way. On the other hand, we show that the correlator is an analytic function of the monodromy v, and the

---

[3]Here and in the rest of the paper we use the shorthand notation $\mu_{\widehat{\Delta}, s} = |b_{\phi\widehat{\mathcal{O}}}|^2$ and $c_{\Delta, \ell} = a_{\mathcal{O}} \lambda_{\phi\bar{\phi}\mathcal{O}}$, where $b_{\phi\widehat{\mathcal{O}}}$, $a_{\mathcal{O}}$, $\lambda_{\phi\bar{\phi}\mathcal{O}}$ are defined in the main text.

transformation $v \to v + 1$ has the interpretation of a change of boundary condition for low-lying defect operators. We also clarify subtleties related to codimension-two defects that had not appeared in the literature. In particular, we obtain conformal blocks for odd-spin bulk operators, which are related to the existence of parity-odd one-point tensor structures when the codimension is $q = 2$. In order to accommodate these operators, we also have to extend the bulk-to-defect Lorentzian inversion formula [266]. These results not only are applicable to monodromy defects, but to any type of codimension-two defect.

Having used the Wilson-Fisher model as a testing ground for our techniques, we move on to the Wess-Zumino (WZ) model, which is the simplest superconformal model preserving four supercharges. This model consists of a complex scalar $\phi(x)$ and a two-component complex fermion $\psi(x)$. The allowed interactions are fully fixed by supersymmetry, so the action depends on a single coupling constant g:

$$L_{\text{WZ}} = (\partial_\mu \bar{\phi})(\partial_\mu \phi) + \psi^\dagger \bar{\sigma}^\mu \partial_\mu \psi + \frac{g}{2}(\psi\psi\phi + \psi^\dagger \psi^\dagger \bar{\phi}) + \frac{g^2}{4}(\phi\bar{\phi})^2 \,. \tag{10.5}$$

Similarly to the WF case, this model has a fixed point in $d = 4 - \varepsilon$ dimensions that can be studied in diagrammatic perturbation theory.[4] Compared to the Wilson-Fisher fixed point, which has gotten a lot of attention from the bootstrap community [92, 94, 135, 136, 146–149], the literature on the Wess-Zumino model using modern conformal bootstrap is much scarcer, the most notable exceptions being [193, 378].

In section 10.3 we take a small detour in order to fill this gap. In this section we forget momentarily about defects, and we start by modifying the original LIF [125] into a formula that directly extracts OPE coefficients of exchanged superconformal primaries. The main virtues of this formula are that it unmixes the contributions of nearly-degenerate operators, and that it applies to general superconformal theories with four supercharges in any number of dimensions. With this newly developed machinery, we carry out the bootstrap program for bulk four-point functions of chiral operators and extract bulk CFT data to leading order in ε. This is the simplest application of our formalism, and we hope to present a more detailed treatment of the Wess-Zumino model using LIF technology elsewhere.

In section 10.4 we put all the pieces together and study monodromy defects in the Wess-Zumino model. We start by reviewing the relevant superconformal blocks [3], and then move on to use the input of section 10.3 and the LIF to bootstrap two-point functions of chiral fields. The final result can be written in a compact form in terms of a class of one-

---

[4]See [383] for a nice summary and introduction to the literature.

and two-variable special functions which are defined by their series expansions. Because these functions might be relevant for future bootstrap calculations, we study some of their analytic properties in more detail. In particular, we explain how to extract their behavior around $x, \bar{x} \sim 1$ given their series expansions around $x, \bar{x} \sim 0$. This amounts to extracting both bulk and defect CFT data to leading order in ε, which was one of the original goals of this work.

10.2 Wilson-Fisher: Monodromy defects

In this section we study monodromy defects in the Wilson-Fisher fixed point, previous work on this subject include [257, 258].[5] Here we present some small improvements by obtaining the full correlation function at order $O(\varepsilon)$ and extracting the bulk CFT data. This model, interesting on its own, is also a good testing ground for our techniques, which we will later apply to the Wess-Zumino model in section 10.4.

   We start this section studying kinematics of codimension-two defects in d-dimensional Euclidean spacetime. Even though kinematics of defect CFTs are well understood in general [259], the case $q = 2$ turns out to be subtle. In particular, we obtain bulk conformal blocks for odd-spin operators, which have not appeared in the literature before. Furthermore, we extend the bulk-to-defect inversion formula of [266], in order to accommodate odd-spin operators for generic $q = 2$ defects. We end the section by bootstrapping two-point functions of bulk scalars $\langle \phi(x_1) \bar{\phi}(x_2) \rangle$ in the presence of monodromy defects, first for free theories, and then for the more interesting case of the Wilson-Fisher fixed point.

10.2.1 Conformal blocks

When considering the correlator $\langle \phi(x_1) \bar{\phi}(x_2) \rangle$ we use a frame where the operators lie on a plane orthogonal to the defect. Furthermore, using a conformal transformation we set $\bar{\phi}(x_2)$ at one and parametrize the plane using complex coordinates $(x, \bar{x})$:

$$x_1 = \left(\tfrac{1}{2}(x + \bar{x}), \tfrac{1}{2i}(x - \bar{x}), \vec{y} \right), \qquad x_2 = (1, 0, \vec{y}). \tag{10.6}$$

The coordinates $(x, \bar{x})$ are the two cross-ratios of our correlation function and play a central role in the discussion below.[6] Let us now look at the two possible OPE channels in defect CFT.

---

[5]See also [390, 391] for other works using methods slightly different to ours.

[6]The cross ratios for a general frame appear in equation (A.2) of [266].

Defect channel

The defect OPE fuses a single bulk field into a sum of defect fields. In the defect OPE limit, i.e. when $x\bar{x} \to 0$, the leading order in the expansion is normalized as

$$\phi(x, \bar{x}, \vec{y}) \sim \sum_{\widehat{\mathcal{O}}} b_{\phi\widehat{\mathcal{O}}} \left(\frac{\bar{x}}{x}\right)^s (x\bar{x})^{(\widehat{\Delta}-\Delta_\phi)/2} \widehat{\mathcal{O}}(\vec{y}) + \dots, \qquad (10.7)$$

where $\vec{y}$ parametrizes the directions along the defect. Inserting (10.7) in the two-point function gives the leading behavior of defect blocks $\hat{f}_{\widehat{\Delta},s}(x, \bar{x}) \sim x^{(\widehat{\Delta}-s)/2}\bar{x}^{(\widehat{\Delta}+s)/2}$. In order to obtain the full dependence on the cross-ratios, one can write down a Casimir equation which is solved by the following conformal block [259]:

$$\hat{f}_{\widehat{\Delta},s}(x, \bar{x}) = x^{(\widehat{\Delta}-s)/2}\bar{x}^{(\widehat{\Delta}+s)/2}{}_2F_1\left(\widehat{\Delta}, d/2 - 1; \widehat{\Delta} + 2 - d/2; x\bar{x}\right). \qquad (10.8)$$

Even though this discussion is general, let us return momentarily to monodromy defects. Since we work in Euclidean signature, the cross ratios are complex conjugates of each other $x^* = \bar{x}$, and moving $\phi(x_1)$ around the defect corresponds to analytically continuing x ($\bar{x}$) around the origin counterclockwise (clockwise). Together with (10.1), we conclude that our correlation function must satisfy the boundary condition

$$\mathcal{G}(x^{\circlearrowleft}, \bar{x}^{\circlearrowleft}) = e^{+2\pi i v}\mathcal{G}(x, \bar{x}). \qquad (10.9)$$

The monodromy (10.9) combined with the form of the defect block (10.8) requires the defect spectrum to consists of non-integer transverse spins:

$$s = -v + n \quad \text{for} \quad n \in \mathbb{Z}. \qquad (10.10)$$

This observation will be important in the discussion that follows.

Bulk channel

Let us now turn to the bulk OPE $\phi \times \bar{\phi}$. Since the two operators are different, the bulk OPE consists of both even and odd spin operators. As is customary, we use index free notation $\mathcal{O}^{(\ell)}(x, u) = \mathcal{O}^{\mu_1 \cdots \mu_\ell}(x)u_{\mu_1} \dots u_{\mu_\ell}$ and assume the following normalization for the OPE[7]

$$\phi(x_1)\bar{\phi}(x_2) \sim \sum_{\mathcal{O}^{(\ell)}} \lambda_{12\mathcal{O}} \, 2^{\ell/2} \frac{\mathcal{O}^{(\ell)}(x_2, x_{12})}{x_{12}^{\Delta_1 + \Delta_2 - \Delta + \ell}} + \dots, \qquad (10.11)$$

---

[7]The awkward factor $2^{\ell/2}$ leads to four-point blocks normalized as $g_{\Delta,\ell}(z, \bar{z}) \sim z^{(\Delta-\ell)/2}\bar{z}^{(\Delta+\ell)/2}$ in the lightcone limit.

where we keep the leading order in the bulk OPE limit $x_{12}^2 \to 0$. A peculiarity of codimension-two defects is that spinning operators with either even or odd spin can have one-point functions:

$$\ell \text{ even:} \qquad \langle \mathcal{O}^{(\ell)}(x,u) \rangle = \frac{2^{\ell/2} a_{\mathcal{O}}}{|x^i|^{\Delta}} \left(\frac{(x^i u^i)^2}{|x^i|^2} - u^i u^i \right)^{\ell/2} ,$$

$$\ell \text{ odd:} \qquad \langle \mathcal{O}^{(\ell)}(x,u) \rangle = -\frac{i \, 2^{\ell/2} a_{\mathcal{O}} \, \varepsilon_{ij} u^i u^j}{|x^i|^{\Delta+1}} \left(\frac{(x^i u^i)^2}{|x^i|^2} - u^i u^i \right)^{(\ell-1)/2} . \tag{10.12}$$

Here ε_{ij} is the two-index antisymmetric epsilon tensor, which is an allowed tensor for $q=2$ defects. Combining the bulk OPE with the form of the one-point function gives the leading order behavior of blocks with even and odd spin:

$$\lim_{x,\bar{x} \to 1} f_{\Delta,\ell}(x,\bar{x}) = \left[(1-x)(1-\bar{x}) \right]^{(\Delta-\ell)/2} (x - \bar{x})^{\ell} . \tag{10.13}$$

It is perhaps surprising that odd-spin bulk blocks are antisymmetric under $x \leftrightarrow \bar{x}$, but it is a direct consequence of the existence of parity-odd one-point functions (10.12). It is also interesting to consider the normalization of bulk blocks in the lightcone limit

$$f_{\Delta,\ell}(x,\bar{x}) = \begin{cases} (1-x)^{(\Delta-\ell)/2}(1-\bar{x})^{(\Delta+\ell)/2} & 0 < 1-x \ll 1-\bar{x} \ll 1 , \\ (-1)^{\ell}(1-\bar{x})^{(\Delta-\ell)/2}(1-x)^{(\Delta+\ell)/2} & 0 < 1-\bar{x} \ll 1-x \ll 1 . \end{cases} \tag{10.14}$$

As usual, the full dependence of $f_{\Delta,\ell}$ on the cross-ratios can be obtained by solving the Casimir differential equation, which has been worked out in [259, 264]. The case of interest for us is $q=2$, when the differential operator in $x, \bar{x}$ coordinates reads

$$\left(D_x + D_{\bar{x}} + (d-2)\frac{(1-x)(1-\bar{x})}{1-x\bar{x}} \left(x\partial_x + \bar{x}\partial_{\bar{x}} \right) - \frac{1}{2}c_2 \right) f_{\Delta,\ell}(x,\bar{x}) = 0 ,$$

$$D_x = (1-x)^2 x\partial_x^2 + (1-x)^2 \partial_x , \tag{10.15}$$

and the Casimir eigenvalue is $c_2 = \Delta(\Delta - d) + \ell(\ell + d - 2)$. The similarity of (10.15) with the Dolan and Osborn differential operator [31, 32] is apparent. Indeed, it was originally pointed out in [259] that in terms of $z, \bar{z}$ coordinates

$$x = 1 - z , \qquad \bar{x} = (1 - \bar{z})^{-1} , \tag{10.16}$$

the two differential operators are the same. By comparing the lightcone limit of the defect block (10.14) with the lightcone limit of four-point blocks, we obtain the precise mapping

$$f_{\Delta,\ell}(x,\bar{x}) = (-1)^{-(\Delta+\ell)/2} g_{\Delta,\ell} \left(1 - x, \frac{\bar{x}-1}{\bar{x}} \right) . \tag{10.17}$$

Our discussion makes it clear that this relation is valid both for even- and odd-spin bulk operators. In the four-dimensional case, which is relevant for the present work, simple closed-form expressions for the four-point blocks are known [16], which in the defect case map to

$$
\begin{aligned}
f_{\Delta,\ell}(x,\bar{x}) &= \frac{(1-x)(1-\bar{x})}{1-x\bar{x}}\left(k^{0,0}_{\Delta-\ell-2}(1-x)k^{0,0}_{\Delta+\ell}(1-\bar{x}) + (-1)^{\ell}(x \leftrightarrow \bar{x})\right), \\
k^{r,s}_{\beta}(x) &= x^{\beta/2}{}_2F_1\left(\frac{\beta-r}{2},\frac{\beta+s}{2},\beta,x\right).
\end{aligned}
\tag{10.18}
$$

It is easy to check that this is normalized according to (10.14). For general space-time dimensions d, one makes an ansatz of the form [124]

$$
f_{\Delta,\ell}(x,\bar{x}) = \sum_{n=0}^{\infty}\sum_{j=-n}^{n} A_{n,j}(\Delta,\ell)(1-x)^{(\Delta-\ell)/2+n}k^{0,0}_{\Delta+\ell+2j}(1-\bar{x}),
\tag{10.19}
$$

and fixes the coefficients recursively with the Casimir equation (10.15). This process can be implemented efficiently using a computer. For the sake of clarity, we present some low-lying coefficients:

$$
A_{0,0}(\Delta,\ell) = 1, \qquad A_{1,0}(\Delta,\ell) = \frac{\Delta-\ell}{4}, \qquad A_{1,-1}(\Delta,\ell) = -\frac{(d-2)\ell}{2\ell+d-4}.
\tag{10.20}
$$

10.2.2   Bulk-to-defect inversion formula

The Lorentzian Inversion Formula (LIF) [125,126] is a central tool for the analytic bootstrap program. In the presence of defects, one can consider a bulk-to-defect LIF [266] and a defect-to-bulk LIF [265]. The bulk-to-defect LIF is of particular importance in this work, as will become clear in subsequent sections. For codimension-two defects, we need a small extension of the formula presented in [266] which we outline below, and we refer the reader to [266] for further details.

The LIF of [266] was derived assuming that the correlator $\mathcal{G}(x,\bar{x})$ is a symmetric function of $x,\bar{x}$, which is true when the external scalars are identical and the theory preserves parity. In our setup, the bulk expansion generically contains even- and odd-spin blocks, which are symmetric and antisymmetric respectively, so the full correlator has no definite symmetry. Furthermore, our derivation is valid for non-integer values of s, which is the relevant situation for monodromy defects.

The central object of this discussion is the function $\mu(\Delta, s)$, which encodes dimensions of defect operators as poles and their OPE coefficients as residues:

$$\mu_{\widehat{\Delta}_*, s} \equiv b^2_{\widehat{\Delta}_*, s} = -\mathrm{Res}_{\widehat{\Delta} = \widehat{\Delta}_*} \mu(\widehat{\Delta}, s) \,. \tag{10.21}$$

Let us introduce coordinates $x = rw$ and $\bar{x} = r/w$, which in Euclidean signature correspond to a radial coordinate r and a phase w. The conformal block (10.8) can be decomposed as $\hat{f}_{\widehat{\Delta}, s}(r, w) = w^{-s} \hat{f}_{\widehat{\Delta}}(r)$, and the correlation function admits a partial wave expansion

$$\mathcal{G}(r, w) = \sum_s \int_{p/2 - i\infty}^{p/2 + i\infty} \frac{d\widehat{\Delta}}{2\pi i} \mu(\widehat{\Delta}, s) w^{-s} \Psi_{\widehat{\Delta}}(r) \,, \quad \Psi_{\widehat{\Delta}}(r) \equiv \frac{1}{2} \left(\hat{f}_{\widehat{\Delta}} + \frac{K_{p-\widehat{\Delta}}}{K_{\widehat{\Delta}}} \hat{f}_{p-\widehat{\Delta}} \right) , \tag{10.22}$$

where the sum runs for all $-\infty < s < \infty$ and we introduced $K_{\widehat{\Delta}} = \Gamma(\widehat{\Delta})/\Gamma(\widehat{\Delta} - p/2)$ and $p = d - 2$. When the partial wave $\Psi_{\widehat{\Delta}}(r)$ has dimension $\widehat{\Delta} = p/2 + i\nu$ it obeys an orthonormality relation [266]:

$$\int_0^1 dr \frac{(1 - r^2)^{d-2}}{r^{d-1}} \Psi_{\widehat{\Delta}_1}(r) \Psi_{\widehat{\Delta}_2}(r) = \frac{\pi}{2} \frac{K_{p-\widehat{\Delta}_2}}{K_{\widehat{\Delta}_1}} [\delta(\nu_1 - \nu_2) + \delta(\nu_1 + \nu_2)] \,. \tag{10.23}$$

Furthermore, we assume the defect spectrum is such that the transverse spins are integer separated $s_1 - s_2 \in \mathbb{Z}$. In this case, we have the orthonormality relation

$$\oint \frac{dw}{2\pi i w} w^{s_1 - s_2} = \delta_{s_1, s_2} \,, \tag{10.24}$$

where the integral is along the unit circle $|w| = 1$. Combining the partial wave decomposition (10.22) with the orthonormality of our basis, one readily obtains the Euclidean inversion formula:

$$\mu(\widehat{\Delta}, s) = \frac{2 K_{\widehat{\Delta}}}{K_{p - \widehat{\Delta}}} \oint \frac{dw}{2\pi i w} w^s \int_0^1 dr \frac{(1 - r^2)^{d-2}}{r^{d-1}} \Psi_{\widehat{\Delta}}(r) \mathcal{G}(r, w) \,. \tag{10.25}$$

Let us stress that this formula is only valid for physical values of the transverse spin s. Now we would like to deform the integration contour of w into Lorentzian kinematics, leading to a formula analytic in s. However, in order to deform the contour safely, one needs the asymptotic behavior of $\mathcal{G}(r, w)$ for large and small w:

$$\mathcal{G}(r, w) \lesssim w^{-s_+^*} \quad \text{as} \quad w \to 0 \,, \qquad \mathcal{G}(r, w) \lesssim w^{s_-^*} \quad \text{as} \quad w \to \infty \,. \tag{10.26}$$

Then we conclude that for $s > s_+^*$ we can contract the contour towards the origin picking up a discontinuity around the cut $w \in [0, r]$. Similarly, for $s < -s_-^*$ we blow up the

contour to infinity, picking a discontinuity around the cut $w \in [1/r, \infty]$. We then rewrite the resulting integral in terms of $x, \bar{x}$, and keep only poles in $\mu(\widehat{\Delta}, s)$ corresponding to the exchanged operator and not its shadow. After the dust settles, we obtain the bulk-to-defect Lorentzian inversion formula in its final form:

$$\mu(\widehat{\Delta}, s) = \begin{cases} \int_0^1 dx \int_1^{1/x} d\bar{x} \, I_{\widehat{\Delta}, s}(x, \bar{x}) \operatorname{Disc}_{\bar{x}} \mathcal{G}(x, \bar{x}) & \text{for} \quad s > s_+^* \\ \int_0^1 d\bar{x} \int_1^{1/\bar{x}} dx \, I_{\widehat{\Delta}, s}(x, \bar{x}) \operatorname{Disc}_x \mathcal{G}(x, \bar{x}) & \text{for} \quad s < -s_-^* \end{cases} . \tag{10.27}$$

In the above formula, the integration kernel and discontinuities are given by:

$$\begin{aligned} I_{\widehat{\Delta}, s}(x, \bar{x}) &= \frac{1}{4\pi i} \, x^{-\frac{\widehat{\Delta} - s + 2}{2}} \bar{x}^{-\frac{\widehat{\Delta} + s + 2}{2}} (1 - x\bar{x})_2 F_1 \left(\begin{matrix} 1 - \widehat{\Delta}, 2 - d/2 \\ d/2 - \widehat{\Delta} \end{matrix} ; x\bar{x} \right), \\ \operatorname{Disc}_x \mathcal{G}(x, \bar{x}) &= \mathcal{G}(x + i0, \bar{x}) - \mathcal{G}(x - i0, \bar{x}), \\ \operatorname{Disc}_{\bar{x}} \mathcal{G}(x, \bar{x}) &= \mathcal{G}(x, \bar{x} + i0) - \mathcal{G}(x, \bar{x} - i0). \end{aligned} \tag{10.28}$$

This is the same formula obtained in [266] for $s > s_+^*$, but one has to exchange the role of $x \leftrightarrow \bar{x}$ to obtain the defect CFT data for for $s < -s_-^*$. Whenever the correlation function $\mathcal{G}(x, \bar{x})$ is a symmetric function, the positive and negative transverse spin Regge trajectories are identical, but this is not true in general, as we will see in section 10.4.

In practical applications, the main virtue of the LIF is that it kills exact double-twist operators. Indeed, only three classes of bulk operators contribute to the inversion formula:

1. The bulk identity.

2. Operators below the double-twist dimension $\Delta < 2\Delta_\phi + \ell$.

3. Double-twist operators with anomalous dimension $\Delta = 2\Delta_\phi + \ell + 2n + \gamma$.

The universal contribution from the bulk identity will be the subject of section 10.2.3. Operators of the second kind appear frequently in large-N CFTs, where they correspond to single-trace operators, but they play no role in our discussion. Finally, the third type of contributions is central in our discussion of the Wilson-Fisher and Wess-Zumino models, and will be treated in more detail there.

10.2.3 GFF monodromy defect

Having developed the necessary techniques, we are ready to study monodromy defects using analytic bootstrap. We start with a generalized free field (GFF) $\phi(x)$ of dimension

Δ_ϕ. It is well known that the bulk spectrum of GFF consists of the identity and double-twist operators $\Delta_{\ell,n} = 2\Delta_\phi + \ell + 2n$, and we just discussed that these do not contribute to the inversion formula. As a result, we can reconstruct the full defect CFT data from the discontinuity of the bulk identity:

$$\mathrm{Disc}_{\bar{x}}\, \mathcal{G}(x, \bar{x}) = \mathrm{Disc}_{\bar{x}} \left(\frac{\sqrt{x\bar{x}}}{(1-x)(1-\bar{x})} \right)^{\Delta_\phi} = 2i\sin(\pi\Delta_\phi) \left(\frac{\sqrt{x}}{1-x} \right)^{\Delta_\phi} \left(\frac{\sqrt{\bar{x}}}{\bar{x}-1} \right)^{\Delta_\phi}.$$

(10.29)

Plugging the discontinuity in the LIF (10.27), one can obtain the defect spectrum and the OPE coefficients. This is worked out in detail in [266], the main result is that the defect spectrum is given by $\Delta_{s,n} = \Delta_\phi + |s| + 2n$ with the following OPE coefficients:

$$\mu^{\mathrm{GFF}}_{s,n}(\Delta_\phi, d) = \frac{(\Delta_\phi + 1 - d/2)_n (\Delta_\phi)_{2n+|s|}}{n!(n+|s|)!(\Delta_\phi + n + |s| + 1 - d/2)_n}.$$

(10.30)

For now we assume that the LIF converges down to $s = 0$, and we come back to the problem of convergence in section 10.2.3. We would like to use the defect data, which is analytic in s, to consider a monodromy defect in a bulk GFF. As pointed out around equation (10.10), one obtains a monodromy defect by allowing the transverse spin to take non-integer values $s \in -v + \mathbb{Z}$. Since we know the full defect CFT data, we can try to resum it and obtain the full correlation function:

$$\mathcal{G}^{\mathrm{GFF}}_{\Delta_\phi, d, v}(x, \bar{x}) = \sum_{n=0}^{\infty} \sum_{s \in \mathbb{Z}-v} \mu^{\mathrm{GFF}}_{s,n}(\Delta_\phi, d) \hat{f}_{\Delta_\phi + |s| + 2n, s}(x, \bar{x}).$$

(10.31)

As a consistency check, we note that the trivial case with no monodromy defect $v = 0$, resums to the bulk identity as one would expect:

$$\mathcal{G}^{\mathrm{GFF}}_{\Delta_\phi, d, v=0}(x, \bar{x}) = \sum_{m=0}^{\infty} \sum_{s \in \mathbb{Z}} \mu^{\mathrm{GFF}}_{m,s}(\Delta_\phi, d) \hat{f}_{\Delta_\phi + s + 2m, s}(x, \bar{x}) = \left(\frac{\sqrt{x\bar{x}}}{(1-x)(1-\bar{x})} \right)^{\Delta_\phi}.$$

(10.32)

In the sections below, we consider three simple cases where the two-point correlator $\mathcal{G}(x, \bar{x})$ can also be obtained in closed form.

Free theory monodromy defect

The first simplification is to consider free bulk fields, which have conformal dimension $\Delta_\phi^{\mathrm{free}} = (d-2)/2$. In this case only the leading transverse-twist trajectory $n = 0$ contributes to the defect expansion, see (10.30). Ideally we would like to find $\mathcal{G}^{\mathrm{free}}_{d,v}(x, \bar{x}) \equiv$

$\mathcal{G}^{\text{GFF}}_{(d-2)/2,d,v}(x,\bar{x})$ for general values of d and v, but this turns out to be hard.[8] Fortunately, for even spacetime dimension $d = 4, 6, \ldots$ the calculation simplifies dramatically and one can obtain closed form expressions. For example, the $d = 4$ correlator is [258]

$$\mathcal{G}^{\text{free}}_{4,v}(x,\bar{x}) = \frac{\sqrt{x\bar{x}}}{(1-x)(1-\bar{x})} \frac{(1-\bar{x})x^v + (1-x)\bar{x}^{1-v}}{1 - x\bar{x}} \,. \tag{10.33}$$

Similar expressions, though more lengthy, can be obtained for higher even values of d. Keeping only the leading terms as $x \to 1$, the expressions simplify and it is possible to guess a formula for the correlator which is analytic in d

$$\mathcal{G}^{\text{free}}_{d,v}(x,\bar{x}) = \left(\frac{\sqrt{x\bar{x}}}{(1-x)(1-\bar{x})} \right)^{\Delta^{\text{free}}_\phi} \Bigg(1 + \tag{10.34}$$

$$+ C^{\text{free}}_{d,v} ((1-x)(1-\bar{x}))^{\Delta^{\text{free}}_\phi} \left[{}_2F_1\left(\begin{matrix} \Delta^{\text{free}}_\phi, \Delta^{\text{free}}_\phi + v \\ d - 1 \end{matrix} ; 1 - \bar{x} \right) + O(1-x) \right] \Bigg),$$

where we introduced the constants

$$C^{\text{GFF}}_{\Delta_\phi,d,v} = -\frac{\Gamma(\Delta_\phi + 1 - v)\Gamma(\Delta_\phi + 1 + v)}{(\Delta_\phi + v)\Gamma(2\Delta_\phi + 1)\Gamma(v)\Gamma(1 - v)} \,, \qquad C^{\text{free}}_{d,v} = C^{\text{GFF}}_{(d-2)/2,d,v} \,. \tag{10.35}$$

Even though (10.34) has been obtained by non-rigorous means, it passes a number of non-trivial consistency checks. It is correct for any even $d = 4, 6, \ldots$, it is consistent with the result [265] for $v = 1/2$ and general d, and it is consistent with the result (10.46) in $d = 4 - \varepsilon$ dimensions.

The power of equation (10.34) is that it captures all the bulk CFT data. Indeed, since the bulk theory is free, the spectrum consists of double-twist operators $\Delta_{\ell,0} = 2\Delta^{\text{free}}_\phi + \ell$, namely

$$\mathcal{G}^{\text{free}}_{d,v}(x,\bar{x}) = \left(\frac{\sqrt{x\bar{x}}}{(1-x)(1-\bar{x})} \right)^{(d-2)/2} \left(1 + \sum_{\ell=0}^{\infty} c^{\text{free}}_\ell f_{\ell+d-2,\ell}(x,\bar{x}) \right) \,. \tag{10.36}$$

Here we remind the reader that we use the shorthand notation $c_{\mathcal{O}} = \lambda_{\phi\bar{\phi}\mathcal{O}} a_{\mathcal{O}}$. Using the bulk blocks (10.19) and comparing (10.34)-(10.36) at leading order in $(1-x)$, one can

---

[8]After this paper was submitted to the `arXiv`, we have been made aware by Y. Linke that there exists a closed form expression for $\mathcal{G}^{\text{free}}_{d,v}(x,\bar{x})$ in terms of Appell F_1 functions. The precise formula can be provided by the authors upon request.

obtain the bulk CFT data order by order in $(1 - \bar{x})$. For the first few coefficients we find

$$
\begin{aligned}
c_0^{\text{free}} &= C_{d,v}^{\text{free}}, & c_2^{\text{free}} &= \frac{(d-2)(v-1)v}{8(d-1)} C_{d,v}^{\text{free}}, \\
c_1^{\text{free}} &= \frac{(d-2)(2v-1)}{4(d-1)} C_{d,v}^{\text{free}}, & c_3^{\text{free}} &= \frac{(d-2)(d+2)(v-1)v(2v-1)}{96(d-1)(d+1)} C_{d,v}^{\text{free}}.
\end{aligned}
\tag{10.37}
$$

The first three coefficients are in perfect agreement with the explicit calculation of [258] up to a difference in normalization.[9] The main advantage of knowing the correlation function is that we can extract the bulk data for very high values of the spin ℓ. In doing this, we observed the CFT data satisfies a simple two-step recursion relation

$$
c_{\ell+2}^{\text{free}} = \frac{(2v-1)(d+2\ell)}{4(\ell+2)(d+\ell)} c_{\ell+1}^{\text{free}} + \frac{(\ell-1)(d+\ell-3)(d+2\ell-2)(d+2\ell)}{16(\ell+2)(d+\ell)(d+2\ell-3)(d+2\ell-1)} c_\ell^{\text{free}},
\tag{10.38}
$$

with the initial conditions as given in (10.37).[10]

Alternate boundary condition

The inversion formula predicts $\Delta_s = \Delta_\phi^{\text{free}} + |s|$ for the free theory defect spectrum. However, as we pointed in section 10.2.2, this result only holds for spins $|s| > s_*$, where the threshold spin s_* cannot be fixed from the bootstrap perspective. In this subsection, we relax the assumption $s_* = 0$ for defects in free theories, which we show is related to continuing the correlator as $v \to v + n$ for $n \in \mathbb{Z}$.

In a free theory, the bulk equations of motion imply the defect spectrum is of the form

$$
\Delta_s^{\pm} = \frac{d-2}{2} \pm |s|.
\tag{10.40}
$$

The positive modes Δ_s^+ are given by the inversion formula, while the negative modes Δ_s^- can arise as low transverse-spin ambiguities for $|s| < s_*$.[11] The negative modes were studied

---

[9]The value of c_3 also agrees with v2 of [258].

[10]For $d = 4$ we managed to obtain a closed-form expression by inverting the exact correlator (10.33):

$$
\begin{aligned}
c_\ell^{\text{free}} \overset{d=4}{=} \frac{\Gamma(\ell-1)\Gamma(\ell+1)^2 \sin^2(\pi v)}{2^{4\ell+1} \pi \Gamma(\ell+\frac{1}{2})\Gamma(\ell+\frac{3}{2})\Gamma(\ell-v+1)\Gamma(\ell+v)} \Bigg[\\
\Gamma(2-v)\Gamma(\ell+v) \, {}_3F_2\left(\begin{matrix} \ell+1, \ell+1, \ell-1 \\ 2(\ell+1), \ell-v+1 \end{matrix} ; 1 \right) + (-1)^\ell \big(v \leftrightarrow 1-v\big) \Bigg].
\end{aligned}
\tag{10.39}
$$

[11]In the setup of [258], the values $\Delta_s^{\pm}$ correspond to the two possible boundary conditions certain KK modes can have on the boundary of hyperbolic space H^{d-1}. We borrow the name of the section from this reference.

in great detail in [294, 295] (see also [292, 390]). The outcome of these works is that if both Δ_s^+ and Δ_s^- are present, the resulting defect is non-trivial. Since we are interested on free defects, let us assume that for $s = -v$ we have a negative mode instead of a positive mode. To obtain the correlator we substract the positive mode and add the negative one:

$$\mathcal{G}_{d,v}^{\text{free},-}(x,\bar{x}) = \mathcal{G}_{d,v}^{\text{free}}(x,\bar{x}) - \frac{\Gamma(\Delta_\phi^{\text{free}} + v)}{\Gamma(\Delta_\phi^{\text{free}})\Gamma(1+v)}\hat{f}_{\Delta_{-v}^+, -v}(x,\bar{x}) + \mu_{-v}^{\text{free},-}\hat{f}_{\Delta_{-v}^-, -v}(x,\bar{x}). \quad (10.41)$$

The OPE coefficient $\mu_{-v}^{\text{free},-}$ is unknown because, by assumption, the inversion formula cannot be trusted for the negative mode $s = -v$. Let us keep this OPE coefficient arbitrary and try to expand the correlator in the bulk channel:

$$\mathcal{G}_{d,v}^{\text{free},-}(x,\bar{x}) = \left(\frac{\sqrt{x\bar{x}}}{(1-x)(1-\bar{x})}\right)^{(d-2)/2}\left(1 + \sum_{\ell=0}^\infty c_\ell^{\text{free},-} f_{\ell+d-2,\ell}(x,\bar{x})\right). \quad (10.42)$$

Perhaps surprisingly, the correlator does not admit a bulk expansion of the above form. Instead, one needs to add extra bulk blocks with unphysical conformal dimensions. The only way for these unphysical operators to drop out is if the defect OPE coefficient takes the following value:

$$\mu_{-v}^{\text{free},-} = \frac{\Gamma(\Delta_\phi^{\text{free}} - v)}{\Gamma(\Delta_\phi^{\text{free}})\Gamma(1-v)}.$$

This is in perfect agreement with the explicit calculation of [258].

Now, the $x \to 1$ limit of the free correlator is given by (10.34), using hypergeometric identities one can combine (10.34) with (10.41) to obtain

$$\mathcal{G}_{d,v}^{\text{free},-}(x,\bar{x}) = \left(\frac{\sqrt{x\bar{x}}}{(1-x)(1-\bar{x})}\right)^{\Delta_\phi^{\text{free}}}\left(1+ \right. \quad (10.43)$$

$$\left. C_{v+1,d}((1-x)(1-\bar{x}))^{\Delta_\phi^{\text{free}}}\left[{}_2F_1\left(\begin{matrix}\Delta_\phi^{\text{free}}, \Delta_\phi^{\text{free}}+v+1\\ d-1\end{matrix}; 1-\bar{x}\right) + O(1-x)\right]\right).$$

Interestingly, this is just the original expression with the replacement $v \to v+1$. Since (10.43) determines completely the bulk CFT data, and the bulk spectrum is independent of v, the full correlators satisfies the same relation:

$$\mathcal{G}_{d,v}^{\text{free},-}(x,\bar{x}) = \mathcal{G}_{d,v+1}^{\text{free}}(x,\bar{x}). \quad (10.44)$$

As a result, the bulk OPE coefficients for alternate boundary conditions are obtained from (10.37) by $v \to v + 1$. For spin $\ell = 0, 2$ we find perfect agreement with explicit calculation [258]:

$$c_0^{\text{free},-} = C_{v+1,d}, \qquad c_1^{\text{free},-} = \frac{(d-2)(2v+1)}{4(d-1)} C_{v+1,d}. \tag{10.45}$$

One can turn on more negative modes in a similar way. Note that in general these violate the defect unitarity bound, but this does not affect the discussion. In particular, if we use negative modes for $s = -v, -v - 1, \ldots, -v - n + 1$, we find that the correlator is given by $\mathcal{G}_{v+n,d}^{\text{free}}(x, \bar{x})$. Similarly, if we turn on negative modes for $s = 1 - v, 2 - v, \ldots, n - v$ the correlator is given by $\mathcal{G}_{v-n,d}^{\text{free}}(x, \bar{x})$. More complicated choices of negative modes do not seem to generate such simple structure.

GFF monodromy defect in $d = 4 - \varepsilon$

In preparation for the analysis of the Wilson-Fisher fixed point, let us study GFF as a perturbation around free theory. Consider a GFF scalar of dimension $\Delta_\phi = 1 - \delta_\phi \varepsilon$ in $d = 4 - \varepsilon$ dimensions. The defect data has been presented in equation (10.30). In order to also extract bulk CFT data, it is necessary to resum the defect expansion. The zeroth order result appears in (10.33), while here we carry out the resummation to leading order in $O(\varepsilon)$. For the leading transverse-twist family, there are contributions at $O(\varepsilon)$ from the OPE coefficients, the defect blocks and the defect dimensions. Furthermore, there are higher-twist families with $n > 0$ that only contribute with tree-level dimensions and OPE coefficients. The complete $O(\varepsilon)$ contribution is then:

$$\begin{aligned}
\mathcal{G}_{1-\delta_\phi\varepsilon,4-\varepsilon,v}^{\text{GFF},O(\varepsilon)}(x, \bar{x}) &= \varepsilon \sum_{n=0}^{\infty} \sum_{s \in -v+\mathbb{Z}} \partial_\varepsilon \left(\mu_{s,n}^{\text{GFF}}(1 - \delta_\phi\varepsilon, 4 - \varepsilon) \hat{f}_{1+|s|-\delta_\phi\varepsilon,s}(x, \bar{x}) \right)_{\varepsilon=0} \\
&= -\delta_\phi\varepsilon \frac{(x\bar{x})^{1/2}}{1 - x\bar{x}} \left[\frac{x^v}{1 - x} \left(\Phi(x, 1, v) + H_{v-1} + \log\left(\frac{\sqrt{x\bar{x}}}{1 - x\bar{x}} \right) \right) \right. \\
&\qquad \left. + \frac{\bar{x}x^v}{1 - \bar{x}} \big(\Phi(x, 1, v) - \Phi(x\bar{x}, 1, v)\big) + (x \leftrightarrow \bar{x}, v \leftrightarrow 1 - v) \right].
\end{aligned} \tag{10.46}$$

The result is written in terms of harmonic numbers H_n and Hurwitz-Lerch zeta function $\Phi(x, 1, v)$, which has nice properties reviewed in appendix 10.A.2. As a consistency check, for a free defect $\delta_\phi = 1/2$, the correlation function (10.46) at leading order in $x \to 1$ agrees

with (10.34) at leading order in ε. Let us also mention that there is a curious non-trivial cancellation of terms such that the final result is proportional to δ_ϕ.

We are now ready to expand in the bulk channel. Once more, since the bulk theory is of the GFF type, the spectrum contains higher-twist families:

$$\mathcal{G}^{\text{GFF}}_{\Delta_\phi,d,v}(x,\bar{x}) = \left(\frac{\sqrt{x\bar{x}}}{(1-x)(1-\bar{x})}\right)^{1-\delta_\phi\varepsilon} \left(1 + \sum_{n=0}^{\infty}\sum_{\ell=0}^{\infty} c^{\text{GFF}}_{\ell,n} f_{2\Delta_\phi+\ell+2n,\ell}(x,\bar{x})\right). \quad (10.47)$$

As explained before, the bulk OPE coefficients can be extracted order by order in $(1-x),(1-\bar{x})$ using the bulk blocks in the form (10.19). Some of the low-lying coefficients are:

$$\begin{aligned}
c^{\text{GFF}}_{0,0} &= C^{\text{GFF}}_{\Delta_\phi,d,v} + O(\varepsilon^2)\,,\\
c^{\text{GFF}}_{1,0} &= \frac{1}{18}C^{\text{GFF}}_{\Delta_\phi,d,v}(2v-1)(3-\delta_\phi\varepsilon) + O(\varepsilon^2)\,,\\
c^{\text{GFF}}_{2,0} &= \frac{1}{36}C^{\text{GFF}}_{\Delta_\phi,d,v}v(v-1)(3-\delta_\phi\varepsilon) + O(\varepsilon^2)\,,\\
c^{\text{GFF}}_{0,1} &= \frac{\varepsilon}{96}(2\delta_\phi-1)v(v-1)\left(v^2-v+4\right) + O(\varepsilon^2)\,.
\end{aligned} \quad (10.48)$$

The interested reader can find more OPE coefficients in the attached `Mathematica` notebook.

10.2.4   Wilson-Fisher monodromy defect

The last model we consider in this section is the $O(2N)$ Wilson-Fisher (WF) fixed point in $d = 4-\varepsilon$ dimensions.[12] Following [257, 258], we impose a monodromy v to the complex scalar $\phi = \phi_1 + i\phi_2$. Besides the defect CFT data, we improve on existing results by computing the two-point function to order $O(\varepsilon)$ and by extracting the bulk CFT data. As already announced, we use the Lorentzian Inversion formula (10.27), which reconstructs defect CFT data from the discontinuity of the correlator $\text{Disc}\,\mathcal{G}(x,\bar{x})$. In perturbative CFTs, the discontinuity can be computed using information which is known from bulk physics at lower orders in perturbation theory.

Let us remind the reader that the identity and double-twist operators with anomalous dimensions contribute to the defect CFT data through the LIF. For the Wilson-Fisher fixed point, there are two important simplifications. One the one hand, the external scalar has dimension $\Delta_\phi = (d-2)/2 + O(\varepsilon^2)$, so the GFF part of the correlator behaves as in free

---

[12]The literature on the WF $O(N)$ model without defects is too vast to review here. However, let us mention the nice references [135, 136], which use analytic bootstrap techniques that inspired our work.

theory. On the other, the leading-twist trajectory has anomalous dimensions starting at order $O(\varepsilon^2)$, i.e. $\Delta = 2\Delta_\phi + \ell + O(\varepsilon^2)$ for $\ell > 0$, and only the $\ell = 0$ operator gets corrected at order $O(\varepsilon)$:

$$\Delta_{\phi\bar\phi} = 2\Delta_\phi + \gamma^{(1)}_{\phi\bar\phi}\varepsilon + O(\varepsilon^2) = 2\Delta_\phi + \frac{N+1}{N+4}\varepsilon + O(\varepsilon^2). \tag{10.49}$$

Our analysis is simplified dramatically, because the discontinuity can be obtained from a single bulk block. In order to compute the discontinuity, we rewrite bulk blocks as

$$f_{\Delta,\ell}(x,\bar x) = \left[(1-x)(1-\bar x)\right]^{(\Delta-\ell)/2}\tilde f_{\Delta,\ell}(x,\bar x). \tag{10.50}$$

The function $\tilde f_{\Delta,\ell}(x,\bar x)$ admits an expansion in integer powers of $(1-x),(1-\bar x)$, so only the prefactor in (10.50) can contribute to the discontinuity. Combining the block with the overall factor $\left(\frac{\sqrt{x\bar x}}{(1-x)(1-\bar x)}\right)^{\Delta_\phi}$ one obtains

$$\begin{aligned}
\mathcal{G}(x,\bar x)|_{\text{singular}} &= \frac{\varepsilon}{2}c_0\gamma^{(1)}_{\phi\bar\phi}(x\bar x)^{\Delta_\phi/2}\log\left[(1-x)(1-\bar x)\right]\tilde f_{2,0}(x,\bar x) \\
&= -\frac{\varepsilon}{2}c_0\gamma^{(1)}_{\phi\bar\phi}\log\left[(1-x)(1-\bar x)\right]\frac{(x\bar x)^{1/2}\log(x\bar x)}{1-x\bar x}\,.
\end{aligned} \tag{10.51}$$

Here $\mathcal{G}(x,\bar x)|_{\text{singular}}$ is the part of the correlator contributing to $\operatorname{Disc}\mathcal{G}(x,\bar x)$ at order $O(\varepsilon)$. Notice it does not include the bulk identity, because it has been studied separately in sections 10.2.3 and 10.2.3. To obtain (10.51) it was necessary to use the closed-form expression (10.18) of the bulk blocks in $d = 4$. The next step in our calculation is to use the definition (10.28) of the discontinuity to obtain

$$\operatorname{Disc}_x \mathcal{G}(x,\bar x) = \operatorname{Disc}_{\bar x} \mathcal{G}(x,\bar x) = 2\pi i\,\frac{\varepsilon}{2}\frac{v(v-1)}{2}\frac{N+1}{N+4}\frac{(x\bar x)^{1/2}\log(x\bar x)}{1-x\bar x}\,. \tag{10.52}$$

The integrand of the LIF is $O(\varepsilon)$, so we can evaluate the integration kernel (10.28) exactly in $d = 4$. The double integral in the LIF is simple to do, for instance when $s > 0$ one obtains

$$\begin{aligned}
\mu(\widehat\Delta, s) &= \varepsilon\frac{v(v-1)}{8}\frac{(N+1)}{(N+4)}\int_0^1 dx\int_1^{1/x}d\bar x\,\log(x\bar x)x^{-\frac{\widehat\Delta-s+1}{2}}\bar x^{-\frac{\widehat\Delta+s+1}{2}} \\
&= -\varepsilon\frac{v(v-1)}{2}\frac{(N+1)}{(N+4)}\frac{1}{s\left(\widehat\Delta-(s+1)\right)^2}\,.
\end{aligned} \tag{10.53}$$

The replacement $s \to |s|$ produces an expression also valid for negative transverse spin. It is well understood that a double-pole in $\widehat\Delta$ indicates defect anomalous dimensions, see [266]

for details. To this, one should add the contribution from the bulk identity. All in all, we conclude that the defect spectrum consists of a single family with the following CFT data:

$$\widehat{\Delta}_s = \frac{d-2}{2} + |s| + \varepsilon \hat{\gamma}_s^{(1)} + O(\varepsilon^2) \,, \qquad \hat{\gamma}_s^{(1)} = \frac{v(v-1)}{2} \frac{(N+1)}{(N+4)} \frac{1}{|s|} \,,$$
$$\mu_s = \frac{(1-\varepsilon/2)_{|s|}}{|s|!} + O(\varepsilon^2) \,, \tag{10.54}$$

which is in perfect agreement with the literature [257, 258].

Let us now extract the bulk OPE coefficients to order $O(\varepsilon)$. As for the free and GFF case, the first step is to resum the defect expansion. The contribution of the bulk identity to the full correlator has been computed in equations (10.33) and (10.46), where one has to set $\delta_\phi = 1/2$ because ϕ behaves as a free field plus $O(\varepsilon^2)$ corrections. There is a contribution which is new for the Wilson-Fisher fixed point, which comes from the defect anomalous dimensions:

$$\mathcal{G}_{\mathrm{WF}}(x, \bar{x}) = \varepsilon \sum_{s \in -v + \mathbb{Z}} b_{|s|}^2 \hat{\gamma}_{|s|}^{(1)} \partial_{\widehat{\Delta}} \hat{f}_{\widehat{\Delta}, s}(x, \bar{x})\big|_{\widehat{\Delta} = |s| + 1}$$
$$= \varepsilon \frac{v(v-1)}{4} \frac{(N+1)}{(N+4)} \frac{(x\bar{x})^{1/2} \log(x\bar{x})}{1 - x\bar{x}} \left[x^v \Phi(x, 1, v) + \bar{x}^{1-v} \Phi(\bar{x}, 1, 1-v) \right] . \tag{10.55}$$

For $v = 1/2$ and $N = 1/2$, this reproduces the Ising $\mathbb{Z}_2$ monodromy defect result [265].

We have obtained the full two-point correlation function to $O(\varepsilon)$, so it is now an easy exercise to extract the bulk OPE coefficients. Besides the twist-two there is also a twist-four family:[13]

$$\mathcal{G}_{d,v}^{\mathrm{free}}(x, \bar{x}) + \mathcal{G}_{\mathrm{WF}}(x, \bar{x}) = \left(\frac{\sqrt{x\bar{x}}}{(1-x)(1-\bar{x})} \right)^{\Delta_\phi} \left(1 + c_{0,0} f_{d-2+\varepsilon\gamma_{\phi\phi}^{(1)},0}(x, \bar{x}) \right.$$
$$\left. + \sum_{\ell=1}^{\infty} c_{\ell,0} f_{\ell+d-2,\ell}(x, \bar{x}) + \sum_{\ell=0}^{\infty} c_{\ell,1} f_{\ell+4,\ell}(x, \bar{x}) \right) . \tag{10.56}$$

The OPE coefficients of the leading-twist trajectory take a particularly simple form after

---

[13]The absence of higher-twist families at this order was suggested in [269] for $\ell = 0$, and then proven in [135].

normalizing by the free piece

$$
\begin{aligned}
c_{0,0} &= c_0^{\text{free}} \left(1 + \frac{\varepsilon}{2} \frac{(N+1)}{(N+4)} (H_{v-1} + H_{-v}) + O(\varepsilon^2) \right), \\
c_{1,0} &= c_1^{\text{free}} \left(1 + \frac{3\varepsilon}{2} \frac{(N+1)}{(N+4)} + O(\varepsilon^2) \right), \\
c_{2,0} &= c_2^{\text{free}} \left(1 + \frac{\varepsilon}{6} \frac{(N+1)}{(N+4)} \frac{(3v-2)(3v-1)}{v(v-1)} + O(\varepsilon^2) \right), \\
c_{3,0} &= c_3^{\text{free}} \left(1 + \frac{\varepsilon}{6} \frac{(N+1)}{(N+4)} \frac{(10v^2 - 10v + 3)}{v(v-1)} + O(\varepsilon^2) \right).
\end{aligned}
\tag{10.57}
$$

On the other hand, the subleading-twist trajectory has the following CFT data:

$$
\begin{aligned}
c_{0,1} &= \frac{\varepsilon}{16} \frac{(N+1)}{(N+4)} v^2 (v-1)^2 + O(\varepsilon^2), \\
c_{1,1} &= \frac{\varepsilon}{144} \frac{(N+1)}{(N+4)} v^2 (v-1)^2 (2v-1) + O(\varepsilon^2), \\
c_{2,1} &= \frac{\varepsilon}{1920} \frac{(N+1)}{(N+4)} v^2 (v-1)^2 \left(5v^2 - 5v + 2 \right) + O(\varepsilon^2).
\end{aligned}
\tag{10.58}
$$

All our results are in perfect agreement with the Ising $\mathbb{Z}_2$ monodromy defect [265]. The interested reader can find the bulk OPE coefficients for higher values of ℓ in the attached `Mathematica` notebook.

10.3 Wess-Zumino: Bulk theory

Superconformal field theories (SCFTs) in non-integer dimensions were studied in [193, 378], where the numerical bootstrap gave evidence that the Wess-Zumino model (10.5) is perhaps the simplest SCFT preserving four supercharges. In this section we study the Wess-Zumino model in $d = 4 - \varepsilon$ dimensions (without defects) using the analytic bootstrap, and the results will be needed for the study of defects in section 10.4. We work to leading order in $O(\varepsilon)$, but the same methods also work at higher orders in ε, a subject that we plan to study in future work. For the reader that is mostly interested on the final results, we present a self-contained summary of the CFT data in section 10.3.4.

10.3.1 Generalities

Let us briefly review some generalities of SCFT in non-integer dimensions, more details can be found in [193].[14] The conformal part of the algebra is generated by the usual operators D, P_i, K_i and M_{ij} with $i = 1, \ldots, d$. There are exactly four Poincaré supercharges Q_α^+ and $Q_{\dot\alpha}^-$ and four conformal supercharges $S^{\dot\alpha +}$ and $S^{\alpha -}$, where the indices take two values $\alpha, \dot\alpha = 1, 2$ regardless of the spacetime dimension. The supercharges obey the usual supersymmetry algebra

$$\{Q_\alpha^+, Q_{\dot\alpha}^-\} = \Sigma_{\alpha\dot\alpha}^i P_i \,, \qquad \{S^{\dot\alpha +}, S^{\alpha -}\} = \bar\Sigma_i^{\dot\alpha\alpha} P_i \,. \tag{10.59}$$

There is also a generator R of $U(1)_R$ symmetry, under which Q_α^+ and $Q_{\dot\alpha}^-$ have charge $+1$ and -1 respectively. The monodromy defects in section 10.4 will be naturally obtained by twisting this $U(1)_R$ symmetry.

In what follows, we focus our attention on chiral-primary operators ϕ and their complex conjugates $\bar\phi$. These operators are killed by supercharges of the same chirality, and the superconformal algebra fixes their conformal dimension in terms of their R-charge:

$$\left[Q_\alpha^+, \phi(0)\right] = \left[Q_{\dot\alpha}^-, \bar\phi(0)\right] = 0 \quad \Rightarrow \quad \Delta_\phi = \Delta_{\bar\phi} = \frac{d-1}{2} R_\phi = -\frac{d-1}{2} R_{\bar\phi} \,. \tag{10.60}$$

In order to bootstrap the Wess-Zumino model without defects, we consider four-point functions of ϕ and $\bar\phi$. If we focus on the s-channel expansion, there are three inequivalent orderings of the external operators:

$$\langle \phi(x_1)\phi(x_2)\bar\phi(x_3)\bar\phi(x_4)\rangle = \frac{\mathcal{F}(z,\bar z)}{(x_{12}^2 x_{34}^2)^{\Delta_\phi}} = \frac{1}{(x_{12}^2 x_{34}^2)^{\Delta_\phi}} \sum_{\Delta,\ell \text{ even}} a_{\Delta,\ell}\, g_{\Delta,\ell}(z,\bar z)\,,$$

$$\langle \phi(x_1)\bar\phi(x_2)\phi(x_3)\bar\phi(x_4)\rangle = \frac{\mathcal{G}(z,\bar z)}{(x_{12}^2 x_{34}^2)^{\Delta_\phi}} = \frac{1}{(x_{12}^2 x_{34}^2)^{\Delta_\phi}} \sum_{\Delta,\ell} b_{\Delta,\ell}\, G_{\Delta,\ell}(z,\bar z)\,, \tag{10.61}$$

$$\langle \bar\phi(x_1)\phi(x_2)\phi(x_3)\bar\phi(x_4)\rangle = \frac{\tilde{\mathcal{G}}(z,\bar z)}{(x_{12}^2 x_{34}^2)^{\Delta_\phi}} = \frac{1}{(x_{12}^2 x_{34}^2)^{\Delta_\phi}} \sum_{\Delta,\ell} (-1)^\ell b_{\Delta,\ell}\, \tilde{G}_{\Delta,\ell}(z,\bar z)\,.$$

In the above formula $a_{\Delta,\ell}$ and $b_{\Delta,\ell}$ are shorthand notation for three-point OPE coefficients

---

[14]A different type of superconformal theories in non-integer dimensions also appear in the context of Parisi-Sourlas supersymmetry [379, 380]

squared. The three orderings above are related to each other by simple crossing relations:

$$
\begin{aligned}
\mathcal{G}(z, \bar{z}) &= \left(\frac{z\bar{z}}{(1-z)(1-\bar{z})} \right)^{\Delta_\phi} \mathcal{G}(1-z, 1-\bar{z}), \\
\mathcal{F}(z, \bar{z}) &= \left(\frac{z\bar{z}}{(1-z)(1-\bar{z})} \right)^{\Delta_\phi} \tilde{\mathcal{G}}(1-z, 1-\bar{z}).
\end{aligned}
\tag{10.62}
$$

The functions $\mathcal{G}(z, \bar{z})$ and $\tilde{\mathcal{G}}(z, \bar{z})$ capture the same CFT data in their s-channel expansion, since they are related by $1 \leftrightarrow 2$.

The constraints of supersymmetry are accounted for by expanding the correlation function in terms of superconformal blocks [193]. It can be shown that in the $\phi \times \phi$ OPE superconformal blocks reduce to regular non-supersymmetric blocks $g_{\Delta, \ell}$. On the other hand, the superblocks $G_{\Delta, \ell}$ are non-trivial for the $\phi \times \bar{\phi}$ OPE. Interestingly, in any dimension the superblocks take the simple form of non-supersymmetric blocks for unequal external operators with a suitable prefactor:

$$
G_{\Delta, \ell}(z, \bar{z}) = (z\bar{z})^{-1/2} g_{\Delta+1, \ell}^{1,1}, \qquad \tilde{G}_{\Delta, \ell}(z, \bar{z}) = (z\bar{z})^{-1/2} g_{\Delta+1, \ell}^{1,-1}.
\tag{10.63}
$$

Superconformal blocks capture the contributions to the OPE of all exchanged operators that belong to the same supermultiplet, which means they should decompose as finite sums of non-supersymmetric blocks with relative coefficients fixed by susy. This is indeed the case

$$
\begin{aligned}
G_{\Delta, \ell}(z, \bar{z}) &= g_{\Delta, \ell} + a_1 \, g_{\Delta+1, \ell+1} + a_2 \, g_{\Delta+1, \ell-1} + a_3 \, g_{\Delta+2, \ell}, \\
\tilde{G}_{\Delta, \ell}(z, \bar{z}) &= g_{\Delta, \ell} - a_1 \, g_{\Delta+1, \ell+1} - a_2 \, g_{\Delta+1, \ell-1} + a_3 \, g_{\Delta+2, \ell},
\end{aligned}
\tag{10.64}
$$

where the explicit coefficients are

$$
\begin{aligned}
a_1 &= \frac{(\Delta + \ell)}{4(\Delta + \ell + 1)}, \\
a_2 &= \frac{\ell(\ell + d - 3)(\Delta - \ell - d + 2)}{(2\ell + d - 4)(2\ell + d - 2)(\Delta - \ell - d + 3)}, \\
a_3 &= \frac{\Delta(\Delta - d + 3)(\Delta + \ell)(\Delta - \ell - d + 2)}{4(2\Delta - d + 4)(2\Delta - d + 2)(\Delta + \ell + 1)(\Delta - \ell - d + 3)}.
\end{aligned}
\tag{10.65}
$$

10.3.2 Inversion formula

The next tool we need are inversion formulas, which reconstruct the CFT data from certain discontinuities of correlators [125]. The main object of interest are functions that encode

dimensions as poles and OPE coefficients as residues:

$$a_{\Delta,\ell} = -\operatorname{Res}_{\Delta'=\Delta} a(\Delta',\ell)\,, \qquad b_{\Delta,\ell} = -\operatorname{Res}_{\Delta'=\Delta} b(\Delta',\ell)\,. \tag{10.66}$$

Let us start with the inversion formula that reconstructs $a(\Delta,\ell)$. Since the $\phi \times \phi$ OPE uses non-supersymmetric blocks, we can use the inversion formula originally derived by Caron-Huot [125]:

$$a(\Delta,\ell) = \frac{1+(-1)^\ell}{4} \kappa^{0,0}_{\Delta+\ell} \int_0^1 \int_0^1 \frac{dz d\bar{z}}{(z\bar{z})^d} |z-\bar{z}|^{d-2} \, g_{\ell+d-1,\Delta+1-d}(z,\bar{z}) \, \mathrm{dDisc}[\mathcal{F}(z,\bar{z})]\,. \tag{10.67}$$

The double discontinuity is defined in the usual way

$$\mathrm{dDisc}[\mathcal{F}(z,\bar{z})] = \mathcal{F}(z,\bar{z}) - \frac{1}{2}\mathcal{F}(z,\bar{z}^{\circlearrowleft}) - \frac{1}{2}\mathcal{F}(z,\bar{z}^{\circlearrowright})\,, \tag{10.68}$$

where the analytic continuation is performed around the branch point $\bar{z} = 1$ in the directions indicated by the arrows. The overall constant has the following value

$$\kappa^{2r,2s}_{2\bar{h}} = \frac{\Gamma(\bar{h}+r)\Gamma(\bar{h}-r)\Gamma(\bar{h}+s)\Gamma(\bar{h}-s)}{2\pi^2 \Gamma(2\bar{h}-1)\Gamma(2\bar{h})}\,. \tag{10.69}$$

Similarly, there exists an inversion formula that reconstructs $b(\Delta,\ell)$. In order to obtain it, note that superconformal blocks are non-supersymmetric blocks with shifted arguments (10.63). Using the inversion formula for completely general external operators [125, 126], after some manipulations we find

$$\begin{aligned}
b(\Delta,\ell) = \frac{\kappa^{1,1}_{\Delta+\ell+1}}{4} \int_0^1 \int_0^1 \frac{dz d\bar{z}}{(z\bar{z})^d} |z-\bar{z}|^{d-2} \Big(& g^{1,1}_{\ell+d-1,\Delta-d+2}(z,\bar{z}) \, \mathrm{dDisc}\left[(z\bar{z})^{1/2}\mathcal{G}(z,\bar{z})\right] \\
& + (-1)^{\ell+1} g^{-1,1}_{\ell+d-1,\Delta-d+2}(z,\bar{z}) \, \mathrm{dDisc}\left[(z\bar{z})^{1/2}\tilde{\mathcal{G}}(z,\bar{z})\right] \Big)\,.
\end{aligned} \tag{10.70}$$

The inversion formula contains t- and u-channel contributions because the external operators are unequal. In principle, one could extract the CFT data using the standard inversion formula (10.67). However, the resulting CFT data is a sum over nearly-degenerate contributions, which would need to be unmixed using the superconformal blocks (10.64). The supersymmetric inversion formula (10.70) elegantly solves this mixing problem.

In practice, it is convenient to expand the integrand of the inversion formulas in the limit $z \to 0$ and integrate term by term. In the limit $z \to 0$ the correlator has an expansion of the following form

$$\mathcal{F}(z,\bar{z}) = \sum_{n=0}^{\infty} \sum_{p=0}^{\infty} z^{\Delta_\phi + n} \log^p z \, \mathcal{F}_{n,p}(\bar{z}) \,, \tag{10.71}$$

and similarly for $\mathcal{G}(z,\bar{z})$ and $\tilde{\mathcal{G}}(z,\bar{z})$. The inversion formula integration kernels can also be expanded in the limit $z \to 0$:

$$\frac{1}{z} \left(\frac{\bar{z}-z}{z\bar{z}} \right)^{d-2} g^{r,s}_{\ell+d-1, \Delta+1-d}(z,\bar{z}) = z^{-(\Delta-\ell)/2} \sum_{m=0}^{\infty} \sum_{j=-m}^{m} \mathcal{C}^{r,s}_{m,j}(\Delta,\ell) z^m k^{r,s}_{\Delta+\ell+2j}(\bar{z}) \,. \tag{10.72}$$

Similarly to equation (10.19), the coefficients in this expansion can be fixed recursively using the four-point Casimir equation. This type of expansion has been described in detail in the appendix of [125, 166]. After expanding the inversion formula as above, the only non-trivial integrals left to do are of the form

$$\begin{aligned}
\mathrm{INV}[g(\bar{z})](\beta) &= \int_0^1 \frac{d\bar{z}}{\bar{z}^2} k_\beta(\bar{z}) \, \mathrm{dDisc}\left[g(\bar{z}) \right] , \\
\mathrm{SINV}^{\pm}[g(\bar{z})](\beta) &= \int_0^1 \frac{d\bar{z}}{\bar{z}^{3/2}} k^{\pm 1,1}_{\beta+1}(\bar{z}) \, \mathrm{dDisc}\left[g(\bar{z}) \right] .
\end{aligned} \tag{10.73}$$

Finally, the last integral in z is elementary and produces poles in Δ.

Collecting the ingredients together, we have obtained new versions of the Lorentzian inversion formula. For $a(\Delta,\ell)$ we find

$$a(\Delta,\ell) = - \sum_{n,p=0}^{\infty} \frac{S_{n,p}(\Delta,\ell)}{(\Delta - \Delta_\phi - \ell - 2n)^{p+1}} \,,$$

$$S_{n,p}(\Delta,\ell) = \left(1 + (-1)^\ell \right) 2^p p! \, \kappa^{0,0}_{\Delta+\ell} \sum_{m=0}^{n} \sum_{k=-m}^{m} \mathcal{C}^{0,0}_{m,k}(\Delta,\ell) \, \mathrm{INV}[\mathcal{F}_{n-m,p}(\bar{z})](\Delta + \ell + 2k) \,.$$

$$\tag{10.74}$$

Similarly, one obtains $b(\Delta, \ell)$ using the following formula:

$$b(\Delta, \ell) = - \sum_{n,p=0}^{\infty} \frac{S_{n,p}(\Delta, \ell)}{(\Delta - \Delta_\phi - \ell - 2n)^{p+1}} \, ,$$

$$S_{n,p}(\Delta, \ell) = 2^p p! \, \kappa_{\Delta+\ell+1}^{1,1} \sum_{m=0}^{n} \sum_{k=-m}^{m} \left[\mathcal{C}_{m,k}^{1,1}(\Delta + 1, \ell) \, \mathrm{SINV}^+[\mathcal{G}_{n-m,p}(\bar{z})](\Delta + \ell + 2k) \right.$$

$$\left. + (-1)^{\ell+1} \mathcal{C}_{m,k}^{-1,1}(\Delta + 1, \ell) \, \mathrm{SINV}^-[\tilde{\mathcal{G}}_{n-m,p}(\bar{z})](\Delta + \ell + 2k) \right].$$

$$(10.75)$$

These new formulas are simpler to use in perturbative settings.

10.3.3 Generalized free field theory

As a first application of the inversion technology, let us consider generalized free field theory (GFF). In order to extract the CFT data $a_{\Delta,\ell}$ in the $\phi \times \phi$ OPE we have to use the GFF correlation function

$$\mathcal{F}(z, \bar{z}) = (z\bar{z})^{\Delta_\phi} + \left(\frac{z\bar{z}}{(1-z)(1-\bar{z})} \right)^{\Delta_\phi}. \tag{10.76}$$

The first term is regular around $\bar{z} = 1$ so it is killed by the discontinuity and it does not contribute to the inversion formula. Expanding in $z \to 0$ and using the definition (10.71) we find

$$\mathcal{F}(z, \bar{z})|_{\mathrm{singular}} = \left(\frac{z\bar{z}}{(1-z)(1-\bar{z})} \right)^{\Delta_\phi} \quad \Rightarrow \quad \mathcal{F}_{n,p}(\bar{z}) = \delta_{p,0} \frac{(\Delta_\phi)_n}{n!} \left(\frac{\bar{z}}{1-\bar{z}} \right)^{\Delta_\phi}. \tag{10.77}$$

The next step is to compute the integral (10.73). A useful trick is to use the Euler representation of the hypergeometric function, and swap the order of integration. The result is [125]:

$$\mathrm{INV}\left[\left(\frac{\bar{z}}{1-\bar{z}} \right)^p \right] (\beta) = 2\pi^2 \frac{\Gamma(\beta)}{\Gamma(\beta/2)^2} \frac{\Gamma(\beta/2 + p - 1)}{\Gamma(p)^2 \Gamma(\beta/2 - p + 1)}. \tag{10.78}$$

All the ingredients can be combined using equation (10.74) to obtain the dimensions and OPE coefficients for low values of n. We find the family of operators $[\phi\phi]_{\ell,n}$ with dimension $\Delta_{\ell,n} = 2\Delta_\phi + \ell + 2n$ and their OPE coefficients agree with the results of [361]:

$$a_{\ell,n}^{\mathrm{GFF}}(\Delta_\phi, d) = \frac{2 \left(\Delta_\phi + 1 - d/2 \right)_n^2 (\Delta_\phi)_{\ell+n}^2}{\ell! n! \, (\ell + d/2)_n \, (2\Delta_\phi + n + 1 - d)_n (2\Delta_\phi + \ell + 2n - 1)_\ell}$$

$$\times \frac{1}{(2\Delta_\phi + \ell + n - d/2)_n}. \tag{10.79}$$

A similar calculation allows one to obtain the OPE coefficients in the $\phi \times \bar{\phi}$ OPE. Now the relevant GFF correlation functions are

$$\mathcal{G}(z,\bar{z}) = 1 + \left(\frac{z\bar{z}}{(1-z)(1-\bar{z})}\right)^{\Delta_\phi}, \qquad \tilde{\mathcal{G}}(z,\bar{z}) = 1 + (z\bar{z})^{\Delta_\phi}. \tag{10.80}$$

Clearly $\mathcal{G}(z,\bar{z})$ has the same singular part as $\mathcal{F}(z,\bar{z})$, see equation (10.77), while $\tilde{\mathcal{G}}(z,\bar{z})$ is regular around $\bar{z} = 1$ and does not contribute to the LIF. Using similar techniques as before one obtains the following integral

$$\mathrm{SINV}^+\left[\left(\frac{\bar{z}}{1-\bar{z}}\right)^p\right](\beta) = 2\pi^2 \frac{\Gamma(\beta+1)}{\Gamma(\beta/2+1)^2} \frac{\Gamma(\beta/2+p)}{\Gamma(p)^2\Gamma(\beta/2-p+1)}. \tag{10.81}$$

Once again, using (10.75) one can obtain the first few OPE coefficients $b_{\ell,n}$ of the operators $[\phi\bar{\phi}]_{\ell,n}$. They are in perfect agreement with the values reported in [193]

$$b_{\ell,n}^{\mathrm{GFF}}(\Delta_\phi, d) = \frac{(\Delta_\phi + 1 - d/2)_n^2 (\Delta_\phi)_{\ell+n}^2}{\ell!n!\,(\ell + d/2)_n (2\Delta_\phi + n + 2 - d)_n (2\Delta_\phi + \ell + 2n)_\ell} \\ \times \frac{1}{(2\Delta_\phi + \ell + n + 1 - d/2)_n}. \tag{10.82}$$

10.3.4   Wess-Zumino model

We are now ready to solve the Wess-Zumino model at leading order in $\varepsilon = 4-d$. There is a well-known Lagrangian formulation for this model (10.5), which consists of a single chiral superfield Φ interacting with cubic superpotential $\mathcal{W} \sim \Phi^3$. In this section we follow a bootstrap approach similar to [135], but it is useful to keep in mind the Lagrangian (10.5). At the end, we check that our results are in perfect agreement with the literature.

A family of solutions to crossing

At order $O(\varepsilon^0)$ the theory consists of a free chiral multiplet in $d = 4$. The spectrum and OPE coefficients can be obtained from the previous section by setting $\Delta_\phi = 1$. In particular, formulas (10.79) and (10.82) imply that only the leading double-twist families $n = 0$ contribute. When we turn on interactions for small ε, the dimension of the external chiral gets corrected $\Delta_\phi = 1 - \delta_\phi\varepsilon + O(\varepsilon^2)$. Furthermore, the operators in the two OPEs $\phi \times \phi$ and $\phi \times \bar{\phi}$ can also get corrected, and new families of operators could appear in the OPEs.

Let us start studying the $\phi \times \phi$ CFT data at the next order $O(\varepsilon)$. The LIF (10.67) reconstructs the CFT data from the discontinuity of $\mathcal{F}(z,\bar{z})$. Using the crossing equation

(10.62), the discontinuity can be computed in terms of the $\phi \times \bar{\phi}$ CFT data. There is one contribution from the bulk identity, which is considered in section 10.3.3, and a contribution from anomalous dimensions. The corrections from anomalous dimensions are of order $O(\varepsilon^2)$ and can be neglected. Since the inversion formula is not expected to converge for low values of ℓ, we should also include a term $\mathcal{H}(z, \bar{z})$ with finite support in spin:

$$\mathcal{F}(z, \bar{z}) = (z\bar{z})^{\Delta_\phi} + \left(\frac{z\bar{z}}{(1-z)(1-\bar{z})}\right)^{\Delta_\phi} + \varepsilon\mathcal{H}(z, \bar{z}). \tag{10.83}$$

Solutions to crossing with finite support in spin were studied in [145], and it was found that around $d = 4$ there is one such solution that takes the form

$$\mathcal{H}(z, \bar{z}) = k\left(1 - \partial_\Delta\right)g_{\Delta,0}^{d=4}(z, \bar{z})\big|_{\Delta=2}. \tag{10.84}$$

For now the constant k should be treated as an unknown, but later its value will be fixed. This correlator has the following decomposition in conformal blocks

$$\mathcal{F}(z, \bar{z}) = \left(a_{0,0}^{(0)} + \varepsilon a_{0,0}^{(1)}\right)g_{2\Delta_\phi + \varepsilon\gamma, 0} + \sum_{\substack{\ell=2 \\ \ell \text{ even}}}^{\infty} a_{\ell,0}g_{2\Delta_\phi + \ell, \ell} + \sum_{\substack{\ell=0 \\ \ell \text{ even}}}^{\infty} a_{\ell,1}g_{2\Delta_\phi + 2 + \ell, \ell}. \tag{10.85}$$

Notice there is a new family of twist-four operators with tree-level OPE coefficients. To the order we are working, we have $a_{\ell,n} = a_{\ell,n}^{\text{GFF}}(\Delta_\phi, d)$. The only exception is the $\ell = n = 0$ case, when the $[\phi\phi]_{0,0}$ operator has the following CFT data:

$$a_{0,0} = 2 + \varepsilon k, \qquad \gamma = -\frac{k}{2}. \tag{10.86}$$

Let us now turn to the CFT data in the $\phi \times \bar{\phi}$ OPE. The inversion formula (10.70) has a t-channel contribution and a u-channel contribution. As before, one uses the crossing equation (10.62) and the OPE expansion to see which terms contribute. The t-channel contribution consists of the identity, which has been studied in section 10.3.3, and anomalous dimensions that contribute at order $O(\varepsilon^2)$. An unfamiliar feature of the supersymmetric inversion formula (10.70) is that the u-channel contribution produces $O(\varepsilon)$ corrections to the CFT data. Using crossing, the part of $\tilde{\mathcal{G}}(z, \bar{z})$ proportional to $\log(1 - \bar{z})$ is given by the $[\phi\phi]_{0,0}$ operator we just studied:[15]

$$\begin{aligned}
\tilde{\mathcal{G}}(z, \bar{z})\big|_{\log(1-\bar{z})} &= \frac{\varepsilon}{2}a_{0,0}\gamma(z\bar{z})^{\Delta_\phi}\log(1 - \bar{z})\tilde{g}_{2,0}(1 - z, 1 - \bar{z}) \\
&= -\frac{\varepsilon}{2}k(z\bar{z})^{\Delta_\phi}\log(1 - \bar{z})\frac{\log z - \log \bar{z}}{z - \bar{z}}.
\end{aligned} \tag{10.87}$$

---

[15]Here $g_{\Delta,\ell}(z, \bar{z}) = (z\bar{z})^{(\Delta-\ell)/2}\tilde{g}_{\Delta,\ell}(z, \bar{z})$ is defined analogously to (10.50).

From this result, it is clear that the only inversions integrals that one needs to do are:

$$\text{SINV}^-\left[\bar{z}^{-n}\log(1-\bar{z})\right](\beta) = \frac{2\pi^2\Gamma(\beta+1)}{\Gamma(\beta/2+1)^2}\,,$$

$$\text{SINV}^-\left[\bar{z}^{-n}\log(1-\bar{z})\log\bar{z}\right](\beta) = 0\,. \tag{10.88}$$

In order to obtain these inversions, we expand the integrand in powers of $(1-\bar{z})/\bar{z}$, integrate term by term, and in the end resum an asymptotic expansion in powers of $1/\beta$. This procedure has been explained in detail in [135, 169], where the reader can find further details. The ingredients (10.87)-(10.88) can be combined using (10.75) to find $b(\Delta,\ell)$. We find that to this order in ε, the $\phi \times \bar{\phi}$ OPE consists only of the leading-twist family

$$\mathcal{G}(z,\bar{z}) = 1 + \sum_{\ell=0}^{\infty} b_{\ell,0} G_{2\Delta_\phi+\ell+\varepsilon\gamma_\ell,\ell} + O(\varepsilon^2)\,, \tag{10.89}$$

where the CFT data can be readily obtained using the inversion formula

$$\gamma_\ell = k\frac{(-1)^{\ell+1}}{\ell+1}\,, \qquad b_{\ell,0} = b_{\ell,0}^{\text{GFF}}(\Delta_\phi,d)\left(1 + k(-1)^{\ell+1}\frac{(H_\ell - H_{2\ell+1})}{(\ell+1)}\varepsilon + O(\varepsilon^2)\right)\,. \tag{10.90}$$

An important observation is that this result makes sense even for spin $\ell = 0$. Furthermore, we expect the Lorentzian inversion formula to have better convergence properties in supersymmetric theories [392]. Thus, we make the plausible assumption that (10.90) is valid for all $\ell \geq 0$.

Fixing the coefficients

We have found a two-parameter family of solutions to crossing which depend on k and δ_ϕ, let us now try to fix these coefficients from basic physical requirements. The first condition is that the stress tensor is conserved. The stress tensor belongs to a short multiplet with a superprimary of dimensions $\Delta = d-1$ and spin $\ell = 1$, as can be seen from the form of the superconformal block:

$$G_{d-1,1} = g_{d-1,1} + \frac{d}{4(d+1)}g_{d,2}\,. \tag{10.91}$$

As a result, conservation of the stress tensor requires that the operator $[\phi\bar{\phi}]_{1,0}$ has dimension $d-1$. This relates δ_ϕ and k as follows

$$2\Delta_\phi + 1 + \varepsilon\gamma_1 = d - 1 \qquad \Rightarrow \qquad \delta_\phi = \frac{k+2}{4}\,. \tag{10.92}$$

On the other hand, the identification of the operator $[\phi\phi]_{0,0}$ allows to fix the remaining free parameter. As it was discussed in [193], this operator can be identified with a chiral-primary operator ϕ^2, in which case:

$$[\phi\phi]_{0,0} = \phi^2 \quad \Rightarrow \quad 2\Delta_\phi + \varepsilon\gamma_0 = 2\Delta_\phi \quad \Rightarrow \quad k = 0, \; \delta_\phi = \frac{1}{2}. \tag{10.93}$$

We conclude that if $[\phi\phi]_{0,0} = \phi^2$ the theory is free in $d = 4 - \varepsilon$ dimensions.

A second possibility discussed in [193] is that $[\phi\phi]_{0,0}$ is a level-two descendant of $\bar{\phi}$:

$$[\phi\phi]_{0,0} = (Q^+)^2\bar{\phi} \quad \Rightarrow \quad 2\Delta_\phi + \varepsilon\gamma_0 = \Delta_\phi + 1 \quad \Rightarrow \quad k = -\frac{2}{3}, \; \delta_\phi = \frac{1}{3}. \tag{10.94}$$

This leads to a non-vanishing k, so we have found a non-trivial supersymmetric CFT in $d = 4 - \varepsilon$ dimensions. In the following section we provide evidence that this CFT is indeed the Wess-Zumino model.

Summary and discussion

Let us summarize our results on the Wess-Zumino model at order $O(\varepsilon)$. The first result of our bootstrap analysis is the dimension of the external chiral field:

$$\Delta_\phi = \frac{d-1}{3}. \tag{10.95}$$

This is actually a well-known result. Recall that the Wess-Zumino model has a cubic superpotential $\mathcal{W} \sim \Phi^3$, which must have R-charge $R_\mathcal{W} = 2$ at the fixed point. As a result, the chiral-primary field $\phi(x)$ must have charge $R_\phi = 2/3$, or equivalently $\Delta_\phi = (d-1)/3$, which means that (10.95) is in fact an exact result to all orders in ε.

The $\phi \times \phi$ OPE consists of double-twist operators $[\phi\phi]_{\ell,n}$, which are of the schematic form $\phi\Box^n\partial_{\mu_1}\ldots\partial_{\mu_\ell}\phi$. The two families $n = 0, 1$ contribute at order $O(\varepsilon)$, with CFT data given by the GFF results in section 10.3.3. The only exception is the $[\phi\phi]_{0,0}$ operator, which has the following CFT data:

$$a_{0,0} = 2 - \frac{2}{3}\varepsilon + O(\varepsilon^2), \qquad \Delta_{0,0} = 2\Delta_\phi + \frac{\varepsilon}{3} + O(\varepsilon^2). \tag{10.96}$$

The first observation is that $\Delta_{0,0} \neq 2\Delta_\phi$ so we cannot interpret $[\phi\phi]_{0,0}$ as a chiral-primary operator ϕ^2. This is consistent because the Wess-Zumino model has a chiral ring relation $\phi^2 = 0$ due to the cubic superpotential. Instead, the correct interpretation is $[\phi\phi]_{0,0} = (Q^+)^2\bar{\phi}$, which agrees with our results since $\Delta_{0,0} = \Delta_\phi + 1$ and the R-charge is conserved.

The presence of such an operator is consistent with the OPE selection rules [193], and it was also suggested by the numerical bootstrap results of [378]. Thus, we expect the relation $\Delta_{0,0} = \Delta_\phi + 1$ to hold to all orders in ε.

The $\phi \times \bar{\phi}$ OPE contains superconformal primaries and superconformal descendants, and their precise contribution can be obtained from the superconformal blocks (10.64). We expect superprimaries of the schematic form $\mathcal{O}_\ell = \phi \partial_{\mu_1} \ldots \partial_{\mu_\ell} \bar{\phi} + \psi \partial_{\mu_1} \ldots \partial_{\mu_{\ell-1}} \sigma^{\mu_\ell} \bar{\psi}$, where the precise relative coefficients should be fixed by demanding $S^\pm \mathcal{O}_\ell = 0$. From our bootstrap analysis we found the following CFT data:

$$
\begin{aligned}
b_\ell &= b_{\ell,0}^{\text{GFF}}(\Delta_\phi, d) \left(1 + (-1)^\ell \frac{2 \left(H_\ell - H_{2\ell+1} \right)}{3(\ell+1)} \varepsilon + \mathcal{O}(\varepsilon^2) \right) , \\
\Delta_\ell &= 2\Delta_\phi + \ell + \frac{2}{3} \frac{(-1)^\ell}{\ell+1} \varepsilon + O(\varepsilon^2) .
\end{aligned}
\tag{10.97}
$$

It is natural to identify the $\ell = 0$ operator with $\phi\bar{\phi}$, which has dimension $\Delta_{\phi\bar{\phi}} = 2 + O(\varepsilon^2)$ [383], in perfect agreement with our results. Finally, using (10.91) one can relate the OPE coefficient b_1 to the central charge[16]

$$
C_T = \frac{d(d+1)}{(d-1)^2} \frac{\Delta_\phi^2}{b_1} = \frac{20}{3} - \frac{17\varepsilon}{9} + O(\varepsilon^2) .
\tag{10.98}
$$

Once again this is in perfect agreement with the literature [383], up to a difference in normalization.

10.4 Wess-Zumino: Monodromy defects

In this section we generalize the analysis of section 10.2 to superconformal theories with four Poincare supercharges. We study half-BPS monodromy defects that preserve two Poincare supercharges and focus on two-point functions of chiral operators. We start the section with general results valid for monodromy defects in arbitrary superconformal theories, and then move on to the specific case of a monodromy defect for the Wess-Zumino model studied in section 10.3.

10.4.1 Superconformal blocks

Let us start by calculating the relevant superconformal blocks. We use techniques originally developed for bulk four-point functions [193, 236] and later applied to superconformal

---

[16]We define the central charge as in [35], such that the stress-tensor contribution to the OPE is of the form: $\langle \phi\bar{\phi}\phi\bar{\phi} \rangle \supset \frac{1}{4} \left(\frac{d}{d-1} \right)^2 \frac{\Delta_\phi^2}{C_T} g_{d,2}$.

boundaries [3]. Here we only give an outline the calculation, the interested reader can find further details in the aforementioned references. We stress again that this section applies to general half-BPS codimension-two defects, which need not be monodromy defects.

Defect superconformal algebra

As in section 10.2, we chose our codimension-two defect to sit at $x^1 = x^2 = 0$. The subalgebra of conformal transformations that preserve the defect is generated by D, P_a, K_a and M_{ab}, where $a, b = 3, \ldots, d$ are indices parallel to the defect. Since translation symmetry is partly broken, at most half of the original supercharges can be preserved by the defect. Following the conventions of section 10.3, we choose the preserved supercharges to be:

$$\mathcal{Q}_1 = Q_1^+ , \qquad \mathcal{Q}_2 = Q_1^- , \qquad \mathcal{S}_1 = S^{1+} , \qquad \mathcal{S}_2 = S^{1-} . \tag{10.99}$$

Using the following Clifford algebra representation $\Sigma^i_{\alpha\dot\alpha} = (\bar\Sigma_i^{\dot\alpha\alpha})^* = (\sigma_1, \sigma_2, \sigma_3, i\mathbb{1})$, it is possible to check in $d = 3$ and $d = 4$ that the supercharges generate a subalgebra of the full superconformal algebra. For non-integer dimensions $3 \leq d \leq 4$ this construction is less rigorous, however we will obtain perfectly consistent results. The anticommutators of the supercharges generate translations and special conformal transformations parallel to the defect:

$$\{\mathcal{Q}_A, \mathcal{Q}_B\} = \widehat{\Sigma}^a_{AB} P_a , \qquad \{\mathcal{S}_A, \mathcal{S}_B\} = \widehat{\Sigma}^a_{AB} K_a , \qquad a = 3, \ldots, d, \quad A, B = 1, 2 . \tag{10.100}$$

Similarly, by considering anticommutators of the form $\{\mathcal{Q}, \mathcal{S}\}$, we observe that the defect does not preserve R–symmetry or transverse rotations independently, but only a particular linear combination of them:[17]

$$\mathcal{M} = M_{12} + \frac{d-1}{2} R . \tag{10.101}$$

With these conventions in mind, we proceed to obtain the superconformal blocks.

Defect channel

Let us start with the defect OPE $\phi(x) \sim \sum \widehat{\mathcal{O}}(\vec{y})$. In this channel only one operator per defect supermultiplet contributes to the OPE, and as a result, the defect superconformal

---

[17]The full subalgebra for $d = 3$ can be found in [181] in conventions slightly different to ours.

blocks $\hat{F}_{\widehat{\Delta},s}(x,\bar{x})$ reduce to bosonic blocks $\hat{f}_{\widehat{\Delta},s}(x,\bar{x})$. In our conventions $\widehat{\Delta}, s$ label the conformal primary exchanged in the OPE, and not the superprimary in the corresponding multiplet.

We justify the above claim following an argument from [65]. Since the chirality condition (10.60) is preserved by the defect supercharges (10.99), it turns out that $[\mathcal{Q}_1, \phi(x)] = [\mathcal{S}_1, \phi(x)] = 0$. Inserting these relations in the OPE implies $[\mathcal{Q}_1, \widehat{\mathcal{O}}(\vec{y})] = [\mathcal{S}_1, \widehat{\mathcal{O}}(\vec{y})] = 0$. However, only one operator in each defect supermultiplet can satisfy both of these conditions, hence superblocks in this channel are just standard bosonic blocks.

Bulk channel

In the bulk channel, up to four conformal primaries in each supermultiplet can contribute to the OPE. Their contributions are organized in superconformal blocks which we now calculate.

Following [31, 194], we characterize superconformal blocks as solutions to the supersymmetric Casimir equation. The superconformal Casimir can be split naturally into a non-supersymmetric and a supersymmetric piece: $C_{\text{full}} = C_{\text{bos}} + C_{\text{susy}}$. The first contribution $\frac{1}{2}C_{\text{bos}}$ leads to the differential operator in equation (10.15). The second contribution is due to supersymmetry:

$$C_{\text{susy}} = -\frac{d-1}{2}R^2 + \frac{1}{2}[S^{\dot{\alpha}+}, Q_{\dot{\alpha}}^-] + \frac{1}{2}[S^{\alpha-}, Q_{\alpha}^+]. \tag{10.102}$$

Following [193], our goal is to massage (10.102) into a differential operator that can be added to (10.15). Using the commutation relations, the chirality properties of ϕ and $\bar{\phi}$, and equation (51) from [193] we find:

$$\left[C_{\text{susy}}, \phi(x_1)\bar{\phi}(x_2)\right]|0\rangle = ix_{12}^\mu \bar{\Sigma}_\mu^{\dot{\alpha}\alpha}\left[Q_{\dot{\alpha}}^-, \phi_1(x_1)\right]\left[Q_\alpha^+, \bar{\phi}_2(x_2)\right]|0\rangle + 4\Delta_\phi \phi(x_1)\bar{\phi}(x_2)|0\rangle. \tag{10.103}$$

Using superconformal Ward identities as in [3, 193] to rewrite the Q-dependent part as a differential operator we get

$$\frac{1}{2}C_{\text{susy}}\langle\phi_1(x_1)\bar{\phi}_2(x_2)\rangle \rightarrow -\left[(1-x)\partial_x + \bar{x}(1-\bar{x})\partial_{\bar{x}}\right]F_{\Delta,\ell}(x,\bar{x}). \tag{10.104}$$

Combining the bosonic equation (10.15), the supersymmetric one (10.104), and using the appropriate supersymmetric eigenvalue $c_2 = \Delta(\Delta - d + 2) + \ell(\ell + d - 2)$, we obtain a

differential equation for the superconformal block $F_{\Delta,\ell}(x,\bar{x})$. In $d = 4$ the solution with correct boundary conditions takes a simple form:

$$F_{\Delta,\ell}(x,\bar{x}) = \frac{\sqrt{(1-x)(1-\bar{x})}}{1-x\bar{x}}\Big(k^{1,-1}_{\Delta-\ell-1}(1-x)k^{1,1}_{\Delta+\ell+1}(1-\bar{x}) \\ + (-1)^{\ell}k^{1,-1}_{\Delta+\ell+1}(1-x)k^{1,1}_{\Delta-\ell-1}(1-\bar{x})\Big). \tag{10.105}$$

For general d, we use an expansion of the form

$$F_{\Delta,\ell}(x,\bar{x}) = \sum_{n=0}^{\infty}\sum_{j=-n}^{n} B_{n,j}(\Delta,\ell)(1-x)^{(\Delta-\ell)/2+n}(1-\bar{x})^{-1/2}k^{1,1}_{\Delta+\ell+1+2j}(1-\bar{x}), \tag{10.106}$$

and we fix the coefficients using the supercasimir equation. The procedure is easy to implement using a computer algebra system. For the first few coefficients we find:

$$B_{0,0}(\Delta,\ell) = 1, \quad B_{1,-1}(\Delta,\ell) = \frac{(2-d)\ell}{d+2\ell-4}, \quad B_{1,1}(\Delta,\ell) = \frac{(2-d)\Delta(\Delta+\ell)(\Delta+\ell+2)}{16(2\Delta+4-d)(\Delta+\ell+1)^2}. \tag{10.107}$$

Finally, let us mention that the superconformal block has a decomposition into a sum of four bosonic blocks:

$$F_{\Delta,\ell}(x,\bar{x}) = f_{\Delta,\ell}(x,\bar{x}) + a_1\,f_{\Delta+1,\ell+1}(x,\bar{x}) - a_2\,f_{\Delta+1,\ell-1}(x,\bar{x}) - a_3\,f_{\Delta+2,\ell}(x,\bar{x}). \tag{10.108}$$

The coefficients can be found in (10.65). The fact that the coefficients are the same as the four-point blocks of chiral operators might seem surprising at first. Actually, with the identification (10.16) the defect bulk blocks $F_{\Delta,\ell}(x,\bar{x})$ are the analytic continuation of the four-point blocks $\tilde{G}_{\Delta,\ell}(z,\bar{z})$ [3]. What we have found is that the close connection between codimension-two defects and four-point functions also holds at the superconformal level.

10.4.2 Free and GFF half-BPS monodromy defect

Armed with the superconformal blocks, we can now bootstrap superconformal monodromy defects. In this section we focus on defects in (generalized) free theories, while we leave the more interesting defect in the Wess-Zumino model for the next section. Fortunately, we can recycle many results from the non-supersymmetric case studied in section 10.2.

Let us start with the case of a free bulk theory preserving four supercharges. Since $\phi(x)$ is a free-field, its correlation function $\mathcal{G}^{\text{free}}_{d,v}(x,\bar{x})$ is independent of the rest of the field content of the theory, so it is given by the non-supersymmetric formulas (10.33)-(10.34).

Moreover, the defect superblocks reduce to non-supersymmetric blocks, so the defect CFT data is given by (10.30). The story is more interesting in the bulk channel, because now in order to obtain the CFT data one must use superconformal blocks:

$$
\mathcal{G}^{\text{free}}_{d,v}(x,\bar{x}) = \left(\frac{\sqrt{x\bar{x}}}{(1-x)(1-\bar{x})} \right)^{(d-2)/2} \left(1 + \sum_{\ell=0}^{\infty} d_\ell^{\text{free}} F_{d-2+\ell,\ell}(x,\bar{x}) \right) . \tag{10.109}
$$

Once again, we use the shorthand notation $d_\mathcal{O} = \lambda_{\phi\bar{\phi}\mathcal{O}} a_\mathcal{O}$. Since the bulk theory is free, only the leading-twist family contributes. Using the series representation (10.106) for the superblocks, we can extract the CFT data order by order in $(1-x)$ and $(1-\bar{x})$. For the first few coefficients we find:

$$
d_0^{\text{free}} = C_{d,v}^{\text{free}}, \quad d_1^{\text{free}} = \frac{(d-2)(v-1)}{2(d-1)} C_{d,v}^{\text{free}}, \quad d_2^{\text{free}} = \frac{(d-2)(v-1)(dv-d+v)}{8(d-1)(d+1)} C_{d,v}^{\text{free}} . \tag{10.110}
$$

Similarly to section 10.2, the coefficients satisfy a two-step recursion relation which can be used to efficiently go to high values of ℓ:[18]

$$
\begin{aligned}
d_{\ell+2}^{\text{free}} &= \frac{(d+2\ell)\left(d^2(v-1) + d(4v-3)\ell + d + (4v-3)\ell^2 - v\right)}{2(\ell+2)(d+\ell)(d+2\ell-1)(d+2\ell+1)} d_{\ell+1}^{\text{free}} \\
&\quad + \frac{\ell(d+\ell-2)(d+2\ell-2)(d+2\ell)}{16(\ell+2)(d+\ell)(d+2\ell-1)^2} d_\ell^{\text{free}} .
\end{aligned} \tag{10.112}
$$

The next simplest example is a monodromy defect in a bulk GFF theory. As in the free case, the full correlator $\mathcal{G}^{\text{GFF}}_{\Delta_\phi,d,v}(x,\bar{x})$ is the same as in the non-supersymmetric theory, and the defect CFT data is given by (10.30). For the bulk data we can use (10.46), which is the leading order correlator in $\varepsilon = 4-d$ around the free value $\Delta_\phi = 1 - \delta_\phi \varepsilon$. Expanding in bulk blocks

$$
\mathcal{G}^{\text{GFF}}_{\Delta_\phi,d,v}(x,\bar{x}) = \left(\frac{\sqrt{x\bar{x}}}{(1-x)(1-\bar{x})} \right)^{\Delta_\phi} \left(1 + \sum_{n=0}^{\infty} \sum_{\ell=0}^{\infty} d_{\ell,n}^{\text{GFF}} F_{2\Delta_\phi+\ell+2n,\ell}(x,\bar{x}) \right) , \tag{10.113}
$$

---

[18]Once again, in the $d=4$ case it is possible to obtain a closed analytic formula:

$$
\begin{aligned}
d_\ell^{\text{free}} \stackrel{d=4}{=} \frac{\Gamma(\ell)\Gamma(\ell+1)\Gamma(\ell+2)\sin^2(\pi v)}{2^{4\ell+3}\pi\Gamma(\ell+3/2)^2} &\left[\frac{\Gamma(2-v)}{\Gamma(\ell-v+2)} {}_3F_2\left(\begin{matrix} \ell,\ell+1,\ell+2 \\ 2\ell+3,\ell-v+2 \end{matrix} ; 1 \right) \right. \\
&\left. + (-1)^{\ell+1} \frac{\Gamma(v)}{\Gamma(\ell+v)} {}_3F_2\left(\begin{matrix} \ell,\ell+1,\ell+1 \\ 2\ell+3,\ell+v \end{matrix} ; 1 \right) \right] .
\end{aligned} \tag{10.111}
$$

267

it is relatively straightforward to extract CFT data up to high values of ℓ and n using the expansion (10.106). Some of the low-lying coefficients are

$$
\begin{aligned}
d_{0,0}^{\mathrm{GFF}} &= C_{\Delta_\phi, d, v} + O(\varepsilon^2)\,, \\
d_{1,0}^{\mathrm{GFF}} &= \frac{1}{9}(v-1)(3 - \delta_\phi \varepsilon) C_{\Delta_\phi, d, v} + O(\varepsilon^2)\,, \\
d_{0,1}^{\mathrm{GFF}} &= \frac{\varepsilon}{96}(2\delta_\phi - 1) v(v-1)(v-2)(v-3) + O(\varepsilon^2)\,,
\end{aligned}
\tag{10.114}
$$

while we give more coefficients in the attached `Mathematica` notebook.

10.4.3   Wess-Zumino model

Finally, we proceed to bootstrap the two-point function of chiral operators in the Wess-Zumino model to order $O(\varepsilon)$ in the ε–expansion. The derivation requires knowledge of the bulk theory derived in section 10.3 and the inversion formula derived in section 10.2.2. Although the calculations for the Wess-Zumino model are similar in spirit to the Wilson-Fisher fixed point, in practice they are more challenging and require extra technology which we develop in the appendix.

Let us remind the reader that the Wess-Zumino model is a theory of a single chiral superfield with cubic superpotential $\mathcal{W} \sim \Phi^3$. At the fixed point, the chiral-primary field $\phi(x)$ must have charge $R_\phi = 2/3$, or equivalently $\Delta_\phi = (d-1)/3$. Since the external dimension differs from free theory at order $O(\varepsilon)$, there is a GFF contribution with $\delta_\phi = 1/3$, which has been discussed in section 10.4.2.

Furthermore, as discussed in section 10.3, the bulk OPE contains double-twist operators $[\phi\bar{\phi}]_{\ell,n}$. Importantly, the leading-twist operators $n = 0$ have OPE coefficients of order $O(1)$ and anomalous dimensions γ_ℓ of order $O(\varepsilon)$, see (10.97). As a result, the entire leading-twist family contributes to $\mathrm{Disc}\,\mathcal{G}(x, \bar{x})$. Indeed, the part of the correlator with non-vanishing discontinuity is

$$
\begin{aligned}
\mathcal{G}(x, \bar{x})|_{\mathrm{singular}} &= \frac{\varepsilon}{2}(x\bar{x})^{\Delta_\phi/2} \log\big[(1-x)(1-\bar{x})\big] \sum_{\ell=0}^{\infty} d_\ell^{\mathrm{free}} \gamma_\ell \tilde{F}_{2\Delta_\phi + \ell, \ell}(x, \bar{x}) \\
&= -\frac{\varepsilon}{3} v(v-1)(x\bar{x})^{1/2} \log\big[(1-x)(1-\bar{x})\big] \frac{h\!\left(\frac{\bar{x}-1}{\bar{x}}\right) - h(1-x)}{1 - x\bar{x}}\,,
\end{aligned}
\tag{10.115}
$$

where we introduced $h(z) = z\,{}_3F_2(1, 1, v+1; 2, 3; z)$. From here it is in principle straightforward to extract the defect CFT data using the bulk-to-defect Lorentzian inversion formula. However, for the sake of clarity, we defer the details to appendix 10.A.1. Below we present

the defect CFT data, which contains contributions from the bulk identity (GFF) and from (10.115).

Leading transverse-twist family: The first family are defect operators of transverse twist approximately one. Since these operators are present in the free theory, their conformal dimensions can get corrected at this order in perturbation theory:

$$\widehat{\Delta}_{s,0} = \frac{d-1}{3} + |s| + \varepsilon\hat{\gamma}_s^{(1)} + O(\varepsilon^2)\,, \qquad \hat{\gamma}_s^{(1)} = \begin{cases} 0 & \text{for } s > 0\,, \\ \frac{2(v-1)}{3|s|} & \text{for } s < 0\,. \end{cases} \tag{10.116}$$

Furthermore, their OPE coefficients also get corrected as follows:

$$\mu_{s>0,0} = 1 + \frac{-(2|s|+1-v)H_{|s|} + (|s|+1-v)H_{|s|+1-v} - (1-v)H_{1-v}}{3|s|}\varepsilon + O(\varepsilon^2)\,,$$

$$\mu_{s<0,0} = 1 + \frac{-(2|s|+v-1)H_{|s|} + (|s|+v-1)H_{|s|+v-1} - (v-1)H_{v-1}}{3|s|}\varepsilon + O(\varepsilon^2)\,.$$

$$\tag{10.117}$$

An important feature of the CFT data is that it is not symmetric under $s \leftrightarrow -s$. Even though this seems surprising at first, it follows because $\phi(x)$ is a complex field, complex conjugation relates positive transverse-spin modes from $\phi(x)$ with the negative modes from $\bar{\phi}(x)$. From a technical point of view, this asymmetry is due to (10.115) not being symmetric under $x \leftrightarrow \bar{x}$. In particular, one would observe a similar phenomena in the $O(N)$ Wilson-Fisher fixed point starting at order $O(\varepsilon^2)$ and $N > 1$.

Subleading transverse-twist families: The next families of defect operators have transverse twist $2n+1$. At this order in perturbation theory, only the tree-level dimensions contribute

$$\widehat{\Delta}_{s,n} = 1 + |s| + 2n + O(\varepsilon) \quad \text{for} \quad n \geq 1\,. \tag{10.118}$$

Notice that these families receive contributions both from the bulk identity and from (10.115), and as a result, the defect OPE coefficients differ from the GFF values:

$$\mu_{s>0,n} = \frac{|s| + 2(1-v)}{6n(|s|+n)}\varepsilon + O(\varepsilon^2)\,, \qquad \mu_{s<0,n} = \frac{|s| + 2(v-1)}{6n(|s|+n)}\varepsilon + O(\varepsilon^2)\,. \tag{10.119}$$

Fractional transverse-twist families: Perhaps surprisingly, there is another family of defect operators with non-integer transverse twist. Indeed, their tree-level conformal dimensions are

$$\widehat{\Delta}^{\mathrm{fr}}_{s>0,n} = 1 + |s| + 2(n+1-v)\,, \quad \widehat{\Delta}^{\mathrm{fr}}_{s<0,n} = 1 + |s| + 2(n+v-1)\,, \qquad \text{for} \quad n \geq 1\,.$$
(10.120)

Notice that this family is generated exclusively from the bulk leading-twist family (10.115). Once more, the tree-level OPE coefficients take a rather simple form:

$$\mu^{\mathrm{fr}}_{s>0,n} = \frac{n}{3(n+1-v)(|s|+n+1-v)}\,, \quad \mu^{\mathrm{fr}}_{s<0,n} = \frac{n}{3(n+v-1)(|s|+n+v-1)}\,.$$
(10.121)

Having reviewed the structure of the defect CFT data, we can now resum the defect-channel expansion in order to obtain the full correlation function at order $O(\varepsilon)$:

$$\mathcal{G}^{\mathrm{GFF}}_{\frac{d-1}{3},d,v}(x,\bar{x}) + \mathcal{G}_{\mathrm{WZ}}(x,\bar{x}) = \sum_{s\in -v+\mathbb{Z}} \left(\sum_{n=0}^{\infty} \mu_{s,n} \hat{f}_{\widehat{\Delta}_{s,n},s}(x,\bar{x}) + \sum_{n=1}^{\infty} \mu^{\mathrm{fr}}_{s,n} \hat{f}_{\widehat{\Delta}^{\mathrm{fr}}_{s,n},s}(x,\bar{x}) \right)\,.$$
(10.122)

The GFF part can be found in equation (10.46) with $\delta_\phi = 1/3$. The contribution which is new from the Wess-Zumino model is significantly harder:

$$
\begin{aligned}
\mathcal{G}_{\mathrm{WZ}}(x,\bar{x}) = -\frac{\varepsilon}{3}\frac{\sqrt{x\bar{x}}}{(1-x\bar{x})}\Bigg[& \\
& + x^v(1-v)\big(j_{2v-1,v}(x) - j_{v,v}(x) - H_{v-1}\Phi_v(x) + \Phi_v(x)\log(x\bar{x})\big) \\
& + \bar{x}^{1-v}(1-v)\big(j_{1-v,1-v}(\bar{x}) - j_{2-2v,1-v}(\bar{x}) + H_{1-v}\Phi_{1-v}(\bar{x})\big) \\
& + x^v \frac{H_{v-1} - H_{2v-2} + \Phi_v(x) - \Phi_{2v-1}(x)}{1-x} \\
& + \bar{x}^{1-v} \frac{H_{-v} - H_{1-2v} + \Phi_{1-v}(\bar{x}) - \Phi_{2-2v}(\bar{x})}{1-\bar{x}} \\
& - x^{1-v}\bar{x}^{2-2v}\left((v-1)J_{2-2v,1-v}(\bar{x},x) + \frac{\Phi_{2-2v}(\bar{x}) - x\Phi_{2-2v}(x\bar{x})}{1-x}\right) \\
& + x^{2v-1}\bar{x}^{v-1}\left((v-1)J_{2v-1,v-1}(x,\bar{x}) - \frac{\Phi_{2v-1}(x) - \bar{x}\Phi_{2v-1}(x\bar{x})}{1-\bar{x}}\right) \\
& - \bar{x}x^{v+1}\left((v-1)J_{v+1,1}(x,\bar{x}) - \frac{\Phi_{v+1}(x) - \bar{x}\Phi_{v+1}(x\bar{x})}{1-\bar{x}}\right) \\
& + x\bar{x}^{2-v}\left((v-1)J_{2-v,1}(\bar{x},x) + \frac{\Phi_{2-v}(\bar{x}) - x\Phi_{2-v}(x\bar{x})}{1-x}\right)\Bigg]\,.
\end{aligned}
$$
(10.123)

We could not express this correlation function in terms of elementary functions. Instead, we introduced the following two special functions

$$j_{a,b}(x) \equiv \sum_{n=0}^{\infty} \frac{x^n H_{n+a}}{n+b} \,, \qquad J_{a,b}(x, \bar{x}) = \sum_{n=0}^{\infty} \sum_{m=0}^{n} \frac{x^n}{(n+a)} \frac{\bar{x}^m}{(m+b)} \,. \qquad (10.124)$$

In appendix 10.A.2 we derive some interesting properties of these functions, in particular we give an efficient algorithm to generate their expansion in powers of $(1-x)$ and $(1-\bar{x})$. This allows us to expand the correlation function in the bulk channel

$$\mathcal{G}_{\mathrm{WZ}}(x, \bar{x}) = \left(\frac{\sqrt{x\bar{x}}}{(1-x)(1-\bar{x})} \right)^{(d-1)/3} \left(1 + \sum_{\ell=0}^{\infty} d_{\ell,n}^{\mathrm{WZ}} F_{\Delta_{\ell,n},\ell}(x, \bar{x}) \right) \,. \qquad (10.125)$$

Once again, we can extract the CFT data using a software like `Mathematica`. Some of the low-lying bulk OPE coefficients are

$$d_{0,0}^{\mathrm{WZ}} = \varepsilon(v-1) \left(\frac{1}{3}(2v-1)\left(H_{-2v} + H_{2v}\right) - \frac{1}{6}(3v-2)\left(H_{-v} + H_v\right) - \frac{5v^2 - v + 1}{6v} \right),$$

$$d_{1,0}^{\mathrm{WZ}} = \varepsilon(v-1)^2 \left(\frac{1}{18}(2v-1)\left(H_{-2v} + H_{2v}\right) - \frac{1}{36}(5v-2)\left(H_{-v} + H_v\right) + \frac{5v^3 + 10v^2 - 12v + 3}{108v(v-1)} \right),$$

$$d_{0,1}^{\mathrm{WZ}} = \frac{\varepsilon}{144} v(v-1) \left(17v^2 - 37v + 18 \right) \,. \qquad (10.126)$$

Let us emphasize that the total OPE coefficients are obtained combining (10.114) and (10.126), namely $d_{\ell,n} = d_{\ell,n}^{\mathrm{WZ}} + d_{\ell,n}^{\mathrm{GFF}}$. As usual, we give a larger list of bulk coefficients in the notebook attached to this publication.

10.5 Conclusions

In this work we used analytical bootstrap techniques to study monodromy defects in the ε–expansion. This program has been highly successful for four-point functions without defects, where CFT data has been extracted up to fourth order in ε for the Wilson-Fisher fixed point [135, 136]. Our analysis can be considered as the first step towards applying these techniques to monodromy defects in CFT. Our main result is equation (10.123), which describes the full leading-order two-point correlator of chiral fields in the Wess-Zumino model. In order to obtain the defect correlator, it was necessary to calculate the leading order CFT data of the Wess-Zumino model without defects (see section 10.3.4), a result that is interesting on its own and that we plan to extend to higher orders in the future.

We also studied monodromy defects in the Wilson-Fisher $O(N)$ model, reproducing and in some cases improving previous results. A natural extension of this work is to consider higher orders in the ε–expansion, although this will require dealing with degeneracies in the bulk spectrum. Another related system is the large-N limit of the $O(N)$ model, which has been studied using bootstrap in [169]. Monodromy defects in the large-N limit have been studied in [258], and they might be good candidates for a bootstrap analysis.

Yet another system in which the techniques used in this paper are directly applicable is a Wilson line defect in $\mathcal{N} = 4$ SYM at strong coupling. The strong-coupling planar spectrum of $\mathcal{N} = 4$ SYM contains double-trace operators which are killed by the discontinuity in the inversion formula. This is very similar to the setup of this paper, and indeed two-point functions of half-BPS operators can be reconstructed by inverting a finite number of conformal blocks [5]. It might also be possible to consider other maximally-supersymmetric models in $3 \le d \le 6$, and bootstrap their defect correlators in suitable limits.

On a more speculative side, the functions studied in appendix 10.A.2 are close cousins of the Hurwitz-Lerch zeta function. Perhaps these functions will find applications in other perturbative calculations or in other branches of mathematical physics. Finally, the study of higher-point functions is one of the long-term goals of the bootstrap. Progress in this direction was made in [388], where higher-point functions in the presence of defects were studied. Eventually, one should be able to obtain the corresponding Lorentzian inversion formulas, and implement the multi-point bootstrap in order to obtain even more restrictive constraints.

10.A   Appendix

10.A.1   Inverting the Wess-Zumino model

In this appendix we explain how to obtain the Wess-Zumino defect spectrum from the discontinuity of the correlator. By means of the inversion formula, it boils down to computing the integral (10.27). An important observation is that since the discontinuity is not symmetric under $x \leftrightarrow \bar{x}$, the integrals are different for $s > 0$ and $s < 0$.

Let us focus on $s > 0$ first, and we summarize $s < 0$ at the end. Since the discontinuity is of order $O(\varepsilon)$, we can evaluate the integration kernel at $d = 4$, when the integral is

dramatically simpler:

$$\mu(\widehat{\Delta}, s) = \varepsilon \frac{v(v-1)}{12} \int_0^1 dx \int_1^{1/x} d\bar{x} \, x^{-(\widehat{\Delta}-s+1)/2} \bar{x}^{-(\widehat{\Delta}+s+1)/2} \left(h\left(\tfrac{\bar{x}-1}{\bar{x}}\right) - h(1-x) \right) . \tag{10.127}$$

Let us remind the reader that $h(z) = z \, {}_3F_2(1,1,v+1;2,3;z)$. The strategy to obtain the CFT data from such an integral is to notice that poles in $\widehat{\Delta}$ come from the region $x \to 0$. Thus, we expand the integrand in powers of x and for each power we have

$$\int_0^1 dx \int_1^{1/x} d\bar{x} \, x^{-(\widehat{\Delta}-s+1)/2} \bar{x}^{-(\widehat{\Delta}+s+1)/2} x^n = -\frac{2}{(s+n)} \frac{1}{(\widehat{\Delta}-s-1-2n)} . \tag{10.128}$$

Physically, each power x^n generates a defect family of dimensions $\widehat{\Delta}_{s,n} = 1 + s + 2n$ and OPE coefficient $\mu_{s,n} \sim 1/(s+n)$. Notice that the function $h(1-x)$ has the following expansion

$$h(1-x) = \frac{2}{v}(1 - H_{1-v}) + \frac{2}{v(v-1)} \sum_{n=1}^{\infty} \left(\frac{(n+v-1)x^n}{n} + \frac{nx^{n+1-v}}{(v-n-1)} \right) . \tag{10.129}$$

Combining this expansion with the inversion (10.128) one obtains the CFT data for $n > 0$, see (10.119) and (10.121). The case $n = 0$ is identical, except one also has to consider contributions from the following integral:

$$\int_0^1 dx \int_1^{1/x} d\bar{x} \, x^{-(\widehat{\Delta}-s+1)/2} \bar{x}^{-(\widehat{\Delta}+s+1)/2} h\left(\frac{\bar{x}-1}{\bar{x}}\right)$$
$$= -\frac{4((s-v+1)(H_{s-v+1} - H_s) + v - 1)}{sv(v-1)(\widehat{\Delta}-s-1)} . \tag{10.130}$$

This integral has been obtained by expanding the integrand around $\bar{x} \to \infty$, integrating term by term, and finally resuming the resulting expression. The final result can be checked numerically to very high precision.

Let us briefly outline the $s < 0$ case. The inversion integral is once again (10.127) where one needs to change $x \leftrightarrow \bar{x}$ in the integration region. The CFT data for $n > 0$ can be read off from the following expansion

$$h\left(\frac{\bar{x}-1}{\bar{x}}\right) = \frac{2}{v}\left(1 - H_{v-1} + \log \bar{x}\right) + \frac{2}{v(v-1)} \sum_{n=1}^{\infty} \left(\frac{(v-n-1)\bar{x}^n}{n} + \frac{n\bar{x}^{n+v-1}}{n+v-1} \right) . \tag{10.131}$$

273

The presence of a $\log \bar{x}$ term leads to the anomalous dimensions (10.116). For the $n = 0$ case, one also needs the integral

$$
\int_0^1 d\bar{x} \int_1^{1/\bar{x}} dx \, x^{-(\widehat{\Delta}-s+1)/2} \bar{x}^{-(\widehat{\Delta}+s+1)/2} h(1-x)
$$

$$
= \frac{4\big(s(s-v+1)\,(H_{-s+v-1} - H_{-s}) + (s+1)(v-1)\big)}{s^2 v(v-1)(\widehat{\Delta}+s-1)},
$$

$$(10.132)$$

which has been computed by expanding around $x = 0$ and integrating term by term.

10.A.2 Defect-channel resummation

In this appendix we present some mathematical results that are useful in order to resum the defect-channel expansion of monodromy defects.

Hurwitz-Lerch zeta function

The first function we consider is the well-known Hurwitz-Lerch zeta function:

$$
\Phi(x,s,a) = \sum_{m=0}^{\infty} \frac{x^m}{(m+a)^s} \,.
$$

$$(10.133)$$

The only case which is relevant in the present work is $s = 1$, when it has a simple expression as a hypergeometric function:

$$
\Phi(x,1,a) = a^{-1} \, {}_2F_1\!\left(\begin{matrix} 1,\, a \\ a+1 \end{matrix} ; x\right).
$$

$$(10.134)$$

The power of the Hurwitz-Lerch zeta function lies in the possibility of writing seemingly complicated infinite sums in terms of them. Defect-channel expansions such as (10.46) or (10.123) can be resummed using the following formulas:

$$
\sum_{n=0}^{\infty} x^n \, (H_{a+n} - H_{a-1}) = \frac{\Phi(x,1,a)}{1-x} \,,
$$

$$
\sum_{n=0}^{\infty} \sum_{m=0}^{n} \frac{x^n \bar{x}^m}{n+a} = \sum_{n=0}^{\infty} x^n \Phi(x\bar{x},1,n+a) = \frac{\Phi(x,1,a) - \bar{x}\Phi(x\bar{x},1,a)}{1-\bar{x}} \,,
$$

$$
\sum_{n=0}^{\infty} \sum_{m=0}^{n} \frac{x^n \bar{x}^m}{m+a} = \frac{\Phi(x\bar{x},1,a)}{1-x} \,.
$$

$$(10.135)$$

For our applications, it is important to expand the Hurwitz-Lerch zeta function around $x = 1$, which allows us to extract the bulk CFT data. Let us note the two elegant expressions

$$\Phi(x, 1, v) = -\sum_{n=0}^{\infty} \frac{(v)_n}{n!}(1 - x)^n \big(\log(1 - x) + H_{v+n-1} - H_n\big),$$

$$x^v \Phi(x, 1, v) = -H_{v-1} - \log(1 - x) + \sum_{n=1}^{\infty} \frac{(-1)^{n+1}(v - n)_n}{n^2(n - 1)!}(1 - x)^n. \tag{10.136}$$

One-variable function

In the study of the Wess-Zumino model, we encountered sums that could not be expressed in terms of simple special functions. The first sum we consider involves a single variable:

$$j_{a,b}(x) \equiv \sum_{n=0}^{\infty} \frac{x^n H_{n+a}}{n + b}. \tag{10.137}$$

It is not hard to relate $j_{a,b}(x)$ to itself after shifting $a \to a \pm 1$ and $b \to b \pm 1$.

Let us consider the case $a = 0$ separately. The function $j_{0,b}(x)$ can be resummed in terms of the incomplete beta function:

$$j_{0,b}(x) = -x^{-b} \left. \frac{\partial B_x(b, a)}{\partial a} \right|_{a=0}. \tag{10.138}$$

In order to generate the series expansion around $x = 1$ efficiently, we note that the function satisfies the differential equation

$$\partial_x (1 - x) \partial_x (1 - x) x^{1-b} \partial_x \big(x^b j_{0,b}(x)\big) = 0. \tag{10.139}$$

Making an ansatz for the series around $x = 1$

$$j_{0,b}(x) = \sum_{i=0}^{\infty} (1 - x)^i \big(a_i + b_i \log(1 - x) + c_i \log^2(1 - x)\big), \tag{10.140}$$

one can fix coefficients recursively using the differential equation (10.139). The initial condition can be obtained from (10.138)

$$a_0 = -\frac{1}{2}\left((H_{b-1})^2 + H_{b-1}^{(2)}\right), \qquad b_0 = 0, \qquad c_0 = \frac{1}{2}. \tag{10.141}$$

Here $H_b^{(r)} = \sum_{n=1}^{b} n^{-r}$ is a generalization of the harmonic number, where the usual continuation to non-integer values of b is assumed.

Let us move on to the general case $a \notin \mathbb{N}$, and define the auxiliary function

$$\tilde{j}_{a,b}(x) = \sum_{n=0}^{\infty} \frac{x^n (H_{n+a} - H_{a-1})}{n+b} = j_{a,b}(x) - H_{a-1} \Phi(x, 1, b) \, . \tag{10.142}$$

Clearly, any property of $\tilde{j}_{a,b}(x)$ can be easily translated to $j_{a,b}(x)$, since the Hurwitz-Lerch zeta function that relates them is well understood. The advantage of the auxiliary function is that it satisfies a simpler differential equation

$$\partial_x (1-x) x^{1-a} \partial_x (1-x) x^{a+1-b} \partial_x \left(x^b \tilde{j}_{a,b}(x) \right) = 0 \, . \tag{10.143}$$

From this differential equation, one can efficiently generate the expansion around $x = 1$ fixing the coefficients in the ansatz

$$j_{a,b}(x) = \sum_{i=0}^{\infty} (1-x)^i \left(d_i + e_i \log(1-x) + f_i \log^2(1-x) \right) \, . \tag{10.144}$$

In order to find the initial conditions d_0, e_0 and f_0, we note that the sum (10.137) can be obtained in `Mathematica` in terms of complicated special functions. Taking the $x \to 1$ limit, and massaging the resulting expressions, we find

$$
\begin{aligned}
d_0 &= -\sum_{n=0}^{\infty} \left(\frac{H_{a-b+n+2}}{n+2} - \frac{H_{a+n+2}}{b+n+2} \right) + \frac{1}{2} \left(H_{a-b} \right)^2 - H_{a-b} + H_a \left(H_b + \frac{1}{b+1} \right) \\
&\quad - \frac{H_b}{a} + \frac{H_{a-b}^{(2)}}{2} + \frac{1}{ab} + \frac{1}{-a+b-1} + \frac{1}{ab+a+b+1} + \frac{\pi^2}{6} \, , \\
e_0 &= H_{a+2} - \frac{1}{a} - \frac{1}{a+1} - \frac{1}{a+2} \, , \\
f_0 &= \frac{1}{2} \, .
\end{aligned}
\tag{10.145}
$$

We have not been able to further simplify the infinite sum in d_0. However, it is interesting to note that when expanding (10.123) in the $x, \bar{x} \to 1$ limit, we have found numerically that the contributions from these infinite sums combine to give zero.

Two-variable function

There is another type of double sum that we have not been able to express in closed form:

$$J_{a,b}(x, \bar{x}) \equiv \sum_{n=0}^{\infty} \sum_{m=0}^{n} \frac{x^n}{(n+a)} \frac{\bar{x}^m}{(m+b)} \, . \tag{10.146}$$

For the bulk channel expansion, we need the series expansion of $J_{a,b}(x,\bar{x})$ around $x,\bar{x}=1$. For simplicity, we always take the limits in the order $|1-x| \ll |1-\bar{x}|$. There is no loss of generality, since in order to expand the function $J_{a,b}(\bar{x},x)$, one can use the relation

$$x J_{a,b}(x,\bar{x}) = \Phi(x,1,a-1)\Phi(\bar{x},1,b) - J_{b,a-1}(\bar{x},x)\,, \tag{10.147}$$

which follows from the definition (10.146). The strategy to expand around around $x,\bar{x}=1$ is to first compute the sum in x, and then expand only in $x \to 1$:

$$J_{a,b}(x,\bar{x}) = \sum_{m=0}^{\infty} \frac{(x\bar{x})^m}{m+b}\Phi(x,1,a+m) \tag{10.148}$$

$$= -\sum_{n=0}^{\infty}(1-x)^n \sum_{m=0}^{\infty}\sum_{p=0}^{n} \frac{\bar{x}^m(-m)_p(a+m)_{n-p}\left(H_{a+m+n-p-1}-H_{n-p}+\log(1-x)\right)}{p!(b+m)(n-p)!}\,.$$

Now we perform that sum in $(1-x)^n$ to the desired order $n_{\max}$. For any finite value of $n_{\max}$, we compute the finite sum in p, and then the sum in m can be computed in terms of rational functions of $(1-\bar{x})$ and the function $j_{a,b}(\bar{x})$. Using the results of section 10.A.2, we finally obtain the expansion in $(1-x)$ and $(1-\bar{x})$ to any desired order. Although it would be hard to do this by hand, the previous algorithm can be implemented efficiently in `Mathematica`. Let us also note that the series expansion contains terms of the form $(1-x)^n(1-\bar{x})^{-m}$ for $n,m \geq 0$. A good sanity check of our implementation is that these spurious powers cancel when they are combined as in (10.123).

Chapter 11

Bootstrapping holographic defect correlators

Abstract

We study two-point functions of single-trace half-BPS operators in the presence of a supersymmetric Wilson line in $\mathcal{N} = 4$ SYM. We use inversion formula technology in order to reconstruct the CFT data starting from a single discontinuity of the correlator. In the planar strong coupling limit only a finite number of conformal blocks contributes to the discontinuity, which allows us to obtain elegant closed-form expressions for two-point functions of single-trace operators $\mathcal{O}_J$ of weight $J = 2, 3, 4$. Our final result passes a number of non-trivial consistency checks: it has the correct discontinuity, it satisfies the superconformal Ward identities, it has a sensible expansion in both defect and bulk OPEs, and is consistent with available results coming from localization. The method is completely algorithmic and can be implemented to calculate correlators of arbitrary weight.

11.1   Introduction

The analytic conformal bootstrap is a powerful tool that has seen significant progress in recent years. The basic proposal made in the original papers [122, 123], is that singular terms in a CFT correlator imply the existence of families of operators at large spin. This observation was later systematized and allowed the calculation of CFT data as a series expansion in inverse powers of the spin variable [393]. This line of thinking led to the

279

Lorentzian inversion formula, that neatly captures the dependence of the CFT data as an analytic function of the spin variable [125]. This formula is a fully non-perturbative result valid for any CFT in any dimension.

Apart from giving us an improved understanding of the structure of CFT, the inversion formula is also a powerful calculational tool. Its power lies on the fact that correlators can be reconstructed from a certain discontinuity, which is in general a simpler object. Inversion formula technology is particularly useful for planar theories at strong coupling, where the discontinuity is captured by only a finite number of conformal blocks, simplifying computations considerably. This approach was carried out successfully for four-point functions of half-BPS operators in $\mathcal{N} = 4$ SYM [170, 394], and confirmed a previous conjecture made in Mellin space [395, 396].

Because the presence of a defect does not change the local physics, the main properties that enable the bootstrap for strong coupling correlators are still present if we add a line defect to the configuration. More precisely, in this paper we consider correlators between single trace half-BPS operators and a supersymmetric Wilson line. These are canonical examples of local and non-local operators in $\mathcal{N} = 4$ SYM. One point-function of half-BPS operators in the presence of a line are fixed by kinematics and the overall coefficient can be calculated exactly using matrix-model techniques [397–400]. Less work has been done on two-point correlators in the presence of a line. This is the first case in which correlators depend non-trivially on conformal invariants and therefore capture an infinite amount of CFT data. The only results on the literature so far are an explicit weak-coupling calculation [286], the extreme strong coupling limit where the correlator becomes the square of a one-point function [401, 402], and special kinematical points where the correlator does not depend on invariants and can be calculated using localization [401, 403]. The goal of this paper is to calculate the full two-point correlator as a function of its cross-ratios, to the first non-trivial order at strong coupling, relying only on analytical bootstrap techniques.

The outline of the paper is as follows. In section 11.2 we review the basic kinematics of our two-point functions, including an interpretation of our bootstrap problem in terms of Witten diagrams. In section 11.3 we compute the two-point function for the stress-tensor multiplet, which is the half-BPS operator of weight $J = 2$, using Lorentzian inversion technology, and present an elegant closed-form expression for the full correlator. In section 11.4 we generalize the analysis for operators of higher weight and present explicit solutions for the cases $J = 3, 4$ as a demonstration of our method. Possible future directions are discussed in section 11.5, while in appendix 11.A we give the bulk and defect conformal

280

blocks needed for the computations.

11.2 Preliminaries

In this section we review the basic properties of the setup under study, before jumping into the technicalities of the computation in section 11.3.

11.2.1 Setup

Consider $\mathcal{N} = 4$ SYM theory with gauge group $U(N)$ in the planar $N \to \infty$ limit. The most important local operators in our discussion are single-trace chiral-primary operators:

$$\mathcal{O}_J(x, u) := (2\pi)^J \frac{2^{J/2}}{\sqrt{J\lambda^J}} \operatorname{tr} \left(u \cdot \phi(x) \right)^J. \tag{11.1}$$

Here u is a six-component null polarization vector $u \cdot u = 0$, such that $\mathcal{O}_J(x, u)$ transforms in a symmetric-traceless representation of the R-symmetry group. These are protected operators that preserve half of the supercharges of the theory. The other important observable in our analysis is the supersymmetric Wilson line (sometimes called the Maldacena-Wilson line):

$$\mathcal{W}_\ell := \frac{1}{N} \operatorname{tr} \mathcal{P} \exp \int_{-\infty}^{\infty} d\tau \left(i\dot{x}^\mu A_\mu + |\dot{x}|\theta \cdot \phi \right). \tag{11.2}$$

This extended operator also preserves half of the supercharges, and has been studied extensively in the literature. Here θ is a unit-normalized six-component vector $\theta \cdot \theta = 1$ that parametrizes a direction in R-symmetry space.

In this work we study correlators of local operators in the presence of the supersymmetric Wilson line:[1]

$$\langle\!\langle \mathcal{O}_{J_1}(x_1, u_1) \mathcal{O}_{J_2}(x_2, u_2) \ldots \rangle\!\rangle := \frac{1}{\langle \mathcal{W}_\ell \rangle} \langle \mathcal{W}_\ell \, \mathcal{O}_{J_1}(x_1, u_1) \, \mathcal{O}_{J_2}(x_2, u_2) \ldots \rangle. \tag{11.3}$$

Even though our configuration breaks some of the $PSU(2, 2|4)$ symmetry of $\mathcal{N} = 4$ SYM, these correlation functions are still restricted by the remaining defect (super)conformal symmetry. It is well understood that in defect CFT one-point functions are kinematically fixed, see for example [259]. The simplest observables in which the coordinate dependence is dynamical and not fixed by symmetry are two-point functions of bulk operators. The

---

[1]The overall normalization is redundant in the present case because $\langle \mathcal{W}_\ell \rangle = 1$, but it would be important for circular Wilson loops.

case $J_1 = J_2 = 2$ was studied recently at weak 't Hooft coupling [286] using standard Feynman diagrams. Here we consider instead a perturbative expansion at large 't Hooft coupling:

$$\langle\!\langle \mathcal{O}_J(x_1, u_1) \mathcal{O}_J(x_2, u_2) \rangle\!\rangle \quad \text{as} \quad N \to \infty, \ \lambda = g^2 N \gg 1 \,. \tag{11.4}$$

To be more precise, our correlator admits a double expansion in powers of $\frac{\lambda}{N^2}$ and $\frac{1}{\sqrt{\lambda}}$ of the form

$$\langle\!\langle \mathcal{O}_J \mathcal{O}_J \rangle\!\rangle = \langle\!\langle \mathcal{O}_J \mathcal{O}_J \rangle\!\rangle^{(0)} + \frac{\lambda}{N^2} \left(\langle\!\langle \mathcal{O}_J \mathcal{O}_J \rangle\!\rangle^{(1)} + \frac{1}{\sqrt{\lambda}} \langle\!\langle \mathcal{O}_J \mathcal{O}_J \rangle\!\rangle^{(2)} + O(\lambda^{-1}) \right) + \dots \,, \tag{11.5}$$

where ... stands for terms starting at $\frac{\lambda^2}{N^4}$. As we will discuss shortly, the first two terms in the expansion are somewhat trivial. Our goal then is to use modern bootstrap methods to calculate the $\langle\!\langle \mathcal{O}_J \mathcal{O}_J \rangle\!\rangle^{(2)}$ contribution. The above perturbative expansion has a natural interpretation in terms of the holographic dual of $\mathcal{N} = 4$ SYM, to which we now turn.

11.2.2   Supergravity interpretation

Thanks to the AdS/CFT correspondence [404–406], the strong coupling limit of $\mathcal{N} = 4$ SYM admits a description in terms of classical IIB supergravity on $AdS_5 \times S^5$. Although we do not use this description to carry out our calculations, it is useful to understand the structure of perturbation theory.[2]

The dual of a supersymmetric Wilson loop is a string worldsheet extending inside AdS_5, whose boundary corresponds to the path of the loop [407, 408]. Graphically

$$\includegraphics = \langle \mathcal{W}_\ell \rangle = 1 \,. \tag{11.6}$$

Here the black circle is the boundary of AdS_5, where the CFT lives, and the blue line corresponds to the string worldsheet. The expectation value of the Wilson loop has been the subject of intense study [341, 409, 410], but here we concentrate on the straight geometry.

We are interested on the interplay between the supersymmetric Wilson line and half-BPS single-trace operators $\mathcal{O}_J$. In the holographic description, $\mathcal{O}_J$ are dual to certain KK modes arising from the compactification of the IIB action on S^5. One of these modes can be sourced at the boundary of AdS_5, propagate through the bulk and be absorbed by the

---

[2]We thank S. Giombi for useful correspondence regarding the holographic calculation.

string worldsheet. This process is dual to the one-point function of $\mathcal{O}_J$ in the presence of the Wilson line. Graphically

$$\text{(diagram)} = \langle\!\langle \mathcal{O}_J(x, u) \rangle\!\rangle = a_J \frac{(u \cdot \theta)^J}{(x^\perp)^J} \,. \tag{11.7}$$

The precise constant a_J has been determined at strong 't Hooft coupling using holography [399, 411], and is consistent with the exact result coming from the matrix-model description. The result is of order $a_J \sim O(\frac{\sqrt{\lambda}}{N})$, as can also be seen by simple power counting arguments.

The focus of the present work is on two-point functions at strong coupling. The leading order contribution corresponds to a disconnected diagram, where the two operators in the boundary of AdS_5 interact through the bulk "ignoring" the string worldsheet:

$$\text{(diagram)} = \langle\!\langle \mathcal{O}_J(x_1, u_1) \mathcal{O}_J(x_2, u_2) \rangle\!\rangle_{\text{disc.}} = \frac{(u_1 \cdot u_2)^J}{(x_{12}^2)^J} \,. \tag{11.8}$$

Following the usual convention in CFT, we normalize this diagram to unity. This corresponds to $\langle\!\langle \mathcal{O}_J \mathcal{O}_J \rangle\!\rangle^{(0)}$ in equation (11.5). The next contribution at strong coupling corresponds to a factorized diagram, where the operators do not interact in the bulk:

$$\text{(diagram)} = \langle\!\langle \mathcal{O}_J(x_1, u_1) \rangle\!\rangle \langle\!\langle \mathcal{O}_J(x_2, u_2) \rangle\!\rangle = a_J^2 \frac{(u_1 \cdot \theta)^J (u_2 \cdot \theta)^J}{(x_1^\perp x_2^\perp)^J} \,. \tag{11.9}$$

From the scaling of the one-point coefficients a_J, it is clear this diagram contributes at order $\frac{\lambda}{N^2}$, so it corresponds to the term $\langle\!\langle \mathcal{O}_J \mathcal{O}_J \rangle\!\rangle^{(1)}$. The first non-trivial correction to the two-point function contains an interaction vertex in the bulk [401]. In the exchanged line one sums over all KK modes that can couple to two $\mathcal{O}_J$'s. Schematically we have

$$\text{(diagram)} \,. \tag{11.10}$$

This is the diagram we calculate in the present work.[3]

Instead of an explicit calculation using the effective action in $AdS_5 \times S^5$, we will bootstrap the result using the bulk-to-defect inversion formula obtained in [266]. The inversion

---

[3] In the case of holographic four-point functions, there exist contact Witten diagrams which are correctly reconstructed from the inversion formula [170, 394]. If such diagrams are present in the defect case, our bootstrap result should capture them. We defer a more detailed study of the explicit holographic calculation for future work.

formula reconstructs a correlator from its singular part, which is mathematically captured by a discontinuity:

$$\text{(diagram)} \sim \int \text{Disc}\,\text{(diagram)}. \tag{11.11}$$

The crucial property of holographic CFT's is that the discontinuity is dramatically simpler than the correlator. In particular, we show below that the discontinuity receives corrections only from a finite number of single-trace operators exchanged in the bulk. Each of these contributions is schematically a product of a tree-level one-point function and a three-point function:

$$\text{(diagram)} \sim \sum_{\substack{\text{single}\\\text{traces}}} \int \text{(diagram)} \times \text{(diagram)}. \tag{11.12}$$

The one- and three-point functions are known from localization, so all is left is to compute a certain integral and sum over finitely many single-trace contributions. In the rest of the paper, we translate this pictorial representation into a concrete bootstrap algorithm, that fully fixes two-point correlators with minimal external input.

11.2.3 Superconformal kinematics

The defect CFT associated with the Wilson line (11.2) preserves an $OSp(4^*|4)$ subgroup of the full $PSU(2,2|4)$ symmetry. From the spacetime perspective, the defect preserves an $SO(2,1) \subset SO(4,2)$ subgroup of the full conformal algebra. Furthermore, the presence of a preferred direction θ preserves only $SO(5)_R \subset SO(6)_R$ of the R-symmetry. The kinematics of non-supersymmetric defects have been thoroughly studied in [259]. Below we only give a brief review, highlighting the new features due to supersymmetry, such as superconformal Ward identities and superconformal blocks.

Two-point function and cross-ratios

A two-point function in a defect CFT depends on two spacetime cross-ratios, while in our setup there is an extra R-symmetry cross-ratio σ:

$$\langle\!\langle \mathcal{O}_J(x_1,u_1)\mathcal{O}_J(x_2,u_2)\rangle\!\rangle = \frac{(u_1\cdot\theta)^J(u_2\cdot\theta)^J}{|x_1^\perp|^J|x_2^\perp|^J}\mathcal{F}^{(J)}(z,\bar z,\sigma). \tag{11.13}$$

For the spacetime part, we use the cross-ratios $z, \bar{z}$ defined in [266]

$$\frac{z + \bar{z}}{2\sqrt{z\bar{z}}} = \frac{x_1^\perp \cdot x_2^\perp}{|x_1^\perp||x_2^\perp|}, \qquad \frac{(1-z)(1-\bar{z})}{\sqrt{z\bar{z}}} = \frac{x_{12}^2}{|x_1^\perp||x_2^\perp|}. \tag{11.14}$$

Geometrically $z, \bar{z}$ are coordinates in a plane orthogonal to the defect. Indeed, placing the first operator at $x_1 = (1, 0, 0, 0)$ and the second one in a xy-plane $x_2 = (x, y, 0, 0)$, then $z = x + iy$ and $\bar{z} = x - iy$. In Lorentzian signature, one would instead find that z and $\bar{z}$ are real and independent. On the other hand, the R-symmetry cross-ratio is defined as

$$\sigma := \frac{(u_1 \cdot u_2)}{(u_1 \cdot \theta)(u_2 \cdot \theta)}. \tag{11.15}$$

The correlator $\mathcal{F}^{(J)}(z, \bar{z}, \sigma)$ is a polynomial of order J in the σ cross-ratio. This reflects the number of different ways to contract u_1, u_2 with each other and with θ, the polarization of the Wilson-line defect. Before moving on, let us point out that one can also consider operators restricted to the line and study the corresponding $1d$ CFT, this configuration has been studied recently by a variety of means [233, 262, 288, 346, 412, 413][4]. In this work we consider bulk operators outside the line, which probes the interplay between local physics and the defect.

Structure of the correlator

As discussed above, the leading contributions at strong coupling to $\langle\!\langle \mathcal{O}_J \mathcal{O}_J \rangle\!\rangle$ take the simple form (11.8) and (11.9). Comparing with the form of the two-point function (11.13) we find

$$\mathcal{F}^{(J)}(z, \bar{z}, \sigma) = \left(\frac{\sigma\sqrt{z\bar{z}}}{(1-z)(1-\bar{z})} \right)^J + a_J^2 + O\left(\frac{\sqrt{\lambda}}{N^2} \right). \tag{11.16}$$

Our goal is to compute the correlation function at the next order $O(\frac{\sqrt{\lambda}}{N^2})$. For simplicity we decompose the correlator at this order in powers of the R-symmetry cross-ratio σ:[5]

$$\mathcal{F}^{(J)}(z, \bar{z}, \sigma)\big|_{O(\frac{\sqrt{\lambda}}{N^2})} = \sum_{j=0}^{J} \sigma^j F_{J-j}^{(J)}(z, \bar{z}). \tag{11.17}$$

Below we use bootstrap methods to reconstruct the functions $F_j^{(J)}(z, \bar{z})$, leading to the final results in equations (11.64), (11.82) and (11.86).

---

[4]Similar setups have also been considered for $3d$ ABJM theories [260, 353, 354].

[5]Note that the definition of $F_j^{(J)}$ in this decomposition is slightly different to the one used in [286]: here the terms are ordered in terms of powers of σ and not Ω. Furthermore, here we keep outside the definition the two leading contributions which are trivial.

Superconformal Ward identities

An important property of our correlator is that it satisfies *superconformal Ward identities*. These were studied in detail for half-BPS boundaries in [285], where it was observed that with a suitable identification of the cross-ratios, they also apply to the half-BPS line defect.[6] In our conventions the Ward identities read

$$\left(\partial_z + \frac{1}{2}\partial_\omega\right)\mathcal{F}^{(J)}(z,\bar{z},\sigma)\Big|_{z=\omega} = 0\,, \quad \left(\partial_{\bar{z}} + \frac{1}{2}\partial_\omega\right)\mathcal{F}^{(J)}(z,\bar{z},\sigma)\Big|_{\bar{z}=\omega} = 0\,, \qquad (11.18)$$

where the natural variable to use is ω, defined by

$$\sigma = -\frac{(1-\omega)^2}{2\omega}\,. \qquad (11.19)$$

It is not hard to check that the two leading terms (11.16) satisfy these equations. Note that the above Ward identities take a form very similar to other setups in the literature [244, 245, 357]. In the case of $\mathcal{N}=4$ SYM without defects, the Ward identities admit a simple closed-form solution in which the different R-symmetry channels are related by algebraic relations. This drastically simplifies the analysis because in the end one can just work with the independent channels. Sadly, the defect setup of this paper is closer to the Ward identities in three dimensions, where such an algebraic relation does no exist [244]. It is possible however to relate the different R-symmetry channels by the action of a non-local operator. This is obviously more cumbersome, but one can still implement it in order to focus only on the independent portions of the correlator [207]. In this paper we work explicitly with all the R-symmetry channels, however finding a better parameterization for our correlators is an interesting problem that should be studied in more detail.

Crossing equation

The last important ingredient for our calculation are the defect CFT crossing equations. Here we only summarize them, and refer the reader to [259] for further details. In any CFT it is possible to fuse two bulk local operators as a sum of bulk operators. This *bulk OPE* is denoted schematically as $\mathcal{O}_J\mathcal{O}_J \sim \sum_\mathcal{O} \lambda_{JJ\mathcal{O}}\mathcal{O}$. On the other hand, the *defect OPE* expands a bulk operator as a sum of defect operators $\mathcal{O}_J \sim \sum_{\hat{\mathcal{O}}} b_{J\hat{\mathcal{O}}}\hat{\mathcal{O}}$. Note that for a bulk one-point function $\langle\!\langle\mathcal{O}\rangle\!\rangle \sim a_\mathcal{O}$, the defect OPE implies $a_\mathcal{O} = b_{\mathcal{O}\hat{1}}$ where $\hat{1}$ is the defect

---

[6]To be precise, $z,\bar{z}$ are mapped to the boundary R-symmetry cross-ratios w_1, w_2, while σ is mapped to the boundary spacetime cross-ratio -2ξ (this factor -2 ensures the correctness of this map).

identity operator. These two expansions can be inserted in a two-point function, resulting in a *crossing equation*

$$\mathcal{F}^{(J)}(z,\bar{z},\sigma) = \left(\frac{\sqrt{z\bar{z}}\,\sigma}{(1-z)(1-\bar{z})}\right)^J \sum_{\mathcal{O}} \lambda_{JJ\mathcal{O}} a_{\mathcal{O}} \mathcal{G}_{\mathcal{O}}^{(J)}(z,\bar{z},\sigma) = \sum_{\hat{\mathcal{O}}} b_{J\hat{\mathcal{O}}}^2 \hat{\mathcal{G}}_{\hat{\mathcal{O}}}^{(J)}(z,\bar{z},\sigma)\,. \quad (11.20)$$

It is important to keep in mind that operators in superconformal theories belong to super-conformal multiplets. For example, in the crossing equation, $\mathcal{O}$ refers to the superconformal primary operator of a $PSU(2,2|4)$ representation, which is labeled by the dimension Δ, the spin ℓ, and an $SO(6)_R$ label K. Similarly, $\hat{\mathcal{O}}$ is the superconformal primary of an $OSp(4^*|4)$ representation labeled by the defect dimension $\widehat{\Delta}$, the transverse-spin s, and an $SO(5)_R$ label $\hat{K}$.[7] Supersymmetry fixes the contributions of superdescendant operators, so the expansion (11.20) is organized in *superconformal blocks*. These are linear combination of non-supersymmetric conformal blocks:

$$\begin{aligned}
\mathcal{G}_{\mathcal{O}}^{(J)}(z,\bar{z},\sigma) &= \sum_{\Delta,\ell,K} c_{\Delta,\ell,K}^{(J)} h_K(\sigma) f_{\Delta,\ell}(z,\bar{z})\,, \\
\hat{\mathcal{G}}_{\hat{\mathcal{O}}}^{(J)}(z,\bar{z},\sigma) &= \sum_{\widehat{\Delta},s,\hat{K}} c_{\widehat{\Delta},s,\hat{K}}^{(J)} \hat{h}_{\hat{K}}(\sigma) \hat{f}_{\widehat{\Delta},s}(z,\bar{z})\,.
\end{aligned} \quad (11.21)$$

The sums range over all operators in the supermultiplets of $\mathcal{O}/\hat{\mathcal{O}}$ that can appear in the bulk/defect OPE of $\mathcal{O}_J$. The function $f_{\Delta,\ell}(z,\bar{z})$ is a bulk-channel conformal block, see (11.91) for a useful series representation. Similarly, $\hat{f}_{\widehat{\Delta},s}(z,\bar{z})$ is a defect-channel conformal block given in (11.94). Finally, $h_K(\sigma)$ and $\hat{h}_{\hat{K}}(\sigma)$ are bulk and defect R-symmetry blocks respectively. They are polynomials in σ with a simple hypergeometric closed form expression (11.95). The precise relative coefficients $c_{\Delta,\ell,K}^{(J)}$ and $c_{\widehat{\Delta},s,\hat{K}}^{(J)}$ have been presented in the appendix of [286].

11.2.4 Topological subsector

An important property of our correlators is that they contain a topological subsector. In terms of the cross-ratios, the topological subsector can be obtained by setting $z = \bar{z} = \omega$. This projects out all the non-protected operators from the bulk and defect OPE and only half-BPS protected operators remain. This topological subsector goes beyond our two-point correlators, and it actually describes a closed-subsector of the operator spectrum of

---

[7]Detailed analysis of the representation theory of these supergroups can be found in the literature [27, 181, 182].

the theory. The CFT data of the topological subsector can be obtained by solving Gaussian multi-matrix models [288, 289, 399, 401]. Some of the explicit results that we present below are necessary to fix overall coefficients in our bootstrap analysis, while others provide non-trivial consistency checks of our calculation.

We start by looking at bulk single-trace half-BPS operators $\mathcal{O}_J$ defined in (11.1). We follow the usual normalization conventions such that their two-point function is unit normalized, and the dynamical information is captured by three-point functions. In our conventions

$$\langle \mathcal{O}_J(x_1, u_1) \mathcal{O}_J(x_2, u_2) \rangle = \frac{(u_1 \cdot u_2)^J}{(x_{12}^2)^J} \, ,$$

$$\langle \mathcal{O}_{J_1}(x_1, u_1) \mathcal{O}_{J_2}(x_2, u_2) \mathcal{O}_{J_3}(x_3, u_3) \rangle = \lambda_{J_1 J_2 J_3} \frac{(u_1 \cdot u_2)^{J_{123}} (u_2 \cdot u_3)^{J_{231}} (u_3 \cdot u_1)^{J_{312}}}{|x_{12}|^{2J_{123}} |x_{23}|^{2J_{231}} |x_{31}|^{2J_{312}}} \, ,$$

$$(11.22)$$

with $J_{ijk} := (J_i + J_j - J_k)/2$. The OPE coefficients $\lambda_{J_1 J_2 J_3}$ were originally computed in [414], and they are independent of the coupling:

$$\lambda_{J_1 J_2 J_3} = \frac{\sqrt{J_1 J_2 J_3}}{N} \, . \tag{11.23}$$

As already discussed, one-point functions of single-trace operators in the presence of the supersymmetric Wilson line are kinematically fixed:

$$\langle\!\langle \mathcal{O}_J(x, u) \rangle\!\rangle = a_J \frac{(u \cdot \theta)^J}{|x^\perp|^J} \, . \tag{11.24}$$

Since the normalization of $\mathcal{O}_J$ is determined by the two point function, the coefficient a_J contains dynamical information about the defect CFT.[8] The precise value can be obtained from a perturbative calculation [397] or from a matrix-model calculation [398–400]

$$a_J = \frac{\sqrt{\lambda J}}{2^{J/2+1} N} \frac{I_J(\sqrt{\lambda})}{I_1(\sqrt{\lambda})} \underset{\lambda \gg 1}{\overset{}{\gtrless}} \frac{\sqrt{\lambda J}}{2^{J/2+1} N} \left(1 - \frac{(J+1)(J-1)}{2\sqrt{\lambda}} + O(\lambda^{-1}) \right) . \tag{11.25}$$

Note that it is also possible to construct half-BPS multi-trace operators. For example, the OPE between the two single-trace operators $\mathcal{O}_J \times \mathcal{O}_J$ must contain the following *double-trace* operator:

$$\mathcal{O}_{(J,J)}(x, u) := (2\pi)^{2J} \frac{2^{J-1/2}}{J \lambda^J} \, \text{tr} \left(u \cdot \phi(x) \right)^J \text{tr} \left(u \cdot \phi(x) \right)^J . \tag{11.26}$$

---

[8]For the particular case $J = 2$ the coefficient a_2 is proportional to the Bremsstrahlung function [342].

The prefactor is chosen to have a unit normalized two-point function. By using the localization techniques of [399, 400, 403], we derived the one-point function of $\mathcal{O}_{(J,J)}$ and its three-point function with single-trace operators. Their product reads

$$a_{(J,J)}\lambda_{JJ(J,J)} = \frac{J\lambda}{2^{J+2}N^2}\frac{I_{2J-1}(\sqrt{\lambda})}{I_1(\sqrt{\lambda})} \stackrel{\lambda\gg 1}{=} \frac{J\lambda}{2^{J+2}N^2}\left(1 - \frac{2J(J-1)}{\sqrt{\lambda}} + O(\lambda^{-1})\right). \quad (11.27)$$

This is all the information we need about bulk protected operators.

The topological sector also captures information involving protected operators localized on the defect. There is a large degeneracy of protected defect operators which has been discussed in [289]. For our purposes, there are two defect operators that play an important role. On the one hand, there are defect operators inserted inside the path-ordering of the Wilson line, which we write as

$$\hat{\mathcal{O}}_{\hat{K}}(\tau, \hat{u}) = \mathcal{W}\left[\left(\hat{u}\cdot\phi(\tau)\right)^{\hat{K}}\right]. \quad (11.28)$$

These operators are in symmetric traceless representations of the $SO(5)_R$ symmetry preserved by the defect. Therefore, $\hat{u}$ is a null polarization vector orthogonal to the Wilson line polarization $\hat{u}\cdot\theta = \hat{u}\cdot\hat{u} = 0$. On the other hand, it is possible to define a similar operator which lives outside the path-ordering

$$\hat{\mathcal{O}}_{(\hat{K})}(\tau, \hat{u}) = \mathcal{W}\,\mathrm{tr}\left(\hat{u}\cdot\phi(\tau)\right)^{\hat{K}}. \quad (11.29)$$

For both of these operators, one should choose a normalization such that their defect two-point functions are unit normalized. The non-trivial dynamical information is then encoded in the bulk-defect two-point function:

$$\langle\!\langle\hat{\mathcal{O}}_{\hat{K}}(\tau_1, \hat{u}_1)\hat{\mathcal{O}}_{\hat{K}}(\tau_2, \hat{u}_2)\rangle\!\rangle = \frac{(\hat{u}_1\cdot\hat{u}_2)^{\hat{K}}}{\tau_{12}^{2\hat{K}}},$$

$$\langle\!\langle\mathcal{O}_J(x_1, u_1)\hat{\mathcal{O}}_{\hat{K}}(\tau_2, \hat{u}_2)\rangle\!\rangle = b_{J\hat{K}}\frac{(u_1\cdot\hat{u}_2)^{\hat{K}}(u_1\cdot\theta)^{J-\hat{K}}}{((x_1^\perp)^2 + \tau_{12}^2)^{\hat{K}}|x_1^\perp|^{J-\hat{K}}}. \quad (11.30)$$

For operators of the first type $\hat{\mathcal{O}}_{\hat{K}}$, the bulk-defect coefficient has been calculated at strong coupling in the planar limit [289]

$$b_{J\hat{K}} = \frac{\lambda^{\frac{2-\hat{K}}{4}}}{N}\frac{2^{\frac{3\hat{K}-J-2}{2}}\sqrt{J}}{\sqrt{\hat{K}!}}\frac{\Gamma(\frac{J+\hat{K}+1}{2})}{\Gamma(\frac{J-\hat{K}+1}{2})}\left(1 + \frac{4 - 4J^2 + 5\hat{K} + \hat{K}^2}{8\sqrt{\lambda}} + O(\lambda^{-1})\right). \quad (11.31)$$

On the other hand, the coefficients $b_{J(\hat{K})}$ have not appeared in the literature. An interesting outcome of our analysis is a prediction for the value of $b_{J(\hat{J})}$. However, let us stress that our correlators also contain information about infinitely many non-protected operators that are not captured by the topological subsector.

Note that the crossing equation given in (11.20) truncate on both sides in the topological sector [285]. This is known as *microbootstrap*, and in some cases the system of equations can be solved exactly [415].

11.3 $\langle\langle \mathcal{O}_2 \mathcal{O}_2 \rangle\rangle$ at strong coupling

In this section we compute the correlator $\langle\langle \mathcal{O}_2 \mathcal{O}_2 \rangle\rangle$ in the strong coupling limit. As explained in section 11.2.2, the two leading contributions are somewhat trivial and take the form given in equations (11.8) and (11.9). As in equation (11.17), we decompose the next correction into three R-symmetry channels:

$$\mathcal{F}^{(2)}(z, \bar{z}, \sigma)\big|_{O(\frac{\sqrt{\lambda}}{N^2})} = \sigma^2 F_0(z, \bar{z}) + \sigma F_1(z, \bar{z}) + F_2(z, \bar{z}). \tag{11.32}$$

For compactness, here and for the rest of this section we drop the superscripts in the functions $F_j^{(J)}(z, \bar{z})$. In what follows we derive this correlator using the Lorentzian inversion formula presented in [266].

11.3.1 Lorentzian inversion formula

The idea of the Lorentzian inversion formula is that the *discontinuity* of the correlator is sufficient to extract the full defect CFT data, which in turn can be used for reconstructing the full correlator. For now we consider general single-trace operators $\mathcal{O}_J(x, u)$, and later we focus on the $J = 2$ case. For a codimension-three defect, such as a Wilson line in four dimensions, the inversion formula reads

$$\begin{aligned} b_j(\hat{\Delta}, s) = \int_0^1 \frac{dz}{2z} z^{-(\hat{\Delta}-s)/2} \int_1^{1/z} \frac{d\bar{z}}{2\pi i} (1 - z\bar{z})(\bar{z} - z)\bar{z}^{-(\hat{\Delta}+s)/2-2} \\ \times \, {}_2F_1\left(\frac{1}{2}, 1 + s, \frac{3}{2} + s; \frac{z}{\bar{z}}\right) {}_2F_1\left(\frac{1}{2}, 1 - \hat{\Delta}, \frac{3}{2} - \hat{\Delta}, z\bar{z}\right) \operatorname{Disc} F_j(z, \bar{z}), \end{aligned} \tag{11.33}$$

where the discontinuity is computed around the branch cut in $\bar{z} \in [1, \infty)$:

$$\operatorname{Disc} F_j(z, \bar{z}) = F_j(z, \bar{z} + i\epsilon) - F_j(z, \bar{z} - i\epsilon), \qquad \bar{z} \geq 1. \tag{11.34}$$

The inversion formula is *bosonic* and thus it should be applied to each R-symmetry channel $F_j(z, \bar{z})$ independently. The defect conformal dimensions are encoded in the poles of $b_j(\widehat{\Delta}, s)$, while the residues are OPE coefficients:

$$b_j(\widehat{\Delta}, s) = -\sum_{n \geq 0} \frac{(b_j^2)_{n,s}}{\widehat{\Delta} - (J + s + 2n + \gamma_{n,s})} \, . \tag{11.35}$$

The coefficients $(b_j)_{n,s}$ capture the normalization of the bulk-defect two-point function $\langle\!\langle \mathcal{O}_J \hat{\mathcal{O}}_{n,s} \rangle\!\rangle$, where the exchanged operators $\hat{\mathcal{O}}_{n,s}$ have dimension $\widehat{\Delta}_{n,s} = J + s + 2n + \gamma_{n,s}$ and transverse-spin s.[9] In the case where (small) anomalous dimensions are relevant, second-order poles are also present in the formula when Taylor expanding:

$$b_j(\widehat{\Delta}, s) = -\sum_{n \geq 0} \left(\frac{(b_j^2)_{n,s}}{\widehat{\Delta} - (J + s + 2n)} + \frac{(b_j^2 \gamma_j)_{n,s}}{(\widehat{\Delta} - (J + s + 2n))^2} + \dots \right) . \tag{11.36}$$

Once the OPE coefficients and the anomalous dimensions have been obtained, the correlator can be expanded in defect spacetime blocks:

$$\tilde{F}_j(z, \bar{z}) = \sum_{s=0}^{\infty} \sum_{n=0}^{\infty} \left((b_j^2)_{n,s} \hat{f}_{J+s+2n,s}(z, \bar{z}) + (b_j^2 \gamma_j)_{n,s} \partial_{\widehat{\Delta}} \hat{f}_{J+s+2n,s}(z, \bar{z}) \right) . \tag{11.37}$$

Note that we have introduced the notation $\tilde{F}_j$ instead of F_j, since the inversion formula might miss contributions from low spins $s < s_*$ [266]. In that case, we must add extra terms with spins $s = 0, 1, \dots, s_*$ to $\tilde{F}_j$ in order to recover the full correlator F_j. This procedure will be described in detail in section 11.3.4. Except for these subtleties, equations (11.33)-(11.37) reconstruct the function F_j using only information in its discontinuity $\mathrm{Disc}\, F_j$.

11.3.2 Computation of the discontinuity

The first step in order to apply the inversion formula (11.33) is to compute the discontinuity. As we now show, the discontinuity can be computed even though the full correlator is not known.

The idea is to expand the correlation functions in the bulk channel. The conformal blocks in (11.91) can be written as $f_{\Delta,\ell}(z, \bar{z}) = [(1 - z)(1 - \bar{z})]^{(\Delta-\ell)/2} \tilde{f}_{\Delta,\ell}(z, \bar{z})$, where the function $\tilde{f}_{\Delta,\ell}(z, \bar{z})$ has an expansion around $z, \bar{z} = 1$ in positive integer powers. As a result,

---

[9]In general the defect spectrum contains degeneracies, in which case the CFT data has to be understood as a sum over degenerate operators.

only the prefactor can have non-vanishing discontinuity. Therefore, the contribution of a single bulk operator $\mathcal{O}$ to the discontinuity is

$$\text{Disc } F_j(z, \bar{z})\big|_{\mathcal{O}} \propto (z\bar{z})^{J/2}(1-z)^{\frac{\Delta-(2J+\ell)}{2}} \tilde{f}_{\Delta,\ell}(z, \bar{z}) \text{ Disc} \left[(1-\bar{z})^{\frac{\Delta-(2J+\ell)}{2}}\right]. \tag{11.38}$$

There are two situations when this discontinuity does not vanish:

1. If Δ is non-integer. This corresponds to $\mathcal{O}$ having an anomalous dimension correcting its tree-level dimension $\Delta = 2J + \ell + 2n + \gamma$.

2. If Δ is integer but $\Delta < 2J + \ell$. This corresponds to $\mathcal{O}$ being a protected single-trace operator, whose dimension is below the double-trace threshold. Note that even though $\text{Disc}(1-\bar{z})^{-n}$ naively vanishes, for $n > 0$ the singularity at $\bar{z} = 1$ gives a finite contribution to the inversion formula.[10]

In our setup the discontinuity only receives contributions of the second type. This claim can be proved by studying the superconformal bulk OPE in detail. From now on we focus on the $J = 2$ case. It was shown in [285] that in the presence of the line defect the OPE $\mathcal{O}_2 \times \mathcal{O}_2$ truncates in the following way:

$$\mathcal{O}_2 \times \mathcal{O}_2 \to \mathbb{1} + \mathcal{B}_{[0,2,0]} + \mathcal{B}_{[0,4,0]} + \sum_{\ell} \mathcal{C}_{[0,2,0],\ell} + \sum_{\Delta,\ell} \mathcal{A}^{\Delta}_{[0,0,0],\ell}. \tag{11.39}$$

These representations correspond to the operators acquiring a non-vanishing one-point function in the presence of a half-BPS line defect (like the supersymmetric Wilson line we study in this work). The operators in the $\mathcal{B}_{[0,2,0]}$ multiplet have integer dimension $\Delta < 4+\ell$, so they have non-vanishing discontinuity. The operators in the $\mathcal{B}_{[0,4,0]}$, $\mathcal{C}_{[0,2,0],\ell}$ multiplets have integer dimension $\Delta \geq 4+\ell$, so they cannot contribute to the discontinuity. Only the unprotected multiplets $\mathcal{A}^{\Delta}_{[0,0,0],\ell}$ can have anomalous dimensions. The scaling dimensions of these multiplets have the following schematic structure [416]

$$\Delta = 2J + 2n + \ell + \frac{1}{N^2}\left(a + \frac{b}{\lambda^{3/2}} + \dots\right) + O(N^{-4}), \tag{11.40}$$

which means anomalous dimensions do not contribute at the order in perturbation theory we are working. This implies all the operators in the bulk OPE (11.39) do not have anomalous dimensions at this order, so the correlator must admit an expansion in integer powers in the limit $z, \bar{z} \to 1$.

---

[10]This will be proved concretely by deriving equation (11.47).

The main consequence of these observations is that only the superblock $\mathcal{G}_{[0,2,0]}$ corresponding to $\mathcal{B}_{[0,2,0]}$ has non-vanishing discontinuity:

$$\operatorname{Disc} \mathcal{F}^{(2)}(z, \bar{z}, \sigma)\Big|_{O(\frac{\sqrt{\lambda}}{N^2})} = \lambda_{222} a_2 \operatorname{Disc} \left(\frac{\sqrt{z\bar{z}}\,\sigma}{(1-z)(1-\bar{z})}\right)^2 \mathcal{G}_{[0,2,0]}(z, \bar{z}, \sigma). \tag{11.41}$$

In the rest of this section we reconstruct the full correlator from the single superblock $\mathcal{G}_{[0,2,0]}$.

11.3.3 Inversion of $\mathcal{B}_{[0,2,0]}$

We now invert the superblock $\mathcal{G}_{[0,2,0]}$ in order to extract the defect CFT data, and by resumming the defect expansions, we obtain the correlators given in (11.54), (11.56) and (11.57).

The superblocks $\mathcal{G}_{[0,K,0]}$ are known and given in equation (11.72). For $K = 2$ they take the form

$$\mathcal{G}_{[0,2,0]}(z, \bar{z}, \sigma) = h_2(\sigma) f_{2,0}(z, \bar{z}) + \frac{1}{180} h_0(\sigma) f_{4,2}(z, \bar{z}), \tag{11.42}$$

where $h_K(\sigma)$ and $f_{\Delta,\ell}(z, \bar{z})$ correspond respectively to R-symmetry and spacetime conformal blocks, which can be found in appendix 11.A. We see that we need to invert two bosonic blocks, namely a scalar block $f_{2,0}$ as well as the stress-tensor block $f_{4,2}$. Using the definition (11.95) for the R-symmetry blocks, we can extract the discontinuities in the three channels:

$$\operatorname{Disc} F_0(z, \bar{z}) = -\lambda_{222} a_2 \operatorname{Disc} \frac{z\bar{z}}{180(1-z)^2(1-\bar{z})^2} (30 f_{2,0}(z, \bar{z}) - f_{4,2}(z, \bar{z})),$$

$$\operatorname{Disc} F_1(z, \bar{z}) = \lambda_{222} a_2 \operatorname{Disc} \frac{z\bar{z}}{(1-z)^2(1-\bar{z})^2} f_{2,0}(z, \bar{z}), \tag{11.43}$$

$$\operatorname{Disc} F_2(z, \bar{z}) = 0.$$

It is convenient to express the blocks using the following variable:

$$\bar{y} := \frac{1-\bar{z}}{\sqrt{\bar{z}}}. \tag{11.44}$$

As discussed in the previous section, only negative powers of $\bar{y}$ are relevant for the discontinuity. Since a factor $\bar{y}^{-2}$ comes from the prefactor in (11.43), we have to expand the bulk blocks to order $O(\bar{y})$ as $\bar{y} \to 0$. Using the methods in appendix 11.A.1 we find

$$f_{2,0}(z, \bar{z}) = -\bar{y} \log z + O(\bar{y}^3),$$

$$f_{4,2}(z, \bar{z}) = \bar{y} \left(\frac{90(z+1)}{z-1} - \frac{30\left(z^2 + 4z + 1\right) \log z}{(z-1)^2}\right) + O(\bar{y}^3). \tag{11.45}$$

Let us now invert an arbitrary power $\bar{y}^{-p}$. In this section we only need the $p = 1$ case, but the case $p \geq 2$ is relevant for section 11.4. For arbitrary powers of $\bar{y}$ the discontinuity (11.34) results in:

$$\text{Disc}\, \bar{y}^{-p} = 2i \sin(p\pi)(-\bar{y})^{-p}. \tag{11.46}$$

In principle now we should compute the inversion integral (11.33). In practice this is too hard, so we expand the integrand as $z \to 0$.[11] Each new power of z will give information of a new defect family with higher transverse-twist $\widehat{\Delta} - s$. In the $z \to 0$ limit the integral over $\bar{z}$ is standard and gives the following result:

$$B_p(\beta) = 2i \sin(\pi p) \int_1^\infty \frac{d\bar{z}}{2\pi i} \bar{z}^{-\beta/2-1}(-\bar{y})^{-p} = \frac{\Gamma\left(\frac{\beta+p}{2}\right)}{\Gamma(p)\Gamma\left(\frac{\beta-p+2}{2}\right)}. \tag{11.47}$$

Although for integer $p > 0$ the discontinuity (11.46) naively vanishes, note that the final result is perfectly finite. This is expected, because the correlator is singular at $\bar{z} \to 1$, and the inversion formula reconstructs the CFT data from this singularity. Note that for $p = 1$ then $B_1(\beta) = 1$, which simplifies our calculations below.

In general the integral over z has the following structure:

$$b(\widehat{\Delta}, s) = \sum_{n \geq 0} \int_0^1 \frac{dz}{2z} z^{-\frac{\widehat{\Delta}-(2+s+2n)}{2}} \left[b^{(0,n)}(\widehat{\Delta}, s) + b^{(1,n)}(\widehat{\Delta}, s) \log z \right]$$

$$= -\sum_{n \geq 0} \left(\frac{b^{(0,n)}(\widehat{\Delta}, s) + 2\partial_{\widehat{\Delta}} b^{(1,n)}(\widehat{\Delta}, s)}{\widehat{\Delta} - (2+s+2n)} + \frac{2 b^{(1,n)}(\widehat{\Delta}, s)}{(\widehat{\Delta} - (2+s+2n))^2} + \dots \right)_{\widehat{\Delta}=2+s+2n}. \tag{11.48}$$

This has to be compared to equation (11.36) in order to obtain the OPE coefficients as well as the product of anomalous dimensions with tree-level OPE coefficients. The presence of logs in equation (11.45) reveals that the scaling dimensions of the defect operators receive anomalous corrections at this order.

In principle the results above are sufficient for extracting the defect CFT data in an algorithmic way and for resumming the correlator using equation (11.37). However, for the $p = 1$ case we can derive a closed-form formula for the defect CFT data corresponding to the bosonic blocks of equation (11.42). In the following we denote by $b_{f_{\Delta,\ell}}(\widehat{\Delta}, s)$ the result of the inversion formula performed for individual bosonic spacetime blocks $f_{\Delta,\ell}$. We begin with the scalar block $f_{2,0}$. Using the inversion formula as well as the integrals (11.47) and

---

[11]As a side effect, the expansion as $z \to 0$ makes the inversion integral convergent order by order in z.

(11.48) we find

$$b_{f_{2,0}}(\widehat{\Delta}, s) = - \sum_{j,k \geq 0} \frac{(s+1)_j (1/2)_j}{j!(s+3/2)_j} \frac{(1-\widehat{\Delta})_k (1/2)_k}{k!(3/2 - \widehat{\Delta})_k} \int_0^1 \frac{dz}{2z} z^{-\frac{\widehat{\Delta}-s-2}{2}} z^{j+k} \log z$$

$$= - \sum_{j,k \geq 0} \frac{(s+1)_j (1/2)_j}{j!(s+3/2)_j} \frac{(1-\widehat{\Delta})_k (1/2)_k}{k!(3/2 - \widehat{\Delta})_k} \frac{-2}{(\widehat{\Delta}-s-2(j+k+1))^2}, \tag{11.49}$$

where we have expanded the hypergeometric functions of equation (11.33). There are only second-order poles present, thus only the coefficients $b^{(1,n)}$ are non-trivial in equation (11.48). The infinite sum can be obtained in closed form

$$\begin{aligned} b^{(0,n)}_{f_{2,0}}(\widehat{\Delta}, s) &= 0\,, \\ b^{(1,n)}_{f_{2,0}}(\widehat{\Delta}, s) &= \mathcal{C}^{(n)}(\widehat{\Delta}, s)\,, \end{aligned} \tag{11.50}$$

where

$$\mathcal{C}^{(n)}(\widehat{\Delta}, s) = -\frac{\Gamma\left(n+\frac{1}{2}\right)(\widehat{\Delta}-n)_n}{n!\sqrt{\pi}\left(\widehat{\Delta}-n-\frac{1}{2}\right)_n} {}_4F_3\left(\begin{array}{c} \frac{1}{2}, -n, s+1, \widehat{\Delta}-n-\frac{1}{2} \\ \frac{1}{2}-n, s+\frac{3}{2}, \widehat{\Delta}-n \end{array}; 1\right). \tag{11.51}$$

The calculation of the stress-tensor block proceeds in an analogous way. Using the integrals given above we obtain

$$\begin{aligned} b^{(0,n)}_{f_{4,2}}(\widehat{\Delta}, s) &= 90\,\mathcal{C}^{(n)}(\widehat{\Delta}, s) + 180 \sum_{m=1}^{n} \mathcal{C}^{(n-m)}(\widehat{\Delta}, s)\,, \\ b^{(1,n)}_{f_{4,2}}(\widehat{\Delta}, s) &= 30\,\mathcal{C}^{(n)}(\widehat{\Delta}, s) + 180 \sum_{m=1}^{n} m\,\mathcal{C}^{(n-m)}(\widehat{\Delta}, s)\,. \end{aligned} \tag{11.52}$$

Putting everything together, with the relative coefficients given by equation (11.43), the bosonic CFT data for $\tilde{F}_0(z, \bar{z})$ reads

$$\begin{aligned} (b_0^2)_{n,s} &= \frac{1}{180}\lambda_{222}a_2 \left(b^{(0,n)}_{f_{4,2}}(\widehat{\Delta}, s) - 60\,\partial_{\widehat{\Delta}} b^{(1,n)}_{f_{2,0}}(\widehat{\Delta}, s) + 2\partial_{\widehat{\Delta}} b^{(1,n)}_{f_{4,2}}(\widehat{\Delta}, s)\right)_{\widehat{\Delta}=J+s+2n}, \\ (b_0^2\gamma_0)_{n,s} &= -\frac{1}{90}\lambda_{222}a_2 \left(30\,b^{(1,n)}_{f_{2,0}}(\widehat{\Delta}, s) - b^{(1,n)}_{f_{4,2}}(\widehat{\Delta}, s)\right)_{\widehat{\Delta}=J+s+2n}. \end{aligned} \tag{11.53}$$

This can be used for resumming the correlator as in equation (11.37). The result takes a very simple form:

$$\tilde{F}_0(z, \bar{z}) = -\lambda_{222}a_2 \frac{z\bar{z}}{2(1-z)(1-\bar{z})} \left[\frac{1+z\bar{z}}{(1-z\bar{z})^2} + \frac{2z\bar{z}\log z\bar{z}}{(1-z\bar{z})^3}\right]. \tag{11.54}$$

The same analysis can be performed for $\tilde{F}_1(z, \bar{z})$, for which we find the following bosonic CFT data

$$
\begin{aligned}
(b_1^2)_{n,s} &= 2\lambda_{222}a_2 \, \partial_{\widehat{\Delta}} b_{f_{2,0}}^{(1,n)}(\widehat{\Delta}, s)\,, \\
(b_1^2\gamma_1)_{n,s} &= 2\lambda_{222}a_2 \, b_{f_{2,0}}^{(1,n)}(\widehat{\Delta}, s)\,,
\end{aligned}
\tag{11.55}
$$

and the resummation gives a compact expression:

$$
\tilde{F}_1(z, \bar{z}) = -\lambda_{222}a_2 \frac{z\bar{z} \log z\bar{z}}{(1-z)(1-\bar{z})(1-z\bar{z})}\,.
\tag{11.56}
$$

Finally, since the discontinuity of $F_2(z, \bar{z})$ vanishes (11.43), we simply find

$$
\tilde{F}_2(z, \bar{z}) = 0\,.
\tag{11.57}
$$

11.3.4 Supersymmetrization of the correlator

The correlation function obtained in the previous section is *not* supersymmetric, i.e. the three R-symmetry channels given in (11.54), (11.56) and (11.57) do not respect the Ward identities given in (11.18). This happens because the inversion formula misses contributions from low-lying spins $s \leq s_*$ as anticipated in section 11.3.1.[12] The value of s_* is related to the behavior of the two-point function in the Regge limit $z/\bar{z} \to 0$ [266], and in principle s_* can be determined by careful analysis of the corresponding Witten diagrams. Instead, in the present work we use the heuristic that s_* should take the minimal value that generates a supersymmetric correlator. As we show below, the resulting correlators make predictions which are in perfect agreement with the expectations from the topological sector.

As we just argued, in order to obtain a supersymmetric correlator, we add defect families with operators of dimensions $\widehat{\Delta} = 0, 1, 2, \ldots$ and low spin $s \leq s_*$. The OPE coefficients of these operators are unknowns that we fix by imposing the Ward identities (11.18). We have found experimentally that the minimal ansatz consists on taking $s_* = 0$ for $\tilde{F}_1(z, \bar{z})$

---

[12] Such a phenomenon has already been observed for bulk correlators. For example, in the bootstrap of the Wilson-Fisher fixed point there is an ambiguity captured by a single $\ell = 0$ block [135, 145]. In supersymmetric theories, one expects the inversion formula to converge better than in non-supersymmetric ones, see [392] for a recent discussion.

and $s_* = 1$ for $\tilde{F}_2(z, \bar{z})$. To be precise, we define the final correlators $F_j(z, \bar{z})$ as

$$F_0(z, \bar{z}) = \tilde{F}_0(z, \bar{z}),$$

$$F_1(z, \bar{z}) = \tilde{F}_1(z, \bar{z}) + \sum_{n=0}^{\infty} \left(k_n \hat{f}_{n,0}(z, \bar{z}) + p_n \partial_{\widehat{\Delta}} \hat{f}_{n,0}(z, \bar{z}) \right),$$

$$F_2(z, \bar{z}) = \tilde{F}_2(z, \bar{z}) + \sum_{s=0,1} \sum_{n=0}^{\infty} \left(q_{n,s} \hat{f}_{n+s,s}(z, \bar{z}) + r_{n,s} \partial_{\widehat{\Delta}} \hat{f}_{n+s,s}(z, \bar{z}) \right). \tag{11.58}$$

As mentioned before, the free coefficients k_n, p_n, $q_{n,s}$ and $r_{n,s}$, can be fixed by requiring that the Ward identities are satisfied. In fact this fixes all the coefficients in terms of $q_{0,0}$ and k_1. Note that $q_{0,0}$ corresponds to the ambiguity $f_{0,0}(z, \bar{z}) = 1$, i.e. the defect identity. However, we know from the Witten diagrams analysis of section 11.2.2 that the defect identity is given by the constant contribution a_2^2, and thus

$$q_{0,0} = a_2^2 \Big|_{O(\frac{\sqrt{\lambda}}{N^2})}. \tag{11.59}$$

On the other hand, the unknown k_1 can be determined by demanding a bulk expansion that is consistent with the observations made in section 11.3.2, i.e. there should not appear anomalous dimensions for bulk operators. This means that the expansion of (11.58) in the limit $z, \bar{z} \to 1$ should take the form of a power series, without spurious $\log(1 - \bar{z})$ terms. Since the defect expansion (11.58) is natural around $z, \bar{z} \sim 0$, this is only possible after fixing the free coefficients and resumming the correlator. We were able to do so, and the remaining spurious term reads:

$$F_1(z, \bar{z}) \sim \frac{1}{2} \left(\lambda_{222} a_2 - k_1 \right) \log(1 - \bar{z}) + \dots \tag{11.60}$$

This fixes the coefficient k_1 to be:

$$k_1 = \lambda_{222} a_2. \tag{11.61}$$

11.3.5 Final result and comparison to localization

We will now present the final result for the correlator $\langle\langle \mathcal{O}_2 \mathcal{O}_2 \rangle\rangle$ using the input of localization for the two remaining free coefficients, namely a_2^2 and $\lambda_{222} a_2$. We can then obtain OPE coefficients of other protected operators which in turn can be checked against the localization data.

The constant contribution a_2^2 from the defect identity can be fixed using equation (11.25):

$$a_2^2 = \frac{\lambda}{N^2} \left(\frac{1}{8} - \frac{3}{8\sqrt{\lambda}} + \dots \right) \tag{11.62}$$

while for the OPE coefficient $\lambda_{222}a_2$ we use the localization results given in equation (11.23) and (11.25):

$$\lambda_{222}a_2 = \frac{\lambda}{N^2}\left(\frac{1}{\sqrt{\lambda}} + \dots\right). \tag{11.63}$$

We thus obtain a correlator without any free coefficient left:

$$
\begin{aligned}
F_0(z, \bar{z}) &= -\frac{\sqrt{\lambda}}{2N^2}\frac{z\bar{z}}{(1-z)(1-\bar{z})}\left[\frac{1+z\bar{z}}{(1-z\bar{z})^2} + \frac{2z\bar{z}\log z\bar{z}}{(1-z\bar{z})^3}\right], \\
F_1(z, \bar{z}) &= \frac{\sqrt{\lambda}}{N^2}\left[\log(1 + \sqrt{z\bar{z}}) + \frac{z\bar{z}}{(1-z\bar{z})^2}\right. \\
&\quad \left. + \frac{z\bar{z}(5z\bar{z} - 2z^2\bar{z}^2 + z^3\bar{z}^3 - (z+\bar{z})(2 - z\bar{z} + z^2\bar{z}^2))\log z\bar{z}}{2(1-z)(1-\bar{z})(1-z\bar{z})^3}\right], \\
F_2(z, \bar{z}) &= \frac{\sqrt{\lambda}}{8N^2}\left[-3 - \frac{2(z+\bar{z})}{\sqrt{z\bar{z}}} + \frac{(z+\bar{z})(1+z\bar{z}) - 4z\bar{z}}{(1-z\bar{z})^2}\right. \\
&\quad + \frac{2((z+\bar{z})(1+z\bar{z}) - 4z\bar{z})\log(1+\sqrt{z\bar{z}})}{z\bar{z}} \\
&\quad \left. + \frac{z\bar{z}((z+\bar{z})(3 - 2z\bar{z} + z^2\bar{z}^2) - 6 + 6z\bar{z} - 4z^2\bar{z}^2)\log z\bar{z}}{(1-z\bar{z})^3}\right].
\end{aligned}
\tag{11.64}
$$

Comparing to (11.98), this correlator predicts the OPE coefficient of the double-trace operator $\mathcal{O}_{(2,2)}$

$$\lambda_{22(2,2)}a_{(2,2)} = \frac{\lambda}{N^2}\left(\frac{1}{8} - \frac{1}{2\sqrt{\lambda}} + \dots\right), \tag{11.65}$$

which matches the localization results given in equation (11.27). We can also extract the defect CFT data for the protected operators:

$$
\begin{aligned}
b_{21}^2 &= \frac{\lambda}{N^2}\left(\frac{1}{\sqrt{\lambda}} + \dots\right), \\
b_{2(2)}^2 &= 1 + \frac{\lambda}{N^2}\left(-\frac{1}{2\sqrt{\lambda}} + \dots\right).
\end{aligned}
\tag{11.66}
$$

The OPE coefficient b_{21}^2 can be compared to the direct computation (see equation (11.31)), and we find a perfect match. The OPE coefficient $b_{2(2)}^2$ corresponds to the operator $\hat{\mathcal{O}}_{(2)}$ introduced in equation (11.29) and is a prediction from our result.[13]

---

[13]The observation that $\hat{\mathcal{O}}_{(2)}$ should appear in this type of correlator was first discussed in appendix A of [289]. In principle the operator $\hat{\mathcal{O}}_2$ should also appear, but it can be seen from equation (11.31) that it is not relevant at the present order.

Moreover, using the superblocks described in [285, 286], the correlator above can also be used for extracting the supersymmetric CFT data for unprotected operators. The resulting CFT data has to be interpreted as a sum over degenerate operators, and one would need to solve a mixing problem similar to the case of $\mathcal{N} = 4$ SYM without defects [170, 363, 417, 418]. Below we provide a few examples, while we postpone the full analysis of the CFT data and the mixing problem to future work. In particular, the product of tree-level coefficients and anomalous dimensions for the unprotected operators at lowest twist $\widehat{\Delta} = s + 2$ reads

$$\hat{F}_{s+2,s}\gamma_{s+2,s}\Big|_{O(\frac{\sqrt{\lambda}}{N^2})} = -\frac{3+2s}{2(1+s)}\frac{\sqrt{\lambda}}{N^2}\,. \tag{11.67}$$

Note that here we use the notation of [286]. It is also possible to obtain a closed form for the OPE coefficients of the semishort operators $(B,1)_{[1,s]}$:

$$\hat{E}_s\Big|_{O(\frac{\sqrt{\lambda}}{N^2})} = -\frac{1+s}{4(1+2s)}\frac{\sqrt{\lambda}}{N^2}\,. \tag{11.68}$$

11.4 General identical operators

In this section we extend the analysis of the previous section for general identical operators $\langle\!\langle \mathcal{O}_J \mathcal{O}_J \rangle\!\rangle$. The calculation of $\langle\!\langle \mathcal{O}_2 \mathcal{O}_2 \rangle\!\rangle$ carries through almost unchanged, as will be described shortly. As a concrete application we obtain closed-form expressions for the $J = 3, 4$ correlators.

11.4.1 General discussion

As discussed in section 11.2, the correlator of interest has the form

$$\mathcal{F}^{(J)}(z, \bar{z}, \sigma) = \left(\frac{\sigma\sqrt{z\bar{z}}}{(1-z)(1-\bar{z})}\right)^J + \frac{J\lambda}{2^{J+2}N^2} + \sum_{j=0}^{J}\sigma^j F_{J-j}^{(J)}(z, \bar{z}) + O\left(\frac{1}{N^2}\right)\,, \tag{11.69}$$

where we used the leading-order result for the one-point function (11.25). Here we give a general prescription to obtain the functions $F_j^{(J)}(z, \bar{z})$ that contribute at order $\frac{\sqrt{\lambda}}{N^2}$.

The central idea is to reconstruct these functions using the Lorentzian inversion formula (11.33). It was discussed in section 11.3.2 that only operators with single-trace dimension can contribute to the discontinuity of the correlator. The bulk OPE of $\mathcal{O}_J$ takes the form [285]

$$\mathcal{O}_J \times \mathcal{O}_J \sim \mathbb{1} + \sum_{k=1}^{J} \mathcal{B}_{[0,2k,0]} + \dots\,, \tag{11.70}$$

where ... contains unprotected multiplets that do not contribute to the discontinuity. Furthermore, $\mathcal{B}_{[0,2J,0]}$ has double-twist dimension and does not contribute. From this it follows that, at the order we are working, the discontinuity of the correlator reads

$$\text{Disc}\,\mathcal{F}^{(J)}(z,\bar{z},\sigma)\Big|_{O(\frac{\sqrt{\lambda}}{N^2})} = \text{Disc}\left[\left(\frac{\sigma\sqrt{z\bar{z}}}{(1-z)(1-\bar{z})}\right)^J \sum_{k=1}^{J-1} \lambda_{JJ2k}a_{2k}\mathcal{G}_{[0,2k,0]}(z,\bar{z},\sigma)\right]. \quad (11.71)$$

The superconformal blocks capture the information of half-BPS operators exchanged in the bulk OPE $\mathcal{O}_J \times \mathcal{O}_J$. They were obtained in [286], and we reproduce them here for simplicity:

$$\mathcal{G}_{[0,K,0]}(z,\bar{z},\sigma) = h_K(\sigma)f_{K,0}(z,\bar{z}) + \frac{(K+2)^2K}{128(K+1)^2(K+3)}h_{K-2}(\sigma)f_{K+2,2}(z,\bar{z})$$
$$+ \frac{(K-2)(K+2)K^2}{16384(K-1)^2(K+1)(K+3)}h_{K-4}(\sigma)f_{K+4,0}(z,\bar{z}). \quad (11.72)$$

Using (11.71) as input to the inversion formula, it is possible to generate a series representation of the correlators $\tilde{F}_j^{(J)}(z,\bar{z})$. In concrete examples, these series expansions do not satisfy the Ward identities, just as we saw for the $\langle\!\langle\mathcal{O}_2\mathcal{O}_2\rangle\!\rangle$ case. This is a result of the inversion formula not converging for low values of the transverse spin s. Empirically we have found that the minimal set of additions is

$$F_j^{(J)}(z,\bar{z}) = \tilde{F}_j^{(J)}(z,\bar{z}) \qquad \text{for} \qquad j = 0,\ldots,J-2\,,$$
$$F_{J-1}^{(J)}(z,\bar{z}) = \tilde{F}_{J-1}^{(J)}(z,\bar{z}) + \sum_{n=0}^{\infty}\left(k_n\hat{f}_{n,0}(z,\bar{z}) + p_n\partial_{\widehat{\Delta}}\hat{f}_{n,0}(z,\bar{z})\right)\,, \quad (11.73)$$
$$F_J^{(J)}(z,\bar{z}) = \tilde{F}_J^{(J)}(z,\bar{z}) + \sum_{s=0,1}\sum_{n=0}^{\infty}\left(q_{n,s}\hat{f}_{n+s,s}(z,\bar{z}) + r_{n,s}\partial_{\widehat{\Delta}}\hat{f}_{n+s,s}(z,\bar{z})\right)\,.$$

Namely, we must add $s=0$ ambiguities to $F_{J-1}^{(J)}(z,\bar{z})$, while we must add $s=0,1$ ambiguities to $F_{J-1}^{(J)}(z,\bar{z})$. Using the Ward identities (11.18), it is possible to fix all the free coefficients k_n, p_n, $q_{n,s}$, $r_{n,s}$ except for $q_{0,0}$ and k_1. As discussed around equation (11.59), $q_{0,0}$ can be identified with the defect identity a_J^2 and is therefore fixed from localization. Furthermore, if one keeps the bulk OPE coefficients $\lambda_{JJK}a_K$ arbitrary, the Ward identities also fix their relative values. For example, the Ward identities together with (11.73) imply

$$\lambda_{JJK}a_K\Big|_{O(\frac{\sqrt{\lambda}}{N^2})} = \frac{K}{2^{K/2}}\lambda_{JJ2}a_2\Big|_{O(\frac{\sqrt{\lambda}}{N^2})} \qquad \text{for} \quad 2 \le K \le J-2\,. \quad (11.74)$$

These results are in perfect agreement with the known values (11.25) at leading order at large λ. This provides evidence that (11.73) is the correct prescription for the low-spin additions.

At this point, it is possible to resum the series expansion representations for $F_j^{(J)}$. These resummed correlators can be expanded in a series around $z, \bar{z} = 1$, which corresponds to the bulk conformal block decomposition. The expansion contains spurious $\log(1 - \bar{z})$ terms, which would imply that bulk operators get anomalous dimensions. These anomalous dimensions should not be present at the order we are working, so canceling the spurious logarithms fixes the remaining free parameter k_1. Finally, one uses a_J^2 and $\lambda_{JJ2}a_2$ coming from localization to write down the final correlator. This correlation function produces all other OPE coefficients in the protected sector, and we find perfect agreement with the literature.

11.4.2 Example 1: $\langle\!\langle \mathcal{O}_3 \mathcal{O}_3 \rangle\!\rangle$

Let us turn our attention to the case of $\langle\!\langle \mathcal{O}_3 \mathcal{O}_3 \rangle\!\rangle$. The purpose of this example is to illustrate the general formalism that we just discussed. Furthermore, we present concrete intermediate results to help the readers interested in reproducing our results.

Inversion of single traces

The first step is to obtain the discontinuity of the correlator, by combining (11.71) and (11.72) with (11.92). For concreteness we look at the coefficient of σ^3, or equivalently we focus on the $F_0^{(3)}(z, \bar{z})$ correlator:

$$
\begin{aligned}
\text{Disc } F_0^{(3)}(z, \bar{z}) = {} & \lambda_{332}a_2 \frac{z^{3/2}\left(z^2 - 2z\log z - 1\right)}{2(1-z)^5} \text{Disc } \frac{1}{\bar{y}^2} \\
& - \lambda_{334}a_4 \frac{z^{3/2}\left(z^3 + 9z^2 - 9z - 1 - 6z(z+1)\log z\right)}{4(1-z)^6} \text{Disc } \frac{1}{\bar{y}}.
\end{aligned}
\tag{11.75}
$$

Similar expressions can be easily obtained for the other $F_j^{(3)}(z, \bar{z})$. The next step is to insert the discontinuity in the inversion formula (11.33), and carry out the inversion order by order as $z \to 0$. Each power z^p induces a defect family with blocks $\hat{f}_{2p+s+2n,s}(z, \bar{z})$ and OPE coefficients given by the poles of $b(\widehat{\Delta}, s)$. Similarly, each power $z^p \log z$ induces defect anomalous dimensions $\partial_{\widehat{\Delta}} \hat{f}_{2p+s+2n,s}(z, \bar{z})$ given by the double poles of $b(\widehat{\Delta}, s)$. All the integrals that are needed are of the form (11.47) with $p = 1, 2$. The resulting defect

expansion for the lowest-lying operators is

$$\tilde{F}_0^{(3)}(z,\bar{z}) = \frac{1}{2}(3\lambda_{332}a_2 - \lambda_{334}a_4)\hat{f}_{3,0}(z,\bar{z}) + \frac{1}{2}(5\lambda_{332}a_2 - \lambda_{334}a_4)\hat{f}_{4,1}(z,\bar{z})$$

$$+ \frac{2}{21}(121\lambda_{332}a_2 - 73\lambda_{334}a_4)\hat{f}_{5,0}(z,\bar{z}) + 2(5\lambda_{332}a_2 - 3\lambda_{334}a_4)\partial_{\widehat{\Delta}}\hat{f}_{5,0}(z,\bar{z})$$

$$+ \frac{1}{2}(7\lambda_{332}a_2 - \lambda_{334}a_4)\hat{f}_{5,2}(z,\bar{z}) + \dots \tag{11.76}$$

Once again, the expansions for other $\tilde{F}_j^{(3)}(z,\bar{z})$ are obtained in an identical manner. Unlike in the $\langle\langle\mathcal{O}_2\mathcal{O}_2\rangle\rangle$ case, we were not able to express the defect CFT data in closed forms. However, the previous calculation can be automatized with a computer, and the expansion can be generated efficiently up to high orders.

Supersymmetrization of the correlator

As for the $\langle\langle\mathcal{O}_2\mathcal{O}_2\rangle\rangle$ case, the $\tilde{F}_j^{(3)}(z,\bar{z})$ do not give a supersymmetric correlator because the Lorentzian inversion formula can miss low transverse-spin contributions. In order for $\tilde{F}_j^{(3)}(z,\bar{z})$ to satisfy the Ward identities (11.18), we add the following $s = 0, 1$ contributions to our correlators

$$F_0^{(3)}(z,\bar{z}) = \tilde{F}_0^{(3)}(z,\bar{z}), \qquad F_1^{(3)}(z,\bar{z}) = \tilde{F}_1^{(3)}(z,\bar{z}),$$

$$F_2^{(3)}(z,\bar{z}) = \tilde{F}_2^{(3)}(z,\bar{z}) + \sum_{n=0}^{\infty}\left(k_n\hat{f}_{n,0}(z,\bar{z}) + p_n\partial_{\widehat{\Delta}}\hat{f}_{n,0}(z,\bar{z})\right), \tag{11.77}$$

$$F_3^{(3)}(z,\bar{z}) = \tilde{F}_3^{(3)}(z,\bar{z}) + \sum_{s=0,1}\sum_{n=0}^{\infty}\left(q_{n,s}\hat{f}_{n+s,s}(z,\bar{z}) + r_{n,s}\partial_{\widehat{\Delta}}\hat{f}_{n+s,s}(z,\bar{z})\right).$$

After this addition, the functions $F_j^{(3)}(z,\bar{z})$ should satisfy the Ward identities (11.18), which are highly constraining. In fact, the only coefficients that remain unfixed are $\lambda_{332}a_2$, k_1 and $q_{0,0}$. In particular, notice that the precise relation between single-trace OPE coefficients is fixed:

$$\lambda_{334}a_4\Big|_{O(\frac{\sqrt{\lambda}}{N^2})} = \lambda_{332}a_2\Big|_{O(\frac{\sqrt{\lambda}}{N^2})}. \tag{11.78}$$

Reassuringly, this relation is consistent with localization (11.25). Again, we believe this is strong evidence for the ansatz (11.77) for low transverse-spin ambiguities to be correct. In the case of $\langle\langle\mathcal{O}_4\mathcal{O}_4\rangle\rangle$ we find a similar result involving $K = 4, 6$, and for general J we expect equation (11.74) to hold.

Fixing free parameters and final result

At this point, we have a supersymmetric correlator depending on three free parameters. Using the series representation of the correlator (11.76) it is possible to find a closed form expression in terms of rational functions and logarithms. In particular, we find

$$F_2^{(3)}(z, \bar{z}) = -\frac{3}{8}(3\lambda_{332}a_2 + 32k_1)\tanh^{-1}\sqrt{z\bar{z}} + \dots \,, \tag{11.79}$$

where ... stand for terms which have an expansion around $z, \bar{z} = 1$ involving only integer powers. On the other hand, $\tanh^{-1}\sqrt{z\bar{z}}$ has an expansion with $\log(1 - \bar{z})$ terms. These logarithms correspond to anomalous dimensions in the bulk, which should be absent by our assumptions. We thus conclude

$$k_1 = -\frac{3}{32}\lambda_{332}a_2 \,. \tag{11.80}$$

In order to fix the last two coefficients we use input from the localization results of the topological sector. Indeed, from (11.25) we have that

$$\lambda_{332}a_2 = \frac{\lambda}{N^2}\left(\frac{3}{2\sqrt{\lambda}} + \dots\right) \,, \quad a_3^2 = \frac{\lambda}{N^2}\left(\frac{3}{32} - \frac{3}{4\sqrt{\lambda}} + \dots\right) \,. \tag{11.81}$$

As discussed around equation (11.59), the coefficient $q_{0,0}$ has a natural interpretation as the defect identity contribution given by a_3^2. We thus conclude $q_{0,0} = -\frac{3\sqrt{\lambda}}{4N^2}$.

The final result with no free parameters takes a reasonably simple form:

$$F_0^{(3)}(z, \bar{z}) = -\frac{6\sqrt{\lambda}}{8N^2}\frac{(z\bar{z})^{3/2}}{[(1-z)(1-\bar{z})]^2}\left[\frac{1+z\bar{z}}{(1-z\bar{z})^2} + \frac{2z\bar{z}\log z\bar{z}}{(1-z\bar{z})^3}\right] \,,$$

$$F_1^{(3)}(z, \bar{z}) = \frac{3\sqrt{\lambda}}{4N^2}\frac{(z\bar{z})^{3/2}}{(1-z)(1-\bar{z})(1-z\bar{z})^4}\left(z^2\bar{z}^2 - 38z\bar{z} + 1\right.$$

$$\left. - \frac{2\left((z+\bar{z})(z\bar{z}+1)\left(z^2\bar{z}^2 - 11z\bar{z} + 1\right) + z\bar{z}(z\bar{z}+5)(5z\bar{z}+1)\right)\log z\bar{z}}{(1-z)(1-\bar{z})(1-z\bar{z})}\right) \,,$$

$$F_2^{(3)}(z, \bar{z}) = -\frac{18\sqrt{\lambda}}{N^2}\frac{(z\bar{z})^{1/2}}{(1-z\bar{z})^2}\left(\frac{z\bar{z}}{(1-z)(1-\bar{z})} - \frac{3(1+z\bar{z})\left(z^2\bar{z}^2 + 6z\bar{z} + 1\right)}{32(1-z\bar{z})^2}\right.$$

$$\left. - \frac{2z\bar{z}\left(7 + 10z\bar{z} + 7z^2\bar{z}^2\right)\log z\bar{z}}{32(1-z\bar{z})^3} + \frac{z\bar{z}(1+z\bar{z})\log z\bar{z}}{2(1-z)(1-\bar{z})(1-z\bar{z})}\right) \,,$$

$$F_3^{(3)}(z, \bar{z}) = -\frac{3\sqrt{\lambda}}{4N^2}\left(1 - \frac{3(z\bar{z})^{1/2}\left((z+\bar{z})\left(z^2\bar{z}^2 + 10z\bar{z} + 1\right) - 3(z\bar{z}+1)^3\right)}{4(1-z\bar{z})^4}\right.$$

$$\left. + \frac{3(z\bar{z})^{3/2}\left(5z^2\bar{z}^2 + 2z\bar{z} + 5 - 3(z+\bar{z})(z\bar{z}+1)\right)\log z\bar{z}}{2(1-z\bar{z})^5}\right) \,. \tag{11.82}$$

In principle, this correlation function contains information of infinitely many unprotected operators, but as for the $\langle\langle\mathcal{O}_2\mathcal{O}_2\rangle\rangle$ case we leave a detailed analysis of the OPE for future work. Instead, we focus on the CFT data captured by the topological sector. Comparing the full correlator (11.69) to equation (11.98) gives the bulk data

$$\lambda_{334}a_4 = \frac{\lambda}{N^2}\left(\frac{3}{2\sqrt{\lambda}}+\dots\right), \quad \lambda_{33(3,3)}a_{(3,3)} = \frac{\lambda}{N^2}\left(\frac{3}{32}-\frac{9}{8\sqrt{\lambda}}+\dots\right), \tag{11.83}$$

while comparing to (11.100) gives the defect data

$$b_{31}^2 = \frac{\lambda}{N^2}\left(\frac{27}{16\sqrt{\lambda}}+\dots\right), \quad b_{32}^2 = O\left(\frac{\lambda^0}{N^2}\right), \quad b_{3(3)}^2 = 1+\frac{\lambda}{N^2}\left(-\frac{3}{4\sqrt{\lambda}}+\dots\right). \tag{11.84}$$

These results are in perfect agreement with the literature, see (11.25), (11.27) and (11.31). Remember that $b_{3(3)}$ cannot be compared to (11.31) because the results of [289] apply to the defect operator $\hat{\mathcal{O}}_3$, while our result applies to the defect operator $\hat{\mathcal{O}}_{(3)}$, see the discussion in footnote 13.

11.4.3   Example 2: $\langle\langle\mathcal{O}_4\mathcal{O}_4\rangle\rangle$

Let us finally consider the $\langle\langle\mathcal{O}_4\mathcal{O}_4\rangle\rangle$ two-point function. Since the calculation is essentially identical to the previous one, we skip most of the details. However, it is important to note that the following input from localization is necessary:

$$\lambda_{442}a_2 = \frac{\lambda}{N^2}\left(\frac{2}{\sqrt{\lambda}}+\dots\right), \quad a_4^2 = \frac{\lambda}{N^2}\left(\frac{1}{16}-\frac{15}{16\sqrt{\lambda}}+\dots\right). \tag{11.85}$$

Following all the steps, which can be automatized with the help of a computer, we obtain the correlation function

$$F_0^{(4)}(z,\bar{z}) = -\frac{\sqrt{\lambda}}{N^2}\frac{(z\bar{z})^2}{[(1-z)(1-\bar{z})]^3}\left[\frac{1+z\bar{z}}{(1-z\bar{z})^2}+\frac{2z\bar{z}\log z\bar{z}}{(1-z\bar{z})^3}\right],$$

$$F_1^{(4)}(z,\bar{z}) = \frac{\sqrt{\lambda}}{N^2}\frac{(z\bar{z})^2}{(1-z)^2(1-\bar{z})^2(1-z\bar{z})^4}\Bigg(z^2\bar{z}^2-38z\bar{z}+1$$
$$-\frac{2\left((z+\bar{z})(z\bar{z}+1)\left(z^2\bar{z}^2-11z\bar{z}+1\right)+z\bar{z}(z\bar{z}+5)(5z\bar{z}+1)\right)\log z\bar{z}}{(1-z)(1-\bar{z})(1-z\bar{z})}\Bigg),$$

$$F_2^{(4)}(z,\bar{z}) = -\frac{3\sqrt{\lambda}}{2N^2}\frac{(z\bar{z})^2}{(1-z)^2(1-\bar{z})^2(1-z\bar{z})^6}\Bigg($$
$$+2(z+\bar{z})(z\bar{z}+1)\left(8z^2\bar{z}^2-91z\bar{z}+8\right)+2z\bar{z}\left(43z^2\bar{z}^2+214z\bar{z}+43\right)$$
$$+\frac{(z\bar{z}+1)(z^4\bar{z}^4+14z^3\bar{z}^3+270z^2\bar{z}^2+14z\bar{z}+1)\log z\bar{z}}{1-z\bar{z}}$$
$$+\frac{(z+\bar{z})(7z^4\bar{z}^4-46z^3\bar{z}^3-222z^2\bar{z}^2-46z\bar{z}+7)\log z\bar{z}}{1-z\bar{z}}\Bigg),$$

$$F_3^{(4)}(z,\bar{z}) = -\frac{\sqrt{\lambda}}{2N^2}\Bigg(\frac{270(z\bar{z})^2(z\bar{z}+1)}{(1-z)(1-\bar{z})(1-z\bar{z})^4}-\frac{z\bar{z}\left(2z^4\bar{z}^4+229z^3\bar{z}^3+438z^2\bar{z}^2+229z\bar{z}+2\right)}{(1-z\bar{z})^6}$$
$$+\frac{90(z\bar{z})^2\left(z^2\bar{z}^2+4z\bar{z}+1\right)\log z\bar{z}}{(1-z)(1-\bar{z})(1-z\bar{z})^5}-4\log\left(1+\sqrt{z\bar{z}}\right)$$
$$-\frac{(z\bar{z})^2\left(2z^5\bar{z}^5-14z^4\bar{z}^4+117z^3\bar{z}^3+325z^2\bar{z}^2+395z\bar{z}+75\right)\log z\bar{z}}{(1-z\bar{z})^7}\Bigg),$$

$$F_4^{(4)}(z,\bar{z}) = \frac{\sqrt{\lambda}}{N^2}\Bigg(-\frac{z+\bar{z}}{2\sqrt{z\bar{z}}}+\frac{(z+\bar{z})(z\bar{z}+1)-4z\bar{z}}{2z\bar{z}}\log\left(1+\sqrt{z\bar{z}}\right)$$
$$+\frac{2(z+\bar{z})(z\bar{z}+1)\left(2z^4\bar{z}^4-11z^3\bar{z}^3+468z^2\bar{z}^2-11z\bar{z}+2\right)}{16(1-z\bar{z})^6}$$
$$-\frac{15z^6\bar{z}^6-74z^5\bar{z}^5+1397z^4\bar{z}^4+924z^3\bar{z}^3+1397z^2\bar{z}^2-74z\bar{z}+15}{16(1-z\bar{z})^6}$$
$$+\frac{(z\bar{z})^2(z+\bar{z})\left(z^5\bar{z}^5-6z^4\bar{z}^4+14z^3\bar{z}^3+56z^2\bar{z}^2+315z\bar{z}+70\right)\log z\bar{z}}{4(1-z\bar{z})^7}$$
$$-\frac{(z\bar{z})^2\left(4z^5\bar{z}^5-28z^4\bar{z}^4+189z^3\bar{z}^3+245z^2\bar{z}^2+385z\bar{z}+105\right)\log z\bar{z}}{4(1-z\bar{z})^7}\Bigg).$$

$$(11.86)$$

Once again, let us compare the predictions of this correlator with the topological sector. We find the bulk data

$$
\lambda_{444}a_4 = \frac{\lambda}{N^2}\left(\frac{2}{\sqrt{\lambda}}+\dots\right), \qquad \lambda_{446}a_6 = \frac{\lambda}{N^2}\left(\frac{3}{2\sqrt{\lambda}}+\dots\right),
$$
$$
\lambda_{44(4,4)}a_{(4,4)} = \frac{\lambda}{N^2}\left(\frac{1}{16}-\frac{3}{2\sqrt{\lambda}}+\dots\right),
$$
(11.87)

while the defect data is given by

$$
b_{41}^2 = \frac{\lambda}{N^2}\left(\frac{2}{\sqrt{\lambda}}+\dots\right), \quad b_{42}^2 = O\left(\frac{\lambda^0}{N^2}\right),
$$
$$
b_{43}^2 = O\left(\frac{\lambda^0}{N^2}\right), \qquad\quad b_{4(4)}^2 = 1 + \frac{\lambda}{N^2}\left(-\frac{1}{\sqrt{\lambda}}+\dots\right).
$$
(11.88)

These results are in perfect agreement with the literature, except for $b_{4(4)}$, which is a new prediction from our calculation.

11.4.4 A conjecture

In the three examples considered in the present paper, the function $F_0^{(J)}(z,\bar{z})$ is very simple:

$$
F_0^{(J)}(z,\bar{z}) = -\frac{J\sqrt{\lambda}}{4N^2}\frac{(z\bar{z})^{J/2}}{\left[(1-z)(1-\bar{z})\right]^{J-1}}\left[\frac{1+z\bar{z}}{(1-z\bar{z})^2}+\frac{2z\bar{z}\log z\bar{z}}{(1-z\bar{z})^3}\right].
$$
(11.89)

It is tempting to conjecture that this relation also holds for $J > 4$. From our bootstrap calculation, (11.89) is a result of a precise combination of the spacetime bulk blocks (11.92), the superblocks (11.72) and the OPE coefficients in the topological sector (11.25). Perhaps from the point of view of the explicit holographic calculation the origin of (11.89) will be more transparent.

Let us also note the similarity between $F_1^{(3)}(z,\bar{z})$ and $F_1^{(4)}(z,\bar{z})$

$$
F_1^{(J)}(z,\bar{z}) = \frac{J\sqrt{\lambda}}{4N^2}\frac{(z\bar{z})^{J/2}}{(1-z)^{J-2}(1-\bar{z})^{J-2}(1-z\bar{z})^4}\left(z^2\bar{z}^2 - 38z\bar{z} + 1\right.
$$
$$
\left.-\frac{2\left((z+\bar{z})(z\bar{z}+1)\left(z^2\bar{z}^2-11z\bar{z}+1\right)+z\bar{z}(z\bar{z}+5)(5z\bar{z}+1)\right)\log z\bar{z}}{(1-z)(1-\bar{z})(1-z\bar{z})}\right).
$$
(11.90)

We do not have enough data points to propose a full analytic formula for any J, however our current results look promising. In the discussions below we speculate on what might be the best possible strategy for the future.

11.5   Conclusions

In this work we have studied the structure of two-point functions of single-trace half-BPS operators in the presence of a supersymmetric Wilson line in $\mathcal{N} = 4$ SYM theory. We used analytical bootstrap techniques in order to reconstruct the correlator at strong coupling. For operators of weight $J = 2, 3, 4$ we obtained fairly simple results presented in (11.64), (11.82), (11.86) which only involve logarithms and rational functions of the cross-ratios.

A natural continuation of our work is the analysis of two-point functions for arbitrary weight $\langle\!\langle \mathcal{O}_{J_1} \mathcal{O}_{J_2} \rangle\!\rangle$. One obvious approach is to keep pushing the algorithm presented in this paper to higher values of J. However there might be better strategies. In $\mathcal{N} = 4$ SYM without defects, explicit closed form expressions for half-BPS operators take a particularly simple form in Mellin space [171, 172, 395, 396]. It would be interesting to transform the explicit formulas presented in this paper to Mellin variables. The Mellin space approach for defect CFT was explored in [419], the hope being that this might be the natural language to write the most general correlator $\langle\!\langle \mathcal{O}_{J_1} \mathcal{O}_{J_2} \rangle\!\rangle$.

Another interesting line of research is to reproduce our results by an explicit holographic calculation using Witten diagrams. Some observables in holographic defect CFTs have been studied perturbatively at strong coupling, for example bulk one-point functions [399, 411], bulk-defect correlators [289] and correlators localized on the defect [260, 288, 346, 420, 421]. The two-point function of bulk operators was studied to order $O(\frac{\lambda}{N^2})$ in [401], and the next order will involve the calculation of the Witten diagram (11.10). The structural understanding presented in this work might give valuable input for this type of calculation.

The idea of reconstructing correlators starting from their discontinuity is powerful. In defect CFT it seems to be as powerful as in the case for homogeneous CFTs. For monodromy defects in the ε–expansion this method was already used to fully bootstrap two-point correlators of chiral fields [4]. In this work we developed an algorithm that in principle can be used to bootstrap an infinite family of half-BPS correlators. We expect that the same method also works in related $\mathcal{N} = 4$ SYM setups, such as the non-supersymmetric Wilson line [420], Wilson lines in more general representations of the gauge group [421], or even higher codimension defects. Furthermore, many half-BPS defects are known to exist in maximally supersymmetric theories in $d = 3, 4, 6$, and all of them might be prime targets for the analytical bootstrap techniques used here.

Acknowledgements

11.A   Appendix

11.A.1   Singular part of bulk blocks

In this appendix, bulk blocks are studied in the limit $\bar{y} = (1 - \bar{z})/\sqrt{\bar{z}} \to 0$. These results provide the necessary input for the inversion formula in sections 11.3 and 11.4. The starting point are the explicit formulas for bulk blocks derived in [264, 265], which we reproduce here for convenience:

$$
\begin{aligned}
f_{\Delta,\ell}(z,\bar{z}) = \sum_{m=0}^{\infty} \sum_{n=0}^{\infty} \frac{4^{m-n}}{m!n!} & \frac{\left(-\frac{\ell}{2}\right)_m^2 \left(\frac{2-\ell-\Delta}{2}\right)_m}{(-\ell)_m \left(\frac{3-\ell-\Delta}{2}\right)_m} \frac{\left(\frac{\Delta-1}{2}\right)_n^2 \left(\frac{\Delta+\ell}{2}\right)_n}{(\Delta-1)_n \left(\frac{\Delta+\ell+1}{2}\right)_n} \frac{\left(\frac{\Delta+\ell}{2}\right)_{n-m}}{\left(\frac{\Delta+\ell-1}{2}\right)_{n-m}} \\
& \times (1-z\bar{z})^{\ell-2m} \, {}_4F_3\left(\begin{array}{c} -n,-m,\frac{1}{2},\frac{\Delta-\ell-2}{2} \\ \frac{2-\Delta-\ell-2n}{2}, \frac{\Delta+\ell-2m}{2}, \frac{\Delta-\ell-1}{2} \end{array} ; 1 \right) \\
& \times [(1-z)(1-\bar{z})]^{\frac{\Delta-\ell}{2}+m+n} \, {}_2F_1\left(\begin{array}{c} \frac{\Delta+\ell}{2}-m+n, \frac{\Delta+\ell}{2}-m+n \\ \Delta+\ell-2(m-n) \end{array} ; 1-z\bar{z} \right).
\end{aligned}
\tag{11.91}
$$

After changing variables from $\bar{z} \to \bar{y}$ and expanding up to order $O(\bar{y}^3)$, we obtain the following formulas:

$$f_{2,0}(z,\bar{z}) \sim -\bar{y} \log z + \bar{y}^3 \left(\frac{z+1}{8(z-1)} - \frac{z \log z}{4(z-1)^2} \right),$$

$$f_{4,0}(z,\bar{z}) \sim \bar{y}^2 \left(-12 + \frac{6(z+1) \log z}{z-1} \right),$$

$$f_{4,2}(z,\bar{z}) \sim \bar{y} \left(\frac{90(z+1)}{z-1} - \frac{30 \left(z^2 + 4z + 1 \right) \log z}{(z-1)^2} \right)$$

$$+ \bar{y}^3 \left(-\frac{15(z+1) \left(z^2 - 20z + 1 \right)}{8(z-1)^3} - \frac{15z \left(z^2 + 7z + 1 \right) \log z}{2(z-1)^4} \right), \tag{11.92}$$

$$f_{6,0}(z,\bar{z}) \sim \bar{y}^3 \left(\frac{90(z+1)}{z-1} - \frac{30 \left(z^2 + 4z + 1 \right) \log z}{(z-1)^2} \right),$$

$$f_{6,2}(z,\bar{z}) \sim \bar{y}^2 \left(-\frac{140 \left(11z^2 + 38z + 11 \right)}{3(z-1)^2} + \frac{140(z+1) \left(z^2 + 8z + 1 \right) \log z}{(z-1)^3} \right),$$

$$f_{8,2}(z,\bar{z}) \sim \bar{y}^3 \left(\frac{525(z+1) \left(5z^2 + 32z + 5 \right)}{(z-1)^3} - \frac{630 \left(z^4 + 16z^3 + 36z^2 + 16z + 1 \right) \log z}{(z-1)^4} \right).$$

The symbol $\sim$ is a reminder that these expressions are valid up to corrections of order $O(\bar{y}^4)$. The same calculation can be carried out to higher orders in $\bar{y}$, as will be necessary to extend the present work to correlators with $J > 4$.

11.A.2   Conformal block normalization

In this appendix we review our normalization conventions for conformal blocks. Furthermore, we study the contribution of half-BPS operators to the bulk and defect OPEs. This allows to extract topological subsector data from correlation functions, and compare to the predictions from section 11.2.4.

The bulk-channel conformal block is given explicitly in (11.91). In the bulk OPE limit $z, \bar{z} \to 1$ it goes like

$$\lim_{z,\bar{z}\to 1} f_{\Delta,\ell}(z,\bar{z}) = [(1-z)(1-\bar{z})]^{(\Delta-\ell)/2}(1-z\bar{z})^{\ell}. \tag{11.93}$$

For the defect-channel conformal block we use the same normalization as [266]

$$\hat{f}_{\widehat{\Delta},s}(z,\bar{z}) = z^{\frac{\widehat{\Delta}-s}{2}} \bar{z}^{\frac{\widehat{\Delta}+s}{2}} \,_2F_1\left(\frac{1}{2}, -s; \frac{1}{2} - s; \frac{z}{\bar{z}} \right) \,_2F_1\left(\frac{1}{2}, \widehat{\Delta}; \widehat{\Delta} + \frac{1}{2}; z\bar{z} \right). \tag{11.94}$$

The asymptotics in the defect OPE limit $z, \bar{z} \to 0$ can be easily extracted. Finally, we use the following form of the R-symmetry blocks:

$$
\begin{aligned}
h_K(\sigma) &= \sigma^{-K/2} {}_2F_1\left(-\frac{K}{2}, -\frac{K}{2}; -K-1; \frac{\sigma}{2}\right), \\
\hat{h}_{\hat{K}}(\sigma) &= \sigma^{\hat{K}} {}_2F_1\left(-\hat{K}-1, -\hat{K}; -2(\hat{K}+1); \frac{2}{\sigma}\right).
\end{aligned}
\tag{11.95}
$$

Using (11.13) and (11.15), it is possible to check that these blocks satisfy the appropriate Casimir equations.

In the discussion of the main text, it is crucial to compare to the predictions in the topological subsector of section 11.2.4. We start showing how to extract the topological bulk CFT data from our correlators. The choice of normalization in (11.22) fixes uniquely the bulk OPE

$$
\mathcal{O}_J(x_1, u_1)\mathcal{O}_J(x_2, u_2)\big|_{\mathcal{O}_K} = \lambda_{JJK} \frac{(u_1 \cdot u_2)^{J-\frac{K}{2}}}{(x_{12}^2)^{J-\frac{K}{2}}} \frac{(u_1 \cdot D_u^{(6)})^{\frac{K}{2}} (u_2 \cdot D_u^{(6)})^{\frac{K}{2}} \mathcal{O}_K(x_2, u)}{K!(K+1)!} + \dots
\tag{11.96}
$$

This is the contribution of a single half-BPS operator $\mathcal{O}_K(x, u)$ to the bulk OPE, and we suppress terms subleading as $x_{12}^2 \to 0$. In order to deal with the R-symmetry polarization, we use the $SO(r)$ Todorov operator

$$
(D_u^{(r)})_\mu = \left(\frac{r}{2} - 1 + u \cdot \frac{\partial}{\partial u}\right) \frac{\partial}{\partial u^\mu} - \frac{1}{2} u_\mu \frac{\partial^2}{\partial u \cdot \partial u}.
\tag{11.97}
$$

One can insert the bulk OPE (11.96) combined with the one-point function (11.24) in the two-point function. Keeping only the leading term as $z, \bar{z} \to 1$ gives

$$
\mathcal{F}^{(J)}(z, \bar{z}, \sigma)\big|_{\mathcal{O}_K} = \left(\frac{\sqrt{z\bar{z}}\,\sigma}{(1-z)(1-\bar{z})}\right)^J \lambda_{JJK} a_K h_K(\sigma)\left[(1-z)(1-\bar{z})\right]^{\frac{K}{2}} + \dots
\tag{11.98}
$$

This is the leading contribution of a protected half-BPS operator to the bulk OPE, and it is equally valid for single- and multi-trace operators. It is reassuring that the contribution is proportional to the R-symmetry block (11.95). This result also justifies our choice of the overall normalization for the bulk superblock (11.72).

The story for the defect OPE works in an identical way. The form of the correlators (11.30) fixes uniquely the bulk-defect expansion

$$
\mathcal{O}_J(x, u)\big|_{\hat{\mathcal{O}}_{\hat{K}}} = b_{J\hat{K}} \frac{(u \cdot \theta)^{J-\hat{K}}}{|x^\perp|^{J-\hat{K}}} \frac{(u \cdot D_{\hat{u}}^{(5)})^{\hat{K}} \hat{\mathcal{O}}_{\hat{K}}(\tau, \hat{u})}{\hat{K}!(3/2)_{\hat{K}}} + \dots
\tag{11.99}
$$

As before, we focus on the contribution of a protected defect operator and keep only the leading-order term as $x^\perp \to 0$. Since the defect operator transforms as an $SO(5)$ symmetric traceless tensor, we use the $r = 5$ version of (11.97). Inserting the defect OPE in the two-point function gives

$$\mathcal{F}^{(J)}(z, \bar{z}, \sigma)\big|_{\hat{\mathcal{O}}_{\hat{K}}} \sim b^2_{J\hat{K}} \hat{h}_{\hat{K}}(\sigma)(z\bar{z})^{\hat{K}/2} + \dots \tag{11.100}$$

This is the leading contribution as $z, \bar{z} \to 0$ of a protected defect operator to the defect OPE.

Part III

Outlook

Chapter 12

Summary and future directions

12.1 Summary

The goal of this thesis was to advance our understanding of conformal bootstrap in the presence of supersymmetry and defects. This goal has been achieved in two different fronts.

First, we have contributed to the numerical and analytical study of SCFT without defects. The single-correlator bounds of chapter 7 have improved the state-of-the-art results for $4d$ $\mathcal{N} = 2$ SCFTs. Furthermore, we performed the first mixed-correlator study that involves Coulomb and Higgs branch operators, two operators ubiquitous in SCFT. Additionally, chapters 9 and 10 studied the Wess-Zumino model, a supersymmetric cousin of the $3d$ Ising CFT. While previous work on the Wess-Zumino model was numerical [193, 378], we focused on analytic methods. Within our framework, we determined the spectrum of the Wess-Zumino model at leading order in the ε–expansion, and in the future, we hope to extend these results beyond the ε–expansion.

Second, this thesis has contributed to the study of conformal and superconformal defects. As a first example, in chapter 8 we studied superconformal line defects in $4d$ $\mathcal{N} = 2$ theories. Our analysis, which considered correlators restricted to the defect, can be viewed as a less-supersymmetric generalization of previous work in $\mathcal{N} = 4$ SYM [233]. The numerical results put general constraints in the space of allowed line defects, while the analytic results solve the crossing equation in the holographic regime. As a second example, in chapters 9-11 we have studied two-point functions of bulk operators in the presence of a conformal defect. Before this thesis, most work on bulk two-point functions considered only non-supersymmetric boundary CFT. In our work, we have generalized this in two ways.

On the one hand, in chapter 9 we added supersymmetry by considering the Wess-Zumino model in the presence of a boundary. On the other hand, using the Lorentzian inversion formula [266] we were able to systematically consider defects of codimension $q > 1$. The inversion formula does not require supersymmetry, but it only applies to perturbative setups, such as the ε–expansion (chapter 10) and holographic CFTs (chapter 11).

12.2 Future directions

After every chapter in part II, we have given an outlook of future directions specific to that context. Instead of summarizing them here, we present more general goals of the conformal bootstrap, that will hopefully be accomplished to some extent in the coming years.

Although the numerical bootstrap is a consolidated technique, there are still prospects of obtaining many interesting results. In the past years, a large effort has led to the determination of critical exponents for the Ising, $O(2)$ and $O(3)$ CFTs to unprecedented accuracy [64, 77, 79]. In the process, the community has developed tools of general applicability [60, 68, 78], so the next natural step is to use these tools to study other $3d$ models relevant to critical phenomena. Another exciting possibility is to use numerical bootstrap to study the fixed points of $4d$ gauge theories such as QCD. Sadly, these models have been elusive in the numerical bootstrap, although some progress has been made recently [96–98]. Finally, a longstanding dream is to combine the developments in the analytic and numerical bootstrap. To be more precise, the goal is to develop numerical bootstrap methods with built-in knowledge of the large-spin behavior predicted by the analytic bootstrap.[1]

These powerful numerical tools can also be used to study SCFT. Although a full classification program for SCFT is unattainable at the moment, perhaps partial results are within reach. For instance, the $3d$ $\mathcal{N} = 1$ super-Ising model appears to be the unique SCFT in a particular corner of theory space [167, 199, 200]. Perhaps the Wess-Zumino model can also be cornered to an island in parameter space, providing stronger evidence that it is the simplest SCFT with four supercharges. To achieve this for the Wess-Zumino model, the natural system of correlators would involve a mix of chiral operators and the lowest-dimension neutral scalar, which is unprotected. However, it has been a longstanding problem to compute superconformal blocks with external unprotected operators. Although there has been significant progress with other correlators [2, 196, 197, 200, 214, 228, 240, 241, 356], the

---

[1]Shortly before this thesis was submitted, [422] appeared which takes a first promising step in this direction.

superblocks that apply to the Wess-Zumino model are not yet known. Finally, the recent work [225] proposed a method to do numerical bootstrap, at the same time requiring that the integrated correlator takes a particular value. The motivation is that in SCFT some integrated correlators can be computed using supersymmetric localization. For $\mathcal{N} = 4$ SYM theory, the combination of integrated correlators, numerical bootstrap and supersymmetric localization gave exciting results [225], which perhaps can be extended to other setups.

In this thesis, our discussion of the conformal bootstrap has been restricted to scalar operators. However, in conformal field theory all four-point functions are crossing symmetric, not only those of scalars. It is thus important to include spinning operators in the crossing equations, as has been done several times in the literature [25, 111–115]. The relative low number of papers considering spinning bootstrap is due to the technical complications that arise in these calculations. However, these complications have been overcome in $3d$ [68, 423], so now is the perfect time to explore in more detail the numerical bootstrap with spinning operators. In the case of superconformal field theories, the extra difficulty is that superconformal blocks involving spinning operators are largely not known, but see [190] for an exception. In the case of defects, two-point functions of spin-ℓ operators are understood kinematically, but only [269] has studied dynamics.

Although exploring spinning correlators is an important endeavor, it is possible that similar or better results can be obtained from higher-point scalar correlators. Higher-point correlators involve five or more external operators, and by means of the OPE, they contain information of spinning exchanged operators. Therefore, crossing of scalar higher-point functions can be equivalent to crossing of spinning four-point functions. Although on paper scalar correlators might appear simpler, the price to pay is that multipoint computations become hard due to the proliferation of conformal cross-ratios. Nevertheless, examples of higher-point correlators have been obtained in perturbation theory [175, 424, 425]. In order to develop the bootstrap program for higher-point functions, the first step is to compute the conformal blocks. Although computing higher-point blocks in full generality is challenging, partial results have appeared in the literature [424, 426–431]. In particular, the kinematics simplify by taking the lightcone limit between consecutive points, facilitating the computation of conformal blocks and allowing analogs of the traditional lightcone bootstrap [425, 432, 433]. However, there are still many unanswered questions. For example, is analyticity in spin preserved for higher-point functions, and if yes, is there an analog of Caron-Huot's Lorentzian inversion formula? On the numerical front, there are no results yet of multipoint numerical bootstrap.

The final topic we want to discuss are conformal defects. Recently, a fruitful idea has been to classify the allowed conformal defects given a free bulk theory [294–296]. The next natural step, which has taken a substantial part of this thesis, is the study of conformal defects in a weakly coupled bulk. However, at the non-perturbative level, it is still an open question how to leverage known properties of the bulk to constrain the space of allowed defects. It is possible that this goal requires imposing crossing symmetry of higher-point correlators such as bulk-bulk-defect. Once again, the kinematics in this setup becomes harder, but recently some of the necessary blocks have been obtained [295, 388]. Although the bootstrap was possible in theories where the bulk is free [294–296], not much progress has been made yet on using bulk-bulk-defect correlators in other setups. Another ambitious idea is to consider correlators involving more than one defect. Besides the expansions mentioned in chapter 6, a defect can be expanded in terms of local operators. By using the defect-local operator expansion, the two-point function of defects can be expanded in conformal blocks [434, 435]. However, in order to find a crossing equation, it is necessary to also consider the expansion of two defects in terms of defects. Unfortunately, it is not clear whether there exists a conformally invariant expansion for the product of two defects, see [436].

This summary shows that, even though there has been amazing progress in the last years, there are still lots of interesting and promising bootstrap questions to answer in the future!

Bibliography

[1] A. Gimenez-Grau and P. Liendo, *Bootstrapping Coulomb and Higgs branch operators*, *JHEP* **01** (2021) 175 [`2006.01847`].

[2] A. Gimenez-Grau and P. Liendo, *Bootstrapping line defects in $\mathcal{N} = 2$ theories*, *JHEP* **03** (2020) 121 [`1907.04345`].

[3] A. Gimenez-Grau, P. Liendo and P. van Vliet, *Superconformal boundaries in $4 - \epsilon$ dimensions*, *JHEP* **04** (2021) 167 [`2012.00018`].

[4] A. Gimenez-Grau and P. Liendo, *Bootstrapping Monodromy Defects in the Wess-Zumino Model*, `2108.05107`.

[5] J. Barrat, A. Gimenez-Grau and P. Liendo, *Bootstrapping holographic defect correlators in $\mathcal{N} = 4$ super Yang-Mills*, `2108.13432`.

[6] A. Gimenez Grau, C. Kristjansen, M. Volk and M. Wilhelm, *A Quantum Check of Non-Supersymmetric AdS/dCFT*, *JHEP* **01** (2019) 007 [`1810.11463`].

[7] A. Gimenez-Grau, C. Kristjansen, M. Volk and M. Wilhelm, *A quantum framework for AdS/dCFT through fuzzy spherical harmonics on S^4*, *JHEP* **04** (2020) 132 [`1912.02468`].

[8] P. A. M. Dirac, *The scientific work of Georges Lemaitre*, *Comment. Pont. Acad. Sci.* **2** (1968) 1.

[9] A. Pelissetto and E. Vicari, *Critical phenomena and renormalization group theory*, *Phys. Rept.* **368** (2002) 549 [`cond-mat/0012164`].

[10] A. Belavin, A. M. Polyakov and A. Zamolodchikov, *Infinite Conformal Symmetry in Two-Dimensional Quantum Field Theory*, *Nucl.Phys.* **B241** (1984) 333.

[11] P. H. Ginsparg, *APPLIED CONFORMAL FIELD THEORY*, in *Les Houches Summer School in Theoretical Physics: Fields, Strings, Critical Phenomena*, 9, 1988, `hep-th/9108028`.

[12] P. Di Francesco, P. Mathieu and D. Senechal, *Conformal field theory*, .

[13] S. Ribault, *Conformal field theory on the plane*, `1406.4290`.

[14] P. Kravchuk, J. Qiao and S. Rychkov, *Distributions in CFT. Part I. Cross-ratio space*, *JHEP* **05** (2020) 137 [`2001.08778`].

[15] P. Kravchuk, J. Qiao and S. Rychkov, *Distributions in CFT. Part II. Minkowski space*, *JHEP* **08** (2021) 094 [`2104.02090`].

[16] F. Dolan and H. Osborn, *Conformal four point functions and the operator product expansion*, *Nucl.Phys.* **B599** (2001) 459 [`hep-th/0011040`].

[17] R. Rattazzi, V. S. Rychkov, E. Tonni and A. Vichi, *Bounding scalar operator dimensions in 4D CFT*, *JHEP* **0812** (2008) 031 [`0807.0004`].

[18] P. Ponte and S.-S. Lee, *Emergence of supersymmetry on the surface of three dimensional topological insulators*, *New J. Phys.* **16** (2014) 013044 [`1206.2340`].

[19] T. Grover, D. N. Sheng and A. Vishwanath, *Emergent Space-Time Supersymmetry at the Boundary of a Topological Phase*, *Science* **344** (2014) 280 [`1301.7449`].

[20] H. Osborn, "Lectures on conformal field theories in more than two dimensions." `https://www.damtp.cam.ac.uk/user/ho/CFTNotes.pdf`, 2019.

[21] D. Simmons-Duffin, *The Conformal Bootstrap*, in *Proceedings, Theoretical Advanced Study Institute in Elementary Particle Physics: New Frontiers in Fields and Strings (TASI 2015): Boulder, CO, USA, June 1-26, 2015*, pp. 1–74, 2017, DOI [`1602.07982`].

[22] M. S. Costa, J. Penedones, D. Poland and S. Rychkov, *Spinning Conformal Correlators*, *JHEP* **1111** (2011) 071 [`1107.3554`].

[23] M. S. Costa, J. Penedones, D. Poland and S. Rychkov, *Spinning Conformal Blocks*, *JHEP* **11** (2011) 154 [`1109.6321`].

[24] M. S. Costa and T. Hansen, *Conformal correlators of mixed-symmetry tensors*, *JHEP* **02** (2015) 151 [`1411.7351`].

[25] L. Iliesiu, F. Kos, D. Poland, S. S. Pufu, D. Simmons-Duffin and R. Yacoby, *Bootstrapping 3D Fermions*, *JHEP* **03** (2016) 120 [`1508.00012`].

[26] G. F. Cuomo, D. Karateev and P. Kravchuk, *General Bootstrap Equations in 4D CFTs*, *JHEP* **01** (2018) 130 [`1705.05401`].

[27] F. A. Dolan and H. Osborn, *On short and semi-short representations for four-dimensional superconformal symmetry*, *Annals Phys.* **307** (2003) 41 [`hep-th/0209056`].

[28] S. Weinberg, *The Quantum theory of fields. Vol. 1: Foundations.* Cambridge University Press, 6, 2005.

[29] D. Pappadopulo, S. Rychkov, J. Espin and R. Rattazzi, *OPE Convergence in Conformal Field Theory*, *Phys.Rev.* **D86** (2012) 105043 [`1208.6449`].

[30] S. Rychkov and P. Yvernay, *Remarks on the Convergence Properties of the Conformal Block Expansion*, *Phys. Lett.* **B753** (2016) 682 [`1510.08486`].

[31] F. Dolan and H. Osborn, *Conformal partial waves and the operator product expansion*, *Nucl.Phys.* **B678** (2004) 491 [`hep-th/0309180`].

[32] F. Dolan and H. Osborn, *Conformal Partial Waves: Further Mathematical Results*, `1108.6194`.

[33] S. Rychkov, *EPFL Lectures on Conformal Field Theory in D¿= 3 Dimensions*, SpringerBriefs in Physics. 2016, 10.1007/978-3-319-43626-5, [`1601.05000`].

[34] S. M. Chester, *Weizmann Lectures on the Numerical Conformal Bootstrap*, `1907.05147`.

[35] D. Poland, S. Rychkov and A. Vichi, *The Conformal Bootstrap: Theory, Numerical Techniques, and Applications*, *Rev. Mod. Phys.* **91** (2019) 015002 [`1805.04405`].

[36] D. Poland and D. Simmons-Duffin, *The conformal bootstrap*, *Nature Phys.* **12** (2016) 535.

[37] J. Polchinski, *Scale and Conformal Invariance in Quantum Field Theory*, *Nucl.Phys.* **B303** (1988) 226.

[38] D. Dorigoni and V. S. Rychkov, *Scale Invariance + Unitarity => Conformal Invariance?*, 0910.1087.

[39] S. El-Showk, Y. Nakayama and S. Rychkov, *What Maxwell Theory in D<>4 teaches us about scale and conformal invariance*, *Nucl. Phys. B* **848** (2011) 578 [1101.5385].

[40] S. a. Meneses, J. a. Penedones, S. Rychkov, J. M. Viana Parente Lopes and P. Yvernay, *A structural test for the conformal invariance of the critical 3d Ising model*, *JHEP* **04** (2019) 115 [1802.02319].

[41] V. Riva and J. L. Cardy, *Scale and conformal invariance in field theory: A Physical counterexample*, *Phys. Lett. B* **622** (2005) 339 [hep-th/0504197].

[42] Y. Nakayama, *Scale invariance vs conformal invariance*, *Phys. Rept.* **569** (2015) 1 [1302.0884].

[43] F. Gliozzi, *More constraining conformal bootstrap*, *Phys.Rev.Lett.* **111** (2013) 161602 [1307.3111].

[44] F. Gliozzi and A. Rago, *Critical exponents of the 3d Ising and related models from Conformal Bootstrap*, *JHEP* **10** (2014) 042 [1403.6003].

[45] F. Gliozzi, P. Liendo, M. Meineri and A. Rago, *Boundary and Interface CFTs from the Conformal Bootstrap*, *JHEP* **05** (2015) 036 [1502.07217].

[46] F. Gliozzi, *Truncatable bootstrap equations in algebraic form and critical surface exponents*, *JHEP* **10** (2016) 037 [1605.04175].

[47] M. Isachenkov and V. Schomerus, *Superintegrability of d-dimensional Conformal Blocks*, *Phys. Rev. Lett.* **117** (2016) 071602 [1602.01858].

[48] V. Schomerus, E. Sobko and M. Isachenkov, *Harmony of Spinning Conformal Blocks*, *JHEP* **03** (2017) 085 [1612.02479].

[49] V. Schomerus and E. Sobko, *From Spinning Conformal Blocks to Matrix Calogero-Sutherland Models*, *JHEP* **04** (2018) 052 [1711.02022].

[50] M. Isachenkov and V. Schomerus, *Integrability of conformal blocks. Part I. Calogero-Sutherland scattering theory*, *JHEP* **07** (2018) 180 [`1711.06609`].

[51] I. Burić, M. Isachenkov and V. Schomerus, *Conformal Group Theory of Tensor Structures*, *JHEP* **10** (2020) 004 [`1910.08099`].

[52] S. Ferrara, R. Gatto and A. F. Grillo, *Positivity Restrictions on Anomalous Dimensions*, *Phys. Rev. D* **9** (1974) 3564.

[53] G. Mack, *All unitary ray representations of the conformal group SU(2,2) with positive energy*, *Commun. Math. Phys.* **55** (1977) 1.

[54] S. Minwalla, *Restrictions imposed by superconformal invariance on quantum field theories*, *Adv. Theor. Math. Phys.* **2** (1998) 783 [`hep-th/9712074`].

[55] F. Caracciolo and V. S. Rychkov, *Rigorous Limits on the Interaction Strength in Quantum Field Theory*, *Phys. Rev. D* **81** (2010) 085037 [`0912.2726`].

[56] D. Poland, D. Simmons-Duffin and A. Vichi, *Carving Out the Space of 4D CFTs*, *JHEP* **05** (2012) 110 [`1109.5176`].

[57] F. Kos, D. Poland and D. Simmons-Duffin, *Bootstrapping the $O(N)$ vector models*, *JHEP* **06** (2014) 091 [`1307.6856`].

[58] F. Kos, D. Poland and D. Simmons-Duffin, *Bootstrapping Mixed Correlators in the 3D Ising Model*, *JHEP* **11** (2014) 109 [`1406.4858`].

[59] D. Simmons-Duffin, *A Semidefinite Program Solver for the Conformal Bootstrap*, *JHEP* **06** (2015) 174 [`1502.02033`].

[60] W. Landry and D. Simmons-Duffin, *Scaling the semidefinite program solver SDPB*, `1909.09745`.

[61] `https://gitlab.com/bootstrapcollaboration/scalar_blocks`.

[62] S. El-Showk, M. F. Paulos, D. Poland, S. Rychkov, D. Simmons-Duffin et al., *Solving the 3D Ising Model with the Conformal Bootstrap*, *Phys.Rev.* **D86** (2012) 025022 [`1203.6064`].

[63] S. El-Showk, M. F. Paulos, D. Poland, S. Rychkov, D. Simmons-Duffin and A. Vichi, *Solving the 3d Ising Model with the Conformal Bootstrap II. c-Minimization and Precise Critical Exponents*, *J. Stat. Phys.* **157** (2014) 869 [1403.4545].

[64] F. Kos, D. Poland, D. Simmons-Duffin and A. Vichi, *Precision Islands in the Ising and $O(N)$ Models*, *JHEP* **08** (2016) 036 [1603.04436].

[65] D. Poland and D. Simmons-Duffin, *Bounds on 4D Conformal and Superconformal Field Theories*, *JHEP* **05** (2011) 017 [1009.2087].

[66] S. El-Showk and M. F. Paulos, *Bootstrapping Conformal Field Theories with the Extremal Functional Method*, *Phys. Rev. Lett.* **111** (2013) 241601 [1211.2810].

[67] M. Go and Y. Tachikawa, *autoboot: A generator of bootstrap equations with global symmetry*, *JHEP* **06** (2019) 084 [1903.10522].

[68] R. S. Erramilli, L. V. Iliesiu, P. Kravchuk, W. Landry, D. Poland and D. Simmons-Duffin, *blocks_3d: software for general 3d conformal blocks*, *JHEP* **11** (2021) 006 [2011.01959].

[69] M. F. Paulos, *JuliBootS: a hands-on guide to the conformal bootstrap*, 1412.4127.

[70] C. Behan, *PyCFTBoot: A flexible interface for the conformal bootstrap*, *Commun. Comput. Phys.* **22** (2017) 1 [1602.02810].

[71] A. Manenti. https://gitlab.com/maneandrea/sailboot.

[72] N. Su. https://gitlab.com/bootstrapcollaboration/simpleboot.

[73] Z. Komargodski and D. Simmons-Duffin, *The Random-Bond Ising Model in 2.01 and 3 Dimensions*, *J. Phys. A* **50** (2017) 154001 [1603.04444].

[74] V. S. Rychkov and A. Vichi, *Universal Constraints on Conformal Operator Dimensions*, *Phys. Rev. D* **80** (2009) 045006 [0905.2211].

[75] R. Rattazzi, S. Rychkov and A. Vichi, *Central Charge Bounds in 4D Conformal Field Theory*, *Phys. Rev. D* **83** (2011) 046011 [1009.2725].

[76] R. Rattazzi, S. Rychkov and A. Vichi, *Bounds in 4D Conformal Field Theories with Global Symmetry*, *J. Phys. A* **44** (2011) 035402 [1009.5985].

[77] S. M. Chester, W. Landry, J. Liu, D. Poland, D. Simmons-Duffin, N. Su et al., *Carving out OPE space and precise O(2) model critical exponents*, 1912.03324.

[78] M. Reehorst, S. Rychkov, D. Simmons-Duffin, B. Sirois, N. Su and B. van Rees, *Navigator Function for the Conformal Bootstrap*, *SciPost Phys.* **11** (2021) 072 [2104.09518].

[79] S. M. Chester, W. Landry, J. Liu, D. Poland, D. Simmons-Duffin, N. Su et al., *Bootstrapping Heisenberg magnets and their cubic instability*, *Phys. Rev. D* **104** (2021) 105013 [2011.14647].

[80] F. Kos, D. Poland, D. Simmons-Duffin and A. Vichi, *Bootstrapping the O(N) Archipelago*, *JHEP* **11** (2015) 106 [1504.07997].

[81] S. M. Chester, S. S. Pufu and R. Yacoby, *Bootstrapping O(N) vector models in 4 < d < 6*, *Phys. Rev. D* **91** (2015) 086014 [1412.7746].

[82] Z. Li and N. Su, *Bootstrapping Mixed Correlators in the Five Dimensional Critical O(N) Models*, *JHEP* **04** (2017) 098 [1607.07077].

[83] Y.-C. He, J. Rong and N. Su, *Non-Wilson-Fisher kinks of O(N) numerical bootstrap: from the deconfined phase transition to a putative new family of CFTs*, *SciPost Phys.* **10** (2021) 115 [2005.04250].

[84] M. Reehorst, *Rigorous bounds on irrelevant operators in the 3d Ising model CFT*, 2111.12093.

[85] S. El-Showk, M. Paulos, D. Poland, S. Rychkov, D. Simmons-Duffin and A. Vichi, *Conformal Field Theories in Fractional Dimensions*, *Phys. Rev. Lett.* **112** (2014) 141601 [1309.5089].

[86] J. Golden and M. F. Paulos, *No unitary bootstrap for the fractal Ising model*, *JHEP* **03** (2015) 167 [1411.7932].

[87] A. Cappelli, L. Maffi and S. Okuda, *Critical Ising Model in Varying Dimension by Conformal Bootstrap*, *JHEP* **01** (2019) 161 [1811.07751].

[88] A. Stergiou, *Bootstrapping hypercubic and hypertetrahedral theories in three dimensions*, *JHEP* **05** (2018) 035 [1801.07127].

[89] S. R. Kousvos and A. Stergiou, *Bootstrapping Mixed Correlators in Three-Dimensional Cubic Theories*, *SciPost Phys.* **6** (2019) 035 [1810.10015].

[90] S. R. Kousvos and A. Stergiou, *Bootstrapping Mixed Correlators in Three-Dimensional Cubic Theories II*, *SciPost Phys.* **8** (2020) 085 [1911.00522].

[91] A. Stergiou, *Bootstrapping MN and Tetragonal CFTs in Three Dimensions*, *SciPost Phys.* **7** (2019) 010 [1904.00017].

[92] J. Henriksson and A. Stergiou, *Perturbative and Nonperturbative Studies of CFTs with MN Global Symmetry*, *SciPost Phys.* **11** (2021) 015 [2101.08788].

[93] S. R. Kousvos and A. Stergiou, *Bootstrapping Mixed MN Correlators in 3D*, 2112.03919.

[94] J. Henriksson, S. R. Kousvos and A. Stergiou, *Analytic and Numerical Bootstrap of CFTs with $O(m) \times O(n)$ Global Symmetry in 3D*, *SciPost Phys.* **9** (2020) 035 [2004.14388].

[95] S. M. Chester and S. S. Pufu, *Towards bootstrapping QED$_3$*, *JHEP* **08** (2016) 019 [1601.03476].

[96] Z. Li and D. Poland, *Searching for gauge theories with the conformal bootstrap*, *JHEP* **03** (2021) 172 [2005.01721].

[97] Y.-C. He, J. Rong and N. Su, *A roadmap for bootstrapping critical gauge theories: decoupling operators of conformal field theories in $d > 2$ dimensions*, *SciPost Phys.* **11** (2021) 111 [2101.07262].

[98] S. Albayrak, R. S. Erramilli, Z. Li, D. Poland and Y. Xin, *Bootstrapping $N_f = 4$ conformal QED$_3$*, 2112.02106.

[99] A. Manenti and A. Vichi, *Exploring $SU(N)$ adjoint correlators in 3d*, 2101.07318.

[100] Y. Pang, J. Rong and N. Su, *ϕ^3 theory with F_4 flavor symmetry in $6 - 2\epsilon$ dimensions: 3-loop renormalization and conformal bootstrap*, *JHEP* **12** (2016) 057 [1609.03007].

[101] J. Rong and J. Zhu, *On the ϕ^3 theory above six dimensions*, *JHEP* **04** (2020) 151 [2001.10864].

[102] J. Rong and N. Su, *Scalar CFTs and Their Large N Limits*, *JHEP* **09** (2018) 103 [1712.00985].

[103] Y.-C. He, J. Rong and N. Su, *Conformal bootstrap bounds for the U(1) Dirac spin liquid and N = 7 Stiefel liquid*, 2107.14637.

[104] Z. Li and N. Su, *3D CFT Archipelago from Single Correlator Bootstrap*, *Phys. Lett. B* **797** (2019) 134920 [1706.06960].

[105] M. Reehorst, M. Refinetti and A. Vichi, *Bootstrapping traceless symmetric O(N) scalars*, 2012.08533.

[106] T. Hartman, D. Mazáč and L. Rastelli, *Sphere Packing and Quantum Gravity*, 1905.01319.

[107] J. Bonifacio and K. Hinterbichler, *Bootstrap Bounds on Closed Einstein Manifolds*, *JHEP* **10** (2020) 069 [2007.10337].

[108] J. Bonifacio, *Bootstrap bounds on closed hyperbolic manifolds*, *JHEP* **02** (2022) 025 [2107.09674].

[109] J. Bonifacio, *Bootstrapping Closed Hyperbolic Surfaces*, 2111.13215.

[110] P. Kravchuk, D. Mazac and S. Pal, *Automorphic Spectra and the Conformal Bootstrap*, 2111.12716.

[111] L. Iliesiu, F. Kos, D. Poland, S. S. Pufu and D. Simmons-Duffin, *Bootstrapping 3D Fermions with Global Symmetries*, *JHEP* **01** (2018) 036 [1705.03484].

[112] D. Karateev, P. Kravchuk, M. Serone and A. Vichi, *Fermion Conformal Bootstrap in 4d*, 1902.05969.

[113] A. Dymarsky, F. Kos, P. Kravchuk, D. Poland and D. Simmons-Duffin, *The 3d Stress-Tensor Bootstrap*, *JHEP* **02** (2018) 164 [1708.05718].

[114] A. Dymarsky, J. Penedones, E. Trevisani and A. Vichi, *Charting the space of 3D CFTs with a continuous global symmetry*, *JHEP* **05** (2019) 098 [1705.04278].

[115] M. Reehorst, E. Trevisani and A. Vichi, *Mixed Scalar-Current bootstrap in three dimensions*, *JHEP* **12** (2020) 156 [1911.05747].

[116] D. Simmons-Duffin, *Projectors, Shadows, and Conformal Blocks*, *JHEP* **04** (2014) 146 [`1204.3894`].

[117] M. Hogervorst and S. Rychkov, *Radial Coordinates for Conformal Blocks*, *Phys. Rev.* **D87** (2013) 106004 [`1303.1111`].

[118] L. Iliesiu, F. Kos, D. Poland, S. S. Pufu, D. Simmons-Duffin and R. Yacoby, *Fermion-Scalar Conformal Blocks*, `1511.01497`.

[119] P. Kravchuk and D. Simmons-Duffin, *Counting Conformal Correlators*, *JHEP* **02** (2018) 096 [`1612.08987`].

[120] D. Karateev, P. Kravchuk and D. Simmons-Duffin, *Weight Shifting Operators and Conformal Blocks*, *JHEP* **02** (2018) 081 [`1706.07813`].

[121] A. L. Fitzpatrick, J. Kaplan and D. Poland, *Conformal Blocks in the Large D Limit*, *JHEP* **08** (2013) 107 [`1305.0004`].

[122] A. L. Fitzpatrick, J. Kaplan, D. Poland and D. Simmons-Duffin, *The Analytic Bootstrap and AdS Superhorizon Locality*, *JHEP* **12** (2013) 004 [`1212.3616`].

[123] Z. Komargodski and A. Zhiboedov, *Convexity and Liberation at Large Spin*, *JHEP* **1311** (2013) 140 [`1212.4103`].

[124] D. Simmons-Duffin, *The Lightcone Bootstrap and the Spectrum of the 3d Ising CFT*, *JHEP* **03** (2017) 086 [`1612.08471`].

[125] S. Caron-Huot, *Analyticity in Spin in Conformal Theories*, *JHEP* **09** (2017) 078 [`1703.00278`].

[126] D. Simmons-Duffin, D. Stanford and E. Witten, *A spacetime derivation of the Lorentzian OPE inversion formula*, *JHEP* **07** (2018) 085 [`1711.03816`].

[127] P. Kravchuk and D. Simmons-Duffin, *Light-ray operators in conformal field theory*, *JHEP* **11** (2018) 102 [`1805.00098`].

[128] S. Rychkov and Z. M. Tan, *The ϵ-expansion from conformal field theory*, *J. Phys. A* **48** (2015) 29FT01 [`1505.00963`].

[129] M. Hogervorst, S. Rychkov and B. C. van Rees, *Unitarity violation at the Wilson-Fisher fixed point in 4-ε dimensions*, *Phys. Rev. D* **93** (2016) 125025 [1512.00013].

[130] P. Liendo, *Revisiting the dilatation operator of the Wilson–Fisher fixed point*, *Nucl. Phys. B* **920** (2017) 368 [1701.04830].

[131] F. Gliozzi, A. Guerrieri, A. C. Petkou and C. Wen, *Generalized Wilson-Fisher Critical Points from the Conformal Operator Product Expansion*, *Phys. Rev. Lett.* **118** (2017) 061601 [1611.10344].

[132] F. Gliozzi, A. L. Guerrieri, A. C. Petkou and C. Wen, *The analytic structure of conformal blocks and the generalized Wilson-Fisher fixed points*, *JHEP* **04** (2017) 056 [1702.03938].

[133] F. Gliozzi, *Anomalous dimensions of spinning operators from conformal symmetry*, *JHEP* **01** (2018) 113 [1711.05530].

[134] J. Henriksson, *The critical O(N) CFT: Methods and conformal data*, 2201.09520.

[135] L. F. Alday, J. Henriksson and M. van Loon, *Taming the ε-expansion with large spin perturbation theory*, *JHEP* **07** (2018) 131 [1712.02314].

[136] J. Henriksson and M. Van Loon, *Critical O(N) model to order ϵ^4 from analytic bootstrap*, *J. Phys.* **A52** (2019) 025401 [1801.03512].

[137] D. Simmons-Duffin, *Analytic bootstrap methods*, Bootstrap School 2018. https://bootstrapcollaboration.com/bootstrap2018/school/.

[138] D. Simmons-Duffin, *Tasi lectures on conformal field theory in lorentzian signature*, TASI 2019. https://gitlab.com/davidsd/lorentzian-cft-notes.

[139] S. Caron-Huot, *Lorentzian and analytic bootstrap*, Bootstrap School 2020. https://projects.iq.harvard.edu/bootstrap2020/videos.

[140] J. Henriksson, *Analytic bootstrap for perturbative conformal field theories*, Ph.D. thesis, University of Oxford, Oxford U., 2020. 2008.12600.

[141] A. Bissi, A. Sinha and X. Zhou, *Selected Topics in Analytic Conformal Bootstrap: A Guided Journey*, 2202.08475.

[142] L. F. Alday and A. Zhiboedov, *Conformal Bootstrap With Slightly Broken Higher Spin Symmetry*, *JHEP* **06** (2016) 091 [`1506.04659`].

[143] L. F. Alday and A. Zhiboedov, *An Algebraic Approach to the Analytic Bootstrap*, *JHEP* **04** (2017) 157 [`1510.08091`].

[144] L. F. Alday, A. Bissi and T. Lukowski, *Large spin systematics in CFT*, *JHEP* **11** (2015) 101 [`1502.07707`].

[145] L. F. Alday, *Solving CFTs with Weakly Broken Higher Spin Symmetry*, *JHEP* **10** (2017) 161 [`1612.00696`].

[146] R. Gopakumar, A. Kaviraj, K. Sen and A. Sinha, *Conformal Bootstrap in Mellin Space*, *Phys. Rev. Lett.* **118** (2017) 081601 [`1609.00572`].

[147] R. Gopakumar, A. Kaviraj, K. Sen and A. Sinha, *A Mellin space approach to the conformal bootstrap*, *JHEP* **05** (2017) 027 [`1611.08407`].

[148] P. Dey, A. Kaviraj and A. Sinha, *Mellin space bootstrap for global symmetry*, *JHEP* **07** (2017) 019 [`1612.05032`].

[149] P. Dey and A. Kaviraj, *Towards a Bootstrap approach to higher orders of epsilon expansion*, *JHEP* **02** (2018) 153 [`1711.01173`].

[150] J. Penedones, J. A. Silva and A. Zhiboedov, *Nonperturbative Mellin Amplitudes: Existence, Properties, Applications*, *JHEP* **08** (2020) 031 [`1912.11100`].

[151] D. Carmi, J. Penedones, J. A. Silva and A. Zhiboedov, *Applications of dispersive sum rules: ε-expansion and holography*, *SciPost Phys.* **10** (2021) 145 [`2009.13506`].

[152] M. Kologlu, P. Kravchuk, D. Simmons-Duffin and A. Zhiboedov, *Shocks, Superconvergence, and a Stringy Equivalence Principle*, *JHEP* **11** (2020) 096 [`1904.05905`].

[153] D. Carmi and S. Caron-Huot, *A Conformal Dispersion Relation: Correlations from Absorption*, *JHEP* **09** (2020) 009 [`1910.12123`].

[154] A.-K. Trinh, *Mixed Correlator Dispersive CFT Sum Rules*, `2111.14731`.

[155] D. Mazac, *Analytic bounds and emergence of AdS_2 physics from the conformal bootstrap*, *JHEP* **04** (2017) 146 [`1611.10060`].

[156] D. Mazac and M. F. Paulos, *The analytic functional bootstrap. Part I: 1D CFTs and 2D S-matrices*, *JHEP* **02** (2019) 162 [1803.10233].

[157] D. Mazac and M. F. Paulos, *The analytic functional bootstrap. Part II. Natural bases for the crossing equation*, *JHEP* **02** (2019) 163 [1811.10646].

[158] D. Mazáč, L. Rastelli and X. Zhou, *A basis of analytic functionals for CFTs in general dimension*, *JHEP* **08** (2021) 140 [1910.12855].

[159] M. F. Paulos, *Analytic functional bootstrap for CFTs in d > 1*, *JHEP* **04** (2020) 093 [1910.08563].

[160] K. Ghosh, A. Kaviraj and M. F. Paulos, *Charging up the functional bootstrap*, *JHEP* **10** (2021) 116 [2107.00041].

[161] S. Caron-Huot, D. Mazac, L. Rastelli and D. Simmons-Duffin, *Dispersive CFT Sum Rules*, *JHEP* **05** (2021) 243 [2008.04931].

[162] R. Gopakumar, A. Sinha and A. Zahed, *Crossing Symmetric Dispersion Relations for Mellin Amplitudes*, *Phys. Rev. Lett.* **126** (2021) 211602 [2101.09017].

[163] A. Kaviraj, *Crossing antisymmetric Polyakov blocks + dispersion relation*, *JHEP* **01** (2022) 005 [2109.02658].

[164] S. Albayrak, D. Meltzer and D. Poland, *More Analytic Bootstrap: Nonperturbative Effects and Fermions*, *JHEP* **08** (2019) 040 [1904.00032].

[165] S. Caron-Huot, Y. Gobeil and Z. Zahraee, *The leading trajectory in the 2+1D Ising CFT*, 2007.11647.

[166] J. Liu, D. Meltzer, D. Poland and D. Simmons-Duffin, *The Lorentzian inversion formula and the spectrum of the 3d O(2) CFT*, *JHEP* **09** (2020) 115 [2007.07914].

[167] A. Atanasov, A. Hillman, D. Poland, J. Rong and N. Su, *Precision Bootstrap for the $\mathcal{N} = 1$ Super-Ising Model*, 2201.02206.

[168] J. Henriksson and T. Lukowski, *Perturbative Four-Point Functions from the Analytic Conformal Bootstrap*, *JHEP* **02** (2018) 123 [1710.06242].

[169] L. F. Alday, J. Henriksson and M. van Loon, *An alternative to diagrams for the critical O(N) model: dimensions and structure constants to order 1/N²*, *JHEP* **01** (2020) 063 [1907.02445].

[170] S. Caron-Huot and A.-K. Trinh, *All tree-level correlators in AdS₅ × S₅ supergravity: hidden ten-dimensional conformal symmetry*, *JHEP* **01** (2019) 196 [1809.09173].

[171] L. F. Alday and X. Zhou, *All Tree-Level Correlators for M-theory on AdS₇ × S⁴*, *Phys. Rev. Lett.* **125** (2020) 131604 [2006.06653].

[172] L. F. Alday and X. Zhou, *All Holographic Four-Point Functions in All Maximally Supersymmetric CFTs*, *Phys. Rev. X* **11** (2021) 011056 [2006.12505].

[173] L. F. Alday, C. Behan, P. Ferrero and X. Zhou, *Gluon Scattering in AdS from CFT*, *JHEP* **06** (2021) 020 [2103.15830].

[174] L. F. Alday, A. Bissi and X. Zhou, *One-loop Gluon Amplitudes in AdS*, 2110.09861.

[175] L. F. Alday, V. Gonçalves and X. Zhou, *Super Gluon Five-Point Amplitudes in AdS Space*, 2201.04422.

[176] C. Behan, P. Ferrero and X. Zhou, *More on holographic correlators: Twisted and dimensionally reduced structures*, *JHEP* **04** (2021) 008 [2101.04114].

[177] A. Bissi, G. Fardelli and A. Georgoudis, *Towards all loop supergravity amplitudes on AdS5 × S5*, *Phys. Rev. D* **104** (2021) L041901 [2002.04604].

[178] A. Bissi, G. Fardelli and A. Georgoudis, *All loop structures in supergravity amplitudes on AdS5 × S5 from CFT*, *J. Phys. A* **54** (2021) 324002 [2010.12557].

[179] S. R. Coleman and J. Mandula, *All Possible Symmetries of the S Matrix*, *Phys. Rev.* **159** (1967) 1251.

[180] W. Nahm, *Supersymmetries and their Representations*, *Nucl. Phys. B* **135** (1978) 149.

[181] N. B. Agmon and Y. Wang, *Classifying Superconformal Defects in Diverse Dimensions Part I: Superconformal Lines*, 2009.06650.

[182] C. Cordova, T. T. Dumitrescu and K. Intriligator, *Multiplets of Superconformal Symmetry in Diverse Dimensions*, *JHEP* **03** (2019) 163 [1612.00809].

[183] M. Flato and C. Fronsdal, *Representations of Conformal Supersymmetry*, *Lett. Math. Phys.* **8** (1984) 159.

[184] V. K. Dobrev and V. B. Petkova, *All Positive Energy Unitary Irreducible Representations of Extended Conformal Supersymmetry*, *Phys. Lett. B* **162** (1985) 127.

[185] H. Osborn, *N=1 superconformal symmetry in four-dimensional quantum field theory*, *Annals Phys.* **272** (1999) 243 [`hep-th/9808041`].

[186] J.-H. Park, *Superconformal symmetry and correlation functions*, *Nucl. Phys.* **B559** (1999) 455 [`hep-th/9903230`].

[187] J.-H. Park, *Superconformal symmetry in three-dimensions*, *J. Math. Phys.* **41** (2000) 7129 [`hep-th/9910199`].

[188] A. A. Nizami, T. Sharma and V. Umesh, *Superspace formulation and correlation functions of 3d superconformal field theories*, *JHEP* **07** (2014) 022 [`1308.4778`].

[189] E. I. Buchbinder, S. M. Kuzenko and I. B. Samsonov, *Superconformal field theory in three dimensions: Correlation functions of conserved currents*, *JHEP* **06** (2015) 138 [`1503.04961`].

[190] A. Manenti, A. Stergiou and A. Vichi, *R-current three-point functions in 4d $\mathcal{N} = 1$ superconformal theories*, *JHEP* **12** (2018) 108 [`1804.09717`].

[191] A. Manenti, *Differential operators for superconformal correlation functions*, *JHEP* **04** (2020) 145 [`1910.12869`].

[192] D. Li and A. Stergiou, *Two-point functions of conformal primary operators in $\mathcal{N} = 1$ superconformal theories*, *JHEP* **10** (2014) 037 [`1407.6354`].

[193] N. Bobev, S. El-Showk, D. Mazac and M. F. Paulos, *Bootstrapping SCFTs with Four Supercharges*, *JHEP* **08** (2015) 142 [`1503.02081`].

[194] A. L. Fitzpatrick, J. Kaplan, Z. U. Khandker, D. Li, D. Poland and D. Simmons-Duffin, *Covariant Approaches to Superconformal Blocks*, *JHEP* **08** (2014) 129 [`1402.1167`].

[195] Z. U. Khandker, D. Li, D. Poland and D. Simmons-Duffin, $\mathcal{N} = 1$ *superconformal blocks for general scalar operators*, *JHEP* **08** (2014) 049 [1404.5300].

[196] I. A. Ramírez, *Towards general super Casimir equations for 4D $\mathcal{N} = 1$ SCFTs*, *JHEP* **03** (2019) 047 [1808.05455].

[197] I. Burić, V. Schomerus and E. Sobko, *Crossing symmetry for long multiplets in 4D $\mathcal{N} = 1$ SCFTs*, *JHEP* **04** (2021) 130 [2011.14116].

[198] M. Lemos and P. Liendo, *Bootstrapping $\mathcal{N} = 2$ chiral correlators*, *JHEP* **01** (2016) 025 [1510.03866].

[199] A. Atanasov, A. Hillman and D. Poland, *Bootstrapping the Minimal 3D SCFT*, *JHEP* **11** (2018) 140 [1807.05702].

[200] J. Rong and N. Su, *Bootstrapping minimal $\mathcal{N} = 1$ superconformal field theory in three dimensions*, 1807.04434.

[201] J. Rong and N. Su, *Bootstrapping the $\mathcal{N} = 1$ Wess-Zumino models in three dimensions*, 1910.08578.

[202] S. M. Chester, L. V. Iliesiu, S. S. Pufu and R. Yacoby, *Bootstrapping $O(N)$ Vector Models with Four Supercharges in $3 \le d \le 4$*, *JHEP* **05** (2016) 103 [1511.07552].

[203] S. M. Chester, S. Giombi, L. V. Iliesiu, I. R. Klebanov, S. S. Pufu and R. Yacoby, *Accidental Symmetries and the Conformal Bootstrap*, *JHEP* **01** (2016) 110 [1507.04424].

[204] J.-B. Bae, D. Gang and J. Lee, *3d $\mathcal{N} = 2$ minimal SCFTs from Wrapped M5-branes*, *JHEP* **08** (2017) 118 [1610.09259].

[205] M. Baggio, N. Bobev, S. M. Chester, E. Lauria and S. S. Pufu, *Decoding a Three-Dimensional Conformal Manifold*, *JHEP* **02** (2018) 062 [1712.02698].

[206] C.-M. Chang, M. Fluder, Y.-H. Lin, S.-H. Shao and Y. Wang, *3d N=4 Bootstrap and Mirror Symmetry*, 1910.03600.

[207] S. M. Chester, J. Lee, S. S. Pufu and R. Yacoby, *The $\mathcal{N} = 8$ superconformal bootstrap in three dimensions*, *JHEP* **09** (2014) 143 [1406.4814].

334

[208] S. M. Chester, J. Lee, S. S. Pufu and R. Yacoby, *Exact Correlators of BPS Operators from the 3d Superconformal Bootstrap*, *JHEP* **03** (2015) 130 [1412.0334].

[209] N. B. Agmon, S. M. Chester and S. S. Pufu, *Solving M-theory with the Conformal Bootstrap*, *JHEP* **06** (2018) 159 [1711.07343].

[210] N. B. Agmon, S. M. Chester and S. S. Pufu, *The M-theory Archipelago*, *JHEP* **02** (2020) 010 [1907.13222].

[211] D. J. Binder, S. M. Chester, M. Jerdee and S. S. Pufu, *The 3d $\mathcal{N}$ = 6 bootstrap: from higher spins to strings to membranes*, *JHEP* **05** (2021) 083 [2011.05728].

[212] M. Berkooz, R. Yacoby and A. Zait, *Bounds on $\mathcal{N}=1$ superconformal theories with global symmetries*, *JHEP* **08** (2014) 008 [1402.6068].

[213] D. Poland and A. Stergiou, *Exploring the Minimal 4D $\mathcal{N}=1$ SCFT*, *JHEP* **12** (2015) 121 [1509.06368].

[214] D. Li, D. Meltzer and A. Stergiou, *Bootstrapping mixed correlators in 4D $\mathcal{N}$ = 1 SCFTs*, *JHEP* **07** (2017) 029 [1702.00404].

[215] Y.-H. Lin, D. Meltzer, S.-H. Shao and A. Stergiou, *Bounds on Triangle Anomalies in (3+1)d*, *Phys. Rev. D* **101** (2020) 125007 [1909.11676].

[216] C. Beem, M. Lemos, P. Liendo, L. Rastelli and B. C. van Rees, *The $\mathcal{N}=2$ superconformal bootstrap*, *JHEP* **03** (2016) 183 [1412.7541].

[217] M. Cornagliotto, M. Lemos and P. Liendo, *Bootstrapping the (A_1, A_2) Argyres-Douglas theory*, *JHEP* **03** (2018) 033 [1711.00016].

[218] A. Bissi, F. Fucito, A. Manenti, J. F. Morales and R. Savelli, *OPE coefficients in Argyres-Douglas theories*, 2112.11899.

[219] M. Lemos, P. Liendo, C. Meneghelli and V. Mitev, *Bootstrapping $\mathcal{N}=3$ superconformal theories*, *JHEP* **04** (2017) 032 [1612.01536].

[220] L. F. Alday and A. Bissi, *The superconformal bootstrap for structure constants*, *JHEP* **09** (2014) 144 [1310.3757].

[221] C. Beem, L. Rastelli and B. C. van Rees, *The $\mathcal{N}=4$ Superconformal Bootstrap*, *Phys. Rev. Lett.* **111** (2013) 071601 [1304.1803].

[222] L. F. Alday and A. Bissi, *Generalized bootstrap equations for $\mathcal{N} = 4$ SCFT*, *JHEP* **02** (2015) 101 [1404.5864].

[223] C. Beem, L. Rastelli and B. C. van Rees, *More $\mathcal{N} = 4$ superconformal bootstrap*, *Phys. Rev. D* **96** (2017) 046014 [1612.02363].

[224] A. Bissi, A. Manenti and A. Vichi, *Bootstrapping mixed correlators in $\mathcal{N} = 4$ super Yang-Mills*, *JHEP* **05** (2021) 111 [2010.15126].

[225] S. M. Chester, R. Dempsey and S. S. Pufu, *Bootstrapping $\mathcal{N} = 4$ super-Yang-Mills on the conformal manifold*, 2111.07989.

[226] Y.-H. Lin, S.-H. Shao, D. Simmons-Duffin, Y. Wang and X. Yin, *$\mathcal{N} = 4$ superconformal bootstrap of the K3 CFT*, *JHEP* **05** (2017) 126 [1511.04065].

[227] Y.-H. Lin, S.-H. Shao, Y. Wang and X. Yin, *(2, 2) superconformal bootstrap in two dimensions*, *JHEP* **05** (2017) 112 [1610.05371].

[228] M. Cornagliotto, M. Lemos and V. Schomerus, *Long Multiplet Bootstrap*, *JHEP* **10** (2017) 119 [1702.05101].

[229] C.-M. Chang, M. Fluder, Y.-H. Lin and Y. Wang, *Spheres, Charges, Instantons, and Bootstrap: A Five-Dimensional Odyssey*, *JHEP* **03** (2018) 123 [1710.08418].

[230] C. Beem, M. Lemos, L. Rastelli and B. C. van Rees, *The (2, 0) superconformal bootstrap*, *Phys. Rev. D* **93** (2016) 025016 [1507.05637].

[231] C.-M. Chang and Y.-H. Lin, *Carving Out the End of the World or (Superconformal Bootstrap in Six Dimensions)*, *JHEP* **08** (2017) 128 [1705.05392].

[232] F. Baume and C. Lawrie, *Bootstrapping (D, D) Conformal Matter*, 2111.02453.

[233] P. Liendo, C. Meneghelli and V. Mitev, *Bootstrapping the half-BPS line defect*, *JHEP* **10** (2018) 077 [1806.01862].

[234] L. Eberhardt, *Superconformal symmetry and representations*, *J. Phys. A* **54** (2021) 063002 [2006.13280].

[235] Z. Li and N. Su, *The Most General 4D $\mathcal{N} = 1$ Superconformal Blocks for Scalar Operators*, *JHEP* **05** (2016) 163 [1602.07097].

[236] N. Bobev, E. Lauria and D. Mazac, *Superconformal Blocks for SCFTs with Eight Supercharges*, *JHEP* **07** (2017) 061 [`1705.08594`].

[237] A. Bissi and T. Łukowski, *Revisiting $\mathcal{N} = 4$ superconformal blocks*, *JHEP* **02** (2016) 115 [`1508.02391`].

[238] F. Baume, M. Fuchs and C. Lawrie, *Superconformal Blocks for Mixed 1/2-BPS Correlators with $SU(2)$ R-symmetry*, *JHEP* **11** (2019) 164 [`1908.02768`].

[239] J.-F. Fortin, K. Intriligator and A. Stergiou, *Current OPEs in Superconformal Theories*, *JHEP* **09** (2011) 071 [`1107.1721`].

[240] I. Buric, V. Schomerus and E. Sobko, *Superconformal Blocks: General Theory*, `1904.04852`.

[241] I. Burić, V. Schomerus and E. Sobko, *The Superconformal Xing Equation*, `2005.13547`.

[242] A. Bissi, G. Fardelli and A. Manenti, *Rebooting quarter-BPS operators in $\mathcal{N} = 4$ Super Yang-Mills*, `2111.06857`.

[243] F. Dolan and H. Osborn, *Superconformal symmetry, correlation functions and the operator product expansion*, *Nucl. Phys. B* **629** (2002) 3 [`hep-th/0112251`].

[244] F. A. Dolan, L. Gallot and E. Sokatchev, *On four-point functions of 1/2-BPS operators in general dimensions*, *JHEP* **09** (2004) 056 [`hep-th/0405180`].

[245] M. Nirschl and H. Osborn, *Superconformal Ward identities and their solution*, *Nucl. Phys.* **B711** (2005) 409 [`hep-th/0407060`].

[246] C. Beem, M. Lemos, P. Liendo, W. Peelaers, L. Rastelli and B. C. van Rees, *Infinite Chiral Symmetry in Four Dimensions*, *Commun. Math. Phys.* **336** (2015) 1359 [`1312.5344`].

[247] P. Liendo, I. Ramirez and J. Seo, *Stress-tensor OPE in $\mathcal{N} = 2$ superconformal theories*, *JHEP* **02** (2016) 019 [`1509.00033`].

[248] M. Lemos and P. Liendo, *$\mathcal{N} = 2$ central charge bounds from 2d chiral algebras*, *JHEP* **04** (2016) 004 [`1511.07449`].

[249] M. Lemos, *Lectures on chiral algebras of $\mathcal{N} \geqslant 2$ superconformal field theories*, 2006.13892.

[250] C. Beem, L. Rastelli and B. C. van Rees, *$\mathcal{W}$ symmetry in six dimensions*, *JHEP* **05** (2015) 017 [1404.1079].

[251] A. S. Galperin, E. A. Ivanov, V. I. Ogievetsky and E. S. Sokatchev, *Harmonic superspace*, Cambridge Monographs on Mathematical Physics. Cambridge University Press, 2007, 10.1017/CBO9780511535109.

[252] J. Padayasi, A. Krishnan, M. A. Metlitski, I. A. Gruzberg and M. Meineri, *The extraordinary boundary transition in the 3d O(N) model via conformal bootstrap*, 2111.03071.

[253] G. Cuomo, Z. Komargodski and M. Mezei, *Localized magnetic field in the $O(N)$ model*, 2112.10634.

[254] A. Kapustin, *Wilson-'t Hooft operators in four-dimensional gauge theories and S-duality*, *Phys.Rev.* **D74** (2006) 025005 [hep-th/0501015].

[255] M. Billó, M. Caselle, D. Gaiotto, F. Gliozzi, M. Meineri and R. Pellegrini, *Line defects in the 3d Ising model*, *JHEP* **07** (2013) 055 [1304.4110].

[256] D. Gaiotto, D. Mazac and M. F. Paulos, *Bootstrapping the 3d Ising twist defect*, *JHEP* **1403** (2014) 100 [1310.5078].

[257] A. Söderberg, *Anomalous Dimensions in the WF $O(N)$ Model with a Monodromy Line Defect*, *JHEP* **03** (2018) 058 [1706.02414].

[258] S. Giombi, E. Helfenberger, Z. Ji and H. Khanchandani, *Monodromy Defects from Hyperbolic Space*, 2102.11815.

[259] M. Billò, V. Goncalves, E. Lauria and M. Meineri, *Defects in conformal field theory*, *JHEP* **04** (2016) 091 [1601.02883].

[260] L. Bianchi, G. Bliard, V. Forini, L. Griguolo and D. Seminara, *Analytic bootstrap and Witten diagrams for the ABJM Wilson line as defect CFT_1*, *JHEP* **08** (2020) 143 [2004.07849].

[261] L. Bianchi, G. Bliard, V. Forini and G. Peveri, *Mellin amplitudes for 1d CFT*, *JHEP* **10** (2021) 095 [2106.00689].

[262] P. Ferrero and C. Meneghelli, *Bootstrapping the half-BPS line defect CFT in N=4 supersymmetric Yang-Mills theory at strong coupling*, *Phys. Rev. D* **104** (2021) L081703 [2103.10440].

[263] E. Lauria, M. Meineri and E. Trevisani, *Radial coordinates for defect CFTs*, *JHEP* **11** (2018) 148 [1712.07668].

[264] M. Isachenkov, P. Liendo, Y. Linke and V. Schomerus, *Calogero-Sutherland Approach to Defect Blocks*, *JHEP* **10** (2018) 204 [1806.09703].

[265] P. Liendo, Y. Linke and V. Schomerus, *A Lorentzian inversion formula for defect CFT*, 1903.05222.

[266] M. Lemos, P. Liendo, M. Meineri and S. Sarkar, *Universality at large transverse spin in defect CFT*, *JHEP* **09** (2018) 091 [1712.08185].

[267] D. McAvity and H. Osborn, *Energy momentum tensor in conformal field theories near a boundary*, *Nucl.Phys.* **B406** (1993) 655 [hep-th/9302068].

[268] D. McAvity and H. Osborn, *Conformal field theories near a boundary in general dimensions*, *Nucl.Phys.* **B455** (1995) 522 [cond-mat/9505127].

[269] P. Liendo, L. Rastelli and B. C. van Rees, *The Bootstrap Program for Boundary CFT_d*, *JHEP* **1307** (2013) 113 [1210.4258].

[270] E. Lauria, M. Meineri and E. Trevisani, *Spinning operators and defects in conformal field theory*, 1807.02522.

[271] C. P. Herzog and A. Shrestha, *Two point functions in defect CFTs*, *JHEP* **04** (2021) 226 [2010.04995].

[272] A. Bissi, T. Hansen and A. Söderberg, *Analytic Bootstrap for Boundary CFT*, *JHEP* **01** (2019) 010 [1808.08155].

[273] D. Mazáč, L. Rastelli and X. Zhou, *An analytic approach to BCFT_d*, *JHEP* **12** (2019) 004 [1812.09314].

[274] A. Kaviraj and M. F. Paulos, *The Functional Bootstrap for Boundary CFT*, *JHEP* **04** (2020) 135 [1812.04034].

[275] P. Dey and A. Söderberg, *On analytic bootstrap for interface and boundary CFT*, *JHEP* **07** (2021) 013 [2012.11344].

[276] V. Procházka and A. Söderberg, *Composite operators near the boundary*, *JHEP* **03** (2020) 114 [1912.07505].

[277] C. P. Herzog and N. Kobayashi, *The $O(N)$ model with ϕ^6 potential in $\mathbb{R}^2 \times \mathbb{R}^+$*, *JHEP* **09** (2020) 126 [2005.07863].

[278] C. P. Herzog, K.-W. Huang, I. Shamir and J. Virrueta, *Superconformal Models for Graphene and Boundary Central Charges*, *JHEP* **09** (2018) 161 [1807.01700].

[279] C. P. Herzog and K.-W. Huang, *Boundary Conformal Field Theory and a Boundary Central Charge*, *JHEP* **10** (2017) 189 [1707.06224].

[280] P. Dey, T. Hansen and M. Shpot, *Operator expansions, layer susceptibility and two-point functions in BCFT*, 2006.11253.

[281] M. Shpot, *Boundary conformal field theory at the extraordinary transition: The layer susceptibility to $O(\varepsilon)$*, 1912.03021.

[282] G. Cuomo, M. Mezei and A. Raviv-Moshe, *Boundary conformal field theory at large charge*, *JHEP* **10** (2021) 143 [2108.06579].

[283] G. Cuomo, Z. Komargodski and A. Raviv-Moshe, *Renormalization Group Flows on Line Defects*, *Phys. Rev. Lett.* **128** (2022) 021603 [2108.01117].

[284] G. Cuomo, Z. Komargodski, M. Mezei and A. Raviv-Moshe, *Spin Impurities, Wilson Lines and Semiclassics*, 2202.00040.

[285] P. Liendo and C. Meneghelli, *Bootstrap equations for $\mathcal{N}=4$ SYM with defects*, *JHEP* **01** (2017) 122 [1608.05126].

[286] J. Barrat, P. Liendo and J. Plefka, *Two-point correlator of chiral primary operators with a Wilson line defect in $\mathcal{N}=4$ SYM*, *JHEP* **05** (2021) 195 [2011.04678].

[287] J. Barrat, P. Liendo, G. Peveri and J. Plefka, *Multipoint correlators on the supersymmetric Wilson line defect CFT*, 2112.10780.

340

[288] S. Giombi and S. Komatsu, *Exact Correlators on the Wilson Loop in $\mathcal{N} = 4$ SYM: Localization, Defect CFT, and Integrability*, *JHEP* **05** (2018) 109 [1802.05201].

[289] S. Giombi and S. Komatsu, *More Exact Results in the Wilson Loop Defect CFT: Bulk-Defect OPE, Nonplanar Corrections and Quantum Spectral Curve*, *J. Phys.* **A52** (2019) 125401 [1811.02369].

[290] L. Bianchi, M. Lemos and M. Meineri, *Line Defects and Radiation in $\mathcal{N} = 2$ Conformal Theories*, *Phys. Rev. Lett.* **121** (2018) 141601 [1805.04111].

[291] F. Galvagno, *Emitted radiation in superconformal field theories*, *Eur. Phys. J. Plus* **137** (2022) 143 [2112.03841].

[292] L. Bianchi and M. Lemos, *Superconformal surfaces in four dimensions*, *JHEP* **06** (2020) 056 [1911.05082].

[293] P. Ferrero, K. Ghosh, A. Sinha and A. Zahed, *Crossing symmetry, transcendentality and the Regge behaviour of 1d CFTs*, *JHEP* **07** (2020) 170 [1911.12388].

[294] E. Lauria, P. Liendo, B. C. Van Rees and X. Zhao, *Line and surface defects for the free scalar field*, 2005.02413.

[295] C. Behan, L. Di Pietro, E. Lauria and B. C. Van Rees, *Bootstrapping boundary-localized interactions*, 2009.03336.

[296] C. Behan, L. Di Pietro, E. Lauria and B. C. van Rees, *Bootstrapping boundary-localized interactions II: Minimal models at the boundary*, 2111.04747.

[297] A. Antunes, *Conformal bootstrap near the edge*, *JHEP* **10** (2021) 057 [2103.03132].

[298] L. Iliesiu, M. Koloğlu, R. Mahajan, E. Perlmutter and D. Simmons-Duffin, *The Conformal Bootstrap at Finite Temperature*, *JHEP* **10** (2018) 070 [1802.10266].

[299] L. Iliesiu, M. Koloğlu and D. Simmons-Duffin, *Bootstrapping the 3d Ising model at finite temperature*, *JHEP* **12** (2019) 072 [1811.05451].

[300] Y. Nakayama and H. Ooguri, *Bulk Local States and Crosscaps in Holographic CFT*, *JHEP* **10** (2016) 085 [1605.00334].

[301] Y. Nakayama, *Bootstrapping critical Ising model on three-dimensional real projective space*, *Phys. Rev. Lett.* **116** (2016) 141602 [1601.06851].

[302] C. Hasegawa and Y. Nakayama, *ϵ-Expansion in Critical ϕ^3-Theory on Real Projective Space from Conformal Field Theory*, *Mod. Phys. Lett. A* **32** (2017) 1750045 [1611.06373].

[303] C. Hasegawa and Y. Nakayama, *Three ways to solve critical ϕ^4 theory on $4 - \epsilon$ dimensional real projective space: perturbation, bootstrap, and Schwinger-Dyson equation*, *Int. J. Mod. Phys. A* **33** (2018) 1850049 [1801.09107].

[304] S. Giombi, H. Khanchandani and X. Zhou, *Aspects of CFTs on Real Projective Space*, *J. Phys. A* **54** (2021) 024003 [2009.03290].

[305] P. Argyres, M. Lotito, Y. Lü and M. Martone, *Geometric constraints on the space of $\mathcal{N} = 2$ SCFTs. Part I: physical constraints on relevant deformations*, *JHEP* **02** (2018) 001 [1505.04814].

[306] P. C. Argyres, M. Lotito, Y. Lü and M. Martone, *Geometric constraints on the space of $\mathcal{N} = 2$ SCFTs. Part II: construction of special Kähler geometries and RG flows*, *JHEP* **02** (2018) 002 [1601.00011].

[307] P. C. Argyres, M. Lotito, Y. Lü and M. Martone, *Expanding the landscape of $\mathcal{N} = 2$ rank 1 SCFTs*, *JHEP* **05** (2016) 088 [1602.02764].

[308] P. Argyres, M. Lotito, Y. Lü and M. Martone, *Geometric constraints on the space of $\mathcal{N} = 2$ SCFTs. Part III: enhanced Coulomb branches and central charges*, *JHEP* **02** (2018) 003 [1609.04404].

[309] P. Argyres and M. Martone, *Construction and classification of Coulomb branch geometries*, 2003.04954.

[310] C. Beem and L. Rastelli, *Vertex operator algebras, Higgs branches, and modular differential equations*, *JHEP* **08** (2018) 114 [1707.07679].

[311] F. Bonetti, C. Meneghelli and L. Rastelli, *VOAs labelled by complex reflection groups and 4d SCFTs*, *JHEP* **05** (2019) 155 [1810.03612].

[312] C. Beem, C. Meneghelli and L. Rastelli, *Free Field Realizations from the Higgs Branch*, *JHEP* **09** (2019) 058 [1903.07624].

[313] C. Beem, C. Meneghelli, W. Peelaers and L. Rastelli, *VOAs and rank-two instanton SCFTs*, 1907.08629.

[314] S. Hellerman, S. Maeda, D. Orlando, S. Reffert and M. Watanabe, *Universal correlation functions in rank 1 SCFTs*, *JHEP* **12** (2019) 047 [`1804.01535`].

[315] A. Grassi, Z. Komargodski and L. Tizzano, *Extremal Correlators and Random Matrix Theory*, `1908.10306`.

[316] M. Baggio, V. Niarchos and K. Papadodimas, *tt^* equations, localization and exact chiral rings in 4d $\mathcal{N}$ =2 SCFTs*, *JHEP* **02** (2015) 122 [`1409.4212`].

[317] M. Baggio, V. Niarchos and K. Papadodimas, *Exact correlation functions in $SU(2)\mathcal{N} = 2$ superconformal QCD*, *Phys. Rev. Lett.* **113** (2014) 251601 [`1409.4217`].

[318] M. Baggio, V. Niarchos and K. Papadodimas, *On exact correlation functions in SU(N) $\mathcal{N} = 2$ superconformal QCD*, *JHEP* **11** (2015) 198 [`1508.03077`].

[319] M. Baggio, V. Niarchos, K. Papadodimas and G. Vos, *Large-N correlation functions in $\mathcal{N} = 2$ superconformal QCD*, *JHEP* **01** (2017) 101 [`1610.07612`].

[320] E. Gerchkovitz, J. Gomis, N. Ishtiaque, A. Karasik, Z. Komargodski and S. S. Pufu, *Correlation Functions of Coulomb Branch Operators*, *JHEP* **01** (2017) 103 [`1602.05971`].

[321] S. Hellerman, D. Orlando, S. Reffert and M. Watanabe, *On the CFT Operator Spectrum at Large Global Charge*, *JHEP* **12** (2015) 071 [`1505.01537`].

[322] S. Hellerman and S. Maeda, *On the Large R-charge Expansion in $\mathcal{N} = 2$ Superconformal Field Theories*, *JHEP* **12** (2017) 135 [`1710.07336`].

[323] M. Beccaria, *On the large R-charge $\mathcal{N} = 2$ chiral correlators and the Toda equation*, *JHEP* **02** (2019) 009 [`1809.06280`].

[324] A. Bourget, D. Rodriguez-Gomez and J. G. Russo, *A limit for large R-charge correlators in $\mathcal{N} = 2$ theories*, *JHEP* **05** (2018) 074 [`1803.00580`].

[325] C. Beem, *Flavor Symmetries and Unitarity Bounds in $\mathcal{N} = 2$ Superconformal Field Theories*, *Phys. Rev. Lett.* **122** (2019) 241603 [`1812.06099`].

[326] P. C. Argyres, M. Plesser, N. Seiberg and E. Witten, *New N=2 superconformal field theories in four-dimensions*, *Nucl. Phys. B* **461** (1996) 71 [`hep-th/9511154`].

[327] P. C. Argyres and M. R. Douglas, *New phenomena in SU(3) supersymmetric gauge theory*, *Nucl. Phys. B* **448** (1995) 93 [`hep-th/9505062`].

[328] K. Maruyoshi and J. Song, $\mathcal{N} = 1$ *deformations and RG flows of* $\mathcal{N} = 2$ *SCFTs*, *JHEP* **02** (2017) 075 [`1607.04281`].

[329] O. Aharony and Y. Tachikawa, *A Holographic computation of the central charges of d=4, N=2 SCFTs*, *JHEP* **01** (2008) 037 [`0711.4532`].

[330] M. Buican and T. Nishinaka, *On the superconformal index of Argyres–Douglas theories*, *J. Phys. A* **49** (2016) 015401 [`1505.05884`].

[331] C. Cordova and S.-H. Shao, *Schur Indices, BPS Particles, and Argyres-Douglas Theories*, *JHEP* **01** (2016) 040 [`1506.00265`].

[332] O. Aharony, A. Fayyazuddin and J. M. Maldacena, *The Large N limit of N=2, N=1 field theories from three-branes in F theory*, *JHEP* **07** (1998) 013 [`hep-th/9806159`].

[333] G. Arutyunov, B. Eden and E. Sokatchev, *On nonrenormalization and OPE in superconformal field theories*, *Nucl. Phys.* **B619** (2001) 359 [`hep-th/0105254`].

[334] J. Song, *Superconformal indices of generalized Argyres-Douglas theories from 2d TQFT*, *JHEP* **02** (2016) 045 [`1509.06730`].

[335] N. Su, "Search methods for the numerical bootstrap." Developments in the Numerical Bootstrap, Nov., 2019.

[336] R. Doobary and P. Heslop, *Superconformal partial waves in Grassmannian field theories*, *JHEP* **12** (2015) 159 [`1508.03611`].

[337] Z. Li, *Superconformal Partial Waves for Stress-tensor Multiplet Correlator in* 4D $\mathcal{N} = 2$ *SCFTs*, `1806.11550`.

[338] I. A. Ramírez, *Mixed OPEs in* $\mathcal{N} = 2$ *superconformal theories*, *JHEP* **05** (2016) 043 [`1602.07269`].

[339] P. Kravchuk, *Unpublished*, .

[340] O. Aharony, N. Seiberg and Y. Tachikawa, *Reading between the lines of four-dimensional gauge theories*, *JHEP* **08** (2013) 115 [`1305.0318`].

344

[341] V. Pestun, *Localization of gauge theory on a four-sphere and supersymmetric Wilson loops*, *Commun. Math. Phys.* **313** (2012) 71 [`0712.2824`].

[342] D. Correa, J. Henn, J. Maldacena and A. Sever, *An exact formula for the radiation of a moving quark in N=4 super Yang Mills*, *JHEP* **1206** (2012) 048 [`1202.4455`].

[343] A. Lewkowycz and J. Maldacena, *Exact results for the entanglement entropy and the energy radiated by a quark*, *JHEP* **05** (2014) 025 [`1312.5682`].

[344] B. Fiol, B. Garolera and A. Lewkowycz, *Exact results for static and radiative fields of a quark in N=4 super Yang-Mills*, *JHEP* **05** (2012) 093 [`1202.5292`].

[345] B. Fiol, E. Gerchkovitz and Z. Komargodski, *Exact Bremsstrahlung Function in $N = 2$ Superconformal Field Theories*, *Phys. Rev. Lett.* **116** (2016) 081601 [`1510.01332`].

[346] S. Giombi, R. Roiban and A. A. Tseytlin, *Half-BPS Wilson loop and AdS_2/CFT_1*, *Nucl. Phys.* **B922** (2017) 499 [`1706.00756`].

[347] M. Cooke, A. Dekel and N. Drukker, *The Wilson loop CFT: Insertion dimensions and structure constants from wavy lines*, *J. Phys.* **A50** (2017) 335401 [`1703.03812`].

[348] M. Cooke, A. Dekel, N. Drukker, D. Trancanelli and E. Vescovi, *Deformations of the circular Wilson loop and spectral (in)dependence*, *JHEP* **01** (2019) 076 [`1811.09638`].

[349] D. Mazáč, *A Crossing-Symmetric OPE Inversion Formula*, *JHEP* **06** (2019) 082 [`1812.02254`].

[350] N. Arkani-Hamed, Y.-T. Huang and S.-H. Shao, *On the Positive Geometry of Conformal Field Theory*, `1812.07739`.

[351] J. Qiao and S. Rychkov, *A tauberian theorem for the conformal bootstrap*, *JHEP* **12** (2017) 119 [`1709.00008`].

[352] L. Frappat, P. Sorba and A. Sciarrino, *Dictionary on Lie superalgebras*, `hep-th/9607161`.

[353] L. Bianchi, L. Griguolo, M. Preti and D. Seminara, *Wilson lines as superconformal defects in ABJM theory: a formula for the emitted radiation*, *JHEP* **10** (2017) 050 [`1706.06590`].

[354] L. Bianchi, M. Preti and E. Vescovi, *Exact Bremsstrahlung functions in ABJM theory*, *JHEP* **07** (2018) 060 [`1802.07726`].

[355] M. Gunaydin and R. J. Scalise, *Unitary Lowest Weight Representations of the Noncompact Supergroup Osp(2m*/2n)*, *J. Math. Phys.* **32** (1991) 599.

[356] F. Kos and J. Oh, *2d small N=4 Long-multiplet superconformal block*, *JHEP* **02** (2019) 001 [`1810.10029`].

[357] P. Liendo, C. Meneghelli and V. Mitev, *On Correlation Functions of BPS Operators in 3d $\mathcal{N} = 6$ Superconformal Theories*, *Commun. Math. Phys.* **350** (2017) 387 [`1512.06072`].

[358] J. D. Hunter, *Matplotlib: A 2d graphics environment*, *Computing in Science & Engineering* **9** (2007) 90.

[359] I. Heemskerk, J. Penedones, J. Polchinski and J. Sully, *Holography from Conformal Field Theory*, *JHEP* **10** (2009) 079 [`0907.0151`].

[360] A. L. Fitzpatrick, E. Katz, D. Poland and D. Simmons-Duffin, *Effective Conformal Theory and the Flat-Space Limit of AdS*, *JHEP* **07** (2011) 023 [`1007.2412`].

[361] A. L. Fitzpatrick and J. Kaplan, *Unitarity and the Holographic S-Matrix*, *JHEP* **10** (2012) 032 [`1112.4845`].

[362] L. F. Alday and A. Bissi, *Loop Corrections to Supergravity on $AdS_5 \times S^5$*, *Phys. Rev. Lett.* **119** (2017) 171601 [`1706.02388`].

[363] F. Aprile, J. M. Drummond, P. Heslop and H. Paul, *Unmixing Supergravity*, *JHEP* **02** (2018) 133 [`1706.08456`].

[364] D. Xie, *Higher laminations, webs and N=2 line operators*, `1304.2390`.

[365] D. Xie, *Aspects of line operators of class S theories*, `1312.3371`.

[366] C. Cordova, D. Gaiotto and S.-H. Shao, *Infrared Computations of Defect Schur Indices*, *JHEP* **11** (2016) 106 [`1606.08429`].

[367] S. Giombi and H. Khanchandani, *$O(N)$ models with boundary interactions and their long range generalizations*, *JHEP* **08** (2020) 010 [`1912.08169`].

[368] L. Di Pietro, D. Gaiotto, E. Lauria and J. Wu, *3d Abelian Gauge Theories at the Boundary*, *JHEP* **05** (2019) 091 [`1902.09567`].

[369] A. Gadde, S. Gukov and P. Putrov, *Walls, Lines, and Spectral Dualities in 3d Gauge Theories*, *JHEP* **05** (2014) 047 [`1302.0015`].

[370] T. Okazaki and S. Yamaguchi, *Supersymmetric boundary conditions in three-dimensional N=2 theories*, *Phys. Rev. D* **87** (2013) 125005 [`1302.6593`].

[371] F. Aprile and V. Niarchos, $\mathcal{N}$ *=2 supersymmetric field theories on 3-manifolds with A-type boundaries*, *JHEP* **07** (2016) 126 [`1604.01561`].

[372] T. Dimofte, D. Gaiotto and N. M. Paquette, *Dual boundary conditions in 3d SCFT's*, *JHEP* **05** (2018) 060 [`1712.07654`].

[373] S. Sugishita and S. Terashima, *Exact Results in Supersymmetric Field Theories on Manifolds with Boundaries*, *JHEP* **11** (2013) 021 [`1308.1973`].

[374] Y. Yoshida and K. Sugiyama, *Localization of 3d $\mathcal{N} = 2$ Supersymmetric Theories on $S^1 \times D^2$*, `1409.6713`.

[375] D. J. Binder and S. Rychkov, *Deligne Categories in Lattice Models and Quantum Field Theory, or Making Sense of $O(N)$ Symmetry with Non-integer N*, *JHEP* **04** (2020) 117 [`1911.07895`].

[376] A. Bilal, *Supersymmetric Boundaries and Junctions in Four Dimensions*, *JHEP* **11** (2011) 046 [`1103.2280`].

[377] I. Brunner, J. Schulz and A. Tabler, *Boundaries and supercurrent multiplets in 3D Landau-Ginzburg models*, *JHEP* **06** (2019) 046 [`1904.07258`].

[378] N. Bobev, S. El-Showk, D. Mazac and M. F. Paulos, *Bootstrapping the Three-Dimensional Supersymmetric Ising Model*, *Phys. Rev. Lett.* **115** (2015) 051601 [`1502.04124`].

[379] A. Kaviraj, S. Rychkov and E. Trevisani, *Random Field Ising Model and Parisi-Sourlas supersymmetry. Part I. Supersymmetric CFT*, *JHEP* **04** (2020) 090 [`1912.01617`].

347

[380] A. Kaviraj, S. Rychkov and E. Trevisani, *Random Field Ising Model and Parisi-Sourlas Supersymmetry II. Renormalization Group*, `2009.10087`.

[381] S. Giombi and H. Khanchandani, *CFT in AdS and boundary RG flows*, `2007.04955`.

[382] S.-S. Lee, *Emergence of supersymmetry at a critical point of a lattice model*, *Phys. Rev. B* **76** (2007) 075103 [`cond-mat/0611658`].

[383] L. Fei, S. Giombi, I. R. Klebanov and G. Tarnopolsky, *Yukawa CFTs and Emergent Supersymmetry*, *PTEP* **2016** (2016) 12C105 [`1607.05316`].

[384] P. Townsend and P. van Nieuwenhuizen, *Dimensional Regularization and Supersymmetry at the Two Loop Level*, *Phys. Rev. D* **20** (1979) 1832.

[385] H. Diehl, *Why boundary conditions do not generally determine the universality class for boundary critical behavior*, *Eur. Phys. J. B* **93** (2020) 195 [`2006.15425`].

[386] D. McAvity, *Integral transforms for conformal field theories with a boundary*, *J. Phys. A* **28** (1995) 6915 [`hep-th/9507028`].

[387] E. Eisenriegler and M. Stapper, *Critical behavior near a symmetry-breaking surface and the stress tensor*, *Phys. Rev. B* **50** (1994) 10009.

[388] I. Burić and V. Schomerus, *Defect Conformal Blocks from Appell Functions*, `2012.12489`.

[389] S. Yamaguchi, *The ϵ-expansion of the codimension two twist defect from conformal field theory*, *PTEP* **2016** (2016) 091B01 [`1607.05551`].

[390] L. Bianchi, A. Chalabi, V. Procházka, B. Robinson and J. Sisti, *Monodromy Defects in Free Field Theories*, `2104.01220`.

[391] J. S. Dowker, *Remarks on spherical monodromy defects for free scalar fields*, `2104.09419`.

[392] M. Lemos, B. C. van Rees and X. Zhao, *Regge trajectories for the (2, 0) theories*, *JHEP* **01** (2022) 022 [`2105.13361`].

[393] L. F. Alday, *Large Spin Perturbation Theory for Conformal Field Theories*, *Phys. Rev. Lett.* **119** (2017) 111601 [`1611.01500`].

[394] L. F. Alday and S. Caron-Huot, *Gravitational S-matrix from CFT dispersion relations*, *JHEP* **12** (2018) 017 [`1711.02031`].

[395] L. Rastelli and X. Zhou, *Mellin amplitudes for $AdS_5 \times S^5$*, *Phys. Rev. Lett.* **118** (2017) 091602 [`1608.06624`].

[396] L. Rastelli and X. Zhou, *How to Succeed at Holographic Correlators Without Really Trying*, *JHEP* **04** (2018) 014 [`1710.05923`].

[397] G. W. Semenoff and K. Zarembo, *More exact predictions of SUSYM for string theory*, *Nucl. Phys. B* **616** (2001) 34 [`hep-th/0106015`].

[398] K. Okuyama and G. W. Semenoff, *Wilson loops in N=4 SYM and fermion droplets*, *JHEP* **06** (2006) 057 [`hep-th/0604209`].

[399] S. Giombi and V. Pestun, *Correlators of local operators and 1/8 BPS Wilson loops on S**2 from 2d YM and matrix models*, *JHEP* **10** (2010) 033 [`0906.1572`].

[400] M. Billo, F. Galvagno, P. Gregori and A. Lerda, *Correlators between Wilson loop and chiral operators in $\mathcal{N} = 2$ conformal gauge theories*, *JHEP* **03** (2018) 193 [`1802.09813`].

[401] S. Giombi and V. Pestun, *Correlators of Wilson Loops and Local Operators from Multi-Matrix Models and Strings in AdS*, *JHEP* **01** (2013) 101 [`1207.7083`].

[402] E. I. Buchbinder and A. A. Tseytlin, *Correlation function of circular Wilson loop with two local operators and conformal invariance*, *Phys. Rev. D* **87** (2013) 026006 [`1208.5138`].

[403] M. Beccaria and A. A. Tseytlin, *On the structure of non-planar strong coupling corrections to correlators of BPS Wilson loops and chiral primary operators*, *JHEP* **01** (2021) 149 [`2011.02885`].

[404] J. M. Maldacena, *The Large N limit of superconformal field theories and supergravity*, *Int.J.Theor.Phys.* **38** (1999) 1113 [`hep-th/9711200`].

[405] E. Witten, *Anti-de Sitter space and holography*, *Adv. Theor. Math. Phys.* **2** (1998) 253 [`hep-th/9802150`].

[406] S. S. Gubser, I. R. Klebanov and A. M. Polyakov, *Gauge theory correlators from noncritical string theory*, *Phys. Lett. B* **428** (1998) 105 [`hep-th/9802109`].

[407] J. M. Maldacena, *Wilson loops in large N field theories*, *Phys. Rev. Lett.* **80** (1998) 4859 [`hep-th/9803002`].

[408] S.-J. Rey and J.-T. Yee, *Macroscopic strings as heavy quarks in large N gauge theory and anti-de Sitter supergravity*, *Eur. Phys. J.* **C22** (2001) 379 [`hep-th/9803001`].

[409] J. K. Erickson, G. W. Semenoff and K. Zarembo, *Wilson loops in N=4 supersymmetric Yang-Mills theory*, *Nucl. Phys. B* **582** (2000) 155 [`hep-th/0003055`].

[410] N. Drukker and D. J. Gross, *An Exact prediction of N=4 SUSYM theory for string theory*, *J. Math. Phys.* **42** (2001) 2896 [`hep-th/0010274`].

[411] D. E. Berenstein, R. Corrado, W. Fischler and J. M. Maldacena, *The Operator product expansion for Wilson loops and surfaces in the large N limit*, *Phys. Rev. D* **59** (1999) 105023 [`hep-th/9809188`].

[412] D. Grabner, N. Gromov and J. Julius, *Excited States of One-Dimensional Defect CFTs from the Quantum Spectral Curve*, *JHEP* **07** (2020) 042 [`2001.11039`].

[413] A. Cavaglià, N. Gromov, J. Julius and M. Preti, *Integrability and conformal bootstrap: One dimensional defect conformal field theory*, *Phys. Rev. D* **105** (2022) L021902 [`2107.08510`].

[414] S. Lee, S. Minwalla, M. Rangamani and N. Seiberg, *Three point functions of chiral operators in D = 4, N=4 SYM at large N*, *Adv. Theor. Math. Phys.* **2** (1998) 697 [`hep-th/9806074`].

[415] J. Barrat, A. Gimenez-Grau and P. Liendo, *Unpublished notes.*

[416] V. Gonçalves, *Four point function of $\mathcal{N} = 4$ stress-tensor multiplet at strong coupling*, *JHEP* **04** (2015) 150 [`1411.1675`].

[417] F. Aprile, J. M. Drummond, P. Heslop and H. Paul, *Quantum Gravity from Conformal Field Theory*, *JHEP* **01** (2018) 035 [`1706.02822`].

[418] F. Aprile, J. M. Drummond, P. Heslop and H. Paul, *Loop corrections for Kaluza-Klein AdS amplitudes*, *JHEP* **05** (2018) 056 [1711.03903].

[419] V. Goncalves and G. Itsios, *A note on defect Mellin amplitudes*, 1803.06721.

[420] M. Beccaria, S. Giombi and A. A. Tseytlin, *Correlators on non-supersymmetric Wilson line in N=4 SYM and AdS_2/CFT_1*, 1903.04365.

[421] S. Giombi, J. Jiang and S. Komatsu, *Giant Wilson loops and $AdS_2/dCFT_1$*, *JHEP* **11** (2020) 064 [2005.08890].

[422] N. Su, *The Hybrid Bootstrap*, 2202.07607.

[423] R. S. Erramilli, L. V. Iliesiu and P. Kravchuk, *Recursion relation for general 3d blocks*, *JHEP* **12** (2019) 116 [1907.11247].

[424] V. Gonçalves, R. Pereira and X. Zhou, 20′ *Five-Point Function from $AdS_5 \times S^5$ Supergravity*, *JHEP* **10** (2019) 247 [1906.05305].

[425] A. Antunes, M. S. Costa, V. Goncalves and J. V. Boas, *Lightcone Bootstrap at higher points*, 2111.05453.

[426] V. Rosenhaus, *Multipoint Conformal Blocks in the Comb Channel*, *JHEP* **02** (2019) 142 [1810.03244].

[427] I. Buric, S. Lacroix, J. A. Mann, L. Quintavalle and V. Schomerus, *From Gaudin Integrable Models to d-dimensional Multipoint Conformal Blocks*, *Phys. Rev. Lett.* **126** (2021) 021602 [2009.11882].

[428] D. Poland and V. Prilepina, *Recursion relations for 5-point conformal blocks*, *JHEP* **10** (2021) 160 [2103.12092].

[429] I. Buric, S. Lacroix, J. A. Mann, L. Quintavalle and V. Schomerus, *Gaudin models and multipoint conformal blocks: general theory*, *JHEP* **10** (2021) 139 [2105.00021].

[430] I. Buric, S. Lacroix, J. A. Mann, L. Quintavalle and V. Schomerus, *Gaudin models and multipoint conformal blocks. Part II. Comb channel vertices in 3D and 4D*, *JHEP* **11** (2021) 182 [2108.00023].

[431] I. Buric, S. Lacroix, J. A. Mann, L. Quintavalle and V. Schomerus, *Gaudin Models and Multipoint Conformal Blocks III: Comb channel coordinates and OPE factorisation*, 2112.10827.

[432] C. Bercini, V. Gonçalves and P. Vieira, *Light-Cone Bootstrap of Higher Point Functions and Wilson Loop Duality*, *Phys. Rev. Lett.* **126** (2021) 121603 [2008.10407].

[433] C. Bercini, V. Gonçalves, A. Homrich and P. Vieira, *The Wilson Loop - Large Spin OPE Dictionary*, 2110.04364.

[434] A. Gadde, *Conformal constraints on defects*, 1602.06354.

[435] N. Kobayashi and T. Nishioka, *Spinning conformal defects*, 1805.05967.

[436] A. Söderberg, *Fusion of conformal defects in four dimensions*, *JHEP* **04** (2021) 087 [2102.00718].